EMERGING INFECTIOUS DISEASES®

Tuberculosis and Other Mycobacteria

March 2024

Paulina Siniatkina (1989–), *Don't Speak*, 2019. Tempera on canvas, 100 in x 105 in/254 cm x 266.7 cm. http://www.paulinasiniatkina.com

EMERGING INFECTIOUS DISEASES®

Emerging Infectious Diseases is published monthly by the Centers for Disease Control and Prevention, 1600 Clifton Rd NE, Mailstop H16-2, Atlanta, GA 30329-4018, USA. Telephone 404-639-1960; email, eideditor@cdc.gov

EMERGING INFECTIOUS DISEASES®

Tuberculosis and Other Mycobacteria **March 2024**

On the Cover

Paulina Siniatkina (1989–), *Don't speak!* Tempera on canvas (2016), 37.4 in × 41.3 in/100 cm × 105 cm. http://www.paulinasiniatkina.com

About the Cover p. 627

Synopsis

Medscape EDUCATION ACTIVITY

Research

438

Dispatches

EMERGING INFECTIOUS DISEASES®

March 2024

Another Dimension

Research Letters

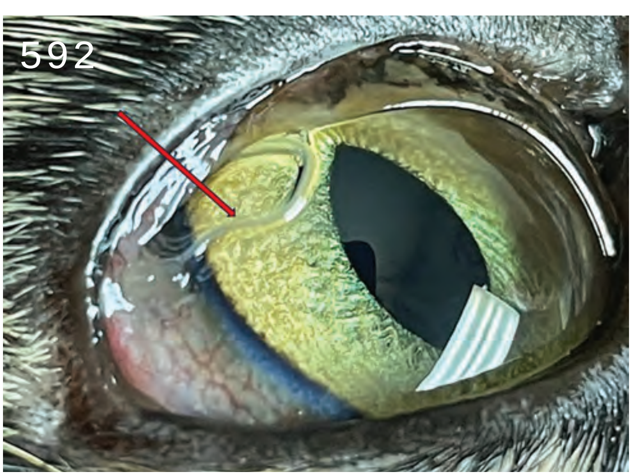

EMERGING INFECTIOUS DISEASES®
March 2024

Books and Media

About the Cover

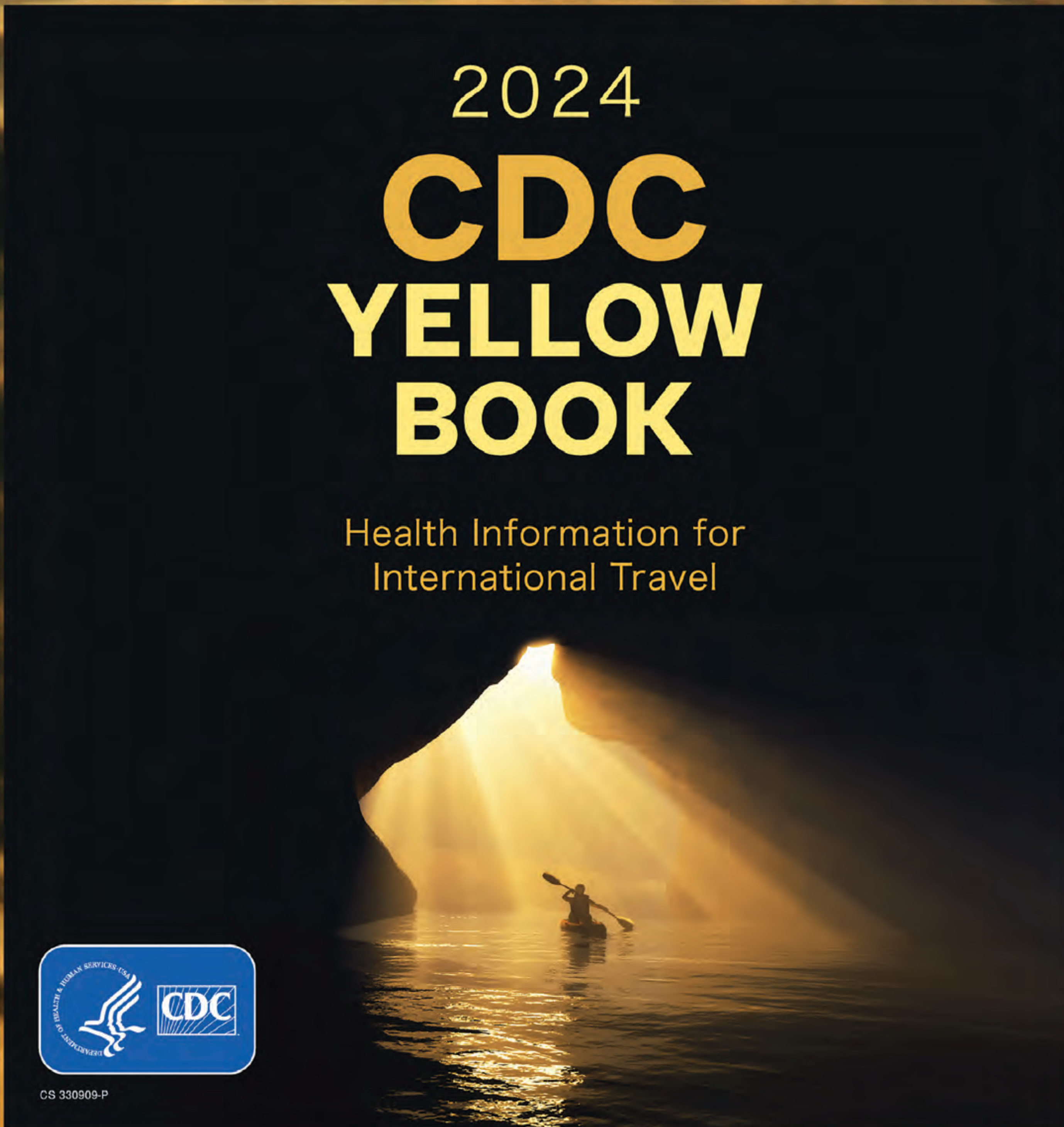

Launch of CDC Yellow Book 2024 – A Trusted Travel Medicine Resource

CDC is pleased to announce the launch of the CDC Yellow Book 2024. The CDC Yellow Book is a source of the U.S. Government's recommendations on travel medicine and has been a trusted resource among the travel medicine community for over 50 years. Healthcare professionals can use the print and digital versions to find the most up-to-date travel medicine information to better serve their patients' healthcare needs.

The CDC Yellow Book is available in print through Oxford University Press and online at www.cdc.gov/yellowbook.

Molecular Epidemiology of Underreported Emerging Zoonotic Pathogen *Streptococcus suis* in Europe

Jaime Brizuela, Thomas J. Roodsant, Qureisha Hasnoe, Boas C.L. van der Putten, Jana Kozakova, Hans-Christian Slotved, Mark van der Linden, Ilse G.A. de Beer-Schuurman, Ewa Sadowy, Juan Antonio Sáez-Nieto, Victoria J. Chalker, Kees C.H. van der Ark, Constance Schultsz

Medscape CME Activity

In support of improving patient care, this activity has been planned and implemented by Medscape, LLC and Emerging Infectious Diseases. Medscape, LLC is jointly accredited with commendation by the Accreditation Council for Continuing Medical Education (ACCME), the Accreditation Council for Pharmacy Education (ACPE), and the American Nurses Credentialing Center (ANCC), to provide continuing education for the healthcare team.

Medscape, LLC designates this Journal-based CME activity for a maximum of 1.00 ***AMA PRA Category 1 Credit(s)*™**. Physicians should claim only the credit commensurate with the extent of their participation in the activity.

Successful completion of this CME activity, which includes participation in the evaluation component, enables the participant to earn up to 1.0 MOC points in the American Board of Internal Medicine's (ABIM) Maintenance of Certification (MOC) program. Participants will earn MOC points equivalent to the amount of CME credits claimed for the activity. It is the CME activity provider's responsibility to submit participant completion information to ACCME for the purpose of granting ABIM MOC credit.

All other clinicians completing this activity will be issued a certificate of participation. To participate in this journal CME activity: (1) review the learning objectives and author disclosures; (2) study the education content; (3) take the post-test with a 75% minimum passing score and complete the evaluation at http://www.medscape.org/journal/eid; and (4) view/print certificate. For CME questions, see page 630.

NOTE: It is Medscape's policy to avoid the use of brand names in accredited activities. However, in an effort to be as clear as possible, the use of brand names should not be viewed as a promotion of any brand or as an endorsement by Medscape of specific products.

Release date: February 22, 2024; Expiration date: February 22, 2025

Learning Objectives

Upon completion of this activity, participants will be able to:

- Assess the worldwide epidemiology of *Streptococcus suis*.
- Distinguish the most common serotype of *S. suis* associated with zoonotic infection.
- Analyze clinical syndromes associated with infection with *S. suis*.
- Evaluate genetic characteristics of *S. suis* isolates in the current study.

CME Editor

Tony Pearson-Clarke, MS, Technical Writer/Editor, Emerging Infectious Diseases. *Disclosure: Tony Pearson-Clarke, MS, has no relevant financial relationships.*

CME Author

Charles P. Vega, MD, Health Sciences Clinical Professor of Family Medicine, University of California, Irvine School of Medicine, Irvine, California. *Disclosure: Charles P. Vega, MD, has the following relevant financial relationships: consultant or advisor for Boehringer Ingelheim Pharmaceuticals, Inc.; GlaxoSmithKline.*

Authors

Jaime Brizuela, MRes; Thomas J. Roodsant, PhD; Qureisha Hasnoe, MSc; Boas C.L. van der Putten, PhD; Jana Kozakova, MD; Hans-Christian Slotved, PhD, DMSc; Mark van der Linden, PhD; Ilse G.A. de Beer-Schuurman, BSc; Ewa Sadowy, PhD, MD; Juan Antonio Sáez-Nieto, PhD; Victoria J. Chalker, PhD; Kees C.H. van der Ark, PhD; Constance Schultsz, PhD, MD.

Author affiliations: Amsterdam University Medical Center, University of Amsterdam, Amsterdam, the Netherlands (J. Brizuela, T.J. Roodsant, Q. Hasnoe, B.C.L. van der Putten, I.G.A de Beer-Schuurman, K.C.H. van der Ark, C. Schultsz); National Institute for Public Health, Prague, Czech Republic (J. Kozakova); Statens Serum Institut, Copenhagen, Denmark (H.-C. Slotved); University Hospital RWTH Aachen, Aachen, Germany (M. van der Linden); National Medicines Institute, Warsaw, Poland (E. Sadowy); Carlos III Health Institute, Madrid, Spain (J.A. Sáez-Nieto); UK Health Security Agency, London, UK (V.J. Chalker).

DOI: https://doi.org/10.3201/eid3003.230348

Streptococcus suis, a zoonotic bacterial pathogen circulated through swine, can cause severe infections in humans. Because human *S. suis* infections are not notifiable in most countries, incidence is underestimated. We aimed to increase insight into the molecular epidemiology of human *S. suis* infections in Europe. To procure data, we surveyed 7 reference laboratories and performed a systematic review of the scientific literature. We identified 236 cases of human *S. suis* infection from those sources and an additional 87 by scanning gray literature. We performed whole-genome sequencing to type 46 zoonotic *S. suis* isolates and combined them with 28 publicly available genomes in a core-genome phylogeny. Clonal complex (CC) 1 isolates accounted for 87% of typed human infections; CC20, CC25, CC87, and CC94 also caused infections. Emergence of diverse zoonotic clades and notable severity of illness in humans support classifying *S. suis* infection as a notifiable condition.

Streptococcus suis is an opportunistic bacterial porcine pathogen that can cause severe disease in humans, most commonly meningitis and sepsis (*1*). Human *S. suis* infections occur both through direct contact with infected pigs and consumption of undercooked contaminated pork (*2*). Human *S. suis* infections have become endemic in Thailand and Vietnam, driven by consumption of traditional raw pork dishes (*1*), and *S. suis* has caused multiple outbreaks in humans with high levels of illness and death in China and Thailand (*3*). In Europe, *S. suis* infections are considered an occupational hazard, mainly occurring among persons with skin lesions working closely with pigs or pork products (*1*). Human infections in Europe account for ≈10% of the global prevalence, but incidence in Europe is likely underestimated because *S. suis* infections are not a notifiable disease (*4*). Togo, Madagascar, Chile, and Indonesia have recently reported zoonotic *S. suis* infections, meaning all continents except Antarctica have now reported human infections (*1*,*5*–*8*).

S. suis is classified into 29 distinct serotypes based on its capsular polysaccharide, as well as 27 novel serotypes based on novel capsular polysaccharide loci. Serotypes 2, 4, 7, and 9 are the most common causes of porcine disease in Europe (*3*); serotype 2 isolates cause ≈95% of human infections and serotype 14 causes ≈4% (*4*). In addition, sporadic infections caused by serotypes 4, 5, 7, 9, 16, 21, 24, and 31 have been reported (*3*,*9*–*11*). *S. suis* genotypes are classified on the basis of sequence types (STs) determined through multilocus sequence typing (MLST), which are grouped into clonal complexes (CCs) (*12*). CC1 with a serotype 2 capsule is the main lineage causing human infections and has expanded worldwide (*3*). Emerging zoonotic lineages, such as CC20, which emerged from CC16 in the Netherlands after acquiring a serotype 2 capsule, also been described (*13*).

We aimed to increase insight into the epidemiology of human *S. suis* infections in Europe and to assess the bacterial population structure and diversity of zoonotic *S. suis* clades (*1*). We assessed the frequency of human *S. suis* infections in Europe through a survey of reference laboratories in top pig-rearing countries in Europe, performed a systematic literature review and explored the gray literature (social media, news accounts, and government reports). In addition, we reconstructed a representative phylogeny of zoonotic *S. suis* isolates in Europe.

This study was not reviewed by an ethics review board, because it was based on anonymized surveillance data. In accordance with Dutch law, approval from a medical ethics committee was not deemed necessary because case-patients were not subject to any actions or rules of conduct. We did not obtain informed consent because our data collection processes were exempted under exceptions formulated in the Dutch Implementation of the European General Data Protection Regulation Act (2016/679).

Methods

Survey

We contacted national reference laboratories in 10 countries in Europe (Czech Republic, Denmark, France, Germany, Hungary, Italy, the Netherlands, Poland, Spain, and the United Kingdom) that included *S. suis* infections within their scope. We asked those laboratories to retrospectively collect data on cases of human *S. suis* infection during 1990–2018 because most human *S. suis* infections have been reported since 1990. We asked participating laboratories to complete a questionnaire collecting patient metadata and bacterial typing and metadata. Anonymized patient metadata were age, sex, clinical signs, and occupation. Bacterial typing encompassed serotype, sequence type (ST), and available whole-genome sequences. Bacterial metadata were date of isolation, source of isolation, and method of identification. In addition, we requested in the questionnaire that reference laboratories share their isolates for further genomic analysis (Appendix, https://wwwnc.cdc.gov/EID/article/30/3/23-0348-App1.pdf).

Systematic Review

We performed a systematic review according to PRISMA (Preferred Reporting Items for Systematic Reviews and Meta-Analyses) guidelines (*14*) to identify cases of human *S. suis* infections in Europe in articles published from 1990 (survey start date) through 2022. We screened PubMed, Web of Science, and Scopus for key terms—*S. suis,* human, and ≥1 country in Europe (as defined by the World Health Organization)—in the titles or abstracts of articles published before April 1, 2022 (Appendix). We removed duplicate references by using Zotero version 6.0.8 (https://www.zotero.org) and manual checking. We included studies containing data on human *S. suis* isolates or case reports describing human *S. suis* infections in Europe; we extracted patient and bacterial metadata for further analysis. We excluded studies that did not include data on zoonotic *S. suis* isolates or human infections, reported isolates not collected in Europe, did not publish original data, were published before 1990, or lacked information on the origin of isolates (Figure 1). To avoid duplication, we excluded from the systematic review isolates reported in both the survey and an article; in addition, if an isolate appeared in multiple articles, we included data only from the original article.

Gray Literature Search

Because *S. suis* is not a notifiable disease, there are no guidelines for reporting such infections. To identify additional cases, we performed a broad scan of gray literature to capture cases of human *S. suis* infections in Europe not identified in the scientific literature or the survey. However, we distinguished cases we identified in the survey, literature review, and official reports from unreported cases (all other cases). We searched X (previously Twitter) and the Google news section using the terms *S. suis,* infection, and human in Dutch, English, French, German, Italian, Portuguese, and Spanish. To complement those data, we scanned ministry of health websites from France, Germany, Italy, the Netherlands,

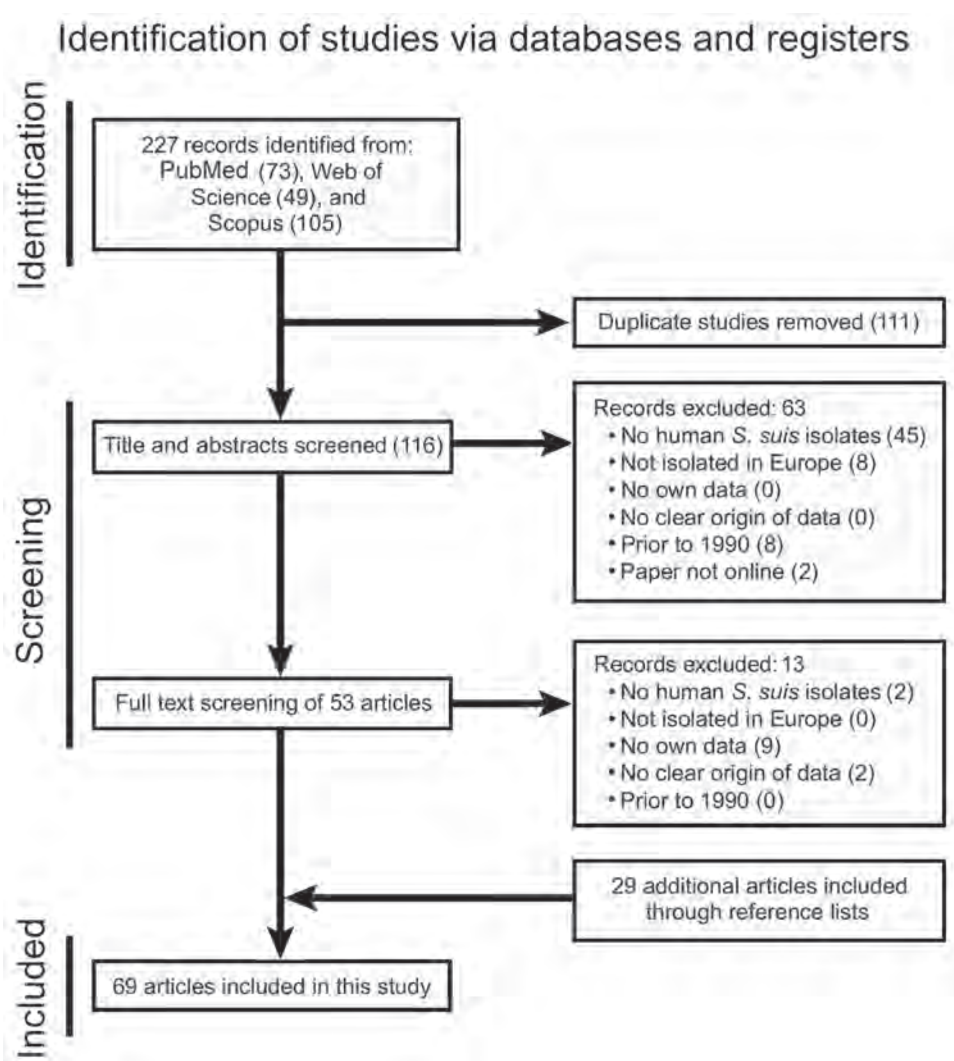

Figure 1. Preferred Reporting Items for Systematic Reviews and Meta-Analyses (PRISMA) search flowchart for systematic review of *Streptococcus suis* in Europe during 1990–2022.

Portugal, Spain, and the United Kingdom for reports on zoonotic bacterial infections related to human *S. suis* infections. To avoid duplication, we compared metadata, when available, with isolate data from the survey and systematic review.

In Silico Typing and Phylogenetic Analysis

We included 74 genomes for whole-genome sequencing (WGS) analysis, 67 from the survey (46 sequenced during this investigation and 21 previously sequenced) and 7 from the systematic review (Appendix Figure 1). We used MLST version 2.19.0 (https://github.com/tseemann/mlst) with the PubMLST database (https://pubmlst.org) to type the MLST profiles of the draft genomes. We submitted profiles for novel STs to PubMLST. We performed in silico serotyping by feeding processed Illumina reads into the *S. suis* serotyping pipeline (*15*). We reconstructed a core genome single-nucleotide polymorphism (SNP) phylogeny using Panaroo version 1.3.0 (*16*) to reconstruct the pangenome and align the core genome. We calculated the number of constant sites in the core genome alignment with SNP-sites version 2.5.1 (*17*) using the flag "-C." We reconstructed the maximum-likelihood (ML) phylogeny by running IQ-TREE version 2.0.3 (*18*) with 1,000 bootstraps and used the general time-reversible plus gamma model with the flag "-fconst" to include the constant sites from SNP-sites. We investigated the presence of 46 accessory genes previously found to be overrepresented in zoonotic isolates (human-pig prevalence ratio >2) using ABRicate (https://github.com/tseemann/abricate) with a custom database and a minimum protein identity and coverage of 80%. We visualized the resulting gene presence/absence matrix in Phandango (*19*,*20*). Raw Illumina sequences can be found in the National Center for Biotechnology Information Short Read Archive (BioProject PRJNA853715). Genome assemblies have been deposited in GenBank and are available under the same BioProject number (Appendix Table 7).

Results

Geographic Distribution of Reported Human *S. suis* Infections across Europe, 1990–2022

Of 10 reference laboratories invited to participate in the survey, 7 laboratories (Spain, Germany, Netherlands, Denmark, Czech Republic, Poland, and United Kingdom) responded and reported 107 unique cases of human *S. suis* infections (Appendix Table 2). In the systematic review, of 119 screened titles and abstracts, we selected 53 articles mentioning human *S. suis* infections in Europe for full-text reading. In addition, we included 29 studies identified by screening reference lists (Figure 1). In total, we extracted data from 129 cases of human *S. suis* infections reported in 69 research articles (Figure 1; Appendix Table 3). Combining both sources, we identified 236 unique cases of human *S. suis* infections across Europe during 1990–2022. Germany, Spain, and the Netherlands, the top pig-rearing countries in Europe (*21*), reported 114/236 (48%) of the cases (Figure 2). Furthermore, 203/236 (86%) of the reported cases originated from just 8 countries (Germany, Spain, the Netherlands, Denmark, Hungary, France, Poland, and the Czech Republic), 6 of which participated in the survey study; sporadic cases reported from 8 additional countries in Europe completed the dataset.

Epidemiology of Human *S. suis* Infections in Europe

Most patients were middle-aged men (Table 1). Of patients with a reported clinical syndrome, meningitis was the main clinical syndrome observed in both the survey (59/71 [83%]) and systematic review (59/86 [68%]), followed by sepsis, which affected 15/71 (21%) in the survey and 21/86 (24%) in the systematic review. Additional clinical signs and symptoms included hearing loss (n = 22), endocarditis (n = 6), and spondylodiscitis (n = 3); 11 patients died. Patient occupation was described as a potential risk factor in 19 cases in the survey and 72 cases in the systematic review (Table 1). Most infections, 78/92 (85%) in the survey and 43/48 (90%) in the systematic review, were caused by serotype 2 isolates, followed by serotype 14 isolates (Table 2). Most isolates (76/87 [78%] in the survey and 14/16 [88%] in the systematic review) belonged to zoonotic lineage CC1. In addition, 11/87 (13%) infections in the survey and 1 in the systematic review were caused by CC20 lineage isolates.

Year of isolation was collected for only 44/129 (34%) isolates from cases in the systematic review (Appendix Table 3). Nonetheless, average number of cases per year in the systematic review and survey increased after 1999, from 2.7 during 1990–1999 to 5.7 during 2000–2009 and 5.0 during 2010–2019 (Appendix Figure 2). Moreover, we calculated crude estimates of *S. suis* incidence in the at-risk population in 6 (Czech Republic, Germany, Hungary, the Netherlands, Poland, and Spain) countries with >5 cases reported in the survey or literature review during 2005–2013. We defined the population at risk as the proportion of the agricultural census involved in pig specialized holdings with a 10% upper margin to account for butchers, hunters, slaughterhouse workers, lorry drivers, and meat factory workers. Incidence

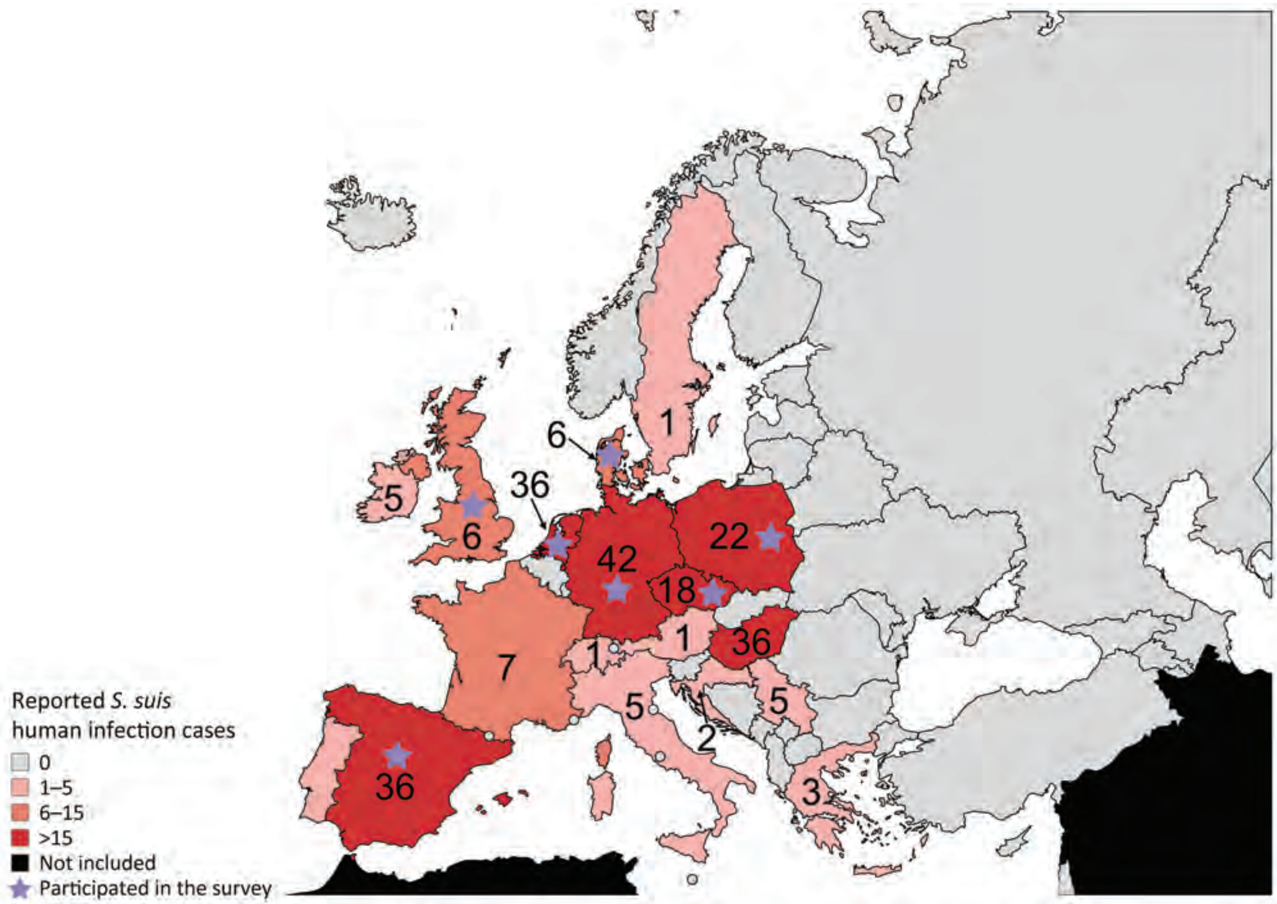

Figure 2. Reported cases of human *Streptococcus suis* infections across Europe during 1990–2022. We pooled reported cases collected in the survey study and systematic search study. The color of the countries represents the relative number of cases: the darker the tone, the higher the number of reported cases. Purple stars indicate reference laboratory participating in the survey study within that country. Scale bar indicated substitutions per site. Countries in black were not included in the study.

range in the at-risk population for those 6 countries during 2005–2013 averaged 0.161–4.945 cases/100,000 persons; Poland had the lowest incidence and the Netherlands the highest (Appendix Table 6).

Scan of Gray Literature

Because no centralized surveillance system exists for human *S. suis* infection and the disease is not notifiable in any country in Europe, the number of infections in Europe has likely been underestimated. We scanned gray literature in search of cases not identified through either the survey or systematic review. Public Health England (now the UK Health Security Agency) included human *S. suis* infections in their annual zoonosis official reports collected from the Veterinary Diagnostic Analysis database of the Animal and Plant Health Agency (*22*). During 1991–2017, those reports recorded 61 human *S. suis* infections in the United Kingdom, 10 times the number of cases identified from the survey and systematic review combined (6 cases). However, those 61 cases might overlap with cases from the survey and systematic review because neither metadata nor identification method were provided (Appendix Table 4). The Netherlands Reference Laboratory for Bacterial Meningitis surveyed 57 medical microbiology laboratories in the Netherlands during 2013 with the aim of identifying cases not reported to the reference laboratory and collected an additional 25 unique cases isolated during 1990–2011 (Appendix Table 5) (*23*). We also found 1 case of *S. suis* meningitis in a butcher in Spain that was reported through X (*24*).

Population Structure of Zoonotic *S. suis* in Europe

To study the population structure of zoonotic *S. suis* isolates in Europe, we reconstructed a core-genome SNP phylogeny of 74 strains from 10 different countries (Figure 3). We identified 5 novel STs, 1660, 1602, 1663, 1707, and 1708. Most strains were part of the major zoonotic clade CC1, which has spread across

Table 1. Patient data collected in survey and systematic review for study of molecular epidemiology of underreported emerging zoonotic pathogen *Streptococcus suis*, Europe*

Patient data	Survey, n = 107	Systematic review, n = 129
Demographic information		
Sex		
M	73	93
F	16	24
NA	18	12
Age		
Median (range), y	52 (0–79)	48 (22–85)
NA	26	54
Clinical symptoms		
Meningitis	59	59
Sepsis	15	21
Hearing loss	0	22
Endocarditis	2	6
Spondylodiscitis	0	3
Death	0	11
NA	36	43
Occupational risk†		
Described	19	72
No risk	0	2
NA	88	55

*Values are no. patients except as indicated. NA, not available.
†Occupational risk: Any job involving close contact with pigs or pork products, including: farmer, butcher, abattoir worker, meat factory worker, hunter, livestock truck driver, or cook.

Europe; ≥1 strain from each country included in the phylogeny was CC1. Most of the CC1 strains had a serotype 2 capsule, and a small subset possessed the structurally similar serotype 14 capsule (*25*). We distinguished 2 subclades within CC1 in a genome-wide SNP phylogeny (Appendix Figure 3). The other zoonotic clades appeared to be more geographically restricted. For example, most of the CC20 strains were isolated in the Netherlands, where the lineage is thought to have emerged (*13*). Two additional CC20 strains were isolated in Germany, forming a serotype 5 outgroup to clonal CC20 serotype 2 strains from the Netherlands. All CC25 strains were recovered in the Czech Republic. The 3 ST25 serotype 2 strains had only 73–116 SNPs across their core genomes, whereas the ST29 strain differed from the ST25 strains by 4,353–4,416 SNPs and had a serotype 7 capsule. Strains from the CC87 clade were identified in Germany and the Czech Republic and possessed a serotype 2 capsule. The 3 strains from Germany were ST19 and highly similar (81–118 SNPs), whereas the strain from the Czech Republic had novel ST1660 and differed from the ST19 clade by 9,411–9,434 SNPs.

Table 2. Bacterial isolate data collected in survey and systematic review for study of molecular epidemiology of underreported emerging zoonotic pathogen *Streptococcus suis*, Europe*

Isolate data	Survey, n = 107	Systematic review, n = 129
Serotype no.		
2	78	43
5	2	1
7	1	0
14	11	4
NA	15	81
Clonal complex no.		
1	68	14
20	11	1
25	4	0
87	3	1
94	1	0
NA	20	113

*NA, not available.

CC1 and CC20 Isolates and Genes Associated with Zoonotic Potential

Overall, strains from clades CC1 and CC20 had a higher number of accessory genes overrepresented in zoonotic isolates than did strains from lineages CC25, CC87, and CC94 (Figure 4). Most genes associated with zoonoses were present in ≥1 of the lineages; only the 2-component signal transduction system *nisK/R* and the fimbria-like adhesin *sssP1* genes were absent from the dataset (Figure 4). Of note, despite its role in adhesion and virulence being extensively studied, muramidase-related protein (*mrp*) was absent from the CC20 clade (*26*). Factor H binding protein (*fhb*), associated with binding factor H and increased translocation across the blood/brain barrier (*27*), was present only in CC1 strains. Differences could be observed within CC1 sublineages; 1 subclade had an additional factor H binding protein (*fhbp*). Last, suilysin (*sly*), a pore-forming hemolysin with a clear role in pathogenesis (*20*), was present in all clades except CC25, which instead carried the hyaluronate lysin A (*hylA*), associated with reduced virulence (Figure 4) (*28*).

Discussion

Despite having caused multiple outbreaks with high levels of illness and death in the past decade and reports of new zoonotic lineages arising on different continents, *S. suis* remains largely excluded from disease surveillance programs (*29*). Although neither carriage in healthy humans nor human-to-human transmission of *S. suis* have been reported to date, systematic surveillance is needed to follow the evolutionary trends of this pathogen in humans and pigs, the main reservoir from which zoonotic lineages emerge (*2*).

Our study included some potential sources of bias. Differences in number of cases between countries should not be attributed only to the size of pig populations. Other factors, such as government policy and disease monitoring and reporting, could contribute to observed differences in reported human *S. suis* cases between countries. For instance, although France has one of the largest pig populations in

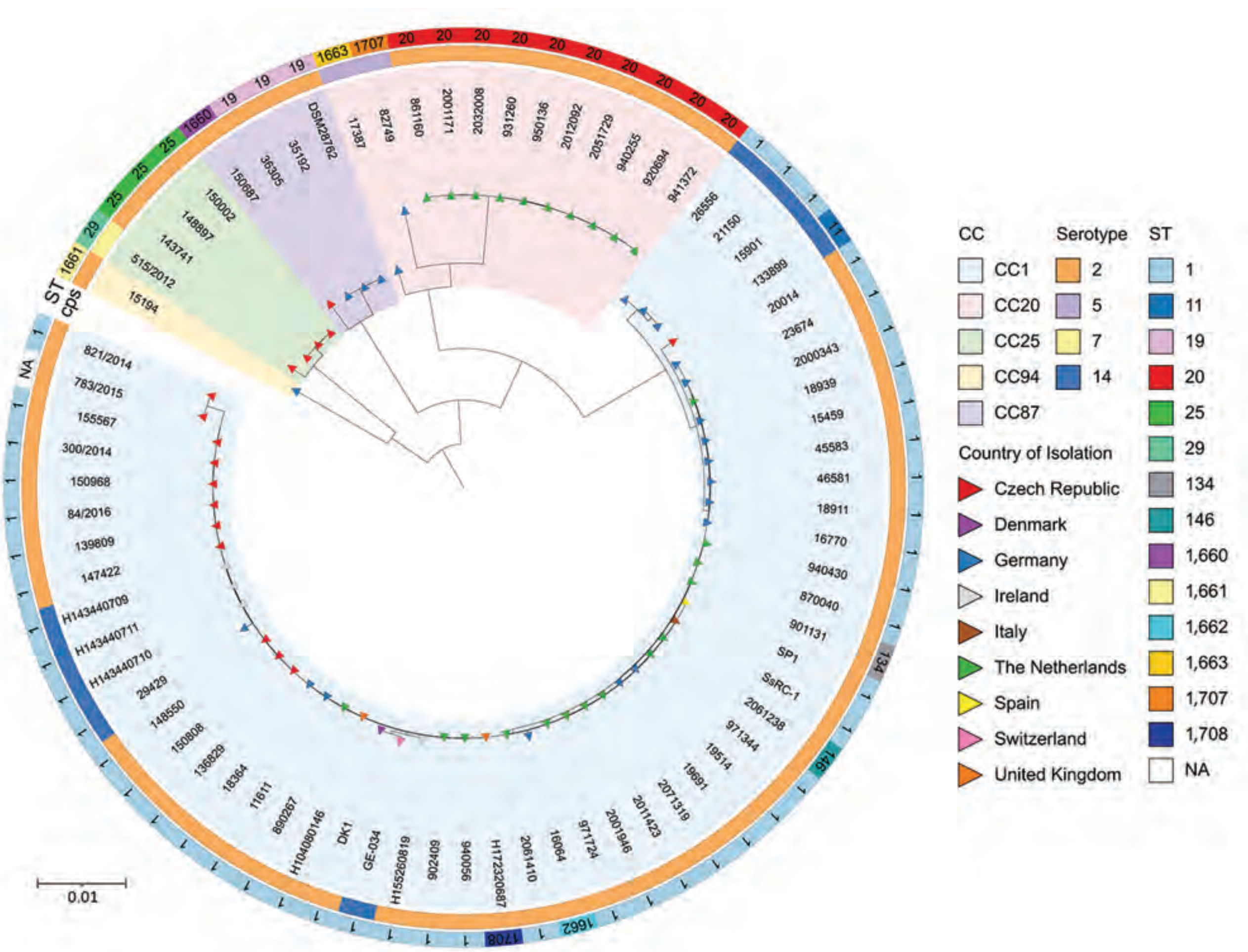

Figure 3. Genome population structure of zoonotic *Streptococcus suis* in Europe. The maximum-likelihood tree was reconstructed using IQ-TREE (18) with a core genome alignment produced with Panaroo (16). Color triangles at branch tips indicate country of collection; color rings indicate lineage (CC). The inner color ring indicates ST and is labeled accordingly. The outer color ring indicates the serotype as determined by the antigenic properties of the cps. We used iTOL (https://itol.embl.de) to visualize the tree. cps, capsular polysaccharide; NA, not available; ST, sequence type.

Europe, only 7 human cases have been reported. In contrast, although they have smaller pig populations, the Czech Republic reported 18 and Poland 22 cases (Figure 2) (*30*). The distribution of clinical symptoms aligns with previous regional and global estimates (*1*). However, clinical data gathered in the survey were potentially biased toward reporting meningitis because several of the surveyed laboratories are reference laboratories for bacterial meningitis (Table 1) (*1*). The systematic review yielded diverse article types (e.g., case reports, surveillance studies) and inconsistent quality of reported metadata. Often, year of isolation and bacterial typing was absent, making it difficult to establish meaningful time trends in the emergence of zoonotic *S. suis* in Europe. Finally, the time frames of the survey, 1990–2018, and systematic review, 1990–2022, were not identical.

The serotype 2 capsule is linked with zoonotic *S. suis* infections, and most worldwide *S. suis* cases are caused by serotype 2 (*4*). While investigating the emergence of the zoonotic clade CC20, 1 study (*13*) proposed that capsule-switching events leading to acquisition of a serotype 2 capsule may be necessary for pathogenic porcine strains to become zoonotic. We observed hints of capsule-switching events, with the CC20 strains from Germany carrying serotype 5 capsule instead of serotype 2, potentially representing an intermediate step in the emergence of zoonotic CC20 from CC16 (*13*). Furthermore, zoonotic strains from CC87 and CC94 lineages were serotype 2, whereas most porcine CC87 strains described in the literature carried a serotype 8 capsule; porcine CC94 strains displayed a wide range of capsules, serotypes 3, 7, and 23 being the most common (*31*). However, the low number of samples collected for CC25, CC87, and CC94 in our study and the fact that they were collected more than a decade ago make it difficult to conclude whether or not these CCs are emerging as zoonotic lineages or are geographically restricted (Appendix Tables 2, 3).

The presence of genes associated with zoonotic potential varied across lineages. Differences in the accessory genome of the zoonotic *S. suis* population, with some well-studied virulence factors such as *sly*, *mrp*, and *fhb* missing from certain pathogenic clades, suggest that, although individual genes might contribute to virulence and zoonotic potential, those genes are not individually essential for *S. suis* to infect humans (*20*,*26*,*27*) (Figure 4). Moreover, simply because a gene is overrepresented in zoonotic isolates does not mean it plays an active role in zoonotic potential, and its role in zoonosis should be explored experimentally. For example, some genes, such as *zmp* and *sp1*, more common in human than porcine *S. suis* isolates, have been shown not to be critical for virulence (*32*,*33*), and others, such as *igdE* and *ideS*, only play a role in evading porcine, not human, immune response (*34*,*35*).

Estimated cumulative prevalence of human *S. suis* infection is substantially higher in southeastern Asia than Europe and the epidemiology of human *S. suis* infections differs significantly between continents (*1*). In Europe, skin injuries and abrasions are thought to be the main point of entry for *S. suis* (*3*), whereas in countries in southeastern Asia with a tradition of raw pork product consumption, the intestinal tract is a notable entry point for infection (*2*,*36*). Differences in exposure routes have led to differences in epidemiology; multiple foodborne human *S. suis* outbreaks with high levels of illness and death have occurred in southeastern Asia in the past 2 decades (*36*,*37*). In Thailand, educational campaigns targeted toward at-risk populations have been shown to reduce incidence of human infections (*36*). Educational campaigns in Europe should be tailored to the different at-risk populations there. Our crude estimates of incidence of *S. suis* human infections in the population at risk for the Czech Republic, Germany, Hungary, the Netherlands, Poland, and Spain are comparable to the incidence of other pathogens causing similar infections in the general population (Appendix). Our estimated incidence in the population at risk for *S. suis*, range 0.161–4.945 cases/100,000 persons across the different countries, was generally higher (except in Poland) than population-wide incidence for *Neisseria meningitidis* (0.42–1.09) and lower than that of *S. pneumoniae* (1.52–14.86) reported by the European Centre for Disease Prevention and Control (*38*) (Appendix Table 6).

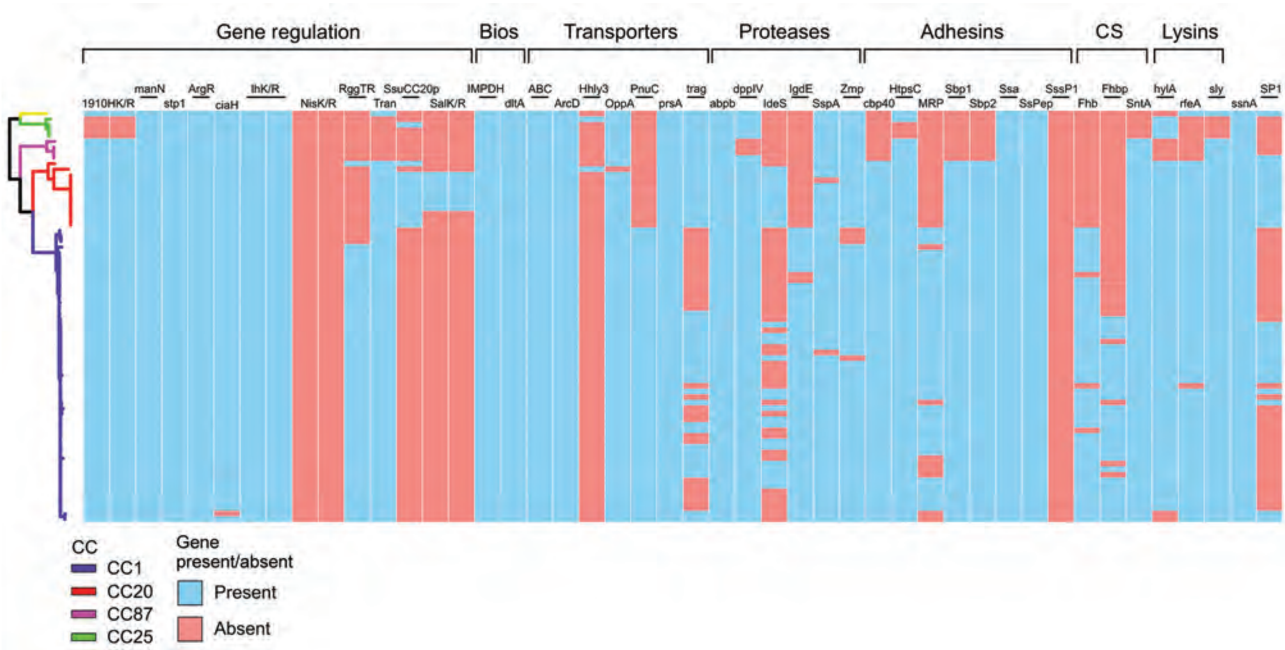

Figure 4. Presence/absence matrix of 46 genes putatively associated with zoonotic potential in study of zoonotic *Streptococcus suis* in Europe. The same phylogenetic tree presented in Figure 3 was used. Blue squares indicate presence of the gene while red squares indicate absence. The colored branches indicate CCs and follow the same pattern as in Figure 3 (blue, CC1; red, CC20; purple, CC87; yellow, CC94; green, CC25). We defined gene presence with 80% protein identity and coverage. We used Phandango (*19*) to visualize the tree. Bios, biosynthesis; CC, clonal complex; CS, complement system evasion.

Furthermore, we found evidence of underreporting in the Netherlands; 25 cases were not reported to the Netherlands Reference Laboratory for Bacterial Meningitis or described in published articles (*23*). The United Kingdom was the only country where human *S. suis* infections were included in official government reports. Those UK reports contained 10 times as many cases within the same timeframe than UK cases from the survey and systematic review combined (*22*) because the survey and systematic review did not capture many unpublished cases. This finding suggest that the number of cases collected in other countries through the survey might also be underestimated. We observed an increase in reported cases after 1999 (Appendix Figure 2); however, this increase could have been caused by heightened awareness after a severe outbreak in China in 2005 and by more precise bacterial identification techniques (*37*). Moreover, in Thailand, a country where *S. suis* is a notifiable disease, reported infections have increased in the past few years (*10*).

In conclusion, despite not being a notifiable disease in Europe, novel zoonotic *S. suis* lineages, including multidrug-resistant lineages, have been detected recently both in Europe and worldwide (*13*,*29*). Moreover, our likely underestimated incidence estimates suggest that risk for *S. suis* infection for the at-risk population is greater than that of *N. meningitidis* and comparable to that of *S. pneumoniae* in the general population. Given the severity of the disease it causes, we propose making *S. suis* infections notifiable in Europe to improve surveillance of emerging zoonotic lineages and evolutionary trends and better detect potential human-to-human transmission.

Our work was funded by the European Union Horizon 2020 grant 727966 (PIGSs).

Author contributions: conceptualization: K.A. and C.S.; data curation: J.B., T.R., Q.H., B.P., J.K., H.C.S., I.B.S., E.S., J.A.S., and V.C.; formal analysis: J.B., B.P., and Q.H.; funding acquisition: C.S.; investigation: J.B., B.P., and Q.H.; methodology: J.B., T.R., Q.H., B.P., K.A., and C.S.; project administration: K.A., C.S., and J.B.; resources: C.S.; software: C.S.; supervision: T.R., B.P., K.A., C.S.; validation: J.B.; visualization: J.B.; writing- original draft: J.B.; writing- reviewing and editing: J.B., T.R., H.Q., B.P., J.K., H.C.S., I.B.S., E.S., J.A.S., V.C., K.A., and C.S.

About the Author

Mr. Brizuela is a PhD student at the Amsterdam UMC, within the context of the Netherlands Centre for One Health project CANVAS, which aims to identify vaccine candidates to prevent *Streptococcus suis* infections in pigs and humans.

References

1. Huong VTL, Ha N, Huy NT, Horby P, Nghia HDT, Thiem VD, et al. Epidemiology, clinical manifestations, and outcomes of *Streptococcus suis* infection in humans. Emerg Infect Dis. 2014;20:1105–14. https://doi.org/10.3201/eid2007.131594
2. Ho DTN, Le TPT, Wolbers M, Cao QT, Nguyen VMH, Tran VTN, et al. Risk factors of *Streptococcus suis* infection in Vietnam. A case-control study. PLoS One. 2011;6:e17604.
3. Segura M, Aragon V, Brockmeier SL, Gebhart C, Greeff A, Kerdsin A, et al. Update on *Streptococcus suis* research and prevention in the era of antimicrobial restriction: 4th International Workshop on *S. suis*. Pathogens. 2020;9:374. https://doi.org/10.3390/pathogens9050374
4. Goyette-Desjardins G, Auger JP, Xu J, Segura M, Gottschalk M. *Streptococcus suis*, an important pig pathogen and emerging zoonotic agent—an update on the worldwide distribution based on serotyping and sequence typing. Emerg Microbes Infect. 2014;3:e45. https://doi.org/10.1038/emi.2014.45
5. Tall H, Njanpop-Lafourcade BM, Mounkoro D, Tidjani L, Agbenoko K, Alassani I, et al. Identification of *Streptococcus suis* meningitis through population-based surveillance, Togo, 2010–2014. Emerg Infect Dis. 2016;22:1262–4. https://doi.org/10.3201/eid2207.151511
6. Raberahona M, Rasoanandrasana S, Rahajamanana VL, Ranaivo-Rabetokotany F, Andriananja V, Rakotomalala FA, et al. Novel *Streptococcus suis* sequence type 834 among humans, Madagascar. Emerg Infect Dis. 2018;24:391–2. https://doi.org/10.3201/eid2402.171138
7. Alarcón L P, Araya R P, Aguayo C, Fernández J, Illesca V, Zaror A, et al. Laboratory confirmation of *Streptococcus suis* in Chile [in Spanish]. Rev Chilena Infectol. 2013;30:539–40. https://doi.org/10.4067/S0716-10182013000500011
8. Susilawathi NM, Tarini NMA, Fatmawati NND, Mayura PIB, Suryapraba AAA, Subrata M, et al. *Streptococcus suis*–associated meningitis, Bali, Indonesia, 2014–2017. Emerg Infect Dis. 2019;25:2235–42. https://doi.org/10.3201/eid2512.181709
9. Kerdsin A, Hatrongjit R, Wongsurawat T, Jenjaroenpun P, Chopjitt P, Boueroy P, et al. Genomic characterization of *Streptococcus suis* serotype 24 clonal complex 221/234 from human patients. Front Microbiol. 2021;12:812436. https://doi.org/10.3389/fmicb.2021.812436
10. Kerdsin A. Human *Streptococcus suis* infections in Thailand: epidemiology, clinical features, genotypes, and susceptibility. Trop Med Infect Dis. 2022;7:359. https://doi.org/10.3390/tropicalmed7110359
11. Liang P, Wang M, Gottschalk M, Vela AI, Estrada AA, Wang J, et al. Genomic and pathogenic investigations of *Streptococcus suis* serotype 7 population derived from a human patient and pigs. Emerg Microbes Infect. 2021;10:1960–74. https://doi.org/10.1080/22221751.2021.1988725
12. King SJ, Leigh JA, Heath PJ, Luque I, Tarradas C, Dowson CG, et al. Development of a multilocus sequence typing scheme for the pig pathogen *Streptococcus suis:* identification of virulent clones and potential capsular serotype exchange. J Clin Microbiol. 2002;40:3671–80. https://doi.org/10.1128/JCM.40.10.3671-3680.2002
13. Willemse N, Howell KJ, Weinert LA, Heuvelink A, Pannekoek Y, Wagenaar JA, et al. An emerging zoonotic clone in the Netherlands provides clues to virulence and zoonotic potential of *Streptococcus suis*. Sci Rep. 2016;6:28984. https://doi.org/10.1038/srep28984
14. Page MJ, McKenzie JE, Bossuyt PM, Boutron I, Hoffmann TC, Mulrow CD, et al. The PRISMA 2020

statement: an updated guideline for reporting systematic reviews. BMJ. 2021;372:n71. https://doi.org/10.1136/bmj.n71
15. Athey TBT, Teatero S, Lacouture S, Takamatsu D, Gottschalk M, Fittipaldi N. Determining *Streptococcus suis* serotype from short-read whole-genome sequencing data. BMC Microbiol. 2016;16:162. https://doi.org/10.1186/s12866-016-0782-8
16. Tonkin-Hill G, MacAlasdair N, Ruis C, Weimann A, Horesh G, Lees JA, et al. Producing polished prokaryotic pangenomes with the Panaroo pipeline. Genome Biol. 2020;21:180. https://doi.org/10.1186/s13059-020-02090-4
17. Page AJ, Taylor B, Delaney AJ, Soares J, Seemann T, Keane JA, et al. SNP-sites: rapid efficient extraction of SNPs from multi-FASTA alignments. Microb Genom. 2016;2:e000056. https://doi.org/10.1099/mgen.0.000056
18. Nguyen LT, Schmidt HA, von Haeseler A, Minh BQ. IQ-TREE: a fast and effective stochastic algorithm for estimating maximum-likelihood phylogenies. Mol Biol Evol. 2015;32:268–74. https://doi.org/10.1093/molbev/msu300
19. Hadfield J, Croucher NJ, Goater RJ, Abudahab K, Aanensen DM, Harris SR. Phandango: an interactive viewer for bacterial population genomics. Bioinformatics. 2018;34:292–3. https://doi.org/10.1093/bioinformatics/btx610
20. Roodsant TJ, Van Der Putten BCL, Tamminga SM, Schultsz C, Van Der Ark KCH. Identification of *Streptococcus suis* putative zoonotic virulence factors: a systematic review and genomic meta-analysis. Virulence. 2021;12:2787–97. https://doi.org/10.1080/21505594.2021.1985760
21. Augère-Granier M-L. European Parliamentary Research Service. The EU pig meat sector [cited 2022 Nov 8]. https://www.europarl.europa.eu/RegData/etudes/BRIE/2020/652044/EPRS_BRI(2020)652044_EN.pdf
22. Public Health England, Department for Environment, Food and Rural Affairs. Zoonoses: UK annual reports: 2017 [cited 2022 Nov 8]. https://www.gov.uk/government/publications/zoonoses-uk-annual-reports
23. National Institute for Public Health and the Environment. Zoonotic infections with *Streptococcus suis* in the Netherlands/IB 11–2013 [in Dutch] [cited 2022 Nov 8]. https://www.rivm.nl/weblog/zoonotische-infecties-met-streptococcus-suis-in-nederland-ib-11-2013
24. @mrvr79. Meningitis due to *Streptococcus suis* in a butcher [in Spanish]. 2020 Dec 19 [cited 2022 Apr 1]. https://twitter.com/mrvr79/status/1340282705439801345
25. Goyette-Desjardins G, Auger JP, Dolbec D, Vinogradov E, Okura M, Takamatsu D, et al. Comparative study of immunogenic properties of purified capsular polysaccharides from *Streptococcus suis* serotypes 3, 7, 8, and 9: the serotype 3 polysaccharide induces an opsonizing IgG response. Infect Immun. 2020;88:e00377-20. https://doi.org/10.1128/IAI.00377-20
26. Wang J, Kong D, Zhang S, Jiang H, Zheng Y, Zang Y, et al. Interaction of fibrinogen and muramidase-released protein promotes the development of *Streptococcus suis* meningitis. Front Microbiol. 2015;6:1001. https://doi.org/10.3389/fmicb.2015.01001
27. Kong D, Chen Z, Wang J, Lv Q, Jiang H, Zheng Y, et al. Interaction of factor H-binding protein of *Streptococcus suis* with globotriaosylceramide promotes the development of meningitis. Virulence. 2017;8:1290–302. https://doi.org/10.1080/21505594.2017.1317426
28. Haas B, Vaillancourt K, Bonifait L, Gottschalk M, Grenier D. Hyaluronate lyase activity of *Streptococcus suis* serotype 2 and modulatory effects of hyaluronic acid on the bacterium's virulence properties. BMC Res Notes. 2015;8:722. https://doi.org/10.1186/s13104-015-1692-9
29. Brizuela J, Kajeekul R, Roodsant TJ, Riwload A, Boueroy P, Pattanapongpaibool A, et al. *Streptococcus suis* outbreak caused by an emerging zoonotic strain with acquired multi-drug resistance in Thailand. Microb Genom. 2023;9:mgen000952. https://doi.org/10.1099/mgen.0.000952
30. Bojarska A, Molska E, Janas K, Skoczyńska A, Stefaniuk E, Hryniewicz W, et al. *Streptococcus suis* in invasive human infections in Poland: clonality and determinants of virulence and antimicrobial resistance. Eur J Clin Microbiol Infect Dis. 2016;35:917–25. https://doi.org/10.1007/s10096-016-2616-x
31. Estrada AA, Gottschalk M, Rossow S, Rendahl A, Gebhart C, Marthaler DG. Serotype and genotype (multilocus sequence type) of *Streptococcus suis* isolates from the United States serve as predictors of pathotype. J Clin Microbiol. 2019;57:e00377–19.
32. Dumesnil A, Auger JP, Roy D, Vötsch D, Willenborg M, Valentin-Weigand P, et al. Characterization of the zinc metalloprotease of *Streptococcus suis* serotype 2. Vet Res. 2018;49:109. https://doi.org/10.1186/s13567-018-0606-y
33. Roy D, Fittipaldi N, Dumesnil A, Lacouture S, Gottschalk M. The protective protein sao (surface antigen one) is not a critical virulence factor for *Streptococcus suis* serotype 2. Microb Pathog. 2014;67-68:31–5. https://doi.org/10.1016/j.micpath.2014.02.002
34. Spoerry C, Seele J, Valentin-Weigand P, Baums CG, von Pawel-Rammingen U. Identification and characterization of IgdE, a novel IgG-degrading protease of *Streptococcus suis* with unique specificity for porcine IgG. J Biol Chem. 2016;291:7915–25. https://doi.org/10.1074/jbc.M115.711440
35. Seele J, Beineke A, Hillermann LM, Jaschok-Kentner B, von Pawel-Rammingen U, Valentin-Weigand P, et al. The immunoglobulin M-degrading enzyme of *Streptococcus suis*, IdeSsuis, is involved in complement evasion. Vet Res. 2015;46:45. https://doi.org/10.1186/s13567-015-0171-6
36. Takeuchi D, Kerdsin A, Akeda Y, Chiranairadul P, Loetthong P, Tanburawong N, et al. Impact of a food safety campaign on *Streptococcus suis* infection in humans in Thailand. Am J Trop Med Hyg. 2017;96:1370–7. https://doi.org/10.4269/ajtmh.16-0456
37. Yu H, Jing H, Chen Z, Zheng H, Zhu X, Wang H, et al.; *Streptococcus suis* study groups. Human *Streptococcus suis* outbreak, Sichuan, China. Emerg Infect Dis. 2006;12:914–20. https://doi.org/10.3201/eid1206.051194
38. European Centre for Disease Prevention and Control. Surveillance atlas of infectious diseases [cited 2023 Jul 27]. https://www.ecdc.europa.eu/en/surveillance-atlas-infectious-diseases

Address for correspondence: Jaime Brizuela, Amsterdam UMC location University of Amsterdam, Department of Medical Microbiology and Infection Prevention, Meibergdreef 9, Amsterdam, the Netherlands; email: j.brizuelagabaldon@amsterdamumc.nl

Multimodal Surveillance Model for Enterovirus D68 Respiratory Disease and Acute Flaccid Myelitis among Children in Colorado, USA, 2022

Kevin Messacar, Shannon Matzinger, Kevin Berg, Kirsten Weisbeck, Molly Butler, Nicholas Pysnack, Hai Nguyen-Tran, Emily Spence Davizon, Laura Bankers, Sarah A. Jung, Meghan Birkholz, Allison Wheeler, Samuel R. Dominguez

Surveillance for emerging pathogens is critical for developing early warning systems to guide preparedness efforts for future outbreaks of associated disease. To better define the epidemiology and burden of associated respiratory disease and acute flaccid myelitis (AFM), as well as to provide actionable data for public health interventions, we developed a multimodal surveillance program in Colorado, USA, for enterovirus D68 (EV-D68). Timely local, state, and national public health outreach was possible because prospective syndromic surveillance for AFM and asthma-like respiratory illness, prospective clinical laboratory surveillance for EV-D68 among children hospitalized with respiratory illness, and retrospective wastewater surveillance led to early detection of the 2022 outbreak of EV-D68 among Colorado children. The lessons learned from developing the individual layers of this multimodal surveillance program and how they complemented and informed the other layers of surveillance for EV-D68 and AFM could be applied to other emerging pathogens and their associated diseases.

Enterovirus D68 (EV-D68) causes epidemics of asthma-like respiratory disease and clusters of cases of the paralytic polio-like disease known as acute flaccid myelitis (AFM) (*1*). During summer/fall seasonal peaks, EV-D68 substantially strains healthcare resources with unexpected surges in emergency department (ED) visits, hospitalizations, and the need for intensive care unit (ICU)–level respiratory support for children (*2*,*3*). Detecting EV-D68–associated AFM cases relies on timely, targeted outreach to ensure prompt diagnosis, appropriate specimen collection and testing, and reporting to public health authorities (*4*). However, because of the inability of clinically available diagnostics to differentiate rhinoviruses from enteroviruses and the lack of widespread availability of EV-D68–specific testing, recognition of waves of EV-D68 infections is often delayed and the associated burden of disease remains substantially underdetected (*5*,*6*). Surveillance for EV-D68 is essential for early warning systems to guide responses to future waves of respiratory disease and AFM.

Although discovered in 1962 (*7*), EV-D68 was rarely detected before clusters of respiratory disease were reported in Europe, Asia, and the United States during 2008–2010 (*8*). In 2014, the largest and most widespread EV-D68 outbreak to date was reported in North America and Europe (*3*,*9*). During 2014–2018, a biennial pattern of circulation in the summer/fall was observed in the United States and Europe; the numbers of reported AFM cases increased with successive outbreaks (*10*–*12*). That biennial circulation pattern was disrupted during the COVID-19 pandemic; no substantial circulation was detected in the United States in 2020–2021, most likely because of the nonpharmaceutical interventions that were directed

Author affiliations: Children's Hospital Colorado, Aurora, Colorado, USA (K. Messacar, M. Butler, H. Nguyen-Tran, S.A. Jung, M. Birkholz, S.R. Dominguez); University of Colorado, Aurora (K. Messacar, H. Nguyen-Tran, S.R. Dominguez); Colorado Department of Public Health and Environment, Denver, Colorado, USA (S. Matzinger, K. Berg, K. Weisbeck, N. Pysnack, E. Spence Davizon, L. Bankers, A. Wheeler)

DOI: https://doi.org/10.3201/eid3003.231223

at curbing the spread of SARS CoV-2 (*13*). Modeling the growth of the population susceptible to EV-D68 during that period of limited activity suggested the potential for a larger outbreak when circulation returned (*14*).

After outbreaks in 2014 (*15*), 2016 (*16*), and 2018 (*17*), we established a multimodal surveillance program in Colorado for EV-D68 and AFM to better define their epidemiology and disease burden and to guide preparedness efforts (Figure 1). Our program included prospective syndromic surveillance for AFM and asthma-like respiratory disease, prospective EV-D68 clinical laboratory surveillance, and retrospective wastewater surveillance. The lessons learned from development and implementation of this multimodal surveillance system during the EV-D68 outbreak in 2022 (18) carry valuable implications for preparedness efforts for EV-D68 and other emerging pathogens.

Methods

AFM Syndromic Surveillance

AFM is a reportable condition statewide in Colorado as part of Centers for Disease Control and Prevention (CDC) nationwide AFM surveillance efforts (*4*). Healthcare providers are required to report suspected AFM cases to the Colorado State Department of Public Health and Environment (CDPHE) within 4 calendar days. Because there are no laboratory criteria for reporting AFM cases, syndromic criteria for reporting to public health authorities include any patient with new onset of focal limb weakness and magnetic resonance images (MRI) showing a spinal cord lesion with at least some gray matter involvement spanning ≥1 vertebral segments (*19*). CDPHE follows the Council of State and Territorial Epidemiologists guidance for AFM case ascertainment. Medical records and MRIs collected by CDPHE are ultimately classified by the CDC AFM neurology panel as confirmed, probable, or suspected in accordance with Council of State and Territorial Epidemiologists criteria.

EV-D68 Respiratory Syndromic Surveillance

Beginning in 2018, we conducted ongoing near–real-time syndromic surveillance of asthma-like respiratory illness at Children's Hospital Colorado (CHCO), a 444-bed quaternary care pediatric hospital in Aurora, Colorado; the hospital catchment area encompassed children in the Denver metropolitan area. Whereas upper and lower respiratory tract infection rates fluctuate with the circulation of many respiratory

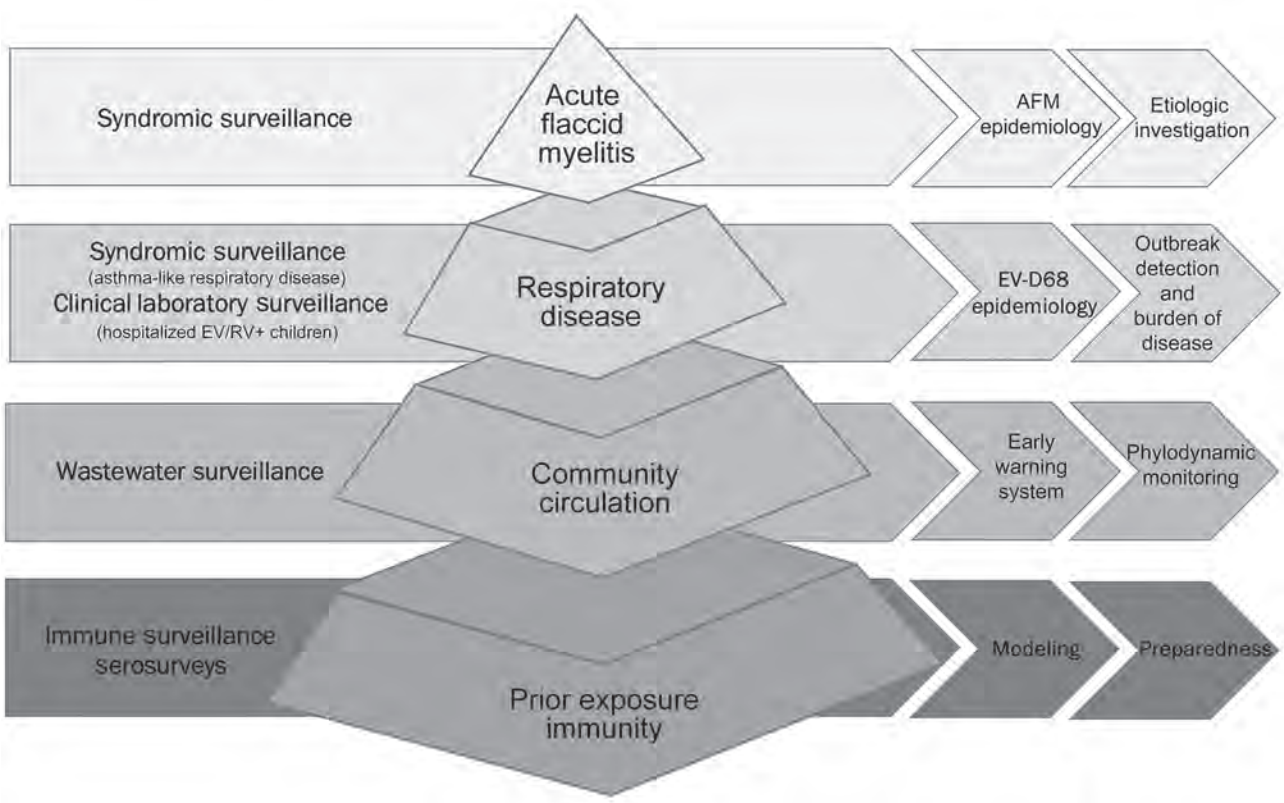

Figure 1. Multimodal surveillance model for enterovirus D68 in Colorado, USA. AFM, acute flaccid myelitis; EV, enterovirus; RV, rhinovirus.

viruses, a surge in cases of asthma-like illness was specifically noted to coincide with the large EV-D68 outbreak in Colorado in 2014 (*2*); thus, medically attended asthma-like illness rates were subsequently tracked for syndromic surveillance of EV-D68 respiratory illness. A de-identified dataset of weekly ED visits with a principal billing diagnosis code of asthma (code J45.XXX from the International Classification of Diseases, 10th Revision, Clinical Modification) from CHCO was collected, and total weekly ED visits served as a denominator. We chose the diagnosis codes to reflect visits associated with an asthma exacerbation or asthma-like episode of wheezing that could be associated with EV-D68. To develop and determine the baseline for the forecast model, we obtained an identical retrospective dataset for the 3 years before the target surveillance year. From those retrospective data, we generated expected counts of weekly ED visits, indirectly standardized by age and sex. We then calculated a standardized morbidity rate for each week by dividing the observed asthma ED visits by the expected count. Our EV-D68 syndromic surveillance system consists of 2 components: a time series forecast model to predict the expected number of asthma ED visits each week and a cumulative sum chart procedure to serve as an alarm to identify potential temporal clusters of elevated weekly asthma ED visits (Appendix, https://wwwnc.cdc.gov/EID/article/30/3/23-1223-App1.pdf).

Clinical Laboratory Surveillance

Clinical laboratory surveillance for EV-D68 respiratory illness was conducted during June–November 2022 among children at CHCO for whom residual respiratory specimens were positive for the enterovirus/rhinovirus target on the BioFire Respiratory Pathogen Panel 2.1 (BioFire Diagnostics, https://www.biofiredx.com). We selected specimens from hospitalized patients with enterovirus/rhinovirus respiratory disease and tested them by using an EV-D68–specific reverse transcription PCR (Appendix). We initially used a primer-probe set designed to target the 2014 B1 strain, in use at CHCO since 2015, for clinical surveillance testing during June–August of 2022. In August 2022, the PCR protocol was updated with primer and probe sequences designed to detect the predominantly circulating strain (subclade B3), as well as previously circulating strains, and used for all clinical laboratory surveillance testing (*20*).

Wastewater Surveillance

We used the digital droplet PCR at the CDPHE laboratory to quantify EV-D68 virus concentration in wastewater samples collected twice weekly during June–December 2022. We used the updated PCR primer-probe set targeting EV-D68 subclade B3 noted above (Appendix). We included 3 sewersheds in the Denver metropolitan area in this analysis, referred to as utilities A, B, and C, which overlap with Adams, Arapahoe, Denver, and Jefferson Counties.

To examine the geospatial overlap in EV-D68 clinical laboratory case detections and detection of EV-D68 in wastewater, we linked residential postal (ZIP) codes of clinical cases to ZIP Code Tabulated Areas (ZCTAs) and conducted a descriptive analysis of the time and spatial relationship between positive clinical and wastewater detection of EV-D68. Our tabulation of positive EV-D68 clinical tests for the 3 select Denver metro area sewersheds where wastewater samples were collected (utilities A, B, and C) was based on the spatial overlap of the sewershed boundary and ZCTA boundary. To estimate allocation of cases to sewershed areas without exact address geolocation data, we split case counts among the sewershed areas (e.g., for a case from a ZCTA that overlapped 2 sewershed areas, we assigned a case value of 0.5 to each area). We used descriptive statistics to compare trends among the different layers of the surveillance system (Appendix).

Results

On August 14, 2022, the Colorado syndromic surveillance system for EV-D68 respiratory illness generated an alarm signal because the cumulative sum output exceeded the threshold for statistical significance during August 14–September 24, 2023 (Figure 2). That alarm signal coincided with an observed uptick in overall CHCO ED visits, hospital ward and ICU admissions, and enterovirus/rhinovirus detections from clinical testing of respiratory specimens. In August 2022, an updated primer-probe set designed against subclade B3 viruses detected EV-D68 in 5 respiratory specimens that the 2014 clade B1-targeted primer-probe set failed to detect (*20*,*21*). On the basis of those results, we converted all EV-D68 surveillance to the updated primer-probe set for all samples tested. Overall, EV-D68 detections were noted at low levels as early as June 19, 2022, increasing substantially the week of August 7, 2022, to a peak positivity rate of 78.6% in selected enterovirus/rhinovirus samples collected during the week of August 21, 2022. In total, 529 enterovirus/rhinovirus–positive clinical specimens were tested during June 15–November 3, 2022, and 121 (22.9%) were positive for EV-D68 (Figure 2).

After clinical laboratory surveillance confirmed EV-D68 as the cause of the enterovirus/rhinovirus

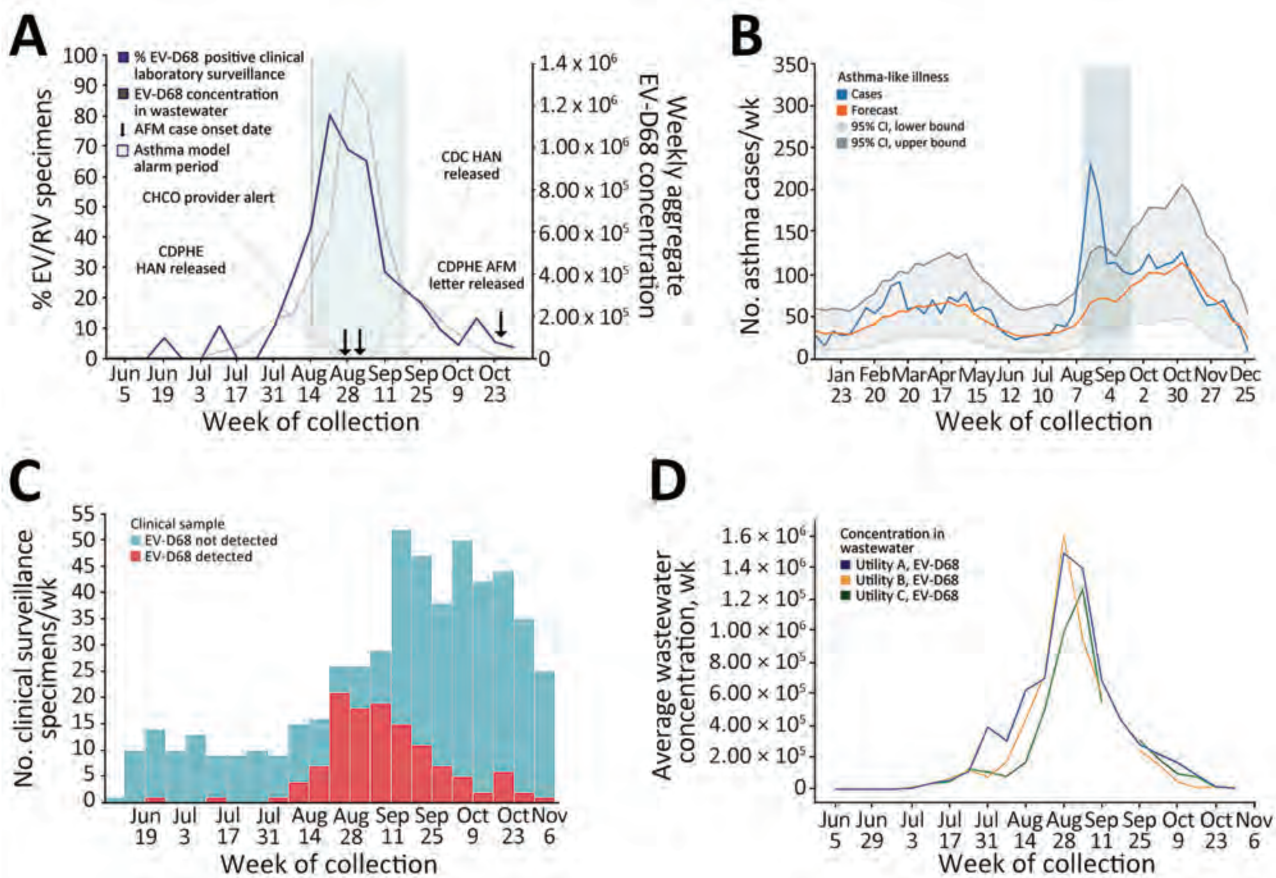

Figure 2. Multimodal surveillance during EV-D68 outbreak in Colorado, USA, 2022. A) Multimodal EV-D68 syndromic, clinical laboratory, and wastewater surveillance. To simplify the presentation of the temporal relationship between clinical positivity rates and the signal in wastewater, the viral concentrations of EV-D68 for the 3 utilities in this study are aggregated. B) Syndromic surveillance for asthma-like respiratory disease. C) Clinical laboratory surveillance for EV-D68 respiratory disease at CHCO. D) Wastewater surveillance for EV-D68 by wastewater utility service area. To generate the line presented in the graph, the concentration values for the 3 utilities were added together and averaged (mean) by sample collection date. The sample collection dates and cadence were uniform over time across all 3 utilities. The data are an estimation of the overall viral signal from the adjacent sewershed areas within the Denver metropolitan region (panel D; Appendix Figure 1, https://wwwnc.cdc.gov/EID/article/30/3/23-1223-App1.pdf). AFM, acute flaccid myelitis; CDC, Centers for Disease Control and Prevention; CHCO, Children's Hospital Colorado; CHPHE, Colorado Department of Public Health and Environment; EV, enterovirus; HAN, Health Alert Network; RV, rhinovirus.

spike in respiratory illness in Colorado, CHCO, CDPHE, and CDC coordinated local, state, and national public health responses. On September 1, 2022, CDPHE issued a statewide Colorado Health Alert Network message about EV-D68 circulation in Colorado, which contained education on AFM and reporting requirements. CHCO leadership activated a plan for emergency surge staffing and hospital bed availability for the expected increase in respiratory illness case volumes. On September 2, 2022, they released systemwide communications alerting providers of the EV-D68 outbreak and potential for AFM cases to follow. Early identification of the outbreak enabled advanced purchasing before the peak of the surge to help secure the CHCO supply chain for pediatric formulations of asthma medications and respiratory support supplies, which subsequently became a nationwide shortage. On September 9, 2022, after being alerted of increases in asthma-like illnesses and detection of sustained EV-D68 circulation by CDPHE and the CDC New Vaccine Surveillance Network sites, CDC released a nationwide Health Alert Network about severe respiratory illnesses associated with enterovirus/rhinovirus infections, including EV-D68 (*22*). In addition, a "Dear Provider" letter was mailed on September 20, 2022, to Colorado medical providers describing signs and symptoms of AFM and providing diagnosis and management recommendations and reporting requirements.

By late September 2022, EV-D68 respiratory syndromic surveillance showed decreasing levels of asthma-like illness cases in the CHCO ED, and clinical laboratory surveillance showed decreasing EV-D68 detection rates. The syndromic alarm signal de-activated, and observed rates returned to expected levels by mid-November in conjunction with EV-D68 clinical laboratory detections decreasing below 10%. The syndromic alarm period coincided with the increased EV-D68 circulation, and the alarm signal disappeared when the EV-D68 outbreak waned, even with a concurrent dramatic increase in CHCO ED visits and admissions resulting from a subsequent and overlapping, early, and large surge in respiratory syncytial virus bronchiolitis cases (Appendix Figure 2) (*23*).

Despite the substantial EV-D68 respiratory illness outbreak in Colorado and throughout the United States in 2022, the number of AFM cases was fewer than would be expected based on increases reported during previous years with substantial EV-D68 circulation. During 2022, CDC classified 4 suspected AFM cases that were reported in Colorado as confirmed or probable cases. In comparison, CDC confirmed 17 AFM cases in Colorado in 2018 and 11 in 2014 during peak years. Similarly, nationwide in the United States, 44 cases of AFM were confirmed in 24 states in 2022, compared with 238 in 42 states in 2018, 153 in 29 states in 2016, and 120 in 34 states in 2014, during peak years correlating with substantial EV-D68 circulation (*24*).

After the 2022 outbreak, CDPHE retrospectively tested wastewater for EV-D68 by using 117 samples from 3 facilities dating back to June 1, 2022, which were banked as part of the CDPHE Wastewater Surveillance Program. EV-D68 was first detected in wastewater on July 5, 2022, shortly after it was initially detected by clinical laboratory surveillance on June 19, 2022. Quantification and preliminary trend analysis of wastewater detection demonstrated an increasing trend in all 3 sampled sewersheds on July 18, 2022, nearly 1 month before the EV-D68 syndrome surveillance alarm was triggered. A similar temporal pattern followed the EV-D68 respiratory syndromic and clinical laboratory surveillance signals by 1–2 weeks (Figure 2) with geospatial and temporal correlation of ZCTA-level clinical laboratory EV-D68 case detections and detection of EV-D68 in wastewater from the corresponding sewersheds (Figures 3,4).

Discussion

We implemented a multimodal surveillance system in Colorado for EV-D68 and AFM, which promptly and accurately detected the large EV-D68 outbreak in the fall of 2022, enabling actionable, real-time surge planning and effective public health messaging. Each layer of surveillance independently provided unique insights into pathogen emergence, disease associations and burden, and community circulation; interdependently, the multiple layers of surveillance complemented each other with the potential to optimize performance and minimize limitations of the other layers in real-time in the future.

Rare, but severe, complications of emerging infectious diseases are often and appropriately the first to be recognized as public health priorities and therefore are typically the initial targets of surveillance to provide information about their epidemiology, etiology, and disease burden. The case definition for AFM was promptly constructed after the initial outbreak was reported in Colorado in 2014 (*25*). Subsequent national syndromic surveillance by CDC has been ongoing since that time; however, the reliance on astute clinicians to recognize, diagnose, and report suspected cases leads to continued case underascertainment (*19*). Substantial public health outreach efforts, including education campaigns (*26*), establishment of guidelines (*4*,*27*), and activation

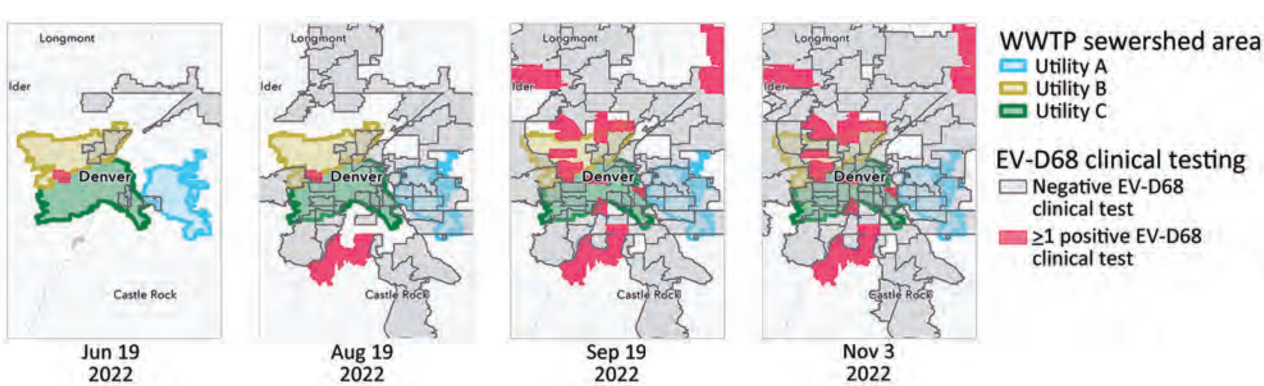

Figure 3. Temporal and geospatial correlation between clinical laboratory confirmed EV-D68 cases and wastewater detections, Colorado, USA, 2022. Cumulative positive EV-D68 clinical cases for June–November 2022 are shown by ZIP Code Tabulated Area overlaying Denver metropolitan area sewersheds. Data source: Children's Hospital Colorado. EV, enterovirus; WWTP, wastewater treatment plant.

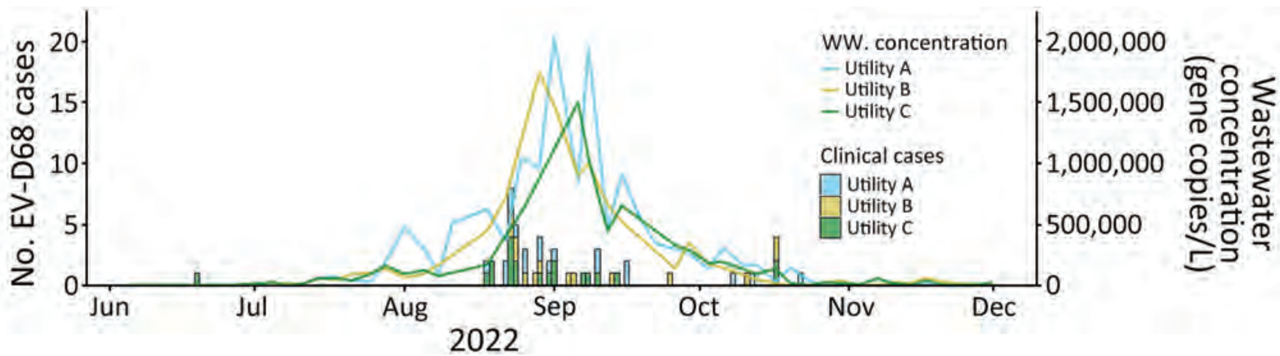

Figure 4. Temporal and geospatial correlation between clinical laboratory confirmed EV-D68 cases and wastewater detections, Colorado, USA, June–December 2022. Data source: Children's Hospital Colorado. EV, enterovirus; WW, wastewater.

of local and state public health authorities and laboratories, have been used to improve recognition, reporting, and testing of AFM cases to support surveillance efforts. Through this pathogen-agnostic surveillance, EV-D68 was identified as the predominant pathogen driving the seasonal, biennial surges in AFM in the United States (*28*).

After a causal association was established (*29*,*30*), public health outreach efforts were focused on timely, targeted AFM education tied to periods of local EV-D68 circulation. Colorado enacted an enhanced AFM outreach program, which included local, state, and national notifications of EV-D68 circulation (*18*) and targeted provider outreach to heighten awareness of AFM during the 2022 outbreak. A large AFM spike was not detected in Colorado or the United States in 2022, which was the first time since 2014 that increased EV-D68 detection was not associated with increased AFM cases. Although much remains to be investigated with regard to the virologic, immunologic, and epidemiologic reasons behind that decoupling, the enhanced AFM surveillance enacted in Colorado was essential for establishing with confidence that the paucity of AFM reports during this period was most likely caused by a true lack of increased AFM cases in the community and not by a lack of recognition or failure to report.

In addition to syndromic surveillance for rare, severe complications, syndromic surveillance for more common presentations of an emerging pathogen can be used to signal outbreaks and improve knowledge of disease burden, especially for pathogens for which widespread testing is not available. During the 2014 outbreak, EV-D68–specific diagnostic testing was available only at CDC on enterovirus/rhinovirus–positive specimens from ICU-level patients with respiratory disease. Retrospectively, we established that syndromic surveillance of resource use for children with asthma-like respiratory diseases provided a better estimate of disease burden (*2*), which was used in an early warning system that sent an alarm as the first sign of an impending outbreak in 2022. Because of continued, limited, and selective sampling and testing for EV-D68, syndromic surveillance for asthma-like illness still provides the best estimate of EV-D68 disease burden. In 2022, that signal was also shown to specifically track with EV-D68, because it did not generate an alarm signal during the subsequent waves of respiratory syncytial virus, SARS-CoV-2, or influenza virus (Appendix Figure 2).

Clinical laboratory surveillance adds key insights into correlating syndromic signals with specific pathogens; however, it is reliant on test availability and performance. Although the enterovirus/rhinovirus signal from clinical testing is a useful early indicator, if this signal is used alone, EV-D68 epidemics can be misattributed to annual fall back-to-school rhinovirus resurgences. Detecting EV-D68 through clinical laboratory surveillance enabled early identification of the 2022 outbreak in Colorado compared with other centers in the United States, where difficulty interpreting the source of the enterovirus/rhinovirus spike on clinical platforms contributed to delayed recognition of the outbreak cause (J. Newland, PedsID ListServ, pers. comm, August 2022).

Until an EV-D68-specific target is included on commercial clinical testing platforms, the additional step of performing EV-D68–specific PCR on enterovirus/rhinovirus–positive specimens is necessary for clinical laboratory surveillance to confirm EV-D68 as the source of a respiratory disease outbreak as well as to detect lower level circulation that would not meet the alarm threshold of syndromic surveillance.

A key limitation of pathogen-specific PCR testing for newly emerging and constantly evolving RNA viruses is that primers must be matched to currently circulating strains to ensure adequate sensitivity. The lack of detection of the 2022 EV-D68 B3 strain by primers directed at the 2014 B1 strain demonstrated the value of the layers of syndromic surveillance in our multimodal system, because a syndromic signal that is not accompanied by PCR detection can alert clinical and public health laboratories to investigate, validate, and update primer-probe sets for detecting actively circulating strains. That iterative modification interdependently informed by our layered multimodal surveillance model enabled us to confirm that EV-D68 was the source of the 2022 respiratory outbreak and to assess the burden of disease among hospitalized children.

Wastewater surveillance and sequencing was initially developed for polio eradication, but scientific advancement has accelerated during the COVID-19 pandemic (*31*), serving as proof-of-principle of its public health utility for emerging pathogens, such as EV-D68 (*32*,*33*). Although our wastewater surveillance for EV-D68 was conducted retrospectively after the 2022 outbreak, we found direct temporal and geospatial correlation with our clinical laboratory surveillance from ZIP codes of hospitalized children with EV-D68 to validate this approach. Wastewater detections temporally preceded our syndromic surveillance alarm signal by 1–2 weeks, demonstrating future potential, if performed in real-time, to serve as the earliest warning of community circulation to detect an impending outbreak at the local level and could be expanded to track regional, national, or international spread.

EV-D68 is thought to be primarily transmitted and shed in respiratory secretions; fecal shedding is less common because most strains are acid-labile and degrade in the gastrointestinal tract (*7*). Our study is consistent with other published studies (*34*,*35*) that have demonstrated that even pathogens that are predominantly shed other than in feces, such as EV-D68, can still be detected and tracked through wastewater because of the high sensitivity of that method. Our study confirms that wastewater surveillance developed for poliovirus can be extended to EV-D68 and in the future probably beyond to other known and emerging enteroviruses associated with AFM. A key limitation to that approach is that enteroviruses, and many other pathogens, can be asymptomatically shed in feces and circulate among the community without causing substantial disease (*36*,*37*). That limitation can be overcome by the multimodal nature of our surveillance model by comparing detected strains in wastewater with those from clinical laboratory surveillance on specimens collected from patients with clinically relevant disease to verify that wastewater pathogen signals are of public health importance.

Last, a future component of multimodal surveillance being developed is the use of immunologic surveillance to assess the underlying immunologic background for an emerging pathogen. As a pathogen emerges, or reemerges, it is important to know the levels of prior exposure and immunity that may protect against future infection and affect transmission dynamics to inform epidemiologic models and predict future circulation patterns (*38*). Serosurveys to determine age-based seroprevalence can also help assess duration of maternal immunity, timing of primary exposure, and durability of humoral immunity (*39*), although they can be affected by antibody cross-reactivity (*40*). Those efforts are currently under way for EV-D68 through the PREMISE EV-D68 pilot study, which serves as proof-of-principle for an immunologic surveillance approach to pandemic preparedness to expedite preemptive development of countermeasures, such as monoclonal antibodies and vaccine candidates (*14*).

The multimodal surveillance system piloted for EV-D68 in Colorado is the culmination of several stepwise surveillance efforts implemented over the previous 8 years, which come with limitations. Differences in implementation timing, particularly the prospective versus retrospective nature, limit the ability to assess actionable effects of each layer. Differences in catchment between surveillance layers may influence correlation between signals. Our pilot surveillance program focused on 1 pathogen in 1 geographic region during 1 outbreak year; the model should be studied for other pathogens across broader regions in a prospective longitudinal manner to determine generalizability. Last, surveillance is meant to be actionable, but delay from signal detection to public health intervention diminishes potential effect and is a potential target for improvement.

Together, the layers of multimodal surveillance enacted in Colorado for EV-D68 rapidly detected the 2022 EV-D68 outbreak and enabled preparedness efforts for an effective local, state, and national response while creating the potential for more advanced future preparedness efforts. Actionable surveillance results enabled surge planning by hospital administration to increase staffing, hospital bed availability, and the supply chain for critical medications and also alerted providers to a potential influx of patients and provided recommendations to improve case recognition and clinical management. Although AFM cases were rare during the EV-D68 outbreak in 2022, our surveillance also demonstrates usefulness as an early warning system to trigger public health outreach efforts to enhance readiness to respond to future outbreaks of enteroviruses associated with AFM. Our multimodal approach, extending from surveillance for rare, severe complications to more common disease presentations and community circulation and immunity, demonstrates the value of investing in surveillance to inform preparedness to respond to the uncertainty that lies ahead with EV-D68 and other emerging pathogens.

Acknowledgments
We acknowledge Carol Wilusz, Susan De Long, and Jim Huang for processing and providing the extracted wastewater RNA for this study.

This study was funded in part by CDC.

About the Author
Dr. Messacar is an associate professor of pediatrics at the University of Colorado School of Medicine in the section of Infectious Diseases and Epidemiology. His clinical research interests involve designing diagnostic and antimicrobial stewardship strategies for the implementation of rapid molecular diagnostic technologies to improve the clinical care of hospitalized children with suspected infections and improving the understanding, diagnostic testing, and treatment of central nervous system infections, including meningitis, encephalitis, and acute flaccid myelitis.

References
1. Messacar K, Abzug MJ, Dominguez SR. The emergence of enterovirus-D68. Microbiol Spectr. 2016;4:4.3.37. https://doi.org/10.1128/microbiolspec.EI10-0018-2016
2. Messacar K, Hawkins SM, Baker J, Pearce K, Tong S, Dominguez SR, et al. Resource burden during the 2014 enterovirus D68 respiratory disease outbreak at Children's Hospital Colorado: an unexpected strain. JAMA Pediatr. 2016; 170:294–7. https://doi.org/10.1001/jamapediatrics. 2015.3879
3. Midgley CM, Watson JT, Nix WA, Curns AT, Rogers SL, Brown BA, et al.; EV-D68 Working Group. Severe respiratory illness associated with a nationwide outbreak of enterovirus D68 in the USA (2014): a descriptive epidemiological investigation. Lancet Respir Med. 2015;3:879–87. https://doi.org/10.1016/S2213-2600(15)00335-5
4. Centers for Disease Control and Prevention. AFM cases and outbreaks [cited 2023 May 17]. https://www.cdc.gov/acute-flaccid-myelitis/cases-in-us.html
5. Centers for Disease Control and Prevention. Enterovirus D68 [cited 2017 Apr 21]. https://www.cdc.gov/non-polio-enterovirus/about/ev-d68.html
6. Kamau E, Harvala H, Blomqvist S, Nguyen D, Horby P, Pebody R, et al. Increase in enterovirus D68 infections in young children, United Kingdom, 2006–2016. Emerg Infect Dis. 2019;25:1200–3. https://doi.org/10.3201/eid2506.181759
7. Oberste MS, Maher K, Schnurr D, Flemister MR, Lovchik JC, Peters H, et al. Enterovirus 68 is associated with respiratory illness and shares biological features with both the enteroviruses and the rhinoviruses. J Gen Virol. 2004;85:2577–84. https://doi.org/10.1099/vir.0.79925-0
8. Centers for Disease Control and Prevention (CDC). Clusters of acute respiratory illness associated with human enterovirus 68—Asia, Europe, and United States, 2008–2010. MMWR Morb Mortal Wkly Rep. 2011;60:1301–4.
9. Holm-Hansen CC, Midgley SE, Fischer TK. Global emergence of enterovirus D68: a systematic review. Lancet Infect Dis. 2016;16:e64–75. https://doi.org/10.1016/S1473-3099(15)00543-5
10. Kujawski SA, Midgley CM, Rha B, Lively JY, Nix WA, Curns AT, et al. Enterovirus D68-associated acute respiratory illness—New Vaccine Surveillance Network, United States, July–October, 2017 and 2018. MMWR Morb Mortal Wkly Rep. 2019;68:277–80. https://doi.org/10.15585/mmwr.mm6812a1
11. McLaren N, Lopez A, Kidd S, Zhang JX, Nix WA, Link-Gelles R, et al. Characteristics of patients with acute flaccid myelitis, United States, 2015–2018. Emerg Infect Dis. 2020;26:212–9. https://doi.org/10.3201/eid2602.191453
12. Park SW, Pons-Salort M, Messacar K, Cook C, Meyers L, Farrar J, et al. Epidemiological dynamics of enterovirus D68 in the United States and implications for acute flaccid myelitis. Sci Transl Med. 2021;13:eabd2400. https://doi.org/10.1126/scitranslmed.abd2400
13. Messacar K, Baker RE, Park SW, Nguyen-Tran H, Cataldi JR, Grenfell B. Preparing for uncertainty: endemic paediatric viral illnesses after COVID-19 pandemic disruption. Lancet. 2022;400:1663–5. https://doi.org/10.1016/S0140-6736(22)01277-6
14. Nguyen-Tran H, Park SW, Messacar K, Dominguez SR, Vogt MR, Permar S, et al. Enterovirus D68: a test case for the use of immunological surveillance to develop tools to mitigate the pandemic potential of emerging pathogens. Lancet Microbe. 2022;3:e83–5. https://doi.org/10.1016/S2666-5247(21)00312-8
15. Messacar K, Schreiner TL, Maloney JA, Wallace A, Ludke J, Oberste MS, et al. A cluster of acute flaccid paralysis and cranial nerve dysfunction temporally associated with an outbreak of enterovirus D68 in children in Colorado, USA. Lancet. 2015;385:1662–71. https://doi.org/10.1016/S0140-6736(14)62457-0
16. Messacar K, Robinson CC, Pretty K, Yuan J, Dominguez SR. Surveillance for enterovirus D68 in Colorado children reveals continued circulation. J Clin Virol. 2017;92:39–41.
17. Messacar K, Pretty K, Reno S, Dominguez SR. Continued biennial circulation of enterovirus D68 in Colorado. J Clin Virol. 2019;113:24–6.
18. Ma KC, Winn A, Moline HL, Scobie HM, Midgley CM, Kirking HL, et al.; New Vaccine Surveillance Network Collaborators. Increase in acute respiratory illnesses among children and adolescents associated with rhinoviruses and enteroviruses, including enterovirus D68—United States, July–September 2022. MMWR Morb Mortal Wkly Rep. 2022;71:1265–70. https://doi.org/10.15585/mmwr.mm7140e1
19. Council of State and Territorial Epidemiologists. Revision to the standardized case definition, case classification, and public health reporting for acute flaccid myelitis. [cited 2015 Oct 30]. https://cdn.ymaws.com/www.cste.org/resource/resmgr/ps/ps2021/21-ID-02_AFM.pdf
20. Ikuse T, Aizawa Y, Takihara H, Okuda S, Watanabe K, Saitoh A. Development of novel PCR assays for improved detection of enterovirus D68. J Clin Microbiol. 2021;59:e0115121. https://doi.org/10.1128/JCM.01151-21
21. Wylie TN, Wylie KM, Buller RS, Cannella M, Storch GA. Development and evaluation of an enterovirus D68

real-time reverse transcriptase PCR assay. J Clin Microbiol. 2015;53:2641–7. https://doi.org/10.1128/JCM.00923-15
22. Centers for Disease Control and Prevention. Severe respiratory illnesses associated with rhinoviruses and/or enteroviruses including EV-D68—multistate, 2022 [cited 2023 May 17]. https://emergency.cdc.gov/han/2022/han00474.asp
23. Rao S, Armistead I, Messacar K, Alden NB, Schmoll E, Austin E, et al. Shifting epidemiology and severity of respiratory syncytial virus in children during the COVID-19 pandemic. JAMA Pediatr. 2023;177:730–2. https://doi.org/10.1001/jamapediatrics.2023.1088
24. Messacar K, Abzug MJ, Dominguez SR. Acute flaccid myelitis surveillance: a signal through the noise. Pediatrics. 2019;144:e20192492. https://doi.org/10.1542/peds.2019-2492
25. Aliabadi N, Messacar K, Pastula DM, Robinson CC, Leshem E, Sejvar JJ, et al. Enterovirus D68 infection in children with acute flaccid myelitis, Colorado, USA, 2014. Emerg Infect Dis. 2016;22:1387–94. https://doi.org/10.3201/eid2208.151949
26. American Academy of Pediatrics. Acute flaccid myelitis [cited 2023 April 5]. https://www.aap.org/en/patient-care/acute-flaccid-myelitis
27. Murphy OC, Messacar K, Benson L, Bove R, Carpenter JL, Crawford T, et al.; AFM working group. Acute flaccid myelitis: cause, diagnosis, and management. Lancet. 2021;397:334–46. https://doi.org/10.1016/S0140-6736(20)32723-9
28. Kidd S, Lopez AS, Konopka-Anstadt JL, Nix WA, Routh JA, Oberste MS. Enterovirus D68–associated acute flaccid myelitis, United States, 2020. Emerg Infect Dis. 2020;26:e201630. https://doi.org/10.3201/eid2610.201630
29. Messacar K, Asturias EJ, Hixon AM, Van Leer-Buter C, Niesters HGM, Tyler KL, et al. Enterovirus D68 and acute flaccid myelitis—evaluating the evidence for causality. Lancet Infect Dis. 2018;18:e239–47. https://doi.org/10.1016/S1473-3099(18)30094-X
30. Dyda A, Stelzer-Braid S, Adam D, Chughtai AA, MacIntyre CR. The association between acute flaccid myelitis (AFM) and enterovirus D68 (EV-D68)—what is the evidence for causation? Euro Surveill. 2018;23:17-00310.
31. O'Reilly KM, Allen DJ, Fine P, Asghar H. The challenges of informative wastewater sampling for SARS-CoV-2 must be met: lessons from polio eradication. Lancet Microbe. 2020;1:e189–90. https://doi.org/10.1016/S2666-5247(20)30100-2
32. Nemudryi A, Nemudraia A, Wiegand T, Surya K, Buyukyoruk M, Cicha C, et al. Temporal detection and phylogenetic assessment of SARS-CoV-2 in municipal wastewater. Cell Rep Med. 2020;1:100098. https://doi.org/10.1016/j.xcrm.2020.100098
33. Mello MM, Meschke JS, Palmer GH. Mainstreaming wastewater surveillance for infectious disease. N Engl J Med. 2023;388:1441–4. https://doi.org/10.1056/NEJMp2301042
34. Erster O, Bar-Or I, Levy V, Shatzman-Steuerman R, Sofer D, Weiss L, et al. Monitoring of enterovirus D68 outbreak in Israel by a parallel clinical and wastewater based surveillance. Viruses. 2022;14:1010. https://doi.org/10.3390/v14051010
35. Tedcastle A, Wilton T, Pegg E, Klapsa D, Bujaki E, Mate R, et al. Detection of enterovirus D68 in wastewater samples from the UK between July and November 2021. Viruses. 2022;14:143. https://doi.org/10.3390/v14010143
36. Brinkman NE, Fout GS, Keely SP. Retrospective surveillance of wastewater to examine seasonal dynamics of enterovirus infections. MSphere. 2017;2:e00099-17. https://doi.org/10.1128/mSphere.00099-17
37. Faleye TOC, Bowes DA, Driver EM, Adhikari S, Adams D, Varsani A, et al. Wastewater-based epidemiology and long-read sequencing to identify enterovirus circulation in three municipalities in Maricopa County, Arizona, southwest United States between June and October 2020. Viruses. 2021;13:1803. https://doi.org/10.3390/v13091803
38. Grenfell BT, Pybus OG, Gog JR, Wood JL, Daly JM, Mumford JA, et al. Unifying the epidemiological and evolutionary dynamics of pathogens. Science. 2004;303:327–32. https://doi.org/10.1126/science.1090727
39. Metcalf CJ, Farrar J, Cutts FT, Basta NE, Graham AL, Lessler J, et al. Use of serological surveys to generate key insights into the changing global landscape of infectious disease. Lancet. 2016;388:728–30. https://doi.org/10.1016/S0140-6736(16)30164-7
40. Rosenfeld AB, Shen EQL, Melendez M, Mishra N, Lipkin WI, Racaniello VR. Cross-reactive antibody responses against nonpoliovirus enteroviruses. MBio. 2022;13:e0366021. https://doi.org/10.1128/mbio.03660-21

Address for correspondence: Kevin Messacar, B055, Children's Hospital Colorado, 13213 E 16th Ave, Aurora, CO 80045, USA; email: kevin.messacar@childrenscolorado.org

Concurrent Clade I and Clade II Monkeypox Virus Circulation, Cameroon, 1979–2022

Delia D. Djuicy, Serge A. Sadeuh-Mba,[1] Chanceline N. Bilounga, Martial G. Yonga, Jules B. Tchatchueng-Mbougua, Gael D. Essima, Linda Esso, Inès M.E. Nguidjol, Steve F. Metomb, Cornelius Chebo, Samuel M. Agwe, Placide A. Ankone, Firmin N.N. Ngonla, Hans M. Mossi, Alain G.M. Etoundi, Sara I. Eyangoh, Mirdad Kazanji, Richard Njouom

During 1979–2022, Cameroon recorded 32 laboratory-confirmed mpox cases among 137 suspected mpox cases identified by the national surveillance network. The highest positivity rate occurred in 2022, indicating potential mpox re-emergence in Cameroon. Both clade I (n = 12) and clade II (n = 18) monkeypox virus (MPXV) were reported, a unique feature of mpox in Cameroon. The overall case-fatality ratio of 2.2% was associated with clade II. We found mpox occurred only in the forested southern part of the country, and MPXV phylogeographic structure revealed a clear geographic separation among concurrent circulating clades. Clade I originated from eastern regions close to neighboring mpox-endemic countries in Central Africa; clade II was prevalent in western regions close to West Africa. Our findings suggest that MPXV re-emerged after a 30-year lapse and might arise from different viral reservoirs unique to ecosystems in eastern and western rainforests of Cameroon.

Monkeypox virus (MPXV) is an emerging zoonotic *Orthopoxvirus* causing mpox in humans, a disease similar to the eradicated smallpox (*1*). Since identification in a monkey in 1958 (*2*) and a human in 1970 (*3*), MPXV-associated outbreaks have occurred primarily in rural rainforests in countries of Central and West Africa (*4*–*6*).

Author affiliations: Centre Pasteur of Cameroon, Yaounde, Cameroon (D.D. Djuicy, S.A. Sadeuh-Mba, M.G. Yonga, J.B. Tchatchueng-Mbougua, G.D. Essima, S.I. Eyangoh, M. Kazanji, R. Njouom); Ministry of Public Health, Yaounde (C.N. Bilounga, L. Esso, I.M.E. Nguidjol, S.F. Metomb, C. Chebo, S.M. Agwe, P.A. Ankone, F.N.N. Ngonla, H.M. Mossi, A.G.M. Etoundi); University of Douala, Cameroon (C.N. Bilounga); University of Bamenda, Cameroon (L. Esso)

DOI: https://doi.org/10.3201/eid3003.230861

Mpox is characterized by an influenza-like syndrome accompanied by adenopathy and maculopapular rashes typically developing on the palms of the hands and soles of the feet (*4*,*7*). For infected persons, supportive care and antiviral treatments, including cidofovir and tecovirimat, are provided (*4*). Cross-immunity with smallpox vaccination and a new generation of smallpox vaccines equally offer some protection (*8*–*10*). However, after smallpox vaccination was discontinued in the early 1980s, herd immunity gradually declined, enabling re-emergence of mpox, which is highlighted by the increased number of cases in Africa during the past 3 decades (*4*,*8*,*11*–*13*). Since early 2022, case counts have surged, and ≈1,215 confirmed mpox cases and 219 deaths were reported in Africa by December 28, 2022 (*14*). Before April 2022, mpox cases in the Western Hemisphere were typically reported from exposure to the exotic pet trade and international travel (*15*–*20*). Since then, MPXV-associated outbreaks have occurred worldwide, affecting >100 countries outside Africa (*4*,*21*) and becoming a global public health concern.

Primary MPXV transmission can occur through direct contact with body fluids or skin lesions of infected animals or indirectly via contaminated fomites. Similar contact with an infected person or with infected respiratory droplets might also lead to human-to-human secondary transmission, the main transmission mode of the 2022 global outbreak (*4*,*22*). Historically, primary zoonotic transmission was more common and mostly involved an at-risk population of hunters, butchers, and bushmeat handlers; secondary transmission was rare, but nosocomial and household transmission have been described (*3*,*13*,*23*–*25*).

[1]Current affiliation: Maryland Department of Agriculture, Salisbury, Maryland, USA.

Phylogenetic studies report 2 distinct MPXV clades: clade I, prevalent in Central Africa, and clade II, endemic to West Africa (*5*,*6*,*26*–*28*). However, Cameroon is an exception, and both clades concurrently circulate in the country (*6*,*29*). Clade I is further subdivided into lineages 1–5 and clade II into subclades IIa and IIb; clade IIb is responsible for the multicountry outbreak that began in 2022 (*27*,*28*,*30*). Globally, MPXV lethality rates vary from 1% to 10%, and clade I is known to have higher mortality rates than clade II (*4*,*24*,*25*). The MPXV animal reservoir has not yet been identified, but the virus can infect a wide range of mammals, and *Funisciurus* squirrels and *Graphiurus lorraineus* mice are thought to be the most probable MPXV reservoirs (*31*–*33*).

In Cameroon, only 4 confirmed mpox cases were documented before the 2022 outbreak, 1 in each 1979, 1980, 1989, and 30 years later in 2018 (*29*,*34*–*36*). According to public health reports, more cases could have occurred and been undocumented in the country, particularly during 2018–2021, and especially in 2022, during which an mpox outbreak of unprecedented magnitude occurred and had recurrent clusters of cases (*37*). However, whether those infections were associated with importations from neighboring countries or from occurrence of indigenous primary or secondary transmission remains unclear (*29*). Overall, data on the epidemiologic features of MPXV occurrence and transmission dynamics in Cameroon are scarce. We investigated the clinical, epidemiologic, and molecular features of MPXV-associated outbreaks in Cameroon.

Methods

Sample Location

Cameroon is in central Africa and is divided into 10 administrative regions. Cameroon is known as Africa in miniature for its diverse agroecologic background: the steppe and savanna in the Far North, North, and Adamawa regions; the coastal zones in the Littoral and Southwest regions; mountain highlands in the Northwest and West regions; and the rainforest in the Centre, South, Southwest, and East regions (*38*). Cameroon has 3 major tropical forests: the Congo Basin Forest that extends across the East, South, and Centre regions; the Guinea moist forest in the western and Adamawa regions; and the Cameroonian Highlands forests in the Northwest and Southwest regions. Those forests are crossed by several waterways, including the Sanaga River, the largest river in Cameroon (*33*–*40*; J. Thia, master's thesis, University of Canterbury, 2014, https://www.researchgate.net/publication/272494772_The_plight_of_trees_in_disturbed_forest_conservation_of_Montane_Trees_Nigeria).

Sample Collection

We defined a suspected case as ≥1 clinical signs or symptoms, including headache, asthenia, adenopathy, myalgia associated with fever, or gradually developing rashes spreading to other parts of the body, including the soles of the feet and palms of the hands. We defined a probable case as clinical manifestations without virologic confirmation but an epidemiologic link with another probable or confirmed case. A confirmed case was any case with laboratory-confirmed MPXV.

We recorded epidemiologic data, including demographic and clinical information, for all suspected cases during 1979–2022. We collected a 5-mL blood sample, vesicle swab, crust samples, or a combination of samples, from case-patients who consented to be tested. We shipped samples under a triple packaging system to the Centre Pasteur du Cameroun (CPC), which is the national reference laboratory for mpox diagnosis in Cameroon. We excluded patients from whom a sample could not be collected.

Laboratory Confirmation of MPXV Infection

At CPC, samples were received, processed, and inactivated in the Biosafety Level 3 laboratory. We purified total DNA by using the QIAamp DNA Mini Kit (QIAGEN, https://www.qiagen.com) according to the manufacturer's instructions. We tested purified DNA for MPXV by the generic real-time PCR Taqman assay, as previously described (*41*). For positive samples displaying a cycle threshold (Ct) value <37, we performed further genotyping by using real-time PCRs specifically targeting MPXV clade I and II (*41*).

We further amplified a subset of 8 positive samples from the 2022 outbreak that had Ct values ≤20 by using a PCR targeting a portion of the MPXV A-type inclusion (*ATI*) gene, according to a previously described protocol (*42*). We used a 1% green-stained agarose gel to reveal resulting amplicons, which we sent to Inqaba Biotechnical Industries (Pretoria, South Africa), a commercial service provider, for Sanger sequencing.

Phylogenetical Analyses

We assembled newly determined sequences and corrected by using CLC Main Workbench software (QIAGEN). We aligned resulting consensus sequences by using MAFFT version 7 (https://mafft.cbrc.jp) and an extended dataset of 56 MPXV reference genomes from GenBank (Appendix Tables 1, 2, https://wwwnc.cdc.gov/EID/article/30/3/23-0861-App1.pdf). We submitted final alignments to the software-integrated Model Finder program (IQ-TREE, http://www.iqtree.org) to select the best evolutionary model based on Bayesian and Akaike information criterion. We used IQ-TREE version 1.6.12 (http://www.iqtree.org) to infer maximum-likelihood phylogenetic trees on MPXV *ATI* sequences based on the Hasegawa-Kishino-Yano plus amino acid substitution model, applying 1,000 bootstrap replicates. We submitted newly determined sequences to GenBank (accession nos. OR038717–24) (Appendix Table 2).

Statistical Analysis and Mapping

To provide a complete picture of the epidemiology of mpox in Cameroon, we added the 4 previously documented mpox cases from Cameroon to our dataset, along with available information collected from the literature and Ministry of Health archives (*29*,*34*–*36*). We summarized sociodemographic and clinical characteristics by using frequencies for categorical variables; we used median and interquartile range (IQR) for quantitative variables. We compared PCR-confirmed cases with nonconfirmed suspected cases by using Pearson χ^2 or Fisher exact tests for categorical variables and Wilcoxon test for quantitative variables. We used univariate logistic regression to identify factors associated with MPXV infection and estimate crude odds ratios (ORs) and 95% CIs. We were unable to infer multivariable analysis models, which failed to converge because too many data were missing (Tables 1, 2). We considered $p<0.05$ statistically significant and $p<0.07$ marginally significant. We performed all analyses in R version 4.1 (The R Foundation for Statistical Computing, https://www.r-project.org). We used Quantum GIS version 3.30.1 (QGIS, https://qgis.org) to analyze and map mpox cases by health zones and geographic data.

Ethics

Sample collection and laboratory analyses were conducted within the framework of the Cameroon national surveillance program. Under that program, we obtained written or oral informed consent from all persons with suspected mpox after we provided detailed information and explanations of the sampling purpose. We obtained informed consent from parents or recognized guardians for persons <15 years of age.

Results

Within the mpox surveillance system in Cameroon, during 1979–2022, we identified 137 suspected mpox cases, including 74 (54.41%) among male and 62 (45.59%) among female persons; 1 case had missing data for sex (Table 1). The median age of case-patients was 11 years (range 2 weeks–75 years; IQR 4–27 years); nearly half (48.18%) were ≤10 years of age (Table 1).

Molecular Diagnostic Results

Mpox virus generic PCR showed 32 (23.36%) laboratory-confirmed mpox cases of 137 patients tested during 1979–2022 in Cameroon (Table 1; Figure 1, panel A; Appendix Table 3). Before 2018, only 3 sporadic cases were confirmed as human MPXV infection. After a 30-year gap without reported mpox cases, the surveillance system continuously identified new mpox cases during 2018–2022. Among suspected cases, only 1 was found in 2018 and 1 in 2019. In 2020 and 2021, 5 laboratory-confirmed cases were recorded each year. During 2022, mpox cases dramatically increased to 17 confirmed cases among 84 suspected cases (Figure 1, panel A; Appendix Table 3).

Genotyping of real-time PCR results identified 12 (9%) patients infected with MPXV clade I and 18 (13%) infected with MPXV clade II among 137 suspected cases; 2 (1%) historic confirmed cases lacked clade determination results (Table 1; Figure 1, panel B; Appendix Tables 2, 3). Among all laboratory-confirmed cases, only 1 death was recorded, in a patient infected with MPXV clade II. Ministry of Health investigation records indicated 2 additional patient deaths among persons with typical mpox clinical manifestations who were epidemiologically linked to 2 confirmed case-patients infected with a clade II MPXV strain. However, no specimens were collected before death; thus, we considered those probable cases. Including the probable cases, the overall case-fatality ratio (CFR) in Cameroon was 2.2% (3/139) among confirmed and suspected cases, and all deaths were associated with viral clade II.

Epidemiology and Clinical Characteristics of Confirmed Mpox Cases

Univariable analysis revealed no statistically significant difference in increased likelihood of infection by sex: 21/74 (28.38%) male and 11/62 (17.74%) female persons had confirmed MPXV infection (Table 1). MPXV-confirmed case-patients had a median age of 21.5 years (range 2 weeks–52 years; IQR 8.5–32.25 years). MPXV infection was more prevalent among adults ≥20 years of age; in all, 35.56% had confirmed MPXV infection, compared with 17.78% among younger MPXV-confirmed case-patients ($p = 0.025$). However, we saw no statistically significant

Table 1. Molecular diagnostic and epidemiologic characteristics of suspected and confirmed mpox cases in a study of concurrent clade I and clade II monkeypox virus circulation, Cameroon, 1979–2022*

Epidemiologic characteristics	MPXV real-time PCR, no. (%) Positive	Negative	Crude OR (95% CI)	p value
Total no. (%), n = 137	32 (23.36)	105 (76.64)		
MPXV clades				
Clade I, n = 12	12 (100.00)	NA	NA	1
Clade II, n = 18	18 (100.00)	NA	NA	
Sex				
M, n = 74	21 (28.38)	53 (71.62)	Referent	**0.142**
F, n = 62	11 (17.74)	51 (82.26)	1.84 (0.81–4.19)	
Age				
Minimum	0	0	NA	**0.075**
1st quartile	8.5	4	NA	
Median	21.5	10	NA	
Mean	21.69	15.64	1.02 (1.00–1.05)	
3rd quartile	32.25	22.5	NA	
Maximum	52	75	NA	
Age group, y				
0–10, n = 66	10 (15.15)	56 (84.85)	Referent	**0.101**
11–20, n = 24	6 (25.00)	18 (75.00)	1.87 (0.60–5.85)	
21–30, n = 18	6 (33.33)	12 (66.67)	2.8 (0.85–9.19)	
>30, n = 27	10 (37.04)	17 (62.96)	3.29 (1.17–9.24)	
Born before 1980				
Y, n = 124	27 (45.45)	97 (54.55)	Referent	**0.092**
N, n = 11	5 (21.77)	6 (78.23)	3.07 (0.86–10.88)	
Born before 2002				
Y, n = 90	16 (17.78)	74 (82.22)	Referent	**0.025**
N, n = 45	16 (35.56)	29 (64.44)	2.55 (1.13–5.77)	
Occupation				
Underage/none, n = 29	6 (20.69)	23 (79.31)	Referent	**0.067**
Pupil/student, n = 54	8 (14.81)	46 (85.19)	0.67 (0.21–2.15)	
Health worker, n = 4	2 (50.00)	2 (50.00)	3.07 (0.84–11.17)	
Farmer, n = 18	8 (44.44)	10 (55.56)	3.83 (0.44- 33.11)	
Others†, n = 14	5 (35.71)	9 (64.28)	2.13 (0.52–8.77)	
Contact with human case				
Y, n = 57	17 (29.82)	40 (70.18)	Referent	0.304
N, n = 56	10 (17.86)	46 (82.14)	0.51 (0.21–1.24)	
Unknown, n = 3	1 (33.33)	2 (66.67)	0.17 (0.10–13.86)	
Contact with animal				
Y, n = 37	12 (32.43)	25 (67.57)	Referent	0.143
N, n = 69	11 (15.94)	58 (84.06)	0.40 (0.15–1.0)	
Unknown, n = 7	2 (28.57)	5 (71.43)	0.88 (0.14–4.93)	
Contact with wild or domestic animal				
Domestic animal, n = 13	3 (23.08)	10 (76.92)	Referent	**0.06**
Wild animal, n = 13	6 (46.15)	7 (53.85)	2.86 (0.53–15.47)	
No contact, n = 69	11 (15.94)	58 (84.06)	0.63 (0.15–2.67)	
Travel history				
Y, n = 21	5 (23.81)	16 (76.19)	Referent	0.831
N, n = 96	25 (26.04)	71 (73.96)	0.89 (0.29–2.67)	
Geographic distribution				
Adamawa, n = 1	0	1 (100.00)	Referent	0.831
Centre, n = 32	11 (34.36)	21 (65.63)	0 to ∞	
East, n = 23	3 (13.04)	20 (86.96)	0 to ∞	
Far-North, n = 2	0	2 (100.00)	0 to ∞	
Littoral, n = 4	1 (25)	3 (75.00)	0 to ∞	
North, n = 1	0	1 (100.00)	0 to ∞	
North-West, n = 25	6 (24.00)	19 (76.00)	0 to ∞	
South, n = 9	1 (11.00)	8 (88.89)	0 to ∞	
South-west, n = 39	10 (25.64)	29 (74.36)	0 to ∞	
Other‡	0	1	0 to ∞	

*Bold text indicates statistical significance. Some categories might not add to 100% because of missing data. Missing data were not accounted for in the statistical analysis. MPXV, monkeypox virus; NA, not applicable; OR, odds ratio.
†Others include teachers, traders, driver or motorbiker, housewife, informal, retired.
‡Equatorial Guinea.

difference for adults born before 1980 than for the rest of the population (p = 0.092). Larger datasets would be needed to confirm the observed trend.

MPXV infection was mostly associated with occupational activities involved in farming (OR 3.83, 95% CI 0.44–33.11) (Table 1). Similarly, potential nosocomial

Table 2. Clinical characteristics of suspected and confirmed mpox cases in a study of concurrent clade I and clade II monkeypox virus circulation, Cameroon, 1979–2022*

Characteristics	MPXV RT-PCR, no. (%) Positive	Negative	Crude OR (95% CI)	p value
Total no. (%), n = 137	32 (23.36)	105 (76.64)		
Active skin lesions				
Lesions, n = 124	29 (23.39)	95 (76.61)	Referent	0.289
No lesions, n = 10	1 (10.00)	9 (90.00)	2.75 (0.33–22.6)	
Lesion progress				
Diffuse, n = 23	5 (21.74)	18 (78.26)	Referent	0.329
Head to limbs, n = 25	4 (16.00)	21 (84.00)	0.69 (0.16–2.95)	
Limbs to head, n = 15	6 (40.00)	9 (60.00)	2.4 (0.57–10.04)	
Others, n = 24	4 (16.67)	20 (83.33)	0.72 (0.17–3.1)	
Lesions at the same stage				
Y, n = 43	13 (30.23)	30 (69.77)	Referent	0.195
N, n = 53	10 (18.87)	43 (81.13)	1.86 (0.72–4.8)	
Lesions of the same size				
Y, n = 49	13 (26.53)	36 (73.47)	Referent	0.546
N, n = 47	10 (21.28)	37 (78.72)	1.34 (0.52–3.43)	
Lesions deep				
Y, n = 42	11 (26.19)	31 (73.81)	Referent	0.767
N, n = 51	12 (23.53)	39 (76.47)	1.15 (0.45–2.97)	
Fever before rash				
Y, n = 86	22 (25.58)	64 (74.42)	Referent	**0.149**
N, n = 30	4 (13.33)	26 (86.67)	2.23 (0.7–7.12)	
Missing	6	15	NA	
Headache				
Y, n = 51	15 (29.41)	36 (70.59)	Referent	**0.1**
N, n = 61	10 (16.39)	51 (83.61)	2.13 (0.86–5.26)	
Cough				
Y, n = 38	13 (34.21)	25 (65.79)	Referent	**0.066**
N, n = 76	14 (18.42)	62 (81.58)	2.3 (0.95–5.59)	
Vomiting, nausea				
Y, n = 15	4 (26.67)	11 (73.33)	Referent	0.722
N, n = 98	22 (22.45)	76 (77.55)	1.26 (0.36–4.34)	
Chills, sweat				
Y, n = 48	18 (37.50)	30 (62.50)	Referent	**0.003**
N, n = 66	9 (13.34)	57 (86.36)	3.8 (1.52–9.48)	
Lymphadenopathy				
Y, n = 29	12 (41.38)	17 (58.62)	Referent	**0.009**
N, n =84	14 (16.37)	70 (83.33)	3.53 (1.38–9.00)	
Sore throat when swallowing				
Y, n = 28	16 (51.14)	12 (42.86)	Referent	**<0.001**
N, n = 85	10 (11.76)	75 (88.24)	10 (3.69–27.12)	
Oral ulcer				
Y, n = 18	11 (61.11)	7 (38.89)	Referent	**<0.001**
N, n = 95	15 (15.79)	80 (84.21)	8.38 (2.80–25.09)	
Itchy lesions				
Y, n = 75	19 (25.33)	56 (74.67)	Referent	0.397
N, n = 43	8 (18.60)	35 (81.40)	1.48 (0.59–3.75)	
Unknown	5	14	NA	
General fatigue				
Y, n = 62	20 (32.25)	42 (67.74)	Referent	**0.016**
N, n = 52	7 (13.46)	45 (86.54)	3.06 (1.17–7.98)	
Myalgia				
Y, n = 29	9 (31.03)	20 (68.97)	Referent	0.244
N, n = 84	17 (20.24)	67 (79.76)	1.77 (0.69–4.59)	
Unknown	6	18	NA	
Conjunctivitis				
Y, n = 14	2 (14.29)	12 (85.71)	Referent	0.385
N, n = 99	24 (24.24)	75 (75.76)	0.52 (0.11–2.49)	

*Bold text indicates statistical significance. Missing data is for patients who did not provide an answer. Unknown is for persons who replied that they did not know. Some categories might not add to 100% because of missing data. Missing data were not accounted for in the statistical analysis. MPXV, monkeypox virus; NA, not applicable; OR, odds ratio.

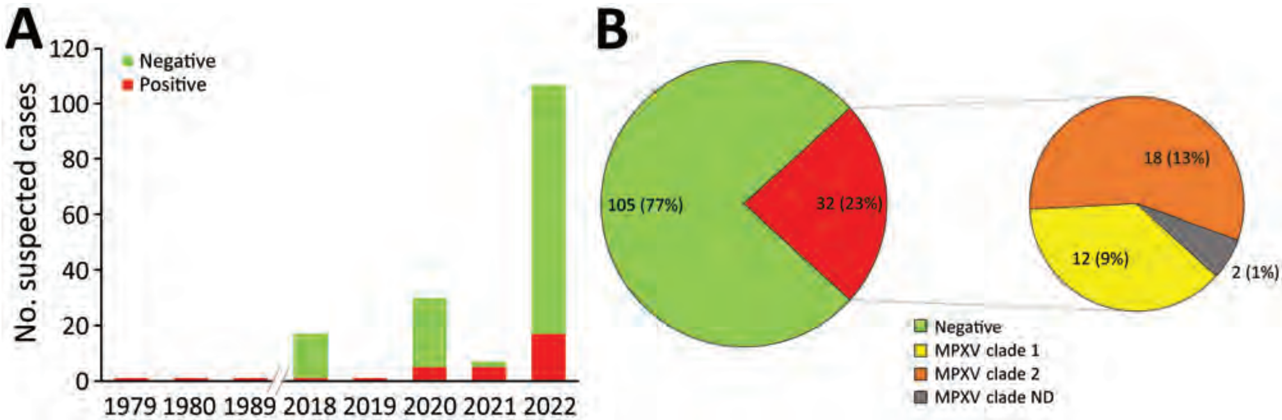

Figure 1. Mpox cases in a study of concurrent clade I and clade II MPXV circulation, Cameroon, 1979–2022. A) Epidemiologic curve of 137 suspected mpox cases. A 30-year gap occurred between the first 3 reported mpox cases and the consecutive cases since 2018, demonstrating increased surveillance in the country. The peak in 2022 corresponds to the worldwide alert raised on mpox, which led to enhanced mpox surveillance in Cameroon. B) Mpox genotyping results showing both clade I and clade II MPXV were identified. MPXV, monkeypox virus; ND, not determined.

transmission was identified in health workers (OR 3.07, 95% CI 0.84–11.17). Other activities, including teaching, trading, or driving, when considered together, also appeared to be potential risk activities for secondary MPXV transmission (OR 2.13, 95% CI 0.52–8.77). However, we found no association for secondary transmission in the 29.82% of MPXV-confirmed cases reporting past contact with persons who had mpox-like clinical signs (Table 1). Because mpox is typically zoonotic, we also assessed antecedent of animal exposures. We observed no association with unspecified animal contacts but observed a higher risk among confirmed cases (6/13 [46.15%]) who reported contact with wild animals (OR 2.86, 95% CI 0.53–15.47) compared with persons reporting contact with domestic animals or having no contact with animals (Table 1). Among wild animal contact, study participants frequently mentioned squirrels, bats, caterpillars, pangolins, rats, porcupines, and monkeys.

As expected from the case definition criterium requiring skin rashes, almost all (124/137 [90.5%]) MPXV-suspected cases had active skin lesions (Table 2; Figure 2; Appendix Table 3). However, we observed no specific difference for lesion progress, deepness, size, or stage among MPXV-confirmed cases compared with MPXV-negative persons (Table 2). Maculopapular lesions were more prevalent in confirmed cases who had lesions on their palms and soles (Figure 2). Clinical data identified cough (OR 2.3, 95% CI 0.95–5.59), chills or sweat (OR 3.8, 95% CI 1.52–9.48), lymphadenopathy (OR 3.53, 95% CI 1.38–9.00), sore throat when swallowing (OR 10, 95% CI 3.69–27.12), mouth ulcers (OR 8.38, 95% CI 2.8–25.09), and general fatigue (OR 3.06, 95% CI 1.17–7.98) as potential symptoms associated with MPXV infection in Cameroon (Table 2; Figure 2). Among all suspected case-patients, ≈26% who reported experiencing fever before skin rashes developed were confirmed for MPXV infection, but we saw no difference between confirmed cases with or without fever. In addition, MPXV-confirmed or -negative cases did not experience differences in headache (Table 2). We noted little difference in clinical severity in cases infected with clade I compared with those infected with clade II (Appendix Table 4). The same was true for the exposure route; we found no association between zoonotic or human-to-human transmission and a specific infecting viral clade (Appendix Table 4). However, because considerable data were missing (Tables 1, 2) we were unable to perform a multivariable analysis. Therefore, concluding interpretations of the epidemiologic and clinical features of mpox infection in Cameroon are difficult to draw.

Geographic and Phylogenetic Analysis

Reported suspected mpox cases originated from 8 administrative regions of Cameroon (Table 1; Figure 3). Most (97.08%) suspected cases were reported from the southern part of the country where all confirmed cases also originated. In particular, 1 (3.13%) case was confirmed in Littoral, 1 (3.13%) in the South, 3 (9.38%) in the East, 6 (18.75%) in the Northwest, 10 (31.25%) in the Southwest, and 11 (34.88%) in the Centre regions (Table 1; Figure 3; Appendix Table 3). Of note, a unique case confirmed in the Littoral region was originally from the Southwest and sought healthcare in Littoral. Genotyping of real-time PCR revealed that all clade I MPXV infections were

Figure 2. Maculopapular lesions in mpox patients from a study of concurrent clade I and clade II monkeypox virus circulation, Cameroon, 1979–2022. A–E) Deep maculopapular lesions of different sizes spread from the head (A, C) to hands (B) and diffuse to the soles of the feet (D) the palm of the hand (E). F) Lesions, including oral lesions and mouth ulcers, in a 3-month-old male baby.

confirmed in patients from the Centre, South, and East regions; all but 1 of clade II MPXV samples were recovered from patients from the Littoral, Northwest, and Southwest regions. Indeed, a clade II MPXV detected in the Centre region was an internally displaced person (IDP) originally from the Northwest region (Table 1; Appendix Table 3). The distribution of mpox cases points toward geographic segregation of the 2 viral clades in Cameroon. Those findings indicate a strong geographic association of MPXV genotypes in southern Cameroon, and that MPXV clade II is associated with the western part and the clade I with the eastern part of the country.

We obtained partial MPXV *ATI* gene sequences from 8 mpox-confirmed cases from 4 regions of Cameroon. We derived the newly determined sequences from samples collected in the Northwest (CPC code 22V-0972), Southwest (CPC codes 22V-07739, 22V-07911, 22V-07968), Centre (CPC codes 22V-05210, 22V-04865, 22V-4639), and South (CPC code 22V-6957) regions. Maximum-likelihood phylogenetic analysis of the 942 nt consensus sequences, including reference sequences (Appendix Tables 1–3), revealed that the 8 MPXV genomes from Cameroon segregated into clade I and clade II. As expected from the geographic association of MPXV isolates we report, MPXV clade I from the Centre and South regions grouped reliably with reference counterparts previously reported from countries in Central Africa, and clade II sequences from the Northwest and Southwest regions grouped consistently with strains from West Africa (Figure 4). Clade II strains from Cameroon clustered reliably within subclade IIb with 83% bootstrap support (Figure 4). Altogether, genotypic and phylogenetic analysis confirmed the concurrent circulation of both MPXV clades I and II in Cameroon with a striking geographic segregation.

Discussion

We examined the clinical, epidemiologic, and molecular patterns of MPXV infection in Cameroon over a 44-year period (1979–2022) as part of mpox surveillance in the country. During 1979–2022, a total of 137 persons were suspected of having mpox, and 32 were confirmed to be MPXV infected. Three persons died (CFR 2.2%) and death was associated with MPXV clade II. That CRF is much lower than those reported in previous studies of MPXV clade I that showed CFRs of 7%–10% (*13*,*43*). Overall, CFRs are lower among patients infected with clade II, including in the 2022 global outbreak settings (*4*,*25*). We were not able to collect information on potential underlying conditions of case-patients to determine whether immunocompromising conditions contributed to death, which would have worsened the clinical disease manifestations, as highlighted by others (*44*). In addition, fatal cases associated with clade I potentially escaped the national surveillance system in Cameroon, which is new and still being improved.

We found that both primary zoonotic and secondary human-to-human MPXV transmission occurs in Cameroon, including nosocomial transmission affecting health workers. Our results are consistent with reports describing secondary transmission chains, including intrafamilial transmission and occupational transmission through trade, transportation, hunting, and healthcare in endemic countries (*24*,*43*,*45*,*46*). This study highlights a common MPXV acquisition pathway in endemic countries, interspecies transmission, and wild animals are presumed reservoirs of the virus (*31*,*32*,*47*). Distinguishing between primary and secondary transmission is difficult because both could occur. Additional data and further investigations are required to clearly understand the underlying drivers of MPXV transmission in Cameroon.

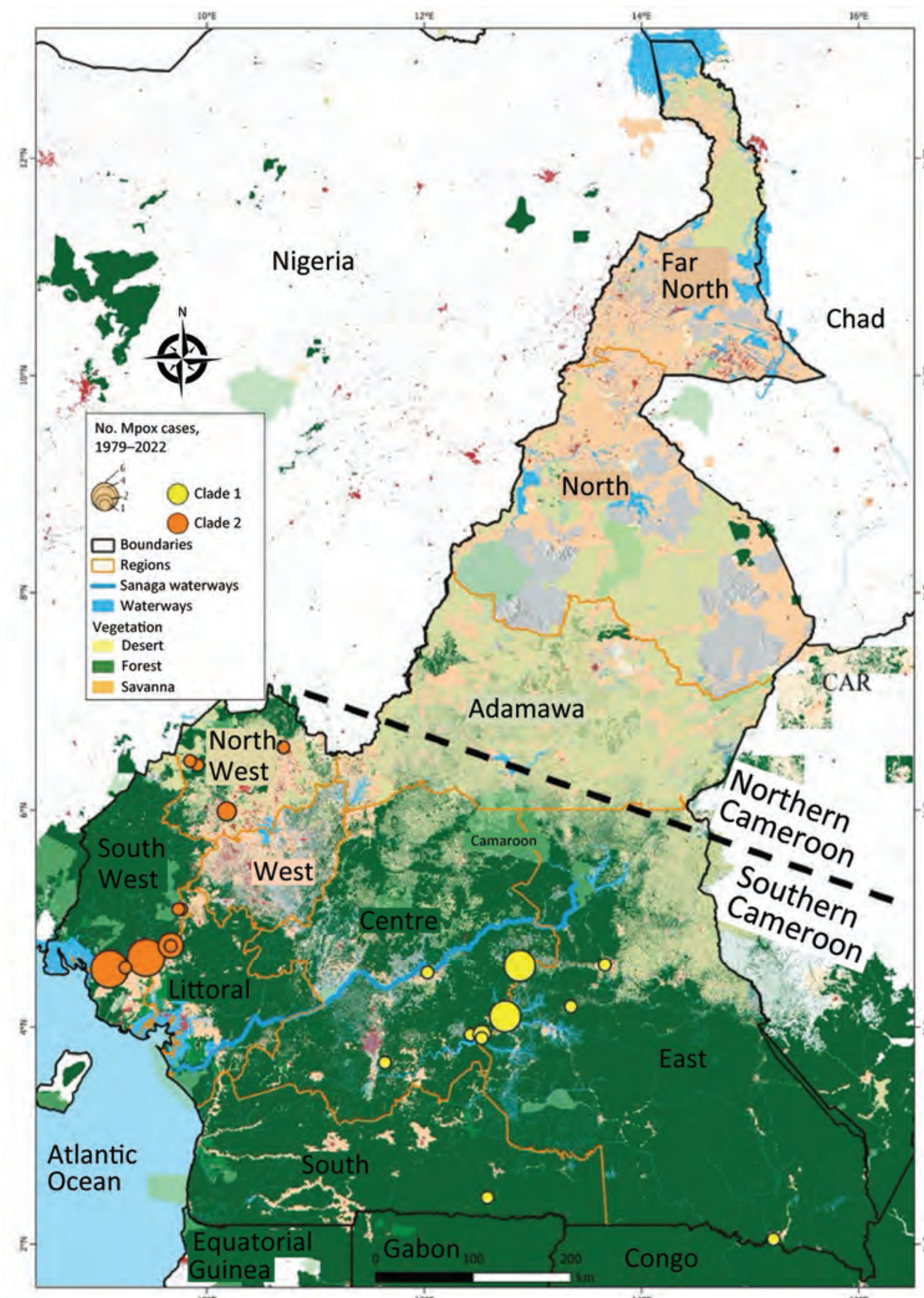

Figure 3. Geographic distribution of confirmed mpox cases and clades in a study of concurrent clade I and clade II monkeypox virus circulation, Cameroon, 1979–2022. A total of 137 suspected mpox cases were reported in the framework of the mpox surveillance system, among which 37 were PCR-confirmed for monkeypox virus infection. Clade I (12 cases) and clade II (18 cases) viral strains were identified circulating in the country. We noted a clear geographic segregation between the Centre, South, and East regions where only clade I (yellow dots) was reported, and the Northwest, and Southwest regions where only clade II (orange dots) was found. The size of each dot is proportional to the number of confirmed cases on the map. The map was designed by using Quantum GIS version 3.30.1 (QGIS, https://qgis.org). CAR, Central African Republic.

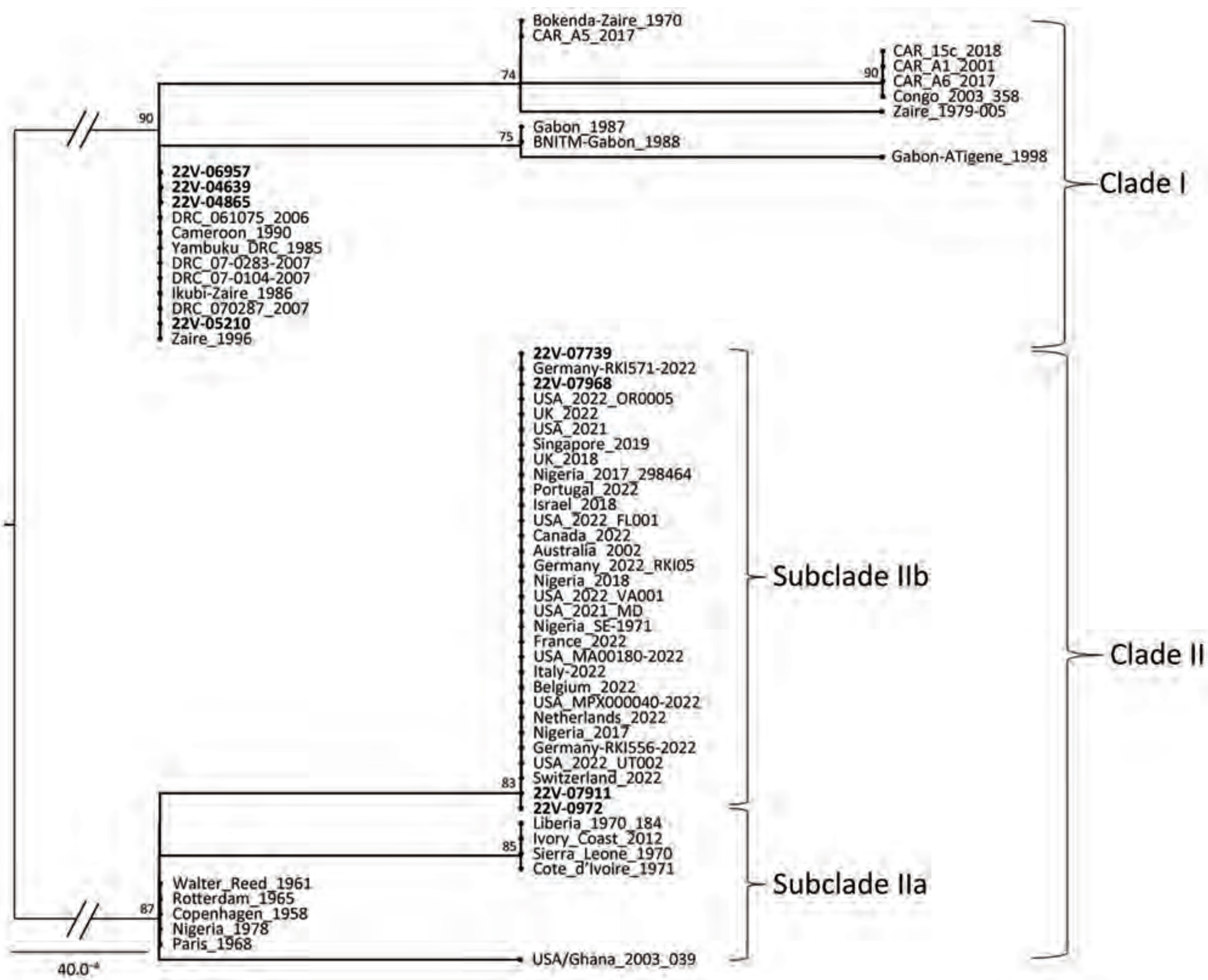

Figure 4. Maximum-likelihood phylogenetic tree of sequences in a study of concurrent clade I and clade II monkeypox virus circulation, Cameroon, 1979–2022. The tree is based on the Hasegawa-Kishino-Yano model inferred from a 942-bp fragment of the *ATI* gene, including 8 virus sequences from Cameroon generated in this work (bold text) and 55 reference sequences from GenBank. The tree with the highest log likelihood (−1,340.35) is shown. To test the robustness of the tree topology, 1,000 bootstrap replicates were performed. For a better display of the tree, the size of the 2 main midpoint rooted branches (represented in gray) that support the differentiation of the 2 monkeypox virus clades have been divided by half. Mpox strains from Cameroon are closely related to clades I and II, especially clade IIb for which a highlighted link to the ongoing global mpox epidemic is noted. Scale bar indicates number of substitutions per site. CAR, Central African Republic; DRC, Democratic Republic of the Congo; USA, United States.

A limitation of this study is our inability to perform more precise analyses to determine the characteristics independently describing the mpox epidemiology in Cameroon. Because the current surveillance system is still handwritten and forms are often incompletely filled, data are missing, as is common in paper-based data collection systems (*48*).

Since 1979, MPXV infections in Cameroon have occurred in 6 of the 10 administrative divisions of the country: Centre, South, East, Littoral, Northwest, and Southwest. All those administrative divisions are in the southern part of the country, which is a forested area encompassed by the lower montane forest of Guinea and the tropical rainforest of the Congo Basin, a favorable ecosystem for potential wildlife hosts. In contrast, northern Cameroon, a dry Sahelian and savannah zone, seems unlikely to be conducive to MPXV transmission because no cases have been confirmed in this region. That ecosystem is probably not suitable for MPXV reservoirs due to the dry environment. In most endemic countries, including Sierra Leone, Nigeria, Liberia, Central African Republic, and the Democratic Republic of the Congo, mpox cases mainly have been reported from forested areas (*24*,*25*,*46*). Most MPXV-confirmed cases in our study originated from the Centre (34 [38%])

and Southwest (31 [25%]) regions, which are the 2 most affected areas in the country. The Northwest region was the third (18 [75%] cases) most affected region. The Northwest and Southwest regions have been most seriously affected by civil unrest since 2017. That civil unrest has increased the number of IDPs in the country, and IDPs often move to different regions and neighboring countries. Furthermore, that situation has greatly increased human contact with wildlife as IDPs seek refuge in makeshift camps in the forest. By living in overlapping natural habitats of wild animals and potential MPXV reservoirs, populations of the Southwest and Northwest regions are under increased threat of zoonotic MPXV acquisition. Indeed, in Africa, civil unrest often leads to increases in mpox cases, and risk for any zoonotic disease is common (*4*,*49*). In several endemic countries, mpox outbreaks in the context of armed conflicts or massive population movements are a typical epidemiologic feature, and those conditions are usually associated with inefficient disease surveillance and control (*4*,*49*).

Genotypic and phylogenetic analyses revealed that both clade I and clade II are concurrently circulating in Cameroon and that a clear geographic segregation appears between the 2 clades. Circulation of both MPXV clades in Cameroon was previously reported in 2 published MPXV sequences from Cameroon (*6*,*29*). However, this study builds on those findings and provides more samples to further confirm that clades I and II concurrently circulate in a single country, a unique feature in MPXV epidemiology.

The geographic segregation of the clades is more perceptible in clade II case 21V-04877 in the Centre region. An epidemiologic investigation revealed that the case-patient was an IDP originating from the Northwest region, where MPXV clade II is endemic. The geographic segregation observed between MPXV strains circulating in Cameroon can be attributed to the natural barriers that potential animal reservoirs might not be able to cross between the Centre, East, and South regions, covered by the Congo Basin tropical forest, and the Northwest and Southwest regions, covered by lower montane moist forest of Guinea (*38*,*40*). Indeed, the Sanaga River, which is the largest river in the country, and the Cameroon highlands region sharply separate the 2 geographic areas into tropical moist forest ecoregions. The Cross-Sanaga-Bioko coastal forests lie to the north between the Sanaga River and the Cross River of Nigeria, and the Atlantic Equatorial coastal forests extends south of the river through southwestern Cameroon and other neighboring countries of central Africa (*38*,*39*). Alternatively, the 2 ecologic environments potentially host different reservoirs. Several studies aimed to identify presumed MPXV reservoirs (*31*,*33*,*47*), but none have emphasized the potential of 2 distinct reservoirs that could be specific to a given ecosystem. Furthermore, MPXV circulation in humans in Cameroon after decades of absence might have resulted from movements of human populations, reservoir hosts, or both from endemic reservoirs in neighboring countries as armed conflicts intensified cross-border movements since 2017. That hypothesis is supported by the clustering of newly sequenced MPXV strains with counterparts originating from neighboring countries that have no physical barrier with the eastern and western parts of Cameroon but have long terrestrial borders.

In summary, this study provides detailed insight into the mpox epidemic in Cameroon during a 44-year period. The epidemiology of mpox in Cameroon involves both primary and secondary transmission. Segregated clade I and II virus strains concurrently circulate, suggesting potential existence of distinct viral reservoirs and cross-border circulation of MPXV. This study can inform the design, optimization, and evaluation of public health interventions for monitoring and controlling mpox in Cameroon and other countries in Africa with similar epidemiologic settings.

Acknowledgments

We thank Africa Centres for Disease Control and Prevention for mpox diagnostic reagents provided to the surveillance system. We thank the patients or their legal guardians who agreed to be enrolled in this study. We thank all the personnel who identified and collected samples from suspected cases included in this study. We thank Huguette Simo for technical review of the manuscript, Landry Messanga for inference of the raw phylogenetic tree, and Hornela Ossombo for QGIS mapping.

This work was supported by the Centre Pasteur of Cameroon.

About the Author

Dr. Djuicy is a research scientist working at the virology department at the Centre Pasteur du Cameroon in Yaoundé, on zoonosis and emerging diseases including viral hemorrhagic fevers. Her research interests focus on developing research axes for emerging and reemerging neglected and poverty-related viral diseases, including mpox, Ebola, Lassa Fever, and Marburg virus.

References

1. Marennikova SS, Moyer RW. Classification of poxviruses and brief characterization of the genus *Orthopoxvirus*. In: Shchelkunov SN, Marennikova SS, Moyer RW, editors. Orthopoxviruses pathogenic for humans. Boston: Springer; 2005. p. 11–8. https://doi.org/10.1007/0-387-25306-8_2
2. von Magnus P, Andersen EK, Petersen KB, Birch-Andersen A. A pox-like disease in cynomolgus monkeys. Acta Pathol Microbiol Scand. 1959;46:156–76. https://doi.org/10.1111/j.1699-0463.1959.tb00328.x
3. Ladnyj ID, Ziegler P, Kima E. A human infection caused by monkeypox virus in Basankusu Territory, Democratic Republic of the Congo. Bull World Health Organ. 1972;46:593–7.
4. Gessain A, Nakoune E, Yazdanpanah Y. Monkeypox. N Engl J Med. 2022;387:1783–93. https://doi.org/10.1056/NEJMra2208860
5. Faye O, Pratt CB, Faye M, Fall G, Chitty JA, Diagne MM, et al. Genomic characterisation of human monkeypox virus in Nigeria. Lancet Infect Dis. 2018;18:246. https://doi.org/10.1016/S1473-3099(18)30043-4
6. Nakazawa Y, Mauldin MR, Emerson GL, Reynolds MG, Lash RR, Gao J, et al. A phylogeographic investigation of African monkeypox. Viruses. 2015;7:2168–84. https://doi.org/10.3390/v7042168
7. McCollum AM, Damon IK. Human monkeypox. Clin Infect Dis. 2014;58:260–7. https://doi.org/10.1093/cid/cit703
8. Rimoin AW, Mulembakani PM, Johnston SC, Lloyd Smith JO, Kisalu NK, Kinkela TL, et al. Major increase in human monkeypox incidence 30 years after smallpox vaccination campaigns cease in the Democratic Republic of Congo. Proc Natl Acad Sci U S A. 2010;107:16262–7. https://doi.org/10.1073/pnas.1005769107
9. Rao AK, Petersen BW, Whitehill F, Razeq JH, Isaacs SN, Merchlinsky MJ, et al. Use of JYNNEOS (smallpox and monkeypox vaccine, live, nonreplicating) for preexposure vaccination of persons at risk for occupational exposure to orthopoxviruses: recommendations of the Advisory Committee on Immunization Practices—United States, 2022. MMWR Morb Mortal Wkly Rep. 2022;71:734–42. https://doi.org/10.15585/mmwr.mm7122e1
10. Eto A, Saito T, Yokote H, Kurane I, Kanatani Y. Recent advances in the study of live attenuated cell-cultured smallpox vaccine LC16m8. Vaccine. 2015;33:6106–11. https://doi.org/10.1016/j.vaccine.2015.07.111
11. Reynolds MG, Damon IK. Outbreaks of human monkeypox after cessation of smallpox vaccination. Trends Microbiol. 2012;20:80–7. https://doi.org/10.1016/j.tim.2011.12.001
12. Simpson K, Heymann D, Brown CS, Edmunds WJ, Elsgaard J, Fine P, et al. Human monkeypox—after 40 years, an unintended consequence of smallpox eradication. Vaccine. 2020;38:5077–81. https://doi.org/10.1016/j.vaccine.2020.04.062
13. Besombes C, Mbrenga F, Schaeffer L, Malaka C, Gonofio E, Landier J, et al. National monkeypox surveillance, Central African Republic, 2001–2021. Emerg Infect Dis. 2022;28:2435–45. https://doi.org/10.3201/eid2812.220897
14. Africa Centres for Disease Control and Prevention. Outbreak brief 24: mpox in Africa Union member states [cited 2023 Nov 23]. https://africacdc.org/disease-outbreak/outbreak-brief-24-mpox-in-africa-union-member-states
15. Erez N, Achdout H, Milrot E, Schwartz Y, Wiener-Well Y, Paran N, et al. Diagnosis of imported monkeypox, Israel, 2018. Emerg Infect Dis. 2019;25:980–3. https://doi.org/10.3201/eid2505.190076
16. Ng OT, Lee V, Marimuthu K, Vasoo S, Chan G, Lin RTP, et al. A case of imported monkeypox in Singapore. Lancet Infect Dis. 2019;19:1166. https://doi.org/10.1016/S1473-3099(19)30537-7
17. Vaughan A, Aarons E, Astbury J, Brooks T, Chand M, Flegg P, et al. Human-to-human transmission of monkeypox virus, United Kingdom, October 2018. Emerg Infect Dis. 2020;26:782–5. https://doi.org/10.3201/eid2604.191164
18. Vaughan A, Aarons E, Astbury J, Balasegaram S, Beadsworth M, Beck CR, et al. Two cases of monkeypox imported to the United Kingdom, September 2018. Euro Surveill. 2018;23:1800509. https://doi.org/10.2807/1560-7917.ES.2018.23.38.1800509
19. Yong SEF, Ng OT, Ho ZJM, Mak TM, Marimuthu K, Vasoo S, et al. Imported monkeypox, Singapore. Emerg Infect Dis. 2020;26:1826–30. https://doi.org/10.3201/eid2608.191387
20. Reed KD, Melski JW, Graham MB, Regnery RL, Sotir MJ, Wegner MV, et al. The detection of monkeypox in humans in the Western Hemisphere. N Engl J Med. 2004;350:342–50. https://doi.org/10.1056/NEJMoa032299
21. Centers for Disease Control and Prevention. 2022–2023 Mpox outbreak global map [cited 2023 May 9]. https://www.cdc.gov/poxvirus/mpox/response/2022/world-map.html
22. Kaler J, Hussain A, Flores G, Kheiri S, Desrosiers D. Monkeypox: a comprehensive review of transmission, pathogenesis, and manifestation. Cureus. 2022;14:e26531. https://doi.org/10.7759/cureus.26531
23. Quiner CA, Moses C, Monroe BP, Nakazawa Y, Doty JB, Hughes CM, et al. Presumptive risk factors for monkeypox in rural communities in the Democratic Republic of the Congo. PLoS One. 2017;12:e0168664. https://doi.org/10.1371/journal.pone.0168664
24. Nakoune E, Lampaert E, Ndjapou SG, Janssens C, Zuniga I, Van Herp M, et al. A nosocomial outbreak of human monkeypox in the Central African Republic. Open Forum Infect Dis. 2017;4:ofx168. https://doi.org/10.1093/ofid/ofx168
25. Yinka-Ogunleye A, Aruna O, Dalhat M, Ogoina D, McCollum A, Disu Y, et al.; CDC Monkeypox Outbreak Team. Outbreak of human monkeypox in Nigeria in 2017–18: a clinical and epidemiological report. Lancet Infect Dis. 2019;19:872–9. https://doi.org/10.1016/S1473-3099(19)30294-4
26. Likos AM, Sammons SA, Olson VA, Frace AM, Li Y, Olsen-Rasmussen M, et al. A tale of two clades: monkeypox viruses. J Gen Virol. 2005;86:2661–72. https://doi.org/10.1099/vir.0.81215-0
27. Happi C, Adetifa I, Mbala P, Njouom R, Nakoune E, Happi A, et al. Urgent need for a non-discriminatory and non-stigmatizing nomenclature for monkeypox virus. PLoS Biol. 2022;20:e3001769. https://doi.org/10.1371/journal.pbio.3001769
28. Isidro J, Borges V, Pinto M, Sobral D, Santos JD, Nunes A, et al. Phylogenomic characterization and signs of microevolution in the 2022 multi-country outbreak of monkeypox virus. Nat Med. 2022;28:1569–72. https://doi.org/10.1038/s41591-022-01907-y
29. Sadeuh-Mba SA, Yonga MG, Els M, Batejat C, Eyangoh S, Caro V, et al. Monkeypox virus phylogenetic similarities between a human case detected in Cameroon in 2018 and the 2017–2018 outbreak in Nigeria. Infect Genet Evol. 2019;69:8–11. https://doi.org/10.1016/j.meegid.2019.01.006
30. Berthet N, Descorps-Declère S, Besombes C, Curaudeau M, Nkili Meyong AA, Selekon B, et al. Genomic history of human monkey pox infections in the Central African

Republic between 2001 and 2018. Sci Rep. 2021;11:13085. https://doi.org/10.1038/s41598-021-92315-8
31. Khodakevich L, Jezek Z, Kinzanzka K. Isolation of monkeypox virus from wild squirrel infected in nature. Lancet. 1986;327:98–9. https://doi.org/10.1016/S0140-6736(86)90748-8
32. Radonić A, Metzger S, Dabrowski PW, Couacy-Hymann E, Schuenadel L, Kurth A, et al. Fatal monkeypox in wild-living sooty mangabey, Côte d'Ivoire, 2012. Emerg Infect Dis. 2014;20:1009–11. https://doi.org/10.3201/eid2006.131329
33. Curaudeau M, Besombes C, Nakouné E, Fontanet A, Gessain A, Hassanin A. Identifying the most probable mammal reservoir hosts for monkeypox virus based on ecological niche comparisons. Viruses. 2023;15:727. https://doi.org/10.3390/v15030727
34. Tchokoteu PF, Kago I, Tetanye E, Ndoumbe P, Pignon D, Mbede J. Variola or a severe case of varicella? A case of human variola due to monkeypox virus in a child from the Cameroon [in French]. Ann Soc Belg Med Trop. 1991;71:123–8.
35. Eozenou P. Retrospective investigation into a case of monkeypox in the United Republic of Cameroon [in French]. Bull OCEAC. 1980;2:23–6.
36. Heymann D. Initial report of an Ebola-Monkeypox investigation in Moloundou (Cameroon, February 1980) [in French]. Bull OCEAC. 1980;7:58–60.
37. Public Health Emergency Operations Coordination Center, Cameroon. Monkeypox [in French] [cited 2023 May 9]. https://www.ccousp.cm/urgences-sanitaires/Mpox/situation-Mpox-cameroun
38. Molua EL, Lambi CM. Climate, hydrology and water resources in Cameroon. Pretoria: The Centre for Environmental Economics and Policy in Africa (CEEPA), University of Pretoria South Africa; 2006.
39. Zébazé Togouet SH, Nyamsi Tchatcho N, Tharme RE, Piscart C. The Sanaga River, an example of biophysical and socio-cultural integration in Cameroon, Central Africa. In: Wantzen KM, editor. River culture: life as a dance to the rhythm of the waters. Paris: United Nations Educational, Scientific and Cultural Organization; 2023. https://doi.org/10.54677/HHMI3947
40. One Earth. Afrotropics [cited 2023 May 9]. https://www.oneearth.org/realms/afrotropics
41. Li Y, Zhao H, Wilkins K, Hughes C, Damon IK. Real-time PCR assays for the specific detection of monkeypox virus West African and Congo Basin strain DNA. J Virol Methods. 2010;169:223–7. https://doi.org/10.1016/j.jviromet.2010.07.012
42. Meyer H, Ropp SL, Esposito JJ. Gene for A-type inclusion body protein is useful for a polymerase chain reaction assay to differentiate orthopoxviruses. J Virol Methods. 1997;64:217–21. https://doi.org/10.1016/S0166-0934(96)02155-6
43. Nolen LD, Osadebe L, Katomba J, Likofata J, Mukadi D, Monroe B, et al. Extended human-to-human transmission during a monkeypox outbreak in the Democratic Republic of the Congo. Emerg Infect Dis. 2016;22:1014–21. https://doi.org/10.3201/eid2206.150579
44. Ogoina D, Iroezindu M, James HI, Oladokun R, Yinka-Ogunleye A, Wakama P, et al. Clinical course and outcome of human monkeypox in Nigeria. Clin Infect Dis. 2020;71:e210–4. https://doi.org/10.1093/cid/ciaa143
45. Larway LZ, Amo-Addae M, Bulage L, Adewuyi P, Shannon F, Wilson W, et al. An outbreak of monkeypox in Doedain District, Rivercess County, Liberia, June, 2017. J Interv Epidemiol Public Heal. 2021;4:8. https://doi.org/10.37432/jieph.2021.4.2.35
46. Besombes C, Gonofio E, Konamna X, Selekon B, Gessain A, Berthet N, et al. Intrafamily transmission of monkeypox virus, Central African Republic, 2018. Emerg Infect Dis. 2019;25:1602–4. https://doi.org/10.3201/eid2508.190112
47. Reynolds MG, Doty JB, McCollum AM, Olson VA, Nakazawa Y. Monkeypox re-emergence in Africa: a call to expand the concept and practice of One Health. Expert Rev Anti Infect Ther. 2019;17:129–39. https://doi.org/10.1080/14787210.2019.1567330
48. Tchatchueng-Mbougua JB, Messanga Essengue LL, Septoh Yuya FJ, Kamtchogom V, Hamadou A, Sadeuh-Mbah SA, et al. Improving the management and security of COVID 19 diagnostic test data with a digital platform in resource-limited settings: The case of PlaCARD in Cameroon. PLOS Digit Health. 2022;1:e0000113. https://doi.org/10.1371/journal.pdig.0000113
49. McPake B, Witter S, Ssali S, Wurie H, Namakula J, Ssengooba F. Ebola in the context of conflict affected states and health systems: case studies of Northern Uganda and Sierra Leone. Confl Health. 2015;9:23. https://doi.org/10.1186/s13031-015-0052-7

Address for correspondence: Richard Njouom, Centre Pasteur du Cameroun, PO Box 1274, Yaounde, Cameroon; email: njouom@pasteur-yaounde.org

Recent Changes in Patterns of Mammal Infection with Highly Pathogenic Avian Influenza A(H5N1) Virus Worldwide

Pablo I. Plaza, Víctor Gamarra-Toledo, Juan Rodríguez Euguí, Sergio A. Lambertucci

We reviewed information about mammals naturally infected by highly pathogenic avian influenza A virus subtype H5N1 during 2 periods: the current panzootic (2020–2023) and previous waves of infection (2003–2019). In the current panzootic, 26 countries have reported ≥48 mammal species infected by H5N1 virus; in some cases, the virus has affected thousands of individual animals. The geographic area and the number of species affected by the current event are considerably larger than in previous waves of infection. The most plausible source of mammal infection in both periods appears to be close contact with infected birds, including their ingestion. Some studies, especially in the current panzootic, suggest that mammal-to-mammal transmission might be responsible for some infections; some mutations found could help this avian pathogen replicate in mammals. H5N1 virus may be changing and adapting to infect mammals. Continuous surveillance is essential to mitigate the risk for a global pandemic.

Since last century, highly pathogenic avian influenza (HPAI) viruses have caused diverse waves of infection (*1*). However, the ongoing panzootic event (2020–2023) caused by HPAI A(H5N1) virus could become one of the most important in terms of economic losses, geographic areas affected, and numbers of species and individual animals infected (*1*–*4*). This pathogen appears to be emerging in several regions of the world (e.g., South America); it has caused death in domestic and wild birds but also in mammals (*2*,*5*,*6*). This trend is of great concern because it may indicate a change in the dynamics of this pathogen (i.e., an increase in their range of hosts and the severity of the disease) (*3*).

H5N1 has affected several mammal species since 2003 (*6*,*7*), thus raising concern because H5N1 mammalian adaptation could represent a risk not only for diverse wild mammals but also for human health (*8*–*10*). Unfortunately, information about this topic, especially related to the current panzootic (2020–2023), is disperse and available often only in gray literature (e.g., databases and official government websites). This fact complicates access and evaluation for many stakeholders working on the front lines (e.g., wildlife managers, conservationists, and public health authorities at regional and local levels).

For this article, we compiled and analyzed information from scientific literature about mammal species, including humans, naturally affected by the current panzootic event and compared those findings with the outcomes of previous waves of H5N1 infection. We focus particularly on the species infected, their habitat, phylogeny, and trophic level, and the sources of infection, virus mutations, clinical signs, and necropsy findings associated with this virus. We also address potential risks for biodiversity and human health.

Methods

We compiled scientific information on mammals infected by H5N1 virus through October 2023. We considered only scientific information on mammal species infected naturally (i.e., experimental studies were not included). We performed 2 systematic searches in Scopus and Google Scholar, first using the terms "H5N1 AND mammal"; this search was divided into 2 periods (1996–2019 and 2020–2023) (Appendix Figure

Author affiliations: Conservation Biology Research Group, Ecotone Laboratory, Institute of Biodiversity and Environmental Research (INIBIOMA), National University of Comahue–National Scientific and Technical Research Council, San Carlos de Bariloche, Argentina (P.I. Plaza, V. Gamarra-Toledo, S.A. Lambertucci); Natural History Museum, National University of San Agustín de Arequipa, Arequipa, Peru (V. Gamarra-Toledo); Ministry of Health of Tierra del Fuego, Ushuaia, Argentina (J. Rodríguez Euguí)

DOI: https://doi.org/10.3201/eid3003.231098

1, 2, https://wwwnc.cdc.gov/EID/article/30/3/23-1098-App1.pdf). We then performed an additional search with no time restriction using the following key terms: “H5N1 OR HPAI OR Highly Pathogenic Avian Influenza AND mammal OR unusual host.” This additional search contributed no new articles on the study topic (Appendix Figure 3). We also adopted a snowball approach, examining all the references in the articles we found in our searches. We included review articles only if they contributed new information about mammal species infected naturally with H5N1; we excluded articles based on serologic surveys because of the difficulty in determining when infection occurred, which can introduce uncertainty into the diagnosis (*11*).

To obtain additional information on the current panzootic event, we also searched the following official databases: World Organisation for Animal Health (*6*), the US Department of Agriculture’s Animal and Plant Health Service (*12*), and the United Kingdom’s Animal and Plant Health Agency (*13*). To obtain information about humans affected by this pathogen we used information provided by the World Health Organization (*14*). We constructed a map with the countries with reports of mammal infections (Figure 1) and the phylogeny of mammal species affected by H5N1 (Figures 2, 3) by using iTOL version 5, following Letunic and Bork (*15*), from DNA sequence data available in Upham et al. (*16*). We retrieved the conservation statuses of infected mammals from International Union for Conservation of Nature Red List of Threatened Species (*17*) and information on their diets from that database and MammalBase (*18*).

Results and Discussion

Scientific Information Available

We found 59 scientific articles on mammals infected naturally by H5N1 virus, 23 from previous waves of infection (up to 2019) and 36 from the current panzootic event (Appendix Figure 1, 2). The articles reporting mammals infected naturally in previous waves were published during 2004–2018, whereas those addressing the current panzootic were published during 2021–2023. The current panzootic has thus generated more articles in 3 years than all the previous waves of infection (published over a 15-year period). This fact suggests increased general interest in emerging pathogens affecting biodiversity and mammals (wild and farmed) and also that the current panzootic event is causing greater concern and having a greater effect than previous ones (considering the geographic regions and mammal species affected) (*4*).

Geographic Localization of Information and Mammal Species Affected

During previous waves of infection, 10 countries reported mammals (not including humans) naturally infected by H5N1 (5 countries in Asia, 3 in Europe, and 2 in Africa) (Figure 1, panel A; Appendix Table). In the current event, 26 countries have reported information on mammals (not including humans) infected by this virus; most information is from Europe (17 countries), followed by South America (5 countries), North America (2 countries), and Asia (2 countries) (Figure 1, panel B; Appendix Table). To the best of our knowledge, for the current outbreak, no information is available on mammals from other parts of the world, which can probably be explained by a lack of testing or reporting of cases. Our review suggests that H5N1 virus is expanding its geographic range to new continents such as North and South America (Figure 1). This fact is of concern because when an emerging pathogen reaches naive populations, the consequences for biodiversity can be catastrophic, especially for threatened species (*19*).

We found that previous waves of infection affected several mammals around the world (*7*,*20*); for example, tigers (*Panthera tigris*), leopards (*Panthera pardus*), domestic cats (*Felis catus*), domestic dogs (*Canis lupus familiaris*), Owston’s palm civet (*Chrotogale owstoni*), stone martens (*Martes foina*), plateau pikas (*Ochotona curzoniae*), minks (*Neovison vison*), and raccoon dogs (*Nyctereutes procyonoides*) (Appendix Table). All the mammal species affected were terrestrial or semiaquatic species (Figure 2, panel A). Most mammals infected during previous waves (75%; n = 9) belong to the order Carnivora, whereas the remainder correspond to the Lagomorpha, Artiodactyla, and Perissodactyla orders (Figure 2, panel B). Infected mammal species included top predators (e.g., tigers and leopards) and some mesopredators (e.g., minks) (Appendix Table). Most species infected in previous waves were carnivores (n = 6) and omnivores (n = 4), followed by herbivores (n = 2) (Figure 2, panel C; Appendix Table).

So far, in the current panzootic, $\geq$48 mammal species from disparate regions of the world have been reported as naturally infected by H5N1 (Appendix Table). Most of those species (n = 35) are terrestrial or semiaquatic mammals (Figure 3, panel A; Appendix Table), but 13 species of marine mammals also were affected, resulting in massive deaths (up to thousands of individual animals) in geographic regions such as Peru, Chile, and Argentina (Figure 3, panel A; Appendix Table). Of the total number of mammals infected, 81% (n = 39) belong to the order

Carnivora, and the remainder correspond to Didelphimorphia, Rodentia, and Cetartiodactyla (Figure 3, panel B). Infected mammal species include top predators (e.g., mountain lion [*Puma concolor*]) and several mesopredators (e.g., red fox [*Vulpes vulpes*]) (Appendix Table). Most mammal species infected are carnivores (n = 34), followed by omnivores (n = 13) and herbivores (n = 1); some of those species (n = 13) also are considered facultative scavengers (i.e., they include in their diet a considerable quantity of carrion; in our case to be a facultative scavenger carrion should be named in the diet) (Figure 3, panel C; Appendix Table).

The species infected in the 2 events show similarities. Most species belong to the order Carnivora and are top or mesopredators with a carnivorous diet; some species also are facultative scavengers. However, in the current panzootic event, the diverse marine mammals affected have suffered massive deaths (e.g., American sea lion [*Otaria flavescens*]) (Appendix Table). Marine mammals have been affected by other influenza viruses such as H10N7 (*21*), but the species

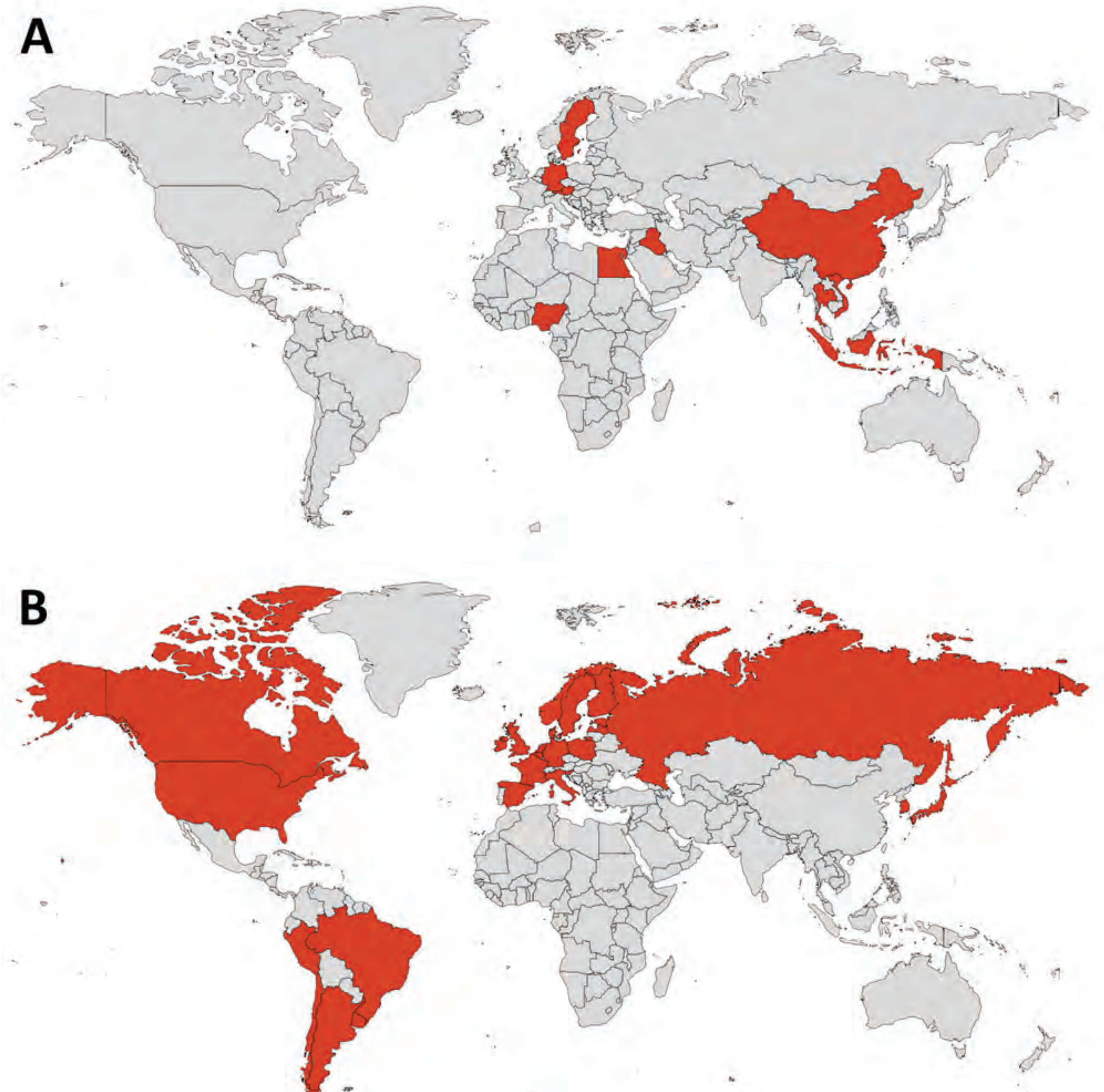

Figure 1. Geographic location of mammal species affected by highly pathogenic influenza virus A(H5N1) in previous waves of infection, 2003–2019 (A), and in the current panzootic, 2020–2023 (B).

affected and the number of dead individual animals attributable to the current event is of great concern (*22*,*23*); for example, the proportion of American sea lions that died in Peru represents 5% of their population there (*22*).

The current panzootic is ongoing, and the number of species being infected naturally is increasing (40 new mammal species have been reported as infected by this pathogen during the current panzootic), so the effect on mammal species may continue to worsen with time. This effect could just be attributable to the current high H5N1 infection rates throughout the world, which means the virus is reaching more areas and mammal species living in these places (i.e., high environmental circulation of this pathogen) (*8*). However, the dynamics of the virus may also be changing (*3*), in which case its infectivity in unusual species such as mammals is probably increasing (*8*). During the final review process of this article, 2 additional species were reported to be infected by this virus in the United States: the Abert's squirrel (*Sciurus aberti*) and the polar bear (*Ursus maritimus*) (newly infected species are not shown in figures or the Appendix Table) (*6*).

Source of Infection

Although the source of infection in mammals is often unknown, most scientific information available during previous and the current H5N1 event suggests that the most plausible source of infection is close contact with infected birds, including their ingestion, which may occur through predation of sick individual animals or scavenging on carcasses. For instance, in the year 2004, a total of 147 tigers and 2 leopards housed in zoos in Thailand became infected and died after consuming infected chicken carcasses (*24*,*25*). In China, this infection source was also associated with the death of a tiger in 2013 (*26*) and a lion in 2016 (*27*). In the current panzootic, the first case of H5N1 infection in minks in Spain was probably caused by contact with infected birds (perhaps gulls) (*9*). Ingestion of infected bird carcasses was probably the route of infection of red foxes in the Netherlands, Finland, and Japan during 2020–2022 (*28*–*31*), American sea lions in Peru in 2023 (*22*), diverse mesocarnivores in Canada during 2021–2022 (*32*) and otters (*Lutra lutra*) and a lynx (*Lynx lynx*) in Finland in 2021–2022 (*31*). Of concern, studies in infected tigers, farmed minks, and social species such as American sea lions, raise an alarm that mammal-to-mammal transmission may have occurred (*9*,*22*,*24*,*33*), but further research is needed to confirm this possibility.

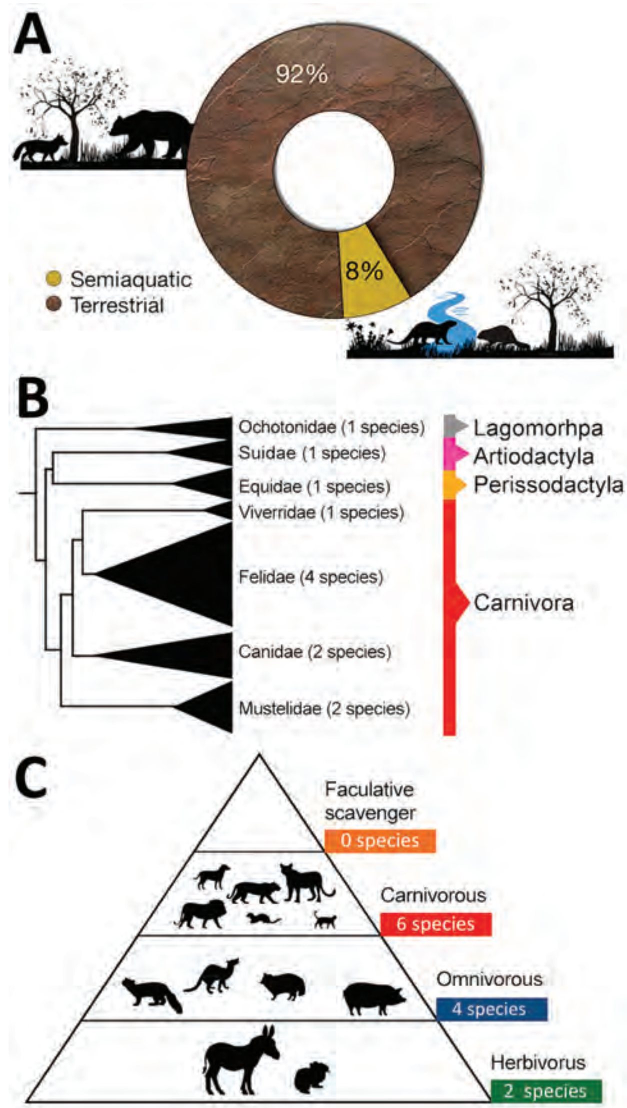

Figure 2. Characteristics of mammal species affected worldwide by highly pathogenic influenza virus A (H5N1) in previous waves of infection (2003–2019). A) Habitat of mammal species affected by H5N1. B) Phylogeny of mammal species affected (tree constructed using iTOL version 5 following Letunic and Bork [*15*], from DNA sequence data available in Upham et al. [*16*]). C) Trophic level (facultative scavenger, carnivore, omnivore, or herbivore) of mammalian species affected worldwide by H5N1.

If mammal-to-mammal transmission occurs during the current H5N1 panzootic, such transmission could imply that the virus mutated to enable virus replication in mammal tissues (*9*). Some researchers have reported mutations compatible with adaptation to mammal replication (*9*,*25*,*33*,*34*), which is concerning and requires attention. However, evaluating whether those mutations happen in wild birds before mammal infections or arise de novo in mammals after infection is important.

Mutations Found

Through sequencing of the H5N1 viruses infecting mammals, some relevant mutations such as E627K in polymerase basic protein 2 (PB2) (PB2-E627K) and D701N in polymerase basic protein 2 (PB2) (PB2-D701N) have been found in previous waves and in the current panzootic (Appendix Table). Those mutations are commonly associated with virulence and efficiency in the replication of this pathogen in mammals (*31*,*33*,*35*). For instance, during 2004–2005, in Thailand, the isolated H5N1 viruses that infected tigers, a domestic cat, a domestic dog, and a leopard contained the PB2-E627K mutation (*25*,*35*,*36*). In the current panzootic, red foxes from the Netherlands also showed the mammalian adaptation of PB2-E627K (*28*). In viruses collected from red foxes, an otter, and a lynx in Finland in 2021–2022, the PB2-E627K and PB2-D701N mutations were identified (the latter mutation was reported in 1 red fox and 1 lynx in Finland) (*31*). Similarly, in the current panzootic, red foxes, otters, and polecats (*Mustela putorius*) in the Netherlands, and red foxes in Canada, and the United States had the PB2-E627K mutation (*8*,*32*,*37*). The PB2-E627K and PB2-D701N mutations were also detected in harbor seals (*Phoca vitulina*) in the United States (*34*), and the latter mutation was found in South American sea lions in Peru (*33*), and in a red fox in Canada (*32*). In both previous and current events, other mutations meriting further research were also found in diverse mammal species, including terrestrial, semiaquatic, and marine mammals (Appendix Table).

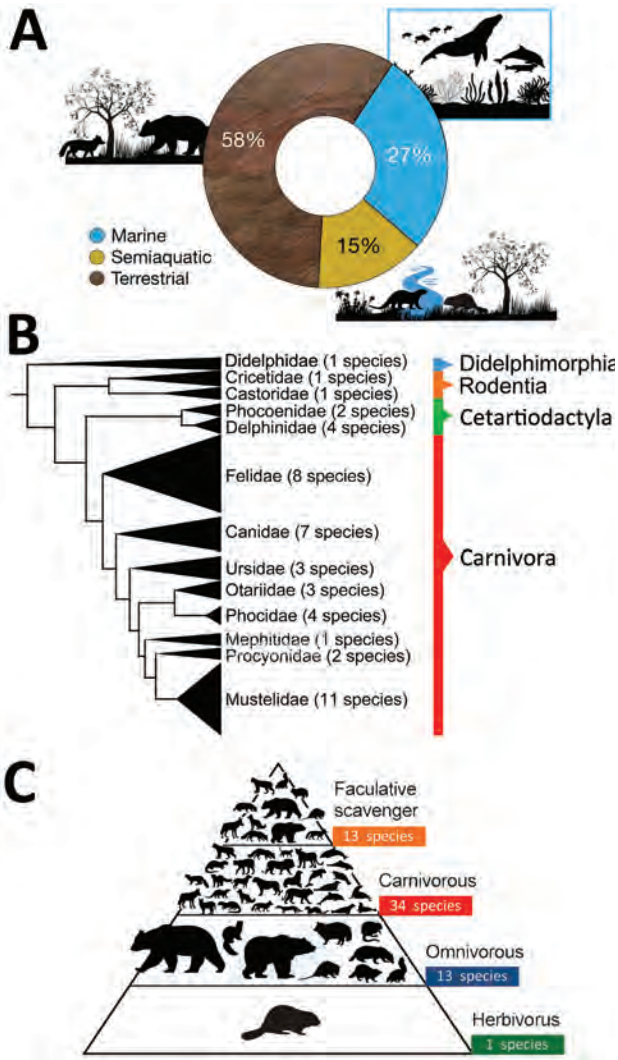

Figure 3. Characteristics of mammal species affected worldwide by highly pathogenic influenza virus A (H5N1) the current panzootic (2020–2023). A) Habitat of mammal species affected by H5N1. B) Phylogeny of mammal species affected (tree constructed using iTOL version 5 following Letunic and Bork [*15*], from DNA sequence data available in Upham et al. [*16*]). C) Trophic level (facultative scavenger, carnivore, omnivore, or herbivore) of mammal species affected worldwide by H5N1. Some of the omnivorous and carnivorous mammals included in the pyramid (n = 13) also consume carrion; thus, they are also considered to be facultative scavengers and are incorporated in the upper part of the pyramid.

Mutations that facilitate replication of the virus in mammal hosts (e.g., enhancing polymerase activity in mammal cells), such as PB2-E627K and PB2-D701N, could be of concern (*8*,*31*,*33*). Potential mutations must be continuously scrutinized to detect whether the H5N1 virus is adapting to mammal-to-mammal transmission. This approach is important for wildlife conservation because if such transmission occurs, the consequences for threatened mammal species could be severe (e.g., threatened South American sea lion deaths in Peru [*22*]). In addition, mutations must be monitored for changes that may favor transmission to and between humans, which would increase the risk for a pandemic.

Clinical Signs of H5N1 in Mammals

The most common clinical signs reported in infected mammals, both in previous waves and the current H5N1 panzootic, are neurologic and respiratory. For instance, in 2005, an infected Owston's civet in Vietnam showed loss of appetite and neurologic signs such as convulsions and paralysis; the same clinical signs were reported in a stone marten in Germany in 2006 (*38*,*39*). Similarly, hundreds of infected tigers in a zoo in Thailand showed respiratory and neurologic signs before they died (*24*). In the current panzootic event, infected minks from Spain manifested loss of appetite, hyper salivation, depression, bloody snout, and neurologic signs such as ataxia and tremors (*9*). American sea lions in Peru and harbor seals in the

United States showed respiratory signs (dyspnea and whitish secretions in nares) and neurologic signs (tremors and convulsions) (*22*,*34*). Red foxes, an otter, a polecat, and a badger (*Meles meles*) in the Netherlands had neurologic signs such as convulsions and head shaking (*8*,*30*). In Finland, an infected otter was also reported to have a set of neurologic signs (*31*). Finally, in the United States and Canada, several mammals manifested neurologic and respiratory signs (*32*,*37*). Those findings suggest that H5N1 virus has neurotropism in mammals, as reported in birds (*6*,*28*), causing severe disease and pathologic lesions (e.g., encephalitis); brain samples should be included in wildlife surveillance programs for reliable detection of the H5N1 virus in mammals (*8*).

Although neurologic and respiratory signs are commonly reported in mammals infected with H5N1, some species and individual animals show subclinical disease. For instance, infected pigs (*Sus scrofa domesticus*) from Indonesia, Nigeria, and China had no signs of influenza but tested positive for H5N1 (*40*–*42*). Similarly, in Austria, infected domestic cats display asymptomatic infections (*43*). Subclinical infections are concerning because they are not easily detected; infected individual animals may be transmitting the virus to other species and even humans, representing a risk to the ecosystem and human health (*40*,*41*).

Necropsy Findings

In previous waves of infection and the current H5N1 panzootic, the most frequently reported anatomopathologic lesions in infected mammals were pneumonia and encephalitis. Those kinds of lesions (e.g., congestion of brain, meningoencephalitis, hemorrhagic lungs, and pleural effusion) were reported in dead tigers in Thailand and China during 2004–2014 (*24*,*26*,*44*), in a lion in China in 2016 (*27*), and in cats and dogs infected naturally in Thailand in 2004 (*45*,*46*). In the current panzootic, for instance, red foxes from the Netherlands had collapsed lungs with a marbled red aspect; histopathologic analyses showed a subacute to chronic purulent granulomatous broncho-interstitial pneumonia and nonsuppurative encephalitis with perivascular cuffing (*28*). Red foxes, polecats, otters, and a badger in the Netherlands also showed nonsuppurative meningitis, encephalitis, or meningoencephalitis, all with differences in severity (*8*). American sea lions in Peru had congestive brains compatible with encephalitis (*22*). A porpoise (*Phocoena phocoena*) in Sweden manifested meningoencephalitis (*47*). Similar findings, meningoencephalitis and pneumonia, were also found in mammals in Finland, the United States, and Canada (*31*,*32*,*37*).

Those findings suggest that respiratory and neurologic lesions are the most common pathologies of necropsied mammals infected with H5N1 in both previous waves of infection and the current panzootic. The lesions largely explain the neurologic and respiratory signs observed in mammals affected by this virus. Complete necropsies of infected mammals may help determine whether those anatomopathologic findings are frequent and pathognomonic for this disease in every species and most individual animals, as preliminary results suggest.

Risks for Biodiversity

The current panzootic is affecting a larger number of species around the world than previous waves of H5N1 infection, and some are of conservation concern. Previous waves affected 2 endangered and 2 vulnerable species (Appendix Table). The current panzootic has so far affected 4 near threatened, 4 endangered, 3 vulnerable, and 1 critically endangered species (Appendix Table); this emerging pathogen may affect species of conservation concern, exacerbating their situation.

In general, most mortality events associated with the current panzootic appear to affect few individual animals and in only certain areas; thus far, large populations have not been affected in the way wild birds have been affected (*4*,*6*). However, this virus is suspected of producing massive deaths in some marine mammals; for example, >20,000 South American sea lions were reported to have died suddenly, and many individual animals tested positive for H5N1 (*6*,*22*,*23*). This fact raises concern as to the potential effect of this virus on the demography of some threatened mammal populations. This emerging pathogen represents a new species invading and impacting new environments and species and could therefore constitute a new threat for diverse species currently threatened by human action (e.g., land use change, contamination, and habitat loss) (*19*,*48*).

Potential Risks for Human Health

During 2003–2023, a total of 878 humans tested positive for the H5N1 virus, and 458 deaths were reported, indicating a lethality of ≈52% (*14*). During 2003–2019, most human cases came from Asia and Africa, particularly from China (n = 53), Egypt (n = 359), and Indonesia (n = 200). From 2020 through July 2023, human cases of H5N1 infection occurred in diverse countries, such as Laos (1 case), India (1 case), United Kingdom (4 cases), China (2 cases), the United States (1 case), Vietnam (1 case), Spain (2 cases), Ecuador (1 case), Chile (1 case), and Cambodia (2 cases) (*14*).

Those recent cases resulted in ≥3 deaths (*14*). Of note, this zoonotic virus has produced human cases in new geographic areas, such as South America.

The spillover to humans has been associated with close contact between humans and infected animals, particularly poultry; this kind of contact is relatively common in some geographic regions (even close contact between dead mammals and humans, as in Peru [*22*]). So far, no evidence indicates human-to-human transmission, and the risk for a pandemic event still seems low (*8*). However, one of the most severe influenza viruses to have affected humans (i.e., Spanish influenza [1918–1919]) developed from an avian influenza virus that adapted to humans (*49*), a fact that should be considered when assessing the spillover risk.

Mutations in the virus found in diverse mammal species, especially in the current panzootic, are of great concern. For instance, the T271A mutation reported in minks in Spain is also present in the H1N1 that produced a pandemic in 2009 (*9*). Similarly, the PB2-E627K mutation found in this virus in diverse geographic areas could indicate an adaptation for replication in mammals (*28*,*31*). Moreover, some infected species, such as minks, may act as a mixing vessel for interspecies transmission between birds, mammals, and humans (*9*). Mutations and infections with H5N1 in potential mixing-vessel species (e.g., minks and wild and domestic pigs) should be followed closely because of the potential risk to human health.

Final Considerations

Given the magnitude of the current H5N1 panzootic, continuous surveillance is necessary to identify any increase in risk to biodiversity and human health. It is therefore essential that all affected countries share all their available information (e.g., genomic data of the H5N1 virus, species, and number of individual animals affected). We urge that all findings be shared quickly. International collaboration must be intensified to obtain rapid results; some less-developed regions have technologic and logistic barriers that hinder the production and analysis of information on the impact of this virus, and they may need help. There is a need for strong collaborative work between countries and institutions in preparation for any spillover that may lead to a mammalian panzootic or human pandemic.

It is fundamental that we rethink the interface between humans, domestic animals, and wild animals to prevent the emergence of dangerous pathogens that affect biodiversity and human health (*48*). Governments must assume responsibility for protecting biodiversity and human health from diseases caused by human activities, particularly diseases originating from intensive production (*50*), such as this H5N1 avian influenza virus. If we hope to conserve biodiversity and protect human health, we must change the way we produce our food (poultry farming, in this specific case) and how we interact with and affect wildlife.

Financial support was provided by Consejo Nacional de Investigaciones Científicas y Técnicas, Agencia Nacional de Promoción Científica y Tecnológica (grant no. PICT-2021-TI-00039), Universidad Nacional del Comahue (project 04/B227, grant to S.A.L.), and Aves Argentinas (grant to P.P.).

About the Author

Dr. Plaza is a veterinarian and research associate at the Conservation Biology Research Group, Ecotone Laboratory, Institute of Biodiversity and Environmental Research (INIBIOMA), National University of Comahue–National Scientific and Technical Research Council, San Carlos de Bariloche, Argentina. His primary research interests include wildlife health and epidemiology, human–wildlife interactions, and animal conservation.

References

1. Shi J, Zeng X, Cui P, Yan C, Chen H. Alarming situation of emerging H5 and H7 avian influenza and effective control strategies. Emerg Microbes Infect. 2023;12:2155072. https://doi.org/10.1080/22221751.2022.2155072
2. Wille M, Barr IG. Resurgence of avian influenza virus. Science. 2022;376:459–60. https://doi.org/10.1126/science.abo1232
3. Harvey JA, Mullinax JM, Runge MC, Prosser DJ. The changing dynamics of highly pathogenic avian influenza H5N1: next steps for management and science in North America. Biol Conserv. 2023;282:110041. https://doi.org/10.1016/j.biocon.2023.110041
4. Adlhoch C, Fusaro A, Gonzales JL, Kuiken T, Mirinaviciute G, Niqueux É, et al.; European Food Safety Authority, European Centre for Disease Prevention and Control, European Union Reference Laboratory for Avian Influenza. Avian influenza overview March–April 2023. EFSA J. 2023;21:e08039.
5. Gamarra-Toledo V, Plaza PI, Angulo F, Gutiérrez R, García-Tello O, Saravia-Guevara P, et al. Highly pathogenic avian influenza (HPAI) strongly impacts wild birds in Peru. Biol Conserv. 2023;286:110272. https://doi.org/10.1016/j.biocon.2023.110272
6. World Organization for Animal Health. WAHIS: World Animal Health Information System. 2023 [cited 2023 Oct 30]. https://wahis.woah.org
7. Reperant LA, Rimmelzwaan GF, Kuiken T. Avian influenza viruses in mammals. Rev Sci Tech. 2009;28:137–59. https://doi.org/10.20506/rst.28.1.1876
8. Vreman S, Kik M, Germeraad E, Heutink R, Harders F, Spierenburg M, et al. Zoonotic mutation of highly pathogenic avian influenza H5N1 virus identified in the brain of multiple wild carnivore species. Pathogens. 2023;12:168. https://doi.org/10.3390/pathogens12020168

9. Agüero M, Monne I, Sánchez A, Zecchin B, Fusaro A, Ruano MJ, et al. Highly pathogenic avian influenza A(H5N1) virus infection in farmed minks, Spain, October 2022. Euro Surveill. 2023;28:2300001. https://doi.org/10.2807/1560-7917.ES.2023.28.3.2300001
10. Kupferschmidt K. Bird flu spread between mink is a 'warning bell'. Science. 2023;379:316–7. https://doi.org/10.1126/science.adg8342
11. Horimoto T, Maeda K, Murakami S, Kiso M, Iwatsuki-Horimoto K, Sashika M, et al. Highly pathogenic avian influenza virus infection in feral raccoons, Japan. Emerg Infect Dis. 2011;17:714–7. https://doi.org/10.3201/eid1704.101604
12. US Departament of Agriculture. 2022–2023 Detections of highly pathogenic avian influenza in mammals [cited 2023 Oct 30]. https://www.aphis.usda.gov/aphis/ourfocus/animalhealth/animal-disease-information/avian/avian-influenza/hpai-2022/2022-hpai-mammals
13. United Kingdom Animal and Plant Health Agency. Confirmed findings of influenza of avian origin in non-avian wildlife [cited 2023 Oct 30]. https://www.gov.uk/government/publications/bird-flu-avian-influenza-findings-in-non-avian-wildlife/confirmed-findings-of-i]nfluenza-of-avian-origin-in-non-avian-wildlife
14. World Health Organization. Cumulative number of confirmed human cases for avian influenza A(H5N1) reported to WHO, 2003–2023, 3 October 2023. 2023 [cited 2023 Oct 30]. https://www.who.int/publications/m/item/cumulative-number-of-confirmed-human-cases-for-avian-influenza-a(h5n1)-reported-to-who--2003-2023--3-october-2023
15. Letunic I, Bork P. Interactive Tree Of Life (iTOL) v5: an online tool for phylogenetic tree display and annotation. Nucleic Acids Res. 2021;49(W1):W293–6. https://doi.org/10.1093/nar/gkab301
16. Upham NS, Esselstyn JA, Jetz W. Inferring the mammal tree: species-level sets of phylogenies for questions in ecology, evolution, and conservation. PLoS Biol. 2019;17:e3000494. https://doi.org/10.1371/journal.pbio.3000494
17. IUCN. IUCN red list of threatened species. 2023 [cited 2023 Oct 30]. https://www.iucnredlist.org
18. MammalBase. Database of recent mammals [cited 2023 Oct 30]. https://www.mammalbase.net/mb
19. Dobson A, Foufopoulos J. Emerging infectious pathogens of wildlife. Philos Trans R Soc Lond B Biol Sci. 2001;356:1001–12. https://doi.org/10.1098/rstb.2001.0900
20. Root J, Shriner S. Avian influenza A virus associations in wild, terrestrial mammals: a review of potential synanthropic vectors to poultry facilities. Viruses. 2020;12:1352. https://doi.org/10.3390/v12121352
21. Bodewes R, Bestebroer TM, van der Vries E, Verhagen JH, Herfst S, Koopmans MP, et al. Avian influenza A(H10N7) virus–associated mass deaths among harbor seals. Emerg Infect Dis. 2015;21:720–2. https://doi.org/10.3201/eid2104.141675
22. Gamarra-Toledo V, Plaza P, Inga G, Gutiérrez R, Garcia-Tello O, Valdivia-Ramirez L, et al. Mass mortality of sea lions caused by highly pathogenic influenza virus (H5N1) in South America. Emerg Infect Dis. 2023;29:2553–6. https://doi.org/10.3201/eid2912.230192
23. OFFLU Ad-Hoc Group on HPAI H5 in Wildlife of South America and Antarctica. Southward expansion of high pathogenicity avian influenza H5 in wildlife in South America: estimated impact on wildlife populations, and risk of incursion into Antarctica. 2023 [cited 2023 Oct 30]. https://www.offlu.org/wp-content/uploads/2023/08/OFFLU-statement-HPAI-wildlife-South-America-20230823.pdf
24. Thanawongnuwech R, Amonsin A, Tantilertcharoen R, Damrongwatanapokin S, Theamboonlers A, Payungporn S, et al. Probable tiger-to-tiger transmission of avian influenza H5N1. Emerg Infect Dis. 2005;11:699–701. https://doi.org/10.3201/eid1105.050007
25. Keawcharoen J, Oraveerakul K, Kuiken T, Fouchier RA, Amonsin A, Payungporn S, et al. Avian influenza H5N1 in tigers and leopards. Emerg Infect Dis. 2004;10:2189–91. https://doi.org/10.3201/eid1012.040759
26. He S, Shi J, Qi X, Huang G, Chen H, Lu C. Lethal infection by a novel reassortant H5N1 avian influenza A virus in a zoo-housed tiger. Microbes Infect. 2015;17:54–61. https://doi.org/10.1016/j.micinf.2014.10.004
27. Chen Q, Wang H, Zhao L, Ma L, Wang R, Lei Y, et al. First documented case of avian influenza (H5N1) virus infection in a lion. Emerg Microbes Infect. 2016;5:e125. https://doi.org/10.1038/emi.2016.127
28. Bordes L, Vreman S, Heutink R, Roose M, Venema S, Pritz-Verschuren SBE, et al. Highly pathogenic avian influenza H5N1 virus infections in wild red foxes (*Vulpes vulpes*) show neurotropism and adaptive virus mutations. Microbiol Spectr. 2023;11:e0286722. https://doi.org/10.1128/spectrum.02867-22
29. Hiono T, Kobayashi D, Kobayashi A, Suzuki T, Satake Y, Harada R, et al. Virological, pathological, and glycovirological investigations of an Ezo red fox and a tanuki naturally infected with H5N1 high pathogenicity avian influenza viruses in Hokkaido, Japan. Virology. 2023;578:35–44. https://doi.org/10.1016/j.virol.2022.11.008
30. Rijks JM, Hesselink H, Lollinga P, Wesselman R, Prins P, Weesendorp E, et al. Highly pathogenic avian influenza A (H5N1) virus in wild red foxes, the Netherlands, 2021. Emerg Infect Dis. 2021;27:2960–2. https://doi.org/10.3201/eid2711.211281
31. Tammiranta N, Isomursu M, Fusaro A, Nylund M, Nokireki T, Giussani E, et al. Highly pathogenic avian influenza A (H5N1) virus infections in wild carnivores connected to mass mortalities of pheasants in Finland [cited 2023 Oct 30]. Infect Genet Evol. 2023;111:105423.
32. Alkie TN, Cox S, Embury-Hyatt C, Stevens B, Pople N, Pybus MJ, et al. Characterization of neurotropic HPAI H5N1 viruses with novel genome constellations and mammalian adaptive mutations in free-living mesocarnivores in Canada. Emerg Microbes Infect. 2023;12:2186608. https://doi.org/10.1080/22221751.2023.2186608
33. Leguia M, Garcia-Glaessner A, Muñoz-Saavedra B, Juarez D, Barrera P, Calvo-Mac C, et al. Highly pathogenic avian influenza A (H5N1) in marine mammals and seabirds in Peru. Nat Commun. 2023;14:5489. https://doi.org/10.1038/s41467-023-41182-0
34. Puryear W, Sawatzki K, Hill N, Foss A, Stone JJ, Doughty L, et al. Highly pathogenic avian influenza A(H5N1) virus outbreak in New England seals, United States. Emerg Infect Dis. 2023;29:786–91. https://doi.org/10.3201/eid2904.221538
35. Amonsin A, Payungporn S, Theamboonlers A, Thanawongnuwech R, Suradhat S, Pariyothorn N, et al. Genetic characterization of H5N1 influenza A viruses isolated from zoo tigers in Thailand. Virology. 2006;344:480–91. https://doi.org/10.1016/j.virol.2005.08.032
36. Amonsin A, Songserm T, Chutinimitkul S, Jam-On R, Sae-Heng N, Pariyothorn N, et al. Genetic analysis of influenza A virus (H5N1) derived from domestic cat and dog in Thailand. Arch Virol. 2007;152:1925–33. https://doi.org/10.1007/s00705-007-1010-5
37. Elsmo EJ, Wunschmann A, Beckmen KB, Broughton-Neiswanger LB, Buckles EL, Ellis J, et al.

Pathology of natural infection with highly pathogenic avian influenza virus (H5N1) clade 2.3.4.4b in wild terrestrial mammals in the United States in 2022. Emerg Infect Dis. 2023;29:2451–60. https://doi.org/10.3201/eid2912.230464
38. Roberton SI, Bell DJ, Smith GJD, Nicholls JM, Chan KH, Nguyen DT, et al. Avian influenza H5N1 in viverrids: implications for wildlife health and conservation. Proc Biol Sci. 2006;273:1729–32. https://doi.org/10.1098/rspb.2006.3549
39. Klopfleisch R, Wolf PU, Wolf C, Harder T, Starick E, Niebuhr M, et al. Encephalitis in a stone marten (*Martes foina*) after natural infection with highly pathogenic avian influenza virus subtype H5N1. J Comp Pathol. 2007;137:155–9. https://doi.org/10.1016/j.jcpa.2007.06.001
40. Nidom CA, Takano R, Yamada S, Sakai-Tagawa Y, Daulay S, Aswadi D, et al. Influenza A (H5N1) viruses from pigs, Indonesia. Emerg Infect Dis. 2010;16:1515–23. https://doi.org/10.3201/eid1610.100508
41. Meseko C, Globig A, Ijomanta J, Joannis T, Nwosuh C, Shamaki D, et al. Evidence of exposure of domestic pigs to highly pathogenic avian influenza H5N1 in Nigeria. Sci Rep. 2018;8:5900. https://doi.org/10.1038/s41598-018-24371-6
42. He L, Zhao G, Zhong L, Liu Q, Duan Z, Gu M, et al. Isolation and characterization of two H5N1 influenza viruses from swine in Jiangsu Province of China. Arch Virol. 2013;158:2531–41. https://doi.org/10.1007/s00705-013-1771-y
43. Leschnik M, Weikel J, Möstl K, Revilla-Fernández S, Wodak E, Bagó Z, et al. Subclinical infection with avian influenza A (H5N1) virus in cats. Emerg Infect Dis. 2007;13:243–7. https://doi.org/10.3201/eid1302.060608
44. Hu T, Zhao H, Zhang Y, Zhang W, Kong Q, Zhang Z, et al. Fatal influenza A (H5N1) virus Infection in zoo-housed tigers in Yunnan Province, China. Sci Rep. 2016;6:25845. https://doi.org/10.1038/srep25845
45. Songserm T, Amonsin A, Jam-on R, Sae-Heng N, Meemak N, Pariyothorn N, et al. Avian influenza H5N1 in naturally infected domestic cat. Emerg Infect Dis. 2006;12:681–3. https://doi.org/10.3201/eid1204.051396
46. Songserm T, Amonsin A, Jam-on R, Sae-Heng N, Pariyothorn N, Payungporn S, et al. Fatal avian influenza A H5N1 in a dog. Emerg Infect Dis. 2006;12:1744–7. https://doi.org/10.3201/eid1211.060542
47. Thorsson E, Zohari S, Roos A, Banihashem F, Bröjer C, Neimanis A. Highly pathogenic avian influenza A(H5N1) virus in a harbor porpoise, Sweden. Emerg Infect Dis. 2023;29:852–5. https://doi.org/10.3201/eid2904.221426
48. Daszak P, Cunningham AA, Hyatt AD. Emerging infectious diseases of wildlife—threats to biodiversity and human health. Science. 2000;287:443–9. https://doi.org/10.1126/science.287.5452.443
49. Taubenberger JK, Reid AH, Lourens RM, Wang R, Jin G, Fanning TG. Characterization of the 1918 influenza virus polymerase genes. Nature. 2005;437:889–93. https://doi.org/10.1038/nature04230
50. Kuiken T, Cromie R. Protect wildlife from livestock diseases. Science. 2022;378:5.

Address for corresponding author: Pablo I. Plaza, Conservation Biology Research Group, Ecotone Laboratory, Institute of Biodiversity and Environmental Research (INIBIOMA), National University of Comahue–National Scientific and Technical Research Council, Quintral 1250 (R8400FRF), San Carlos de Bariloche, Argentina; email: plazapablo@comahue-conicet.gob.ar

Monitoring and Characteristics of Mpox Contacts, Virginia, USA, May–November 2022

Eleanor N. Field, Elizabeth McCarty, Dawn Saady, Brandy Darby

During 2022, a global outbreak of mpox resulted primarily from human-to-human contact. The Virginia Department of Health (Richmond, VA, USA) implemented a contact tracing and symptom monitoring system for residents exposed to monkeypox virus, assessed their risk for infection, and offered interventions as needed. Among 991 contacts identified during May 1–November 1, 2022, import records were complete for 943 (95.2%), but 99 (10.0%) were not available for follow-up during symptom monitoring. Mpox developed in 28 (2.8%) persons; none were healthcare workers exposed at work (n = 275). Exposure risk category and likelihood of developing mpox were strongly associated. A total of 333 persons received ≥1 dose of JYENNOS (Bavarian Nordic, https://www.bavarian-nordic.com) vaccine, most (n = 295) administered after virus exposure. Median time from exposure to vaccination was 8 days. Those data tools provided crucial real-time information for public health responses and can be used as a framework for other emerging diseases.

Mpox is an emerging viral disease characterized by a prodromal illness followed by vesiculopustular rash (*1*). Since monkeypox virus (MPXV) was first isolated in 1970 from a child in the Democratic Republic of the Congo, cases of mpox have been documented across 15 countries, primarily Africa (*1*). Sporadic cases outside of those countries were usually epidemiologically linked to international travel or animal importation (*2*). However, during 2022, a global outbreak of mpox began that was driven by human-to-human transmission (*3*,*4*); ≈87,000 cases from 110 countries have been reported to the World Health Organization since January 2022 through May 2023 (*5*). Before 2022, no mpox case had been reported in Virginia, USA; however, by the end of December 2022, Virginia reported 568 cases and was among the top 15 US states for mpox case burden (*6*).

Author affiliations: Centers for Disease Control and Prevention, Atlanta, Georgia, USA (E.N. Field); Virginia Department of Health, Richmond, Virginia, USA (E.N. Field, E. McCarty, D. Saady, B. Darby)

DOI: https://doi.org/10.3201/eid3003.230609

In Virginia, mpox is reportable as an Unusual Occurrence of Disease of Public Health Concern. Local public health departments have 24 hours from case notification to begin an investigation, initiate contact tracing to identify exposed persons, and offer medical countermeasures to halt further transmission. The 2-dose vaccine series (JYNNEOS; Bavarian Nordic, https://www.bavarian-nordic.com) was offered for persons at increased risk for MPXV exposure or after a known or presumed exposure to MPXV (*7*). The Centers for Disease Control and Prevention (CDC) recommends that vaccine be given as soon as possible, ideally within 4 days after exposure; administration 4–14 days after exposure may still provide some protection against mpox and should still be offered (*7*). The second dose should be administered 28–35 days after the first dose, although completing the series at any time thereafter is recommended (*7*).

The changing epidemiology of MPXV transmission from primarily zoonotic to primarily human-to-human during an outbreak of unprecedented scale provided a unique public health challenge. We describe how the Virginia Department of Health (VDH; Richmond, VA, USA) adapted an existing data collection tool for tracing contacts and monitoring symptoms of persons affected by an emerging disease and how those data were used to assess contact characteristics, MPXV exposures, vaccine uptake, and timeliness of postexposure vaccination.

Our study received ethics approval from the Virginia Department of Health Institutional Review Board (study #50284). The study was also reviewed by CDC and conducted consistent with federal law and CDC policy (*45 C.F.R. part 46, 21 C.F.R. part 56; 42 U.S.C. Sect. 241(d); 5 U.S.C. Sect. 552a; 44 U.S.C. Sect. 3501 et seq.).

Materials and Methods

Cohort Design

The objective of VDH mpox contact tracing was to identify close contacts, advise them of the virus exposure, and offer vaccination to prevent illness or reduce disease severity to those eligible. Symptom monitoring was implemented to expedite early laboratory testing and case identification to reduce further transmission. To be included in the study, a person needed to have either self-reported an MPXV exposure or have been notified by VDH of a recent exposure. Persons who were not residents of Virginia were not eligible for participation. VDH may have been notified of an mpox case by an in-state healthcare provider, clinic, or laboratory; by another state; or by CDC.

We recorded persons with confirmed and probable mpox identified during the symptom monitoring period as persons in whom mpox developed. We defined a confirmed mpox case as positive detection of MPXV through either molecular testing or genomic sequencing. We defined a probable case as detection of orthopoxvirus by molecular testing and no laboratory evidence of another nonvariola orthopoxvirus, detection of orthopoxvirus by immunohistochemistry or genomic sequencing, or detection of orthopoxvirus IgM in a person with no recent history of vaccination (*8*).

Mpox Contact Tracing and Symptom Monitoring Data Collection

Local health department staff used REDCap (Research Electronic Data Capture, https://www.project-redcap.org) to collect information on mpox close contacts and symptom monitoring during case and contact interviews. Some hospitals monitored their own employees and provided information to local health departments about their healthcare workers (HCWs) exposed at work. Information was entered into a contact import form that included patient demographics, MPXV exposure (e.g., date of last exposure, exposure risk category, location description and setting), mpox vaccination status, HCW status, immunosuppression status, and public health interviewer details. We also linked close contact to a daily mpox monitoring form, which collected information about mpox symptoms (e.g., temperature, rash, chills, swollen lymph nodes), medications taken, and final disposition. The daily mpox monitoring form was completed and submitted by the contact over text message, email, or by phone with a local health department staff member.

The REDCap project also included a case report form, which was adapted from CDC recommendations (*9*). The form consisted of 248 fields asking about the interaction(s) that may have been the source(s) of infection, mpox vaccination status, mpox hospitalization, mpox symptoms, date of illness onset, residence, demographics (including sexual orientation and gender identity), recent trips and contacts with whom the person had interacted (and the nature of the interactions), laboratory information about the diagnosis, and interview details.

Contact information obtained from case interviews was recorded in the database, but participation in daily mpox symptom monitoring and exposure or case interviews with the local health department was voluntary. Symptom monitoring lasted for 21 days from a person's last reported exposure.

Cohort Analyses

We conducted a retrospective cohort study for persons enrolled in the VDH mpox close contact monitoring cohort during May 1–November 1, 2022 (Figure 1). We excluded data for 16 persons who had not completed symptom monitoring within the study time frame and for 1 person for whom duplicate, conflicting information was recorded. For all analyses, we used R Statistical Software version 4.2.2 (The R Foundation for Statistical Computing, https://www.r-project.org).

Mpox Exposure Analysis

We extracted information regarding demographics, MPXV exposure details, assigned exposure risk category (*10*), monitoring participation, and outcome (disease did vs. did not develop) of persons included in the monitoring cohort. Exposure settings were mutually exclusive because of limitations in the structure of data collection forms. Exposure risk categories (high, intermediate, lower, and none) characterizing personal risk from the nature of the exposure using criteria defined by CDC (*10*) were assigned by local health department personnel in the contact import form.

We used descriptive statistics to describe select demographic and exposure data for the full cohort, for persons within the cohort in whom mpox developed, and for HCWs exposed at work (Figure 1). Calculated percentages exclude missing values. We used χ^2 analysis to evaluate the association between exposure risk category (excluding the none category) and development of mpox.

Mpox Vaccination Analysis

Mpox vaccine administration is mandatorily reported to the Virginia Immunization Information System

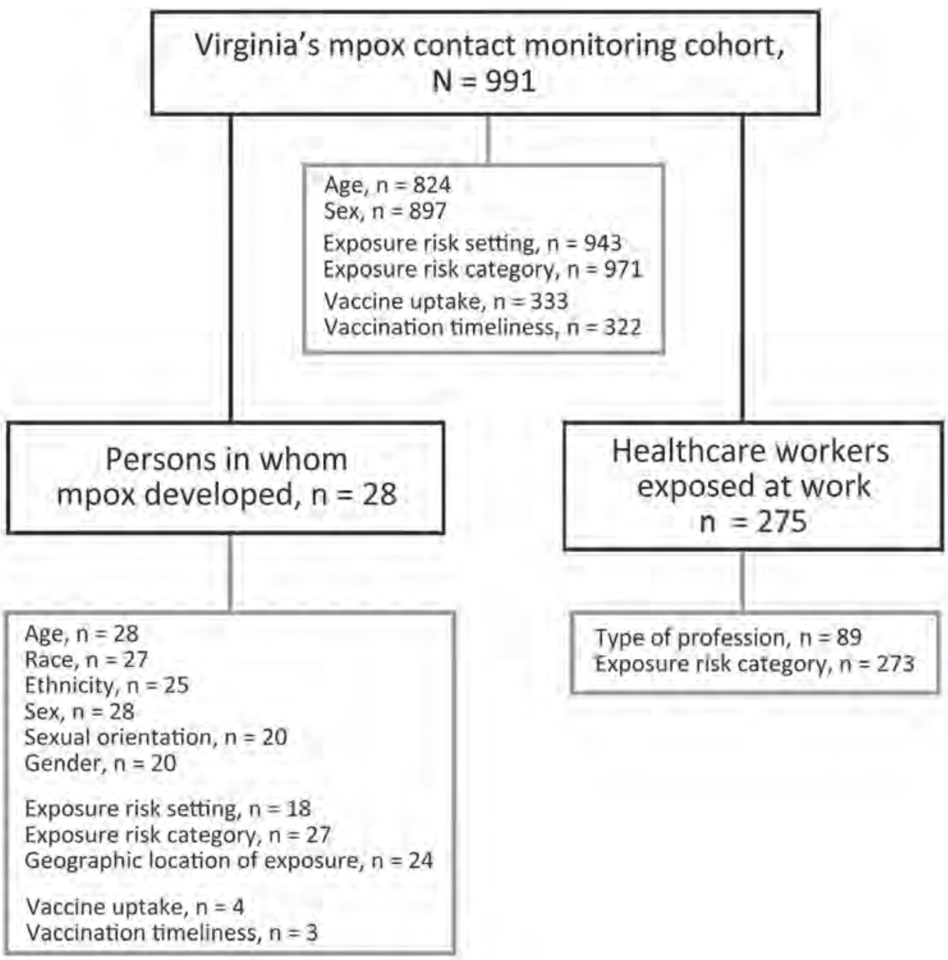

Figure 1. Mpox contact tracing and symptom monitoring cohort (n = 991), Virginia, USA, May 1–November 1, 2022. Analyzed subcohorts included persons in whom mpox developed (n = 28) and healthcare workers exposed at work (n = 275).

(https://viis.vdh.virginia.gov); we used this system to determine which persons received in-state mpox vaccine(s) and the date(s) of administration. Matching was completed by using exact date of birth, postal (ZIP) code, and the first 3 letters of first and last names.

To assess vaccine uptake, we described how many and what percentage of persons within the cohort received $\geq$1 dose of an mpox vaccine. We used those descriptive statistics to measure completion of the 2-dose series. We also specifically assessed vaccine uptake for persons within the cohort in whom mpox developed. Last, to determine if there were differences across exposure risk categories, we measured vaccine uptake by exposure risk category.

We measured vaccination timeliness as time in days from reported MPXV exposure to first dose of an mpox vaccine for the full cohort and for persons in whom mpox developed. We did not analyze preexposure vaccination timeliness. We also assessed timeliness by using CDC postexposure recommendations (7), describing how many doses were administered within 4 and 14 days of the reported exposure.

Results

Cohort Characteristics

During May 1–November 1, 2022, a total of 991 persons were enrolled in Virginia's mpox close contact monitoring cohort and ended their 21-day monitoring period during the study period. Among the 932 persons for whom data about their method of participation were available, 491 (52.7%) used email, 239 (25.6%) reported directly to their local health department, 143 (15.3%) self-monitored, and 59 (0.06%) used text messaging to access surveys. Of 991 contact records, 943 (95.2%) were complete and 48 (4.8%) were incomplete. During symptom monitoring, 99 (10.0%) contacts were not available for follow-up and 20 (2.2%) declined or no longer needed monitoring (e.g., their reported exposure was beyond the 21-day symptom monitoring period, not determined to be a close contact, or from a person later determined to be MPXV negative). Eleven (1.1%) contact investigations were transferred to another jurisdiction. Of the 28 persons in the close contact monitoring cohort in whom mpox developed, 26 (92.9%) completed their case interview. Among 897 persons in the cohort for whom sex was recorded, 494 (55.1%) were male and 403 (44.9%) female (Table 1). Age information was available for 824 persons; median age was 35 (interquartile range [IQR] 26–49) years.

Persons with Mpox Cohort Characteristics

Within the cohort of 991 persons, mpox developed in 28 (2.8%) while they were being monitored for symptoms (Figure 1); 27 cases were confirmed and 1 was probable. Twenty-seven (96.4%) persons were recorded as male and 1 (3.6%) as female (Table 1). The median age was 36 (IQR 31–40) years. Among 27 persons with mpox who reported their race, 15 (55.6%) self-identified as White, 11 (40.7%) as Black, and 1 (3.7%) as Native Hawaiian or Other Pacific Islander. Among 25 persons with mpox who reported ethnicity, 8 (32.0%) self-identified as Hispanic. Information on sexual orientation and gender identity was available for 20 persons with mpox; 19 (94.7%) self-identified as bisexual or gay cisgender men, and 1 (5%) self-identified as a straight cisgender woman.

Reported Mpox Exposure Settings

Exposure information was available for 943 persons in the cohort (Figure 1). Of those, 326 (34.5%) were exposed in households, 310 (32.9%) in healthcare settings, 145 (15.4%) at private gatherings or parties, 58 (6.2%) in workplaces, 52 (5.5%) in an airport or airplane, 33 (3.5%) in a school, 14 (1.5%) in other congregate settings, and 5 (0.5%) in a long-term-care facility (Figure 2).

Reported Mpox Exposures in Persons in Whom Mpox Developed

Reported exposure setting information was available for 18 of the 28 persons in whom mpox developed; 10 reported MPXV exposures from a household (55.6%) and 7 from a private gathering or party (38.9%). One (5.6%) person was being monitored for exposure on an airplane or in an airport, but investigators later determined that that was not the most likely source of infection (Figure 2).

Among the 25 persons in whom mpox developed and who provided additional information about their MPXV exposure, 22 (88.0%) reported recent sexual activity. Seven men reported sexual activity with multiple male partners, and 3 of them reported that their partners were anonymous. Mpox developed in 1 straight cisgender woman within the cohort after a reported sexual exposure from a male household contact. Of the 3 persons in whom mpox developed without their having reported recent sexual contact, 2 persons reported that their exposure was from a congregate setting (specifically, a prison and a convention event) and 1 person reported close nonsexual contact. Geographic exposure location was available for 24 persons: 18 (75.0%) reported in-state exposures and 6 (25.0%) reported exposures during out-of-state domestic travel (to Georgia, North Carolina, New York, and Massachusetts) or international travel (Mexico).

Mpox Exposure Risk Categories

Among 971 persons for whom exposure risk categories were assigned by using CDC criteria (*10*) (Figure 1), 374 (38.5%) were assigned intermediate risk, 360 (37.1%) lower risk, 225 (23.2%) higher risk, and 12 (1.2%) no risk (Table 2). Among the 28 persons in

Table 1. Characteristics of 991 persons enrolled in mpox contact tracing and symptom monitoring cohort, Virginia, USA, May 1–November 1, 2022*

	No. (%) persons		
Characteristic	Total	Persons without mpox	Persons with mpox
Total	991	963	28
Sex assigned at birth			
M	494 (55.1)	467 (53.7)	27 (96.4)
F	403 (44.9)	402 (46.3)	1 (3.6)
Missing	94	94	0
Age group, y			
0–9	32 (3.9)	32 (4.0)	0 (0)
10–19	48 (5.8)	48 (6.0)	0
20–29	130 (15.8)	128 (16.1)	2 (7.1)
30–39	205 (24.9)	193 (24.2)	12 (42.9)
40–49	155 (18.8)	145 (18.2)	10 (35.7)
50–59	101 (12.3)	99 (12.4)	2 (7.1)
60–69	103 (12.5)	101 (12.7)	2 (7.1)
70–79	0 (4.4)	36 (4.5)	0
≥80	14 (1.7)	14 (1.8)	0
Missing	167	167	0

*Calculated percentages exclude missing values.

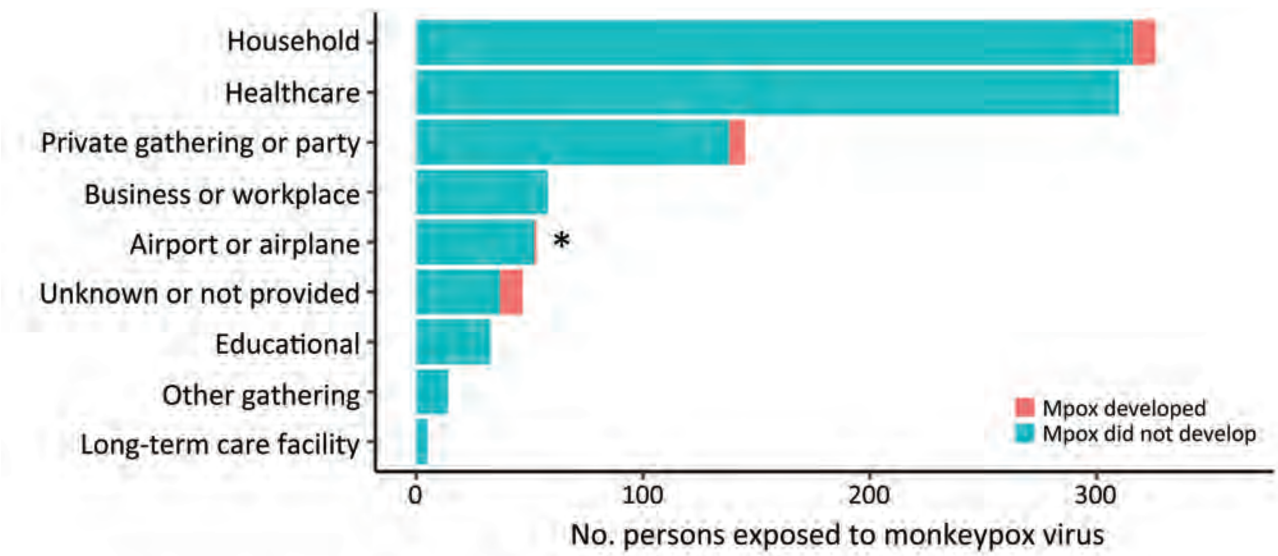

Figure 2. Reported monkeypox virus exposure setting categories from mpox contact tracing and symptom monitoring cohort (n = 991), Virginia, USA, May 1–November 1, 2022. For persons in whom mpox developed while being monitored (n = 28), asterisk indicates where initial reported exposure setting differed from most likely infection source.

whom mpox developed for whom an exposure risk category was assigned, 20 (71.4%) exposures were categorized as high risk, 4 (14.3%) as intermediate risk, and 3 (10.7%) as lower risk; 1 person (3.6%) was not assigned an exposure risk category (Table 2). The degree of association between assigned exposure risk category and likelihood of mpox development was high (p<0.001) (Table 2).

HCW Occupational Exposures

A total of 275 persons self-identified as HCWs who were exposed at work (Figure 1). Among the HCWs who reported their role, 2 (2.1%) were administrators, 14 (15.4%) worked in emergency medical services, 1 (1.1%) was an imaging technician, 27 (29.7%) were nurses, 7 (7.7%) were nurse assistants, 14 (15.4%) worked as other direct care HCWs, 1 (1.1%) worked as an other nondirect care HCW, 21 (23.1%) were health-care providers, and 3 (3.3%) worked in registration. Among 273 HCWs exposed at work for whom an exposure risk category was assigned, 34 (12.5%) exposures were categorized as high risk, 48 (17.6%) as intermediate risk, 180 (65.9%) as low risk, and 11 (4.0%) as no risk (e.g., personal protective equipment was appropriately worn during exposure encounter[s]).

Vaccine Uptake

Of the 991 persons in the cohort, 333 (33.6%) received ≥1 vaccine dose that was recorded in Virginia's Immunization Information System (Table 3; Figure 1). In addition, 212 received a second dose, representing 63.7% of those available for follow-up and indicating that 21.4% of the cohort completed the mpox series during May–November 2022.

Of the 225 persons identified as having had a high-risk exposure, 121 (53.8%) received ≥1 dose. A total of 166 (44.3%) of 374 persons who had intermediate risk exposures received ≥1 dose, and 35 (9.7%) of 360 persons self-identified as having lower exposure risk received ≥1 dose.

Information about exposure and vaccination dates were available for 322 of the 333 vaccinated

Table 2. Exposure risk categories and likelihood of developing mpox among 991 persons included in mpox contact tracing and symptom monitoring cohort, Virginia, USA, May 1–November 1, 2022*

	No. (%) persons				
Risk category	Total	Persons without mpox	Persons with mpox	χ^2 (d.f.)†	p value
None	12 (1.2)	12 (1.3)	0		
Lower	360 (37.1)	357 (37.8)	3 (11.1)	39.7 (2)	<0.001
Intermediate	374 (38.5)	370 (39.2)	4 (14.8)		
High	225 (23.2)	205 (21.7)	20 (74.1)		
Missing	20	19	1		

*Calculated percentages exclude missing values. Predetermined categories were defined by the nature of the exposure using criteria defined by the Centers for Disease Control and Prevention (*10*).
†χ^2 analysis excludes persons in the none category.

Table 3. Vaccine uptake and postexposure timeliness in mpox contact tracing and symptom monitoring cohort, Virginia, USA, May 1–November 1, 2022*

Characteristic	Value
All persons	991
Received ≥1 dose	333 (33.6)
Before exposure	27 (8.4)
After exposure	295 (91.6)
Unable to determine	10
Received 2 doses	212 (63.7)
Persons vaccinated after exposure	295
Median time from exposure to first dose, d	8 (range 4–12)
No. receiving 1st dose within <4 days of exposure	82 (27.8)
No. receiving 1st dose within <14 days of exposure	252 (85.4)

*Values are no (%) except as indicated. Calculated percentages exclude missing values.

persons. A total of 295 (91.6%) persons received postexposure vaccination, and 27 (8.4%) received preexposure prophylaxis (Table 3).

Timeliness of Postexposure Vaccination

Among the 295 persons who received postexposure vaccination, the median time of first vaccine administration after MPXV exposure was 8 (IQR 4–12) days (Table 3). In terms of timeliness of recommended postexposure administration, 82 (27.8%) persons were vaccinated <4 days after MPXV exposure and 252 (85.4%) were vaccinated ≤14 days after exposure (Table 3). Information on exposure and vaccination dates were available for 3 of the vaccinated persons in whom mpox developed; all had received postexposure prophylaxis within 14 days (4, 11, and 12 days).

Discussion

The data tool that we used enabled flexibility and for real-time review of data from personnel at the local and state health department level to track the number of persons who had been exposed to MPXV and offer interventions to persons at high risk for exposure to stop transmission. Contact lists were easily exported so that health department personnel could cross-check against Virginia's vaccine registry to encourage vaccination completion. The overall high completion rate of contact records and low number of persons not available for follow-up during symptom monitoring demonstrates successful implementation and use of the VDH mpox close contact monitoring response.

We found no cases of mpox in HCWs exposed at work. Most exposures for HCWs were lower risk, potentially suggesting either some use of personal protective equipment or minimal contact with the patient. Details about high-risk exposures in medical settings were not provided and could be an area of further research. Similarly, mpox did not develop in any persons exposed in businesses, workplaces, or educational settings. We do report mpox development after household exposures, but case interviews more specifically identified that the source of infection was from sexual contact in a household environment rather than cohabitation with an infected person. That finding is consistent with results from a recent study of undiagnosed mpox prevalence in the United States (*11*).

The high degree of association between assigned exposure risk category and likelihood of mpox development suggests that risk categories are useful for public health officials identifying persons to prioritize for interventions. Our cohort analysis identified 3 persons who were labeled lower risk but in whom mpox developed. One person disclosed sexual contact unrelated to known exposure, and it is likely that the assigned classification instead reflected the exposure for which the person was being monitored. One person disclosed recent sexual contact without other potential exposure sources and represents a misclassification of exposure risk category, underrepresenting mpox risk. The third person did not complete an interview, so it is unclear how that risk category was assigned.

Overall vaccine uptake in this cohort was low; only one third of the cohort received ≥1 dose and one fifth completed the 2-dose series. Just over half of persons who were identified as having had a high-risk exposure received a vaccine. However, more persons categorized as having high-risk exposure were vaccinated than were persons in other exposure risk categories, which might suggest higher motivation to receive vaccination or success in vaccine prioritization.

Timely vaccine uptake for postexposure prophylaxis was low; <30% of persons were vaccinated within the recommended 4 days after a known or presumed MPXV exposure. However, most (85%) persons who received postexposure vaccine received it within 14 days of their exposure, which may confer some protection (*6*). Factors such as reduced patient access to diagnostic testing may have delayed the initial mpox case-patient's diagnosis, affecting exposure notification to contacts. In addition, vaccine availability might have affected vaccination timeliness.

Among the limitations of our retrospective cohort analysis, persons exposed to MPXV or who had mpox might have been missed by official VDH reporting channels, and we were unable to estimate how well our cohort captured these populations. Also, persons with mpox interviewed by public health personnel may have been hesitant to discuss sexual exposure details, leading to underreporting and lack of follow-up with contacts or misclassification of infection risk.

In conclusion, our study describes mpox contact tracing and symptom monitoring in Virginia and evaluated characteristics of persons with reported exposures and can be used to inform public health preparedness and response measures. The flexible data collection tools and real-time access to data used by VDH in the mpox response can serve as a framework for future emerging diseases.

Acknowledgments

We thank Jonathan Falk and Tessa Dewalt for guidance on mpox monitoring response details and REDCap forms. We thank local health department personnel who led investigations and all who participated in the monitoring cohort. We thank Katie Labgold, Bruce Gutelius, and Laurie Forlano for their thoughtful guidance throughout the creation of this manuscript.

This work was completed at the Virginia Department of Health, 109 Governor Street, Richmond, Virginia.

About the Author

Dr. Field is an Epidemic Intelligence Service Officer with the Centers for Disease Control and Prevention, hosted at the Virginia Department of Health. Dr. Field's primary research interest is vectorborne and zoonotic diseases.

References

1. Alakunle E, Moens U, Nchinda G, Okeke MI. Monkeypox virus in Nigeria: infection biology, epidemiology, and evolution. Viruses. 2020;12:1257. https://doi.org/10.3390/v12111257
2. Kumar N, Acharya A, Gendelman HE, Byrareddy SN. The 2022 outbreak and the pathobiology of the monkeypox virus. J Autoimmun. 2022;131:102855. https://doi.org/10.1016/j.jaut.2022.102855
3. Philpott D, Hughes CM, Alroy KA, Kerins JL, Pavlick J, Asbel L, et al.; CDC Multinational Monkeypox Response Team. Epidemiologic and clinical characteristics of monkeypox cases—United States, May 17–July 22, 2022. MMWR Morb Mortal Wkly Rep. 2022;71:1018–22. https://doi.org/10.15585/mmwr.mm7132e3
4. Thornhill JP, Barkati S, Walmsley S, Rockstroh J, Antinori A, Harrison LB, et al.; SHARE-net Clinical Group. Monkeypox virus infection in humans across 16 countries—April–June 2022. N Engl J Med. 2022;387:679–91. https://doi.org/10.1056/NEJMoa2207323
5. World Health Organization. 2022–-2023 Mpox (monkeypox) outbreak: global trends [cited 2023 Apr 6]. https://who.int/emergencies/situations/monkeypox-oubreak-2022
6. Centers for Disease Control and Prevention. 2022–2023 U.S. map & case count [cited 2023 Dec 1]. https://www.cdc.gov/poxvirus/mpox/response/2022/us-map.html
7. Centers for Disease Control and Prevention. Vaccination [cited 2023 Jan 11]. https://www.cdc.gov/poxvirus/monkeypox/interim-considerations/overview.html
8. Centers for Disease Control and Prevention. Monkeypox virus infection case definition [cited 2023 Feb 22]. https://ndc.services.cdc.gov/case-definitions/monkeypox-virus-infection
9. Centers for Disease Control and Prevention. 2022/2023 U.S. mpox outbreak short case report form. [cited 2023 Nov 10]. https://www.cdc.gov/poxvirus/mpox/pdf/scrf-short-form.pdf
10. Centers for Disease Control and Prevention. Monitoring and risk assessment for persons exposed in the community [cited 2022 Dec 13]. archive.cdc.gov/www_cdc_gov/poxvirus/mpox/clinicians/monitoring.html
11. Minhaj FS, Singh V, Cohen SE, Townsend MB, Scott H, Szumowski J, et al. Prevalence of undiagnosed monkeypox virus infections during global mpox outbreak, United States, June–September 2022. Emerg Infect Dis. 2023;29:2307–14. https://doi.org/10.3201/eid2911.230940

Address for correspondence: Eleanor Field, Virginia Department of Health, 109 Governor's St, Richmond, VA 23219, USA; email: eleanor.field@vdh.virginia.gov

Expansion of *Neisseria meningitidis* Serogroup C Clonal Complex 10217 during Meningitis Outbreak, Burkina Faso, 2019

Joann F. Kekeisen-Chen, Felix T. Tarbangdo, Shalabh Sharma, Daya Marasini, Henju Marjuki, Janelle L. Kibler, Heather E. Reese, Seydou Ouattara, Flavien H. Ake, Issaka Yameogo, Issa Ouedraogo, Emmanuel Seini, Robert L. Zoma; Issa Tonde, Mahamoudou Sanou, Ryan T. Novak,[1] Lucy A. McNamara[1]

During January 28–May 5, 2019, a meningitis outbreak caused by *Neisseria meningitidis* serogroup C (NmC) occurred in Burkina Faso. Demographic and laboratory data for meningitis cases were collected through national case-based surveillance. Cerebrospinal fluid was collected and tested by culture and real-time PCR. Among 301 suspected cases reported in 6 districts, *N. meningitidis* was the primary pathogen detected; 103 cases were serogroup C and 13 were serogroup X. Whole-genome sequencing revealed that 18 cerebrospinal fluid specimens tested positive for NmC sequence type (ST) 10217 within clonal complex 10217, an ST responsible for large epidemics in Niger and Nigeria. Expansion of NmC ST10217 into Burkina Faso, continued NmC outbreaks in the meningitis belt of Africa since 2019, and ongoing circulation of *N. meningitidis* serogroup X in the region underscore the urgent need to use multivalent conjugate vaccines in regional mass vaccination campaigns to reduce further spread of those serogroups.

Burkina Faso is a landlocked country within the meningitis belt of sub-Saharan Africa that experiences hyperendemic bacterial meningitis and an elevated risk for recurrent meningitis outbreaks (*1*). Commonly characterized by headache, fever, stiff neck, and altered consciousness, bacterial meningitis can lead to permanent disability or death if not quickly detected and treated.

Historically, meningitis epidemics within the meningitis belt of Africa have been caused primarily by *Neisseria meningitidis* serogroup A (NmA) (*2*–*4*). In 2010, Burkina Faso was the first of many meningitis-belt countries to introduce the novel monovalent meningococcal serogroup A conjugate vaccine, MenAfriVac, nationwide. After MenAfriVac introduction, meningitis cases and outbreaks caused by NmA were no longer reported (*2*,*4*). However, seasonal meningitis outbreaks and epidemics still occur in the region because of non-NmA serogroups, including *N. meningitidis* serogroup C (NmC), X (NmX), and W (*5*). In particular, NmC has caused several large outbreaks both within and outside the meningitis belt in the past several years (*6*).

Meningitis caused by NmC had been generally uncommon in the meningitis belt of Africa. Occasional NmC outbreaks and epidemics have been reported in the belt during the past 50 years, including an NmC epidemic in 1975 in northern Nigeria and small, localized outbreaks in Burkina Faso in 1979, Mali during 1988–1992, and Nigeria during 2013–2014 (*7*–*11*). In 2015, however, NmC emerged as a serious public health threat after a focal NmC infection outbreak in northern Nigeria spread to neighboring Niger, where a large NmC epidemic that had 9,367 suspected cases and 549 deaths was reported (*12*). In 2017, the largest recorded meningitis epidemic caused by NmC occurred in northern Nigeria; 14,518 suspected cases and 1,166 deaths were reported (*13*). Through molecular typing, the recent epidemics in Niger and Nigeria were shown to be caused by a new NmC strain,

Author affiliations: Centers for Disease Control and Prevention, Atlanta, Georgia, USA (J.F. Kekeisen-Chen, S. Sharma, D. Marasini, H. Marjuki, J.L. Kibler, H.E. Reese, R.T. Novak, L.A. McNamara); Davycas International, Ouagadougou, Burkina Faso (F.T. Tarbangdo, F.H. Ake, R.L. Zoma); Ministère de la Santé, Ouagadougou (S. Ouattara, I. Yameogo, I. Ouedraogo, E. Seini); Centre Hospitalier Universitaire Pédiatrique Charles de Gaulle, Ouagadougou (I. Tonde, M. Sanou); Université Joseph Ki-Zerbo, Ouagadougou (I. Tonde, M. Sanou)

DOI: https://doi.org/10.3201/eid3003.221760

[1]These senior authors contributed equally to this article.

sequence type (ST) 10217 belonging to clonal complex (CC) 10217 (*12*,*14*). Comparative genomic analysis suggested that NmC ST10217 emerged from a meningococcal strain previously identified in nasopharyngeal specimens of asymptomatic human carriers after acquiring virulence genes (*15*).

In January 2019, a cluster of unexplained deaths was reported from the Boutou commune of Diapaga District in Burkina Faso's Est administrative region. The Est region shares its northern border with Niger and southern border with Benin and Togo. The chief medical officer, regional director of health, and director of population health protection were alerted, which led to epidemiologic investigations in Diapaga that confirmed a meningitis outbreak caused by NmC. Because of the rise of NmC cases in neighboring countries, recent large NmC outbreaks in the region, concern for the spread of NmC ST10217, and limited availability of NmC vaccines, outbreak investigation was critical to elucidate the evolving epidemiology of meningitis within the region (*16*). We describe the 2019 meningitis outbreak in Burkino Faso, the outbreak response, and microbiologic features of the NmC strain driving the outbreak.

Methods

Meningitis Surveillance

Population-based meningitis surveillance exists in 2 complementary systems in Burkina Faso (*17*). First, district-level aggregate reports of clinically defined (suspected) meningitis cases and meningitis-related deaths are transmitted weekly by the Telegramme Lettre Official Hebdomadaire (TLOH). The TLOH system has been functional in Burkina Faso since 1997 but does not hold any laboratory or demographic information aside from that obtained from the administrative district reporting cases (*17*). Second, the TLOH system is complemented by nationwide case-based surveillance (CBS), conducted by using the cloud-based System for Tracking Epidemiologic Data and Laboratory Specimens (STELAB). STELAB collects detailed case-level demographic, clinical, and laboratory data and assigns barcodes to each case report form and collected specimen, enabling real-time tracking of a specimen's journey from the district laboratory to the regional laboratory, then finally to a national reference laboratory (NRL) (*1*). National meningitis CBS data collected during 2018–2020 were validated in June 2021 and used for this analysis.

Alert and epidemic thresholds were defined according to published World Health Organization (WHO) guidelines. The alert threshold was defined as ≥3 suspected cases per week/100,000 inhabitants; the epidemic threshold was defined as ≥10 suspected cases per week/100,000 inhabitants (*18*). A suspected case was defined according to WHO guidelines as a sudden onset of fever (≥38.5°C) accompanied by neck stiffness, altered consciousness, or other meningeal signs, including flaccid neck, bulging fontanelle, or convulsions in children <2 years of age (*18*). A confirmed bacterial meningitis case was defined as any suspected or probable case that was laboratory confirmed by culturing or by identifying a bacterial pathogen (*N. meningitidis*, *Streptococcus pneumoniae*, *Haemophilus influenzae type b*) in the cerebrospinal fluid (CSF) or blood by PCR as previously described (*18*).

Laboratory

CSF specimens were collected from patients with suspected meningitis as part of routine surveillance. Confirmatory testing and serogrouping were performed by direct real-time PCR at the NRL. We performed further serogroup confirmation and molecular characterization for 18 CSF specimens at the Bacterial Meningitis Laboratory, National Center for Immunization and Respiratory Diseases, Centers for Disease Control and Prevention (CDC) (Atlanta, GA, USA). We enriched the specimens by using selective whole-genome amplification procedures and assessed the amplification by real-time PCR of the superoxide dismutase gene, *sodC*, as previously described (*19*). We performed whole-genome sequencing of all 18 CSF specimens that yielded a PCR cycle threshold of <16 for *sodC* after enrichment; the resulting genome assembly containing ≥1,400 core-genome multilocus sequence typing loci (*20*). We analyzed sequencing data by using the analysis pipeline developed in-house (*19*). We determined clonal complex and sequence types and characterized the gene locus encoding the polysaccharide capsule and peptide typing loci as previously described (*19*). For *N. meningitidis* CC10217 phylogenetic analysis, we compared 278 high-quality genome assemblies from isolates collected from Africa during 2012–2019 and the 18 Burkina Faso outbreak samples from 2019. All whole-genome sequencing data from this outbreak are publicly available in the PubMLST database (https://pubmlst.org/neisseria) (Appendix Table, https://wwwnc.cdc.gov/EID/article/30/3/22-1760-App1.xlsx).

Epidemiologic Analyses

We calculated cumulative incidence as the number of reported suspected meningitis cases in CBS data per 100,000 inhabitants by using 2019 health district population data. District populations in 2019 were provided as part of the TLOH line list by the Burkina Faso Ministry of Health. We extracted details of events prompting outbreak investigations from investigative reports provided by health districts under the supervision of the Ministry of Health. We determined the timing of key events related to the outbreak according to WHO weekly meningitis surveillance bulletin reports derived from TLOH data during the period of interest. We then analyzed CBS data in parallel to confirm the chronology of events and provide case-level laboratory and demographic information for each suspected case. We collected dates, administrative coverage, and vaccine type for reactive vaccination campaigns in each affected district from vaccination campaign reports provided by the Direction de la Protection de la Santé de la Population under Burkina Faso's Ministry of Health.

We used shapefiles of the national, regional, and health district boundaries obtained from the Direction de la Protection de la Santé de la Population to show the geographic distribution of cases during the outbreak. We defined the spatial location of cases as the patient's reported district of residence. The Diapaga health district is divided into 8 communes and has 37 health facilities that each serve a population covering ≈11 km^2 of land. For surveillance purposes, the district has been subdivided into 4 epidemiologic surveillance zones that have ≈100,000 inhabitants per

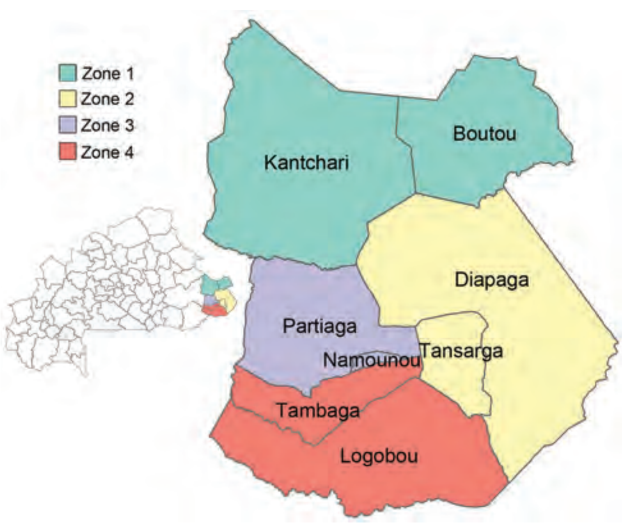

Figure 1. Meningitis surveillance zones in study of expansion of *Neisseria meningitidis* serogroup C clonal complex 10217 during meningitis outbreak, Burkina Faso, January 28–May 5, 2019. Main map indicates Diapaga health district divided into 8 communes within Tapoa Province of Burkina Faso. Inset map indicates the location of Tapoa Province in Burkina Faso. Colors indicate subdivision of the health district into 4 epidemiologic surveillance zones that have ≈100,000 inhabitants per zone.

zone (Figure 1). For our analysis, we mapped Diapaga's zones according to each commune's corresponding health facility zoning in 2019. We maintained datasets and analytic results in Microsoft Excel version 2108 (https://www.microsoft.com) and performed data analyses and mapping by using R version 4.1.3 (The R Project for Statistical Computing, https://www.r-project.org). This work was reviewed by CDC and conducted consistent with applicable federal law and CDC policy (e.g., 45 Code of Federal Regulation part 46, 21 Code of Federal Regulation part 56; 42 United States Code [U.S.C.] §241(d); 5 U.S.C. §552a; 44 U.S.C. §3501 et seq.).

Results

Outbreak and Response Timelines

During January 28–January 31, 2019, a total of 19 suspected cases (zone 1, 17 cases; zone 2, 2 cases) were reported from Diapaga; CSF samples were collected from each patient (Figure 1). On January 31, PCR testing was performed on 12 of 19 specimens; 7 were confirmed positive for NmC. The remaining 7 samples were tested on February 11, confirming 3 additional NmC cases. All 10 confirmed cases came from zone 1. A reactive vaccination campaign was conducted during February 9–13 in 11 health facilities located within zone 1 of Diapaga by using the national stockpile of plain polysaccharide MenACWY vaccine. The campaign targeted persons who were 2–29 years of age and achieved an estimated 108% administrative coverage of the targeted population. No additional confirmed meningitis cases caused by any pathogen were reported from zone 1 during the 2019 epidemic season after February 11.

From the end of February through April, the outbreak spread to Diapaga zones 2, 3, and 4 and to neighboring districts (Pama in the Est region and Sebba and Gayeri in the Sahel region) (Figures 1, 2). A vaccine request was submitted to WHO's International Coordinating Group (ICG) on Vaccine Provision on March 8; vaccines were delivered to affected areas on March 27 and, during March 29–April 2, a second vaccination campaign with conjugate MenACWY vaccines obtained through ICG was conducted in health facilities within Diapaga zones 2, 3, and 4 (Figure 3, panel A). The campaign targeted persons 1–29 years of age and achieved an estimated 111% administrative coverage. An additional ICG vaccine request was submitted on April 14 to cover Sebba and Gayeri. Plain polysaccharide MenACW vaccines were obtained through ICG, and a third campaign targeting persons 2–29 years of age was conducted during June 13–17, achieving an estimated 80% administrative coverage in Sebba and 87% in Gayeri (Figure 3, panel A). The second and third reactive vaccination campaigns were conducted in locations that either crossed the epidemic threshold (Diapaga zone 2, Sebba) or were considered to be at risk for outbreak expansion (Diapaga zones 3 and 4, Gayeri).

Epidemiologic Characterization of the Outbreak

During January 28–May 5, 2019, a total of 301 meningitis cases were reported from 6 districts in the Est (Diapaga, Gayeri, Pama, and Bogandé) and Sahel (Sebba and Dori) regions through Burkina Faso's national meningitis CBS, corresponding to a cumulative incidence of 17 cases/100,000 population during this 14-week period (Figure 3). Diapaga experienced the highest disease burden during the outbreak; the cumulative incidence was 29 cases/100,000 population. Cumulative incidences per 100,000 population were 27 cases in Sebba, 15 in Pama, 14 in Gayeri, and 6 each in Dori and Bogandé (Figure 2). We calculated all cumulative incidence rates according to suspected cases. Of the total reported cases, 290 (96%) had specimens collected; among those specimens, 286 (99%) were transported to an NRL and tested by PCR or culture. During the outbreak, the total case-fatality rate reported through CBS in the 6 districts was 5.6%. Of the 301 suspected meningitis cases, the pathogen was confirmed for 137 (46%): 103 (75%) cases were caused by NmC, 16 (12%) by *S. pneumoniae*, 13 (9%) by NmX, 3 (2%) by non–type b *H. influenzae*, and 2 (1%) by *H. influenzae* type b (Tables 1, 2).

Among the 103 persons with confirmed NmC infection, 83 (86%) persons were 5–29 years of age, representing a narrower age distribution than suspected case-patients, of whom only 50% were in this age range (Figure 4). A preponderance of confirmed NmX was observed among cases reported in Dori; although only 23 (7.6%) suspected cases were reported from Dori, 6 (46%) of the 13 confirmed NmX cases were reported from this district.

Molecular Typing and Phylogeny

A total of 18 clinical specimens from the outbreak, collected during January 28–May 6 from Diapaga zones 1–3 (9 specimens from zone 1, 6 from zone 2, 3 from zone 3), were whole-genome sequenced at the CDC Bacterial Meningitis Laboratory. The patients from whom the specimens were collected came from 13 different villages. All 18 *N. meningitidis* strains belonged to serogroup C and ST10217, the core ST of CC10217. In addition, all specimens shared the same variant type: PorA type P1.21-15,16; FetA type F1–7; and PorB type 3–463. Phylogenetic analysis (Figure 5) indicated the *N. meningitidis* strain from Burkina Faso shared a common ancestor with ST10217 strains that have been causing disease in Niger and Nigeria since 2013. The strains most closely related to those from Burkina Faso were isolates collected from Niger in 2017.

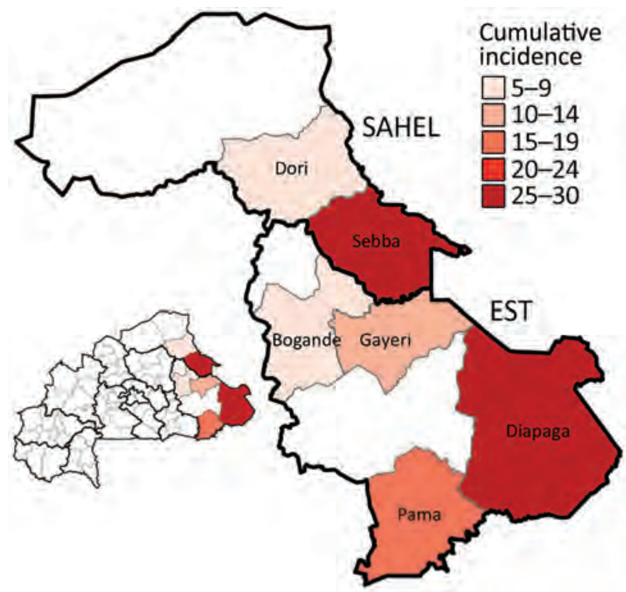

Figure 2. Meningitis cumulative incidence (cases/100,000 population) across 6 affected districts in the Sahel and Est regions of Burkina Faso in study of expansion of *Neisseria meningitidis* serogroup C clonal complex 10217 during meningitis outbreak, January 28–May 5, 2019. Colors indicate incidence of meningitis cases per 100,000 population. Inset map shows location of surveilled regions in Burkina Faso.

Discussion

We report an NmC ST10217 outbreak in Burkina Faso, which occurred during the 2019 epidemic season, that demonstrates the expansion of this epidemic-prone strain into and within Burkina Faso. Despite a history of this strain causing large epidemics, the 2019 outbreak in Burkina Faso remained relatively small, possibly because of the responsive national surveillance system and rapid implementation of reactive vaccination campaigns.

According to the ICG's performance indicator for timely outbreak response, a country should take <28 days from the time of crossing the meningitis epidemic threshold to implementing a reactive vaccination campaign. Both vaccination campaigns in Diapaga exceeded this indicator; the first vaccination campaign using national vaccine stock in zone 1 was initiated in 6 days, and the second campaign in zones 2, 3, and 4 was initiated 26 days after crossing the epidemic threshold. However, the third vaccination

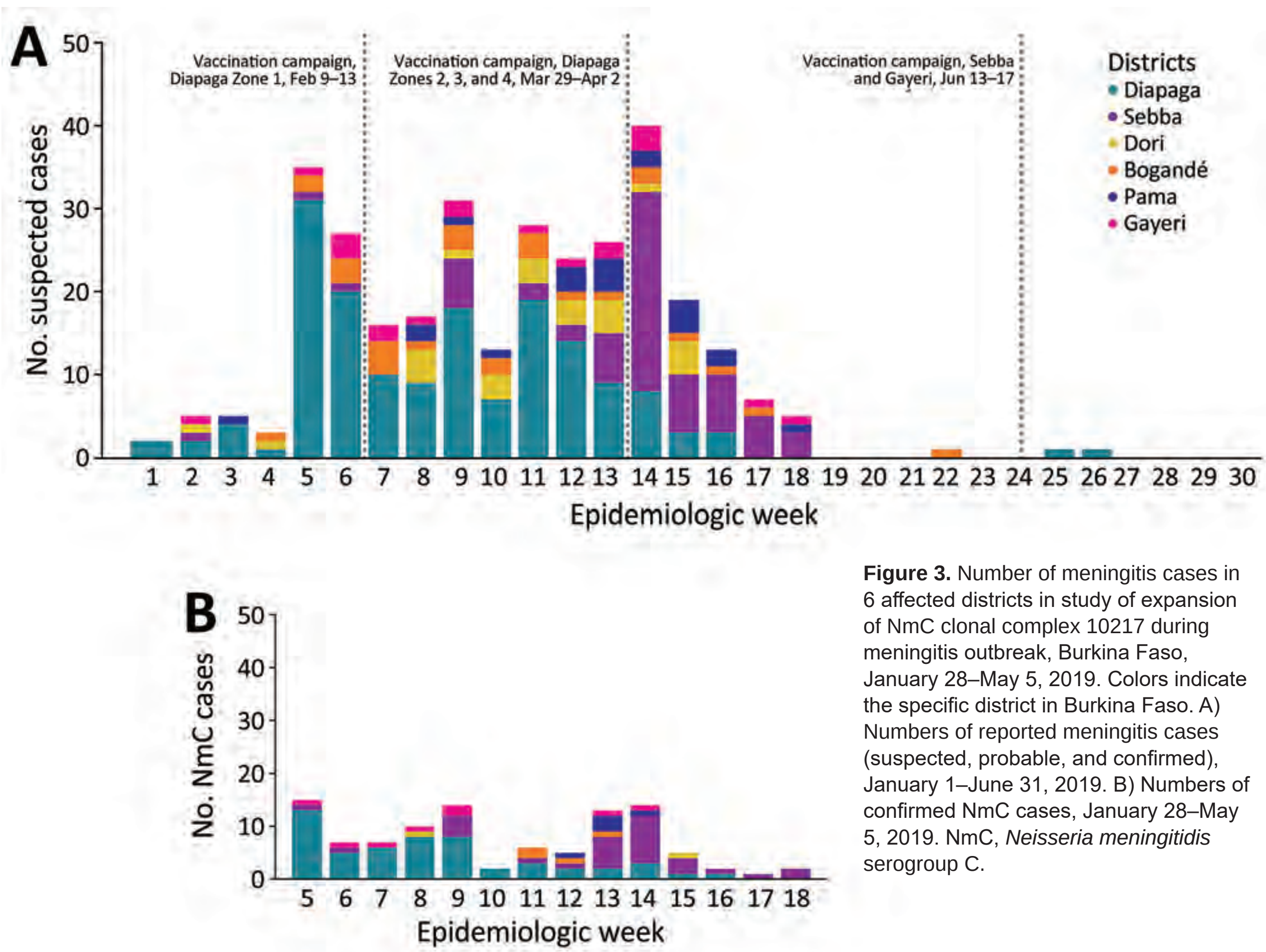

Figure 3. Number of meningitis cases in 6 affected districts in study of expansion of NmC clonal complex 10217 during meningitis outbreak, Burkina Faso, January 28–May 5, 2019. Colors indicate the specific district in Burkina Faso. A) Numbers of reported meningitis cases (suspected, probable, and confirmed), January 1–June 31, 2019. B) Numbers of confirmed NmC cases, January 28–May 5, 2019. NmC, *Neisseria meningitidis* serogroup C.

campaign in Sebba and Gayeri was delayed and was implemented 67 days after crossing the epidemic threshold. Key factors affecting vaccination campaign plans in Sebba and Gayeri were geographic barriers and insecurity that made some of the target areas difficult to access. The high proportion of collected specimens, rapid specimen transport to and confirmatory testing at the NRL, and rapid transmission of available surveillance data through STELAB enabled swift outbreak confirmation and coordination of response efforts. Furthermore, the availability of vaccines in the national stockpile likely expedited the particularly rapid response (6 days) for the first vaccination campaign in Diapaga zone 1, highlighting the utility of having decentralized vaccine stockpiles at national and regional levels. This strategy might become more feasible once a sufficient stock of the upcoming NmCV-5 pentavalent conjugate vaccine covering serogroups A, C, Y, W, and X becomes available (*21*). The NmCV-5 vaccine was prequalified in July 2023 and is expected to be available in ICG's emergency stockpile in early 2024.

Recognizing NmC ST10217's potential to cause explosive outbreaks and continued expansion, at-risk countries in the region should continue prioritizing, investing, and building a responsive meningitis surveillance and laboratory network to rapidly guide vaccination response in outbreak

Table 1. Number of PCR-confirmed bacterial meningitis cases during January 28–May 5, 2019, in study of *Neisseria meningitidis* serogroup C clonal complex 10217 expansion in Burkina Faso*

Bacteria	No. (%) cases
Neisseria meningitidis	
Serogroup A	0
Serogroup B	0
Serogroup C	103 (75)
Serogroup W	0
Serogroup X	13 (9)
Serogroup Y	0
Streptococcus pneumoniae	16 (12)
Haemophilus influenzae	
Type b	2 (1)
Non-b	3 (2)
Total	137

*Cases were from Diapaga, Sebba, Dori, Bogandé, Sebba, and Gayeri districts.

Table 2. Number of reported cases of meningitis according to causative pathogen during January 28–May 5, 2019, in study of *Neisseria meningitidis* serogroup C clonal complex 10217 expansion in Burkina Faso*

Characteristics	Suspected/probable cases†	Confirmed cases, n = 137			
		NmC	NmX	*Streptococcus pneumoniae*	*Haemophilus influenzae*
Total no. cases	164	103	13	16	5
Patient sex					
F	92 (56)	45 (44)	3 (23)	5 (31)	3 (60)
M	72 (44)	58 (56)	10 (77)	11 (69)	2 (40)
Districts reporting cases					
Diapaga	87 (53)	54 (52)	6 (46)	2 (13)	2 (40)
Sebba	33 (20)	30 (29)	0	1 (6)	0
Dori	13 (8)	2 (2)	6 (46)	2 (13)	0
Bogandé	14 (9)	4 (4)	0	4 (25)	3 (60)
Pama	10 (6)	5 (5)	0	5 (31)	0
Gayeri	7 (4)	8 (8)	1 (8)	2 (13)	0

*Values are no. (%). A total of 301 cases were reported. NmC, *Neisseria meningitidis* serogroup C; NmX, *Neisseria meningitidis* serogroup X.
†Includes 3 cases that met the definition of a probable case as previously described (*18*).

settings. Smaller focal *N. meningitidis* outbreaks should not be overlooked because a characteristic pattern of meningococcal disease is for a local outbreak to presage a large widespread epidemic (*22*). Before the rollout of MenAfriVac, large epidemic waves caused by NmA were observed over several decades; small, focal outbreaks preceded an explosive epidemic every 5–12 years (*23*,*24*). The major variation in incidence observed with those epidemic waves is believed to be unique to meningococcus (*24*). Thus, despite the smaller magnitude of the 2019 NmC meningitis outbreak compared with those in 2015 and 2017, NmC will likely not disappear from the region without vaccine intervention. NmC continued to be detected in the meningitis belt during 2020–2023 (*25*). Awareness of potential increases in NmC meningitis cases during the next meningitis season will be critical. Although not the dominant pathogens detected, meningitis cases caused by *S. pneumoniae* and *H. influenzae* were also reported during this outbreak. Burkina Faso introduced the *H. influenzae* type b conjugate vaccine in 2006 and the 13-valent pneumococcal conjugate vaccine in 2013. Further analyses of serotype data will help strengthen surveillance and monitoring of invasive disease caused by those bacteria.

The pattern and manifestation of the 2019 meningitis outbreak during the dry season, which is dominated by the Harmattan winds, is consistent with the typical seasonality of meningococcal meningitis outbreaks in the region (*26*–*28*). Similarly, the age distribution of patients with confirmed NmC infections did not differ much from what has been typically observed for meningococcal disease; 86% of patients with confirmed NmC were 5–29 years of age (*11*). However, the difference in age distribution between confirmed NmC and suspected cases during the 2019 outbreak suggests that a substantial percentage of the suspected cases are likely not false negatives but might represent other pathogens or indicate increased care-seeking among certain age groups. The difference is expected because the suspected case definition is designed to have high sensitivity but low specificity, and

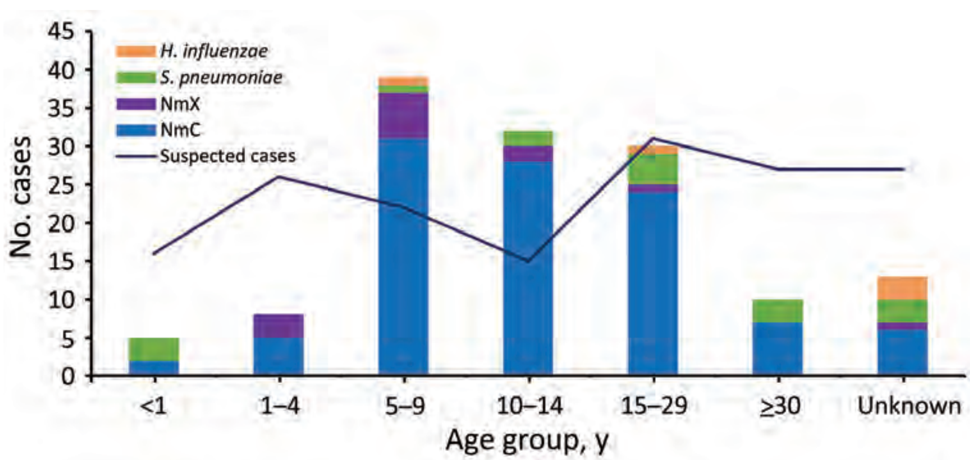

Figure 4. Age distribution of patients with suspected and confirmed meningitis in study of expansion of NmC clonal complex 10217 during meningitis outbreak, Burkina Faso, January 28–May 5, 2019. Data are from districts of Diapaga, Sebba, Dori, Bogandé, Sebba, and Gayeri, Colors indicate the confirmed cause of meningitis; black line indicates number of suspected cases for each age group. The number of suspected cases includes 3 cases that met the definition of a probable case as previously described (*18*). NmC, *Neisseria meningitidis* serogroup C; NmX, *N. meningitidis* serogroup X.

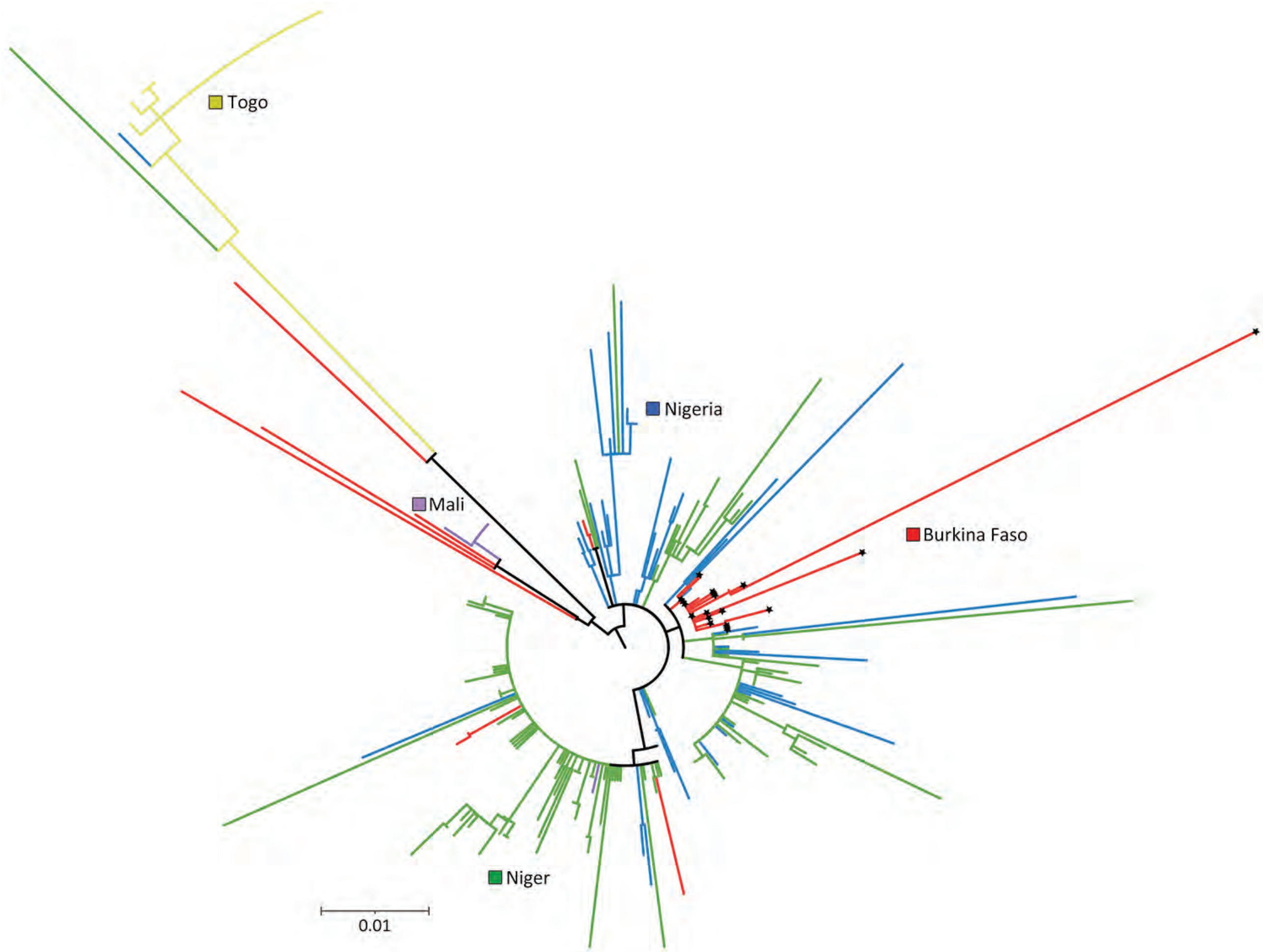

Figure 5. Phylogenetic analysis of *Neisseria meningitidis* clonal complex 10217 isolates from invasive meningitis cases collected during 2012–2019 in Mali, Nigeria, Burkina Faso, Togo, and Niger used in study of expansion of *N. meningitidis* serogroup C during meningitis outbreak, Burkina Faso, January 28–May 5, 2019. Colors indicate the major clades/subclades found in each country. Solid black stars on nodes indicate isolates from the Burkina Faso outbreak in 2019. Scale bar indicates nucleotide substitutions per site.

many other diseases manifest symptoms similar to bacterial meningitis.

Three key limitations affected the analysis of the 2019 NmC infection outbreak. First, the ongoing humanitarian crisis in Burkina Faso caused by clashes between armed extremist groups has resulted in a greater need for resources to implement public health interventions. Security concerns have led to large-scale internal displacement of citizens, as well as health facility closures (*29*). During the 2019 meningitis season, this crisis affected several of the areas that reported NmC cases. The humanitarian crisis might have reduced the likelihood of symptomatic persons effectively seeking healthcare and, thus, reduced the number of reported cases. In addition, incidence estimates relied on population projections from 2010, which were unable to account for major population movements, such as those caused by internal displacement. Second, data discrepancies between STELAB and TLOH were observed. In TLOH, 292 suspected cases were reported during the outbreak (compared with 301 in CBS), and a case-fatality rate of 8.2% was reported (compared with 5.6% in CBS). Data discrepancies and potential underreporting suggest that outbreak characteristics and cases reported in this study are not fully representative of all NmC cases that occurred during the outbreak. Third, administrative vaccine coverage estimates, which were used to approximate reactive vaccination coverage after the outbreak, can be biased because of inaccurate numerators or denominators (*30*). Coverage estimates for all 3 vaccination campaigns conducted during this outbreak are likely overestimates because inflated numerators caused by population movement were heavily affected by the ongoing humanitarian crisis.

In conclusion, meningococcal meningitis remains a serious public health threat within the meningitis belt of Africa. The 2019 NmC outbreak in Burkina Faso shows that a responsive national surveillance system and laboratory network providing timely, spatially explicit case-level data can strengthen outbreak monitoring, response efforts, and tracking of bacteria strains across the region. Detection of NmC ST10217, the strain responsible for previous large-scale epidemics in Niger and Nigeria and the cause of the 2019 Burkina Faso meningitis outbreak, reaffirms the capacity for novel strains to cross geographic boundaries. Preventive mass vaccination campaigns using a long-lasting meningococcal conjugate vaccine have proved effective in dramatically reducing disease, as demonstrated by the national rollout of the MenAfriVac vaccine across the belt. Since the 2019 outbreak in Burkina Faso, 3 consecutive NmC outbreaks have occurred in neighboring Niger during the 2020–2023 epidemic seasons (*25*). The NmC outbreak in Niger during the 2022–23 season also spread to neighboring districts in Nigeria (*31*). Continued NmC outbreaks documented in the belt since the 2019 outbreak and circulation of other *N. meningitidis* non-A serogroups in the region indicate a crucial need for the NmCV-5 vaccine (*21*). In particular, stocking this vaccine at the regional or national level would help ensure that vaccines are immediately ready for use in regional vaccination campaigns when needed. This vaccine strategy could substantially reduce disease caused by nonserogroup A meningococcal pathogens and serves as a key step toward eliminating meningitis outbreaks in the meningitis belt.

Acknowledgments

We thank the Burkina Faso Ministry of Health and the Burkina Faso national health system, including all participating health centers, laboratories, and patients, for their contributions to this article.

About the Author

Ms. Kekeisen-Chen is an epidemiologist in the Meningitis and Vaccine Preventable Diseases Branch, Division of Bacterial Diseases, National Center for Immunization and Respiratory Diseases, Centers for Disease Control and Prevention, Atlanta, Georgia, USA. Her research interests focus on bacterial meningitis, vaccine evaluation, and utilizing implementation science to strengthen bacterial meningitis outbreak response efforts in Africa.

References

1. Diallo AO, Kiemtoré T, Bicaba BW, Medah I, Tarbangdo TF, Sanou S, et al. Development and implementation of a cloud-based meningitis surveillance and specimen tracking system in Burkina Faso, 2018. J Infect Dis. 2019;220:S198–205. https://doi.org/10.1093/infdis/jiz376
2. Patel JC, Soeters HM, Diallo AO, Bicaba BW, Kadadé G, Dembélé AY, et al.; MenAfriNet Consortium. MenAfriNet: a network supporting case-based meningitis surveillance and vaccine evaluation in the meningitis belt of Africa. J Infect Dis. 2019;220:S148–54. https://doi.org/10.1093/infdis/jiz308
3. Greenwood B. Manson lecture. Meningococcal meningitis in Africa. Trans R Soc Trop Med Hyg. 1999;93:341–53. https://doi.org/10.1016/s0035-9203(99)90106-2
4. Lingani C, Bergeron-Caron C, Stuart JM, Fernandez K, Djingarey MH, Ronveaux O, et al. Meningococcal meningitis surveillance in the African meningitis belt, 2004–2013. Clin Infect Dis. 2015;61:S410–5. https://doi.org/10.1093/cid/civ597
5. Alderson MR, LaForce FM, Sobanjo-Ter Meulen A, Hwang A, Preziosi MP, Klugman KP. Eliminating meningococcal epidemics from the African meningitis belt: the case for advanced prevention and control using next-generation neningococcal conjugate vaccines. J Infect Dis. 2019;220:S274–8. https://doi.org/10.1093/infdis/jiz297
6. Continuing risk of meningitis due to Neisseria meningitidis serogroup C in Africa: revised recommendations from a WHO expert consultation. Wkly Epidemiol Rec. 2017;92:612–7.
7. Whittle HC, Evans-Jones G, Onyewotu I, Adjukiewicz A, Turunen U, Crockford J, et al. Group-C meningococcal meningitis in the northern savanna of Africa. Lancet. 1975;305:1377. https://doi.org/10.1016/S0140-6736(75)92281-3
8. Broome CV, Rugh MA, Yada AA, Giat L, Giat H, Zeltner JM, et al. Epidemic group C meningococcal meningitis in Upper Volta, 1979. Bull World Health Organ. 1983;61:325–30.
9. Koumare B, Achtman M, Cisse M, Wang JF, Giovanna M, Doumbia T. Etude antigénique de 337 souches de *Neisseria meningitidis* isolées au Mali. Intérêt épidémiologique et vaccinal. Med Mal Infect. 1995;25:1132–6. https://doi.org/10.1016/S0399-077X(05)80403-2
10. Chow J, Uadiale K, Bestman A, Kamau C, Caugant DA, Shehu A, et al. Invasive meningococcal meningitis serogroup C outbreak in northwest Nigeria, 2015—third consecutive outbreak of a new strain. PLoS Curr. 2016;8: ecurrents.outbreaks.06d10b6b4e690917d8b0a04268906143. https://doi.org/10.1371/currents.outbreaks.06d10b6b4e690917d8b0a04268906143
11. Funk A, Uadiale K, Kamau C, Caugant DA, Ango U, Greig J. Sequential outbreaks due to a new strain of *Neisseria meningitidis* serogroup C in northern Nigeria, 2013–14. PLoS Curr. 2014;6:ecurrents.outbreaks.b50c2aaf1032b3ccade0fca0b63ee518. https://doi.org/10.1371/currents.outbreaks.b50c2aaf1032b3ccade0fca0b63ee518
12. Sidikou F, Zaneidou M, Alkassoum I, Schwartz S, Issaka B, Obama R, et al.; MenAfriNet consortium. Emergence of epidemic *Neisseria meningitidis* serogroup C in Niger, 2015: an analysis of national surveillance data. Lancet Infect Dis. 2016;16:1288–94. https://doi.org/10.1016/S1473-3099(16)30253-5
13. Nnadi C, Oladejo J, Yennan S, Ogunleye A, Agbai C, Bakare L, et al. Large outbreak of *Neisseria meningitidis* serogroup C—Nigeria, December 2016–June 2017. MMWR Morb Mortal Wkly Rep. 2017;66:1352–6. https://doi.org/10.15585/mmwr.mm6649a3
14. Kretz CB, Retchless AC, Sidikou F, Issaka B, Ousmane S, Schwartz S, et al.; Niger Response Team. Whole-genome

characterization of epidemic *Neisseria meningitidis* serogroup C and resurgence of serogroup W, Niger, 2015. Emerg Infect Dis. 2016;22:1762–8. https://doi.org/10.3201/eid2210.160468
15. Brynildsrud OB, Eldholm V, Bohlin J, Uadiale K, Obaro S, Caugant DA. Acquisition of virulence genes by a carrier strain gave rise to the ongoing epidemics of meningococcal disease in West Africa. Proc Natl Acad Sci USA. 2018;115:5510–5. https://doi.org/10.1073/pnas.1802298115
16. World Health Organization. WHO and partners provide vaccines to control meningitis C in Nigeria. April 13, 2017 [cited 2022 Feb 10]. https://www.who.int/news/item/13-04-2017-who-and-partners-provide-vaccines-to-control-meningitis-c-in-nigeria
17. Novak RT, Kambou JL, Diomandé FV, Tarbangdo TF, Ouédraogo-Traoré R, Sangaré L, et al. Serogroup A meningococcal conjugate vaccination in Burkina Faso: analysis of national surveillance data. Lancet Infect Dis. 2012;12:757–64. https://doi.org/10.1016/S1473-3099(12)70168-8
18. World Health Organization. Standard operating procedures for surveillance of meningitis preparedness and response to epidemics in Africa. October 2018 [cited 2022 Feb 10]. https://apps.who.int/iris/bitstream/handle/10665/312141/9789290234241-eng.pdf
19. Itsko M, Retchless AC, Joseph SJ, Norris Turner A, Bazan JA, Sadji AY, et al. Full molecular typing of *Neisseria meningitidis* directly from clinical specimens for outbreak investigation. J Clin Microbiol. 2020;58:e01780-20. https://doi.org/10.1128/JCM.01780-20
20. Dolan Thomas J, Hatcher CP, Satterfield DA, Theodore MJ, Bach MC, Linscott KB, et al. sodC-based real-time PCR for detection of *Neisseria meningitidis*. PLoS One. 2011;6:e19361. https://doi.org/10.1371/journal.pone.0019361
21. Katz S, Townsend-Payne K, Louth J, Lee-Jones L, Trotter C, Dan Dano I, et al.; MenAfriCar Consortium. Validation and use of a serum bactericidal antibody assay for *Neisseria meningitidis* serogroup X in a seroprevalence study in Niger, West Africa. Vaccine. 2022;40:6042–7. https://doi.org/10.1016/j.vaccine.2022.08.013
22. World Health Organization. Control of epidemic meningococcal disease. WHO practical guidelines. 2nd edition. March 22, 1998 [cited 2022 Feb 10]. https://www.who.int/publications/i/item/control-of-epidemic-meningococcal-disease
23. Teyssou R, Muros-Le Rouzic E. Meningitis epidemics in Africa: a brief overview. Vaccine. 2007;25:A3–7. https://doi.org/10.1016/j.vaccine.2007.04.032
24. Mueller JE, Gessner BD. A hypothetical explanatory model for meningococcal meningitis in the African meningitis belt. Int J Infect Dis. 2010;14:e553–9. https://doi.org/10.1016/j.ijid.2009.08.013
25. World Health Organization Regional Office for Africa. Enhanced surveillance of meningitis in Africa, Republic of Congo, 2020–2023 [cited 2023 Aug 1]. https://app.powerbi.com/view?r=eyJrIjoiMzExZTUzZDAtMmQ5Ni00YjkxLWFmZmItODljOWZhOTMyM2Y3IiwidCI6ImY2MTBjMGI3LWJkMjQtNGIzOS04MTBiLTNkYzI4MGFmYjU5MCIsImMiOjh9
26. Sultan B, Labadi K, Guégan JF, Janicot S. Climate drives the meningitis epidemics onset in West Africa. PLoS Med. 2005;2:e6. https://doi.org/10.1371/journal.pmed.0020006
27. Molesworth AM, Cuevas LE, Connor SJ, Morse AP, Thomson MC. Environmental risk and meningitis epidemics in Africa. Emerg Infect Dis. 2003;9:1287–93. https://doi.org/10.3201/eid0910.030182
28. Palmgren H. Meningococcal disease and climate. Glob Health Action. 2009;2:1. https://doi.org/10.3402/gha.v2i0.2061
29. Norwegian Refugee Council. Burkina Faso: almost 2 million people displaced amid worst food crisis in a decade. Sep 5, 2022 [cited 2022 Oct 5]. https://www.nrc.no/news/2022/september/burkina-faso-almost-2-million-people--now-displaced-amid-worst-food-crisis-in-a-decad
30. World Health Organization. Assessing and improving the accuracy of target population estimates for immunization coverage. 2015 [cited 2022 Jun 1]. https://www.who.int/publications/m/item/assessing-and-improving-the-accuracy-of-target-population-estimates-for-immunization-coverage
31. Nigeria Centre for Disease Control and Prevention. Cerebrospinal meningitis situation report, report 06, epidemiological week 23–26 (June 5–July 2, 2023) [cited 2023 Aug 1]. https://ncdc.gov.ng/diseases/sitreps/?cat=6&name=An%20Update%20of%20Meningitis%20Outbreak%20in%20Nigeria

Address for correspondence: Joann F. Kekeisen-Chen, Centers for Disease Control and Prevention, 1600 Clifton Rd NE, Mailstop H24-6, Atlanta, GA 30329-4018, USA; email: pvv4@cdc.gov

Microsporidia (*Encephalitozoon cuniculi*) in Patients with Degenerative Hip and Knee Disease, Czech Republic

Bohumil Sak, Petra Gottliebová, Elka Nyčová, Nikola Holubová, Jana Fenclová, Marta Kicia, Żaneta Zajączkowska, Martin Kváč

Total joint arthroplasty is a commonly used surgical procedure in orthopedics. Revision surgeries are required in >10% of patients mainly because of prosthetic joint infection caused by bacteria or aseptic implant loosening caused by chronic inflammation. *Encephalitozoon cuniculi* is a microsporidium, an obligate intracellular parasite, capable of exploiting migrating proinflammatory immune cells for dissemination within the host. We used molecular detection methods to evaluate the incidence of *E. cuniculi* among patients who had total hip or knee arthroplasty revision. Out of 49 patients, *E. cuniculi* genotypes I, II, or III were confirmed in joint samples from 3 men and 2 women who had implant loosening. Understanding the risks associated with the presence of microsporidia in periprosthetic joint infections is essential for proper management of arthroplasty. Furthermore, *E. cuniculi* should be considered a potential contributing cause of joint inflammation and arthrosis.

Microsporidia are a group of obligate intracellular parasites comprising ≈1,300 species within >200 genera (*1*). Microsporidia are considered to be closely related to fungi (*2*,*3*) and infect a broad range of invertebrates and vertebrates, from protists to humans (*4*). Because of improved detection methods and greater awareness, microsporidia have been detected in a broad range of human populations, including children, travelers, elderly persons, and organ transplant recipients (*5*). Persons with high exposure to animals and contaminated soil and water are considered at risk for microsporidiosis (*6*). Of the several species of microsporidia that infect humans, *Encephalitozoon cuniculi* is the most common (*7*). Four genotypes of *E. cuniculi* have been identified on the basis of variable repeats in the rRNA internal transcribed spacer; however, human infections are mostly associated with genotypes I and II (*8*).

The digestive tract is an entrance point for microsporidia and subsequent spreading of infection occurs in all parts of the intestine. Within weeks, infection spreads to other tissues and organs, most commonly the kidney, liver, spleen, lung, and brain, depending on the species-specific interaction with the host (*8*). However, the unique mechanism of host cell invasion involving a highly specialized structure, the 10–50 µm long polar filament, enables only limited spread over short distances within the host. Therefore, the dissemination rate suggests the possible engagement of macrophages or other immune cells involved in inflammatory responses, which can serve as vehicles transporting microsporidia to foci outside of the intestine (*9*,*10*). Microsporidia are often overlooked in clinical samples because of problematic diagnoses, increasing the likelihood of hidden infections that can cause extensive tissue damage and various nonspecific pathologies and that often go without effective treatment (*11*).

Total joint arthroplasty is one of the most common surgical procedures in orthopedics to replace joints in patients with degenerative diseases (*12*). Revision surgeries are required in >10% of those patients because of implant failure caused mainly by prosthetic joint infection and aseptic implant loosening from inflammation (*13*,*14*). Whereas prosthetic joint infection is caused by bacterial infection (e.g.,

Author affiliations: Biology Centre of the Czech Academy of Sciences, České Budějovice, Czech Republic (B. Sak, N. Holubová, J. Fenclová, M. Kváč); Bulovka Hospital, Prague, Czech Republic (P. Gottliebová, E. Nyčová); University of South Bohemia, České Budějovice (J. Fenclová, M. Kváč); Wroclaw Medical University, Wroclaw, Poland (M. Kicia, Ż. Zajączkowska)

DOI: https://doi.org/10.3201/eid3003.231263

Staphylococcus aureus, *Streptococcus* spp., and *Enterococcus faecalis*) and pathologic growth around the prosthetic joint (*15*), aseptic implant loosening results from chronic inflammation caused by activation of resident immune cells in contact with implant wear debris or allergic reactions to metal ions derived from implant materials (*16*). However, the classification of aseptic implant loosening might be misleading because other pathogens are often overlooked, and the condition is potentially mislabeled as aseptic (*17*).

E. cuniculi is considered a cause of osteolysis in hip periprosthetic tissue (*17*), and connections between proinflammatory immune responses and concentration of *E. cuniculi* in inflammatory foci have been reported (*9,10*). Understanding the risks for microsporidiosis within periprosthetic joints is essential for proper arthroplasty management. We evaluated the incidence of generally neglected microsporidia among patients who had total hip or knee arthroplasty revision.

Methods

Patients

We investigated samples obtained from immunocompetent patients who were hospitalized or who visited the orthopedic clinic at Bulovka Hospital (Prague, Czech Republic) during May 2020–September 2021. The first group of patients had undergone a hip puncture/total hip revision arthroplasty, and the second group had undergone a knee puncture/knee revision arthroplasty (in 1 case, the patient only underwent a knee arthroscopy). We assigned patients to 3 diagnostic groups according to microbiologic cultures and criteria of the Infectious Diseases Society of America or the Musculoskeletal Infection Society for periprosthetic joint infection according to the judgement of the treating physician: periprosthetic joint infection, aseptic implant loosening (aseptic loosening was diagnosed when signs of implant loosening were present, but infection was not the cause), and other diagnosis (patients who did not fit into the first 2 groups) (*18,19*).

Sample Collection

Fragments of periprosthetic hip and knee tissues and joint fluids were collected intraoperatively; joint aspirates were collected during knee or hip punctures. Samples for microbiologic culture (i.e., samples of joint tissues, joint fluids, and surgical swabs from the endoprosthesis, tissues, or joints) were gathered intraoperatively. The number of samples collected was at the discretion of the orthopedic surgeon. Surgical swabs or other samples with insufficient volumes were excluded from the study. All samples were collected under sterile conditions. Each sample was placed in a separate sterile container and delivered at room temperature (20°–25°C) to the Department of Clinical Microbiology at Bulovka Hospital. Samples collected outside of laboratory working hours were maintained at room temperature (20°–25°C) overnight and then processed.

Samples were processed in a laminar flow cabinet for microbiologic culture; aliquots were stored without preservatives at −20°C for further molecular investigation and sent to the Biology Centre of the Czech Academy of Sciences for microsporidia screening. For *Neisseria* identification, we inoculated samples onto GO blood agar (LabMediaServis s.r.o., https://www.labmediaservis.cz) and 5% sheep blood agar, and incubated at 37°C in 5% CO_2 for 24 h for GO blood agar and 48 h for 5% sheep blood agar. We cultured samples on Endo agar, in liver broth, and on sheep blood agar (containing 10% NaCl) at 37°C in an aerobic atmosphere for 24 h and 48 h (blood agar). After 24 h, we subcultured the liver broth on 5% sheep blood agar in a 5% CO_2 atmosphere and Endo agar in an aerobic atmosphere for another 24 h. We examined cultures for bacterial growth after 24 h and 48 h (GO blood agar). If no growth occurred, we incubated the 5% sheep blood agar and GO blood agar cultures for 7 d. For anaerobic cultures, we inoculated patient samples onto Schaedler agar and in thioglycolate broth and cultured in an anaerobic atmosphere for 48 h and a total of 7 d. Depending on the microbiologist's decision, we subcultured the thioglycolate broth cultures onto Schaedler agar. We identified all bacteria by using standard laboratory procedures, including biochemical testing, by using the BD Phoenix system (Becton Dickinson, https://www.bd.com), and, in the case of *Salmonella* Enteritidis, by serotyping. We performed antimicrobial drug susceptibility testing by using European Committee on Antimicrobial Susceptibility Testing methodology (https://www.eucast.org). We prepared fungal cultures on Sabouraud agar only when requested by the orthopedic surgeon; those plates were incubated aerobically at 37°C for 48 h, examined, and then cultured for a total of 7 d.

DNA Isolation

We used aliquots of tissue and primary materials from joint aspirates and fluids from each patient for DNA isolation. We homogenized a total of 200 mg of tissue or aspirate sediment by using bead disruption on a FastPrep-24 instrument (MP Biomedicals, https://www.mpbio.com) at a speed of 5.5 m/s for 1 min. We extracted total DNA by using the DNeasy Blood and Tissue Kit (QIAGEN, https://www.qiagen.com) according to the manufacturer's instructions. We included an extraction negative control to each DNA extraction series to ensure the absence of contamination in reagents, consumables, and the environment. We stored extracted DNA at −20°C until PCR amplification. We isolated control DNA from purified *E. intestinalis* spores by using the same methods.

Molecular Examination

We amplified a partial sequence of the 16S rRNA gene that included the entire internal transcribed spacer by using nested PCR protocols with microsporidia-specific primers (*9*). We used DNA obtained from *E. intestinalis* spores as a positive PCR control and ultrapure water (without template) as a negative control in each PCR run. We evaluated the PCR products by gel electrophoresis.

We processed DNA from microsporidia PCR-positive samples by using a real-time quantitative PCR protocol that amplified a 268-bp region of the *E. cuniculi* 16S rRNA gene (*9*). We used negative controls comprising unspiked specimens and diluent blanks for each PCR. We determined positive results according to mathematical algorithms included with the LightCycler System (Roche, https://www.roche.com); results were positive when the cycle threshold was ≤43. We calculated the total number of spores in 1 g of sample according to a standard curve derived from spore DNA that was serially diluted in water; dilutions ranged from 1 to 1×10^8 ($R^2 = 0.9903$).

Phylogenetic Analyses

We purified PCR amplicons by using the QIAquick Gel Extraction Kit (QIAGEN), and sequencing was performed in both directions at SeqMe (https://www.seqme.eu). Amplification and sequencing of each positive sample was repeated 3 times.

We manually edited the nucleotide sequences by using ChromasPro 2.1.4 (Technelysium, https://www.technelysium.com.au) and aligned the sequences with references from GenBank by using MAFFT version 7 (http://mafft.cbrc.jp). We performed phylogenetic analysis by using the maximum-likelihood method and evolutionary models selected by MEGA X software (MEGA, https://www.megasoftware.net). We inferred the evolutionary history for partial sequences of the 16S rRNA gene, the entire internal transcribed spacer region, and a partial sequence of the 5.8S rRNA gene by using neighbor-joining analyses and computed relationships between sequences by using the Tamura 3-parameter method, gamma distribution, and parametric bootstrap analysis of 1,000 replicates in MEGA X software.

Microscopic Examination

We examined microsporidia PCR-positive samples microscopically. We prepared slides by mechanically homogenizing tissue samples with a mortar and pestle and centrifuged aspirates at 13,000 × *g* for 10 min; we stained aspirate sediments and homogenized tissues with Calcofluor M2R (Sigma Aldrich, https://www.sigmaaldrich.com) (*17*).

Ethics Statement

We analyzed existing specimens beyond routine microbiologic screening, focusing on verifying the association between inflammatory disease and the presence of microsporidia in inflammatory foci. Because the study was performed by using samples with no human intervention arm, patient consent was not required.

Results

We screened a total of 94 samples from 49 patients who were 41–96 (median 71) years of age for microsporidia infection in tissues surrounding the operated hip and knee joints. The mean age was 71 (SD±9.3; range 41–84) among hip replacement patients and 70 (SD±9.0; range 62–96) years among knee replacement patients. The male to female ratio was 12 (36%) to 21 (64%) in the hip replacement group and 9 (56%) to 7 (44%) in knee replacement group. Most patients had prosthetic joint infections; only 3 patients had other diagnoses, and the remaining patients had aseptic implant loosening (Table 1). Laboratory examinations showed physiologic indicators were within reference ranges for all patients. Patients did not undergo immunosuppressive treatment during the study period.

Among screened patients, 16 underwent knee arthroplasty providing 36 samples, and 33 underwent hip arthroplasty providing 58 samples (Table 1). The number of samples obtained from patients was 1–7; multiple samples mostly represented more sample types (Figure 1). Most (n = 28) patients underwent primary revision, then secondary and further revisions (9 each); 3 patients underwent repeated surgery: primary/secondary revision (patient no. 24) and primary/third and further revision (patient nos. 9 and 19) (Figure 1).

Of the 94 samples examined, most (61) were microbiologically sterile, whereas 12 samples were positive for *S. aureus* (5 were methicillin resistant), 6 were positive for *Escherichia coli*, 3 were positive for *E. faecalis*, 3 were positive for *Salmonella* Enteritidis,

Table 1. Sample types, age of patients, surgical procedures, and diagnoses in study of microsporidia (*Encephalitozoon cuniculi*) in patients with degenerative hip and knee disease, Czech Republic*

	Periprosthetic joint infection			Aseptic implant loosening			Other diagnosis		
Sample type	NP/NS	PR/SR/TR	Mean age (SD)	NP/NS	PR/SR/TR	Mean age (SD)	NP/NS	PR/SR/TR	Mean age (SD)
Knees									
Joint fluid	7/8	4/2/1	72.7 (5.7)	NA	NA	NA	NA	NA	NA
Puncture aspirate	9/12	5/2/2	76.3 (8.9)	1/1	0/1/0	74	1/1	1/0/0	78
Joint tissue	9/14	5/1/3	73.0 (6.9)	NA	NA	NA	NA	NA	NA
Hips									
Joint fluid	11/13	6/2/3	68.3 (9.4)	9/9	5/3/1	69.1 (8.5)	NA	NA	NA
Puncture aspirate	7/8	6/0/1	66.9 (12.7)	1/1	1/0/0	74	NA	NA	NA
Joint tissue	10/17	5/2/3	71.9 (6.1)	6/8	5/1/0	70.5 (7.7)	2/2	0/0/2	69.5 (0.5)

*Samples were collected from immunocompetent patients during May 2020–September 2021 at Bulovka Hospital in Prague, Czech Republic. NA, not applicable; NP, number of patients; NS, number of samples; PR, primary revision; SR, secondary revision; TR, third and further revision.

2 were positive for *Staphylococcus epidermidis*, and 2 were positive for group G beta-hemolytic *Streptococcus*. *Streptococcus agalactiae*, *Corynebacterium tuberculostearicum*, *Pseudomonas aeruginosa*, or *Enterococcus faecium* were detected in the remaining samples.

Encephalitozoon-specific DNA was confirmed in samples from 3 men and 2 women who were 63–78 years of age. Phylogenetic analyses revealed *E. cuniculi* genotypes I, II, and III. The 5 sequences obtained in this study were 100% identical to GenBank sequences for *E. cuniculi* genotype I (accession no. KJ941140), II (accession no. MF062430), and III (accession no. KF736984) (Figure 2).

We detected microsporidia in knee or hip aspirates obtained during ambulatory puncture and joint fluids and tissues recovered intraoperatively for all 5 *Encephalitozoon*-positive patients (Table 2). Of those 5 patients, 3 had periprosthetic joint infection, and 2 had aseptic implant loosening. *E. cuniculi* genotype I was most often detected, in 8 knee and hip samples from 3 patients; the number of spores ranged from 12 to 5,600 per gram of sample. We detected *Encephalitozoon cuniculi* genotype II in a hip sample (260 spores/g sample) from 1 patient, and genotype III in a knee sample (6.9 spores/g sample) from 1 other patient (Table 2). Microscopic analysis of Calcofluor M2R–stained smears confirmed the presence of spores (2–5 spores per slide) in tissue samples obtained from patient nos. 2 and 29 who tested positive for *Encephalitozoon* DNA (Figure 3). Samples from the other 3 patients were microscopically negative for spores. Microbiologic tests showed bacterial infections within the tissues of 3 patients: group G beta-hemolytic *Streptococcus* in the knee of patient no. 1, *E. faecalis* in the knee of patient no. 29, and methicillin-resistant *S. aureus* in the hip of patient no. 2; the other 2 patients were clinically classified as aseptic (Table 2).

Discussion

Primary hip and knee arthroplasty ranks among the top 5 most common procedures performed and among the top 5 fastest growing procedures each year across all surgical disciplines (*20*). Total joint replacement improves function, reduces pain, and improves quality of life for patients, and is cost-effective (*21*,*22*). Despite the high success rate of modern total joint arthroplasty (*23*) and technologic advances designed to extend the lifetime of primary implants (*24*–*26*), modern implant bearings and well-fixed components have a finite lifespan

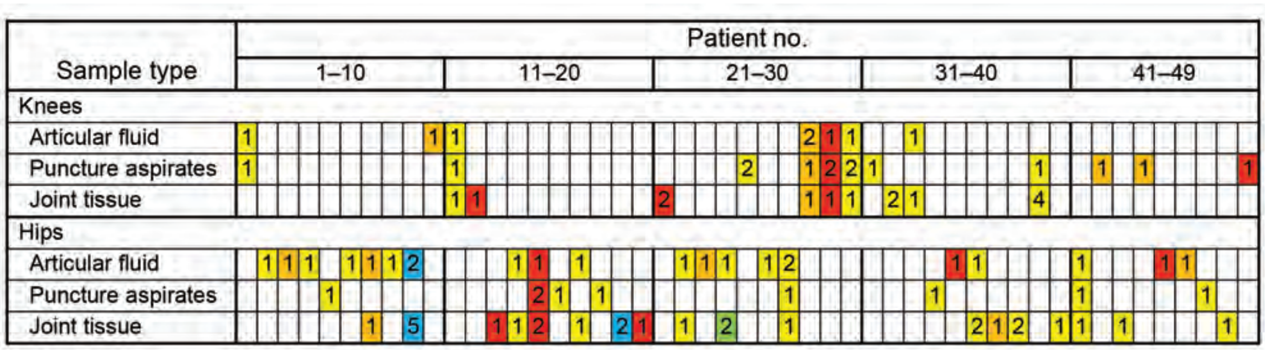

Figure 1. Samples obtained from each patient during revision surgery in study of microsporidia (*Encephalitozoon cuniculi*) in patients with degenerative hip and knee disease, Czech Republic. Samples were collected from immunocompetent patients during May 2020–September 2021 at Bulovka Hospital in Prague, Czech Republic. Numbers indicate the number of collected samples for each patient. Colors indicate the type of revision surgery: yellow, primary revision; orange, secondary revision; red, third and further revision; blue, both primary and third and further revision; green, both primary and secondary revision.

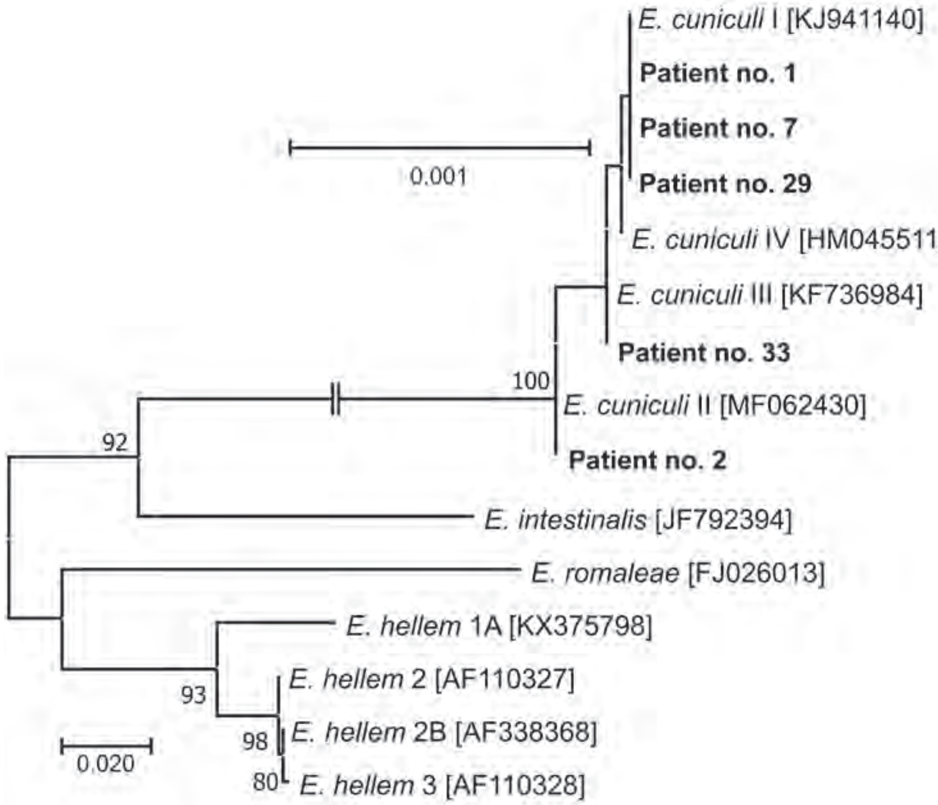

Figure 2. Phylogenetic analysis of *Encephalitozoon cuniculi* genotypes recovered from immunocompetent patients in study of microsporidia in patients with degenerative hip and knee disease, Czech Republic. Samples were collected from patients during May 2020–September 2021 at Bulovka Hospital in Prague. Partial sequences of 16S rRNA gene, the entire internal transcribed spacer region, and a partial sequence of 5.8S rRNA gene were inferred by using neighbor-joining analyses, and relationships were computed by using the Tamura 3-parameter method with gamma distribution and parametric bootstrap analysis of 1,000 replicates in MEGA X software (MEGA, https://www.megasoftware.net). Bold type indicates sequences obtained in this study, identified by patient number. Sequences for comparisons were obtained from GenBank; accession numbers are in brackets. Scale bar indicates nucleotide substitutions per site.

(*27*). Total joint replacements because of osteoarthritis require a revision procedure in 10% of patients, ≈4% within 10 years of initial surgery (*13*,*14*). Risk for revision increases in younger, more active patients and in those who have a higher body mass index (*28*). The most common reasons for revision surgery are infection, fracture around the implant, and loosening of the implant, which can occur soon after joint replacement or after decades of good function (*29*).

Prosthetic joint infection was detected in 34 (69.3%) of 49 patients we screened. Gram-positive cocci, such as *S. aureus*, coagulase-negative staphylococci, and *E. faecalis* are the major prosthetic joint infection-related microorganisms, after which Gram-negative bacilli are common (*30*–*32*); however, other pathogens are often overlooked, leading to an aseptic joint diagnosis. Microsporidia are often overlooked, fungus-related, obligate intracellular parasites occurring worldwide and infecting various vertebrate and invertebrate hosts, including humans (*33*,*34*); 17 species have been reported in humans, causing more severe symptoms in immunocompromised persons than in immunocompetent counterparts (*35*,*36*). *E. cuniculi* was the first microsporidium identified in mammals and the best-studied, forming the foundation of knowledge about microsporidia. *E. cuniculi* is typically described as a chronic, slow-acting pathogen and, thus, is considered less virulent than other pathogen groups; however, it can multiply successfully and extensively without any obvious signs of infection in immunocompetent hosts (*37*–*39*). *E. cuniculi* infects a wide spectrum of host cells, including epithelial cells, vascular endothelial cells, kidney tubule cells, and can be found in most tissues, having a propensity toward brain and kidneys (*40*). *E. cuniculi* is responsible for various pathologies depending on the infection site, affecting the nervous system as well as the respiratory and digestive tracts and causing hepatitis, peritonitis, pneumonitis, cystitis, nephritis, and encephalitis (*41*,*42*). Most documented cases originated from HIV/AIDS patients and transplant recipients. Whereas infection with *E. cuniculi* genotype I and II is common, occurrence of genotypes III and IV in humans is rare (*43*). As researchers and clinicians become more aware of those pathogens and are able to diagnose infections caused by them, new associations between microsporidia parasites and common infections have been reported (*17*,*44*). Moreover, *E. cuniculi* is able to survive and replicate in a variety of immune cells, including resident and migratory macrophages and

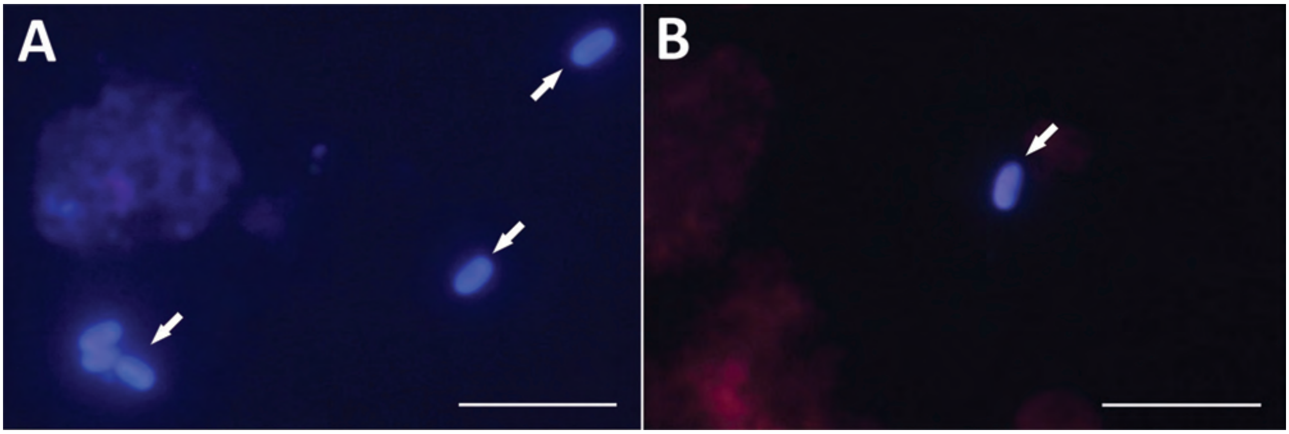

Figure 3. Microscopic analysis of *Encephalitozoon cuniculi* spores isolated from immunocompetent patients in study of microsporidia in patients with degenerative hip and knee disease, Czech Republic. Samples were collected from patients who tested positive for *Encephalitozoon* DNA during May 2020–September 2021 at Bulovka Hospital in Prague. Visualization of *E. cuniculi* from sample of knee joint fluid from patient no. 29 (A) and hip joint fluid from patient no. 2 (B). Arrows indicate *E. cuniculi* spores stained with Calcofluor M2R (Sigma Aldrich, https://www.sigmaaldrich.com) and viewed after fluorescence excitation at 490 nm wavelength. Scale bars are 10 µm.

other phagocytic cells, such as neutrophils, eosinophils, monocytes, and dendritic cells; thus, those immune cells might contribute to dissemination of *E. cuniculi* throughout the host organism (*45*,*46*).

The most common route of microsporidia transmission is the fecal-oral route; spores are passed in the urine or feces of infected persons into the environment and transmitted mostly through contaminated water sources (*43*). Microsporidia spores have been identified in wastewater, and in surface, irrigation, and drinking water. Moreover, several studies have reported foodborne transmission through fresh produce, such as strawberries, raspberries, lettuce, celery, parsley, and oranges, including orange juice. Recently, *E. cuniculi* has been reported in milk from dairy cows and goats, and the possibility of *E. cuniculi* transmission through pasteurized cow's milk, fermented pork products, and fresh goat cheese has been experimentally documented (*43*). Furthermore, infection in the respiratory tract suggests airborne transmission by contaminated aerosols (*43*).

E. cuniculi can survive and persist in immunocompetent hosts, even after chemotherapeutic treatment (*47*–*49*), and a latent infection can be activated by inflammation in the host body (*9*). A role for proinflammatory immune cells in the expansion of *E. cuniculi* infection in host tissues has been suggested because of the occurrence of microsporidia in inflamed tissues (*17*) and the targeted migration toward inflammatory foci seen after experimental induction of inflammation (*9*,*10*). Thus, the incidence of microsporidia infections might be much higher than previously reported, and microsporidia might represent a neglected etiologic agent for more common diseases, including prosthetic joint infection.

Table 2. Characteristics of immunocompetent patients and patient samples in study of microsporidia (*Encephalitozoon cuniculi*) in patients with degenerative hip and knee disease, Czech Republic*

Patient no.	Age, y/sex	Samples: Origin	Pathology	Total/no. positive†	Genotype‡	No. spores/g sample (Ct)§	Microbiology
1	78/M	Knee, PR, puncture aspirate, fluid	PJI	2/2	I	74 (37)	Group G beta-hemolytic *Streptococcus*
29	76/M	Knee, TR, 2 puncture aspirates, fluid, tissue	PJI	4/4	I	5,600 (33)	*Enterococcus faecalis*
33	63/F	Knee, PR, fluid, tissue	AIL	2/2	III	6.9 (39)	Aseptic
2	75/M	Hip, PR, fluid	PJI	1/1	II	260 (35)	*Staphylococcus aureus* (MRSA)
7	71/F	Hip, PR, fluid, tissue	AIL	2/2	I	12 (38)	Aseptic

*Samples were collected during May 2020–September 2021 at Bulovka Hospital in Prague, Czech Republic. AIL, aseptic implant loosening; Ct, cycle threshold; MRSA, methicillin-resistant *Staphylococcus aureus*; PJI, periprosthetic joint infection; PR, primary revision; TR, third and further revision.
†Total number of samples/number of *E. cuniculi*-positive samples.
‡*E. cuniculi* genotype was determined by nested PCR of partial sequence of the 16S rRNA gene that included the entire internal transcribed spacer.
§Number of spores was determined by quantitative real-time PCR of a 268-bp region of the *E. cuniculi* 16S rRNA gene. DNA was isolated from tissue or aspirate sediment.

We confirmed periprosthetic *E. cuniculi* infection in 3 patients who had prosthetic joint infection and 2 who had aseptic implant loosening. Moreover, the molecular data were supported by microscopy in 2 patients who had the highest spore loads. The other 3 *E. cuniculi* PCR-positive patients had negative microscopic results; those results were likely caused by limited sensitivity of microscopy in samples with low spore load rather than laboratory contamination of PCR. Because we obtained uniform results from multiple samples from specific patients by using both PCR and quantitative PCR, it is unlikely that contamination occurred in all samples from a particular patient at the same time and not in other samples. Laboratory contamination was excluded as a possible reason for our results because the samples were taken and PCR was performed under sterile conditions by the same trained personnel, and the PCR diagnostics workspace is structurally divided into separate areas adhering to a one-direction workflow.

Whether microsporidia infection occurred in the affected joint areas before the onset of inflammatory processes or whether they entered the affected areas secondarily through macrophages or other cells involved in inflammation remains unclear. Nevertheless, not only infective agents can induce inflammation. Implant-derived wear particles can also induce host inflammatory responses via opsonization by danger-associated molecular pattern molecules and recognition by Toll-like receptors (*50*). Therefore, *E. cuniculi* spores likely were transported to the joints within immune cells associated with proinflammatory immune responses.

In conclusion, *E. cuniculi* can occupy unusual extraintestinal locations, such as joint fluid or tissue, and should be considered a contributing cause of joint inflammation and arthrosis. However, the role of this pathogen in causing osteolysis and subsequent implant loosening needs to be clarified. The presence of microsporidia spores and DNA in periprosthetic tissue of immunocompetent hosts indicates active infection in those patients and should be considered in the history of the disease. In addition, microsporidia should be considered as a potential cause of periprosthetic osteolysis and implant destabilization after hip replacement.

This work was supported by grants from the Grant Agency of the Czech Republic (grant nos. 20-10706S and 23-06571S) and National Science Centre, Poland (grant no. 2020/39/O/NZ6/02313). The funders had no role in study design, data collection and analysis, decision to publish, or preparation of the manuscript.

About the Author

Dr. Sak is a research scientist at the Biology Centre of the Czech Academy of Sciences. His research interests focus on the detection of parasites, such as microsporidia, and diagnostics, isolation, in vitro cultivation, experimental infections, and morphologic and molecular characterization of parasites.

References

1. Cali A, Becnel JJ, Takvorian PM. Microsporidia. In: Archibald JM, Simpson AGB, Slamovits CH, editors. Handbook of the protists, 2nd edition. Cham (CH): Springer; 2017. p. 1559–618.
2. Edlind TD, Li J, Visvesvara GS, Vodkin MH, McLaughlin GL, Katiyar SK. Phylogenetic analysis of beta-tubulin sequences from amitochondrial protozoa. Mol Phylogenet Evol. 1996;5:359–67. https://doi.org/10.1006/mpev.1996.0031
3. Keeling PJ, Doolittle WF. Alpha-tubulin from early-diverging eukaryotic lineages and the evolution of the tubulin family. Mol Biol Evol. 1996;13:1297–305. https://doi.org/10.1093/oxfordjournals.molbev.a025576
4. Wittner M. Historic perspective on the microsporidia: expanding horizons. In: Wittner M, Weiss LM, editors. The microsporidia and microsporidiosis. Washington DC: American Association of Microbiology; 1999. p. 1–6.
5. Didier ES, Didier PJ, Snowden KF, Shadduck JA. Microsporidiosis in mammals. Microbes Infect. 2000;2:709–20. https://doi.org/10.1016/s1286-4579(00)00354-3
6. Sak B, Kučerová Z, Kváč M, Květoňová D, Rost M, Secor EW. Seropositivity for *Enterocytozoon bieneusi*, Czech Republic. Emerg Infect Dis. 2010;16:335–7. https://doi.org/10.3201/eid1602.090964
7. Didier ES. Microsporidiosis: an emerging and opportunistic infection in humans and animals. Acta Trop. 2005;94:61–76. https://doi.org/10.1016/j.actatropica.2005.01.010
8. Didier ES, Weiss LM. Microsporidiosis: not just in AIDS patients. Curr Opin Infect Dis. 2011;24:490–5. https://doi.org/10.1097/QCO.0b013e32834aa152
9. Brdíčková K, Sak B, Holubová N, Květoňová D, Hlásková L, Kicia M, et al. *Encephalitozoon cuniculi* genotype II concentrates in inflammation foci. J Inflamm Res. 2020;13:583–93. https://doi.org/10.2147/JIR.S271628
10. Sak B, Holubová N, Květoňová D, Hlásková L, Tinavská J, Kicia M, et al. Comparison of the concentration of *Encephalitozoon cuniculi* genotypes I and III in inflammatory foci under experimental conditions. J Inflamm Res. 2022;15:2721–30. https://doi.org/10.2147/JIR.S363509
11. Lallo MA, da Costa LFV, de Castro JM. Effect of three drugs against *Encephalitozoon cuniculi* infection in immunosuppressed mice. Antimicrob Agents Chemother. 2013;57:3067–71. https://doi.org/10.1128/AAC.00157-13
12. Kurtz SM, Lau E, Ong K, Zhao K, Kelly M, Bozic KJ. Future young patient demand for primary and revision joint replacement: national projections from 2010 to 2030. Clin Orthop Relat Res. 2009;467:2606–12. https://doi.org/10.1007/s11999-009-0834-6
13. Sloan M, Premkumar A, Sheth NP. Projected volume of primary total joint arthroplasty in the U.S., 2014 to 2030. J Bone Joint Surg Am. 2018;100:1455–60. https://doi.org/10.2106/JBJS.17.01617
14. Malchau H, Garellick G, Berry D, Harris WH, Robertson O, Kärrlholm J, et al. Arthroplasty implant registries over the past five decades: development, current, and future impact.

J Orthop Res. 2018;36:2319–30. https://doi.org/10.1002/jor.24014
15. Fernandez-Sampedro M, Salas-Venero C, Fariñas-Álvarez C, Sumillera M, Pérez-Carro L, Fakkas-Fernandez M, et al. 26Postoperative diagnosis and outcome in patients with revision arthroplasty for aseptic loosening. BMC Infect Dis. 2015;15:232. https://doi.org/10.1186/s12879-015-0976-y
16. Hodges NA, Sussman EM, Stegemann JP. Aseptic and septic prosthetic joint loosening: impact of biomaterial wear on immune cell function, inflammation, and infection. Biomaterials. 2021;278:121127. https://doi.org/10.1016/j.biomaterials.2021.121127
17. Kicia M, Wesolowska M, Kopacz Z, Kvác M, Sak B, Sokulska M, et al. Disseminated infection of *Encephalitozoon cuniculi* associated with osteolysis of hip periprosthetic tissue. Clin Infect Dis. 2018;67:1228–34. https://doi.org/10.1093/cid/ciy256
18. Osmon DR, Berbari EF, Berendt AR, Lew D, Zimmerli W, Steckelberg JM, et al.; Infectious Diseases Society of America. Diagnosis and management of prosthetic joint infection: clinical practice guidelines by the Infectious Diseases Society of America. Clin Infect Dis. 2013;56:e1–25. https://doi.org/10.1093/cid/cis803
19. Fillingham YA, Della Valle CJ, Suleiman LI, Springer BD, Gehrke T, Bini SA, et al. Definition of successful infection management and guidelines for reporting of outcomes after surgical treatment of periprosthetic joint infection: from the workgroup of the Musculoskeletal Infection Society (MSIS). J Bone Joint Surg Am. 2019;101:e69. https://doi.org/10.2106/JBJS.19.00062
20. Fingar KR, Stocks C, Weiss AJ, Steiner CA. Statistical brief #186. Most frequent operating room procedures performed in U.S. Hospitals, 2003–2012. In Healthcare Cost and Utilization Project (HCUP) statistical briefs. Rockville (MD): Agency for Healthcare Research and Quality; 2006.
21. Price AJ, Longino D, Rees J, Rout R, Pandit H, Javaid K, et al. Are pain and function better measures of outcome than revision rates after TKR in the younger patient? Knee. 2010;17:196–9. https://doi.org/10.1016/j.knee.2009.09.003
22. Dakin H, Gray A, Fitzpatrick R, MacLennan G, Murray D; KAT Trial Group. Rationing of total knee replacement: a cost-effectiveness analysis on a large trial data set. BMJ Open. 2012;2:e000332. PubMed https://doi.org/10.1136/bmjopen-2011-000332
23. Quintana JM, Arostegui I, Escobar A, Azkarate J, Goenaga JI, Lafuente I. Prevalence of knee and hip osteoarthritis and the appropriateness of joint replacement in an older population. Arch Intern Med. 2008;168:1576–84. https://doi.org/10.1001/archinte.168.14.1576
24. Lim SJ, Jang SP, Kim DW, Moon YW, Park YS. Primary ceramic-on-ceramic total hip arthroplasty using a 32-mm ceramic head with a titanium-alloy sleeve. Clin Orthop Relat Res. 2015;473:3781–7. https://doi.org/10.1007/s11999-015-4374-y
25. Delaunay CP, Putman S, Puliéro B, Bégin M, Migaud H, Bonnomet F. Cementless total hip arthroplasty with Metasul bearings provides good results in active young patients: a concise followup. Clin Orthop Relat Res. 2016;474:2126–33. https://doi.org/10.1007/s11999-016-4920-2
26. Sobieraj M, Marwin S. Ultra-high-molecular-weight polyethylene (UHMWPE) in total joint arthroplasty. Bull Hosp Jt Dis (2013). 2018;76:38–46.
27. Schwartz AM, Farley KX, Guild GN, Bradbury TL Jr. Projections and epidemiology of revision hip and knee arthroplasty in the United States to 2030. J Arthroplasty. 2020;35:S79–85. https://doi.org/10.1016/j.arth.2020.02.030
28. Bayliss LE, Culliford D, Monk AP, Glyn-Jones S, Prieto-Alhambra D, Judge A, et al. The effect of patient age at intervention on risk of implant revision after total replacement of the hip or knee: a population-based cohort study. Lancet. 2017;389:1424–30. https://doi.org/10.1016/S0140-6736(17)30059-4
29. Rabiu AR, Rasidovic D, Parsons H, Wall PDH, Metcalfe A, Bruce J. Surgical interventions for failed primary knee replacement. Cochrane Database Syst Rev. 2020;2020:CD013681. https://doi.org/10.1002/14651858.CD013681
30. Zimmerli W, Trampuz A, Ochsner PE. Prosthetic-joint infections. N Engl J Med. 2004;351:1645–54. https://doi.org/10.1056/NEJMra040181
31. Martínez-Pastor JC, Muñoz-Mahamud E, Vilchez F, García-Ramiro S, Bori G, Sierra J, et al. Outcome of acute prosthetic joint infections due to gram-negative bacilli treated with open debridement and retention of the prosthesis. Antimicrob Agents Chemother. 2009;53:4772–7. https://doi.org/10.1128/AAC.00188-09
32. Hsieh PH, Lee MS, Hsu KY, Chang YH, Shih HN, Ueng SW. Gram-negative prosthetic joint infections: risk factors and outcome of treatment. Clin Infect Dis. 2009;49:1036–43. https://doi.org/10.1086/605593
33. Snowden KF. Microsporidia in higher vertebrates. In: Weiss LM, Becnel JJ, editors. Microsporidia: pathogens of opportunity, 1st edition. Chichester (UK): John Wiley & Sons, Inc.; 2014. p. 469–91.
34. Fayer R, Santin–Duran M. Epidemiology of microsporidia in human Infections. In: Weiss LM, Becnel JJ, editors. Microsporidia: pathogens of opportunity. Chichester (UK): John Wiley & Sons, Inc.; 2014. p. 135–64.
35. Vávra J, Lukeš J. Microsporidia and 'the art of living together'. Adv Parasitol. 2013;82:253–319. https://doi.org/10.1016/B978-0-12-407706-5.00004-6
36. Didier ES, Khan IA. The immunology of microsporidiosis in mammals. In: Weiss LM, Becnel JJ, editors. Microsporidia: pathogens of opportunity. Chichester (UK): John Wiley & Sons, Inc.; 2014. p. 307–26.
37. Sak B, Kotková M, Hlásková L, Kváč M. Limited effect of adaptive immune response to control encephalitozoonosis. Parasite Immunol. 2017;39:e12496. https://doi.org/10.1111/pim.12496
38. Sak B, Brdíčková K, Holubová N, Květoňová D, Hlásková L, Kváč M. *Encephalitozoon cuniculi* genotype III evinces a resistance to albendazole treatment in both immunodeficient and immunocompetent mice. Antimicrob Agents Chemother. 2020;64:e00058-20. https://doi.org/10.1128/AAC.00058-20
39. Kotková M, Sak B, Kváč M. Differences in the intensity of infection caused by *Encephalitozoon cuniculi* genotype II and III—comparison using quantitative real-time PCR. Exp Parasitol. 2018;192:93–7. https://doi.org/10.1016/j.exppara.2018.07.019
40. Gannon J. A survey of *Encephalitozoon cuniculi* in laboratory animal colonies in the United Kingdom. Lab Anim. 1980;14:91–4. https://doi.org/10.1258/002367780780942917
41. Mertens RB, Didier ES, Fishbein MC, Bertucci DC, Rogers LB, Orenstein JM. *Encephalitozoon cuniculi* microsporidiosis: infection of the brain, heart, kidneys, trachea, adrenal glands, and urinary bladder in a patient with AIDS. Mod Pathol. 1997;10:68–77.
42. Weber R, Bryan RT, Schwartz DA, Owen RL. Human microsporidial infections. Clin Microbiol Rev. 1994;7:426–61. https://doi.org/10.1128/CMR.7.4.426
43. Sak B, Kváč M. Chronic infections in mammals due to microsporidia. Exp Suppl. 2022;114:319–71. https://doi.org/10.1007/978-3-030-93306-7_12

44. Ditrich O, Chrdle A, Sak B, Chmelík V, Kubále J, Dyková I, et al. *Encephalitozoon cuniculi* genotype I as a causative agent of brain abscess in an immunocompetent patient. J Clin Microbiol. 2011;49:2769–71. https://doi.org/10.1128/JCM.00620-11
45. Couzinet S, Cejas E, Schittny J, Deplazes P, Weber R, Zimmerli S. Phagocytic uptake of *Encephalitozoon cuniculi* by nonprofessional phagocytes. Infect Immun. 2000;68:6939–45. https://doi.org/10.1128/IAI.68.12.6939-6945.2000
46. Nassonova ES, Tokarev YS, Trammer T, Entzeroth R, Sokolova YY. Phagocytosis of *Nosema grylli* (Microsporida, Nosematidae) spores in vivo and in vitro. J Eukaryot Microbiol. 2001;48:83S–4S. https://doi.org/10.1111/j.1550-7408.2001.tb00462.x
47. Sak B, Brady D, Pelikánová M, Květoňová D, Rost M, Kostka M, et al. Unapparent microsporidial infection among immunocompetent humans in the Czech Republic. J Clin Microbiol. 2011;49:1064–70. https://doi.org/10.1128/JCM.01147-10
48. Sak B, Kváč M, Kučerová Z, Květoňová D, Saková K. Latent microsporidial infection in immunocompetent individuals—a longitudinal study. PLoS Negl Trop Dis. 2011;5:e1162. https://doi.org/10.1371/journal.pntd.0001162
49. Kotková M, Sak B, Květoňová D, Kváč M. Latent microsporidiosis caused by *Encephalitozoon cuniculi* in immunocompetent hosts: a murine model demonstrating the ineffectiveness of the immune system and treatment with albendazole. PLoS One. 2013;8:e60941. https://doi.org/10.1371/journal.pone.0060941
50. Konttinen YT, Pajarinen J, Takakubo Y, Gallo J, Nich C, Takagi M, et al. Macrophage polarization and activation in response to implant debris: influence by "particle disease" and "ion disease". J Long Term Eff Med Implants. 2014;24:267–81. https://doi.org/10.1615/jlongtermeffmedimplants.2014011355

Address for correspondence: Bohumil Sak, Institute of Parasitology, Biology Centre of the Czech Academy of Sciences, Branišovská 31, České Budějovice 37005, Czech Republic; email: casio@paru.cas.cz

etymologia revisited

Salmonella

[sal′′mo-nel′ə]

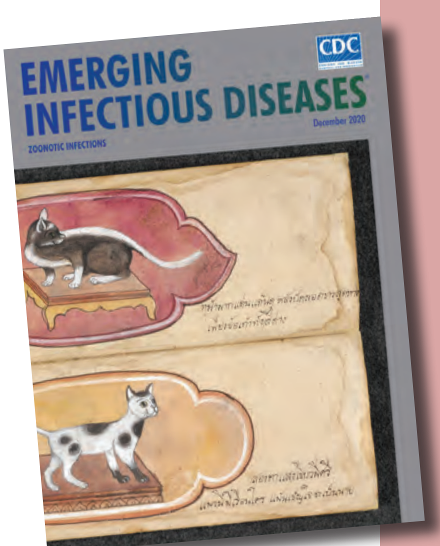

Originally published in December 2020

Named in honor of Daniel Elmer Salmon, an American veterinary pathologist, *Salmonella* is a genus of motile, gram-negative bacillus, nonspore-forming, aerobic to facultatively anaerobic bacteria of the family Enterobacteriaceae. In 1880, Karl Joseph Eberth was the first to observe *Salmonella* from specimens of patients with typhoid fever (from the Greek *typhōdes* [like smoke; delirious]), which was formerly called *Eberthella typhosa* in his tribute. In 1884, Georg Gaffky successfully isolated this bacillus (later described as *Salmonella* Typhi) from patients with typhoid fever, confirming Eberth's findings. Shortly afterward, Salmon and his assistant Theobald Smith, an American bacteriologist, isolated *Salmonella* Choleraesuis from swine, incorrectly assuming that this germ was the causative agent of hog cholera. Later, Joseph Lignières, a French bacteriologist, proposed the genus name *Salmonella* in recognition of Salmon's efforts.

References:

1. Dorland's Illustrated Medical Dictionary. 32nd ed. Philadelphia: Elsevier Saunders; 2012.
2. Gossner CM, Le Hello S, de Jong B, Rolfhamre P, Faensen D, Weill FX, et al. Around the world in 1,475 Salmonella geo-serotypes [Another Dimension]. Emerg Infect Dis. 2016;22:1298–302.
3. Issenhuth-Jeanjean S, Roggentin P, Mikoleit M, Guibourdenche M, de Pinna E, Nair S, et al. Supplement 2008-2010 (no. 48) to the White-Kauffmann-Le Minor scheme. Res Microbiol. 2014;165:526–30.
4. Salmon DE. The discovery of the germ of swine-plague. Science. 1884;3:155–8.
5. Su LH, Chiu CH. Salmonella: clinical importance and evolution of nomenclature. Chang Gung Med J. 2007;30:210–9.

Population-Based Evaluation of Vaccine Effectiveness against SARS-CoV-2 Infection, Severe Illness, and Death, Taiwan

Cheng-Yi Lee, Hung-Wei Kuo, Yu-Lun Liu, Jen-Hsiang Chuang, Jih-Haw Chou

Taiwan provided several COVID-19 vaccine platforms: mRNA (BNT162b2, mRNA-1273), adenoviral vector-based (AZD1222), and protein subunit (MVC-COV1901). After Taiwan shifted from its zero-COVID strategy in April 2022, population-based evaluation of vaccine effectiveness (VE) became possible. We conducted an observational cohort study of 21,416,151 persons to examine VE against SARS-CoV-2 infection, moderate and severe illness, and death during March 22, 2021–September 30, 2022. After adjusting for age and sex, we found that persons who completed 3 vaccine doses (2 primary, 1 booster) or received MVC-COV1901 as the primary series had the lowest hospitalization incidence (0.04–0.20 cases/100,000 person-days). We also found 95.8% VE against hospitalization for 3 doses of BNT162b2, 91.0% for MVC-COV1901, 81.8% for mRNA-1273, and 65.7% for AZD1222, which had the lowest overall VE. Our findings indicated that protein subunit vaccines provide similar protection against SARS-CoV-2–associated hospitalization as mRNA vaccines and can inform mix-and-match vaccine selection in other countries.

In response to the worldwide COVID-19 pandemic, most countries adopted vaccination policies on the basis of clinical trial outcomes and scientific evidence for vaccine procurement and policy planning frameworks. Studies suggested that after Omicron variants emerged, persons receiving 2 COVID-19 vaccine doses might not be adequately protected against severe illness and death (*1*–*8*). Research indicated that persons who completed a primary vaccine series would need a booster dose for better protection against new SARS-CoV-2 variants (*9*–*13*). Moreover, many countries provided several COVID-19 vaccine platform combinations (mix-and-match) of mRNA, protein subunit, and viral vector–based vaccines. However, few studies adopted population-level datasets and national vaccination registry records to examine the VE of mix-and-match COVID-19 vaccine regimens against SARS-CoV-2 infection, severe illness, and death.

Author affiliations: Taiwan Centers for Disease Control, Taipei, Taiwan (C.-Y. Lee, H.-W. Kuo, Y.-L. Liu, J.-H. Chuang); Ministry of Health and Welfare, Taipei (J.-H. Chou)

DOI: https://doi.org/10.3201/eid3003.230893

Government agencies, including the UK Health Security Agency (*14*), the US Centers for Disease Control and Prevention (*7*), Health Canada (*15*), and the Public Health Agency of Sweden (*16*), adopted sampling or regional data to routinely evaluate COVID-19 VE in real-world settings. Those authorities review VE for national vaccination strategies to improve public policy implementation and provide evidence to encourage vulnerable groups and at-risk populations to get vaccinated. However, most countries worldwide have experienced several waves of the COVID-19 pandemic, and VE results could be affected by natural humoral immunity due to SARS-CoV-2 infection among populations. Thus, previous VE might be biased because of persons who were infected and vaccinated, reporting schemes, and fundamental distinctions among groups with different vaccination statuses.

Taiwan offers various COVID-19 vaccines for the public, including mRNA (Pfizer-BioNTech BNT162b2 [https://www.pfizer.com] and Moderna mRNA-1273 [https://www.modernatx.com]), protein subunit (Medigen MVC-COV1901 [https://www.medigenvac.com]), and Novavax NVX-CoV2373 [https://www.novavax.com]), and viral vector-based vaccines (Oxford–AstraZeneca AZD1222 [https://www.astrazeneca.com]). In Taiwan, AZD1222 was introduced on March 22, 2021, mRNA-1273 on June 8, 2021, MVC-COV1901 on August 23, 2021, and BNT162b2 on

September 22, 2021. Government-funded COVID-19 vaccines were provided and prioritized by risk groups, such as healthcare workers, COVID-19 control staff (e.g., frontline health authority, customs, immigration, and quarantine staff, and security workers), caregivers in social welfare facilities, and high-risk groups (such as persons receiving kidney dialysis, older adults, pregnant women, and patients with rare diseases, catastrophic illnesses, or chronic diseases). No preferential recommendations for specific vaccine platforms were offered, and COVID-19 vaccines were provided to risk groups on the basis of availability. Persons could choose and reserve any available COVID-19 vaccine platforms at the vaccination stations.

In Taiwan, after authorities investigated COVID-19 cases, most were classified as imported, and few autochthonous cases were reported until April 2022. Community outbreaks did not begin until May 2021 and all were controlled within 3 months (*17*,*18*). Moreover, the national COVID-19 vaccination program was initiated in March 2021 (*19*), and vaccine coverage was <1% of the population when community outbreaks occurred in May 2021. Those outbreaks were mainly an Alpha subvariant of SARS-CoV-2 and was well controlled under the country's zero-COVID policy. The Taiwan Centers for Disease Control (Taiwan CDC) conducted a seroprevalence survey on blood donors whose samples were obtained during January–April 2022. The national nucleocapsid protein positivity rate was 0.00%–0.94%, showing that the population maintained a low level of COVID-19 infection. When a major outbreak of the SARS-CoV-2 Omicron BA.2 variant began in April 2022, the population could be regarded as SARS-CoV-2 immune naive. Thus, evaluating the nationwide VE of COVID-19 vaccines and vaccine combinations among a population-based cohort became realistic after April 2022.

We launched this study and used national vaccination registration records and a mandatory patient-level COVID-19 reporting dataset to estimate real-world VE of mRNA, protein subunit, and viral vector-based vaccines against infection, severe disease, and death in this predominantly infection-naive population during Omicron BA.2 variant predominance in Taiwan, mainly April–September 2022. This study also aimed to provide an overview and review of the performance of various COVID-19 vaccine platforms and vaccine combinations against the SARS-CoV-2–associated severe illness and to provide evidence for the vaccination strategy and guidance for areas and countries where various vaccine types are available.

Methods

Ethics Considerations

Taiwan CDC performed this study as a public policy analysis and evaluation. According to the Communicable Disease Control Act, Personal Data Protection Act, and regulations issued by the Ministry of Health and Welfare (reference no. 1010265083), the requirement of informed consent was waived from the study subjects because data were collected and obtained from Taiwan CDC. This study was approved by the Taiwan CDC institutional review board for health policy analysis research (reference no. 112103) and received an exempt review certificate of approval.

Study Design and Data Sources

We conducted a population-based retrospective cohort study to assess the VE of mRNA (BNT162b2 and mRNA-1273), protein subunit (MVC-COV1901), and vector-based (ChAdOx1-S -AZD1222) COVID-19 vaccines in Taiwan during March 22, 2021–September 30, 2022. Our analysis included citizens and permanent residents of Taiwan.

Registration in the National Immunization Information System (NIIS) is mandatory for all vaccinated persons and includes patient-level records of each government-funded vaccine administered. We retrieved the official database of the NIIS, which included vaccine types, vaccination dates of each dose, and vaccine combinations (i.e., mix-and-match) statuses for all vaccinees. We obtained information on SARS-CoV-2 infection notifications, moderate and severe illness (i.e., hospitalization), and death outcomes from the National Infectious Disease Reporting System (NIDRS). NIDRS also included information on eligible persons who were not vaccinated (i.e., received zero doses). At enrollment, NIIS and NDRS collected demographic information, such as age and sex, and information on enrollees' residential districts. On November 10, 2022, we retrieved analytic datasets from Taiwan CDC systems that stored integrated data that integrated NIIS, NIDRS, and case information. To ensure that persons were alive at the start of the cohort, we verified personal identification numbers against the death registry and census database from the Ministry of the Interior.

The second booster (i.e., fourth dose) campaign for certain older adults and vulnerable groups began on May 16, 2022. Because persons who had 2 booster doses might have stronger immunity, we excluded persons whose records showed they had received a fourth dose (i.e., second booster) to avoid any possible bias. In addition to MVC-COV1901, Novavax

(Nuvaxovid) is also a protein subunit vaccine. However, Novavax had limited availability and only specific population groups were eligible to receive it, so most persons could not receive Novavax in their primary vaccine series; thus, we excluded persons vaccinated with Novavax. Most COVID-19 case notifications occurred during April–September 2022, but the bivalent Moderna vaccine was not provided until September 2022; therefore, we excluded persons who received the Moderna bivalent vaccine. Of note, VE comparison of monovalent and bivalent vaccines was not the main goal of the study.

Statistical Analysis

Although the COVID-19 vaccine program launched on March 22, 2021, and most cases occurred after April 2022, sporadic outbreaks and community transmission still occurred and were attributed to imported cases during the zero-COVID strategy timeframe. Therefore, we estimated the overall VE of COVID-19 vaccines and aimed to provided VE of various mix-and-match vaccine platforms in Taiwan during March 22, 2021–September 30, 2022. Moreover, to address the timeframe between vaccination dates and events, we estimated the incidence rate and explored time from vaccination to infection, hospitalization, or death. We removed the total follow-up days and at-risk population if the outcome of interest occurred. We also explored incidence rates of outcomes of interest (i.e., confirmed infection, hospitalization, and death) for comparison. We considered persons protected at 14 days after a vaccine dose, the time required to develop an immune response. We calculated the person-days between the date of vaccination and event dates for infection, hospitalization, or death (Appendix, https://wwwnc.cdc.gov/EID/article/30/3/23-0893-App1.pdf).

We used logistic regression models to calculate odds ratios (ORs) and 95% CIs of hospitalization and death outcomes. We included vaccination status in the analysis and considered the demographic characteristics of sex and age as covariates. We defined VE as (1 – adjusted OR) × 100% to estimate the risk probability of outcomes of interest among persons who had 0, 1, 2, or 3 vaccine doses. We compared VEs of persons who had 1–3 vaccination doses to unvaccinated (i.e., 0 vaccines) persons as the reference group. We also measured the absolute VE of various vaccine combinations against an unvaccinated reference (control) group. We excluded persons who received ≥4 vaccine doses from the analysis to avoid bias.

We stratified VE estimates by 3 age groups, all ages, 18–64 years of age, and ≥65 years of age, and by vaccine platform combinations (i.e., mix-and-match). Taiwan CDC guidelines did not restrict the brand of vaccines used as the primary series and encouraged eligible groups to receive vaccines when products were available. After a physician's consultation, persons could choose their vaccine type and brand (Appendix). Because the array of combinations was infinite, to reduce confusion, we limited our analysis to 27 specific vaccine combinations, determined by the number of persons vaccinated. We performed all analyses in SAS version 9.4 (SAS Institute, Inc., https://www.sas.com) and SPSS Statistics 26.0 (IBM, https://www.ibm.com).

Results

Our analysis included 23,933,482 unique persons, from which 2,516,382 persons were excluded because they received ≥4 vaccine doses during the study period; 949 persons were excluded because of incomplete national immunization and reporting system records. We found that 3,373,548 (15.8%) persons were unvaccinated, 1,183,138 (5.5%) received 1 dose, 3,287,659 (15.4%) received 2 doses, and 13,571,806 (63.4%) completed 3 doses (Table). The mean age was 41.0 years for unvaccinated persons, 28.7 years for persons with 1 vaccine dose, 31.8 years for persons with 2 doses, and 42.5 years for persons with 3 doses.

SARS-CoV-2 infection rates were 24.3% for unvaccinated (0 dose) persons, 31.4% for persons with

Table. Vaccination status and outcomes in a population-based evaluation of vaccine effectiveness against SARS-CoV-2 infection, severe illness, and death, Taiwan

Vaccination status and outcomes	Total population	Unvaccinated	No. doses: 1	2	3
No. (%) cases	21,416,151 (100)	3,373,548 (15.8)	1,183,138 (5.5)	3,287,659 (15.4)	13,571,806 (63.4)
Mean age (SD)	39.9 (21.5)	41.0 (30.6)	28.7 (25.7)	31.8 (22.4)	42.5 (16.8)
Sex					
M	10,644,720	1,720,573	644,365	1,741,738	6,538,044
F	10,771,431	1,652,975	538,773	1,545,921	7,033,762
SARS-CoV-2 infection					
No. confirmed cases (%)	5,830,809 (27.2)	819,991 (24.3)	371,202 (31.4)	903,475 (27.5)	3,736,141 (27.5)
COVID-19 prognosis					
No. moderate and severe cases (%)	28,840 (0.13)	14,674 (0.43)	2,575 (0.22)	3,700 (0.11)	7,891 (0.06)
No. deaths (%)	10,667 (0.05)	5,342 (0.16)	989 (0.08)	1,305 (0.04)	3,031(0.02)

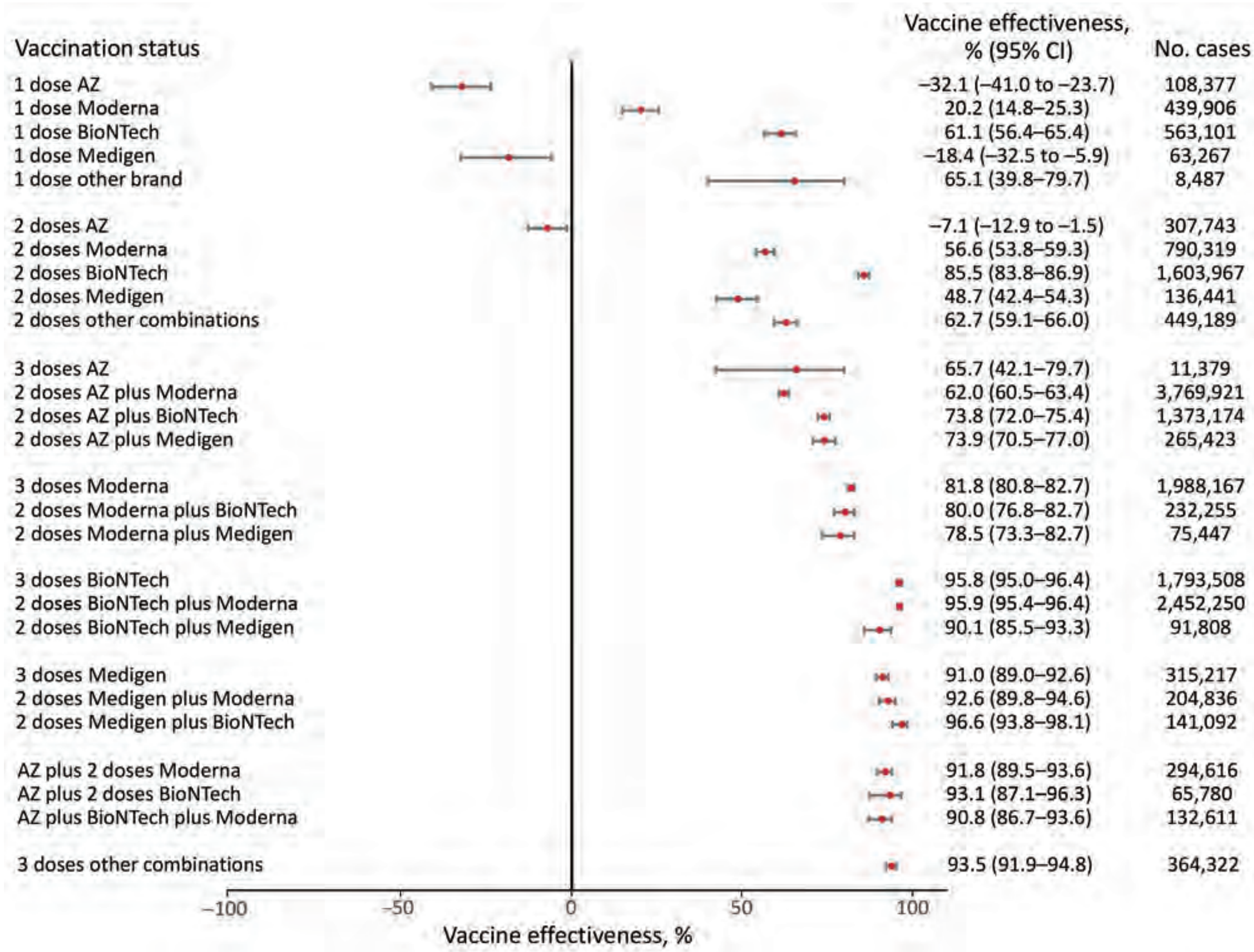

Figure 1. Vaccine effectiveness against hospitalization among all age groups in a population-based evaluation of vaccine effectiveness against SARS-CoV-2 infection, severe illness, and death, Taiwan, March 22, 2021–September 30, 2022. The study investigated various vaccine types: mRNA (Pfizer-BioNTech BNT162b2 [https://www.pfizer.com] and Moderna mRNA-1273 [https://www.modernatx.com]), protein subunit (Medigen MVC-COV1901 [https://www.medigenvac.com]), and viral vector–based vaccines (Oxford-AstraZeneca AZD1222 [https://www.astrazeneca.com]). The forest plot demonstrates effectiveness of different vaccination regimens status against moderate and severe illness defined by hospitalization for all age groups. Red dots indicate percentage effectiveness; bars indicate 95% CIs. AZ, AstraZeneca vaccine.

1 dose, 27.5% for persons with 2 doses, and 27.5% for persons with 3 doses. We found that 0.43% of unvaccinated persons had moderate to severe illness, which we defined by hospitalization, and 0.16% died. In contrast, 0.22% of 1-dose vaccinees were hospitalized and 0.08% died; 0.11% of 2-dose vaccinees were hospitalized and 0.04% died. Among persons who completed 3 doses, 0.06% were hospitalized and 0.02% died, which was the lowest death rate in our cohort.

We categorized 27 groups of vaccine combinations because of the complexity of mix-and-match combinations; we compiled the number of cases and patient characteristics and calculated the incidence of SARS-CoV-2 infection, hospitalization, and death (Appendix Table 1). Most persons who completed a 3-dose regimen received a combination of vaccines, most (3,769,921 [17.6%]) of which were 2 doses of AZD1222 and 1 dose of mRNA-1273.

For hospitalization risk comparison among 3-dose mix-and-match vaccine recipients, persons receiving MVC-COV1901 as the primary series had the lowest hospitalization incidence of 0.04–0.20/100,000 person-days, followed by BNT162b2 (0.06–0.20/100,000 person-days), mRNA-1273 (0.40–0.66/100,000 person-days), and AZD1222 (0.06–0.20/100,000 person-days). We observed a similar pattern in among patient deaths.

Among 3-dose vaccinees using the same brand, 3 doses of MVC-COV1901 had the lowest infection incidence (116.05 cases/100,000 person-days), followed by mRNA-1273 (138.11 cases/100,000 person-days), BNT162b2 (149.26 cases/100,000 person-days), and AZD1222 (152.62 cases/100,000 person-days). For COVID-19–associated hospitalization outcomes, 3 doses of BNT162b2 had the lowest incidence (0.06/100,000 person-days), followed by MVC-COV1901 (0.20/100,000 person-days), mRNA-1273 (0.48/100,000 person-days), and AZD1222 (0.71/100,000 person-days). We observed a similar pattern among patient deaths.

We categorized 3 age groups, all ages, 18–64 years of age, and ≥65 years of age, to show VE against COVID-19–associated hospitalization and death (Appendix Tables 2, 3). We used unvaccinated persons as the reference group and adjusted for age and sex when calculating VE in multivariate models (Figures 1–6). For VE against hospitalization, a booster dose generally provided higher protection (Figures 1–3). VE in persons who received mRNA vaccines as a primary series showed a similar pattern to persons who received protein-based vaccines as a primary series. We noted a 95.8% (95% CI 95.0%–96.4%) point estimate of VE for 3 doses of BNT162b2, an 81.8% (95% CI 80.8%–82.7%) point estimate for mRNA-1273, a 91.0% (95% CI 90.9%–92.6%) point estimate for MVC-COV1901, and a lower VE (65.7%; 95% CI 42.1%–79.9%) for 3 doses of AZD1222. In contrast, AZD1222 plus 2 doses of mRNA vaccines provided a higher (90.8%–93.1%) VE against hospitalization than 3 doses of AZD1222.

Among persons 18–64 years of age receiving only 1 dose, we observed no statistically significant protection against death for AZD1222 (−29.5%; 95% CI

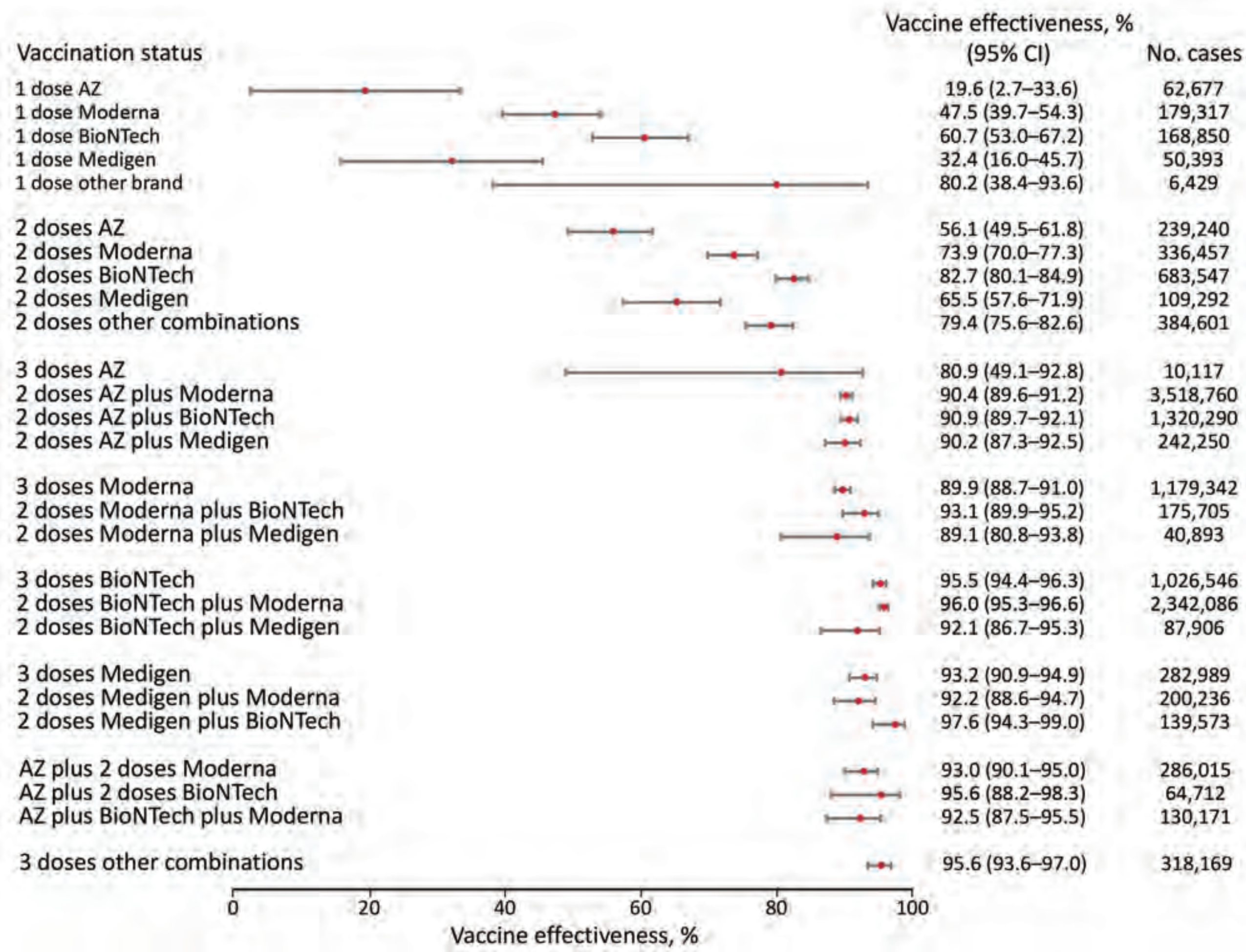

Figure 2. Vaccine effectiveness against hospitalization among persons 18–64 years of age in a population-based evaluation of vaccine effectiveness against SARS-CoV-2 infection, severe illness, and death, Taiwan, March 22, 2021–September 30, 2022. The study investigated various vaccine types: mRNA (Pfizer-BioNTech BNT162b2 [https://www.pfizer.com] and Moderna mRNA-1273 [https://www.modernatx.com]), protein subunit (Medigen MVC-COV1901 [https://www.medigenvac.com]), and viral vector–based vaccines (Oxford-AstraZeneca AZD1222 [https://www.astrazeneca.com]). The forest plot demonstrates effectiveness of different vaccination regimens status against moderate and severe illness defined by hospitalization for persons 18–64 years of age. Red dots indicate percentage effectiveness; bars indicate 95% CIs. AZ, AstraZeneca vaccine.

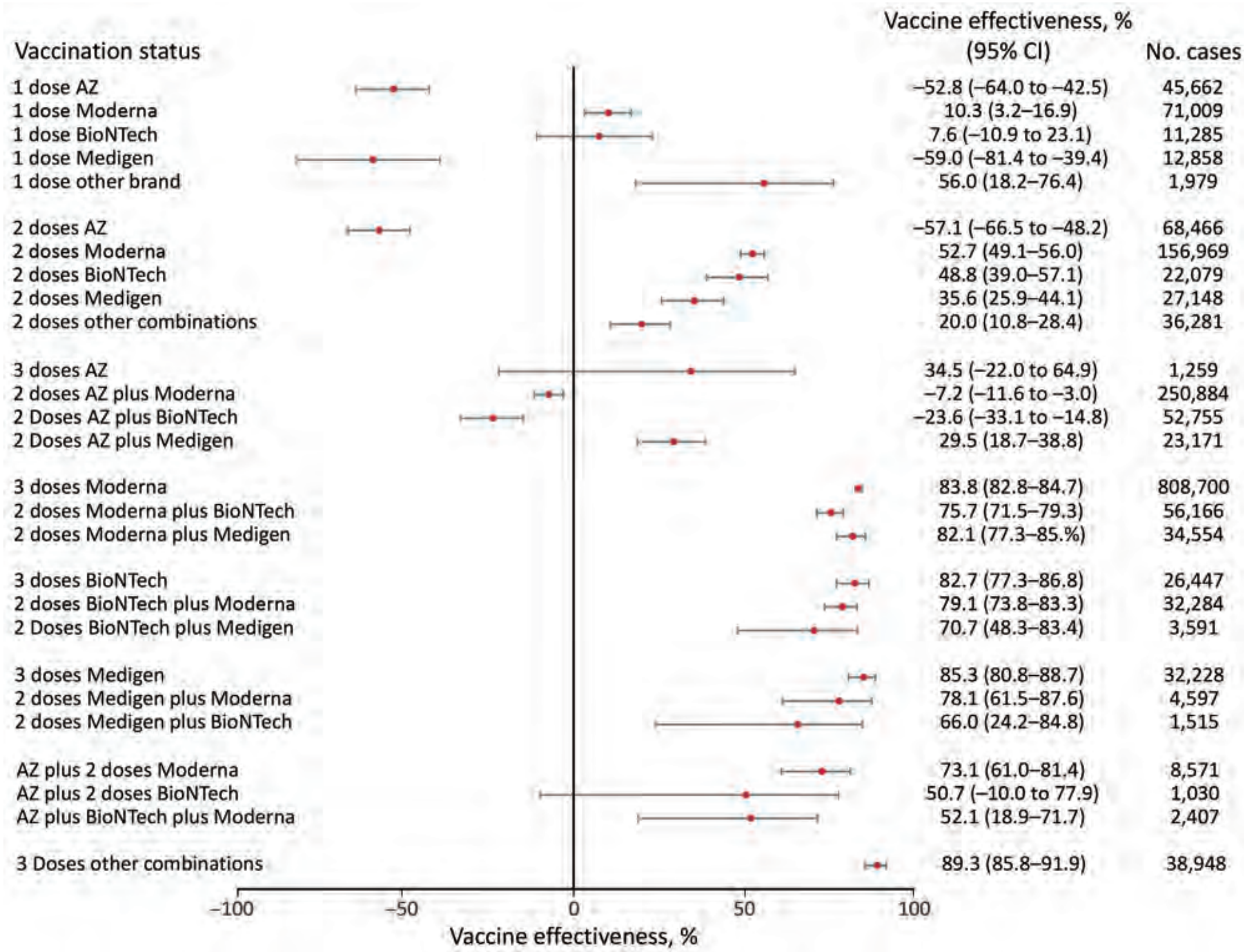

Figure 3. Vaccine effectiveness against hospitalization among persons ≥65 years of age in a population-based evaluation of vaccine effectiveness against SARS-CoV-2 infection, severe illness, and death, Taiwan, March 22, 2021–September 30, 2022. The study investigated various vaccine types: mRNA (Pfizer-BioNTech BNT162b2 [https://www.pfizer.com] and Moderna mRNA-1273 [https://www.modernatx.com]), protein subunit (Medigen MVC-COV1901 [https://www.medigenvac.com]), and viral vector-based vaccines (Oxford-AstraZeneca AZD1222 [https://www.astrazeneca.com]). The forest plot demonstrates effectiveness of different vaccination regimens status against moderate and severe illness defined by hospitalization for persons ≥65 years of age. Red dots indicate percentage effectiveness; bars indicate 95% CIs. AZ, AstraZeneca vaccine.

−77.9% to –5.7%), mRNA-1273 (11.8%; 95% CI −10.4% to 29.6%), BNT162b2 (65.5%; 95% CI 47.8%–77.2%), and MVC-COV1901 (19.4%; 95% CI –21.9% to 46.7%) (Figure 2). We observed a higher level of protection with 2 doses of mRNA; BNT162b2 reached 79.1% (95% CI 72.4%–84.25%) and mRNA-1273 reached 72.0% (95% CI 63.0%–78.7%). VE for protein-based vaccine MVC-COV1901 was 62.6% (95% CI 43.9%–75.1%). By comparison, the VE was the lowest, 37.3% (95% CI 19.3%–51.3%), for 3 AZD1222 doses.

We found higher VE was obtained among persons 18–64 years of age who had a booster dose. In addition, 3 doses of mRNA or protein-based vaccines provided similar protection against COVID-19–associated death: 94.9% (95% CI 92.2%–96.7%) for BNT162b2, 92.0% (95% CI 89.7%–93.8%) for mRNA-1273, and 92.0% (95% CI 86.1%–95.4%) for MVC-COV1901 (Figure 2). The combination of 1 AZD1222 and 2 doses of mRNA vaccines provided high (81.9%–93.5%) protection, as well. However, we observed little protection from death after 3 doses of AZD1222, with a point estimate of 78.4% (95% CI −53.6% to 97.0%).

For persons ≥65 years of age who received 3 vaccine doses, 3 doses of mRNA or protein-based vaccines provided similar protection against death: 86.6% (95% CI 85.2%–87.9%) for mRNA-1273, 83.6% (95% CI 74.3%–89.6%) for BNT162b2, and 85.2% (95% CI 77.5%–90.3%) for MVC-COV1901 (Figure 6). However, 3 doses of AZD1222 provided low protection against death and had a point estimate of 21.6% (95%

CI −88.8% to 67.5%). However, because of the relatively small population, we did not examine the combination of 1 AZD1222 and 2 doses of mRNA vaccines and other brands for this age group.

Discussion

We adopted population-based data to evaluate effectiveness for different COVID-19 vaccine platforms among a predominately immune-naive population in Taiwan, which had minimal circulation of SARS-CoV-2 before March 2022. In April 2022, a major epidemic of Omicron BA.2 variant led the government to abandon its zero-COVID policy, which had been in effect since January 2020 (*20*). The nationwide vaccine campaign was initiated in March 2021. However, before the end of March 2022, the cumulative confirmed domestic cases were <0.3% of the total population. Therefore, evaluating nationwide COVID-19 vaccine effectiveness among this immune-naive population became possible in April 2022. According to nationwide community subvariant surveillance during April 2021–September 2022, the BA.2 Omicron SARS-CoV-2 variant predominated and accounted for 85%–90% of all subvariants; the rest were BA.5, BA.2.75, and others (*21*). Previous studies indicated that COVID-19 infection could induce natural immunity that can be as effective as vaccines for certain amount of time after infection (*22*–*25*). However, our study offers baseline immunity values of the effectiveness of various vaccine platform combinations, primarily induced by vaccines. In addition, our findings provide further data on vaccine-induced immunity against Omicron variants and VE of various mix-and-match vaccine platforms, rather than immunity from previous

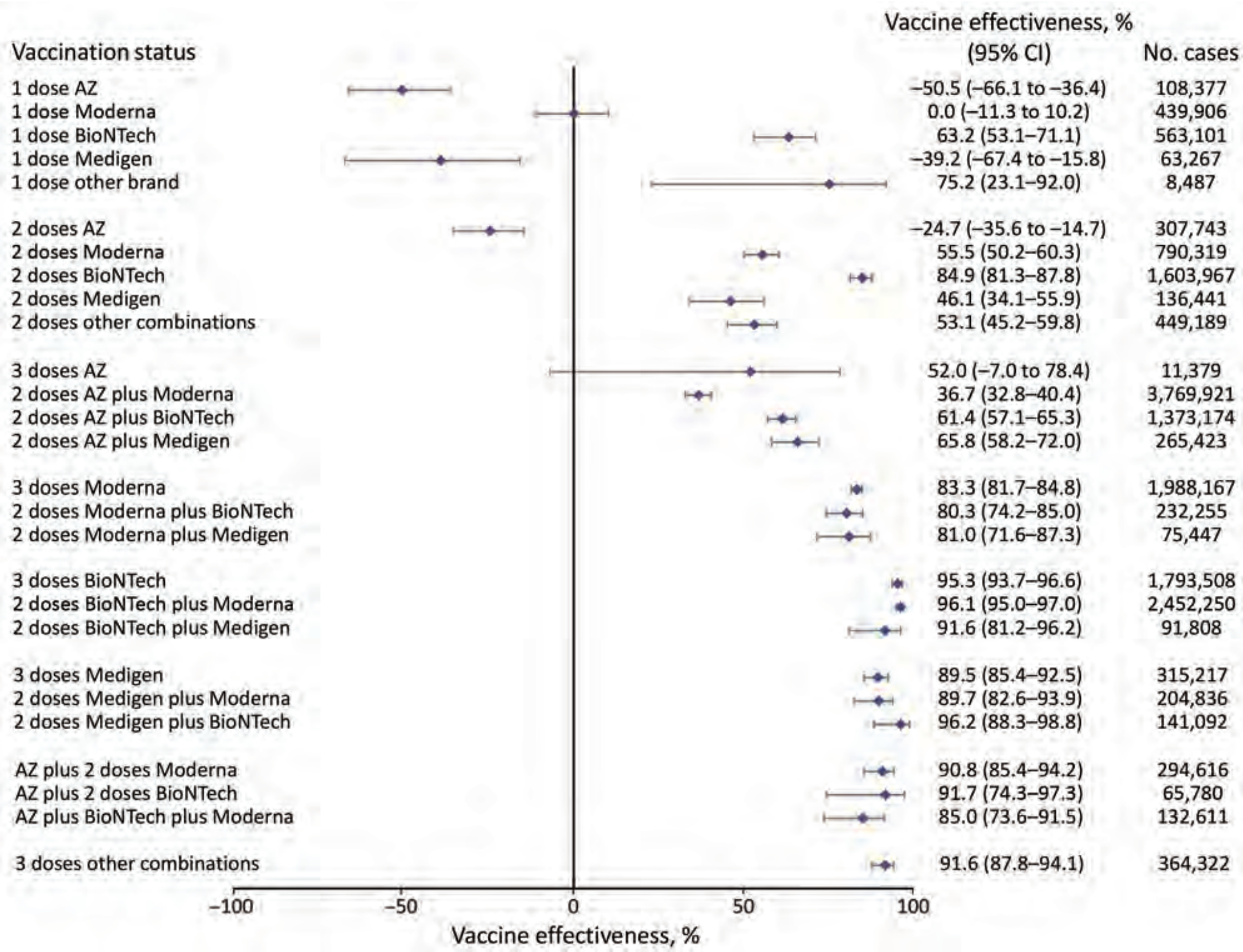

Figure 4. Vaccine effectiveness against death among all age groups in a population-based evaluation of vaccine effectiveness against SARS-CoV-2 infection, severe illness, and death, Taiwan, March 22, 2021–September 30, 2022. The study investigated various vaccine types: mRNA (Pfizer-BioNTech BNT162b2 [https://www.pfizer.com] and Moderna mRNA-1273 [https://www.modernatx.com]), protein subunit (Medigen MVC-COV1901 [https://www.medigenvac.com]), and viral vector-based vaccines (Oxford-AstraZeneca AZD1222 [https://www.astrazeneca.com]). The forest plot demonstrates effectiveness of different vaccination regimens status against death for all age groups. Blue diamonds indicate percentage effectiveness; bars indicate 95% CIs. AZ, AstraZeneca vaccine.

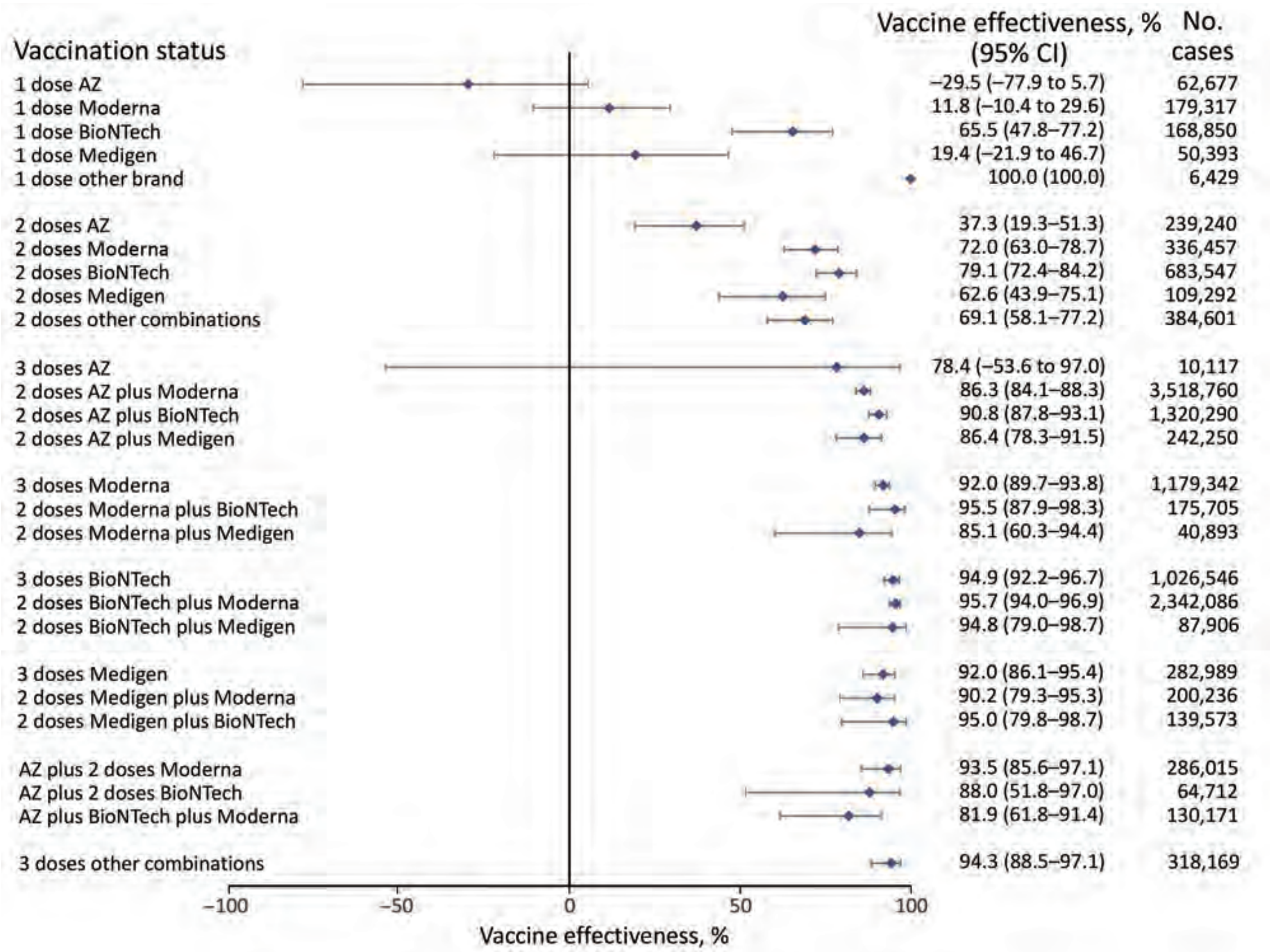

Figure 5. Vaccine effectiveness against death among persons 18–64 years of age in a population-based evaluation of vaccine effectiveness against SARS-CoV-2 infection, severe illness, and death, Taiwan, March 22, 2021–September 30, 2022. The study investigated various vaccine types: mRNA (Pfizer-BioNTech BNT162b2 [https://www.pfizer.com] and Moderna mRNA-1273 [https://www.modernatx.com protein subunit (Medigen MVC-COV1901 [https://www.medigenvac.com]), and viral vector–based vaccines (Oxford-AstraZeneca AZD1222 [https://www.astrazeneca.com]). The forest plot demonstrates effectiveness of different vaccination regimens status against death for persons 18–64 years of age. Blue diamonds indicate percentage effectiveness; bars indicate 95% CIs. AZ, AstraZeneca vaccine.

natural infection or a hybrid combination of protective effectiveness from vaccination and infection.

We found that persons who completed 3 vaccine doses and received mRNA platform vaccines (mRNA-1273 and BNT162b2) as the primary series had VE against COVID-19–associated hospitalization of 80.0%–95.9%, and the VE against COVID-19–associated death was 80.3%–96.1%. For persons whose primary series doses were the protein subunit platform MVC-COV1901, VE against hospitalization was 91.0%–96.6%, and the VE against death was 89.5%–96.2%. For persons whose primary series doses were vector-based AZD1222, the VE against hospitalization was 62.0%–73.9%, and the VE against death was 36.7%–65.8%. The VE of mRNA and protein subunit vaccines against COVID-19 hospitalization and death were similar, but the VE of the vector-based vaccine was lower (Figures 1–6).

A randomized, double-blind, active-controlled trial was conducted in Paraguay to evaluate immunogenicity of the protein subunit vaccine (*26*). Results from that study showed that MVC-COV1901 exhibited superiority in neutralizing antibody titers and noninferiority of seroconversion rates compared with the AZD1222 (*26*). A study on the protein recombinant vaccine NVX-CoV2373 (Novavax) in the general population of Italy found that VE against symptomatic COVID-19 was 31% (95% CI 16%–44%) in partially vaccinated (1 dose only) persons and 50% (95% CI 40%–58%) in fully vaccinated (2 doses) persons (*27*). Neither of those studies of protein vaccines reported VE against hospitalization and death. Our research might add insights and provide a reference for countries adopting MVC-COV1901 vaccines.

Our study provides additional information about VE among specific age groups and guidance for persons who might need second booster doses for better immunity, including persons whose primary series doses were AZD1222. For persons 18–64 years of age, our findings suggested that VE against COVID-19–associated hospitalization averaged ≈90%. However, VE against hospitalization and death for persons who received AZD1222 as primary series doses was lower than for those who received mRNA and protein subunit platform vaccines, suggesting vaccine-induced immunity waned more quickly for AZD1222 than for other vaccine types. That finding also might suggest that AZD1222 was not a proper choice for booster doses to induce sufficient immunity against SARS-CoV-2 Omicron variant, which is similar to a finding published by UK Health Security Agency (*28*). Our results indicated persons 18–64 years of age who completed 3 doses might have sufficient protection because VE against hospitalization was 80.9%–97.6% for that group, and the VE against death was 78.4%–95.7%. For persons ≥65 years of age, our findings indicated that persons whose primary series was AZD1222 had a VE against COVID-19–associated hospitalization ranging from −23.6% to 34.5%, which was much lower than for persons receiving mRNA or subunit protein vaccine. Real-world data from Brazil showed similar results; among persons ≥60 years of age, VE against hospitalization for those receiving AZD1222 was lower than for those receiving mRNA

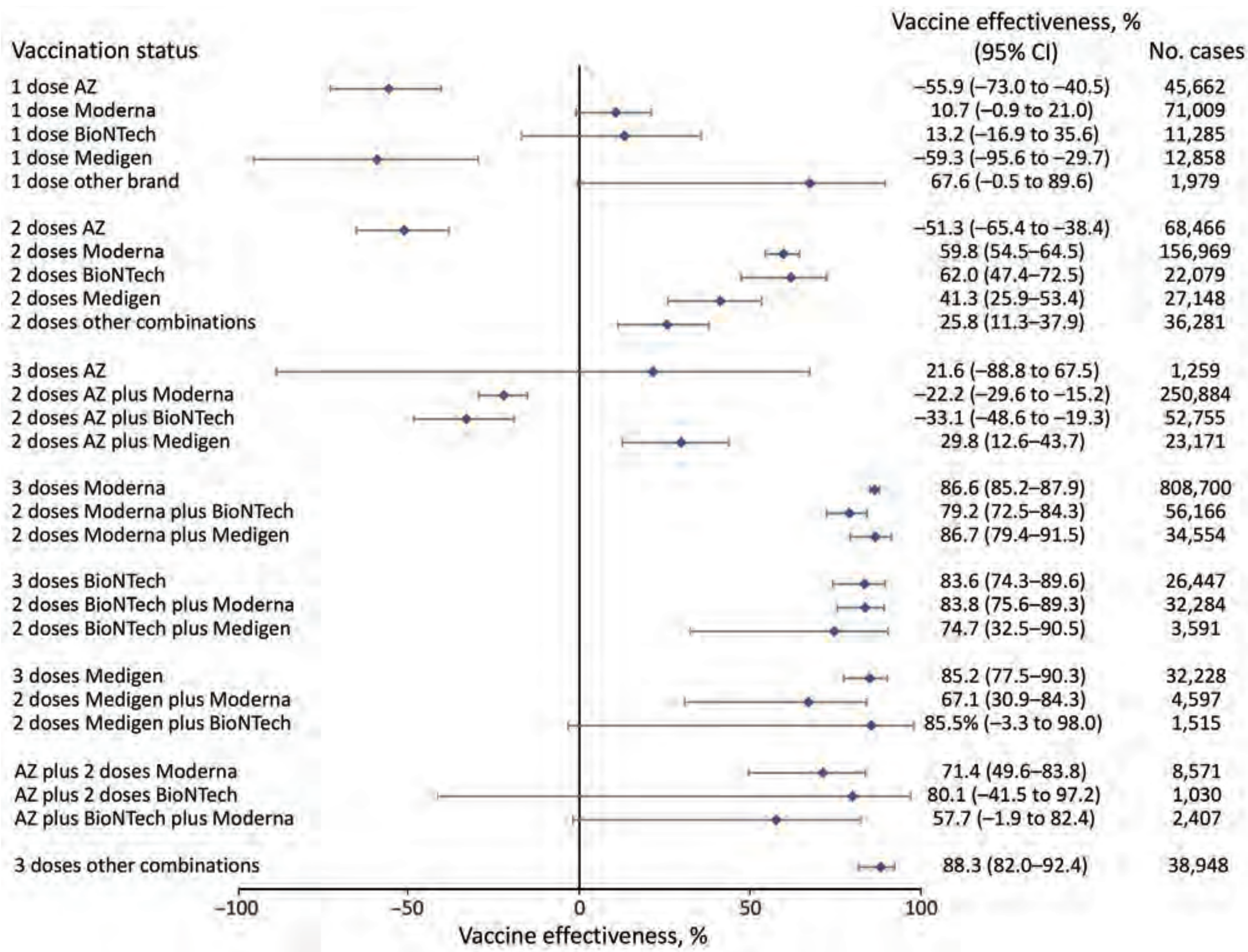

Figure 6. Vaccine effectiveness against death among persons ≥65 years of age in a population-based evaluation of vaccine effectiveness against SARS-CoV-2 infection, severe illness, and death, Taiwan, March 22, 2021–September 30, 2022. The study investigated various vaccine types: mRNA (Pfizer-BioNTech BNT162b2 [https://www.pfizer.com] and Moderna mRNA-1273 [https://www.modernatx.com]), protein subunit (Medigen MVC-COV1901 [https://www.medigenvac.com]), and viral vector–based vaccines (Oxford-AstraZeneca AZD1222 [https://www.astrazeneca.com]). The forest plot demonstrates effectiveness of different vaccination regimens status against death for persons ≥65 years of age. Blue diamonds indicate percentage effectiveness; bars indicate 95% CIs. AZ, AstraZeneca vaccine.

platform, and waning immunity was reported (*29*). Future studies could explore whether persons receiving AZD1222 are at higher risk for waning immunity, hospitalization, and death compared with persons receiving other vaccine platforms.

The World Health Organization Strategic Advisory Group of Experts updated COVID-19 vaccination guidance in March 2023 (*30*). The advisory group indicated high-priority groups, which were mainly evaluated on the basis of risk for severe COVID-19 and death. Our study suggested that the protection and immunity induced by vaccines among persons ≥65 years of age might not be sufficient, which is supported by previous studies in real-world settings (*28*,*31*,*32*). Therefore, the priority for future vaccine campaigns should emphasize persons ≥65 years of age, especially those whose primary series vaccines were AZD1222. The policy implication is that if a nationwide vaccine campaign was implemented with limited resources, the government could focus on the age groups and vaccine types that had lower VE rather than advocating for vaccination of the general population.

Our findings suggested that VE of the protein subunit vaccine MVC-COV1901 provides similar protection against COVID-19–associated hospitalization and death as mRNA vaccines BNT162b2 and mRNA-1273. Because both vaccine types could provide effective immunity against Omicron BA.2–associated severe outcomes, SARS-CoV-2 vaccine guidance in Taiwan recommend those vaccine types (*33*). VE of protein subunit and mRNA vaccines were also recognized by Indonesia, Palau, New Zealand, Belize, Somaliland, Thailand, Estonia, Paraguay, Malaysia, and Saint Kitts and Nevis (*33*). The similar VE of protein subunit and mRNA vaccines might provide the public with alternative vaccine types for primary series or booster shots. It also provides alternatives other than mRNA vaccines.

We provide population-level VE evaluation of protein subunit vaccines against severe outcomes. However, other studies have reported the efficacy a similar vaccine, NVX-CoV2373 (Novavax), from clinical trials and VE against symptomatic infection (*27*,*34*). For public implications, the results from this study could enhance the autonomy of individual preferences. In addition, because the Medigen MVC-COV1901 vaccine was locally innovated and produced in Taiwan, fewer issues of availability might arise in the evolving pandemic.

The first limitation of this study is that in estimating VE, although we used age and sex for model adjustments, information on underlying conditions, medication, treatment status and history, health behaviors, and potential unmeasurable factors were unavailable for individual cases; thus, we could not include those confounding factors as variables. Second, because of variations in healthcare seeking behaviors, notification records might be underestimated, especially for mild or asymptomatic cases. Third, Taiwan CDC received hospitalization records from the clinical status, documentation, notification and investigation, and case reports from the NIIS and NIDRS rather than mandatory reporting; thus, moderate and severe illness (hospitalization) could have been underreported. Fourth, an expert committee reviewed each death case to verify whether the death was SARS-CoV-2–associated according to medical records and death certificates obtained by national cause of death registry. Therefore, the death case numbers might be underestimated compared with studies that defined SARS-CoV-2 death within a specific timeframe.

In summary, this study provides scientific evidence for countries that use several COVID-19 vaccine platform combinations (mix-and-match) of mRNA, protein subunit, and viral vector-based vaccines. The study identified which vaccine combinations have lower VE and might require additional booster shots or attention. We found that persons who received AZD1222 as their primary series vaccines might not be adequately protected against COVID-19–associated hospitalization and death, even if they received a booster dose. We also found that the protein subunit vaccine MVC-COV1901 provided similar protection against severe SARS-CoV-2 outcomes as mRNA vaccines. Our findings can help inform vaccine selection for various age groups and at-risk populations during future COVID-19 vaccination campaigns, especially if resources are limited.

Acknowledgments

We thank the special COVID-19 vaccine effectiveness consultant committee led by Shan-Chwen Chang for their sharing of expertise on various vaccine platforms and supporting the study. We also thank the officers managing the National Immunization Information System, National Infectious Disease Reporting System and the Communicable Disease Data Warehouse for their technical assistance.

This research was supported by the COVID-19 Central Epidemic Command Center, directed by former Minister Shih-Chung Chen and successor Deputy Minister Pi-Sheng Wang and Minister Jui-Yuan Hsueh. This study was conducted by National COVID-19 Vaccine Effectiveness Analysis team, whose members are all government officials in Taiwan CDC. This research received no funding from other agencies, and Taiwan CDC provided a national COVID-19 vaccination registry and mandatory notification dataset for this study. The funders of the study (Taiwan CDC) had no role in the study design, data analysis, data interpretation, or writing of the report. All authors had full access to the whole dataset in the study and had responsibility for the decision to submit for publication.

Author contributions: All authors meet the criteria of the International Committee of Medical Journal Editors (ICMJE) for authorship. C.-Y.L. and H.-W.K. conceived and designed this research; C.-Y.L., H.-W.K., and Y.-L.L. collected the data. Y.-L.L. retrieved the dataset, C.-Y.L. performed the data analysis, and H.-W.K. verified the results. All authors interpreted the results. C.-Y.L. drafted the original manuscript. All authors have read and provided revision comments concerning the context. All authors have approved the manuscript being submitted and have approved its submission for publication.

About the Author

Dr. Lee is an associate research fellow and infectious disease epidemiologist with the Taiwan Centers for Disease Control and a senior officer in Taiwan's World Health Organization International Health Regulations Focal Point Office. His research interests include health policy evaluation, vaccine effectiveness research, COVID-19, excess mortality, and health economics.

References

1. Lauring AS, Tenforde MW, Chappell JD, Gaglani M, Ginde AA, McNeal T, et al.; Influenza and Other Viruses in the Acutely Ill (IVY) Network. Clinical severity of, and effectiveness of mRNA vaccines against, covid-19 from omicron, delta, and alpha SARS-CoV-2 variants in the United States: prospective observational study. BMJ. 2022;376:e069761. https://doi.org/10.1136/bmj-2021-069761
2. McMenamin ME, Nealon J, Lin Y, Wong JY, Cheung JK, Lau EHY, et al. Vaccine effectiveness of one, two, and three doses of BNT162b2 and CoronaVac against COVID-19 in Hong Kong: a population-based observational study. Lancet Infect Dis. 2022;22:1435–43. https://doi.org/10.1016/S1473-3099(22)00345-0
3. Sheikh A, Kerr S, Woolhouse M, McMenamin J, Robertson C; EAVE II Collaborators. Severity of omicron variant of concern and effectiveness of vaccine boosters against symptomatic disease in Scotland (EAVE II): a national cohort study with nested test-negative design. Lancet Infect Dis. 2022;22:959–66. https://doi.org/10.1016/S1473-3099(22)00141-4
4. Baum U, Poukka E, Leino T, Kilpi T, Nohynek H, Palmu AA. High vaccine effectiveness against severe COVID-19 in the elderly in Finland before and after the emergence of Omicron. BMC Infect Dis. 2022;22:816. https://doi.org/10.1186/s12879-022-07814-4
5. Thompson MG, Natarajan K, Irving SA, Rowley EA, Griggs EP, Gaglani M, et al. Effectiveness of a third dose of mRNA vaccines against COVID-19–associated emergency department and urgent care encounters and hospitalizations among adults during periods of Delta and Omicron variant predominance—VISION Network, 10 States, August 2021–January 2022. MMWR Morb Mortal Wkly Rep. 2022;71:139–45. https://doi.org/10.15585/mmwr.mm7104e3
6. Lai FTT, Yan VKC, Ye X, Ma T, Qin X, Chui CSL, et al. Booster vaccination with inactivated whole-virus or mRNA vaccines and COVID-19-related deaths among people with multimorbidity: a cohort study. CMAJ. 2023;195:E143–52. https://doi.org/10.1503/cmaj.221068
7. Adams K, Rhoads JP, Surie D, Gaglani M, Ginde AA, McNeal T, et al.; Influenza and other Viruses in the AcutelY ill (IVY) Network. Vaccine effectiveness of primary series and booster doses against covid-19 associated hospital admissions in the United States: living test negative design study. BMJ. 2022;379:e072065. https://doi.org/10.1136/bmj-2022-072065
8. Bloomfield LE, Ngeh S, Cadby G, Hutcheon K, Effler PV. SARS-CoV-2 vaccine effectiveness against Omicron variant in infection-naive population, Australia, 2022. Emerg Infect Dis. 2023;29:1162–72. https://doi.org/10.3201/eid2906.230130
9. Tsang NNY, So HC, Cowling BJ, Leung GM, Ip DKM. Effectiveness of BNT162b2 and CoronaVac COVID-19 vaccination against asymptomatic and symptomatic infection of SARS-CoV-2 omicron BA.2 in Hong Kong: a prospective cohort study. Lancet Infect Dis. 2023;23:421–34. https://doi.org/10.1016/S1473-3099(22)00732-0
10. Vietri MT, D'Elia G, Caliendo G, Passariello L, Albanese L, Molinari AM, et al. Antibody levels after BNT162b2 vaccine booster and SARS-CoV-2 Omicron infection. Vaccine. 2022;40:5726–31. https://doi.org/10.1016/j.vaccine.2022.08.045
11. Ochoa-Hein E, Leal-Morán PE, Nava-Guzmán KA, Vargas-Fernández AT, Vargas-Fernández JF, Díaz-Rodríguez F, et al. Significant rise in SARS-CoV-2 reinfection rate in vaccinated hospital workers during the Omicron wave: a prospective cohort study. Rev Invest Clin. 2022;74:175–80. https://doi.org/10.24875/RIC.22000159
12. Yang SL, Teh HS, Suah JL, Husin M, Hwong WY. SARS-CoV-2 in Malaysia: a surge of reinfection during the predominantly Omicron period. Lancet Reg Health West Pac. 2022;26:100572. https://doi.org/10.1016/j.lanwpc.2022.100572
13. Patalon T, Saciuk Y, Peretz A, Perez G, Lurie Y, Maor Y, et al. Waning effectiveness of the third dose of the BNT162b2 mRNA COVID-19 vaccine. Nat Commun. 2022;13:3203. https://doi.org/10.1038/s41467-022-30884-6
14. UK Health Security Agency. COVID-19 vaccine surveillance report Week 40. London: Public Health England, UK Health Security Agency; 2022.
15. Ontario Agency for Health Protection and Promotion (Public Health Ontario). Confirmed cases of COVID-19 following vaccination in Ontario: December 14, 2020 to April 23, 2023. Toronto (ON): King's Printer for Ontario; 2023.
16. Public Health Agency of Sweden. Protection by a third and fourth dose of vaccine against COVID-19 among persons aged 65 years and older: based on Swedish data from February to August 2022. Östersund (Sweden): The Agency; 2022.
17. Taiwan Centers for Disease Control. CECC raises epidemic warning to Level 3 nationwide from May 19 to May 28; strengthened measures and restrictions introduced across Taiwan to reduce community transmission [in Taiwanese]

[cited 2023 Jun 8]. https://www.cdc.gov.tw/En/Bulletin/Detail/VN_6yeoBTKhRKoSy2d0hJQ
18. Taiwan Centers for Disease Control. CECC extends nationwide Level 3 epidemic alert until July 26 to safeguard disease prevention efforts in the community; CECC to partially relax restrictions starting July 13 [in Taiwanese] [cited 2023 Jun 8]. https://www.cdc.gov.tw/En/Bulletin/Detail/vlmAORqyqEntz1Tr_Ls7DQ
19. Taiwan Centers for Disease Control. Taiwan to start COVID-19 vaccination with AstraZeneca vaccine on March 22 [in Taiwanese] [cited 2023 Jun 8]. https://www.cdc.gov.tw/Category/ListContent/EmXemht4IT-IRAPrAnyG9A
20. De Guzman C. Taiwan is abandoning its zero-COVID strategy in favor of a 'new model' of coronavirus containment. Time. 2022 May 12 [cited 2023 Apr 6]. https://time.com/6174132/taiwan-covid-strategy
21. Taiwan Centers for Disease Control. Community variants and genomic surveillance for SARS-CoV-2 in Taiwan [in Taiwanese]. Center for Diagnostic and Vaccine Development, editor. Taipei: The Centers; 2022 [cited 2023 Jun 8]. https://www.cdc.gov.tw/Bulletin/Detail/CvcKJh_3GBr7CpYQHY8TEA
22. Tsang NNY, So HC, Cowling BJ, Leung GM, Ip DKM. Effectiveness of BNT162b2 and CoronaVac COVID-19 vaccination against asymptomatic and symptomatic infection of SARS-CoV-2 omicron BA.2 in Hong Kong: a prospective cohort study. Lancet Infect Dis. 2023;23:421–34. https://doi.org/10.1016/S1473-3099(22)00732-0
23. Centers for Disease Control and Prevention. Science brief: SARS-CoV-2 infection-induced and vaccine-induced immunity. Atlanta: The Centers; 2020.
24. Chemaitelly H, Ayoub HH, AlMukdad S, Coyle P, Tang P, Yassine HM, et al. Protection from previous natural infection compared with mRNA vaccination against SARS-CoV-2 infection and severe COVID-19 in Qatar: a retrospective cohort study. Lancet Microbe. 2022;3:e944–55. https://doi.org/10.1016/S2666-5247(22)00287-7
25. Chen Q, Zhu K, Liu X, Zhuang C, Huang X, Huang Y, et al. The protection of naturally acquired antibodies against subsequent SARS-CoV-2 infection: a systematic review and meta-analysis. Emerg Microbes Infect. 2022;11:793–803. https://doi.org/10.1080/22221751.2022.2046446
26. Torales J, Cuenca-Torres O, Barrios L, Armoa-Garcia L, Estigarribia G, Sanabria G, et al. An evaluation of the safety and immunogenicity of MVC-COV1901: results of an interim analysis of a phase III, parallel group, randomized, double-blind, active-controlled immunobridging study in Paraguay. Vaccine. 2023;41:109–18. https://doi.org/10.1016/j.vaccine.2022.10.030
27. Mateo-Urdiales A, Sacco C, Petrone D, Bella A, Riccardo F, Del Manso M, et al.; Italian National COVID-19 Integrated Surveillance System and the Italian COVID-19 vaccines registry. Estimated effectiveness of a primary cycle of protein recombinant vaccine NVX-CoV2373 against COVID-19. JAMA Netw Open. 2023;6:e2336854. https://doi.org/10.1001/jamanetworkopen.2023.36854
28. Andrews N, Stowe J, Kirsebom F, Toffa S, Rickeard T, Gallagher E, et al. Covid-19 vaccine effectiveness against the Omicron (B.1.1.529) variant. N Engl J Med. 2022;386:1532–46. https://doi.org/10.1056/NEJMoa2119451
29. Santos CVBD, Valiati NCM, Noronha TG, Porto VBG, Pacheco AG, Freitas LP, et al. The effectiveness of COVID-19 vaccines against severe cases and deaths in Brazil from 2021 to 2022: a registry-based study. Lancet Reg Health Am. 2023;20:100465. https://doi.org/10.1016/j.lana.2023.100465
30. World Health Organization. SAGE updates COVID-19 vaccination guidance [cited 2023 Jun 8]. https://www.who.int/news/item/28-03-2023-sage-updates-covid-19-vaccination-guidance
31. Suah JL, Tng BH, Tok PSK, Husin M, Thevananthan T, Peariasamy KM, et al. Real-world effectiveness of homologous and heterologous BNT162b2, CoronaVac, and AZD1222 booster vaccination against Delta and Omicron SARS-CoV-2 infection. Emerg Microbes Infect. 2022;11:1343–5. https://doi.org/10.1080/22221751.2022.2072773
32. Nogareda F, Regan AK, Couto P, Fowlkes AL, Gharpure R, Loayza S, et al.; REVELAC-i Working Group. Effectiveness of COVID-19 vaccines against hospitalisation in Latin America during three pandemic waves, 2021–2022: a test-negative case-control design. Lancet Reg Health Am. 2023;27:100626. https://doi.org/10.1016/j.lana.2023.100626
33. Taiwan Central News Agency. A total of ten countries recognized the COVID-19 vaccine effectiveness of Medigen: Taiwan's Deputy Minister [in Taiwanese] [cited 2023 Jun 8]. https://www.cna.com.tw/news/ahel/202210200215.aspx
34. Heath PT, Galiza EP, Baxter DN, Boffito M, Browne D, Burns F, et al. Safety and efficacy of the NVX-CoV2373 coronavirus disease 2019 vaccine at completion of the placebo-controlled phase of a randomized controlled trial. Clin Infect Dis. 2023;76:398–407. https://doi.org/10.1093/cid/ciac803

Address for correspondence: Hung-Wei Kuo, Epidemic Intelligence Center, Taiwan Centers for Disease Control, Ministry of Health and Welfare, Fl 2, No. 6 Lin-shen South Rd, Taipei City, 10050, Taiwan; email: hwkuo@cdc.gov.tw

Effect of Pneumococcal Conjugate Vaccine on Pneumonia Incidence Rates among Children 2–59 Months of Age, Mongolia, 2015–2021

Claire von Mollendorf, Munkhchuluun Ulziibayar, Cattram D. Nguyen, Purevsuren Batsaikhan, Bujinlkham Suuri, Dashtseren Luvsantseren, Dorj Narangerel, John de Campo, Margaret de Campo, Bilegtsaikhan Tsolmon, Sodbayar Demberelsuren, Eileen M. Dunne, Catherine Satzke, Tuya Mungun, E. Kim Mulholland

Starting in June 2016, the 13-valent pneumococcal conjugate vaccine (PCV13) was introduced into the routine immunization program of Mongolia by using a 2+1 dosing schedule, phased by district. We used prospective hospital surveillance to evaluate the vaccine's effect on pneumonia incidence rates among children 2–59 months of age over a 6-year period. Of 17,607 children with pneumonia, overall adjusted incidence rate ratios showed decreased primary endpoint pneumonia, very severe pneumonia, and probable pneumococcal pneumonia until June 2021. Results excluding and including the COVID-19 pandemic period were similar. Pneumonia declined in 3 districts that introduced PCV13 with catch-up campaigns but not in the 1 district that did not. After PCV13 introduction, vaccine-type pneumococcal carriage prevalence decreased by 44% and nonvaccine-type carriage increased by 49%. After PCV13 introduction in Mongolia, the incidence of more specific pneumonia endpoints declined in children 2–59 months of age; additional benefits were conferred by catch-up campaigns.

Globally, the most common infectious cause of death among children 1–59 months of age is lower respiratory tract infection (1). Despite vaccine availability, *Streptococcus pneumoniae* causes a substantial proportion of severe pneumonia cases, attributed to 18.3% of severe pneumonia episodes and 32.7% of all pneumonia deaths in children globally (2). Pneumonia disease burden is highest among younger children and in certain regions such as southern Asia and Africa (2).

Mongolia is a lower-middle-income country in central Asia. Half of the Mongolia population of 3.3 million live in the capital city of Ulaanbaatar (3). Similar to other low- and middle-income countries (LMICs), several demographic and socioeconomic factors in Mongolia increase the risk for childhood pneumonia (4). Rapid urbanization with expansion of informal living areas and coal use during winter has resulted in poor air quality in Ulaanbaatar (5). Air pollution exacerbates respiratory diseases such as asthma and increases the risk for pneumonia (6).

In the past 2 decades, pneumococcal conjugate vaccines (PCVs) have had a substantial public health effect globally; effectiveness against hospitalization for invasive pneumococcal disease, clinical pneumonia, and radiologically confirmed pneumonia has been demonstrated (7,8). Modeling has estimated that, in children <5 years of age, introduction of 13-valent PCV (PCV13) resulted in a reduction of 175 million cases of pneumococcal disease and 625,000 associated deaths worldwide over 10 years (9). Among those cases, 14 million illnesses and 374,550 deaths

Author affiliations: Murdoch Children's Research Institute, Melbourne, Victoria, Australia (C. von Mollendorf, C.D. Nguyen, J. de Campo, M. de Campo, E.M. Dunne, C. Satzke, E.K. Mulholland); The University of Melbourne, Melbourne (C. von Mollendorf, C.D. Nguyen, J. de Campo, M. de Campo, E.M. Dunne, C. Satzke, E.K. Mulholland); National Center for Communicable Diseases, Ulaanbaatar, Mongolia (M. Ulziibayar, P. Batsaikhan, B. Suuri, D. Luvsantseren, B. Tsolmon, T. Mungun); Ministry of Health, Ulaanbaatar (D. Narangerel); Mongolian National University of Medical Sciences, Ulaanbaatar (B. Tsolmon); World Health Organization, Ulaanbaatar (S. Demberelsuren); Peter Doherty Institute for Infection and Immunity, Melbourne (C. Satzke); London School of Hygiene and Tropical Medicine, London, UK (E.K. Mulholland)

DOI: https://doi.org/10.3201/eid3003.230864

resulted from pneumococcal pneumonia (9); however, 6 countries in Asia have yet to introduce PCV into their national immunization programs, and in 2021, >25 million children in those regions still did not have access to the vaccines (10). Data from Asia with regard to pneumonia burden and PCV effect are lacking; only 2 studies have demonstrated the effect of PCV13 (11,12).

Starting in 2016, PCV13 was introduced into the routine infant immunization program of Mongolia, phased by district, in the context of an expanded pneumonia surveillance program to monitor vaccine effect (13). Baseline data estimated that clinical pneumonia incidence among children 2–59 months was 31.8 cases/1,000 population and for severe pneumonia was 19.2 cases/1,000 population (14). To ensure sustainability of the program in Mongolia, PCV13 was introduced in stages because the country was transitioning from Gavi funding (15).

Our study goal was to estimate the effect of PCV13 introduction on clinical and radiologic pneumonia endpoints among hospitalized children 2–59 months of age living in 4 districts of Ulaanbaatar, Mongolia, over a 6-year period. The study was approved by the Medical Ethics Review Committee at the Mongolian Ministry of Health and the Royal Children's Hospital Human Research Ethics Committee (HREC 33203). Written informed consent was obtained from all parents/caregivers for enrolled children before any study procedures were conducted.

Methods

Study Setting

Expanded hospital-based pneumonia surveillance was initiated in 4 districts of Ulaanbaatar in April 2015 as previously described (13,14). Mongolia introduced PCV13 into the national immunization program in a 2+1 schedule (2, 4, and 9 months) by district: June 2016 (Songinokhairkhan [SKD] and Sukhbaatar [SBD]), July 2017 (Bayanzurkh [BZD]), and March 2018 (Chingeltei [CHD]). Catch-up campaigns were instituted in the districts in which PCV13 was introduced in 2016 and 2017 (13,14). During 2017–2021, PCV13 coverage among the target age group from all introduced districts was reported to be 95%–98% (16).

Study Population and Design

During April 2015–June 2021, we enrolled children 2–59 months of age who were admitted to 1 of 4 four participating district hospitals (or the tertiary hospital if they resided in one of the relevant districts) and met the specific study case definition for clinical pneumonia. We excluded patients with bronchiolitis and bronchitis. Protocol details have been previously published (13) (Appendix, https://wwwnc.cdc.gov/EID/article/30/3/23-0864-App1.pdf). Bloodsamples, nasopharyngeal swab samples, and chest radiographs were collected for all enrolled patients or for whom consent was provided. To ensure that no eligible patients were missed, dedicated study staff ensured that patients were correctly enrolled by clinical hospital staff.

The primary study outcome was World Health Organization (WHO)–defined primary endpoint pneumonia (PEP) (17). Secondary outcomes were clinical pneumonia (all cases); severe pneumonia (WHO 2005 case definition [18]); very severe pneumonia (severe cases complicated by empyema, intensive care unit admission, persistent severe disease after discharge, hypoxia, or death [14]); hypoxic pneumonia (oxygen saturation <90%); probable pneumococcal pneumonia (PPP) (19) (elevated C-reactive protein with either PEP [19] or high pneumococcal nasopharyngeal carriage); or definite pneumococcal pneumonia (positive blood or pleural fluid culture) and pneumococcal carriage (13).

Sample Collection and Laboratory Procedures

We adhered to WHO recommended methods for nasopharyngeal sample collection, handling, and transport (20). We tested nasopharyngeal swab samples for pneumococci by using *lytA* real-time quantitative PCR and molecular serotyping by DNA microarray (Appendix) (21). We tested 1,000 patients/year for pneumococci, including all patients with PEP (primary objective) and a random sample of remaining patients.

Statistical Analyses

We summarized categorical variables with frequency counts and percentages and demographic variables by district and overall. To determine changes before and after PCV13 introduction, we compared characteristics of children during the 2 periods. We calculated crude annual incidence rates for April–March because surveillance started in April 2015 and pneumonia was highly seasonal and most cases were identified during winter. We obtained annual population estimates for denominators from the Mongolian Ministry of Health. We calculated CIs for incidence estimates by using a Poisson distribution. We based the definitions of pre-PCV13 and post-PCV13 periods on month of vaccine introduction at the district level. We calculated crude incidence rates and incidence rate ratios (IRRs) comparing pre-PCV13 and post-PCV13 periods for all patients and stratified them by district and age group.

We calculated adjusted IRRs (aIRRs) for different pneumonia endpoints comparing pre-PCV13 and post-PCV13 periods by using negative binomial regression with separate models for data until February 2020 (excluding the COVID-19 pandemic period) and June 2021 (end of study). All models included terms for PCV13 introduction, district, age group, and a categorical variable for each calendar month elapsed (to account for secular trends), with log-transformed population denominators included as an offset. To allow for a differential effect between districts, we included an interaction term between PCV13 and district for district-specific effects. The model coefficients were exponentiated to obtain IRRs with 95% CIs. We calculated percent reduction in pneumonia rates as (1 – IRR) × 100%. We conducted 2 sensitivity analyses for IRR calculations. We first introduced a 1-year lag period for effect of PCV introduction and then stratified IRRs by age group (2–23 months and 24–59 months).

We used univariable and multivariable log-binomial regression to estimate crude and adjusted prevalence ratios (aPR) for overall, PCV13-type and non-PCV13–type prevalence of pneumococcal carriage. To adjust prevalence ratios, we used a common set of confounders, selected by using a directed acyclic graph based on current literature (Appendix Figure 1). We calculated prevalence ratios by comparing the post-PCV13 with the pre-PCV13 period for all endpoints. Reductions in PCV13 carriage were calculated as (1 – aPR) × 100%. We used Stata statistical software 17.0 (StataCorp LLC, https://www.stata.com) to analyze data.

Results

During April 1, 2015–June 30, 2021, a total of 55,691 children 2–59 months of age with acute lower respiratory tract infections were admitted to one of the study hospitals; 17,688 (32%) were assessed according to the study case definition, received study consent, and were enrolled (Appendix Figure 2). Among the 17,607 confirmed to meet all study eligibility criteria, 71% were 2–23 months of age, 54% were male and 46% female, and most were admitted during autumn and winter (Appendix Table 1). More than two thirds of households had single children <5 years of age, and 21% of children attended kindergarten. Most participants (15,248 [87%]) had a risk-factor questionnaire completed by a parent or caregiver; 81% (14,184), underwent chest radiography; and 87% (15,411) had nasopharyngeal swab samples collected and processed, of which 6,545 swabs were tested for pneumococci. Of 13,602 children for whom complete data were available to assess PPP, 11% met the case definition. Blood cultures were performed for 15,232 (87%) children, but only 14 (0.1%) were culture-positive for *S. pneumoniae*. For 2 children, *S. pneumoniae* was cultured from pleural fluid; and for 1 child, blood culture was also positive.

The highest numbers of patients were enrolled from the largest districts, SKD and BZD. Differences were observed between the 4 study districts (Appendix Table 1). Most households in CHD (2,984/3,703 [81%]) and SKD (3,259/4,568 [71%]) used coal or wood as the main fuel source, and only half of the households in SBD and BZD used those smoky fuels. The highest proportions of participants living in crowded households were in CHD (32%) and SKD (36%) or living in informal housing were also in those same 2 districts (39% for CHD and 45% for SKD). Overall, 77% of participants had severe pneumonia; proportions were slightly higher in CHD (79%) and SKD (81%). A total of 37% of participants had very severe pneumonia; percentages were highest in BZD (43%) and CHD (46%). Of 13,755 children with interpretable chest radiographs, 1,813 (13%) had PEP (Appendix Table 1).

Pneumonia incidence rates were highly seasonal; case numbers were highest during winter (October–February) (Figure 1; Appendix Figure 3). After PCV13 introduction, peak incidence of all clinical pneumonia decreased, except in CHD, which had no PCV catch-up campaign (Figure 1). Pneumonia incidence decreased from February 2020 through June 2021, when COVID-19 restrictions, including kindergarten/school closures, were in place. No winter peak was observed during the 2020–21 season (Figure 1; Appendix Figure 3). Overall, 32% of admitted patients met the study case definition, which was intended to exclude patients with milder pneumonia (Appendix Figure 4).

The profile of participants differed before and after introduction of PCV13 (Appendix Table 2). Compared with the pre-PCV13 period, percentages were lower for children previously admitted (48% before vs. 42% after; p<0.0001), with hypoxia (22% before vs. 17% after; p<0.0001), or with primary endpoint pneumonia (14% before vs. 13% after; p = 0.007) in the post-PCV13 period. The percentage of children with severe and very severe pneumonia in the post-PCV13 period was also reduced (Appendix Table 2).

By March 2020 (early COVID-19 pandemic restrictions), changes for crude IRRs varied by pneumonia diagnosis and district (Appendix Table 3). For all districts combined, IRR was reduced for all patients

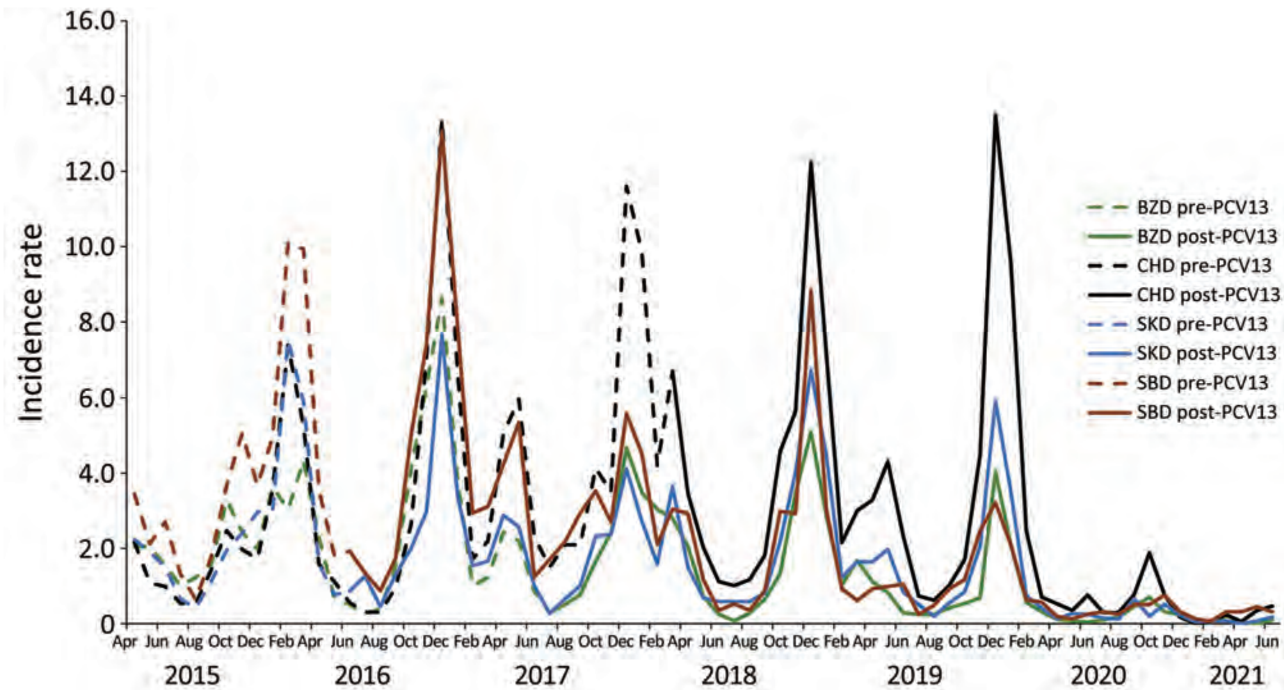

Figure 1. All clinical pneumonia incidence rates (cases/1,000 population) by month and district in children 2–59 months of age, Ulaanbaatar, Mongolia, April 2015–June 2021. BZD, Bayanzurkh District; CHD, Chingeltei District; PCV13, 13-valent pneumococcal conjugate vaccine; SBD, Sukhbaatar District; SKD, Songinokhairkhan District.

with all clinical pneumonia (21%, 95% CI 18%–23%), PEP (20%, 95% CI 12%–27%), severe pneumonia (23%, 95% CI 20%–25%), very severe pneumonia (26%, 95% CI 22%–29%), hypoxic pneumonia (34%, 95% CI 29%–39%), and PPP (38%, 95% CI 31%–44%). Individual districts mainly showed reductions, except for CHD, which showed increases in IRRs in cases of all clinical, severe, and very severe pneumonia. By March 2021, which included a period of COVID-19 restrictions, additional reductions were observed in line with reduced case numbers, and PEP was reduced by 36% (95% CI 29%–42%) (Appendix Table 3). We found some variability by age group; slightly larger reductions were observed for the 24–59-month age group compared with the younger age group (Appendix Table 4). Annual incidence rates were highest in 2016 in SKD, SBD, and BZD, but CHD showed high incidence rates until 2019 (Appendix Table 5).

To account for secular trends and district effect not accounted for in crude IRRs, we calculated aIRRs for different pneumonia endpoints until February 2020 before extensive COVID-19 lockdown measures (Figure 2; Appendix Table 6). Those aIRRs showed a reduction in all clinical pneumonia rates in 3 of the districts (BZD 0.71, 95% CI 0.59–0.85; SKD 0.86, 95% CI 0.70–1.07; SBD 0.64, 95% CI 0.51–0.79) and an increase in 1 district (CHD 1.68, 95% CI 1.41–2.01) where PCV13 was introduced last without a catch-up campaign. The trends observed in the other pneumonia endpoints were similar across districts. For all districts combined by February 2020, aIRRs showed a reduction in PEP (0.72, 95% CI 0.56–0.93), very severe pneumonia (0.77, 95% CI 0.64–0.93), and PPP (0.77, 95% CI 0.61–0.97); however, reductions were not shown for severe pneumonia (0.97, 95% CI 0.82–1.15), hypoxic pneumonia (0.83, 95% CI 0.67–1.04), or all clinical pneumonia (1.01, 95% CI 0.87–1.17) (Figure 2; Appendix Table 6). Reductions were similar until June 2021 (Figure 3, Appendix Table 6).

A total of 6,545 samples were tested for pneumococci. Overall, 3,056 (47%) were positive for pneumococcal carriage and 2,557 (84%) were culturable and had serotyping results, of which 1,058 (41%) had PCV13-type serotypes, 1,267 (50%) had non–PCV13-type serotypes, and 232 (9%) had both types of serotype identified. In all districts combined, overall pneumococcal carriage prevalence (any serotype) did not change between the pre-PCV13 (48%) and post-PCV13 (46%) periods (adjusted prevalence ratio [aPR] 0.98, 95% CI 0.92–1.04) overall or in the individual districts (Table). PCV13-type carriage overall was reduced by 44% (aPR 0.56, 95% CI 0.51–0.62) and in each district ranging from 41% in BZD and SBD to 50% in SKD. Non–PCV13-type carriage increased overall (aPR 1.49, 95% CI 1.32–1.67) and significantly in 2 districts (Table).

Sensitivity Trends

We calculated aIRRs, assuming a delay of 1 year for the effect of PCV13 introduction among all children 2–59 months of age (Appendix Table 7). Results for PEP were similar to those of the main analysis (26% [95% CI 4%–43%] reduction). We observed a greater reduction in clinical pneumonia (24%, 95% CI 9%–36%), severe pneumonia (24%, 95% CI 8%–38%), and very severe pneumonia (30%, 95% CI 14%–44%) compared with the main analyses.

Stratification by age group (2–23 months and 24–59 months) demonstrated a greater reduction in most endpoints among older children. All clinical pneumonia cases were reduced by 12% (95% CI −7% to 27%) (negative numbers indicate an increase), PEP a 38% (95% CI 10%–57%) reduction, severe pneumonia a 13% (95% CI −9% to 30%) reduction, very severe pneumonia a 39% (95% CI 21%–52%) reduction, and hypoxic pneumonia a 31% (95% CI 7%–48%) reduction in all districts combined (Appendix Table 7).

Discussion

In our large-scale surveillance study in Mongolia, a country with a high burden of respiratory disease, we demonstrated the effect of PCV13 introduction on children hospitalized for pneumonia. We found that phased introduction of PCV13 in 4 districts of Ulaanbaatar resulted in reduced disease incidence, with some variability by district, age, and pneumonia endpoint used. Overall, PCV13 led to similar reductions in cases of PEP (28%), very severe pneumonia (23%), and PPP (23%) but no significant reduction of all clinical pneumonia or severe pneumonia. Reductions were observed in 3 districts in which catch-up campaigns were conducted at the time of vaccine introduction. PCV13-type pneumococcal carriage declined overall (44%) and in each individual district. Non–PCV13-type carriage increased overall and significantly in 2 districts. Our surveillance program is one of few programs reporting PCV13 effect on pneumonia for a high-burden LMIC in Asia.

Many countries have used invasive pneumococcal disease (IPD) to determine PCV effect. Because IPD is rare and requires robust laboratory capacity, using IPD is often not possible in LMICs, nor is it an ideal metric in countries such as Mongolia with small populations and few annual IPD cases detected. Pneumonia surveillance can be an indicator of PCV effect. A challenge in studying PCV effect on pneumonia is that young children do not produce sputum, very few cases are bacteremic, and no diagnostic tests are available for nonbacteremic pneumococcal pneumonia in this age group.

In Fiji, a time-series analysis 5 years after PCV10 introduction found a reduction in pediatric hospitalizations for pneumonia, varying by age and pneumonia endpoint (22). Similar to the Fiji study, we found that compared with younger children, the reduction of pneumonia was greater among children 24–59 months of age, although a lower proportion of children in that group were fully vaccinated. It is likely that a higher percentage of cases in the older group were caused by pneumococcus and in the younger (<2 years of age) group by respiratory syncytial virus (23).

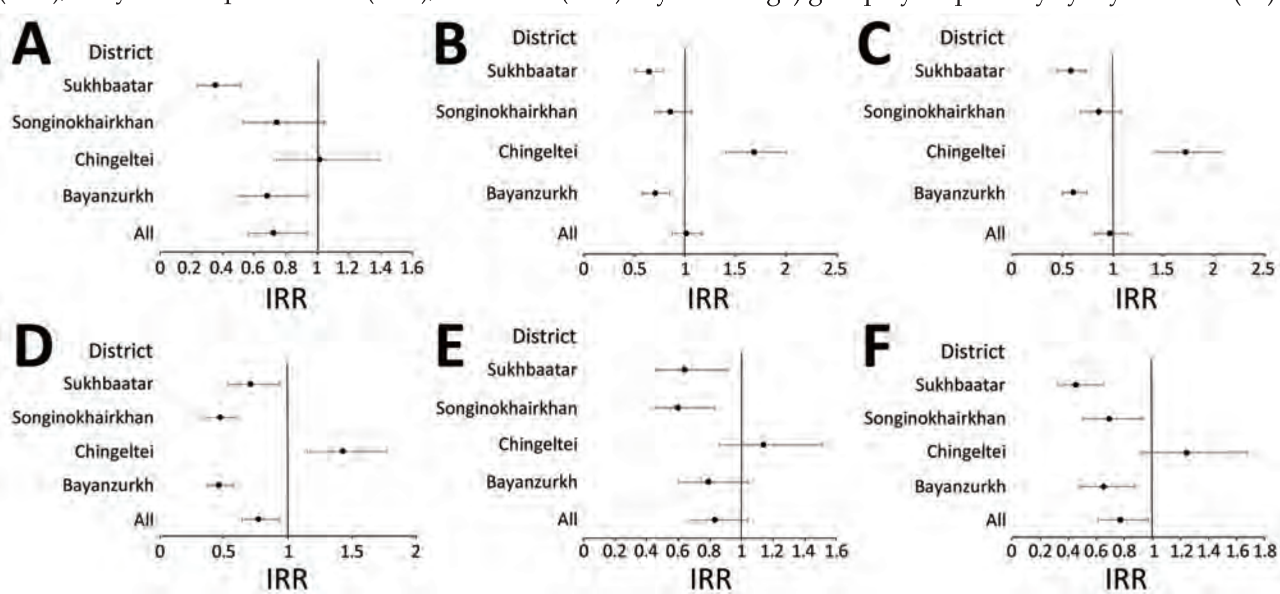

Figure 2. Adjusted IRRs for pneumonia endpoints for pre-vaccine period (April 2015–February 2020, excluding COVID-19 pandemic period) in study of effect of pneumococcal conjugate vaccine on pneumonia incidence rates among children 2–59 months of age, Mongolia, 2015–2021. A) Primary endpoint pneumonia; B) all pneumonia; C) severe pneumonia; D) very severe pneumonia; E) hypoxic pneumonia; F) probable pneumococcal pneumonia. Error bars indicate 95% CIs. IRR, incidence rate ratio.

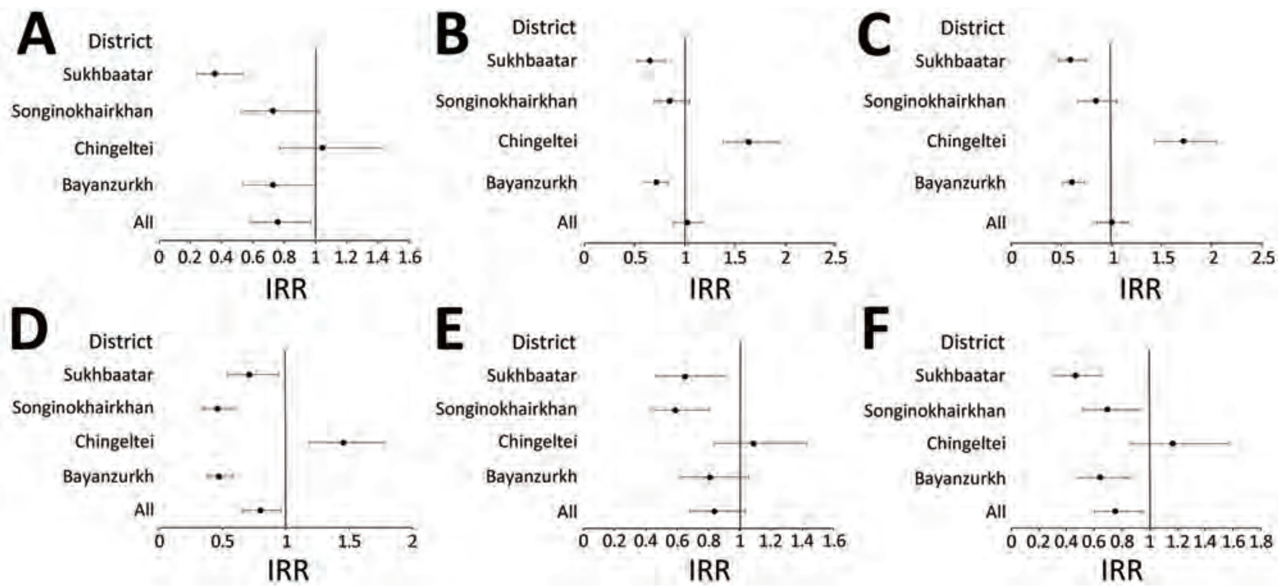

Figure 3. Adjusted IRRs for pneumonia endpoints post-vaccine period (April 2015–June 2021, including COVID-19 pandemic period) in study of effect of pneumococcal conjugate vaccine on pneumonia incidence rates among children 2–59 months of age, Mongolia, 2015–2021. A) Primary endpoint pneumonia; B) all pneumonia; C) severe pneumonia; D) very severe pneumonia; E) hypoxic pneumonia; F) probable pneumococcal pneumonia. Error bars indicate 95% CIs. IRR, incidence rate ratio.

A recent systematic review found a decline in pneumonia hospitalization incidence among children after PCV introduction, although the magnitude of the decline across different endpoints and settings displayed heterogeneity (24). The review demonstrated that PCV effect tended to increase as the pneumonia outcome increased in diagnostic specificity for pneumococcal disease (24). We observed substantial declines in carriage of PCV13 serotypes as well as declines in pneumonia outcomes considered more likely to be caused by pneumococcus, such as PEP and very severe pneumonia.

The decrease in pneumonia cases during 2020 and 2021 probably results from measures put in place to combat the COVID-19 pandemic. Mongolia instituted kindergarten/school closures from the end of January 2020 until September 2021, except for a brief period during late 2020 (25,26). In addition, travel bans, multiple hard lockdowns, and other public health nonpharmaceutical interventions were instituted (25,27), and COVID-19 vaccines were available starting in February 2021 (27). Studies from other countries have shown that restrictions instituted during the COVID-19 pandemic reduced childhood infections (28,29).

The use of catch-up campaigns has been encouraged by WHO as a strategy to increase herd immunity (30). Observational data from LMICs documenting the effect of catch-up campaigns are limited. A transmission dynamic model using data from Kenya indicated that a catch-up campaign among children <5 years of age prevented additional IPD cases and used fewer doses per case averted than routine introduction only (31). In our surveillance program, PCV introduction included a catch-up campaign in 3 of the 4 study districts. Pneumonia incidence was not significantly reduced in the district without catch-up (CHD) but was reduced, especially for more severe pneumonia endpoints, in the other districts. Of note, CHD was the last district to introduce PCV13, and no significant increase in non–PCV13-type carriage was demonstrated. The average annual coverage in eligible age groups in CHD was similar to routine coverage in BZD, where PCV13 was introduced in 2017.

In addition to catch-up campaigns, other explanations for different results between districts are variable smoke exposure, levels of poverty, housing type, crowding, and other factors reflective of known risk factors for pneumonia (4). Movement between districts and migration may also have varied over the study period. A previous publication from Mongolia found evidence of direct and indirect vaccine effects on carriage, which varied by formal and informal living conditions (32). We observed a reduction (46%) in vaccine-type pneumococcal carriage 3–5 years after introduction in 4 districts. We identified residual circulation of vaccine serotypes (17%) despite high PCV coverage, similar to findings in Malawi and South Africa (33,34).

One study strength is establishment of an expanded active pneumonia surveillance program on preexisting WHO invasive bacterial disease surveillance

Table. Carriage prevalence and prevalence ratios for pneumococcal carriage among 6,545 children with pneumonia before and after PCV13 availability, 4 districts, Mongolia, 2015–2021*

Pneumococcal type	Pre-PCV13, no./total	Pre-PCV13 prevalence, % (95% CI)	Post-PCV13 no./total	Post-PCV13 prevalence, % (95% CI)	Unadjusted prevalence ratio (95% CI)	Adjusted prevalence ratio (95% CI)†
Overall pneumococci						
All districts	882/1,837	48.0 (45.7–50.3)	2,174/4,708	46.2 (44.7–47.6)	0.96 (0.91–1.02)	0.98 (0.92–1.04)
Bayanzurkh	263/657	40.0 (36.2–43.9)	363/905	40.1 (36.9–43.4)	1.00 (0.89–1.13)	1.06 (0.93–1.21)
Chingeltei	341/592	57.6 (53.5–61.6)	565/1,194	47.3 (44.4–50.2)	0.82 (0.75–0.90)	0.81 (0.73–0.90)
Songinokhairkhan	184/368	50.0 (44.8–55.2)	953/1,891	50.4 (48.1–52.7)	1.01 (0.90–1.13)	1.00 (0.89–1.12)
Sukhbaatar	94/220	42.7 (36.1–49.5)	293/718	40.8 (37.2–44.5)	0.95 (0.80–1.14)	0.95 (0.79–1.14)
PCV13 serotypes						
All districts	548/1,742	31.4 (29.3–33.7)	742/4,304	17.2 (16.1–18.4)	0.55 (0.50–0.60)	0.56 (0.51–0.62)
Bayanzurkh	161/614	26.2 (22.8–29.9)	119/830	14.3 (12.0–16.9)	0.55 (0.44–0.68)	0.59 (0.47–0.75)
Chingeltei	200/566	35.3 (31.4–39.4)	205/1,077	19.0 (16.7–21.5)	0.54 (0.46–0.64)	0.53 (0.44–0.63)
Songinokhairkhan	127/354	35.9 (30.9–41.1)	306/1,737	17.6 (15.8–19.5)	0.49 (0.41–0.58)	0.50 (0.42–0.61)
Sukhbaatar	60/208	28.8 (22.8–35.5)	112/660	17.0 (14.2–20.0)	0.59 (0.45–0.77)	0.59 (0.44–0.78)
Non-PCV13 serotypes						
All districts	329/1,742	18.9 (17.1–20.8)	1,170/4,304	27.2 (25.8–28.5)	1.44 (1.29–1.60)	1.49 (1.32–1.67)
Bayanzurkh	76/614	12.4 (9.9–15.2)	193/830	23.2 (20.4–26.3)	1.88 (1.47–2.40)	1.95 (1.49–2.55)
Chingeltei	152/566	26.8 (23.2–30.7)	286/1,077	26.5 (23.9–29.3)	0.99 (0.83–1.17)	0.96 (0.79–1.17)
Songinokhairkhan	69/354	19.5 (15.5–24.0)	550/1,737	31.7 (29.5–33.9)	1.62 (1.30–2.03)	1.57 (1.24–1.99)
Sukhbaatar	32/208	15.4 (10.8–21.0)	141/660	21.4 (18.3–24.7)	1.39 (0.98–1.97)	1.26 (0.88–1.81)

*Overall, PCV13 serotypes and non-PCV13 serotypes. PCV13, 13-valent pneumococcal conjugate vaccine.
†Adjusted by using a common set of confounders: age, informal housing, other children <5 y of age in the home, coal used for fuel, household income, crowding, maternal education, season, and antimicrobial drug receipt 48 h before admission.

in 4 districts of Ulaanbaatar. All patients admitted for pneumonia were screened daily by clinical staff, and they were enrolled if they met a prespecified case definition. The case definition selected for more severe cases. To ensure that all eligible patients were identified, dedicated study staff monitored weekly enrollments performed by clinical staff. Any eligible patients that were missed were enrolled retrospectively, ensuring a high inclusion rate. The 6-year study included a considerable number of patients admitted for respiratory conditions. A structured questionnaire was completed for participants, and most underwent chest radiography and specimen collection. The radiographs were reread by 2 experienced independent radiologists using WHO guidelines (17), and sensitive molecular methods were used to measure pneumococcal carriage and determine serotypes (20). In Mongolia, hospitalization is free for all children <5 years of age, which reduces bias associated with access to care. In addition, Mongolia has a structured public healthcare system in which most patients flow from primary care to district hospitals, enabling population-based estimates. The adherence of patients to this referral pathway can sometimes vary, however, by socioeconomic status and setting (35).

The first limitation our study was that although we had only 1 year of pre-PCV13 data in all districts, because of a phased PCV13 introduction, we had 2–3 years of data before vaccine introduction in half of the districts. Second, the study included only 4 Ulaanbaatar districts, so the results may not be generalizable to all children in Mongolia, although the included districts are the largest in Ulaanbaatar and half the country's population live in this city. Third, we did not collect data for a nonrespiratory control condition and could not account for other interventions, such as air pollution measures, which may have affected pneumonia trends. Fourth, the COVID-19 pandemic affected case numbers; however, adjusted IRRs were similar before or including this period. Last, ongoing internal migration of inhabitants and a possible increase in unregistered migrants during a migration ban (2017–2020) (36) may have potentially affected denominators and thus incidence rates. In addition, urban redevelopment of traditional tented housing (ger) districts resulted in the temporary relocation of inhabitants from ger to other subdistricts (37). Redevelopment and relocation were reported in the ger subdistricts of CHD during 2016 and 2017 (37), which may have resulted in lower case numbers reported in these years, because of patients accessing alternative district hospitals, and contributed to an overall rate increase.

In conclusion, PCV13 introduction into the childhood immunization schedule in Mongolia, with catch-up vaccination in 3 districts, resulted in substantially reduced pneumonia incidence. The decreases were more prominent for more severe disease endpoints and in PCV13-type pneumococcal colonization. Other countries that have satisfactory PCV coverage can expect decreased severe pneumonia cases and vaccine-type carriage after vaccine introduction. Countries should consider offering catch-up vaccination when introducing PCV and should monitor changes in disease burden and pneumococcal serotypes through surveillance. Our study adds to limited data available on PCV effects for Asia and for countries transitioning from Gavi financial support.

This article was published as a preprint at https://www.ssrn.com/abstract=4485625.

Acknowledgments

We acknowledge the Ministry of Health in Mongolia, the WHO country and regional offices, and colleagues at UNICEF for their support for this project; Stephen Lacey for his assistance with the review of radiologic equipment and training of radiology staff in Mongolia; and the study staff, laboratory staff in Mongolia and Murdoch Children's Research Institute, and participating families.

This project was funded by the Gavi Alliance (contract no. PP61690717A2). C.S. was supported by a National Health and Medical Research Council Career Development Fellowship (1087957) and a veski inspiring women fellowship. Authors affiliated with Murdoch Children's Research Institute were supported by the Victoria government Operational Infrastructure Support Program. The funders had no role in study design, data collection and analysis, decision to publish, or preparation of the manuscript.

C.v.M., M.U., C.D.N, P.B., B.S., D.L., C.S., T.M., and E.K.M. are investigators on a Pfizer collaborative research project outside this work. E.M.D. is employed by Pfizer. C.S., E.K.M., and C.D.N. are investigators on a Merck Investigator Studies Program grant funded by MSD outside this work. The other authors have no relevant conflicts of interest to declare.

E.K.M., C.v.M., and C.S. are responsible for conception/design of the work; C.v.M., T.M., E.K.M., B.T., D.N., and S.D. for study oversight; M.U., B.S., D.L., P.B., and T.M. for acquisition of data; and C.S. and E.M.D. for oversight of pneumococcal carriage data acquisition. C.v.M, T.M., E.M.D., E.K.M., C.S., J.d.C., and M.d.C supported interpretation of the data; C.v.M., and C.N. devised the analysis plan; C.v.M. analyzed the data and drafted the manuscript. All authors were involved in data interpretation and review of the final manuscript.

About the Author

Dr. von Mollendorf is a medical epidemiologist at the Murdoch Children's Research Institute and an associate professor at the University of Melbourne, Melbourne, Australia. Her research interests include infectious diseases, pneumococcal and other vaccines, and global health.

References

1. Perin J, Mulick A, Yeung D, Villavicencio F, Lopez G, Strong KL, et al. Global, regional, and national causes of under-5 mortality in 2000–19: an updated systematic analysis with implications for the Sustainable Development Goals. Lancet Child Adolesc Health. 2022;6:106–15. https://doi.org/10.1016/S2352-4642(21)00311-4
2. Walker CLF, Rudan I, Liu L, Nair H, Theodoratou E, Bhutta ZA, et al. Global burden of childhood pneumonia and diarrhoea. Lancet. 2013;381:1405–16. https://doi.org/10.1016/S0140-6736(13)60222-6
3. Center for Health Development, World Health Organization. Health Indicators 2019 [cited 2022 Mar 13]. http://hdc.gov.mn/media/uploads/2021-05/Health_Indicator_2019_ENG.pdf
4. Marangu D, Zar HJ. Childhood pneumonia in low-and-middle-income countries: an update. Paediatr Respir Rev. 2019;32:3–9.
5. Ganbat G, Soyol-Erdene T-O, Jadamba B. Recent improvement in particulate matter (PM) pollution in Ulaanbaatar, Mongolia. Aerosol Air Qual Res. 2020;20:2280–8. https://doi.org/10.4209/aaqr.2020.04.0170
6. Kurt OK, Zhang J, Pinkerton KE. Pulmonary health effects of air pollution. Curr Opin Pulm Med. 2016;22:138–43. https://doi.org/10.1097/MCP.0000000000000248
7. Wahl B, O'Brien KL, Greenbaum A, Majumder A, Liu L, Chu Y, et al. Burden of *Streptococcus pneumoniae* and Haemophilus influenzae type b disease in children in the era of conjugate vaccines: global, regional, and national estimates for 2000-15. Lancet Glob Health. 2018;6:e744–57. https://doi.org/10.1016/S2214-109X(18)30247-X
8. Cohen O, Knoll MD, O'Brien KL, Ramakrishnan M, Constenla D, Privor-Dumm L, et al. Pneumococcal conjugate vaccine (PCV) review of impact evidence (PRIME) summary of findings from systematic review [cited 2022 Mar 11]. https://terrance.who.int/mediacentre/data/sage/SAGE_Docs_Ppt_Oct2017/9_session_PCV/Oct2019_session9_PCV_PRIMEsummary.pdf
9. Chapman R, Sutton K, Dillon-Murphy D, Patel S, Hilton B, Farkouh R, et al. Ten year public health impact of 13-valent pneumococcal conjugate vaccination in infants: a modelling analysis. Vaccine. 2020;38:7138–45. https://doi.org/10.1016/j.vaccine.2020.08.068
10. International Vaccine Access Center, VIEW-hub. Pneumococcal conjugate vaccine introduction and use [cited 2023 Feb 12]. https://view-hub.org/map
11. Weaver R, Nguyen CD, Chan J, Vilivong K, Lai JYR, Lim R, et al. The effectiveness of the 13-valent pneumococcal conjugate vaccine against hypoxic pneumonia in children in Lao People's Democratic Republic: an observational hospital-based test-negative study. Lancet Reg Health West Pac. 2020;2:100014. https://doi.org/10.1016/j.lanwpc.2020.100014
12. Blyth CC, Britton KJ, Nguyen CD, Sapura J, Kave J, Nivio B, et al. Effectiveness of 13-valent pneumococcal conjugate vaccine against hypoxic pneumonia and hospitalisation in Eastern Highlands Province, Papua New Guinea: an observational cohort study. Lancet Reg Health West Pac. 2022;22:100432. https://doi.org/10.1016/j.lanwpc.2022.100432
13. La Vincente SF, von Mollendorf C, Ulziibayar M, Satzke C, Dashtseren L, Fox KK, et al. Evaluation of a phased pneumococcal conjugate vaccine introduction in Mongolia using enhanced pneumonia surveillance and community carriage surveys: a study protocol for a prospective observational study and lessons learned. BMC Public Health. 2019;19:333. https://doi.org/10.1186/s12889-019-6639-y

14. von Mollendorf C, La Vincente S, Ulziibayar M, Suuri B, Luvsantseren D, Narangerel D, et al. Epidemiology of pneumonia in the pre-pneumococcal conjugate vaccine era in children 2–59 months of age, in Ulaanbaatar, Mongolia, 2015-2016. PLoS One. 2019;14:e0222423. https://doi.org/10.1371/journal.pone.0222423
15. Kallenberg J, Mok W, Newman R, Nguyen A, Ryckman T, Saxenian H, et al. Gavi's transition policy: moving from development assistance to domestic financing of immunization programs. Health Aff (Millwood). 2016;35:250–8. https://doi.org/10.1377/hlthaff.2015.1079
16. World Health Organization. Immunization Mongolia 2023 country profile [cited 2023 Dec 4]. https://www.who.int/publications/m/item/immunization-mongolia-2023-country-profile
17. Cherian T, Mulholland EK, Carlin JB, Ostensen H, Amin R, de Campo M, et al. Standardized interpretation of paediatric chest radiographs for the diagnosis of pneumonia in epidemiological studies. Bull World Health Organ. 2005;83:353–9.
18. World Health Organization. Handbook IMCI: integrated management of childhood illness [cited 2022 Jun 16]. https://apps.who.int/iris/bitstream/handle/10665/42939/9241546441.pdf
19. Madhi SA, Klugman KP. World Health Organisation definition of "radiologically-confirmed pneumonia" may under-estimate the true public health value of conjugate pneumococcal vaccines. Vaccine. 2007;25:2413–9. https://doi.org/10.1016/j.vaccine.2006.09.010
20. Satzke C, Turner P, Virolainen-Julkunen A, Adrian PV, Antonio M, Hare KM, et al. Standard method for detecting upper respiratory carriage of *Streptococcus pneumoniae:* updated recommendations from the World Health Organization Pneumococcal Carriage Working Group. Vaccine. 2013;32:165–79.
21. von Mollendorf C, Dunne EM, La Vincente S, Ulziibayar M, Suuri B, Luvsantseren D, et al. Pneumococcal carriage in children in Ulaanbaatar, Mongolia before and one year after the introduction of the 13-valent pneumococcal conjugate vaccine. Vaccine. 2019;37:4068–75. https://doi.org/10.1016/j.vaccine.2019.05.078
22. Reyburn R, Tuivaga E, Nguyen CD, Ratu FT, Nand D, Kado J, et al. Effect of ten-valent pneumococcal conjugate vaccine introduction on pneumonia hospital admissions in Fiji: a time-series analysis. Lancet Glob Health. 2021;9:e91–8. https://doi.org/10.1016/S2214-109X(20)30421-6
23. von Mollendorf C, Berger D, Gwee A, Duke T, Graham SM, Russell FM, et al.; ARI Review Group. Aetiology of childhood pneumonia in low- and middle-income countries in the era of vaccination: a systematic review. J Glob Health. 2022;12:10009. https://doi.org/10.7189/jogh.12.10009
24. Reyburn R, Tsatsaronis A, von Mollendorf C, Mulholland K, Russell FM; ARI Review Group. Systematic review on the impact of the pneumococcal conjugate vaccine ten valent (PCV10) or thirteen valent (PCV13) on all-cause, radiologically confirmed and severe pneumonia hospitalisation rates and pneumonia mortality in children 0–9 years old. J Glob Health. 2023;13:05002. https://doi.org/10.7189/jogh.13.05002
25. Erkhembayar R, Dickinson E, Badarch D, Narula I, Warburton D, Thomas GN, et al. Early policy actions and emergency response to the COVID-19 pandemic in Mongolia: experiences and challenges. Lancet Glob Health. 2020;8:e1234–41. https://doi.org/10.1016/S2214-109X(20)30295-3
26. Ministry of Health (Mongolia). Mongolia Ministry of Health and Social Protection COVID-19 2020–2022 [cited 2-22 Oct 28]. https://ghdx.healthdata.org/record/mongolia-ministry-health-and-social-protection-covid-19-situation-report
27. Ganzon JG, Lin X, Shehata DJ, Gandour G, Turay FU, Bah AS, et al. A perspective on impeding the COVID-19 pandemic: lessons from Mongolia's comprehensive countermeasure. Health Sci Rep. 2022;6:e1017. https://doi.org/10.1002/hsr2.1017
28. Kuitunen I, Artama M, Mäkelä L, Backman K, Heiskanen-Kosma T, Renko M. Effect of social distancing due to the COVID-19 pandemic on the incidence of viral respiratory tract infections in children in Finland during early 2020. Pediatr Infect Dis J. 2020;39:e423–7. https://doi.org/10.1097/INF.0000000000002845
29. Kadambari S, Goldacre R, Morris E, Goldacre MJ, Pollard AJ. Indirect effects of the covid-19 pandemic on childhood infection in England: population based observational study. BMJ. 2022;376:e067519. https://doi.org/10.1136/bmj-2021-067519
30. World Health Organization. Pneumococcal vaccines WHO position paper—2012. Wkly Epidemiol Rec. 2012;87:129–44.
31. Flasche S, Ojal J, Le Polain de Waroux O, Otiende M, O'Brien KL, Kiti M, et al. Assessing the efficiency of catch-up campaigns for the introduction of pneumococcal conjugate vaccine: a modelling study based on data from PCV10 introduction in Kilifi, Kenya. BMC Med. 2017;15:113. https://doi.org/10.1186/s12916-017-0882-9
32. Chan J, Mungun T, Batsaixan P, Ulziibayar M, Suuri B, Otgonbayar D, et al.; PneuCAPTIVE Mongolia Research Group. Direct and indirect effects of 13-valent pneumococcal conjugate vaccine on pneumococcal carriage in children hospitalised with pneumonia from formal and informal settlements in Mongolia: an observational study. Lancet Reg Health West Pac. 2021;15:100231. https://doi.org/10.1016/j.lanwpc.2021.100231
33. Swarthout TD, Fronterre C, Lourenço J, Obolski U, Gori A, Bar-Zeev N, et al. High residual carriage of vaccine-serotype *Streptococcus pneumoniae* after introduction of pneumococcal conjugate vaccine in Malawi. Nat Commun. 2020;11:2222. https://doi.org/10.1038/s41467-020-15786-9
34. Madhi SA, Nzenze SA, Nunes MC, Chinyanganya L, Van Niekerk N, Kahn K, et al. Residual colonization by vaccine serotypes in rural South Africa four years following initiation of pneumococcal conjugate vaccine immunization. Expert Rev Vaccines. 2020;19:383–93. https://doi.org/10.1080/14760584.2020.1750377
35. World Health Organization. Primary Health Care Systems (PRIMASYS): comprehensive case study from Mongolia [cited 2023 Feb 9]. https://iris.who.int/bitstream/handle/10665/341092/WHO-HIS-HSR-17.34-eng.pdf
36. International Organization for Migration. Research study on assessing the effectiveness of migration restrictions in Ulaanbaatar City and migrants' vulnerability. Ulaanbaatar (Mongolia); The Organization; 2021.
37. Asian Development Bank. Mongolia: Ulaanbaatar Urban Services and Ger Areas Development Investment Program: revised facility administration manual [cited 2023 Dec 18]. https://www.adb.org/projects/documents/mon-45007-003-fam-0

Address for correspondence: Claire von Mollendorf, Murdoch Children's Research Institute, The Royal Children's Hospital, 50 Flemington Rd, Parkville, VIC 3052 Australia; email: claire.vonmollendorf@mcri.edu.au

Spatial Analysis of Drug-Susceptible and Multidrug-Resistant Cases of Tuberculosis, Ho Chi Minh City, Vietnam, 2020–2023

Ruan Spies, Hanh N. Hong, Phu P. Trieu, Luong K. Lan, Kim Lan, N.N. Hue, Nguyen T.L. Huong, Tran T.L.N. Thao, Nguyen L. Quang, Thu D.D. Anh, Truong V. Vinh, Dang T.M. Ha, Phan T. Dat, Nguyen P. Hai, Le H. Van, Guy E. Thwaites, Nguyen T.T. Thuong, James A. Watson,[1] Timothy M. Walker[1]

We characterized the spatial distribution of drug-susceptible (DS) and multidrug-resistant (MDR) tuberculosis (TB) cases in Ho Chi Minh City, Vietnam, a major metropolis in southeastern Asia, and explored demographic and socioeconomic factors associated with local TB burden. Hot spots of DS and MDR TB incidence were observed in the central parts of Ho Chi Minh City, and substantial heterogeneity was observed across wards. Positive spatial autocorrelation was observed for both DS TB and MDR TB. Ward-level TB incidence was associated with HIV prevalence and the male proportion of the population. No ward-level demographic and socioeconomic indicators were associated with MDR TB case count relative to total TB case count. Our findings might inform spatially targeted TB control strategies and provide insights for generating hypotheses about the nature of the relationship between DS and MDR TB in Ho Chi Minh City and the wider southeastern region of Asia.

Tuberculosis (TB) causes more deaths worldwide than any other infectious disease. Progress in reducing the global burden of TB stalled during the COVID-19 pandemic; an estimated 10.6 million persons became ill from TB in 2021, and 1.6 million died (*1*). The number of persons with multidrug-resistant TB (MDR TB), defined by resistance to rifampin and isoniazid, is estimated to have increased by 3.1% since 2020 (*1*), including an estimated 450,000 incident cases in 2021. MDR TB remains underdiagnosed and is associated with worse treatment outcomes than for drug-susceptible TB (DS TB) (*1*,*2*).

TB is spatially heterogeneous both globally and locally. Thirty low- and middle-income countries account for nearly 90% of the global burden of disease (*1*), but an unequal distribution of disease has also been described more locally (*3*–*12*). Although poorly understood, the drivers of geographic heterogeneity in TB are believed to reflect the complex interplay between the infectious and susceptible host, the infecting organism, the physical environment, and distal determinants such as poverty (*13*).

The World Health Organization (WHO) recognizes Vietnam as a high-burden country for TB and MDR TB; estimated incidence is 173 (95% CI 112–247) cases/100,000 population for TB and 9.1 (95% CI 5.5–13) cases/100,000 population for MDR TB (*1*,*14*). The highest incidence is seen in the southern parts of the country, especially in Ho Chi Minh City (*15*,*16*). Patients with MDR TB in Ho Chi Minh City can have acquired their disease through selection of drug-resistance mutations while receiving first-line TB drug treatment or directly from others through transmission (*17*). Comparison of the spatial distributions of DS and MDR TB across this high-incidence city has the potential to offer insights into relative contributions of each to MDR TB burden. For example, the observation of distinct spatial distributions of DS and MDR TB might support the hypothesis that MDR TB is transmitted in networks independent

Author affiliations: University of Oxford, Oxford, UK (R. Spies, G.E. Thwaites, N.T.T. Thuong, J.A. Watson, T.M. Walker); Oxford University Clinical Research Unit, Ho Chi Minh City, Vietnam (H.N. Hong, P.P. Trieu, L.K. Lan, K. Lan, N.N. Hue, N.T.L. Huong, T.L.T.N. Thao, N.L. Quang, T.D.D. Anh, L.H. Van, G.E. Thwaites, N.T.T. Thuong, J.A. Watson, T.M. Walker); Pham Ngoc Thach Hospital, Ho Chi Minh City (T.V. Vinh, D.T.M. Ha, P.T. Dat, N.P. Hai)

DOI: https://doi.org/10.3201/eid3003.231309

[1]These authors contributed equally to this article.

from circulating DS TB. Alternatively, sporadic MDR TB cases among clusters of DS TB cases might be more indicative of de novo emergence of MDR TB through inadequate treatment and selection. Clarifying hyperlocal patterns of disease might also contribute to spatially targeted interventions, such as active case finding and healthcare facility planning (*18*–*21*), and to the design of and recruitment into clinical trials and other studies. In this study, we aimed to characterize the spatial distribution of DS and MDR TB in Ho Chi Minh City and to explore demographic and socioeconomic factors associated with local TB burden.

Methods

Study Setting

Ho Chi Minh City has a total population of ≈10 million persons and is subdivided into 24 districts, 19 urban and 5 rural (Appendix Figure 1, https://wwwnc.cdc.gov/EID/article/30/3/23-1309App1.pdf), of which 3 were combined to form a municipal city, Thủ Đức City, in 2021. Districts of Ho Chi Minh City are further subdivided into 322 administrative subunits consisting of wards, townlets, and communes (hereafter wards); median population is ≈22,000 persons. This study includes data from before 2021 and therefore references the previous 24-district subdivision of Ho Chi Minh City.

Public-sector community-based TB care in Ho Chi Minh City is coordinated through 24 district treatment units (DTUs), where persons with suspected TB are referred for testing and treatment. Once given a diagnosis of TB, patients are registered with the National TB Program (NTP). All persons given a diagnosis of MDR TB in the public sector initiate treatment through the city's lung hospital, Phạm Ngọc Thạch, and then continue outpatient care through the DTUs. Phạm Ngọc Thạch Hospital is the regional center for MDR TB treatment in southern Vietnam and provides treatment for ≈80% of all MDR TB cases in Vietnam (*22*).

Study Population

The study population included all persons who registered for TB treatment in the public sector in 23 of the districts of Ho Chi Minh City during January 1, 2020–April 30, 2023. The study excluded TB cases from Cần Giờ, a rural district comprising 7 wards with a population of 71,527 persons (0.8% of the population Ho Chi Minh City) (*23*), because data were not available. For the ecologic analysis, 315 residential wards constituting 23 of the districts of Ho Chi Minh City formed the units of analysis.

Data Sources

We accessed data for participants with DS TB from the Vietnam TB Information Management Electronic System, a web-based surveillance system that records TB notifications and treatment outcomes for the NTP (*24*). This system includes data on all persons in Ho Chi Minh City initiated on first-line TB therapy in the public sector. At treatment initiation, patient details are added to a paper-based register, which is electronically transcribed by DTU staff at monthly intervals. Data extracted from the electronic register for this study included participant age, sex, home address, HIV status, and history of previous TB. We obtained data for participants with MDR TB from an ongoing cohort study conducted through the Oxford University Clinical Research Unit. Participants included all persons initiating treatment for MDR TB at Phạm Ngọc Thạch Hospital. We selected the Oxford University Clinical Research Unit cohort study database as the data source for MDR TB cases because it provided identical case coverage to the NTP-based register, with less missing data.

We obtained district-level and ward-level demographic and socioeconomic indicators from published regional data collected as part of the 2019 Vietnam census (*23*). Extracted indicators that were available at only the district level were population age structure, unemployment rate, proportion of households that had a computer, and number of persons living with HIV. All wards within a district were assigned the district value for indicators available only at the district level. For example, District 1 had an HIV prevalence of 1.5%; this value was subsequently assigned to each of the constituent wards of District 1. Extracted indicators, which were available at the ward level, were total population, population by sex, population density, average number of persons per household, literacy rate, and residence type (urban or rural). Location was labeled as city center if wards were located in the central commercial, commuting, and socializing hubs of Ho Chi Minh City and as peripheral if wards were located outside those areas (Appendix).

Design and Analysis

We used individual-level data for a descriptive, cross-sectional analysis of the burden of TB in Ho Chi Minh City and the characteristics of TB cases. We used an ecologic design, using ward-level data, to describe ward-level factors associated with TB burden. The outcomes for the ecologic analysis were total TB incidence and burden of MDR TB relative to total TB.

Descriptive Analysis

We summarized participant characteristics with mean and SD for continuous variables and as counts and proportions for categorical variables. Participant home addresses were deidentified and converted to latitude and longitude coordinates by using the Google geocoding service and the tidygeocoder package in R (*25*). We obtained spatial polygons for the administrative units of Ho Chi Minh City from the Database of Global Administrative Areas (*26*). We mapped and aggregated individual TB cases and calculated average annual incidence of DS and MDR TB by ward.

Spatial Autocorrelation

We assessed the presence, strength, and direction of spatial autocorrelation over the entire study area separately for DS and MDR TB incidence through the calculation of the global Moran I statistic. We assessed local spatial autocorrelation in these parameters through the calculation of the Getis-Ord Gi* statistic and Anselin Local Moran I. We used the Getis-Ord Gi* statistic to define spatial hot spots and cold spots relative to the null hypothesis of spatial randomness over the entire study area. In this analysis, we considered each ward in the context of its neighboring wards, forming a neighborhood. We compared the local sum of the values for the given parameter (e.g., DS TB incidence) for each of the wards in a neighborhood proportionally to the sum of the parameter values for all the wards in the study area. We designated neighborhoods with significantly higher parameter values than the entire study area as hot spots and neighborhoods with significantly lower parameter values than the entire study area as cold spots (*27*). The analysis using Anselin Local Moran I value further compared each ward to its neighborhood. We designated wards with high parameter values within neighborhoods with high values as high–high clusters, wards with high values within neighborhoods with low values as high–low outliers, wards with low values within neighborhoods with low values as low–low clusters, and wards with low values within neighborhoods with high values as low–high outliers (*28*). We applied false-discovery rate correction for multiple testing and spatial dependency to both local spatial autocorrelation analyses.

Ecologic Analysis

We summarized continuous ward-level indicators with mean and SD or median and interquartile range, depending on skew. We summarized categorical indicators as counts and proportions. Exploratory analyses evaluated the relationship between ward-level demographic and socioeconomic indicators and total TB incidence and MDR TB case count relative to total TB case count. We assessed univariate associations between ward-level indicators and the natural logarithm of total TB incidence through the inspection of scatter plots and the calculation of the Spearman ρ for continuous indicators and by the Wilcoxon rank-sum test and analysis of variance for categorical indicators. We categorized continuous indicators with nonlinear associations with the outcome into tertiles. We included indicators associated with total TB incidence ($p<0.05$) in a multivariable negative binomial regression model for each outcome. We modeled ward-level TB incidence by including ward-level TB case count as the dependent variable with an offset term for ward population. We modeled ward-level MDR TB case count as a proportion of all TB cases by using MDR TB case count as the dependent variable with an offset term for total TB case count. Visualization of spatial autocorrelation in the residuals for each negative binomial regression model (measured by using the Moran I) demonstrated positive spatial autocorrelation in the residuals for both models, violating the assumption of independence. To account for that finding, we added a spatially autocorrelated random effects term to each model (using the centroid of each ward as latitude and longitude), assuming a Matérn covariance structure. We assessed additional assumptions, including the absence of multicollinearity and inequality in outcome means and variances. We compared model fit for the mixed-effects models and standard models using Akaike information criterion and scatter plots of the observed versus fitted values.

We conducted a sensitivity analysis to estimate the association between ward-level demographic and socioeconomic indicators and both outcomes using conditional autoregressive modeling. In contrast to the main analysis, in which spatial information was formatted as point data (i.e., latitude and longitude coordinates for the centroid of each ward), in the sensitivity analysis we reformatted spatial information as areal data, each ward represented by a spatial polygon surrounded by an administrative boundary. We defined ward neighbors by contiguity in administrative boundaries and converted neighborhood lists to an adjacency matrix by using binary weights to indicate the presence (1) or absence (0) of a neighbor. We incorporated the adjacency matrix into the negative binomial regression model as a random effects term to account for spatial autocorrelation between neighboring wards.

We conducted statistical analyses using R Studio (The R Foundation for Statistical Computing, https://www.r-project.org). We calculated statistics and conducted mapping by using ArcGIS Online (Environmental Systems Research Institute, https://www.esri.com).

Results

Descriptive Analysis

During January 1, 2020–April 30, 2023, a total of 36,089 persons registered for DS TB treatment and 1,451 persons for MDR TB treatment in Ho Chi Minh City. Of those, 49 participants with DS TB (0.1%) and 12 participants with MDR TB (0.8%) provided residential addresses outside Ho Chi Minh City and were excluded from the spatial analysis. Of the 37,540 total persons who registered treatment, 25,463 (67.7%) were male and 12,117 (32.3%) female; 30,268 (81%) were urban dwelling, and the mean (SD) age was 45 (16.5) years (Table 1). HIV co-infection was present in 5% of all participants (n = 1,692); this proportion was similar for both DS and MDR TB groups. Previous TB infection was reported by 4,721 (13%) of the participants given treatment for DS TB and 795 (55%) of the participants given treatment for MDR TB, although it is unknown how many previous infections were caused by drug-resistant TB.

Among 31,999 case-patients who had no history of TB, 640 (2%) registered for MDR TB treatment; 772 (14%) of the 5,516 case-patients who had a history of TB registered for MDR TB treatment. Asymmetric population pyramids demonstrated a greater DS and MDR TB burden among middle-aged to late middle-aged men, although the sex distributions were more symmetric in persons <40 years of age (Figure 1). The average annual incidence of notified DS TB in Ho Chi Minh City during this period was 121.4 (95% CI 119.1–123.7) cases/100,000 persons and of MDR TB was 4.8 (95% CI 4.4–5.4) cases/100,000 persons.

We observed substantial spatial heterogeneity in DS and MDR TB average annual incidence across Ho Chi Minh City wards (Figures 2, 3). DS TB incidence (per 100,000 persons) ranged from 26.7 in Bình Lợi (District Bình Chánh) to 1,345.3 in An Khánh (District 2). Thirty-two wards recorded 0 MDR TB cases during the study period; ward 8 (District 11) showed MDR TB incidence of 31.7 cases/100,000 persons. In the overall study population, 3.9% (95% CI 3.7%–4.1%) of all TB cases were given treatment for MDR TB.

Spatial Autocorrelation

The global Moran I statistic was 0.14 (p<0.001) for DS TB and MDR TB incidence, demonstrating weak positive global spatial autocorrelation for each parameter. This finding demonstrated that over the entire study area, wards with similar values for the above parameters (e.g., similar DS TB incidences) were located closer to each other than would be expected if the wards were randomly arranged (i.e., there was evidence of some spatial clustering for each parameter). However, the global Moran I provided no information about where these clustered wards were located or how the clustering of DS TB related to the clustering of MDR TB. We provide results of the hot spot analysis using the Getis-Ord Gi* statistic (Figure 4). Hot spots were evident in the central parts of Ho Chi Minh City for DS TB and MDR TB and cold spots to the north of the city center. Like the hot spots, the DS and MDR TB cold spots largely overlapped spatially. We provide Anselin Local Moran I to demonstrate wards in which TB incidence was congruent with the surrounding neighborhood (clusters) and wards in which TB

Table 1. Characteristics of persons registered for TB treatment stratified by TB type, Ho Chi Minh City, Vietnam, January 1, 2020–April 30, 2023*

Characteristic	DS TB, n = 36,089	MDR TB, n = 1,451	Overall, n = 37,540
Age, y, mean (SD)	44.9 (16.6)	45.7 (14.1)	44.9 (16.5)
Sex, no. (%)			
F	11,732 (32.5)	385 (26.5)	12,117 (32.3)
M	24,357 (67.5)	1,066 (73.5)	25,423 (67.7)
HIV status, no. (%)			
Negative	27,745 (76.9)	1,333 (91.9)	29,078 (77.5)
Positive	1,609 (4.5)	83 (5.7)	1,692 (4.5)
Unknown	6,735 (18.7)	35 (2.4)	6,770 (18.0)
TB history, no. (%)			
No	31,344 (86.9)	655 (45.1)	31,999 (85.2)
Yes	4,721 (13.1)	795 (54.8)	5,516 (14.7)
Unknown	24 (0.1)	1 (0.1)	25 (0.1)
Residence type, no. (%)			
Urban	29,086 (80.6)	1,182 (81.5)	30,268 (80.6)
Rural	6,948 (19.3)	246 (17.0)	7,194 (19.2)

*DS TB, drug-susceptible tuberculosis; MDR TB, multidrug-resistant tuberculosis; TB, tuberculosis.

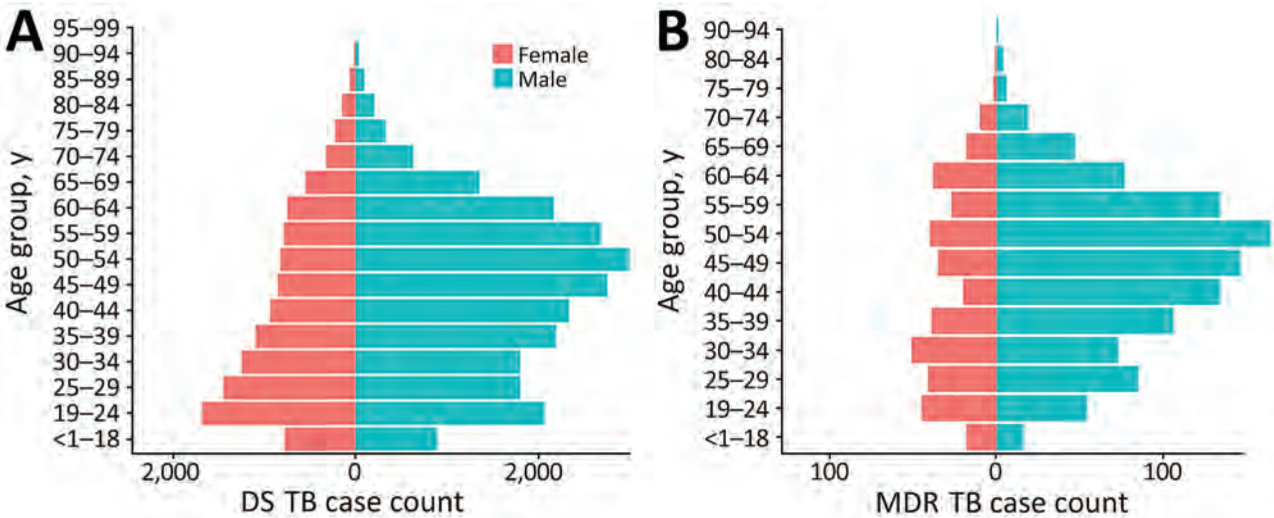

Figure 1. Population pyramids of age and sex distributions of participants registered for TB treatment in Ho Chi Minh City, Vietnam, January 1, 2020–April 30, 2023. A) DS TB; B) MDR TB. DS, drug-susceptible; MDR, multidrug-resistant; TB, tuberculosis.

incidence contrasted the surrounding neighborhood (outliers) (Figure 5). Heterogeneity in incidence, for DS TB and MDR TB, was evident even within hot spots and cold spots. For DS TB, most of the wards in the city center hot spot, when considered separately from their neighborhood, were low–high outliers. A greater number of the wards that constituted the MDR TB hot spot were high–high clusters, indicating more homogeneity within the MDR TB hot spots.

Ward-Level Factors Associated with TB Burden

Wards in the highest tertile of TB incidence had the lowest male proportion of the population (47.6%), although the range of male proportion of the population between wards in the highest and lowest tertiles was small (47.6%–48.1%). Literacy rate (98.8%), proportion of homes that had a computer (65.2%), and lowest unemployment rate (2.8%) were also lowest in those wards (Table 2). Those wards had the highest

Figure 2. Choropleth map displaying geographic variation in average annual incidence (cases/100,000 persons) for DS TB, subdivided by ward, Ho Chi Minh City, Vietnam, January 1, 2020–April 30, 2023. Map does not include Cần Giờ district. Inset map shows location of study area in Vietnam. DS TB, drug-susceptible tuberculosis.

Figure 3. Choropleth map displaying geographic variation in average annual incidence (cases/100,000 persons) for MDR TB, subdivided by ward, Ho Chi Minh City, Vietnam, January 1, 2020–April 30, 2023. Map does not include Cần Giờ district. Inset map shows location of study area in Vietnam. MDR TB, multidrug-resistant tuberculosis.

proportion of the population 30–59 years of age (45.5%), population density (32,117 persons/km^2), number of persons per household (3.6), and HIV prevalence (0.9%). Indicators strongly associated with TB incidence in the univariate analyses, and subsequently included in the final multivariable models, were male proportion of the population, proportion of the population 30–59 years of age, average number

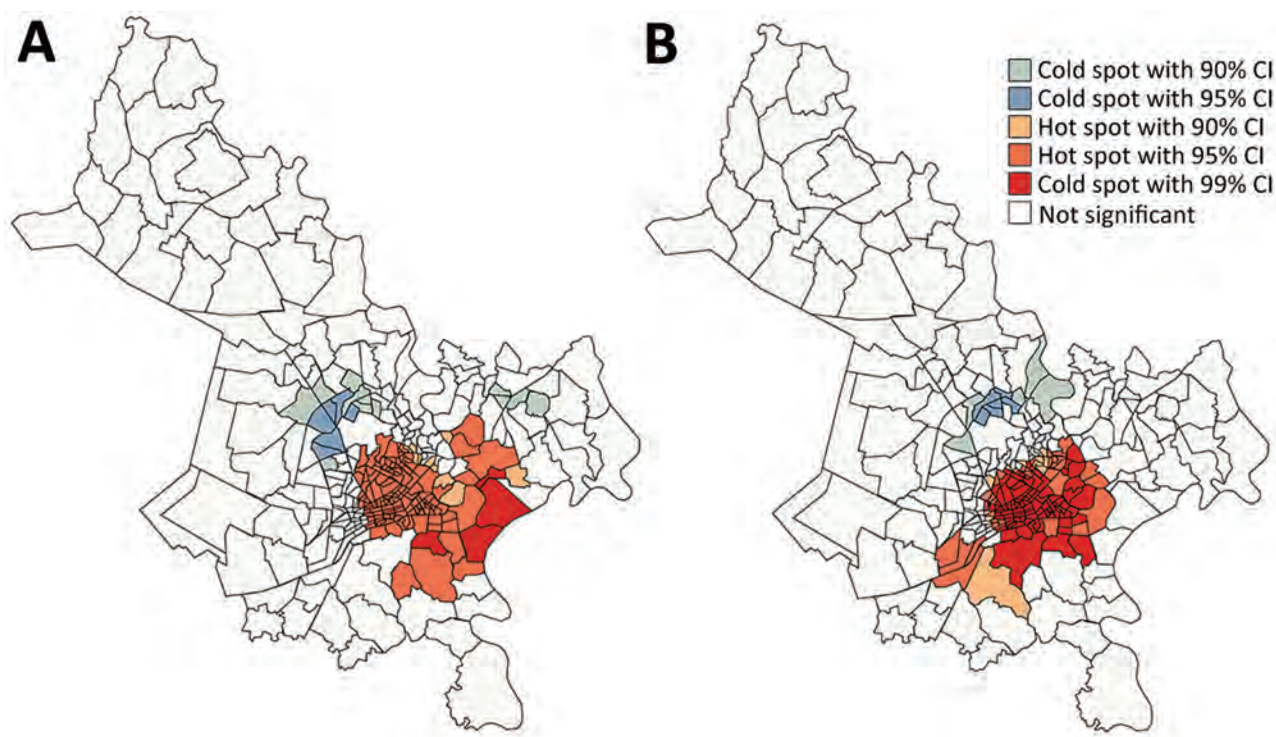

Figure 4. Spatial clustering of drug-susceptible (A) and multidrug-resistant (B) tuberculosis incidence, Ho Chi Minh City, Vietnam, January 1, 2020–April 30, 2023, based on the Getis-Ord GI* statistic.

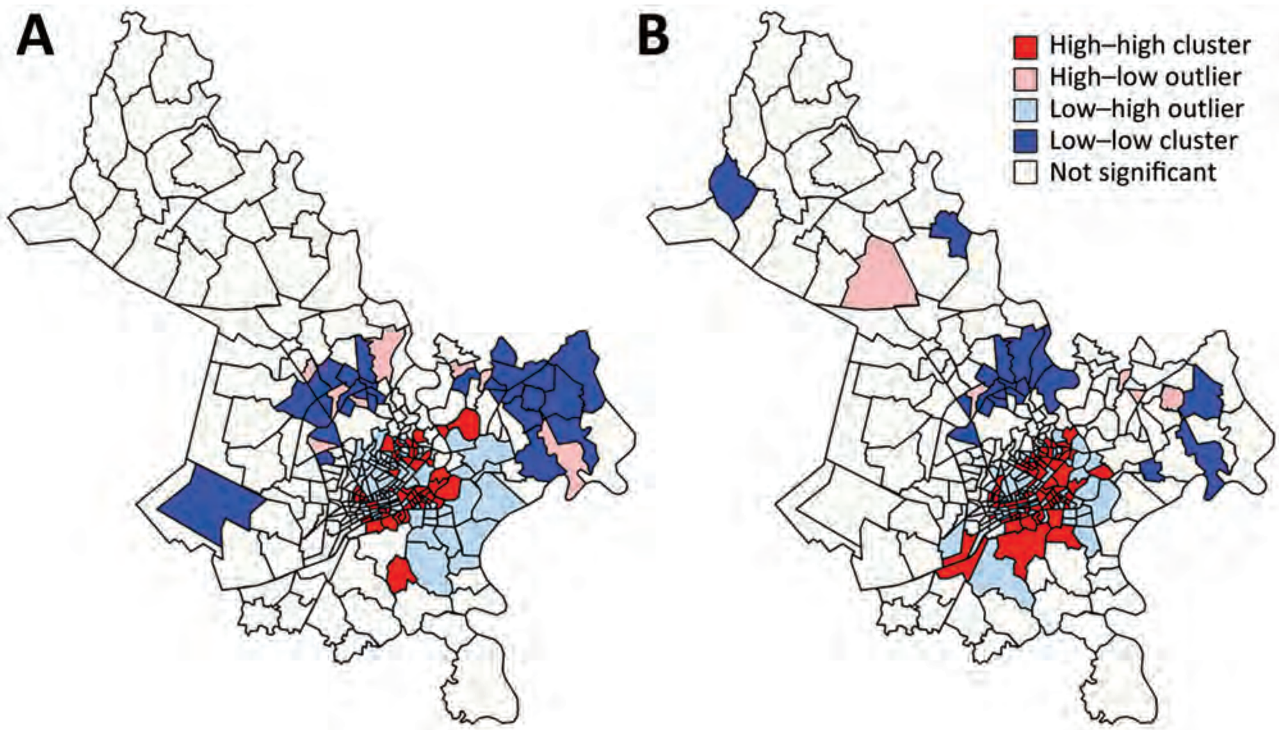

Figure 5. Spatial clusters and outliers of drug-susceptible (A) and multidrug-resistant (B) tuberculosis incidence, Ho Chi Minh City, Vietnam, January 1, 2020–April 30, 2023, based on the Anselin Local Moran I statistic.

of persons per household, literacy rate, unemployment rate, and HIV prevalence (Appendix).

In a multivariable negative binomial regression model with mixed effects, in contrast to the unadjusted association, the male proportion of the population was strongly associated with total TB incidence (incidence rate ratio 1.05, 95% CI 1.02–1.08), and each percentage increase in HIV prevalence was associated with a 77% increase in TB incidence (incidence rate ratio 1.77, 95% CI 1.54–2.03) (Table 3). None of the

Table 2. Ward-level demographic and socioeconomic indicators stratified by tertiles of overall TB incidence, Ho Chi Minh City, Vietnam, January 1, 2020–April 30, 2023*

Indicator	Overall TB incidence: 1st tertile, median incidence 84/100,000 persons, n = 105	2nd tertile, median incidence 120/100,000 persons, n = 105	3rd tertile, median incidence 187/100,000 persons, n = 105	Overall, n = 315
Male proportion of population, mean (SD)	48.1 (1.86)	48.2 (1.82)	47.6 (2.78)	48.0 (2.21)
Proportion of population 30–59 years old, mean (SD)	44.1 (2.23)	44.2 (2.02)	45.5 (1.52)	44.6 (2.04)
Residence type, no. (%)				
Urban	86 (81.9)	89 (84.8)	88 (83.8)	263 (83.5)
Rural	19 (18.1)	16 (15.2)	17 (16.2)	52 (16.5)
Location, no. (%)				
City center	23 (21.9)	22 (21)	24 (22.9)	69 (22)
Peripheral	82 (78.1)	83 (79)	81 (77.1)	246 (78)
Total population, median (IQR)	26,050 (12,402–40,289)	25,575 (13,354–42,067)	16,911 (11,190–25,068)	22,383 (12,397–36,880)
Population density, persons/km^2, median (IQR)	27,537 (9,203–44,241)	20,810 (6,323–41,535)	32,117 (13,005–46,854)	27,781 (8,233–44,812)
Average no. persons per household, mean (SD)	3.51 (0.319)	3.55 (0.269)	3.62 (0.321)	3.56 (0.307)
Literacy rate, median (IQR)	99.3 (98.7–99.6)	99.3 (98.7–99.6)	98.8 (97.7–99.3)	99.2 (98.5–99.6)
Unemployment rate, mean (SD)	3.25 (1.17)	3.10 (1.05)	2.76 (0.747)	3.04 (1.02)
Proportion of homes that had a computer, median (IQR)	71.7 (55.4–77.6)	71.0 (59.3–76.5)	65.2 (59.3–73.2)	71.0 (59.3–76.3)
HIV prevalence, median (IQR)	0.49 (0.34–0.84)	0.48 (0.34–0.93)	0.93 (0.45–1.29)	0.49 (0.36–0.95)

*IQR, interquartile range; TB, tuberculosis.

Table 3. Adjusted incidence rate ratios for association between ward-level indicators and total TB incidence and MDR TB case count relative to total TB case count, Ho Chi Minh City, Vietnam, January 1, 2020–April 30, 2023*

Indicator	Total TB incidence (95% CI)	MDR TB case count (95% CI)†
Male proportion of population, %	1.05 (1.02–1.08)	0.99 (0.94–1.05)
Proportion of population 30–59 years old, %	1.02 (0.99–1.04)	1.03 (0.98–1.08)
Average no. persons per household	1.13 (0.98–1.31)	0.97 (0.76–1.25)
Literacy rate		
1st tertile	Referent	Referent
2nd tertile	1.06 (0.96–1.18)	1.05 (0.89–1.26)
3rd tertile	0.96 (0.86–1.07)	1.01 (0.83–1.25)
Unemployment rate, %	0.96 (0.92–1.00)	0.95 (0.87–1.03)
HIV prevalence, %	1.77 (1.54–2.03)	1.08 (0.85–1.38)

*MDR TB, multidrug-resistant tuberculosis; TB, tuberculosis.
†Relative to total TB case count.

selected indicators were significantly associated with MDR TB case counts relative to total TB case counts. The mixed-effects models including spatially autocorrelated random effects terms demonstrated better fit than the standard models, and estimates from the sensitivity analysis were similar to those of the main analysis (Appendix).

Discussion

We characterized the burden of TB in Ho Chi Minh City with granular, ward-level descriptions of DS and MDR TB burden. Both DS and MDR TB were heterogeneously distributed throughout Ho Chi Minh City, forming geographic clusters of high incidence, predominantly concentrated in the city's center. Total TB incidence at the ward level was strongly associated with HIV prevalence and more weakly associated with the proportion of the population that is male.

The asymmetric age and sex distributions among TB cases in Ho Chi Minh City we describe are consistent with the findings from the second Vietnam national TB prevalence survey, which confirmed prevalence of bacteriologically TB was 4 times greater in male than female patients and increased with age (*29*). Studies from Vietnam have also demonstrated a greater prevalence of latent TB in men than in women (*30*). However, the magnitude of this difference in prevalence by sex is smaller for latent TB than for active TB, emphasizing the role of sex differences in risk factors for disease progression. A recent substudy from the national TB prevalence survey specifically noted the stark differences in the prevalence of smoking (45% of men vs. 1% of women) (*31*) and drinking (44% of men vs. 1% of women) (*32*) in Vietnam as likely contributors to observed differences in the prevalence of active TB by sex (*33*). Sex differences, for both latent and active disease, remain incompletely understood but likely reflect the complex interplay between biologic, behavioral, and environmental factors (*34*). We demonstrated a 5% greater TB incidence per percentage increase in the proportion of the population that is male, suggesting sex-specific differences in risk might manifest at the population level.

We observed a 5% prevalence of TB and HIV co-infection, approximating previous regionally representative estimates (*14*,*35*). TB incidence was substantially greater with each percentage increase in HIV prevalence, emphasizing the potential contribution of HIV to the TB epidemic, even in settings with relatively low HIV prevalence.

Our incidence estimates for DS and MDR TB, derived from TB notifications, are markedly lower than the estimates of WHO for Vietnam (TB incidence 173 cases/100,000 persons, MDR TB 9.1 cases/100,000 persons) (*14*), despite evidence that Ho Chi Minh City has some of the highest TB incidences in the country (*15*,*16*). The WHO estimates are derived from multiple data sources, including prevalence surveys, case notification data, expert opinion about case detection gaps, and dynamic modeling (*36*). The differences between incidence estimates likely reflect a limitation of this study, the diagnostic gap—the difference between the true number of persons who became ill with TB and the number of persons who were registered for TB treatment (*1*). The diagnostic gap is a well-described barrier to TB control in Vietnam and has recently been exacerbated by COVID-19–related health system disruptions; <50% of predicted TB case-patients enrolled for treatment in 2021 (*1*).

TB incidence in Ho Chi Minh City was not associated with measures of poverty (literacy rates; unemployment rates; and proportion of homes that had a computer, a proxy for material wealth), even though poverty is a well-established risk factor (37). The central concentration of TB burden in Ho Chi Minh City was instead, in our data, related to factors such as sex distribution and HIV prevalence. This lack of association might reflect the poor representation of poverty and social deprivation by the variables included in our analysis (i.e., literacy rates are high across Ho Chi Minh City, even in poorer and rural areas [23]). It might also be that rapid equitable economic growth in

Vietnam, coupled with a reduction in TB prevalence over the past 20 years, contributed to a reduction of the concentration of TB among poor households (38).

Our spatial analysis demonstrated substantial overlap in geographic clusters of DS and MDR TB incidence, raising interesting questions about the relationship between DS and MDR TB burden. Those findings might be consistent with the hypothesis that drug resistance largely emerges from DS TB de novo, and distributions of DS and MDR TB therefore related. Alternatively, the overlapping distributions might also be consistent with the hypothesis that most MDR TB is transmitted and that factors associated with the transmission of TB in general are geographically clustered. The lack of association between any demographic and socioeconomic indicators and MDR TB burden relative to total TB burden we describe potentially supports the latter hypothesis. Ultimately, it is likely that both de novo and transmitted resistance contribute to MDR TB burden. Enrichment of spatial data with genetic data will better demonstrate the relative contributions of each mechanism (*39*).

The first limitation of this study is that we used public sector registry data to identify TB cases and therefore excluded persons who had undiagnosed TB, potentially biasing our sample selection toward groups who are more likely to manifest signs or symptoms when symptomatic. Furthermore, we had no data on private-sector TB diagnoses, estimated to represent 8% of all TB cases in Ho Chi Minh City (*40*). Participants in our study were only geolocated through their home addresses. However, several studies have demonstrated the role of transmission outside the home with the emergence of genetic data demonstrating geographically unrelated, cryptic transmission networks mediated by mobility-linked locations in high-burden settings (*41*,*42*). Future work on the transmission of TB in Ho Chi Minh City will benefit from whole-genome sequencing–derived genetic data being generated by a parallel, related study. The degree to which our findings are relevant to other settings is uncertain, but it is likely that the dynamics in Ho Chi Minh City are not markedly different from other major cities with similar economic metrics in Southeast Asia, where nearly half the world's TB patients reside (*1*).

In summary, we characterized the demographic profile of persons with DS and MDR TB in Ho Chi Minh City and mapped parts of the city most affected. Our findings provide a starting point for deeper research into TB acquisition and transmission dynamics and spatially informed TB control interventions in Ho Chi Minh City, Vietnam, and the greater southeastern region of Asia.

Acknowledgments

We thank Truong Thi Bich Le for providing district and ward socioeconomic and demographic data for Ho Chi Minh City.

This study was approved by the Oxford Tropical Research Ethics Committee (reference no. 51–19) and the Institutional Review Board at Pham Ngoc Thach Hospital (643/PNT-HDDD).

This study was supported in whole, or in part, by the Wellcome Trust (206724/Z/17/Z, 223253/Z/21/Z, and 214560/Z/18/Z]). R.S. is supported by the Rhodes Trust. N.T.T.T. is a Wellcome Intermediate Fellow in Public Health and Tropical Medicine (206724/Z/17/Z). J.A.W. is a Sir Henry Dale Fellow supported by the Wellcome Trust (223253/Z/21/Z). T.M.W. is a Wellcome Trust Clinical Career Development Fellow (214560/Z/18/Z).

About the Author

Dr. Spies is a physician and doctoral candidate at the Nuffield Department of Medicine, University of Oxford, Oxford, UK, and the Oxford University Clinical Research, Ho Chi Minh City, Vietnam. His primary research interest is the molecular epidemiology of multidrug-resistant tuberculosis.

References

1. World Health Organization. Global tuberculosis report 2022 [cited 2023 Dec 8]. https://www.who.int/publications-detail-redirect/9789240061729
2. World Health Organization. WHO consolidated guidelines on tuberculosis. Module 4: Treatment. Drug-resistant tuberculosis treatment 2020 [cited 2023 Dec 8]. https://www.who.int/publications-detail-redirect/9789240007048
3. Jenkins HE, Plesca V, Ciobanu A, Crudu V, Galusca I, Soltan V, et al. Assessing spatial heterogeneity of multidrug-resistant tuberculosis in a high-burden country. Eur Respir J. 2013;42:1291–301. https://doi.org/10.1183/09031936.00111812
4. Oliveira O, Ribeiro AI, Krainski ET, Rito T, Duarte R, Correia-Neves M. Using Bayesian spatial models to map and to identify geographical hotspots of multidrug-resistant tuberculosis in Portugal between 2000 and 2016. Sci Rep. 2020;10:16646. https://doi.org/10.1038/s41598-020-73759-w
5. Aturinde A, Farnaghi M, Pilesjö P, Mansourian A. Spatial analysis of HIV-TB co-clustering in Uganda. BMC Infect Dis. 2019;19:612. https://doi.org/10.1186/s12879-019-4246-2
6. Ding P, Li X, Jia Z, Lu Z. Multidrug-resistant tuberculosis (MDR-TB) disease burden in China: a systematic review and spatio-temporal analysis. BMC Infect Dis. 2017;17:57. https://doi.org/10.1186/s12879-016-2151-5
7. Alene KA, Viney K, McBryde ES, Clements AC. Spatial patterns of multidrug resistant tuberculosis and relationships to socio-economic, demographic and household factors in northwest Ethiopia. PLoS One. 2017;12:e0171800. https://doi.org/10.1371/journal.pone.0171800

8. Mashamba MA, Tanser F, Afagbedzi S, Beke A. Multi-drug-resistant tuberculosis clusters in Mpumalanga Province, South Africa, 2013–2016: A spatial analysis. Trop Med Int Health. 2022;27:185–91. https://doi.org/10.1111/tmi.13708
9. Sy KT, Leavitt SV, de Vos M, Dolby T, Bor J, Horsburgh CR Jr, et al. Spatial heterogeneity of extensively drug resistant-tuberculosis in Western Cape Province, South Africa. Sci Rep. 2022;12:10844. https://doi.org/10.1038/s41598-022-14581-4
10. Chirenda J, Gwitira I, Warren RM, Sampson SL, Murwira A, Masimirembwa C, et al. Spatial distribution of *Mycobacterium tuberculosis* in metropolitan Harare, Zimbabwe. PLoS One. 2020;15:e0231637. https://doi.org/10.1371/journal.pone.0231637
11. Lima SV, Dos Santos AD, Duque AM, de Oliveira Goes MA, da Silva Peixoto MV, da Conceição Araújo D, et al. Spatial and temporal analysis of tuberculosis in an area of social inequality in northeast Brazil. BMC Public Health. 2019;19:873. https://doi.org/10.1186/s12889-019-7224-0
12. Zaidi SM, Jamal WZ, Mergenthaler C, Azeemi KS, Van Den Berge N, Creswell J, et al. A spatial analysis of TB cases and abnormal X-rays detected through active case-finding in Karachi, Pakistan. Sci Rep. 2023;13:1336. https://doi.org/10.1038/s41598-023-28529-9
13. Trauer JM, Dodd PJ, Gomes MG, Gomez GB, Houben RM, McBryde ES, et al. The importance of heterogeneity to the epidemiology of tuberculosis. Clin Infect Dis. 2019;69:159–66. https://doi.org/10.1093/cid/ciy938
14. World Health Organization. Tuberculosis profile: Viet Nam [cited 2023 Dec 8]. https://worldhealthorg.shinyapps.io/tb_profiles/?_inputs_&entity_type=%22country%22&lan=%22EN%22&iso2=%22VN%22
15. Bonell A, Contamin L, Thai PQ, Thuy HT, van Doorn HR, White R, et al. Does sunlight drive seasonality of TB in Vietnam? A retrospective environmental ecological study of tuberculosis seasonality in Vietnam from 2010 to 2015. BMC Infect Dis. 2020;20:184. https://doi.org/10.1186/s12879-020-4908-0
16. Dao TP, Hoang XH, Nguyen DN, Huynh NQ, Pham TT, Nguyen DT, et al. A geospatial platform to support visualization, analysis, and prediction of tuberculosis notification in space and time. Front Public Health. 2022; 10:973362. https://doi.org/10.3389/fpubh.2022.973362
17. Srinivasan V, Ha VT, Vinh DN, Thai PV, Ha DT, Lan NH, et al. Sources of multidrug resistance in patients with previous isoniazid-resistant tuberculosis identified using whole genome sequencing: a longitudinal cohort study. Clin Infect Dis. 2020;71:e532–9. https://doi.org/10.1093/cid/ciaa254
18. Theron G, Jenkins HE, Cobelens F, Abubakar I, Khan AJ, Cohen T, et al. Data for action: collection and use of local data to end tuberculosis. Lancet. 2015;386:2324–33. https://doi.org/10.1016/S0140-6736(15)00321-9
19. Shrestha S, Chatterjee S, Rao KD, Dowdy DW. Potential impact of spatially targeted adult tuberculosis vaccine in Gujarat, India. J R Soc Interface. 2016;13:20151016. https://doi.org/10.1098/rsif.2015.1016
20. Yuen CM, Amanullah F, Dharmadhikari A, Nardell EA, Seddon JA, Vasilyeva I, et al. Turning off the tap: stopping tuberculosis transmission through active case-finding and prompt effective treatment. Lancet. 2015; 386:2334–43. https://doi.org/10.1016/S0140-6736(15)00322-0
21. Cudahy PG, Andrews JR, Bilinski A, Dowdy DW, Mathema B, Menzies NA, et al. Spatially targeted screening to reduce tuberculosis transmission in high-incidence settings. Lancet Infect Dis. 2019;19:e89–95. https://doi.org/10.1016/S1473-3099(18)30443-2
22. Hoa NB, Khanh PH, Chinh NV, Hennig CM. Prescription patterns and treatment outcomes of MDR-TB patients treated within and outside the National Tuberculosis Programme in Pham Ngoc Thach hospital, Viet Nam. Trop Med Int Health. 2014;19:1076–81. https://doi.org/10.1111/tmi.12347
23. Ho Chi Minh City Statistics Office. Statistical yearbook of Ho Chi Minh City, 2021 [cited 2023 Dec 8]. https://www.gso.gov.vn/en/data-and-statistics/2022/08/statistical-yearbook-of-2021
24. Thai LH, Nhat LM, Shah N, Lyss S, Ackers M. Sensitivity, completeness and agreement of the tuberculosis electronic system in Ho Chi Minh City, Viet Nam. Public Health Action. 2017;7:294–8. https://doi.org/10.5588/pha.17.0081
25. Cambon J, Hernangómez D, Belanger C, Possenriede D. tidygeocoder: an R package for geocoding. J Open Source Softw. 2021;6:3544. https://doi.org/10.21105/joss.03544
26. Global Administrative Areas. Vietnam Administrative Areas [cited 2023 Dec 8]. https://gadm.org/download_country.html
27. Ord JK, Getis A. Local spatial autocorrelation statistics: distributional issues and an application. Geogr Anal. 1995;27:286–306. https://doi.org/10.1111/j.1538-4632.1995.tb00912.x
28. Anselin L. Local indicators of spatial association—LISA. Geogr Anal. 1995;27:93–115. https://doi.org/10.1111/j.1538-4632.1995.tb00338.x
29. Nguyen HV, Tiemersma EW, Nguyen HB, Cobelens FG, Finlay A, Glaziou P, et al. The second national tuberculosis prevalence survey in Vietnam. PLoS One. 2020;15:e0232142. https://doi.org/10.1371/journal.pone.0232142
30. Marks GB, Nhung NV, Nguyen TA, Hoa NB, Khoa TH, Son NV, et al. Prevalence of latent tuberculous infection among adults in the general population of Ca Mau, Viet Nam. Int J Tuberc Lung Dis. 2018;22:246–51. https://doi.org/10.5588/ijtld.17.0550
31. Van Minh H, Giang KB, Ngoc NB, Hai PT, Huyen DT, Khue LN, et al. Prevalence of tobacco smoking in Vietnam: findings from the Global Adult Tobacco Survey 2015. Int J Public Health. 2017;62(Suppl 1):121–9. https://doi.org/10.1007/s00038-017-0955-8
32. Tran QB, Hoang VM, Vu HL, Biu PL, Kim BG, Pham QN, et al. Risk factors for non-communicable diseases among adults in Vietnam: findings from the Vietnam STEPS Survey 2015. J Glob Health Sci. 2020;2:e7. https://doi.org/10.35500/jghs.2020.2.e7
33. Nguyen HV, Brals D, Tiemersma E, Gasior R, Nguyen NV, Nguyen HB, et al. Influence of sex and sex-based disparities on prevalent tuberculosis, Vietnam, 2017–2018. Emerg Infect Dis. 2023;29:967–76. https://doi.org/10.3201/eid2905.221476
34. Long NH. Gender specific epidemiology of tuberculosis in Vietnam. Doctoral thesis. Department of Public Health Sciences, Karolinska Institute, Stockholm, Sweden, 2000 [cited 2023 Dec 8]. https://openarchive.ki.se/xmlui/handle/10616/44375
35. Trinh QM, Nguyen HL, Do TN, Nguyen VN, Nguyen BH, Nguyen TV, et al. Tuberculosis and HIV co-infection in Vietnam. Int J Infect Dis. 2016;46:56–60. https://doi.org/10.1016/j.ijid.2016.03.021
36. Glaziou P, Arinaminpathy N, Dodd PJ, Dean A, Floyd K. Methods used by WHO to estimate the global burden of TB disease 2023 [cited 2023 Dec 8]. https://www.who.int/publications/m/item/methods-used-by-who-to-estimate-the-global-burden-of-tb-disease-2022
37. Wingfield T, Tovar MA, Huff D, Boccia D, Saunders MJ, Datta S, et al. Beyond pills and tests: addressing the social

determinants of tuberculosis. Clin Med (Lond). 2016; 16(Suppl 6):s79–91. https://doi.org/10.7861/clinmedicine.16-6-s79

38. Foster N, Nguyen HV, Nguyen NV, Nguyen HB, Tiemersma EW, Cobelens FG, et al. Social determinants of the changing tuberculosis prevalence in Viet Nam: analysis of population-level cross-sectional studies. PLoS Med. 2022;19:e1003935. https://doi.org/10.1371/journal.pmed.1003935
39. Liebenberg D, Gordhan BG, Kana BD. Drug resistant tuberculosis: implications for transmission, diagnosis, and disease management. Front Cell Infect Microbiol. 2022;12:943545. https://doi.org/10.3389/fcimb.2022.943545
40. Hoa NB, Cobelens FG, Sy DN, Nhung NV, Borgdorff MW, Tiemersma EW. Diagnosis and treatment of tuberculosis in the private sector, Vietnam. Emerg Infect Dis. 2011;17:562–4. https://doi.org/10.3201/eid1703.101468
41. Wang W, Mathema B, Hu Y, Zhao Q, Jiang W, Xu B. Role of casual contacts in the recent transmission of tuberculosis in settings with high disease burden. Clin Microbiol Infect. 2014;20:1140–5. https://doi.org/10.1111/1469-0691.12726
42. Brown TS, Robinson DA, Buckee CO, Mathema B. Connecting the dots: understanding how human mobility shapes TB epidemics. Trends Microbiol. 2022;30:1036–44. https://doi.org/10.1016/j.tim.2022.04.005

Address for correspondence: Ruan Spies, Brasenose College, University of Oxford, Radcliffe Square, Oxford OX1 4AJ, UK; email: ruan.spies@ndm.ox.ac.uk

Disseminated Leishmaniasis, a Severe Form of *Leishmania braziliensis* Infection

Paulo R.L. Machado, Alexsandro Lago, Thiago M. Cardoso, Andréa Magalhaes, Lucas P. Carvalho, Tainã Lago, Augusto M. Carvalho, Rúbia Costa, Edgar M. Carvalho

Medscape CME Activity

In support of improving patient care, this activity has been planned and implemented by Medscape, LLC and Emerging Infectious Diseases. Medscape, LLC is jointly accredited with commendation by the Accreditation Council for Continuing Medical Education (ACCME), the Accreditation Council for Pharmacy Education (ACPE), and the American Nurses Credentialing Center (ANCC), to provide continuing education for the healthcare team.

Medscape, LLC designates this Journal-based CME activity for a maximum of 1.00 ***AMA PRA Category 1 Credit(s)™***. Physicians should claim only the credit commensurate with the extent of their participation in the activity.

Successful completion of this CME activity, which includes participation in the evaluation component, enables the participant to earn up to 1.0 MOC points in the American Board of Internal Medicine's (ABIM) Maintenance of Certification (MOC) program. Participants will earn MOC points equivalent to the amount of CME credits claimed for the activity. It is the CME activity provider's responsibility to submit participant completion information to ACCME for the purpose of granting ABIM MOC credit.

All other clinicians completing this activity will be issued a certificate of participation. To participate in this journal CME activity: (1) review the learning objectives and author disclosures; (2) study the education content; (3) take the post-test with a 75% minimum passing score and complete the evaluation at http://www.medscape.org/journal/eid; and (4) view/print certificate. For CME questions, see page 631.

NOTE: It is Medscape's policy to avoid the use of brand names in accredited activities. However, in an effort to be as clear as possible, the use of brand names should not be viewed as a promotion of any brand or as an endorsement by Medscape of specific products.

Release date: February 23, 2024; Expiration date: February 23, 2025

Learning Objectives

Upon completion of this activity, participants will be able to:

- Assess the epidemiology and parasitology of disseminated leishmaniasis (DL)
- Analyze cure rates of DL treated with meglumine antimoniate
- Distinguish variables associated with a higher number of lesions in cases of DL
- Compare cure rates of different treatment regimens for DL

CME Editor

Jill Russell, BA, Technical Writer/Editor, Emerging Infectious Diseases. *Disclosure: Jill Russell, BA, has no relevant financial relationships.*

CME Author

Charles P. Vega, MD, Health Sciences Clinical Professor of Family Medicine, University of California, Irvine School of Medicine, Irvine, California. *Disclosure: Charles P. Vega, MD, has the following relevant financial relationships: consultant or advisor for Boehringer Ingelheim; GlaxoSmithKline.*

Authors

Paulo R. L. Machado, MD, PhD; Alexsandro Lago, PhD; Thiago M. Cardoso, PhD; Andréa Magalhaes, PhD; Lucas P. Carvalho, PhD; Tainã Lago, PhD; Augusto M. Carvalho, PhD; Rúbia Costa, PhD; Edgar M. Carvalho, MD, PhD.

Author affiliations: Federal University of Bahia, Salvador, Brazil (P.R.L. Machado, A. Lago, A. Magalhaes, L.P. Carvalho, T. Lago, R. Costa, E.M. Carvalho); National Institute of Science and Technology of Tropical Diseases (INCT-DT), Brasília, Brazil (P.R.L. Machado, L.P. Carvalho, A.M. Carvalho, E.M. Carvalho); Fiocruz, Salvador (T.M. Cardoso, A. Magalhaes, L.P. Carvalho, A.M. Carvalho, R. Costa, E.M. Carvalho)

DOI: https://doi.org/10.3201/eid3003.230786

Disseminated leishmaniasis (DL) is an emergent severe disease manifesting with multiple lesions. To determine the relationship between immune response and clinical and therapeutic outcomes, we studied 101 DL and 101 cutaneous leishmaniasis (CL) cases and determined cytokines and chemokines in supernatants of mononuclear cells stimulated with leishmania antigen. Patients were treated with meglumine antimoniate (20 mg/kg) for 20 days (CL) or 30 days (DL); 19 DL patients were instead treated with amphotericin B, miltefosine, or miltefosine and meglumine antimoniate. High levels of chemokine ligand 9 were associated with more severe DL. The cure rate for meglumine antimoniate was low for both DL (44%) and CL (60%), but healing time was longer in DL (p = 0.003). The lowest cure rate (22%) was found in DL patients with >100 lesions. However, meglumine antimoniate/miltefosine treatment cured all DL patients who received it; therefore, that combination should be considered as first choice therapy.

Disseminated leishmaniasis (DL) is an aggressive form of tegumentary leishmaniasis associated with multiple and polymorphic cutaneous lesions (acneiform and inflammatory papules, nodules, and ulcers) in ≥2 body regions (*1*). DL has been mainly described in Brazil in patients infected with *Leishmania (Viannia) braziliensis*, but the disease is documented in other countries of South America and in the Old World. The disease may be caused by other species of *Leishmania*, including *L. mexicana amazonensis*, *L. (V) guyanensis*, *L. tropica*, and *L. major* (*2*–*5*). DL is an emerging disease and is highly endemic in the area of *L. braziliensis* transmission in northeastern Brazil. The frequency of the disease has increased >20 times in the past 30 years (*1*,*6*). When DL was initially described in this leishmaniasis-endemic area in northeastern Brazil, *L. amazonensis* was the most frequent causal agent, detected in 56.2% of the cases (*7*,*8*). However, more recently, *L. amazonensis* has not been isolated from patients in this area, and *L. braziliensis* is the only species identified in patients with American tegumentary leishmaniasis (*9*). Making distinctions between DL and diffuse cutaneous leishmaniasis (DCL) is key. Whereas DL might be caused by several *Leishmania* species, DCL is caused by *L. amazonensis* in the Americas and *L. aethiopica* in Africa. DL manifests in multiple types of lesions, such as papules, superficial nodules, and ulcerations, with few parasites in situ, whereas DCL is associated with infiltrated plaques and nodules along with a high number of parasites in the lesions (*10*).

Both parasite and host factors participate in the pathogenesis of DL. *L. braziliensis* is polymorphic, and genotypic differences in chromosomes 28 and 42 are associated with DL (*11*). Those genotypic differences among isolates of *L. braziliensis* have been associated with different clinical forms and with the severity of American tegumentary leishmaniasis and its failure to respond to meglumine antimoniate (*12*,*13*). Regarding host factors, macrophages from DL patients allow for greater parasite multiplication than cutaneous leshmaniasis (CL) cells (*14*). A parasite dissemination as observed in visceral leishmaniasis and DCL is associated with an impairment in the T-cell response (*15*,*16*). However, no clear evidence exists demonstrating that impairment in the T-cell response is the cause of parasite dissemination in DL. Approximately 20% of DL patients might experience a negative delayed-type hypersensitivity test to leishmania antigens (*17*). Although peripheral blood lymphocytes from DL patients produce fewer Th1 cytokines than those of patients with CL (*1*), immunochemistry studies of the lesions in CL and DL patients do not show differences in the cell populations and cytokine expression in those 2 forms of the disease (*17*,*18*).

Case reports of DL indicate that after a single lesion develops, dissemination occurs in ≥1 weeks (*1*,*8*). The number of lesions can vary widely; some patients have 10–20, and others can have >100–1,000 lesions. Nasal mucosa involvement occurs in ≈40% of DL patients (*1*,*7*,*8*).

DL is associated with high therapeutic failure of meglumine antimoniate treatment. Studies are scarce comparing therapeutic responses to antimony in DL versus CL, as are studies investigating the efficacy of miltefosine and amphotericin B. Moreover, clinic and immunologic risk factors associated with DL are not well known. In this article, we investigated miltefosine and amphotericin B treatment of DL and CL, the phenotypic heterogeneity among DL patients when grouped by the number of lesions, and associations with distinct immunologic responses and different clinical and therapeutic outcomes.

Materials and Methods

The study participants were 202 patients, half with DL and half with CL. All were from the leishmaniasis-endemic region of Corte de Pedra in the southeast of Bahia, Brazil. All DL patients (N = 101) whose illness was diagnosed during 2016–2020 at the Corte de Pedra Health Post were included in the study. CL patients (N = 101) were randomly assigned to the study without age or sex matching at a ratio of 1:1 DL and CL cases. The primary goal was to determine whether the number of lesions influenced the clinical outcome and response to therapy. We compared DL patients who have >50 cutaneous lesions with DL cases who have <40 lesions at the time of diagnosis.

Case Definition and Inclusion Criteria

A DL case was defined as the presence of ≥10 or more cutaneous lesions over 2 or more noncontiguous body areas in a patient (*1*) (Figure 1). CL was defined by the presence of 1–3 ulcerated lesions with raised borders in any body location. The diagnosis of DL and CL was confirmed by a positive PCR result for *L. braziliensis*. We counted the cutaneous lesions and measured the diameter of the largest lesion. An ear, nose, and throat (ENT) specialist performed a nasal and pharyngeal examination to evaluate mucosal involvement.

Skin Lesion Biopsies for Histopathology and PCR

We took skin biopsy specimens from the border of the original ulcer in both DL and CL patients. The skin fragment was obtained using a 4 mm–diameter punch after the application of a local anesthetic. The biopsy specimens were placed in formol for histopathologic studies and in RNAlater for PCR techniques. Leishmania species was determined by a serial real-time quantitative PCR system (*19*).

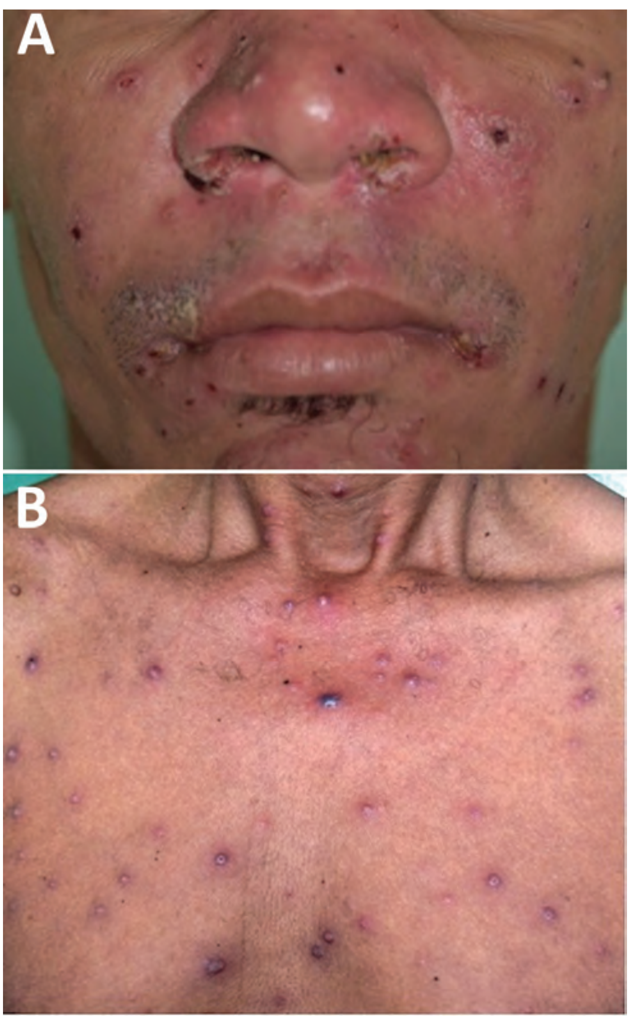

Figure 1. Clinical manifestation of disseminated leishmaniasis in male patient with multiple acneiform lesions, inflammatory and crusted papules in the face (A) and trunk (B), Brazil.

Leishmania Antigen and Skin Test

We prepared soluble *Leishmania* antigen (SLA) as previously described (*20*). We inoculated 25 µg in 0.1 mL of SLA in the forearm and induration was determined after 48 hours. A skin test result was considered positive when the induration was ≥5 mm.

Determination of Cytokines and Chemokines

We isolated peripheral blood mononuclear cells (PBMC) from heparin-treated venous blood by Ficoll-Hypaque gradient centrifugation and stimulated them with SLA as previously described (*21*). In brief, after washing 3 times in 0.9% NaCl, we resuspended cells in RPMI 1640 Medium (ThermoFisher Scientific) supplemented with 10% fetal bovine serum, 100 IU/mL penicillin, and 100 µg/mL streptomycin. Cells were adjusted to 3×10^6 cells/mL, put in 24-well plates, and stimulated with SLA (5 µg/mL). After incubation for 72 hours at 37°C and 5% CO_2, we collected and stored supernatants at –20°C. The levels of interferon (IFN) γ, tumor necrosis factor (TNF), interleukin (IL) 1β, IL-10, chemokine ligand (CXCL) 9, and CXCL-10 were measured by the ELISA sandwich method with reagents from BD Bioscience and the results were expressed as picograms per milliliter (*22*).

Treatment and Cure Criteria

As recommended by the Brazil Ministry of Health, the standard therapy was meglumine antimoniate (20 mg/kg) for 30 days for DL and 20 days for CL. However, DL is common in patients >50 years of age, and those patients should be treated with amphotericin B or miltefosine to reduce adverse reactions. Of the 202 study participants, 82 DL and all 101 CL patients were treated with meglumine antimoniate. We evaluated patients every 30 days until cure. We registered the number and size of lesions and noted appearance of new lesions, occurrence of mucosal disease, and adverse reactions at each visit. We defined cure as complete epithelization of all lesions without infiltrated borders 90 days after initiating therapy.

Age of >50 years, heart disease, and kidney failure are contraindications for the use of meglumine antimoniate. In this study, 19 DL patients did not receive meglumine antimoniate and were treated with available alternative drugs: 3 patients received deoxycholate amphotericin B (20–30 mg/kg weight;

6 patients received liposomal amphotericin B (35–40 mg/kg weight; 5 patients received miltefosine (2.5 mg/kg/d [maximum dose 150 mg/d] for 28 days); and 5 patients received miltefosine (same dosing) combined with meglumine antimoniate (20 mg/kg weight for 30 d). Patients who failed to respond to meglumine antimoniate received a second course of the same dose. Those who failed to respond to miltefosine or amphotericin B received liposomal amphotericin B (35 mg/kg weight).

Ethical Considerations

This study was approved by the Institutional Review Board of the Federal University of Bahia (document of approval CAAE 62974916.8.0000.5577). Written consent was obtained from all participants.

Results

Clinical Profile of DL and CL Patients

DL patients were older than CL patients; men predominated in both groups, but the percentage of men was substantially higher in the DL group (Table 1). The duration of disease before diagnosis was longer in patients with DL. Both the frequency of patients with positive leishmania skin test (p = 0.0001) and the induration size (p = 0.0001) were higher for CL than for DL. After 1 course of meglumine antimoniate therapy, 44% of DL patients were cured, compared with 60% of CL patients. The healing time was significantly shorter for CL than for DL (110.8 ± 7.7 vs. 177 ± 19.6 days; p = 0.001). Mucosal disease associated with cutaneous lesions was observed in 33 (40.7%) of 81 DL patients, as determined by an ENT specialist. Those lesions were characterized as nodular or superficial ulcers in the nasal mucosa.

Cytokine and Chemokine Profile in DL

We have previously shown that DL patients produce lower levels of IFN-γ and TNF in supernatants of PBMC stimulated with SLA than do CL patients (*21*). To better understand the pathogenesis of DL and to determine whether the number of lesions in DL was associated with cytokine production, we measured IFN-γ, TNF, IL-1β, IL-10, CXCL-9, and CXCL-10 in supernatants of PBMC cultures stimulated with SLA in DL patients who had <40 lesions (DL<40) and in those with >50 lesions (DL>50) (Figure 2). No difference was noted regarding the production of IFN-γ, TNF, IL-1β, IL-10, and CXCL-9 between the 2 groups, but CXCL-10 was higher (p = 0.0034) in supernatants of lymphocyte cultures of DL>50 patients (1,742 ± 1,206 pg/mL) than in DL<40 patients (626 ± 684.4 pg/mL).

Demographic and Clinical Features of DL>50 Patients and DL<40 Patients

During the study period, we diagnosed DL>50 in 40 patients and DL<40 in 55 patients (Table 2). DL>50 was associated with older age and shorter duration of illness. The time between the appearance of the first lesion and dissemination was similar in the 2 groups. Systemic symptoms such as fever, chills, and headache were present in most cases (76% of DL>50 cases and 70% of DL<40). Although not a significant difference, the frequency of mucosal disease was higher in DL>50 patients (44%) than in DL<40 patients (31%). Cure rate was 30% in DL>50 patients and 56% in DL<40 patients after a single course of meglumine antimoniate (p = 0.03). Moreover, the healing time in DL>50 patients was longer (p = 0.001) than in DL<40 patients.

Table 1. Demographic, clinical, laboratory, and therapeutic characteristics of DL and CL patients in study of leishmaniasis immune response and clinical and therapeutic outcomes, Corte de Pedra Health Post, Brazil, 2016–2019*

Characteristic	DL, n = 101	CL, n = 101	p value
Age, y	39.5 ± 14.8	32 ± 13.3	0.0002†
Sex, no. (%) patients			
M	88 (87)	69 (68)	0.04‡
F	13 (13)	23 (32)	0.04‡
Duration of disease until diagnosis, d	52.7 ± 2.7	41 ± 1.7	0.0003†
No. lesions	113.6 ± 210	1.4 ± 0.7	<0.0001†
Biggest lesion size, mm^2	775.6 ± 2,190	392.7 ± 283.4	NS
Lymphadenopathy, no. positive/no. tested (%)	47/93 (50.5)	61/101 (60.4)	NS
LST size, mm^2	102.3 ± 96.5	213.6 ± 126.9	0.0001†
LST , no. positive/no. tested (%)	64/97 (66)	101/101 (100)	0.0001‡
PCR. no. positive/no. tested (%)	84/91 (92)	101/101 (100)	NS
Cure rate, no. cured/no. treated (%)§	34/78 (44)¶	44/101 (60)	NS
Healing time, d§	177 ± 19.6	110.8 ± 7.7	0.001†

*Values are mean ± SD unless otherwise indicated. CL, cutaneous leishmaniasis; DL, disseminated leishmaniasis; LST, *Leishmania* skin test, NS, not significant.
†By unpaired t-test.
‡By Fisher exact test.
§After 1 standard course of meglumine antimoniate (20 mg/kg/d) for 20 d (CL) or 30 d (DL).
¶Six patients had no outcome data, irregular use, or discontinuation.

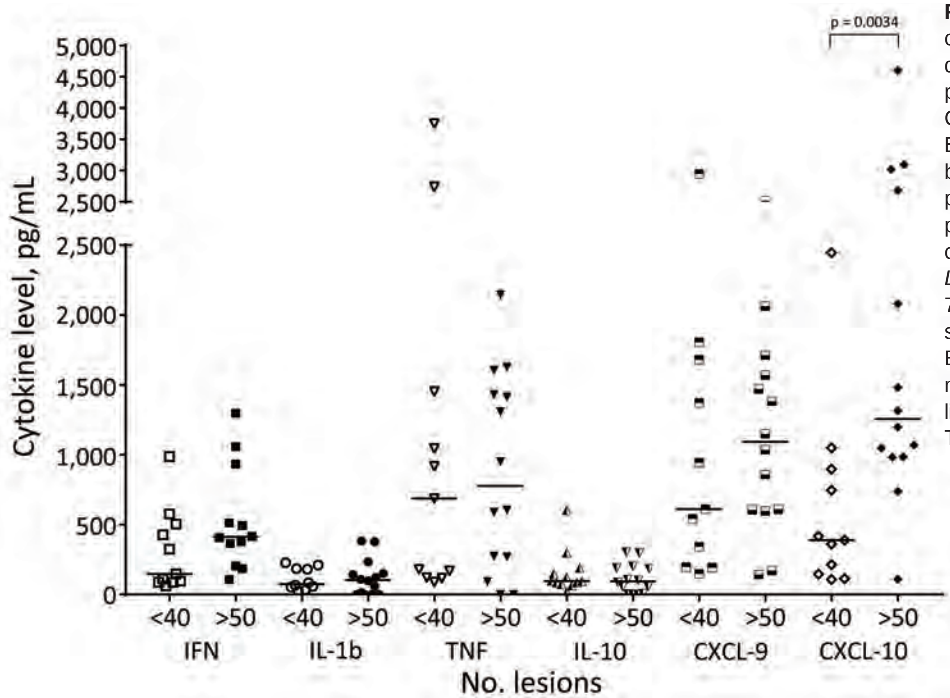

Figure 2. Systemic production of chemokines and cytokines among disseminated leishmaniasis (DL) patients with >50 and <40 lesions, Corte de Pedra Health Post, Brazil, 2016–2019. Peripheral blood mononuclear cells from 11 patients with <40 lesions and 14 patients with >50 lesions were cultured in the presence of soluble *Leishmania* antigen (5 µg/mL) for 72 hours. Cytokine levels in culture supernatants were measured by ELISA. Horizontal lines represent median values. CXCL, chemokine ligand; IFN, interferon; IL, interleukin; TNF, tumor necrosis factor.

Because the classification of the 2 patient groups was arbitrary, we performed other comparisons to better evaluate the effect of the number of lesions in therapeutic response to meglumine antimoniate. The cure rate in persons with DL who had <20 lesions was 65% and for DL patients with >100 lesions was 22% (p = 0.003). The cure rate in patients with DL<40 (56%) was higher than in patients with DL with >100 lesions (22%) (p = 0.006). The cure rate progressively decreased according to the number of lesions; the cure rate was 65% in patients with <20 lesions, 56% in patients with <40 lesions, 30% in patients with >50 lesions, and 22% in persons with >100 lesions. The Kaplan-Meyer curve (Figure 3) shows that DL<40 patients healed in less time than did DL>50 patients.

Therapeutic Response of DL to Amphotericin B and Miltefosine

We demonstrate the clinical features, cure rate at day 90, and healing time of patients who were treated with amphotericin B, miltefosine, or miltefosine combined with meglumine antimoniate and in those

Table 2. Demographic, clinical, laboratory, and therapeutic aspects of DL patients according to number of lesions in study of leishmaniasis immune response and clinical and therapeutic outcomes, Corte de Pedra Health Post, Brazil, 2016–2019*

Characteristic	DL with >50 lesions, n = 40	DL with <40 lesions, n = 55	p value
Age, y	44.5 ± 13.3	35.3 ± 14.2	0.0018†
Sex			
M	34 (85)	49 (89)	NS
F	6 (15)	6 (11)	NS
Duration of disease, d	46 ± 3.4	58 ± 4.0	0.031†
Dissemination time, d	21 ± 2.3	26 ± 4.4	0.40†
Systemic symptoms, no. positive/no. tested (%)	29/38 (76)	28/40 (70)	NS
No. lesions	252 ± 45.1	22 ± 1.0	<0.0001†
Largest lesion area, mm^2	1181 ± 581.2	905 ± 415.3	0.69#
Lymphadenopathy, no. positive/no. tested (%)	13/26 (50)	25/51 (49)	NS
Mucosal involvement, no. positive/no. tested (%)	16/36 (44.4)	12/39 (31)	NS
LST area, mm^2	156 ± 84.7	141 ± 71.4	0.47†
LST, no. positive/no. tested (%)	24/39 (62)	36/54 (67)	NS
PCR, no. positive/no. tested (%)	24/26 (92)	44/49 (90)	NS
Cure rate, no. cured/no. treated (%)‡	7/21 (33)	23/41 (56)	0.03§
Healing time, d	218 ± 203	109 ± 95	0.0018†

*Values are no. (%) or mean ± SD unless otherwise indicated. DL, disseminated leishmaniasis; LST, *Leishmania* skin test, NS, not significant.
†By unpaired t-test.
‡After 1 standard course of meglumine antimoniate (20 mg/kg/d) for 30 d.
§By Fisher exact test.

who only received meglumine antimoniate (Table 3). The demographic and clinical features were similar in the 4 groups of patients; the number of lesions was lower in patients treated with miltefosine alone. The healing time was shorter (p<0.01) for persons who received meglumine antimoniate plus miltefosine than for patients in the other groups. Moreover, all patients who received the combined therapy were cured before day 90, and 4 (80%) of them were cured on day 60.

Discussion

DL is a severe disease caused by *L. braziliensis* that is characterized by a large number of cutaneous lesions, occurrence of both skin and nasal mucosal disease, and high rate of therapeutic failure to meglumine antimoniate, the drug that is recommended to treat leishmaniasis in Latin America (*17*). The pathogenesis of DL is not completely understood; clinical findings and response to therapy is based on case series consisting of small numbers of patients (*7*,*8*). We compared clinical features and response to therapy in 101 CL patients and 101 DL patients and evaluated the association between number of lesions with clinical findings, cytokine production, and outcome of therapy. We confirmed that DL patients are predominantly male, that DL is highly associated with mucosal disease, and that treatment with meglumine antimoniate has a high rate of failure. The number of lesions in DL cases was variable; increased numbers of lesions were associated with age, duration of illness, long healing time, and production of CXCL-10 in PBMC supernatants stimulated with SLA. Moreover, in a small number of patients, we observed that combined therapy with miltefosine and meglumine antimoniate resulted in a higher cure rate of DL than other forms of therapy.

In this study, DL patients were older than CL patients, but we also identified a large number of DL case-patients <50 years of age and many women with DL, which differed from previous reports (*7*,*14*). The cases of DL in our leishmaniasis-endemic area have spread from inner regions to other parts, suggesting parasites that cause DL are spreading and that transmission is occurring in peridomicile areas rather than only in farms, as previously described (*11*,*23*). Those changes in epidemiology might have influenced the increasing occurrence of DL in young patients and in women. The low cure rate of CL with meglumine antimoniate is a major public health problem in our area; the failure rate has increased from 10% to >50% in the past 40 years (*24*–*27*). In this study, the cure rate by meglumine antimoniate was similar in CL and DL cases, but the healing time was longer for DL patients than for CL patients.

The immune response at the lesion site and histopathologic features are similar in DL and CL, but frequency of positive *Leishmania* skin test was lower in DL than in CL (*17*,*18*,*28*). In addition to the less frequent positive skin tests, the size of the skin test reaction was smaller in DL than in CL. The contrast between the similarity of the immune response at the lesion site in DL and CL and the poor Th1 immune

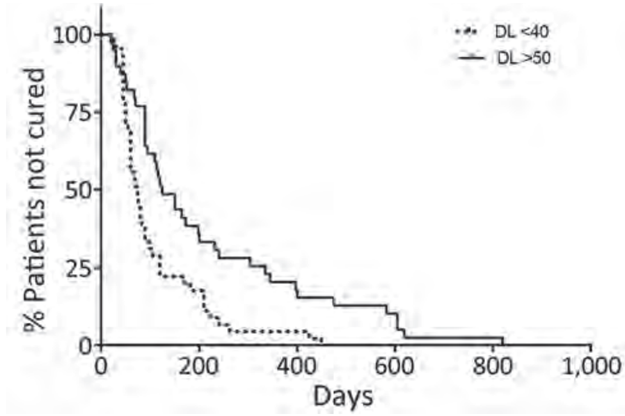

Figure 3. Kaplan-Meyer curve showing time to cure in the 2 groups of DL patients treated with meglumine antimoniate in monotherapy, Corte de Pedra Health Post, Brazil, 2016–2019. Patients with >50 lesions (n = 40) and <40 lesions (n = 55) were treated with meglumine antimoniate (20 mg/kg/d) for 20 days (p = 0.0012 by log-rank test). DL, disseminated leishmaniasis.

Table 3. Clinical profile and response to therapy of disseminated leishmaniasis patients treated with amphotericin b, miltefosine, and miltefosine plus meglumine antimoniate in study of leishmaniasis immune response and clinical and therapeutic outcomes, Corte de Pedra Health Post, Brazil, 2016–2019*

Treatment†	Age, y	% Men	Illness duration, d	No. lesions	Cure rate on day 90	Healing time
Amphotericin B, n = 9	59 ± 5.1	88.8%	54 ± 16.9	350 ± 489.1	55.5%	137 ± 1113
Miltefosine, n = 5	54 ± 9.2	100%	54 ± 9.2	49 ± 18.8	40%	96 ± 27.9
Miltefosine + MA, n = 5	57 ± 9.3	80%	42 ± 7.5	181 ± 204.2	100%	53 ± 18.3
MA, n = 78	39 ± 16.7	84.6%	53 ± 6.1	116 ± 217.3	44%	177 ± 19.6
p value	0.51‡	0.47§	0.32¶	0.26¶	NA	0.01¶

*Values are mean ± SD unless otherwise indicated. MA, meglumine antimoniate; NA, not applicable.
†The total number of disseminated leishmaniasis cases with therapeutic outcome was 97. We have no follow-up data for 4 patients.
‡By student t-test.
§Fisher exact test.
¶Kruskal-Wallis test.

response observed in DL in vivo and in vitro tests to evaluate T-cell response argue against an impairment in the Th1 immune response (*17*). Because of migration of most antigen-reactive cells to the multiple infected skin lesions, it is likely those cells are lacking in peripheral blood and in the other tissues, decreasing T-cell responses in the delayed-type hypersensitivity test and in blood cells.

Regarding the histopathology and cytokine production, DL lesions have fewer granuloma and higher frequencies of B cells and plasma cells than CL ulcers (*8*,*29*). More recently, we have shown that SLA IgG and IgG2 titers are higher in DL than in CL (*30*). Moreover, we demonstrated a correlation between number of lesions and *L. braziliensis* IgG2 production in DL patients (*29*). In this study, most cytokine levels were similar in the supernatants of PBMC stimulated with SLA from DL and CL, as well in supernatants of cells from DL patients with >50 lesions or <40 lesions, but CXCL-10 levels were higher in DL patients with >50 lesions. The inflammatory response is exaggerated in DL patients (*14*). CXCL-10 is expressed in blood cells, and its receptor, chemokine receptor 3, is expressed in tissues. The interaction of those chemokines enables macrophages and T cells to pass to the lesion site, increasing the inflammatory response (*30*,*31*), which suggests that CXCL-10 might contribute to the inflammatory response in DL patients and to parasite dissemination.

The high number of cutaneous lesions and the concomitant occurrence of cutaneous and mucosal involvement is a hallmark of DL. We compared the clinical features and cure rate in DL patients who had <40 lesions with patients who had >50 lesions. We left a gap between 40 and 50 lesions because very small lesions might be missed on routine clinical examination. Patients with >50 lesions were older and had shorter duration of illness, but we found no difference between the 2 groups of patients regarding symptoms associated with systemic manifestations. The frequency of mucosal leishmaniasis was similar in those with >50 and <40 lesions, indicating that the number of lesions is not a biomarker of mucosal disease in DL patients. Mucosal leishmaniasis is one of the more severe forms of *L. braziliensis* infection, characterized by ulcerated lesions, rupture of the nasal septum, and destruction of the facial structure (*32*). Mucosal leishmaniasis usually occurs weeks or even years after a cutaneous ulcer, but in a recent large series of patients with mucosal leishmaniasis, we found that 30% of cases had concomitant cutaneous and mucosal disease (*33*,*34*). The severity of mucosal disease in *L. braziliensis* infection has been classified by stages ranging from 1 to 5 (*35*). A nodule is the first sign of mucosal involvement, followed by superficial and deep ulcer cutaneous, nasal septum perforation, and destruction of the facial structure. In DL, patients' mucosal disease is characterized by nodules and superficial ulcers; the mild mucosal disease and the initiation of therapy before nasal tissue is destroyed might contribute to the curing of mucosal lesions in ≤60 days for most DL patients.

The cure rate in patients who had >50 lesions was significantly lower than for persons with <40 lesions; only 30% of patients with >50 lesions were cured with 90 days of therapy. Moreover, a higher number of lesions was associated with prolonged healing time. Most DL patients were treated with meglumine antimoniate, but a limited number of patients were treated with amphotericin B, miltefosine, or miltefosine combined with meglumine antimoniate. We have previously shown that miltefosine is more effective than meglumine antimoniate in CL patients (*27*,*36*). However, monotherapy with miltefosine only cured 40% of DL patients. All 5 patients who used miltefosine plus meglumine antimoniate were cured, and healing time was short. Amphotericin B is known to be the best drug for therapy in American tegumentary leishmaniasis, and liposomal amphotericin B in a total dose ranging from 17 to 37 mg/kg cured 70% of DL patients by day 90 (*37*). In this study, only 4 of 9 patients treated with this drug did not achieve cure by day 90, although all were eventually cured without the use of other drugs. Patients taking amphotericin B who did not achieve cure by day 90 had more severe disease; in 3 of those patients, the number of lesions ranged from 405 to 1,500.

The limitations of this study are that not all patients had an ENT examination, follow-up care was not completed in ≈8% of DL patients treated with meglumine antimoniate, and alternative therapies were only used in a limited number of patients. Moreover, treatment with amphotericin B is very difficult in this leishmaniasis-endemic area, and the effective dose of this drug was only achieved 60–90 days after initiating therapy. However, this study followed a much larger number of DL patients prospectively than previous studies, and new information was obtained. Most DL patients were <40 years of age, and despite mucosal disease occurring in a high frequency, the mucosal lesions were mild and responded well to therapy. Despite an increase in failure of meglumine antimoniate therapy observed in CL patients in this area, healing time was longer for DL patients than for CL patients, and the number of lesions in DL patients was associated with increased treatment failure. In addition, we extend previous observations regarding the therapeutic response in DL. The high rate of therapeutic failure and the long healing time of DL patients treated with meglumine antimoniate indicates that alternative drugs or polychemotherapy should be used for the treatment of DL. Although further testing in a large number of DL patients is needed, our preliminary observation of a high cure rate in patients who received meglumine antimoniate combined with miltefosine supports use of those drugs as first choice therapy.

Acknowledgments

We thank Cristiano Sampaio Franco for assistance in the preparation of this manuscript.

This work was supported by National Institutes of Health grant AI136032 (Tropical Medicine Research Center}, Brazilian Ministry of Science, Technology, and Innovation #465229/2014-0 (CNPq) and the Fundação de Amparo à Pesquisa do Estado da Bahia (FAPESB) INC 0003/2019.

About the Author

Dr. Machado is the head of the Immunology Service at the University Hospital Edgar Santos, Federal University of Bahia. His research is mainly focused in immunological, clinical, and therapeutic aspects of American tegumentary leishmaniasis and leprosy.

References

1. Turetz ML, Machado PR, Ko AI, Alves F, Bittencourt A, Almeida RP, et al. Disseminated leishmaniasis: a new and emerging form of leishmaniasis observed in northeastern Brazil. J Infect Dis. 2002;186:1829–34. https://doi.org/10.1086/345772
2. Calvopina M, Gomez EA, Uezato H, Kato H, Nonaka S, Hashiguchi Y. Atypical clinical variants in New World cutaneous leishmaniasis: disseminated, erysipeloid, and recidiva cutis due to *Leishmania (V.) panamensis*. Am J Trop Med Hyg. 2005;73:281–4. https://doi.org/10.4269/ajtmh.2005.73.281
3. Alborzi A, Pouladfar GR, Fakhar M, Motazedian MH, Hatam GR, Kadivar MR. Isolation of *Leishmania tropica* from a patient with visceral leishmaniasis and disseminated cutaneous leishmaniasis, southern Iran. Am J Trop Med Hyg. 2008;79:435–7. https://doi.org/10.4269/ajtmh.2008.79.435
4. Rincón MY, Silva SY, Dueñas RE, López-Jaramillo P. A report of two cases of disseminated cutaneous leishmaniasis in Santander, Colombia [in Spanish]. Rev Salud Publica (Bogota). 2009;11:145–50. https://doi.org/10.1590/S0124-00642009000100015
5. Newlove T, Robinson M, Meehan SA, Pomerantz R. Old World cutaneous leishmaniasis. Dermatol Online J. 2012;18:32. https://doi.org/10.5070/D36J84K1FN
6. Jirmanus L, Glesby MJ, Guimarães LH, Lago E, Rosa ME, Machado PR, et al. Epidemiological and clinical changes in American tegumentary leishmaniasis in an area of *Leishmania (Viannia) braziliensis* transmission over a 20-year period. Am J Trop Med Hyg. 2012;86:426–33. https://doi.org/10.4269/ajtmh.2012.11-0378
7. Costa JM, Marsden PD, Llanos-Cuentas EA, Netto EM, Carvalho EM, Barral A, et al. Disseminated cutaneous leishmaniasis in a field clinic in Bahia, Brazil: a report of eight cases. J Trop Med Hyg. 1986;89:319–23.
8. Carvalho EM, Barral A, Costa JM, Bittencourt A, Marsden P. Clinical and immunopathological aspects of disseminated cutaneous leishmaniasis. Acta Trop. 1994;56:315–25. https://doi.org/10.1016/0001-706X(94)90103-1
9. Rosa AC, Cuba CC, Vexenat A, Barreto AC, Marsden PD. Predominance of *Leishmania braziliensis braziliensis* in the regions of Três Braços and Corte de Pedra, Bahia, Brazil. Trans R Soc Trop Med Hyg. 1988;82:409–10. https://doi.org/10.1016/0035-9203(88)90138-1
10. Machado GU, Prates FV, Machado PRL. Disseminated leishmaniasis: clinical, pathogenic, and therapeutic aspects. An Bras Dermatol. 2019;94:9–16. https://doi.org/10.1590/abd1806-4841.20198775
11. Queiroz A, Sousa R, Heine C, Cardoso M, Guimarães LH, Machado PR, et al. Association between an emerging disseminated form of leishmaniasis and *Leishmania (Viannia) braziliensis* strain polymorphisms. J Clin Microbiol. 2012;50:4028–34. https://doi.org/10.1128/JCM.02064-12
12. Guimarães LH, Queiroz A, Silva JA, Silva SC, Magalhães V, Lago EL, et al. Atypical manifestations of cutaneous leishmaniasis in a region endemic for *Leishmania braziliensis*: clinical, immunological and parasitological aspects. PLoS Negl Trop Dis. 2016;10:e0005100. https://doi.org/10.1371/journal.pntd.0005100
13. Silva J, Queiroz A, Moura I, Sousa RS, Guimarães LH, Machado PRL, et al. Dynamics of American tegumentary leishmaniasis in a highly endemic region for *Leishmania (Viannia) braziliensis* infection in northeast Brazil. PLoS Negl Trop Dis. 2017;11:e0006015. https://doi.org/10.1371/journal.pntd.0006015
14. Oliveira WN, Dórea AS, Carneiro PP, Nascimento MT, Carvalho LP, Machado PRL, et al. The influence of infection by different *Leishmania (Viannia) braziliensis* isolates on the pathogenesis of disseminated leishmaniasis. Front Cell Infect Microbiol. 2021;11:740278.
15. Petersen EA, Neva FA, Barral A, Correa-Coronas R, Bogaert-Diaz H, Martinez D, et al. Monocyte suppression of antigen-specific lymphocyte responses in diffuse cutaneous leishmaniasis patients from the Dominican Republic. J Immunol. 1984;132:2603–6. https://doi.org/10.4049/jimmunol.132.5.2603
16. Christensen SM, Belew AT, El-Sayed NM, Tafuri WL, Silveira FT, Mosser DM. Host and parasite responses in human diffuse cutaneous leishmaniasis caused by *L. amazonensis*. PLoS Negl Trop Dis. 2019;13:e0007152. https://doi.org/10.1371/journal.pntd.0007152
17. Machado PR, Rosa ME, Costa D, Mignac M, Silva JS, Schriefer A, et al. Reappraisal of the immunopathogenesis of disseminated leishmaniasis: in situ and systemic immune response. Trans R Soc Trop Med Hyg. 2011;105:438–44. https://doi.org/10.1016/j.trstmh.2011.05.002
18. Dantas ML, Oliveira JM, Carvalho L, Passos ST, Queiroz A, Guimarães LH, et al. Comparative analysis of the tissue inflammatory response in human cutaneous and disseminated leishmaniasis. Mem Inst Oswaldo Cruz. 2014;109:202–9. https://doi.org/10.1590/0074-0276130312
19. Weirather JL, Jeronimo SMB, Gautam S, Sundar S, Kang M, Kurtz MA, et al. Serial quantitative PCR assay for detection, species discrimination, and quantification of *Leishmania* spp. in human samples. J Clin Microbiol.

2011;49:3892–904. https://doi.org/10.1128/JCM.r00764-11
20. Reed SG, Badaró R, Masur H, Carvalho EM, Lorenco R, Lisboa A, et al. Selection of a skin test antigen for American visceral leishmaniasis. Am J Trop Med Hyg. 1986;35:79–85. https://doi.org/10.4269/ajtmh.1986.35.79
21. Bacellar O, Lessa H, Schriefer A, Machado P, Ribeiro de Jesus A, Dutra WO, et al. Up-regulation of Th1-type responses in mucosal leishmaniasis patients. Infect Immun. 2002;70:6734–40. https://doi.org/10.1128/IAI.70.12.6734-6740.2002
22. Leopoldo PTG, Machado PRL, Almeida RP, Schriefer A, Giudice A, de Jesus AR, et al. Differential effects of antigens from *L. braziliensis* isolates from disseminated and cutaneous leishmaniasis on in vitro cytokine production. BMC Infect Dis. 2006;6:75. https://doi.org/10.1186/1471-2334-6-75
23. Schriefer A, Guimarães LH, Machado PRL, Lessa M, Lessa HA, Lago E, et al. Geographic clustering of leishmaniasis in northeastern Brazil. Emerg Infect Dis. 2009;15:871–6. https://doi.org/10.3201/eid1506.080406
24. Correia D, Macêdo VO, Carvalho EM, Barral A, Magalhães AV, de Abreu MV, et al. Comparative study of meglumine antimoniate, pentamidine isethionate and aminosidine sulfate in the treatment of primary skin lesions caused by *Leishmania (Viannia) braziliensis* [in Portugese]. Rev Soc Bras Med Trop. 1996;29:447–53. https://doi.org/10.1590/S0037-86821996000500007
25. Machado PRL, Ampuero J, Guimarães LH, Villasboas L, Rocha AT, Schriefer A, et al. Miltefosine in the treatment of cutaneous leishmaniasis caused by *Leishmania braziliensis* in Brazil: a randomized and controlled trial. PLoS Negl Trop Dis. 2010;4:e912. https://doi.org/10.1371/journal.pntd.0000912
26. Prates FVO, Dourado MEF, Silva SC, Schriefer A, Guimarães LH, Brito MD, et al. Fluconazole in the treatment of cutaneous leishmaniasis caused by *Leishmania braziliensis*: a randomized controlled trial. Clin Infect Dis. 2017;64:67–71. https://doi.org/10.1093/cid/ciw662
27. Machado PRL, Prates FVO, Boaventura V, Lago T, Guimarães LH, Schriefer A, et al. A double-blind, randomized trial to evaluate miltefosine and topical granulocyte macrophage colony-stimulating factor in the treatment of cutaneous leishmaniasis caused by *Leishmania braziliensis* in Brazil. Clin Infect Dis. 2021;73:e2465–9. https://doi.org/10.1093/cid/ciaa1337
28. Carvalho EM, Correia Filho D, Bacellar O, Almeida RP, Lessa H, Rocha H. Characterization of the immune response in subjects with self-healing cutaneous leishmaniasis. Am J Trop Med Hyg. 1995;53:273–7. https://doi.org/10.4269/ajtmh.1995.53.273
29. Vieira MGS, Oliveira F, Arruda S, Bittencourt AL, Barbosa AA Jr, Barral-Netto M, et al. B-cell infiltration and frequency of cytokine producing cells differ between localized and disseminated human cutaneous leishmaniases. Mem Inst Oswaldo Cruz. 2002;97:979–83. https://doi.org/10.1590/S0074-02762002000700009
30. Magalhães A, Carvalho LP, Costa R, Pita MS, Cardoso TM, Machado PRL, et al. Anti-*Leishmania* IgG is a marker of disseminated leishmaniasis caused by *Leishmania braziliensis*. Int J Infect Dis. 2021;106:83–90. https://doi.org/10.1016/j.ijid.2021.02.016
31. Lee JH, Kim B, Jin WJ, Kim HH, Ha H, Lee ZH. Pathogenic roles of CXCL10 signaling through CXCR3 and TLR4 in macrophages and T cells: relevance for arthritis. Arthritis Res Ther. 2017;19:163. https://doi.org/10.1186/s13075-017-1353-6
32. Miranda Lessa M, Andrade Lessa H, Castro TWN, Oliveira A, Scherifer A, Machado P, et al. Mucosal leishmaniasis: epidemiological and clinical aspects. Rev Bras Otorrinolaringol (Engl Ed). 2007;73:843–7. https://doi.org/10.1016/S1808-8694(15)31181-2
33. Cincurá C, de Lima CMF, Machado PRL, Oliveira-Filho J, Glesby MJ, Lessa MM, et al. Mucosal leishmaniasis: a retrospective study of 327 cases from an endemic area of *Leishmania* (*Viannia*) *braziliensis*. Am J Trop Med Hyg. 2017;97:761–6. https://doi.org/10.4269/ajtmh.16-0349
34. Cincura C, Costa RS, De Lima CMF, Oliveira-Filho J, Rocha PN, Carvalho EM, et al. Assessment of immune and clinical response in patients with mucosal leishmaniasis treated with pentavalent antimony and pentoxifylline. Trop Med Infect Dis. 2022;7:383. https://doi.org/10.3390/tropicalmed7110383
35. Lessa HA, Lessa MM, Guimarães LH, Lima CM, Arruda S, Machado PR, et al. A proposed new clinical staging system for patients with mucosal leishmaniasis. Trans R Soc Trop Med Hyg. 2012;106:376–81. https://doi.org/10.1016/j.trstmh.2012.03.007
36. Machado PRL, Penna G. Miltefosine and cutaneous leishmaniasis. Curr Opin Infect Dis. 2012;25:141–4. https://doi.org/10.1097/QCO.0b013e3283509cac
37. Machado PRL, Rosa MEA, Guimarães LH, Prates FV, Queiroz A, Schriefer A, et al. Treatment of disseminated leishmaniasis with liposomal amphotericin B. Clin Infect Dis. 2015;61:945–9. https://doi.org/10.1093/cid/civ416

Address for correspondence: Paulo R.L. Machado, Immunology Service of University Hospital Professor Edgard Santos, Federal University of Bahia, Rua Augusto Viana, snº, Canel, 40110-060 Salvador, Bahia, Brazil; email: 19pmachado@gmail.com

Systematic Review of Scales for Measuring Infectious Disease–Related Stigma

Amy Paterson, Ashleigh Cheyne, Benjamin Jones, Stefan Schilling, Louise Sigfrid, Jeni Stolow, Lina Moses, Piero Olliaro, Amanda Rojek

Infectious disease outbreaks are associated with substantial stigma, which can have negative effects on affected persons and communities and on outbreak control. Thus, measuring stigma in a standardized and validated manner early in an outbreak is critical to disease control. We reviewed existing scales used to assess stigma during outbreaks. Our findings show that many different scales have been developed, but few have been used more than once, have been adequately validated, or have been tested in different disease and geographic contexts. We found that scales were usually developed too slowly to be informative early during an outbreak and were published a median of 2 years after the first case of an outbreak. A rigorously developed, transferable stigma scale is needed to assess and direct responses to stigma during infectious disease outbreaks.

Infectious disease outbreaks are typically accompanied by stigma (*1*–*4*). Stigma can be defined as the denial of social acceptance to a person or group due to an attribute deemed discrediting by their community or society (*5*,*6*). That umbrella term includes the cognitive or affective endorsement of negative stereotypes, referred to as prejudice; negative behavioral manifestations, referred to as discrimination; and medically unwarranted avoidance or neglect of affected persons (*6*,*7*) (Figure 1).

Stigma associated with infectious disease outbreaks reduces affected persons' opportunities for physical, social, and psychological well-being, contributing to social and health inequalities (*8*–*11*). COVID-19 and Ebola virus disease (EVD) stigmatization have specifically been proven predictors of severe psychological distress, depression, anxiety, and posttraumatic stress disorder symptoms (*1*,*11*–*13*). Stigma can also impede efforts to control disease outbreaks by fueling fear, decreasing uptake of preventive measures (including vaccination), discouraging health-seeking behavior such as seeking testing and treatment, and reducing adherence to care (*6*,*8*,*10*,*14*).

Furthermore, outbreak-related public health interventions can affect the stigma associated with a disease (*10*). In a systematic review of the psychological effects of quarantine, persistent stigma was a central theme (*15*). Contact tracing has been found to lead to linear blaming of affected persons (*10*). Vaccination status can be a source of social stigma (*16*–*18*), as can decisions about mask-wearing (*19*). Although evidence of the exacerbation of stigma might not fully undermine the value of these public health interventions, those outcomes highlight the need for the inadvertent social consequences to be considered and minimized where possible.

A range of stigma reduction interventions have been described in the literature (*6*–*8*,*14*). However, without robust stigma scales, determining where these interventions are most needed and evaluating their effectiveness in outbreak settings is difficult (*11*). Stigma scales have been used in other infectious disease contexts (most routinely HIV) and could be similarly helpful when applied to emerging and reemerging disease outbreaks (*11*).

We identified disease-associated stigma scales used in outbreak settings and described the commonalities, strengths, and limitations of those scales. The results of this review are intended to improve the development and use of stigma scales in infectious disease outbreaks and inform the design of a

Author affiliations: University of Oxford, Oxford, UK (A. Paterson, A. Cheyne, B. Jones, S. Schilling, L. Sigfrid, P. Olliaro, A. Rojek); Tulane University, New Orleans, Louisiana, USA (J. Stolow, L. Moses); Global Outbreak Alert and Response Network, World Health Organization, Geneva, Switzerland (J. Stolow, L. Moses); The Royal Melbourne Hospital, Melbourne, Victoria, Australia (A. Rojek)

DOI: https://doi.org/10.3201/eid3003.230934

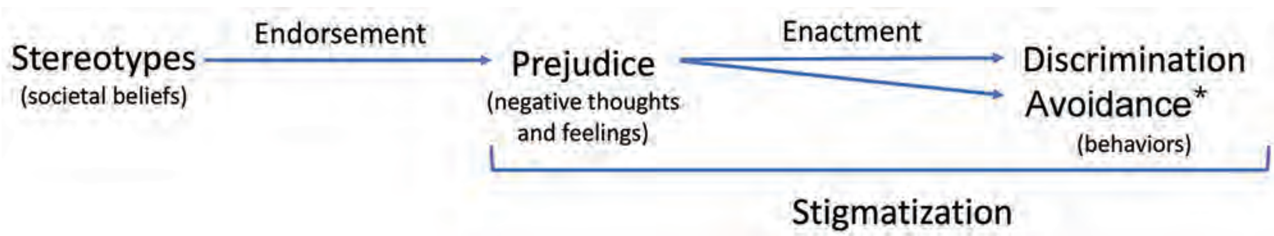

Figure 1. Conceptualization of stigma used in a systematic review of scales for measuring infectious disease–related stigma. Graphic is based on N. Jones and P.W. Corrigan (*6*) and M.G. Weiss (*7*). Asterisk (*) indicates cases where avoidance is medically unwarranted.

transferable scale that can be used across different infectious disease outbreaks.

Methods

Review Strategy

We conducted a review to determine what scales have been used for measuring stigma due to outbreaks in affected communities through January 31, 2023. We assessed the common content themes within those scales; methods used to develop and validate scales; psychometric properties (i.e., validity and reliability) of available scales; transferability of scales; and limitations in the development, validation, and use of those scales.

We defined an outbreak as a rapid, unexpected increase in disease case numbers. Therefore, stigma associated with endemic, chronic diseases, such as HIV and tuberculosis, were outside the scope of this review.

We reported this review in line with the PRISMA (Preferred Reporting Items for Systematic Reviews and Meta-Analyses) 2020 checklist (*20*). Our review was informed by the COSMIN guideline for systematic reviews of patient reported outcome measures (*21*). The review protocol is registered on PROSPERO (registration no. CRD42023396387).

Search Strategy and Eligibility Criteria

We formulated a search strategy with a librarian. The search strategy combined terms for the key components "stigma," "infectious disease outbreaks," and "prevalence scale" by using the Boolean operator "AND" (Appendix Figure, https://wwwnc.cdc.gov/EID/article/30/3/23-0934-App1.pdf). We searched MEDLINE, PsycINFO (https://www.apa.org/pubs/databases/psycinfo), CABI Global Health, Embase, Web of Science, and Cochrane Library databases with no language restrictions. We retrieved all records published though January 31, 2023. We also screened bibliographies of relevant systematic reviews and included additional studies that met the eligibility criteria.

Study Selection

We assessed the retrieved records according to our eligibility criteria (Table 1). We uploaded all citations

Table 1. Eligibility criteria used in a systematic review of scales for measuring infectious disease–related stigma

Criteria	Inclusion	Exclusion
Population	Involved community members of any age affected by infectious disease outbreaks with or without a personal history of the disease	Focused exclusively on healthcare workers
Concept	Described the development, validation, or use of a stigma scale, such as a survey, questionnaire or other instrument consisting of ≥2 closed-end questions that form a composite score and aim to measure outbreak-related stigma prevalence	Focused on broader measurements of intersectional stigma during, but not due to, the outbreak of concern*
Context	Related to infectious disease outbreaks	Focused on non-communicable diseases or chronic infectious diseases
Study types	Cross-sectional or cohort studies	Interventional studies without a pre-intervention survey
	Studies describing scale development, piloting, or validation	Studies investigating stigma exclusively through qualitative methods
	Interventional studies which include pre-interventional surveys providing observational data.	Protocols, guidelines, book sections, case-reports, opinion pieces (editorials, viewpoints, commentaries) conference abstracts, preprints, and unpublished literature
Minimum validity of scale	Use of stigma scales that, at a minimum, have been assessed for face validity†	Not applicable

*Includes scales that assessed stigma associated with race, sexual orientation, mental health, weight, or class during an outbreak or epidemic but not in direct relation to the outbreak disease. For example, scales that assessed race-based discrimination unrelated to association with COVID-19 during the pandemic.
†For instance, scales were at least superficially reviewed by potential end-users, experts, or both to confirm that the scale appears to reflect the concept of stigma in the relevant contexts (*21*).

to EndNote 20.5 (https://endnote.com) and removed duplicates, after which we uploaded titles and abstracts to Rayyan systematic review software (https://www.rayyan.ai). Two independent reviewers screened a random 10% of titles and abstracts and we used Cohen's kappa (κ) to calculate inter-rater reliability. For conflicts, the 2 reviewers discussed the studies and agreed or asked a third reviewer to provide a final decision, then clarified or refined the eligibility criteria. We repeated this process until κ showed excellent agreement (*22*), after which all further titles and abstracts were divided and screened by 1 reviewer.

The reviewer screened eligible full text publications by using the same process. We achieved the required κ after the second round of title and abstract screening (κ = 0.76) and the second round of full text screening (κ = 0.82). Where complete stigma scales were not available, we emailed corresponding authors to request access. If the scale was still not provided, we excluded the study. For non-English stigma scales, we used a professional translation service to translate the scale into English (Appendix). Where multiple articles described the same study activities, we included the article with the most available information on the relevant stigma scale.

Data Extraction and Analysis

One reviewer extracted data by using Excel 2021 (Microsoft, https://www.microsoft.com). Another reviewer independently extracted a random 10% sample of the data to ensure reliability.

We assessed the psychometric properties (i.e., validity and reliability) of scales according to COSMIN guidelines (*21*) (Table 2). We assessed transferability for each scale by using a previously described cross-cultural equivalence framework (*23*) (Appendix Table 1).

We used framework synthesis to identify the domains of stigma included in the scales (*24*). That method of evidence synthesis is used increasingly for health-related reviews and combines framework and thematic analysis techniques (*24*). The method involves starting with an a priori conceptual framework and coding all included studies against that framework (*24*). New themes, or in this case stigma domains, are generated from evidence not captured by the a priori framework (*24*). The approach thereby adopts a mixed deductive and inductive approach to produce a revised conceptual framework (*24*).

We used a previously developed stigma typology (*6*) as the a priori framework for our analysis (Appendix Table 3). We then adjusted and added to the framework throughout the analysis as new domains

Table 2. Definitions of psychometric properties used in a systematic review of scales for measuring infectious disease–related stigma*

Domain	Property	Aspect of property	Definition
Validity			The degree to which an instrument measures the constructs it purports to measure
	Content validity		The degree to which the content of an instrument is an adequate reflection of the construct to be measured
		Face validity	The degree to which an instrument looks as though it reflects the construct to be measured
	Construct validity		The degree to which the scores of an instrument are consistent with hypotheses (for instance regarding internal relationships, relationships to scores of other instruments, or differences between relevant groups) based on the assumption that the instrument validly measures the construct to be measured
		Structural validity	The degree to which the scores of an instrument are an adequate reflection of the dimensionality of the construct to be measured
		Hypotheses testing	The degree to which the scores of an instrument are consistent with hypotheses on relationships to scores of other instruments
		Cross-cultural validity	The degree to which an instrument accurately measures the same construct in different population groups.
	Criterion validity†		The degree to which the scores of an instrument are an adequate reflection of a gold standard
Reliability			The degree to which the measurement is free from measurement error
	Internal consistency		The degree of the interrelatedness among the items
	Test-retest reliability		The amount of the total variance in two sets of measurements which is due to 'true' differences between respondents
	Measurement error		The systematic and random error of a respondent's score that is not attributed to true changes in the construct to be measured
Responsiveness			The ability of an instrument to detect change over time in the construct to be measured

*Table adapted from COSMIN definitions of domains, measurement properties, and aspects of measurement properties, which uses the term "gold standard" (*21*).
†Criterion validity assessment was not considered in this review because no standard for stigma assessment is available.

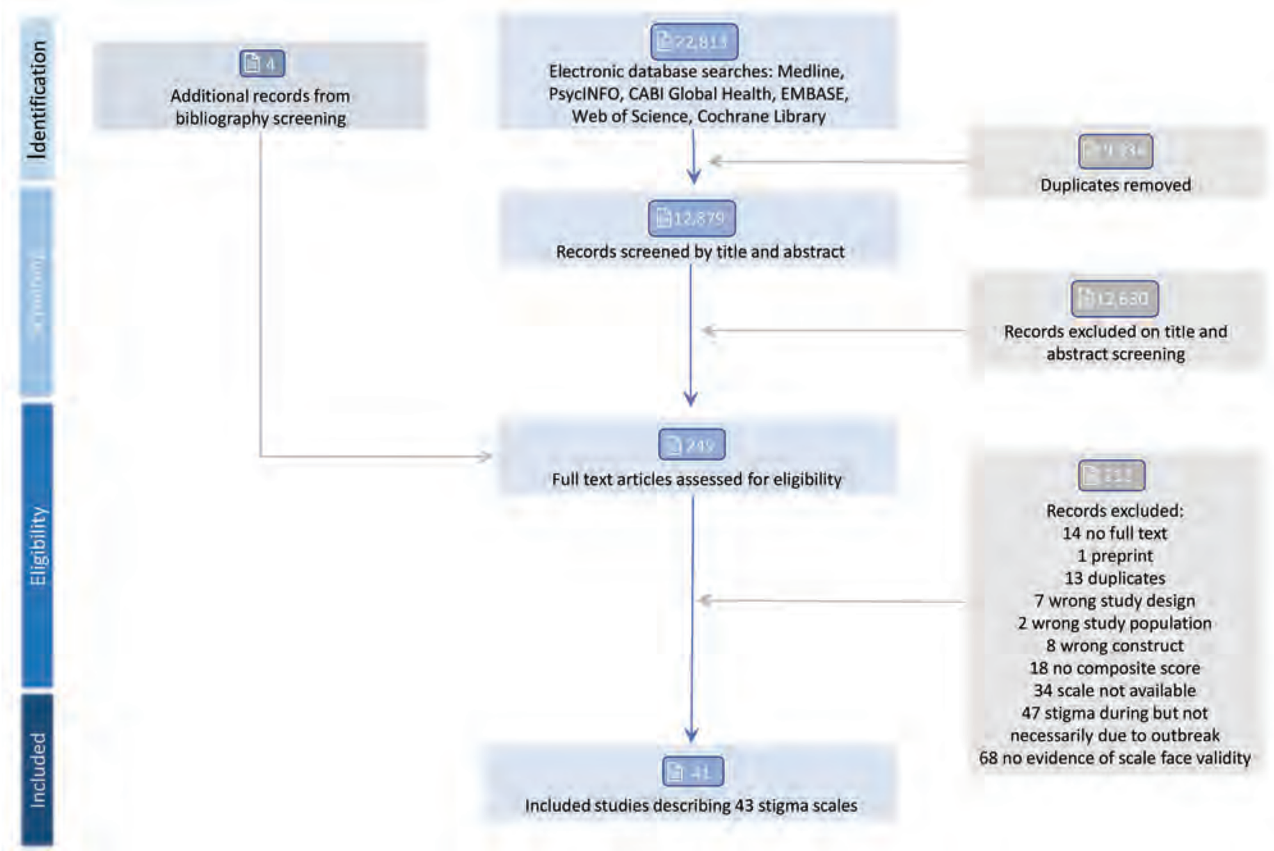

Figure 2. Diagram of studies included in and excluded from a systematic review of scales for measuring infectious disease–related stigma. Reviews were performed in accordance with PRISMA (Preferred Reporting Items for Systematic reviews and Meta-Analyses) guidelines (*20*). PsycINFO is a database of the American Psychiatric Association (https://www.apa.org/pubs/databases/psycinfo).

emerged that were not captured by the existing framework. For example, many scales included questions about stigmatization by employers and coworkers but did not fit into the existing framework; therefore, we added a new domain, termed workplace stigma, to the framework. All authors discussed and agreed upon each addition or adjustment to the framework. We used the same approach for identifying themes in acknowledged limitations.

Quality Assessment

We assessed the quality of each study by using the COSMIN Risk of Bias Checklist (*25*). That checklist uses a modular approach dependent on whether the study was intended for scale development or validation and the aspects of the scale the study set out to validate. The quality of each relevant method is given a rating using by using a worst score counts principle (*25*).

Results

Our search strategy retrieved 12,879 records after deduplication (Figure 2). We excluded most records at title and abstract screening because the search term “discriminat*” referred to the discriminatory ability of prediction models or tests, rather than social discrimination.

We found 249 records eligible for full-text review. Of those, we found 41 studies that described the development, validation, or use of 43 unique outbreak disease–associated stigma scales that met the inclusion criteria. We included those 43 scales in this review.

Overview of Scales

Of the 43 included scales, 42 (98%) were newly developed specifically for the outbreaks of concern (Appendix Table 4); 38 (88%) were used only once in the published literature. The scales were used in 27 different countries.

Thirty-two (74%) scales focused on COVID-19–associated stigma, 7 (16%) assessed EVD-associated stigma, 2 (5%) were SARS-associated, and 1 (2%) scale each was used in Lassa fever, long COVID, and Zika virus disease. Those scales were published a median of 25 (interquartile range 18–30) months after the first case of a given outbreak.

Almost half (21 [49%]) of the scales were based on HIV literature and existing HIV stigma scales (Appendix Table 4). Only 9 (21%) scales included primary qualitative data in the scale development processes. The Long COVID Stigma Scale (*26*), was the only scale explicitly codeveloped with affected community members.

Content of Scales

We identified 24 domains of stigma in the included scales by using the framework synthesis process (Table 3). Those domains included 3 distinct stigma experiences: prejudice, discrimination, and avoidance of persons beyond suggested public health measures. Those stigma experiences were enacted by different groups, including family and friends (social stigma), broader community and strangers (public stigma), colleagues and employers (occupational stigma), service providers (provider-related stigma), and institutions (structural stigma). Our final framework also included the internalization of stigma (self-stigma), avoidance of stigma (anticipated stigma), and stigmatization of persons associated with the disease but not directly infected (stigma-by-association). The most common domains were public prejudice, public discrimination, and self-prejudice. Provider-related, occupational, and anticipated prejudice were infrequently included in the scales (Figure 3).

Table 3. Definitions and example scale items for each domain identified in a systematic review of scales for measuring infectious disease–related stigma*

Action-oriented stigma domains†	Experiential stigma domains		
	Prejudice‡	Discrimination§	Medically unwarranted avoidance¶
Social: stigmatization by friends and family	"I feel blamed by relatives or friends," Self-stigma Scale (SSS-15)	"[I was] forced to change residence because of social alienation," 7-item EVD-related stigma index	"People I cared for stopped calling or interacting after learning that I was infected/suspected," COVID-19 Stigma Scale
Public: stigmatization by broader community and strangers	"Most people think that a person who has had Ebola is disgusting," Ebola/COVID-19–related Stigma Survey	"I have been insulted/discriminated because of my history of being infected/suspected," COVID-19 Stigma Scale	"Some people avoid touching me even after my recovery once they knew I was infected with/suspected," COVID-19 stigma scale
Workplace: stigmatization by colleagues and employers	"My feeling of job security has been affected by my illness," COVID-19 Perceived Stigma Scale-22 (CPSS-22)	"I will dismiss my employee who recovers from COVID-19," Social stigma and discriminatory attitudes scale	"Someone refused to buy products from you," Stigmatization related to EVD and COVID-19 scale
Provider-related: stigmatization by service providers	"You feel it is not worthwhile for you to serve persons who contracted COVID-19" - Stigma Discrimination Scale (SDS-11)	"[I was] treated unfairly by healthcare professionals," COVID-19 Experienced DISCrimination Scale (CEDISC)	"I was denied health care services when the doctors found out I was infected /suspected," COVID-19 Stigma Scale
Structural: stigmatization by institutions	NA	"The first COVID-19 patient in each city should be identified and penalised due to their role in spreading the disease," COVID-19-related enacted Stigma Questionnaire	"At the hospital/clinic, I was made to wait until the last," Ebola-related stigma instrument
Self: internalization of stigma	"Having had COVID-19 infection makes me feel that I am a bad person," COVID-19-related Stigma Survey	"I stopped eating with other people," Ebola-related stigma instrument	NA
Anticipated; disclosure concerns or avoidance due to fear of stigma	"I worry that people may judge me negatively when they find out I have long Covid," Long COVID Stigma Scale (LCSS)	"You have avoidance behaviours such as staying home for fear of being stigmatised or rejected," Stigmatization related to EVD and COVID-19 scale	NA
Stigma-by-association; stigmatization of those societally associated with the disease or infected persons but not personally infected	"If they knew about it would your neighbors, colleagues or others in your community think less of your family because of your COVID-19 infection?" Arabic Explanatory Model Interview Catalogue (EMIC)	"A school refused to accept your children," Stigmatization related to EVD and COVID-19 scale	"If a person was infected with COVID-19, it is better to avoid his/her family members," Community COVID-19 Stigma Scale

*Framework based on stigma typology from Jones and Corrigan (*6*). EVD, Ebola virus disease; NA, not applicable.
†Domains adopted from Pescosolido and Martin (*27*).
‡Negative thoughts and feelings toward stigmatized persons.
§Enactment of prejudice or differential treatment of stigmatized persons.
¶Neglect of stigmatized persons.

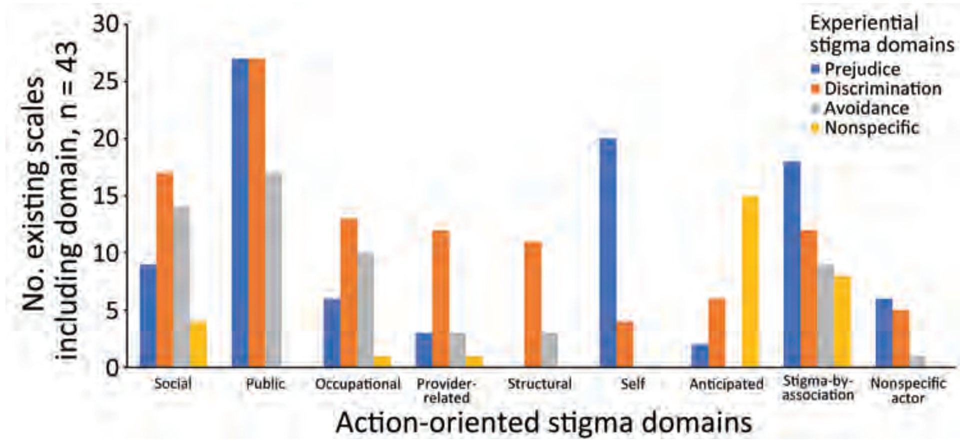

Figure 3. Frequency of inclusion of domains of stigma in a systematic review of scales for measuring infectious disease–related stigma. Graph displays existing scales from framework synthesis. Action-oriented stigma domains included the following: social, stigmatization by friends and family; public, stigmatization by broader community and strangers; occupational, stigmatization by colleagues and employers; provider-related, stigmatization by service providers; structural, stigmatization by institutions; self, internalized stigma; anticipated, disclosure concerns or avoidance due to fear of stigma; nonspecific actor, item does not specify who is enacting stigma.

More than one quarter (14 [28%]) of scales included items that deviated from widely accepted definitions of stigma, including the definition used in this review (Figure 1). Those scales considered adoption of recommended preventive measures (e.g., people should stay away from those infected with COVID-19) and limited knowledge of disease (e.g., COVID-19 only affects the elderly) as evidence of stigmatization.

Sixteen (37%) scales asked participants whether they endorsed or participated in stigmatization toward others, 15 (35%) ask about participants' own experiences of stigmatization, and 4 (9%) enquired about participants' observations of stigmatization toward others in their community. Eight (19%) scales included items from a mixture of those perspectives.

Psychometric Evaluation of Scales

Psychometric evaluation (i.e., assessment of validity and reliability) of scales was notably limited (Appendix Table 5). Among the scales that underwent validation processes, none consistently met the COSMIN criteria for sufficient validity and reliability (*21*).

Approximately half (24 [56%]) the scales were assessed by both relevant professionals and community members before administration. Only 3 studies (*28–30*) reported formal content validity scores. According to the COSMIN criteria (*21*), all scales had indeterminate or inconsistent content validity by our definitions (Table 2).

Among included scales, 20 (47%) had been tested for structural validity, and 12 (60%) met the COSMIN criteria for sufficient validity (*21*). Five (12%) scales had been evaluated for construct validity using hypotheses testing, all of which met the sufficiency criteria (*21*). Six (14%) scales had been assessed for test-retest reliability, and 3 (50%) were deemed sufficient (*21*). No studies assessed responsiveness, that is, the ability of an instrument to detect change in a construct over time (*21*).

For 32 (74%) scales, authors had reported on internal consistency, and most used Cronbach α coefficients. However, because the structural validity of a scale needs to be confirmed before internal consistency can be tested (*21*), we could only consider 17 (53%) of those scores. Of those 17 scales, 4 (24%) had $\alpha<0.7$, suggesting inadequate internal consistency (*31*).

Transferability of Scales

Only 1 scale, the Stigmatization Related to EVD and COVID-19 Scale (*1*), was used across different outbreaks. However, that scale is not publicly available, and we had to request it. In addition, the COVID-19–Related Stigma Survey administered in India and Bangladesh (*32*,*33*) is closely related to the Ebola-Related Stigma Scale administered in Liberia (*34*) and adopted 14 of the original scale's 16 items. Three scales were administered in >1 country. Six scales were used across different participant profiles (i.e., community members with and without lived experience of the disease). No scales had sufficient evidence of cross-cultural equivalence when we reviewed them using a cross-cultural equivalence framework (*23*) (Table 4).

Acknowledged Limitations of Included Studies

Authors of the included studies commonly acknowledged inadequate validation of the stigma scales as a limitation. Most studies also noted the inability to establish causality because of the adoption of a cross-sectional study design. In addition, more than half of the studies expressed concern about the generalizability of their findings because they used nonrepresentative sampling techniques and had undercoverage bias for certain subpopulations.

Quality Assessment of Studies

For 35 studies that described scale development, we found that 7 (20%) received a doubtful quality rating for those methods according to the COSMIN Risk of Bias Checklist (*25*), and we rated the rest inadequate (Appendix Table 5). We found similar ratings for studies that aimed to content validate an existing scale. Conversely, we found that structural validity, internal consistency, test-retest reliability, and hypotheses testing methods more commonly received very good or adequate quality ratings, but those methods were infrequently conducted.

Discussion

We found that numerous scales have been developed to assess outbreak-related stigma and that those scales have been used in a wide range of geographic settings. That finding illustrates a global recognition and concern about the stigma associated with infectious disease outbreaks and potential adverse impacts of stigma. However, shortcomings in the development, validation, and use of those scales mean that stigma is

Table 4. Transferability of scales determined by a systematic review of scales for measuring infectious disease–related stigma*

	Transferability		
Scale name	Cross-national	Cross-outbreak	Participant profile†
Stigmatization related to EVD and COVID-19 scale	Used; IE	Used; IE	Not used; A
Ebola-related Stigma Scale	Not used; U	Not used; A	Not used; A
COVID-19–related Stigma Survey	Used; IE	Not used; A	Not used; A
COVID-19 Stigma Scale	Not used; U	Not used; U	Not used; A
Community COVID-19 Stigma Scale	Not used; U	Not used; U	Not used; A
7-item EVD-related Stigma Index	Used; IE	Not used; A	Used; IE
Eight-item Stigma Scale	Not used; U	Not used; A	Not used; A
Arabic Explanatory Model Interview Catalogue (EMIC)	Not used; U	Not used; U	Not used; A
COVID-19 Stigma Instrument-Patients (CSI-P2)	Not used; A	Not used; A	Not used; A
The Perceived Courtesy Stigma Sub-scale	Not used; U	Not used; A	Not used; U
The Affiliate Stigma Sub-scale	Not used; A	Not used; U	Not used; A
Modified 12-item HIV Stigma Scale	Not used; U	Not used; A	Not used; A
Ebola-related Stigma Instrument	Not used; A	Not used; U	Not used; A
Stigma Discrimination Scale (SDS-11)	Not used; U	Not used; A	Used; IE
Self-stigma Scale (SSS-15)	Not used; A	Not used; A	Not used; A
COVID-19 Bullying Scale	Not used; U	Not used; U	Used; IE
COVID-19 Experienced DISCrimination Scale (CEDISC)	Not used; U	Not used; U	Not used; A
Covid-19 Internalised Stigma Scale (COINS)	Not used; U	Not used; U	Not used; A
COVID-19 Responsibility Attribution Scale	Not used; A	Not used; A	Not used; A
COVID-19 Attitudes Scale	Not used; A	Not used; A	Not used; A
SARS Social Life and Services Stigma Self-report Questionnaire	Not used; A	Not used; A	Used; IE
SARS Discrimination in the Workplace Self-report Questionnaire	Not used; A	Not used; A	Used; IE
Stigma toward EVD Survivors Scale	Not used; U	Not used; U	Not used; U
EVD Stigma Index	Not used; U	Not used; U	Not used; A
COVID-19-related Enacted Stigma Questionnaire	Not used; A	Not used; A	Not used; A
Discrimination in Medical Settings Scale	Not used; U	Not used; U	Not used; A
30-item Bullying during the COVID-19 Pandemic Questionnaire	Not used; A	Not used; U	Not used; U
Stigmatising Attitudes Scale	Not used; A	Not used; A	Not used; A
COVID-19 Stigma Scale (COVID19SS)	Not used; A	Not used; U	Not used; U
COVID-19 Perceived Stigma Scale-22 (CPSS-22)	Not used; U	Not used; U	Not used; A
Public Attitudes toward Stigma Questionnaire	Not used; A	Not used; A	Not used; A
Perceived Stigmatization of COVID-19 Scale	Not used; A	Not used; A	Not used; A
Modified Version of the KAP Survey Tool on Zika Virus Disease	Not used; U	Not used; U	Not used; U
Public COVID-19-related Stigma toward Patients Measure	Not used; U	Not used; U	Not used; U
Public COVID-19-related Stigma toward Wuhan People Measure	Not used; A	Not used; A	Not used; U
EVD-related Stigma Scale	Not used; A	Not used; U	Used; IE
COVID-19 Public Stigma Scale	Not used; U	Not used; A	Not used; A
Social Stigma and Discriminatory Attitudes Scale	Not used; U	Not used; U	Not used; A
Long COVID Stigma Scale (LCSS)	Not used; U	Not used; A	Not used; A
Modified Measure of Disease-Related Stigma (MDRS) Scale	Not used; A	Not used; A	Not used; A
Lassa Fever-associated Stigmatization Scale	Not used; U	Not used; A	Not used; U
The Social Stigma Scale	Not used; A	Not used; A	Not used; A
COVID-19 related Social Stigma Scale	Not used; A	Not used; A	Not used; A

*Insufficient evidence (IE) indicates insufficient evidence of cross-cultural equivalence and transferability as assessed using cross-cultural equivalence framework devised by S.A.M. Stevelink and W.H. Van Brakel (*23*) (Appendix Table 1, https://wwwnc.cdc.gov/EID/article/30/3/23-0934-App1.pdf). A, substantial adaptations anticipated for cross-cultural use; U, appears readily usable.
†Usability for persons with and without a personal history of the disease.

Table 5. Recommendations for future outbreak stigma scales determined by a systematic review of scales for measuring infectious disease–related stigma

Area	Recommendations
Design	A theoretical framework of stigma should be applied from conception of the scale to ensure all relevant domains of stigma are represented. Future scales should be co-designed with persons with lived experience of outbreak-associated stigma. Scale items should be informed by qualitative research alongside existing scales. When resources allow, scale design should be informed by a range of outbreak diseases and settings to enhance transferability of the scale. This should be facilitated by large public health institutions. Established best practices for ensuring cross-cultural equivalence (e.g., [*23*]) should be followed when translating and adapting scales for cross-contextual use.
Validation	Scale items should be formally assessed for content validity (including clarity, relevance, and comprehensiveness) by both experts in the field and relevant community members with lived experience of stigma. Confirmation of the structural validity of scales should precede internal consistency testing. Other forms of reliability, including test-retest reliability, should be routinely assessed alongside internal consistency. The cross-cultural validity of scales should be assessed across countries, diseases, and respondent profiles using multi-group factor analyses or Differential Item Functioning analyses. The responsiveness of scales should be assessed to ensure they have the ability to detect changes in stigma over time.
Use	Scales should be used in longitudinal and pre- and post-interventional studies to assess stigma trends over the course of an outbreak, rather than limited to cross-sectional use. When possible, representative sampling techniques should be adopted in administration of stigma scales. The results of studies assessing stigma during outbreaks, as well as the stigma scales used, need to be rapidly publicly disseminated with minimal access barriers such as paywalls.

being incompletely and unreliably measured during outbreaks and that comparison of experience across outbreaks is not possible.

We found that, according to the COSMIN Risk of Bias Checklist (*25*), the quality of scale development and content validation methods were inadequate or doubtful for all studies. Similarly, several other forms of psychometric assessment (e.g., test-retest reliability) were not performed on most scales, which could be because of shortcuts taken in best practices in research methods because of the perceived urgency of an outbreak. However, those shortcuts compromise the validity of study findings. Thus, psychometric validation using best-practice guidelines (*31*,*35*) should be more rigorously applied to stigma scales and routinely reported. Of the scales reviewed, the Perceived Courtesy Stigma Scale and the Affiliate Stigma Scale (*36*) had the most evidence of sufficient validity and reliability, although the content and cross-cultural validity and responsiveness should be assessed during future use of those scales.

In addition, we noted a lack of repeated use of scales across diseases and settings, despite similarity in scale content and derivation from the same HIV-related stigma scales. That finding represents a missed opportunity to maximize scale development efforts, strengthen the evidence base of a scale, and expand understanding of the common impacts of stigma across outbreaks (*11*,*14*,*18*).

The fact that half the scales were derived from HIV scales also raises concerns about scale validity when applied to acute outbreaks. For example, stigma-by-association questions specific to sexual partners or groups at high risk for HIV infection might not be appropriate in other outbreaks. Similarly, questions about avoidance might not account for mandated isolation of affected persons in certain outbreaks, which could explain the misuse of items such as "people should stay away from those infected with COVID-19" and other key preventive measures as markers of stigma in more than one fourth of scales we reviewed. That misuse could be avoided by adopting theoretical frameworks in scale design by using formal content validity scoring processes (*31*) and ensuring that the scales are informed by qualitative data from in-depth or semistructured interviews with end users and other stakeholders (*25*).

Stigma scales tended to capture more advanced forms of stigmatization, such as public discrimination and the internalization of persistent stigma (i.e., self-stigma). Poor detection of the potential precursors of those forms of stigma, such as social, occupational, or provider-based prejudice, were not investigated; however, if identified, those precursors could be targeted before action, thereby reducing the detrimental effects of stigma on outbreak control and patient well-being (*8*).

In addition, the high frequency of stigma-by-association as a theme in the reviewed scales recognizes that noninfected community members are not only potential stigmatizers but might also be stigmatized. Therefore, the current practice, which gives scales about stigma experiences to persons who have had the disease but gives noninfected community members scales asking about endorsement of stigma, is a false dichotomy. Persons can be both a stigmatizer and be stigmatized (*8*). That false dichotomy could be overcome by using items that are distanced (i.e., less personal) from the respondent, such as case vignettes or questions about third-person observations (*37*). Those types of items enable all community members, regardless of disease status, to answer a wider range of questions while reducing social desirability bias. Another option, drawing from the HPTN 071 (PopART) trial (*38*), is to use multiple scales in parallel to separately ask persons with lived experience of the disease, healthcare workers, and other community members about experienced and endorsed stigma.

Of note, the median time from the start of an outbreak to publication of a relevant stigma scale was 2 years. That timeframe can be partially attributed to the traditionally slow peer-reviewed publication process, which is a recognized obstacle to efficient translational science in emerging outbreaks (*39*). However, the delay can also be attributed to the lengthy process involved in stigma scale development and implementation, which often results in outbreak-related stigma being investigated retrospectively, rather than early in an outbreak, when the scale has the greatest potential to inform response interventions and risk communication. The lack of early identification of stigma is also a major omission in the existing research because evidence suggests stigma can be most detrimental early in an outbreak because of heightened isolation (*3*,*10*).

Together, our findings demonstrate that the model of de novo scale development for each outbreak does not work in the context of emerging infectious diseases and leads to small, overlapping, methodologically weak, and slow outcomes, despite the best intentions of developers. As is the case with clinical research on emerging diseases (*39*), overcoming the challenge of stigma scale development requires an innovative approach.

A critical need exists for preemptive development of a methodologically rigorous stigma scale that can be easily adapted for new outbreaks. Such a scale would enable outbreak responders to immediately integrate stigma assessment into surveillance activities at the onset of an outbreak. That measure should be developed or endorsed by international and national public health institutions to ensure adequate funding and reach of the scale, aid in cross-learning, and reduce duplication of efforts.

The feasibility of a standardized scale is supported by the similarities in stigma manifestations across disease and geographic contexts. Those similarities are noted both in this review and in previous stigma literature (*8*,*11*,*14*). A modular approach to the scale, whereby additional context- and disease-specific items can be included as appropriate, could capture stigma specific to distinct outbreak settings.

Within pandemic preparedness in other fields, such as vaccine development and clinical research, efforts to ensure rapid outbreak response includes solving for disease X, a hypothetical, undefined pathogen of potential consequence (*40*). We suggest the preemptive stigma scale development and validation process mirror that process.

To optimize adoption and usefulness, a stigma scale needs to be publicly available and used in longitudinal, preinterventional, and postinterventional studies, rather than restricted to cross-sectional use. In turn, results of those studies need to be effectively disseminated to policymakers, response actors, and affected communities, which could inform the adaptation of response interventions to minimize associated stigma (*8*,*10*).

The limitations of this systematic review include that the screening strategy relied on inclusion of stigma or a similar term in the title or abstract. Therefore, studies that used a stigma scale but did not report it in their abstract might have been missed. Second, because the review was not limited to scales in the English language, the local meaning and relevance of some of the items might have been distorted with translation. Finally, this review did not include healthcare worker–specific scales, which might more frequently include occupational- and provider-related stigma items. Nonetheless, this review included an extensive search of the literature, without language or date restrictions, and provides a meaningful summary of the uses, validity, and transferability of existing outbreak stigma scales.

In conclusion, rapid and methodologically sound assessment of stigma is a critical and urgently needed aspect of outbreak response. This review demonstrates a range of readily implementable improvements that could be made to outbreak stigma scale design and use (Table 5). The data and recommendations we provide can be used to design valid and versatile stigma scales for ongoing and future outbreaks.

Acknowledgment

We thank Nia Roberts for her assistance in developing the search strategy for the review.

About the Author

Dr. Paterson is a clinician-researcher and a PhD candidate at the University of Oxford. Her research interests focus on the stigma due to infectious disease outbreaks.

References

1. Cénat JM, Rousseau C, Bukaka J, Dalexis RD, Guerrier M. Severe anxiety and PTSD symptoms among Ebola virus disease survivors and healthcare workers in the context of the COVID-19 pandemic in Eastern DR Congo. Front Psychiatry. 2022;13:767656. https://doi.org/10.3389/fpsyt.2022.767656
2. Gregorio ER Jr, Medina JRC, Lomboy MFTC, Talaga ADP, Hernandez PMR, Kodama M, et al. Knowledge, attitudes, and practices of public secondary school teachers on Zika virus disease: a basis for the development of evidence-based Zika educational materials for schools in the Philippines. PLoS One. 2019;14:e0214515. https://doi.org/10.1371/journal.pone.0214515
3. Lee S, Chan LY, Chau AM, Kwok KP, Kleinman A. The experience of SARS-related stigma at Amoy Gardens. Soc Sci Med. 2005;61:2038–46. https://doi.org/10.1016/j.socscimed.2005.04.010
4. Usifoh SF, Odigie AE, Ighedosa SU, Uwagie-Ero EA, Aighewi IT. Lassa fever-associated stigmatization among staff and students of the University of Benin, Nigeria. J Epidemiol Glob Health. 2019;9:107–15. https://doi.org/10.2991/jegh.k.190514.001
5. Goffman E. Stigma: notes on the management of spoiled identity. New York: J. Aronson; 1974.
6. Jones N, Corrigan PW. Understanding stigma. In: Corrigan PW, editor. The stigma of disease and disability. Understanding causes and overcoming injustices. Washington: American Psychological Association; 2014. p. 9–34.
7. Weiss MG. Stigma and the social burden of neglected tropical diseases. PLoS Negl Trop Dis. 2008;2:e237. https://doi.org/10.1371/journal.pntd.0000237
8. Stangl AL, Earnshaw VA, Logie CH, van Brakel W, Simbayi LC, Barré I, et al. The health stigma and discrimination framework: a global, crosscutting framework to inform research, intervention development, and policy on health-related stigmas. BMC Med. 2019;17:31. https://doi.org/10.1186/s12916-019-1271-3
9. Major B, Dovidio JF, Link BG, Calabrese SK. Stigma and its implications for health: introduction and overview. In: Major B, Dovidio JF, Link BG, editors. The Oxford handbook of stigma, discrimination, and health. New York: Oxford University Press; 2018. p. 3–28.
10. Trinh DH, McKinn S, Nguyen AT, Fox GJ, Nguyen AT, Bernays S. Uneven stigma loads: community interpretations of public health policies, 'evidence' and inequities in shaping Covid-19 stigma in Vietnam. SSM Popul Health. 2022;20:101270. https://doi.org/10.1016/j.ssmph.2022.101270
11. Van Brakel WH. Measuring health-related stigma—a literature review. Psychol Health Med. 2006;11:307–34. https://doi.org/10.1080/13548500600595160
12. Cénat JM, Noorishad PG, Kokou-Kpolou CK, Dalexis RD, Hajizadeh S, Guerrier M, et al. Prevalence and correlates of depression during the COVID-19 pandemic and the major role of stigmatization in low- and middle-income countries: a multinational cross-sectional study. Psychiatry Res. 2021;297:113714. https://doi.org/10.1016/j.psychres.2021.113714
13. Cénat JM, Noorishad PG, Dalexis RD, Rousseau C, Derivois D, Kokou-Kpolou CK, et al. Prevalence and risk factors of depression symptoms among rural and urban populations affected by Ebola virus disease in the Democratic Republic of the Congo: a representative cross-sectional study. BMJ Open. 2022;12:e053375. https://doi.org/10.1136/bmjopen-2021-053375
14. Nyblade L, Stockton MA, Giger K, Bond V, Ekstrand ML, Lean RM, et al. Stigma in health facilities: why it matters and how we can change it. BMC Med. 2019;17:25. https://doi.org/10.1186/s12916-019-1256-2
15. Rajkumar E, Rajan AM, Daniel M, Lakshmi R, John R, George AJ, et al. The psychological impact of quarantine due to COVID-19: a systematic review of risk, protective factors and interventions using socio-ecological model framework. Heliyon. 2022;8:e09765. https://doi.org/10.1016/j.heliyon.2022.e09765
16. Li L, Wang J, Leng A, Nicholas S, Maitland E, Liu R. Will COVID-19 vaccinations end discrimination against COVID-19 patients in China? New evidence on recovered COVID-19 patients. Vaccines (Basel). 2021;9:490. https://doi.org/10.3390/vaccines9050490
17. Mazzagatti R, Riva MA. Monkeypox vaccine–related stigma. Public Health Pract (Oxf). 2022;4:100336. https://doi.org/10.1016/j.puhip.2022.100336
18. Logie CH. What can we learn from HIV, COVID-19 and mpox stigma to guide stigma-informed pandemic preparedness? J Int AIDS Soc. 2022;25:e26042. https://doi.org/10.1002/jia2.26042
19. Kwon S. Mask wearing and perceived discrimination associated with COVID-19 in the United States from March 2020 to May 2021: three-level longitudinal analyses. Health Educ Behav. 2022;49:200–9. https://doi.org/10.1177/10901981221076396
20. Page MJ, McKenzie JE, Bossuyt PM, Boutron I, Hoffmann TC, Mulrow CD, et al. The PRISMA 2020 statement: an updated guideline for reporting systematic reviews. BMJ. 2021;372:n71. https://doi.org/10.1136/bmj.n71
21. Prinsen CAC, Mokkink LB, Bouter LM, Alonso J, Patrick DL, de Vet HCW, et al. COSMIN guideline for systematic reviews of patient-reported outcome measures. Qual Life Res. 2018;27:1147–57. https://doi.org/10.1007/s11136-018-1798-3
22. Cicchetti DV, Sparrow SA. Developing criteria for establishing interrater reliability of specific items: applications to assessment of adaptive behavior. Am J Ment Defic. 1981;86:127–37.
23. Stevelink SAM, van Brakel WH. The cross-cultural equivalence of participation instruments: a systematic review. Disabil Rehabil. 2013;35:1256–68. https://doi.org/10.3109/09638288.2012.731132
24. Carroll C, Booth A, Leaviss J, Rick J. "Best fit" framework synthesis: refining the method. BMC Med Res Methodol. 2013;13:37. https://doi.org/10.1186/1471-2288-13-37
25. Mokkink LB, de Vet HCW, Prinsen CAC, Patrick DL, Alonso J, Bouter LM, et al. COSMIN risk of bias checklist for systematic reviews of patient-reported outcome measures. Qual Life Res. 2018;27:1171–9. https://doi.org/10.1007/s11136-017-1765-4
26. Pantelic M, Ziauddeen N, Boyes M, O'Hara ME, Hastie C, Alwan NA. Long Covid stigma: estimating burden and validating scale in a UK-based sample. PLoS One. 2022;17:e0277317. https://doi.org/10.1371/journal.pone.0277317
27. Pescosolido BA, Martin JK. The stigma complex. Annu Rev Sociol. 2015;41:87–116. https://doi.org/10.1146/annurev-soc-071312-145702
28. Alchawa M, Naja S, Ali K, Kehyayan V, Haddad PM, Bougmiza I. COVID-19 perceived stigma among survivors: a cross-sectional study of prevalence and predictors. Eur J Psychiatry. 2023;37:24–35. https://doi.org/10.1016/j.ejpsy.2022.08.004
29. Mlouki I, Zammit N, Ghammem R, Ben Fredj S, Bannour R, El Echi A, et al. Validity and reliability of a modified short

version of a stigma scale for use among Tunisian COVID-19 patients after quarantine: a cross-sectional study. Health Sci Rep. 2022;5:e520. https://doi.org/10.1002/hsr2.520
30. Nair S, Joshi A, Aggarwal S, Adhikari T, Mahajan N, Diwan V, et al. Development & validation of scales to assess stigma related to COVID-19 in India. Indian J Med Res. 2022;155:156–64. https://doi.org/10.4103/ijmr.ijmr_2455_21
31. Boateng GO, Neilands TB, Frongillo EA, Melgar-Quiñonez HR, Young SL. Best practices for developing and validating scales for health, social, and behavioral research: a primer. Front Public Health. 2018;6:149. https://doi.org/10.3389/fpubh.2018.00149
32. Dar SA, Khurshid SQ, Wani ZA, Khanam A, Haq I, Shah NN, et al. Stigma in coronavirus disease-19 survivors in Kashmir, India: a cross-sectional exploratory study. PLoS One. 2020;15:e0240152. https://doi.org/10.1371/journal.pone.0240152
33. Kibria MG, Islam T, Islam MT, Kabir R, Ahmed S, Sultana P. Stigma and its associated factors among patients with COVID-19 in Dhaka City: evidence from a cross-sectional investigation. PeerJ. 2022;10:e14092. https://doi.org/10.7717/peerj.14092
34. Overholt L, Wohl DA, Fischer WA II, Westreich D, Tozay S, Reeves E, et al. Stigma and Ebola survivorship in Liberia: results from a longitudinal cohort study. PLoS One. 2018;13:e0206595. https://doi.org/10.1371/journal.pone.0206595
35. Mokkink LB, Prinsen CA, Patrick DL, Alonso J, Bouter LM, de Vet HCW, et al. COSMIN study design checklist for patient-reported outcome measurement instruments 2019 [cited 2023 Nov 3] https://www.cosmin.nl/wp-content/uploads/COSMIN-study-designing-checklist_final.pdf
36. Li T, Bu H, Duan W. A brief measure of perceived courtesy and affiliate stigma on COVID-19: a study with a sample from China. Pers Individ Dif. 2021;180:110993. https://doi.org/10.1016/j.paid.2021.110993
37. Al-Zamel LA, Al-Thunayan SF, Al-Rasheed AA, Alkathiri MA, Alamri F, Alqahtani F, et al. Validation and cultural adaptation of Explanatory Model Interview Catalogue (EMIC) in assessing stigma among recovered patients with COVID-19 in Saudi Arabia. Int J Environ Res Public Health. 2021;18:8261. https://doi.org/10.3390/ijerph18168261
38. Stangl AL, Lilleston P, Mathema H, Pliakas T, Krishnaratne S, Sievwright K, et al.; HPTN 071 (PopART) Study Team. Development of parallel measures to assess HIV stigma and discrimination among people living with HIV, community members and health workers in the HPTN 071 (PopART) trial in Zambia and South Africa. J Int AIDS Soc. 2019;22:e25421. https://doi.org/10.1002/jia2.25421
39. Sigfrid L, Maskell K, Bannister PG, Ismail SA, Collinson S, Regmi S, et al. Addressing challenges for clinical research responses to emerging epidemics and pandemics: a scoping review. BMC Med. 2020;18:190. https://doi.org/10.1186/s12916-020-01624-8
40. World Health Organization. Prioritizing diseases for research and development in emergency contexts [cited 2023 Nov 3]. https://www.who.int/activities/prioritizing-diseases-for-research-and-development-in-emergency-contexts

Address for correspondence: Amy Paterson, Pandemic Sciences Institute, New Richards Building, Old Road Campus, Roosevelt Dr, Headington, Oxford OX3 7DQ, UK; email: amy.paterson@ndm.ox.ac.uk

Wastewater Surveillance for Identifying SARS-CoV-2 Infections in Long-Term Care Facilities, Kentucky, USA, 2021–2022

James W. Keck,[1] Reuben Adatorwovor, Matthew Liversedge,[2] Blazan Mijotavich, Cullen Olsson, William D. Strike, Atena Amirsoleimani, Ann Noble, Soroosh Torabi, Alexus Rockward, Mohammad Dehghan Banadaki, Ted Smith, Parker Lacy, Scott M. Berry

Persons living in long-term care facilities (LTCFs) were disproportionately affected by COVID-19. We used wastewater surveillance to detect SARS-CoV-2 infection in this setting by collecting and testing 24-hour composite wastewater samples 2–4 times weekly at 6 LTCFs in Kentucky, USA, during March 2021–February 2022. The LTCFs routinely tested staff and symptomatic and exposed residents for SARS-CoV-2 using rapid antigen tests. Of 780 wastewater samples analyzed, 22% (n = 173) had detectable SARS-CoV-2 RNA. The LTCFs reported 161 positive (of 16,905) SARS-CoV-2 clinical tests. The wastewater SARS-CoV-2 signal showed variable correlation with clinical test data; we observed the strongest correlations in the LTCFs with the most positive clinical tests (n = 45 and n = 58). Wastewater surveillance was 48% sensitive and 80% specific in identifying SARS-CoV-2 infections found on clinical testing, which was limited by frequency, coverage, and rapid antigen test performance.

Persons living in long-term care facilities (LTCFs) have experienced disproportionate illnesses and deaths from the COVID-19 pandemic. By June 2020, >50,000 COVID-19 deaths had occurred in LTCF residents in the United States, an estimated 43% of all US COVID-19 deaths in a group comprising <1% of the US population (*1*). Nearly 2 years later, the COVID-19 pandemic continues to cause disproportionate illnesses and deaths in this vulnerable population and is responsible for >200,000 LTCF resident deaths in the United States (*2*).

Early detection of SARS-CoV-2 infection in LTCF staff or residents is an important strategy to mitigate SARS-CoV-2 transmission. Routine symptom screening of LTCF employees and residents was the primary strategy to detect infections early in the pandemic. However, symptom screening misses persons with presymptomatic or asymptomatic SARS-CoV-2 infection (*3*) and performs similarly to the flip of a coin for identifying persons with SARS-CoV-2 infection (*4*). Clinical testing, which was heavily constrained early in the pandemic, became the preferred screening approach as testing capacity increased in 2020. Federal and state guidance encouraged routine clinical testing of unvaccinated asymptomatic LTCF staff with the frequency determined by the level of community transmission (*5*). However, routine clinical testing of large numbers of asymptomatic persons is expensive, invasive, and inefficient and may be inaccurate depending on the type of clinical test used.

Wastewater surveillance provides an alternative strategy for SARS-CoV-2 detection by evaluating samples of wastewater for the presence of viral biomarkers like RNA (*6*). Persons infected with SARS-CoV-2 shed virus in their feces (*7*); early in the pandemic, scientists reported detecting the virus in the wastewater of urban areas (*8*,*9*). Many municipalities

Author affiliations: University of Kentucky, Lexington, Kentucky, USA (J.W. Keck, R. Adatorwovor, M. Liversedge, C. Olsson, W.D. Strike, A. Amirsoleimani, A. Noble, S. Torabi, A. Rockward, M. Dehghan Banadaki, S.M. Berry); University of Louisville, Louisville, Kentucky, USA (T. Smith); Trilogy Health Services, LLC, Louisville (P. Lacy)

DOI: http://doi.org/10.3201/eid3003.230888

[1]Current affiliation: WWAMI School of Medical Education, University of Alaska Anchorage, Anchorage, Alaska, USA.

[2]Current affiliation: College of Medicine, University of Cincinnati, Cincinnati, Ohio, USA.

across the United States surveilled wastewater at treatment plants for SARS-CoV-2, while universities tested wastewater at the building level; researchers used the collected data to trigger enhanced clinical testing that led to identifying persons with previously unknown SARS-CoV-2 infections (*10*,*11*). We implemented wastewater surveillance to detect SARS-CoV-2 infection at LTCFs and assessed its performance using routine clinical testing data.

Methods

Study Population and Site Selection

We collaborated with a LTCF organization that manages >100 LTCFs across the upper Midwest of the United States. We identified LTCF study sites on the basis of their proximity to our research laboratory in Lexington, Kentucky; their sewer system design allowing for facility-specific sampling; and presence of SARS-CoV-2 infections. We selected 3 LTCFs in Lexington and 3 LTCFs in Louisville, Kentucky; each facility served 67–160 residents and had 76–117 staff. The University of Kentucky Institutional Review Board approved this study (IRB no. 62384).

Wastewater Collection

We collected 24-hour composite LTCF effluent wastewater samples 2–3 times/week at Louisville sites and 3–4 times/week at Lexington sites. We initiated wastewater sampling in both cities on March 19, 2021, and concluded wastewater collection on December 17, 2021, at the Louisville sites and on February 18, 2022, at the Lexington sites. We installed Teledyne ISCO GLS composite autosamplers (https://www.teledyneisco.com/water-and-wastewater/gls-compact) with 12V batteries in effluent sewer pipes via the manhole access closest to the LTCF. The autosamplers collected 100 mL of wastewater effluent every 20 minutes for 24 hours. Ice packed around the autosampler collection jug cooled the wastewater to a target temperature <4°C to minimize degradation of nucleic acids. After a 24-hour cycle of composite sampling, we transported 250 mL of the composite wastewater sample on ice to the laboratory for analysis and disposed of the remaining sample in the sewer.

Before initiating wastewater surveillance at one LTCF, we flushed RNA encoding for jellyfish-derived enhanced green fluorescent protein (eGFP) into a toilet and collected 5-minute fractionated wastewater samples to measure the durability of the RNA signal in the wastewater effluent. We used real-time PCR to measure eGFP RNA in the fractionated wastewater samples. We detected eGFP in the initial wastewater fraction collected 3 minutes after flushing and in most of the wastewater fractions (11/16) over the 2-hour collection window; those findings supported the use of a 20-minute sampling cadence.

Quantification of SARS-CoV-2 in Wastewater

We extracted RNA from wastewater samples on the same day as sample collection. To address the heterogeneous distribution of biologic material in wastewater, we analyzed 8 replicates of 250 µL from each wastewater sample. We used exclusion-based sample preparation (ESP) to extract nucleic acids from the wastewater replicates. We previously published a detailed description of this method for analysis of SARS-CoV-2 RNA in wastewater (*12*). In brief, we lysed samples and added paramagnetic particles (PMPs) (SeraSil-Mag; Cytiva, https://www.cytivalifesciences.com). We vortexed the samples, heated them at 50°C for 20 minutes, and then tumbled them for 20 minutes. We loaded these samples into an ESP device (Extractman; Gilson, Inc., https://www.gilson.com) with wash buffers and processed the replicates as previously described. We heated the purified PMP-RNA complexes for 20 minutes at 70°C to elute the RNA. We tracked RNA extraction efficiency using negative wastewater samples spiked with known concentrations of whole SARS-CoV-2 virus (BEI Resources, https://www.beiresources.org).

We amplified and quantified ESP-purified RNA via real-time quantitative PCR using the CDC-recommended SARS-CoV-2 N1 gene primer and probe sequences (*13*). We used positive and negative controls with each PCR plate for quality assurance of the PCR process. For the positive control, we added SARS-CoV-2 RNA (BEI Resources) to the reaction. We calculated wastewater SARS-CoV-2 concentrations on the basis of quantification cycle (Cq) values and the Roche LightCycler 2nd derivative maximum algorithm (https://diagnostics.roche.com). We translated Cq values into SARS-CoV-2 genomic concentrations using a standard curve ($r^2 = 0.985$) constructed from serial dilutions of the BEI positive-control RNA. We reported wastewater SARS-CoV-2 values as the arithmetic average of 8 aliquots (or the number of aliquots with valid results) from a given sample in units of genome copies per milliliter of wastewater (gc/mL).

Clinical Testing

Clinical testing of LTCF staff and residents for SARS-CoV-2 occurred in accordance with LTCF policy and

Table 1. Characteristics of clinical and wastewater testing for SARS-CoV-2 at 6 long-term care facilities, Kentucky, USA, 2021–2022*

Site	Person	Population†	Total no. clinical tests (% RAT†)	SARS-CoV-2 positive, no. (%)	WW surveillance duration, d	WW samples	WW SARS-CoV-2 detection, no. (%)
A	Resident	75	558 (94.8)	3 (0.5)	338	160	32 (20.0)
	Staff	89	1,607 (92.8)	24 (1.5)			
B	Resident	65	525 (94.3)	14 (2.7)	338	160	42 (26.3)
	Staff	85	1,475 (87.1)	31 (2.1)			
C	Resident	95	2,736 (99.4)	17 (0.6)	338	160	43 (26.9)
	Staff	117	3,808 (95.4)	41 (1.1)			
D	Resident	160	730 (98.9)	6 (0.8)	274	102	18 (17.6)
	Staff	106	1,965 (93.6)	12 (0.6)			
E	Resident	91	625 (96.8)	1 (0.2)	274	100	18 (18.0)
	Staff	98	1,951 (93.6)	7 (0.4)			
F	Resident	67	94 (43.6)	1 (1.1)	274	98	20 (20.4)
	Staff	76	831 (85.9)	4 (0.5)			
All	Resident	553	5,268 (97.0)	42 (0.8)	274–338	780	173 (22.2)
	Staff	571	11,637 (92.7)	119 (1.0)			
	All	1,124	16,905 (94.0)	161 (1.0)			

*RAT, rapid antigen test; WW, wastewater.
†Population at time of study conclusion.

at the discretion of individual staff choosing to test outside the workplace. We received deidentified positive and negative clinical test results from staff and residents during the study period from the 6 facilities with wastewater testing. The LTCF organization used antigen-based point of care SARS-CoV-2 tests (Binax Now; Abbott, https://www.abbott.com) for routine staff screening. Employees who sought SARS-CoV-2 testing outside of their employer's testing program were required to report their test results to the LTCF organization.

Testing frequency of staff and residents followed federal and state guidance (https://chfs.ky.gov/cv19/LTCFSurveillanceTestingFAQs.pdf). In accordance with that guidance, LTCF-based clinical testing happened routinely for unvaccinated staff working onsite, for symptomatic residents and employees, and for all residents and staff after a positive test result in a resident or staff member at the facility. Frequency of testing asymptomatic unvaccinated staff depended on the level of SARS-CoV-2 transmission in the county in which the facility was located and varied from 2 times/week (high transmission) to weekly (substantial transmission) to monthly (moderate/low transmission) according to a color-coded map (https://chfs.ky.gov/agencies/os/oig/dhc/Pages/cvltc.aspx) based on CDC transmission risk criteria (https://covid.cdc.gov/covid-data-tracker/#county-view).

Data Analysis

We provide a descriptive summary of the wastewater RNA concentrations and clinical test data using counts, proportions, means, medians, and SDs. When a person had 2 consecutive SARS-CoV-2 positive clinical test results within 21 days of each other, we excluded the second test result from the final analytic dataset because it likely represented the same SARS-CoV-2 infection. We defined a cluster of cases when >1 LTCF resident from the same facility tested positive for SARS-CoV-2 within 14 days. To evaluate whether wastewater testing identified SARS-CoV-2 in LTCFs earlier than routine clinical screening, we conducted a lead/lag time correlational analysis. We estimated the correlation between the wastewater RNA concentration and the number of identified positive clinical SARS-CoV-2 infections at each LTCF and offset clinical testing data by 1–7 days before and after the wastewater data collection date.

We estimated the SARS-CoV-2 wastewater contribution per known clinical case by dividing wastewater concentrations by the number of clinical cases to obtain an average wastewater viral concentration per clinical case. We used weekly averaged wastewater SARS-CoV-2 concentrations and total weekly clinical cases for this calculation to moderate differences in sampling and testing frequency between facilities. We excluded weeks when there were no clinical cases because this would result in dividing by 0.

We estimated the concentration of SARS-CoV-2 RNA in wastewater corresponding to ≥1 clinically confirmed case at an LTCF by fitting a negative binomial regression model to the weekly average number of positive clinical tests (Appendix, https://wwwnc.cdc.gov/EID/article/30/3/23-0888-App1.pdf). During the model fitting procedure, we used the log-link function and the total number of LTCF residents as the exposure variable. We used the incidence density ratios for positive SARS-CoV-2 test results for each LTCF to estimate the incidence rate or probability

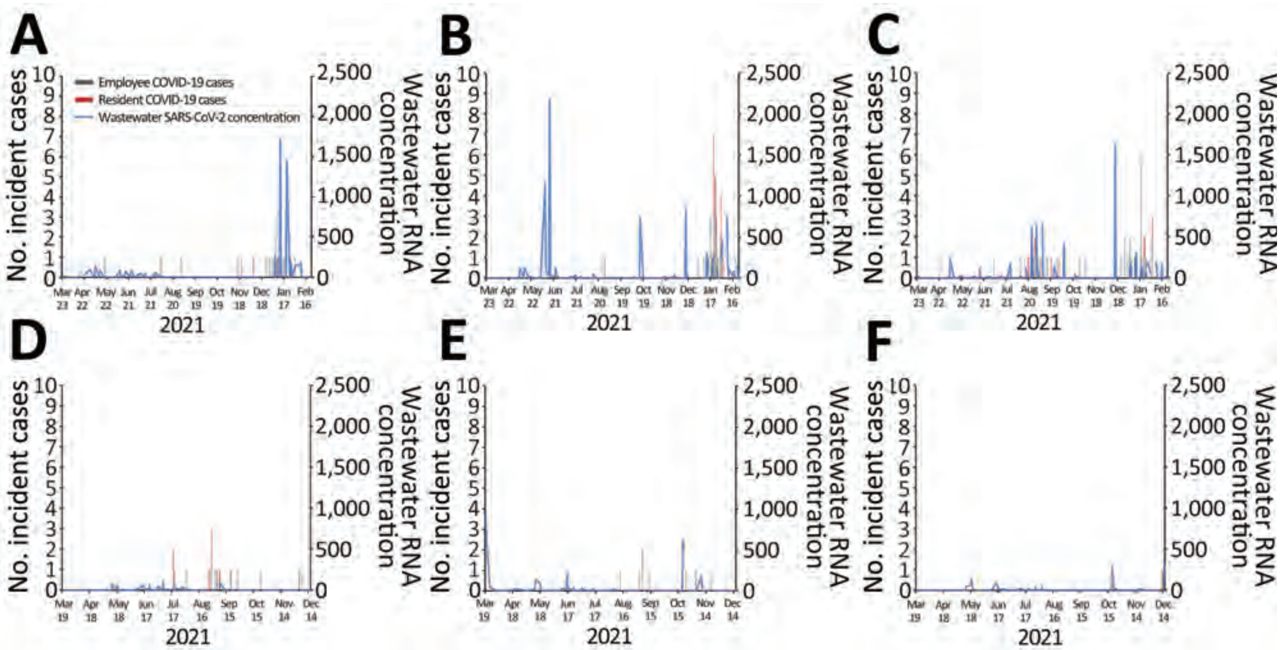

Figure 1. Wastewater SARS-CoV-2 concentrations (genome copies/mL; blue line) and incident cases of positive clinical SARS-CoV-2 tests (red bars for residents, gray bars for staff) from 6 long-term care facilities (A–F), Kentucky, USA, March 2021–February 2022.

of identifying a clinical case in an LTCF during the surveillance period based on the wastewater signal. We assumed that SARS-CoV-2 RNA detected in the wastewater during the surveillance day correlated with symptomatic or asymptomatic persons infected and shedding SARS-CoV-2 virus into the wastewater. We used weekly RNA wastewater averages because of the limited number of wastewater samples collected during the week.

Last, we evaluated the sensitivity and specificity of wastewater surveillance for detecting SARS-CoV-2 infections identified through clinical testing. We categorized wastewater samples categorized as either positive or negative using various SARS-CoV-2 RNA concentration threshold values (0–250 gc/mL). In our analysis, we defined clinical test positivity as a positive clinical test result observed during the 1-week window after each wastewater measurement at that facility. We constructed 2 × 2 contingency tables to allocate positive and negative wastewater and clinical testing results and calculated the sensitivity and specificity of wastewater testing at each wastewater SARS-CoV-2 RNA concentration threshold. The primary analysis used SARS-CoV-2 infections identified in staff and residents; a secondary analysis used only resident case data because staff may not defecate at work and they isolated at home following a positive test. We used SAS version 9.4 (SAS Institute Inc., https://www.sas.com) for the statistical analyses.

Results

During March 19, 2021–February 18, 2022, we collected and analyzed 780 composite wastewater

Table 2. SARS-CoV-2 case clusters and associated wastewater signal characteristics at 4 long-term care facilities, Kentucky, USA, 2021–2022*

Characteristic	Facility B	Facility C	Facility C	Facility D
Case cluster				
No. residents infected	14	10	7	4
Duration, d	15	47	24	13
Wastewater signal				
Period since previous positive signal, d	6	5	6	23
Magnitude of previous signal, genome copies/mL	250.7	29.8	177.9	6.8
Signal on day of initial positive clinical test, genome copies/mL	208.1	NA	53.5	NA
Time from initial case to positive signal, d	0	2	0	12
Signal range, genome copies/mL	0–467	0–663	0–687	0–39
Fraction of samples with SARS-CoV-2 detected	6/8	12/26	8/13	1/4

*Case clusters were defined as >1 resident testing positive for SARS-CoV-2 within 14 d at the same facility. Two clusters occurred at the same facility at different time points. NA, not applicable because no wastewater sample collected that day.

samples from the 6 LTCFs (98–160 samples per facility (Table 1). An additional 31 wastewater samples were collected but not processed due to reagent shortages (n = 21), processing delays following winter storms (n = 9), or contamination during laboratory extraction (n = 1). We identified

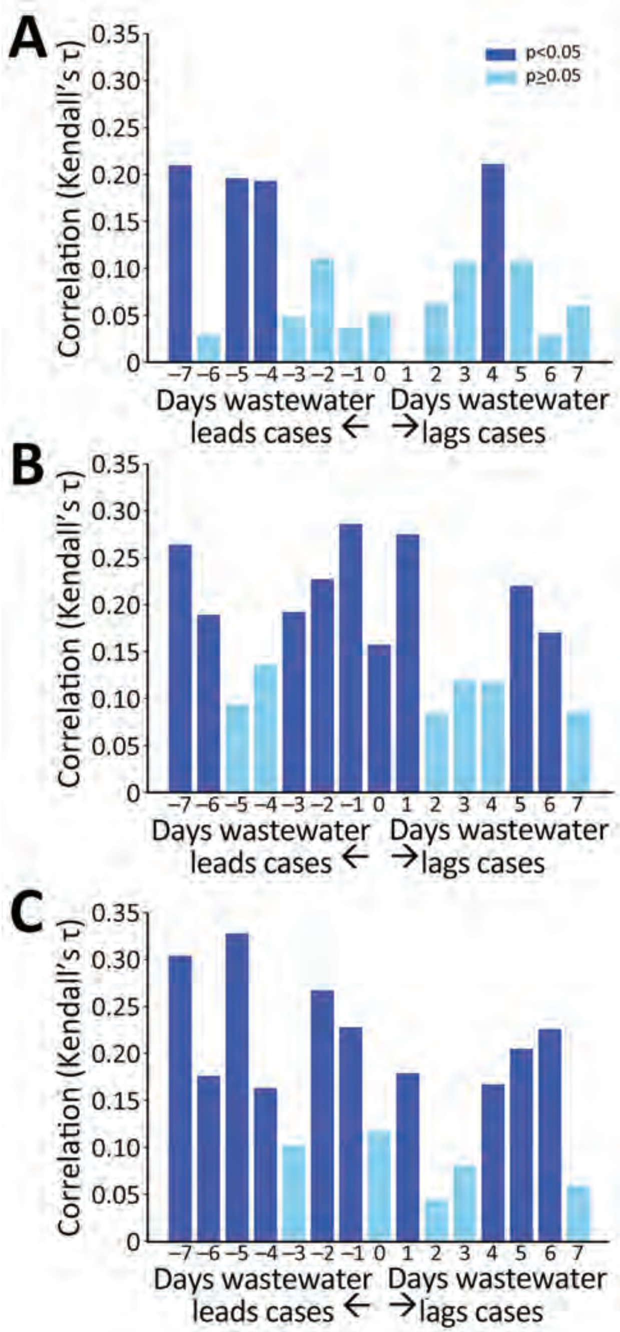

Figure 2. Time shifted (−7 to +7 days) correlation between wastewater SARS-CoV-2 signal and positive SARS-CoV-2 clinical tests at 3 long-term care facilities with >20 positive clinical tests (facility A = 27, facility B = 58, and facility C = 45), Kentucky, USA, March 2021–February 2022.

SARS-CoV-2 RNA in 18%–27% of wastewater samples at each facility at levels of 0–1,726 gc/mL. The SARS-CoV-2 wastewater signal varied over time and across facilities (Figure 1); positivity was greater during December 2022–January 2023, which also was when most of the positive SARS-CoV-2 clinical tests were reported from facilities A–C that had ongoing wastewater surveillance.

During the wastewater surveillance period, the LTCF organization reported the results of 16,905 COVID-19 tests from residents (n = 5,268) and staff (n = 11,637) at the 6 facilities (Table 1). Residents had 42 (0.8%) positive tests and staff had 119 (1.0%) positive tests. In 4 instances, >1 LTCF resident from the same facility tested positive for SARS-CoV-2 within 14 days, which we designated as a cluster of cases. Clusters included 4–14 residents and lasted 13–47 days. Wastewater positivity varied in these clusters; 25%–75% of samples had measurable SARS-CoV-2 RNA (Table 2).

The wastewater signal had a statistically significant correlation with clinical testing results. Facilities with <20 positive clinical tests showed poor correlation with the wastewater signal. However, at the 3 facilities with >20 known cases, we observed significant correlations across time shifts of the wastewater data from 7 days before to 6 days after clinical test dates (Figure 2). The strongest correlations occurred with the wastewater signal shifted 1–6 days before the clinical test dates.

On average, each identified clinical case corresponded to a wastewater concentration of 26.9 gc/mL. Using a log-linear incidence density model, we estimated the wastewater concentration associated with a probability of ≥0.5 clinically confirmed cases to 206–743 gc/mL (Figure 3); the estimate at the 3 facilities with the largest number of clinically confirmed cases was 206–336 gc/mL.

A positive wastewater SARS-CoV-2 signal (>0 gc/mL) was 30.6% (95% CI 24.4%–36.9%) sensitive and 79.7% (95% CI 76.4%–82.9%) specific in identifying a positive clinical test result when we included test data from staff and residents (Figure 4). Wastewater sensitivity improved to 48.0% (95% CI 36.5%–59.4%) and specificity to 79.9% (95% CI 77.0%–82.9%) when we considered only clinical test data from residents. Higher wastewater signal thresholds resulted in lower sensitivity and higher specificity. A wastewater signal threshold of 30 gc/mL resulted in a sensitivity of 39.7% (95% CI 28.5%–51.0%) and specificity of 92% (95% CI 89.5%–93.6%) for identifying a LTCF resident with a positive SARS-CoV-2 test.

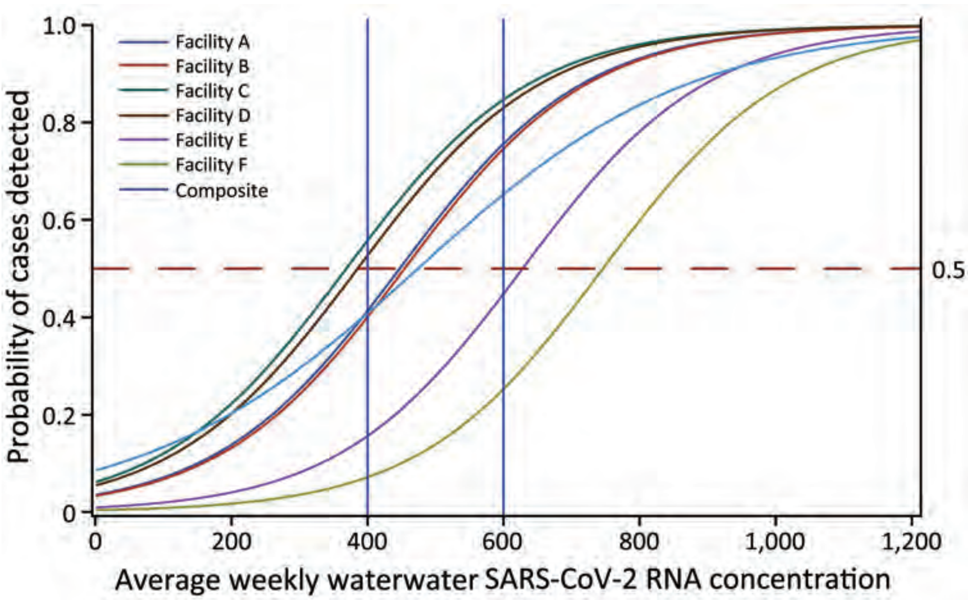

Figure 3. The probability of a positive SARS-CoV-2 clinical test by long-term care facility as a function of the average weekly wastewater SARS-CoV-2 concentration (genome copies/mL) at that facility, Kentucky, USA, March 2021–February 2022. Facility-specific curves are A–F; the final curve is a composite curve that uses data from all 6 facilities. Vertical blue lines at 400 and 600 gc/mL serve as reference points to identify site-specific wastewater signal thresholds when the probably of detecting a SARS-CoV-2 case is >0.5.

Discussion

We collected and analyzed >700 wastewater samples for SARS-CoV-2 from 6 LTCFs during the second year of the COVID-19 pandemic. By pairing the wastewater data with clinical testing results from staff and residents at the 6 facilities, we evaluated the performance of wastewater surveillance for detecting clinical SARS-CoV-2 cases in this vulnerable population. Wastewater surveillance demonstrated statistically significant correlations with clinical test results, and the estimated correlation was stronger when considering the wastewater signal as leading clinical case identification; those findings suggest its potential as an early warning indicator of infection in a facility. Wastewater surveillance performance in discriminating the presence of a positive clinical SARS-CoV-2 test varied depending on the wastewater signal threshold selected and it demonstrated better specificity than sensitivity.

Several factors affected the performance of LTCF wastewater surveillance and challenged the interpretation of the wastewater data. The population that contributed to the wastewater at an LTCF was dynamic and difficult to track. Residents were admitted and discharged, staff turnover was frequent, staff worked across multiple facilities, residents were visited by family members and friends, and visitors passed through the facilities. The frequency with which staff, visitors, and residents contributed waste to the LTCF sewer system was not known. In addition, the sewer access at facility B was where the facility's effluent sewage joined the sewage from an adjacent apartment complex. Facility B wastewater samples may have inadvertently included wastewater from persons living in or visiting the apartment complex, which is the likely reason for the high SARS-CoV-2 RNA concentrations measured in June 2021 in the absence of identified SARS-CoV-2 infections at the facility (*14*).

Negative wastewater samples observed at facilities with known SARS-CoV-2–infected residents could be attributed to residents wearing adult briefs secondary to fecal incontinence. For example, during a cluster of 10 resident SARS-CoV-2 infections over 13 weeks (Table 2), 3 of the residents were completely incontinent and wore adult briefs. The feces from those residents were disposed in biomedical waste receptacles rather than in the sewer system. Three other residents were partially incontinent. Feces from those residents also may not have entered the sewer system. Diversion of LTCF resident waste may reduce the sensitivity of wastewater surveillance in this setting.

Another likely cause of a negative wastewater signal in the presence of known infections is the variability with which SARS-CoV-2–infected persons shed virus in their feces. Studies done early in the pandemic detected virus in stool samples of 29%–59% of persons with COVID-19 (*15*–*17*). The patients in those studies were hospitalized and presumably infected with nonvariant SARS-CoV-2 virus. Shedding frequency may differ in persons with milder or asymptomatic illness, of different ages, or infected with SARS-CoV-2 variants. In addition, it is unknown how vaccination status and previous SARS-CoV-2 infection affect fecal shedding. Viral shedding frequency, intensity, and duration may have outsized effects on building-level wastewater surveillance because of the small numbers of persons contributing to the wastewater.

To optimize our ability to detect SARS-CoV-2 in LTCF wastewater, we collected 24-hour composite samples using a 20-minute sampling cadence. As described in the Methods section, the results of our spiking experiment suggested that a 20-minute sampling cadence would capture RNA associated with a bowel movement flushed into the sewer system at an LTCF. Our sample collection schedule meant that we obtained wastewater samples from 37% of days in Louisville and 47% of days in Lexington during our surveillance period. Because an infected person shedding virus is likely to do so for many days, a sampling frequency of 3–4 days per week should detect the case-patients who shed virus into a facility's wastewater system if they remain onsite during the duration of their illness.

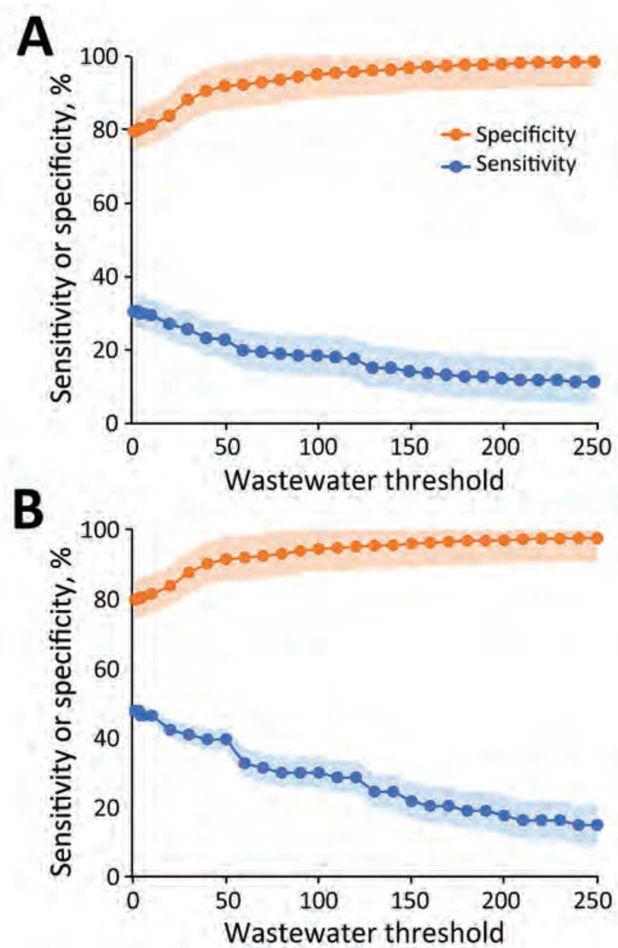

Figure 4. Sensitivity and specificity of SARS-CoV-2 wastewater surveillance for identifying positive SARS-CoV-2 clinical tests as a function of the wastewater SARS-CoV-2 signal strength in 6 long-term care facilities, Kentucky, USA, March 2021–February 2022. A) Staff and residents; B) residents only. Shaded areas indicate 95% CIs.

Two additional properties of the wastewater samples may have affected our results. First, there were likely inhibitors (i.e., factors that degrade RNA, reduce PCR efficiency, or both) in the wastewater of the LTFCs because of laundry, kitchen, and janitorial activities. Detergents decreased the detectable signal of extracted RNA by ≈100-fold in 1 study (*18*), and detergents used by LTCF staff may have degraded RNA in the sewer system. We did not assess for the presence of specific inhibiting compounds and do not know how substantial their burden and effects were on our laboratory analyses. Second, wastewater is a highly heterogeneous matrix, and although we made reasonable efforts to homogenize wastewater samples (collecting composite samples, mixing composite sample before aliquoting sample for laboratory analysis, mixing laboratory sample before aliquoting for replicate analysis), variation in RT-PCR results across the 8 replicates from each composite sample suggests a heterogeneous distribution of SARS-CoV-2 virus within wastewater. Strike et al. demonstrated that our laboratory method combined with 8 replicates reliably detected SARS-CoV-2 RNA concentrations down to 100 gc/mL, and lower concentrations were observed after averaging zero and nonzero datapoints (*12*). In our study, many samples contained a mixture of positive and negative replicates. In those cases, positive replicates were averaged together with negative measurements (e.g., 0 gc/mL), often yielding average values <100 gc/mL.

We evaluated the performance of wastewater surveillance against the results of intermittent and incomplete clinical testing of LTCF staff and residents. Our LTCF partner implemented clinical testing strategies that aligned with state and federal COVID-19 guidance, which yielded pragmatic clinical testing data. Two limitations of the clinical testing protocols may have affected data quality and completeness. First, asymptomatic LTCF residents were not routinely tested; testing occurred when the resident had a known or suspected contact with a case-patient, such as a facility staff member who had tested positive. Similarly, vaccinated staff were not routinely screened. Untested but infected asymptomatic residents or vaccinated staff or a visitor to the facility may have caused a positive wastewater signal that was interpreted as a false positive, given the absence of known cases at the facility. This scenario would decrease the estimated specificity of wastewater surveillance. The second limitation was the LTCF organization's use of rapid antigen-based SARS-CoV-2 tests for screening staff and residents. The poor sensitivity of antigen-based tests, particularly in asymptomatic persons (58% by a Cochrane meta-analysis [*19*]), likely resulted in some false-negative clinical screening tests, which would decrease the estimated specificity of wastewater surveillance.

Our study adds to the sparse literature on SARS-CoV-2 wastewater surveillance at LTCFs. A team in Italy surveilled wastewater from 5 LTCFs for several months at the end of 2020 and intermittently detected SARS-CoV-2 RNA in the wastewater of 4 of the facilities (*20*). As in our study, the presence of residents with identified COVID-19 infection only intermittently resulted in a positive wastewater signal. Researchers in Spain consistently detected SARS-CoV-2 in the wastewater effluent from an elderly residence when there were known clinical cases in the building; however, the number of known cases in a week was typically >10 (*21*). An alternative environmental surveillance approach in Canada using analysis of floor swab samples for SARS-CoV-2 demonstrated good discriminatory ability to identify COVID-19 outbreaks LTCFs (*22*).

In summary, we found that wastewater surveillance for SARS-CoV-2 performed moderately well when compared with clinical testing. Our correlational analysis indicated that a SARS-CoV-2 wastewater signal may precede the identification of clinical cases at LTCFs, which suggests that such testing could provide an early warning to trigger enhanced clinical testing or infection prevention activities, such as physical distancing. Optimizing wastewater collection and analysis methods may improve surveillance performance; however, viral and contextual factors such as fecal shedding rates, PCR inhibitors in the LTCF wastewater, and use of adult briefs likely limit wastewater surveillance performance in this setting. Improved understanding of the many potential contributors to wastewater signal variability will enhance the interpretation of this emerging surveillance strategy, which can augment traditional infection detection and prevention activities in vulnerable LTCF populations.

This work was funded by the Centers for Disease Control and Prevention (contract BAA 75D301-20-R-68024).

S.B. has an ownership interest in Salus Discovery, LLC, which has licensed the ESP technology described in the text.

About the Author

Dr. Keck was faculty in the department of family and community medicine at the University of Kentucky during this study and is now based in Alaska at the Alaska Native Tribal Health Consortium and University of Alaska Anchorage. His primary research interest is environmental disease surveillance, to protect the health of vulnerable, remote, and rural communities.

References

1. Kamp J, Mathews AW. As U.S. nursing-home deaths reach 50,000, states ease lockdowns. The Wall Street Journal. 2020 Jun 16 [cited 2022 May 3]. https://www.wsj.com/articles/coronavirus-deaths-in-u-s-nursing-long-term-care-facilities-top-50-000-11592306919
2. Chidambaram P. Over 200,000 residents and staff in long-term care facilities have died from COVID-19. Kaiser Family Foundation; 2022 Feb 3 [cited 2022 May 3]. https://www.kff.org/policy-watch/over-200000-residents-and-staff-in-long-term-care-facilities-have-died-from-covid-19
3. Arons MM, Hatfield KM, Reddy SC, Kimball A, James A, Jacobs JR, et al.; Public Health–Seattle and King County and CDC COVID-19 Investigation Team. Presymptomatic SARS-CoV-2 infections and transmission in a skilled nursing facility. N Engl J Med. 2020;382:2081–90. https://doi.org/10.1056/NEJMoa2008457
4. Keck JW, Bush M, Razick R, Mohammadie S, Musalia J, Hamm J. Performance of formal smell testing and symptom screening for identifying SARS-CoV-2 infection. PLoS One. 2022;17:e0266912. https://doi.org/10.1371/journal.pone.0266912
5. Centers for Disease Control and Prevention. Interim infection prevention and control recommendations for healthcare personnel during the coronavirus disease 2019 (COVID-19) pandemic. 2019 [cited 2022 Oct 9]. https://www.cdc.gov/coronavirus/2019-ncov/hcp/infection-control-recommendations.html
6. Orive G, Lertxundi U, Barcelo D. Early SARS-CoV-2 outbreak detection by sewage-based epidemiology. Sci Total Environ. 2020;732:139298. https://doi.org/10.1016/j.scitotenv.2020.139298
7. Chen Y, Chen L, Deng Q, Zhang G, Wu K, Ni L, et al. The presence of SARS-CoV-2 RNA in the feces of COVID-19 patients. J Med Virol. 2020;92:833–40. https://doi.org/10.1002/jmv.25825
8. Wurtzer S, Marechal V, Mouchel JM, Maday Y, Teyssou R, Richard E, et al. Evaluation of lockdown effect on SARS-CoV-2 dynamics through viral genome quantification in waste water, Greater Paris, France, 5 March to 23 April 2020. Euro Surveill. 2020;25:2000776. https://doi.org/10.2807/1560-7917.ES.2020.25.50.2000776
9. Ahmed W, Angel N, Edson J, Bibby K, Bivins A, O'Brien JW, et al. First confirmed detection of SARS-CoV-2 in untreated wastewater in Australia: a proof of concept for the wastewater surveillance of COVID-19 in the community. Sci Total Environ. 2020;728:138764. https://doi.org/10.1016/j.scitotenv.2020.138764
10. Betancourt WQ, Schmitz BW, Innes GK, Prasek SM, Pogreba Brown KM, Stark ER, et al. COVID-19 containment on a college campus via wastewater-based epidemiology, targeted clinical testing and an intervention. Sci Total

Environ. 2021;779:146408. https://doi.org/10.1016/j.scitotenv.2021.146408
11. Harris-Lovett S, Nelson KL, Beamer P, Bischel HN, Bivins A, Bruder A, et al. Wastewater surveillance for SARS-CoV-2 on college campuses: initial efforts, lessons learned and research needs. Int J Environ Res Public Health. 2021;18:4455. https://doi.org/10.3390/ijerph18094455
12. Strike W, Amirsoleimani A, Olaleye A, Noble A, Lewis K, Faulkner L, et al. Development and validation of a simplified method for analysis of SARS-CoV-2 RNA in university dormitories. ACS ES T Water. 2022;2:1984–91. https://doi.org/10.1021/acsestwater.2c00044
13. Centers for Disease Control and Prevention. CDC's influenza SARS-CoV-2 multiplex assay. [cited 2020 Sep 6]. https://archive.cdc.gov/www_cdc_gov/coronavirus/2019-ncov/lab/multiplex.html
14. Keck JW, Lindner J, Liversedge M, Mijatovic B, Olsson C, Strike W, et al. Wastewater surveillance for SARS-CoV-2 at long-term care facilities: mixed methods evaluation. JMIR Public Health Surveill. 2023;9:e44657. https://doi.org/10.2196/44657
15. Wu Y, Guo C, Tang L, Hong Z, Zhou J, Dong X, et al. Prolonged presence of SARS-CoV-2 viral RNA in faecal samples. Lancet Gastroenterol Hepatol. 2020;5:434–5. https://doi.org/10.1016/S2468-1253(20)30083-2
16. Zheng S, Fan J, Yu F, Feng B, Lou B, Zou Q, et al. Viral load dynamics and disease severity in patients infected with SARS-CoV-2 in Zhejiang province, China, January–March 2020: retrospective cohort study. BMJ. 2020;369:m1443. https://doi.org/10.1136/bmj.m1443
17. Wang W, Xu Y, Gao R, Lu R, Han K, Wu G, et al. Detection of SARS-CoV-2 in different types of clinical specimens. JAMA. 2020;323:1843–4. https://doi.org/10.1001/jama.2020.3786
18. Robinson CA, Hsieh HY, Hsu SY, Wang Y, Salcedo BT, Belenchia A, et al. Defining biological and biophysical properties of SARS-CoV-2 genetic material in wastewater. Sci Total Environ. 2022;807:150786. https://doi.org/10.1016/j.scitotenv.2021.150786
19. Dinnes J, Deeks JJ, Berhane S, Taylor M, Adriano A, Davenport C, et al.; Cochrane COVID-19 Diagnostic Test Accuracy Group. Rapid, point-of-care antigen and molecular-based tests for diagnosis of SARS-CoV-2 infection. Cochrane Database Syst Rev. 2021;3:CD013705. https://doi.org/10.1002/14651858.CD013705.pub2
20. Davó L, Seguí R, Botija P, Beltrán MJ, Albert E, Torres I, et al. Early detection of SARS-CoV-2 infection cases or outbreaks at nursing homes by targeted wastewater tracking. Clin Microbiol Infect. 2021;27:1061–3. https://doi.org/10.1016/j.cmi.2021.02.003
21. Pico-Tomàs A, Mejías-Molina C, Zammit I, Rusiñol M, Bofill-Mas S, Borrego CM, et al. Surveillance of SARS-CoV-2 in sewage from buildings housing residents with different vulnerability levels. Sci Total Environ. 2023;872:162116. https://doi.org/10.1016/j.scitotenv.2023.162116
22. Fralick M, Nott C, Moggridge J, Castellani L, Raudanskis R, Guttman DS, et al. Detection of COVID-19 outbreaks using built environment testing for SARS-CoV-2. NEJM Evid. 2023;2. https://doi.org/10.1056/EVIDoa2200203

Address for correspondence: James W. Keck, WWAMI School of Medical Education, University of Alaska Anchorage, 3900 Ambassador Dr, Ste 201, Anchorage, AK 99508, USA; email: jwkeck@alaska.edu

Estimates of Incidence and Predictors of Fatiguing Illness after SARS-CoV-2 Infection

Quan M. Vu, Annette L. Fitzpatrick, Jennifer R. Cope, Jeanne Bertolli, Nona Sotoodehnia, T. Eoin West, Nikki Gentile, Elizabeth R. Unger

This study aimed to estimate the incidence rates of post–COVID-19 fatigue and chronic fatigue and to quantify the additional incident fatigue caused by COVID-19. We analyzed electronic health records data of 4,589 patients with confirmed COVID-19 during February 2020–February 2021 who were followed for a median of 11.4 (interquartile range 7.8–15.5) months and compared them to data from 9,022 propensity score–matched non–COVID-19 controls. Among COVID-19 patients (15% hospitalized for acute COVID-19), the incidence rate of fatigue was 10.2/100 person-years and the rate of chronic fatigue was 1.8/100 person-years. Compared with non–COVID-19 controls, the hazard ratios were 1.68 (95% CI 1.48–1.92) for fatigue and 4.32 (95% CI 2.90–6.43) for chronic fatigue. The observed association between COVID-19 and the significant increase in the incidence of fatigue and chronic fatigue reinforces the need for public health actions to prevent SARS-CoV-2 infections.

According to the Household Pulse Survey conducted by the US Centers for Disease Control and Prevention in January 2023, up to 15% of all US adults had experienced ≥1 symptoms of post–COVID-19 conditions (PCC), also known as long COVID or postacute sequelae of SARS-CoV-2 infection (PASC) (*1*). Among persons with PCC, fatigue is frequently reported in both hospitalized and nonhospitalized patients (*2*,*3*). A recent prospective cohort study reported 85% of patients who met its PASC definition had fatigue (*4*). A substantial percentage of patients with fatigue remain ill for many months with an illness similar to myalgic encephalomyelitis/chronic fatigue syndrome (ME/CFS) (*5*), an unexplained syndrome sometimes seen after infections that is characterized by functional limitations that impair patients' ability to maintain daily activities and is associated with profound fatigue (*6*).

The burden, distribution, and trend of PCC can theoretically be measured by using prevalence and incidence. The prevalence of PCC is a useful measure of overall disease burden at a specific time but is dependent on recovery, deaths, and incidence. The incidence of PCC measures the rate of new cases over a certain period and can be valuable for informing public health actions to reduce new illnesses. Numerous studies have estimated PCC prevalence, but very few have attempted to estimate PCC incidence because the incidence estimate requires information on timing of incident event and a well-defined population at risk that does not include prevalent cases (*7*). Both requirements are challenging in the context of PCC because they consist of a range of conditions and symptoms, most of which are not specific to PCC. To date, no diagnostic biomarkers are available, and recognition of PCC requires integrating medical history and clinical findings. Recent studies also emphasize the importance of an equivalent, concurrent, non–COVID-19 comparison group so that the effects of COVID-19 will not be overestimated (*8*). Given the central role of fatigue in PCC and the lack of data on incidence of fatigue among patients who have had COVID-19, we conducted a study of incident fatigue diagnoses among patients with and without COVID-19. Our objectives were to estimate the incidence rates of fatigue and chronic fatigue; quantify the additional incident fatigue caused by COVID-19; assess factors associated with incident fatigue; and describe deaths and hospitalizations among patients with incident fatigue after SARS-CoV-2 infection.

Author affiliations: Centers for Disease Control and Prevention, Atlanta, Georgia, USA (Q.M. Vu, J.R. Cope, J. Bertolli, E.R. Unger); University of Washington, Seattle, Washington, USA (A.L. Fitzpatrick, N. Sotoodehnia, T.E. West, N. Gentile)

DOI: https://doi.org/10.3201/eid3003.231194

Methods

This study was designed as a retrospective cohort analysis. We analyzed electronic health records (EHR) data collected from the University of Washington (UW) that included 3 hospitals (Harborview Medical Center, UW Medical Center Northwest, and UW Medical Center Montlake) and >300 primary care and specialty clinics providing healthcare services across the state of Washington, USA.

Case and Control Classification

COVID-19 patients consisted of adults (≥18 years of age) having either a positive PCR test result for SARS-CoV-2 or a clinical diagnosis of COVID-19 during February 2020–February 2021 (*9*). A clinical diagnosis of COVID-19 was defined by an International Classification of Diseases, 10th Revision, Clinical Modification (ICD-10-CM), diagnostic code of B97.29, other coronavirus as the cause of diseases classified elsewhere; or U07.1, COVID-19, recorded in the EHR during February 2020–February 2021 (*10*). The index date was defined as the date of the first positive PCR result or the first clinical diagnosis, whichever was earlier.

Non–COVID-19 control patients were defined as adults who did not belong to the COVID-19 group and had ≥1 negative PCR for SARS-CoV-2 during February 2020–February 2021. The first negative test date is referred to as the index date. We excluded from this group persons with suspected COVID-19 or evidence of past COVID-19, including persons with any of the following ICD-10-CM codes: B34.2, coronavirus infection, unspecified; J12.82, pneumonia due to COVID-19; Z86.16, personal history of COVID-19; U09.9, post COVID-19 condition. We also excluded persons with a positive result on SARS-CoV-2 IgG.

Inclusion and Exclusion Criteria

Patients in both COVID-19 case and non–COVID-19 control groups were required to survive the first 30 days from index date; access care ≥1 time on or after the day 30 from the index date, defined by having a diagnosis code or a laboratory test; access care ≥1 time during the 18 months before the index date for evaluation of preexisting fatigue diagnoses; and not be diagnosed with any codes used to define fatigue during the 18 months before the index date. During February 2020–February 2021, a total of 11,503 unique patients received a COVID-19 diagnosis. A total of 4,608 COVID-19 patients were eligible for matching (Figure 1).

We extracted data from 15,834 non–COVID-19 patients by querying the study database using the previously described inclusion and exclusion criteria, as well as the same requirements for accessing care. After data cleaning, 15,485 non–COVID-19 patients were determined to be eligible for matching.

Propensity Score Matching

We used propensity score matching to achieve balance in selected characteristics for COVID-19 and non–COVID-19 groups (*11*). We estimated propensity score using logistic regression with 22 input variables of age, sex, race, ethnicity, and whether the person had comorbidities derived from the Charlson Comorbidity Index (CCI) during the 18-month period before the index date (Table 1) (*12*). We then matched patients on the logit of propensity score using the greedy method with a caliper of 0.2 SD of the logit of the score.

Among 4,608 patients with COVID-19 who were eligible for matching, 19 (0.4%) had no matched controls. Among 4,589 patients with COVID-19 who had ≥1 match with 9,022 non–COVID-19 controls, 4,433 patients (96.6%) had 2 matched controls and 156 (3.4%) had 1. After matching, the standardized differences for 22 input variables used for estimating propensity score and for the index date were all <0.1, indicating between-group balances in these variables (*13*).

Outcome Measures

Outcome events of interest were patients with ≥1 diagnostic codes for fatigue or chronic fatigue recorded in the EHR during the postacute period. The postacute period was defined as the time between the 30th day since the index date and the last follow-up date up to January 2022.

Fatigue was defined by any of the following ICD-10-CM or International Classification of Diseases, 9th Revision, Clinical Modification (ICD-9-CM), diagnostic codes recorded in EHR during the postacute period: G93.3, postviral fatigue syndrome; R53.82, chronic fatigue, unspecified; R53.83, other fatigue; 780.71, chronic fatigue syndrome/postviral fatigue syndrome; or 780.79, malaise and fatigue. We defined incident fatigue as a patient who had ≥1 diagnostic code for fatigue during the postacute period.

In this study, chronic fatigue is a subset of fatigue, defined as having any of the following 3 ICD-10-CM or ICD-9-CM codes recorded in the EHR during the postacute period: G93.3, postviral fatigue syndrome; R53.82, chronic fatigue, unspecified; and 780.71, chronic fatigue syndrome/postviral fatigue syndrome. We defined incident chronic fatigue as a patient who had ≥1 diagnostic code for chronic fatigue during the postacute period.

Follow-Up Time and Censoring

The last follow-up date was defined as the death date or the last date of having a clinical diagnosis or laboratory test up to January 2022. The follow-up time was calculated as time from the index date to the date of the first incident event for patients with an event, or as time from the index date to the last follow-up date for those without an event (right censoring).

Statistical Methods

We estimated incidence rates of fatigue and chronic fatigue for COVID-19 case and non–COVID-19 control groups using frequencies of events during the follow-up time, assuming a Poisson distribution of events. To quantify the attribution of COVID-19 to fatigue and chronic fatigue diagnoses, we used proportional hazards models that employed robust variance estimators to adjust for dependences associated with matching (*14*).

To examine potential predictors of incident fatigue among 4,589 patients with COVID-19, we used the Clinical Classifications Software Refined to aggregate diseases and conditions diagnosed within 18 months before COVID-19 into clinically meaningful categories (*15*). We analyzed data for categories with prevalence ≥1% and used the log-rank test to compare survival functions for each of the categories. We used multivariable proportional hazards models to identify factors associated with incident fatigue, adjusting for age, sex, and total number of comorbidities derived from the CCI (*12*,*16*). To assess the assumption of proportional hazards, we generated time-dependent covariates as a function of the predictors and follow-up time then evaluated the covariates in the model. We used proportions and crude relative risk (RR) to compare proportions of deaths and hospitalizations among patients with COVID-19 with fatigue versus those without fatigue. We performed all analyses using SAS 9.4 (SAS Institute, Inc., https://www.sas.com).

Human Subjects Considerations

This analysis is part of Project RELIEF (Research on COVID-19 Long-Term Effects). This activity was reviewed by the Centers for Disease Control and Prevention and was conducted consistent with applicable federal law and center policy. All protocols, procedures, and consent processes used in Project RELIEF were reviewed and approved by the University of Washington Institutional Review Board Committee A (STUDY00014595).

Results

Patients

The study population had a mean age of 49.5 years for cases and 49.0 years for controls (Table 1). Approximately half of the patients were women. The most common comorbidities were diabetes and chronic obstructive pulmonary disease, each with 14% prevalence. Approximately 55% of the population had no comorbidities, and 6% had 4–10 comorbidities derived from the CCI.

Fatigue

During the total of 4,241.9 person-years of follow-up of 4,589 COVID-19 cases (median 11.4 months, range 1–21.4 months), 434 (9.5%) incident fatigue cases were identified, resulting in an incidence rate of 10.2/100 person-years. Of the 434 case-patients, 241 (55.5%) were women, the mean age was 52.6 (SD 17.3) years, and 165 (38.0%) patients did not have comorbidities.

The incidence rate of fatigue diagnosis was higher among women than among men and increased with advancing age (Table 2). We noted no strong

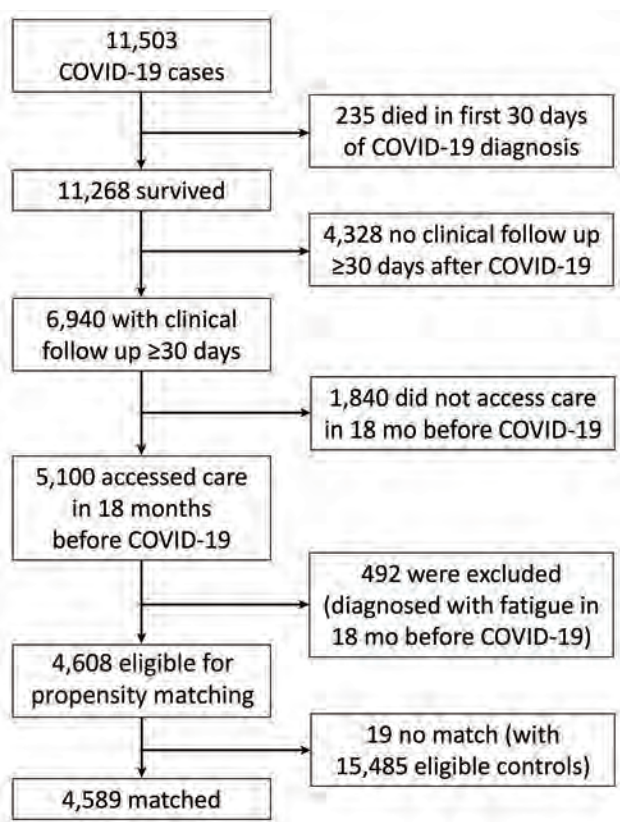

Figure 1. Data flow for COVID-19 cases in study of incidence and predictors of fatiguing illness after SARS-CoV-2 infection, Washington, USA, February 2020–February 2021.

Table 1. Characteristics of patients with COVID-19 and matched controls in study of incidence and predictors of fatiguing illness after SARS-CoV-2 infection, Washington, USA, February 2020–February 2021*

Description	Patients, n = 4,589	Controls, n = 9,022
Age, y, mean (SD)	49.5 (17.8)	49.0 (18.0)
Sex		
F	2,248 (49.0)	4,447 (49.3)
M	2,341 (51.0)	4,575 (50.7)
Race		
Asian	418 (9.1)	807 (8.9)
Black	704 (15.3)	1136 (12.6)
Indian/Alaska native	97 (2.1)	153 (1.7)
Native Hawaiian Pacific	82 (1.8)	119 (1.3)
White	2,942 (64.1)	5,825 (64.6)
Missing	346 (7.5)	982 (10.9)
Ethnicity		
Hispanic/Latino	613 (13.4)	1,166 (12.9)
Not Hispanic/Latino	3,709 (80.8)	7,033 (78.0)
Missing	267 (5.8)	823 (9.1)
Underlying conditions†		
Acute myocardial infarction	90 (2.0)	147 (1.6)
History of myocardial infarction	97 (2.1)	149 (1.7)
Congestive heart failure	289 (6.3)	490 (5.4)
Peripheral vascular disease	257 (5.6)	451 (5.0)
Cerebrovascular disease	231 (5.0)	410 (4.5)
COPD	667 (14.5)	1,259 (14.0)
Dementia	73 (1.6)	122 (1.4)
Hemiplegia or paraplegia	99 (2.2)	178 (2.0)
Diabetes	678 (14.8)	1,262 (14.0)
Diabetes with complications	354 (7.7)	635 (7.0)
Moderate–severe renal disease	400 (8.7)	715 (7.9)
Mild liver disease	318 (6.9)	559 (6.2)
Moderate–severe liver disease	46 (1.0)	81 (0.9)
Peptic ulcer disease	43 (0.9)	71 (0.8)
Rheumatologic disease	81 (1.8)	128 (1.4)
HIV/AIDS	129 (2.8)	218 (2.4)
Any malignancy, except skin	382 (8.3)	677 (7.5)
Metastatic solid tumor	111 (2.4)	193 (2.1)

*Values are no. (%) except as indicated. Race includes no information on Hispanic ethnicity. COPD, chronic obstructive pulmonary disease.
†Diagnosed in the 18 mo before date of COVID-19 confirmation or date of negative test.

evidence of a racial or ethnic difference in incidence of fatigue, except a slightly lower incidence among Black patients. Persons with more comorbidities experienced higher incidence rates than did persons without comorbidities. However, even among younger persons (18–29 years of age), those without comorbidities, and those who were not hospitalized for acute COVID-19, the incidence of fatigue was only slightly reduced (7.3/100 person-years for younger persons, 7.4/100 person-years for persons without comorbidities, and 9.9/100 person-years for persons who were not hospitalized).

During the total of 7,939.1 person-years of follow-up of 9,022 non–COVID-19 controls (median 11.5 months, range 1–21.5 months), we identified 477 incident fatigue cases, resulting in an incidence rate of 6.0/100 person-years. The risk of incident fatigue was 68% higher among COVID-19 cases than among non–COVID-19 controls (hazard ratio 1.68, 95% CI 1.48–1.92; p<0.001) (Figure 2, panel A).

Chronic Fatigue

We next examined the incidence of chronic fatigue diagnosis, a subset of fatigue. During follow-up, 81 COVID-19 patients received a diagnosis of incident chronic fatigue, resulting in an incidence rate of 1.82 (95% CI 1.47–2.27)/100 person-years. The incidence rate of chronic fatigue among non–COVID-19 controls was 0.42 (95% CI 0.29–0.58)/100 person-years. The risk of developing chronic fatigue was significantly higher for COVID-19 cases compared with non–COVID-19 controls (HR 4.32, 95% CI 2.90–6.43; p<0.001). The difference between cumulative incidence for COVID-19 patients and non–COVID-19 controls continued to increase without apparent plateau >12 months after the index date (Figure 2, panel B).

Predictors of Incident Fatigue

Women were 39% more likely to have a fatigue diagnosis than men were after adjusting for age group and comorbidities (Table 2). Persons of advancing age groups were more likely than young adults 18–29 years of age to have a fatigue diagnosis in an unadjusted model. After adjusting for sex and comorbidities, the HRs for advancing age groups were still elevated, but the differences were no longer statistically significant. Those with comorbidities were significantly more likely to have incident fatigue compared with those with no comorbidities.

Among 36 diseases and conditions diagnosed in the 18 months before COVID-19 with a prevalence ≥1% that show difference in incident fatigue (log-rank p<0.05), 21 conditions remained associated (p<0.05) with incident fatigue when each was included in a multivariable proportional hazards model that adjusted for age, sex, and number of comorbidities. Obesity was associated with incident fatigue in the simple model, but the association became nonsignificant in the adjusted model. The risk for incident fatigue that was significantly higher for other diseases and conditions (Table 3) ranged from 27% increased risk for persons with hypertension to 93% increased risk for persons with gastritis and duodenitis.

Deaths and Hospitalizations

Patients with COVID-19 in whom incident fatigue developed had far worse clinical outcomes, as evidenced by deaths and hospitalizations, than patients without fatigue (Figure 3). Among 434 COVID-19 patients in whom fatigue developed, 111 (25.6%) were hospitalized ≥1 times during the postacute period, whereas

13.6% of 4,155 patients without incident fatigue were hospitalized (RR 1.88, 95% CI 1.57–2.24; p<0.001). Moreover, COVID-19 patients with incident fatigue were at higher risk of dying (23/434, 5.3%) during the postacute period than were COVID-19 patients without incident fatigue (94/4,155 [2.3%]; RR 2.34, 95% CI 1.50–3.66; p<0.001).

Discussion

In this community-based cohort study of >4,500 adults followed for an average of 11.4 months after COVID-19 infection, fatigue developed in 9%. Even among persons not hospitalized for acute COVID-19 or those without comorbidities, the incidence of post–COVID-19 fatigue approached 10% per year. COVID-19 patients had 1.68 times the risk for fatigue in the follow-up period compared with concurrent, matched non–COVID-19 controls. The risk for chronic fatigue was even more marked: patients with COVID-19 had 4.32 times the risk for chronic fatigue than did controls.

This study provides new estimates of the incidence rate of fatigue using person-years of follow-up of at-risk patients after COVID-19 infection. Our data can be put in the context of previous reports. A retrospective study of EHR data reported 12.8% of patients had received a diagnosis of incident fatigue within 6 months of COVID-19 infection (*17*). That report had a different follow-up time and did not describe whether preexisting fatigue cases were excluded from the incident fatigue counts, which might explain their higher proportion than our estimate of 9.5%. In another retrospective study of insurance claims where preexisting fatigue diagnoses were excluded from the incident event count, 4.6% of COVID-19 patients received a diagnosis of fatigue during the follow-up of ≤6 months (*18*). That proportion approaches our estimate of 5% cumulative incidence of fatigue for 6 months.

An incidence rate of 4.2/100 person-years for post–COVID-19 fatigue was reported from Germany (*19*). That study counted cases occurring from 3 months after infection, which potentially contributed to lower event counts. Of note, follow-up times for patients with an incident event were assigned on the basis of the calendar quarter of the insurance claim submission, and the follow-up times for patients without events were not described. A combination of those methodological differences might have contributed to the lower incidence estimate in that study.

Table 2. Incidence rate of fatigue among patients with COVID-19 in study of incidence and predictors of fatiguing illness after SARS-CoV-2 infection, by selected characteristics, Washington, USA, February 2020–February 2021*

Description	No. (%) patients	Incidence rate/100 person-years		Proportional hazards model	
		Estimate (95% CI)	p value	HR (95% CI)	aHR (95% CI)
All patients	4,589 (100.0)	10.2 (9.3–11.2)			
Sex					
F	2,248 (49.0)	11.6 (10.2–13.1)	<0.01	1.29 (1.07–1.56)	1.39 (1.15–1.69)
M	2,341 (51.0)	9.0 (7.8–10.3)	Referent	Referent	Referent
Age group, years					
18–29	771 (16.8)	7.3 (5.5–9.7)	Referent	Referent	Referent
30–59	2,344 (51.1)	10.3 (9–11.7)	0.03	1.39 (1.02–1.90)	1.23 (0.90–1.69)
≥60	1,474 (32.1)	11.6 (9.9–13.5)	<0.01	1.56 (1.13–2.14)	1.21 (0.86–1.69)
Race					
Asian	418 (9.1)	11.1 (8.2–15)	0.93	1.02 (0.74–1.41)	
Black	704 (15.3)	7.8 (5.9–10.2)	0.03	0.71 (0.53–0.96)	
American Indian/Alaska Native	97 (2.1)	15.4 (9.1–25.9)	0.21	1.41 (0.83–2.41)	
Native Hawaiian/Pacific Islander	82 (1.8)	6.3 (2.6–15)	0.22	0.56 (0.23–1.37)	
White	2,942 (64.1)	10.9 (9.8–12.2)	Referent	Referent	
Missing	346 (7.5)	7.5 (4.9–11.4)	0.09	0.69 (0.45–1.06)	
Ethnicity					
Hispanic/Latino	613 (13.4)	11.2 (8.8–14.4)	0.54	1.09 (0.83–1.42)	
Not Hispanic/Latino	3,709 (80.8)	10.3 (9.3–11.5)	Referent	Referent	
Missing	267 (5.8)	6.2 (3.7–10.5)	0.06	0.61 (0.36–1.04)	
Hospitalized first 30 d					
Yes	689 (15.0)	12.1 (9.6–15.2)	0.13	1.22 (0.95–1.57)	
No	3,900 (85.0)	9.9 (9.0–11.0)	Referent	Referent	
No. underlying conditions†					
0	2,511 (54.7)	7.4 (6.3–8.6)	Referent	Referent	Referent
1–3	1,780 (38.8)	12.9 (11.3–14.7)	<0.01	1.73 (1.42–2.12)	1.73 (1.40–2.13)
4–10	298 (6.5)	16.4 (12.3–21.9)	<0.01	2.21 (1.59–3.06)	2.30 (1.63–3.24)

*Blank cells in aHR column indicate variables not included in multivariable model. aHR, adjusted HR, obtained from multivariable proportional hazards model; HR, hazard ratio, obtained from simple proportional hazards model.
†Any of the following conditions diagnosed within 18 mo before COVID-19: acute myocardial infarction, history of myocardial infarction, congestive heart failure, peripheral vascular disease, cerebrovascular disease, chronic obstructive pulmonary disease, dementia, hemiplegia or paraplegia, diabetes, diabetes with complications, moderate–severe renal disease, mild liver disease, moderate–severe liver disease, peptic ulcer disease, rheumatologic disease, HIV/AIDS, any malignancy except skin, metastatic solid tumor.

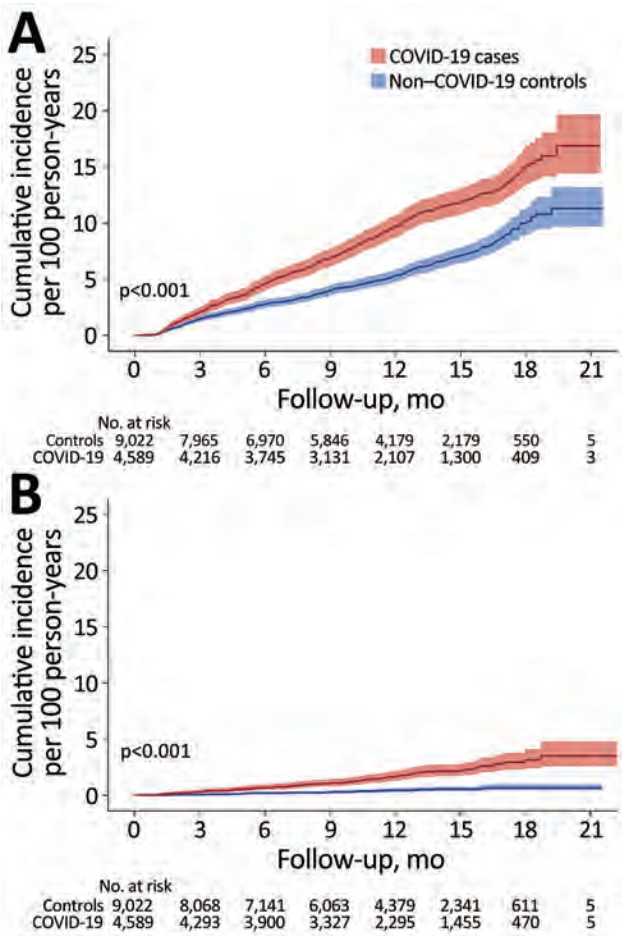

Figure 2. Cumulative incidence of fatigue (A) and chronic fatigue (B) among 4,589 COVID-19 cases and 9,022 non–COVID-19 controls in study of fatiguing illness after SARS-CoV-2 infection, Washington, USA, February 2020–February 2021. Shading around data lines indicates 95% CIs.

The excess risk for fatigue attributable to COVID-19 estimated in our study is in range of previous estimates. Specifically, our hazard ratio for fatigue of 1.68 (95% CI 1.48–1.92) indicates that when compared with a concurrent control population without COVID-19, COVID-19 contributes to a 68% increase in the rate of incident fatigue. This finding mirrors the previous estimates in studies using EHR data (HR 1.65) or administrative claims data (HR 2.20, 95% CI 1.48–3.27) in the United States or in Germany (incidence rate ratio [IRR] 1.97, 95% CI 1.89–2.06) (*17*–*19*).

This study also provides new estimates of incidence rate of chronic fatigue, including ME/CFS after COVID-19 illness. The incidence rate of 1.8/100 person-years is notable, as is the observation that chronic fatigue diagnoses continued in the 18 months of follow-up after COVID-19 detection. The extended period of incident chronic fatigue occurrences suggests a persistent effect but could also indicate a delay in diagnosing fatigue as a separate symptom or diagnosis. The hazard ratio for chronic fatigue (4.32, 95% CI 2.90–6.43) indicates that COVID-19 illness results in 4.3 times the risk for chronic fatigue compared with non–COVID-19 group. That increase is similar to findings from a study of chronic fatigue syndrome in Germany (IRR 3.04, 95% CI 2.66–3.48) (*19*). Although chronic fatigue is not the same as chronic fatigue syndrome or ME/CFS, which requires additional symptoms for diagnosis, including activity limitation, postexertional malaise, unrefreshing sleep, and either cognitive impairment or orthostatic intolerance (*20*), the ICD-9 and ICD-10 codes used for the diagnosis of ME/CFS were included in the diagnostic codes used to define the chronic fatigue diagnosis. The recently implemented diagnostic code G93.32 for ME/CFS when used in conjunction with code U09.9, post COVID-19 condition, will be instrumental in identifying COVID-19–related ME/CFS in future research (*21*).

We found many diseases and conditions to be associated with post–COVID-19 fatigue. Those associations might provide useful prognostic information for the assessment of patients with COVID-19. Patients with mood disorders were previously reported to be at higher risk for illness and death during acute COVID-19 and increased risk of needing postacute care (*22*). Our findings indicate that patients with a history of mood disorders are also at increased risk for post–COVID-19 fatigue. The association of post–COVID-19 fatigue with pain syndromes and sleep disorders is supported by previous research in non–COVID-19 populations (*23*).

Our study has several strengths, including addressing a critical data gap in incidence measure of post–COVID-19 fatigue; robust application of cohort methodologies in incidence estimation using EHR data; that the EHR data were collected from a comprehensive, multiclinic, multihospital health system; a well-defined population at risk for identifying the incident event; and the rigorous selection of concurrent non–COVID-19 matched controls. However, several limitations deserve consideration. First, because we used EHR data for this study, our findings apply only to patients who access care. Future studies are needed to understand the incidence of post-COVID fatigue among those who do not access care, which would likely require different methods. Second, data on exact date of onset, duration, and severity of fatigue or related functional limitations are unavailable for further characterization. The date of fatigue documented in EHR does not necessarily represent the date of symptom onset. In addition, providers might continue to document fatigue or carry forward the diagnosis. Therefore, relying on coding for chronic fatigue without an exact date of symptom onset might underestimate incidence of chronic fatigue. Moreover, the sense of fatigue is subjective and can be underrecorded if it is being considered as part of a disease process. The introduction of code U09.9, post COVID-19 condition, in October 2021 would not change results because it would need to be coded in conjunction with fatigue. Third, data on COVID-19 vaccination were not recorded for most patients, precluding further analysis. Fourth, the relatively small number of patients with fatigue who experienced hospitalization or death during follow-up precluded further multivariable analyses to adjust for potential confounders. The unadjusted association between fatigue and hospitalization or death might have been the result of the greater comorbidities seen in persons with fatigue. Fifth, this article is focused on post–COVID-19 fatigue, but PCC is generally experienced with multisystem symptom clusters. This study was not designed to capture symptom clusters, such as postexertional malaise or symptoms other than fatigue that might also be associated with subsequent outcomes. Last, our data were limited to persons who were tested or received a diagnosis in the first 13 months of the pandemic in Washington, which was 3 months before the Delta variant was detected and 9 months before Omicron was detected (*24*). Early research indicates that the prevalence of post–COVID-19 fatigue was similar across pre-Delta variants, Delta variants, and Omicron variants, but the prevalence of severe fatigue after infections with pre-Delta variants was slightly higher than for other variants (*25*). Future research is needed to estimate incidence rates of fatigue after infections with Delta and Omicron variants and compare them with the findings from this study.

Table 3. Associations between incident fatigue and diseases and conditions diagnosed in 18 months before SARS-CoV-2 infection among 4,589 patients with COVID-19 in study of incidence and predictors of fatiguing illness after SARS-CoV-2 infection, Washington, USA, February 2020–February 2021*

	Proportional hazards model			
	Simple		Multivariable†	
Description	HR (95% CI)	p value	aHR (95% CI)	p value
Circulatory system				
Essential hypertension	1.53 (1.27–1.86)	<0.001	1.27 (1.01–1.59)	0.043
Digestive system				
Biliary tract disease	2.27 (1.43–3.59)	<0.001	1.71 (1.06–2.74)	0.027
Gastroesophageal reflux disease and other esophageal disorders	1.53 (1.23–1.90)	<0.001	1.29 (1.02–1.62)	0.032
Gastritis and duodenitis	2.10 (1.38–3.20)	<0.001	1.93 (1.26–2.94)	0.002
Endocrine				
Hypothyroidism and other thyroid disorders	1.84 (1.41–2.39)	<0.001	1.44 (1.09–1.89)	0.011
Nutritional deficiency, including vitamin D, B, iron	1.86 (1.35–2.56)	<0.001	1.55 (1.12–2.15)	0.008
Obesity	1.55 (1.19–2.02)	0.001	1.22 (0.93–1.61)	0.156
Musculoskeletal system and connective tissue				
Low back pain	1.60 (1.27–2.01)	<0.001	1.42 (1.13–1.79)	0.003
Musculoskeletal pain, not low back pain	1.74 (1.44–2.10)	<0.001	1.58 (1.31–1.92)	<0.001
Osteoarthritis	1.88 (1.46–2.41)	<0.001	1.61 (1.23–2.09)	<0.001
Neoplasms				
Neoplasms of unspecified nature or uncertain behavior	2.2 (1.56–3.11)	<0.001	1.87 (1.31–2.66)	<0.001
Nervous system				
Headache, including migraine	1.82 (1.33–2.49)	<0.001	1.67 (1.22–2.29)	0.002
Nerve and nerve root disorders	1.91 (1.31–2.78)	<0.001	1.74 (1.19–2.53)	0.004
Nervous system pain and pain syndromes	1.61 (1.30–1.99)	<0.001	1.39 (1.12–1.74)	0.003
Sleep disorders	1.85 (1.49–2.28)	<0.001	1.59 (1.27–1.99)	<0.001
Psychiatry				
Anxiety and fear-related disorders	1.68 (1.35–2.10)	<0.001	1.57 (1.25–1.97)	<0.001
Depressive disorders	1.82 (1.47–2.25)	<0.001	1.62 (1.30–2.01)	<0.001
Trauma- and stressor-related disorders	1.59 (1.16–2.17)	0.004	1.46 (1.07–2.00)	0.018
Otolaryngology				
Otitis media	1.89 (1.04–3.44)	0.037	1.84 (1.01–3.34)	0.047
Respiratory system				
Acute upper respiratory infection	1.63 (1.30–2.04)	<0.001	1.62 (1.29–2.03)	<0.001
Allergic rhinitis	2.01 (1.50–2.71)	<0.001	1.80 (1.33–2.43)	<0.001
Sinusitis	1.55 (1.07–2.25)	0.021	1.56 (1.08–2.26)	0.019

*Reference for all categories is patients without the given disease/condition. Underlying conditions: acute myocardial infarction, history of myocardial infarction, congestive heart failure, peripheral vascular disease, cerebrovascular disease, chronic obstructive pulmonary disease, dementia, hemiplegia or paraplegia, diabetes, diabetes with complications, moderate-severe renal disease, mild liver disease, moderate-severe liver disease, peptic ulcer disease, rheumatologic disease, HIV/AIDS, any malignancy except skin, metastatic solid tumor. aHR, adjusted HR; HR, hazard ratio.
†Multivariable proportional hazards regression models adjusting for age, sex, and number of underlying conditions, unless otherwise noted.

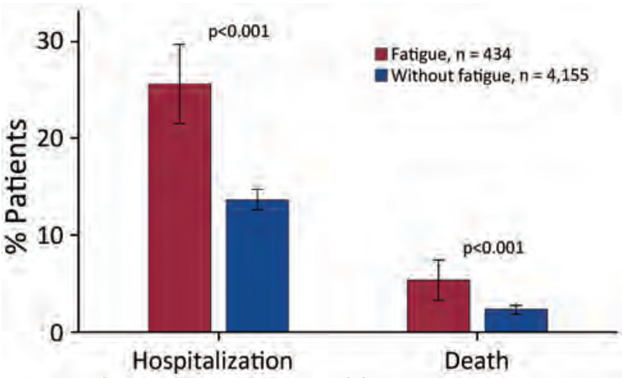

Figure 3. Clinical outcomes among COVID-19 patients with and without incident fatigue after SARS-CoV-2 infection in study of fatiguing illness after SARS-CoV-2 infection, Washington, USA, February 2020–February 2021.

In our unadjusted analyses, patients with COVID-19 who had incident fatigue were at higher risk for hospitalization and death than were persons without incident fatigue. The severe outcome is likely driven, at least in part, by some of the comorbidities and predictors identified in this study. Elevated death rate was previously reported among fatigued patients without COVID-19 (HR 1.45) (*26*). Increased awareness of fatigue and other PCC is warranted to enable patients to seek early care when needed. Further research is also warranted to investigate the causes and preventive measures for the severe outcomes associated with post-COVID fatigue.

In conclusion, our data indicate that COVID-19 is associated with a significant increase in new fatigue diagnoses, and physicians should be aware that fatigue might occur or be newly recognized >1 year after acute COVID-19. Future study is needed to better understand the possible association between fatigue and clinical outcomes. The high incidence rates of fatigue reinforce the need for public health actions to prevent infections, to provide clinical care to those in need, and to find effective treatments for post–acute COVID-19 fatigue.

This work was supported by a contract with the Centers for Disease Control and Prevention (contract no. 75D30121C10207).

About the Author

Dr. Vu is an epidemiologist in the Division of High-Consequence Pathogens and Pathology, National Center for Emerging and Zoonotic Infectious Diseases, Centers for Disease Control and Prevention. His primary research interests are infectious diseases and postinfectious sequelae.

References

1. Centers for Disease Control and Prevention. Long COVID—household pulse survey [cited 2023 Feb 6]. https://www.cdc.gov/nchs/covid19/pulse/long-covid.htm
2. Carfì A, Bernabei R, Landi F; Gemelli Against COVID-19 Post-Acute Care Study Group. Persistent symptoms in patients after acute COVID-19. JAMA. 2020;324:603–5. https://doi.org/10.1001/jama.2020.12603
3. O'Mahoney LL, Routen A, Gillies C, Ekezie W, Welford A, Zhang A, et al. The prevalence and long-term health effects of Long Covid among hospitalised and non-hospitalised populations: A systematic review and meta-analysis. EClinicalMedicine. 2022;55:101762. https://doi.org/10.1016/j.eclinm.2022.101762
4. Thaweethai T, Jolley SE, Karlson EW, Levitan EB, Levy B, McComsey GA, et al.; RECOVER Consortium. Development of a definition of postacute sequelae of SARS-CoV-2 infection. JAMA. 2023;329:1934–46. https://doi.org/10.1001/jama.2023.8823
5. Bateman L, Bested AC, Bonilla HF, Chheda BV, Chu L, Curtin JM, et al. Myalgic Encephalomyelitis/chronic fatigue syndrome: essentials of diagnosis and management. Mayo Clin Proc. 2021;96:2861–78. https://doi.org/10.1016/j.mayocp.2021.07.004
6. Choutka J, Jansari V, Hornig M, Iwasaki A. Unexplained post-acute infection syndromes. Nat Med. 2022;28:911–23. https://doi.org/10.1038/s41591-022-01810-6
7. Horberg MA, Watson E, Bhatia M, Jefferson C, Certa JM, Kim S, et al. Post-acute sequelae of SARS-CoV-2 with clinical condition definitions and comparison in a matched cohort. Nat Commun. 2022;13:5822. https://doi.org/10.1038/s41467-022-33573-6
8. Wisk LE, Gottlieb MA, Spatz ES, Yu H, Wang RC, Slovis BH, et al.; INSPIRE Group. Association of initial SARS-CoV-2 test positivity with patient-reported well-being 3 months after a symptomatic illness. JAMA Netw Open. 2022;5:e2244486. https://doi.org/10.1001/jamanetworkopen.2022.44486
9. Centers for Disease Control and Prevention. ICD-10-CM official coding and reporting guidelines: April 1, 2020 through September 30, 2020 [cited 2023 Aug 25]. https://www.cdc.gov/nchs/data/icd/covid-19-guidelines-final.pdf
10. Centers for Disease Control and Prevention. Co-occurrence of other respiratory illnesses for hospital confirmed COVID-19 encounters by week from selected hospitals [cited 2023 Mar 10]. https://www.cdc.gov/nchs/covid19/nhcs/other-respiratory-illnesses.htm
11. Rosenbaum PR, Rubin DB. The central role of the propensity score in observational studies for causal effects. Biometrika. 1983;70:41–55. https://doi.org/10.1093/biomet/70.1.41
12. Charlson ME, Pompei P, Ales KL, MacKenzie CR. A new method of classifying prognostic comorbidity in longitudinal studies: development and validation. J Chronic Dis. 1987;40:373–83. https://doi.org/10.1016/0021-9681(87)90171-8
13. Zhang Z, Kim HJ, Lonjon G, Zhu Y; written on behalf of AME Big-Data Clinical Trial Collaborative Group. Balance diagnostics after propensity score matching. Ann Transl Med. 2019;7:16. https://doi.org/10.21037/atm.2018.12.10
14. Lin DY, Wei LJ. The robust inference for the Cox proportional hazards model. J Am Stat Assoc. 1989;84:1074–8. https://doi.org/10.1080/01621459.1989.10478874
15. Agency for Healthcare Research and Quality. Clinical Classifications Software Refined (CCSR) [cited 2023 Jan 19]. https://www.hcup-us.ahrq.gov/toolssoftware/ccsr/ccs_refined.jsp

16. Quan H, Li B, Couris CM, Fushimi K, Graham P, Hider P, et al. Updating and validating the Charlson comorbidity index and score for risk adjustment in hospital discharge abstracts using data from 6 countries. Am J Epidemiol. 2011;173:676–82. https://doi.org/10.1093/aje/kwq433
17. Taquet M, Dercon Q, Luciano S, Geddes JR, Husain M, Harrison PJ. Incidence, co-occurrence, and evolution of long-COVID features: a 6-month retrospective cohort study of 273,618 survivors of COVID-19. PLoS Med. 2021;18:e1003773. https://doi.org/10.1371/journal.pmed.1003773
18. Daugherty SE, Guo Y, Heath K, Dasmariñas MC, Jubilo KG, Samranvedhya J, et al. Risk of clinical sequelae after the acute phase of SARS-CoV-2 infection: retrospective cohort study. BMJ. 2021;373:n1098. https://doi.org/10.1136/bmj.n1098
19. Roessler M, Tesch F, Batram M, Jacob J, Loser F, Weidinger O, et al. Post-COVID-19-associated morbidity in children, adolescents, and adults: a matched cohort study including more than 157,000 individuals with COVID-19 in Germany. PLoS Med. 2022;19:e1004122. https://doi.org/10.1371/journal.pmed.1004122
20. Institute of Medicine. Beyond myalgic encephalomyelitis/chronic fatigue syndrome: redefining an illness. Washington: The National Academies; 2015.
21. Centers for Disease Control and Prevention. Myalgic encephalomyelitis/chronic fatigue syndrome: ICD-10-CM codes [cited 2023 Dec 15]. https://www.cdc.gov/me-cfs/healthcare-providers/diagnosis/icd-10.html
22. Castro VM, Gunning FM, McCoy TH, Perlis RH. Mood disorders and outcomes of COVID-19 hospitalizations. Am J Psychiatry. 2021;178:541–7.
23. Thomas KS, Motivala S, Olmstead R, Irwin MR. Sleep depth and fatigue: role of cellular inflammatory activation. Brain Behav Immun. 2011;25:53–8. https://doi.org/10.1016/j.bbi.2010.07.245
24. Washington State Department of Health. SARS-CoV-2 sequencing and variants in Washington state [cited 2023 May 5]. https://doh.wa.gov/sites/default/files/2022-02/420-316-SequencingAndVariantsReport.pdf
25. Gottlieb M, Wang RC, Yu H, Spatz ES, Montoy JCC, Rodriguez RM, et al.; Innovative Support for Patients with SARS-CoV-2 Infections Registry (INSPIRE) Group. Severe fatigue and persistent symptoms at 3 months following severe acute respiratory syndrome coronavirus 2 infections during the pre-Delta, Delta, and Omicron time periods: a multicenter prospective cohort study. Clin Infect Dis. 2023;76:1930–41. https://doi.org/10.1093/cid/ciad045
26. Goklemez S, Saligan LN, Pirsl F, Holtzman NG, Ostojic A, Steinberg SM, et al. Clinical characterization and cytokine profile of fatigue in hematologic malignancy patients with chronic graft-versus-host disease. Bone Marrow Transplant. 2021;56:2934–9. https://doi.org/10.1038/s41409-021-01419-2

Address for correspondence: Quan M. Vu, Centers for Disease Control and Prevention, 1600 Clifton Rd NE, Mailstop H24-12, Atlanta, GA 30329-4018, USA; email: vaq2@cdc.gov

etymologia revisited

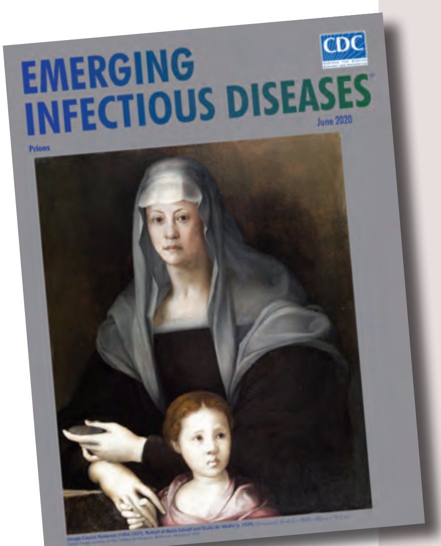

Originally published in June 2020

Scrapie

[skra′pe]

Scrapie is a fatal neurodegenerative disease of sheep and goats that was the first of a group of spongiform encephalopathies to be reported (1732 in England) and the first whose transmissibility was demonstrated by Cuille and Chelle in 1936. The name resulted because most affected sheep develop pruritis and compulsively scratch their hides against fixed objects. Like other transmissible spongiform encephalopathies, scrapie is associated with an alteration in conformation of a normal neural cell glycoprotein, the prion protein. The scrapie agent was first described as a prion (and the term coined) by Stanley Prusiner in 1982, work for which he received the Nobel Prize in 1997.

References:

1. Brown P, Bradley R. 1755 and all that: a historical primer of transmissible spongiform encephalopathy. BMJ. 1998;317:1688–92.
2. Cuillé J, Chelle PL. The so-called “trembling” disease of sheep: is it inoculable? [in French]. Comptes Rendus de l’Académie Sciences. 1936;203:1552.
3. Laplanche J-L, Hunter N, Shinagawa M, Williams E. Scrapie, chronic wasting disease, and transmissible mink encephalopathy. In: Prusiner SB, editor. Prion biology and diseases. Cold Spring Harbor (NY): Cold Spring Harbor Laboratory Press; 1999. p. 393–429.
4. Prusiner SB. Novel proteinaceous infectious particles cause scrapie. Science. 1982;216:136–44.

https//wwwnc.cdc.gov/eid/article/26/6/et-2606_article

RESEARCH

Geographic Variation and Environmental Predictors of Nontuberculous Mycobacteria in Laboratory Surveillance, Virginia, USA, 2021–2023[1]

Brendan Mullen, Eric R. Houpt, Josh Colston, Lea Becker, Sharon Johnson, Laura Young, Jasie Hearn, Joe Falkinham III, Scott K. Heysell

Because epidemiologic and environmental risk factors for nontuberculous mycobacteria (NTM) have been reported only infrequently, little information exists about those factors. The state of Virginia, USA, requires certain ecologic features to be included in reports to the Virginia Department of Health, presenting a unique opportunity to study those variables. We analyzed laboratory reports of *Mycobacterium avium* complex (MAC) and *M. abscessus* infections in Virginia during 2021–2023. MAC/*M. abscessus* was isolated from 6.19/100,000 persons, and 2.37/100,000 persons had MAC/*M. abscessus* lung disease. *M. abscessus* accounted for 17.4% and MAC for 82.6% of cases. Saturated vapor pressure was associated with MAC/*M. abscessus* prevalence (prevalence ratio 1.414, 95% CI 1.011–1.980; p = 0.043). Self-supplied water use was a protective factor (incidence rate ratio 0.304, 95% CI 0.098–0.950; p = 0.041). Our findings suggest that a better understanding of geographic clustering and environmental water exposures could help develop future targeted prevention and control efforts.

Nontuberculous mycobacteria (NTM) infections are increasing globally and have thus become pathogens of substantial public health concern (*1*). However, because of scarce public health reporting, little is known about epidemiologic and environmental risk factors for NTM. Virginia is one of the few states in the United States where NTM infections are reported to a statewide public health agency (*2*); those data are uniquely suited to study the NTM bacterial complex. In addition, Virginia, which has areas of varying population density and a relatively large population using self-supplied domestic water (e.g., well water, rainwater captured in cisterns), presents a particularly advantageous location to study the environmental epidemiology of NTM, given its location in the southeastern United States, a region previously described as having a relatively high burden of NTM disease and that has areas of various geographic and climatic conditions: the Coastal Plains (Tidewater), Piedmont, Blue Ridge Mountains, Valley and Ridge, and Appalachian Plateau regions (*3*,*4*).

Exposure to environmental and in-home water sources, soil conditions and metallic content, climate, and coexisting medical conditions are thought to play complex roles in the acquisition and development of NTM infection (*5*). Numerous risk factors for NTM disease have been identified, including coexisting conditions such as compromised immunity, cystic fibrosis, prior cavitary lung disease, and bronchiectasis; atmospheric water vapor content has also been identified as a predictor of NTM rates across cystic fibrosis centers (*6*,*7*).

Previous studies of NTM epidemiology, often relying on data from retrospective review of electronic medical record databases, suggest NTM are increasing in incidence; the most common pathogens of clinical respiratory disease belong to *Mycobacterium avium* complex (MAC) and *Mycobacterium abscessus* (*8*–*10*).

Author affiliations: University of Virginia, Charlottesville, Virginia, USA (B. Mullen, E.R. Houpt, J. Colston, L. Becker, S. Johnson, S.K. Heysell); Virginia Department of Health, Richmond, Virginia, USA (L. Young, J. Hearn); Virginia Polytechnic Institute and State University, Blacksburg, Virginia, USA (J. Falkinham III)

DOI: https://doi.org/10.3201/eid3003.231162

[1]Preliminary results from this study were presented at the Union-North America Region (NAR) conference, February 22–25, 2023, Vancouver, British Columbia, Canada.

To date, information for epidemiologic research from laboratory surveillance for NTM such as MAC and *M. abscessus* has not been accessed as frequently as for some other pathogens of public health concern (*11–15*). Despite this, population-based studies of NTM have found that 86% of patients meeting the American Thoracic Society/Infectious Diseases Society of America microbiologic definition of NTM lung disease also met full clinical criteria for that disease, suggesting microbiologic laboratory-based data could be used for public health surveillance (*16*). We aimed to characterize the geographic distribution of MAC/*M. abscessus* isolates that met microbiologic criteria for NTM lung disease across Virginia to determine geographic clustering and model population-level determinants of prevalence at the county level. For this epidemiologic study, we used demographic and microbiologic data from routine electronic laboratory reports made to the Virginia Department of Health during June 2021–March 2023, as part of a prospective surveillance study approved by human subject review boards at the University of Virginia (#HSR 200234) and Virginia Department of Health.

Methods

The time period for our study encompassed multiple years of inherent seasonality inclusive of all months for which complete data were available from the state health department. These reports included any culture positive for MAC or *M. abscessus* from any laboratory within the state of Virginia. For all positive cultures, we obtained the person's age, sex, and residential ZIP (postal) code, as well as the anatomic site of sample isolation and date of test result. Case counts were aggregated to the county level based on residential postal codes.

To investigate potential climatic and geographic factors associated with MAC/*M. abscessus* prevalence, we obtained mean annual saturated vapor pressure, mean daily maximum temperature, and mean annual precipitation data for each county in Virginia during 2021–2022 from Weather Source (https://weathersource.com). We extracted the percentage of each county using self-supplied groundwater from US Geological Survey data from 2018, the most recent data available (*4*). Based on a recent US Geological Survey analysis, water source data from Virginia has been reliably recorded and relatively stable over time (*17*).

Case Definitions

We defined cases of MAC/*M. abscessus* lung disease using 2020 American Thoracic Society/Infectious Diseases Society of America microbiologic criteria for NTM pulmonary disease (*18*). Case-patients had either a single MAC or *M. abscessus* culture isolated from bronchoalveolar lavage, pleural fluid, or lung tissue or ≥2 cultures from sputum. For persons with multiple cultures collected over time, we included case data only from the earliest culture meeting these criteria. We excluded data from mixed MAC and *M. abscessus* cultures or from successive cultures testing positive for one then the other. We excluded cases not meeting the microbiologic criteria for lung disease in which only 1 sputum culture contained MAC or *M. abscessus*. We excluded data from lung disease cases diagnosed based on nonrespiratory samples. We also excluded data from persons residing outside of Virginia.

Statistical Analyses

We analyzed differences in age of MAC and *M. abscessus* case-patients using Mann-Whitney U tests and differences in sex using χ^2 tests. We obtained US Census Bureau data on population size, median age, and population density for each Virginia county from 2022, the midpoint of the study period (*19*). We calculated average annual prevalence of MAC/*M. abscessus* lung disease captured by laboratory surveillance during 2021–2023 for the entire state of Virginia and for each county and independent city. Average annual prevalence was reported as rate per 100,000 population.

We generated choropleth maps to visualize total county-level MAC/*M. abscessus*, MAC, and *M. abscessus* infections, saturated vapor pressure, and percentage of county population using self-supplied water. Self-supplied water comes from nonpublic groundwater or surface water sources, such as wells or rainwater captured in cisterns. To assess clustering, we calculated Moran *I* for each map as a measure of spatial autocorrelation. We analyzed factors potentially associated with prevalence of MAC/*M. abscessus* infections in each county using negative binomial regression, a generalization of Poisson regression, to account for overdispersion. We adjusted population numbers using the natural log of person-years as an offset variable. We defined person-years as the given population (e.g., statewide, county) multiplied by 3 years (i.e., length of the study period). We included additional variables in the final model as potentially relevant epidemiologic confounders and environmental factors noted in previous investigations of NTM: sex, median age, population density, mean saturated vapor pressure, mean maximum temperature, mean daily precipitation, and percentage of population using self-supplied water (*3*,*6*,*8*,*10*). We reported exponentiated coefficients from the model as prevalence ratios. We analyzed data using SPSS Statistics 28.0 (IBM, https://www.ibm.com) and generated maps using ArcGIS 3.0 (Environmental Systems Research Institute, https://www.esri.com).

Results

Statewide Results

We identified 874 persons with ≥1 MAC or *M. abscessus* pulmonary cultures during the 2021–2023 data collection period. We excluded 10 persons who resided outside of Virginia, leaving data from 864 persons to evaluate. We categorized 714 persons (82.6%) with MAC and 150 (17.4%) with *M. abscessus*; 331/864 (38.3%) of those met microbiologic criteria for NTM lung disease.

Case Demographics

Median age was 69 (interquartile range [IQR] 58–76) years among case-patients identified with MAC/*M. abscessus* infections overall, median 64 (IQR 46–75) years among those with *M. abscessus*, and median 69 (IQR 60–77) years among those with MAC. Only 18 case-patients (2.1%) were <18 years of age, and 534 (61.8%) were >65 years of age. Sex distribution for all case-patients was 497 (57.5%) female and 366 (42.5%) male (Table 1). We found no difference in sex distribution between total MAC and *M. abscessus* case-patients of all ages (p = 0.934). Prevalences of MAC, *M. abscessus*, and total MAC/*M. abscessus* cases were higher for female than male case-patients >65 years of age but were similar compared with all other case-patients <65 years (Figure 1).

Geographic Distribution

Rates of MAC/*M. abscessus* infections varied significantly by locality, driven by differences in distribution of MAC infections (Figure 2). MAC/*M. abscessus* cases clustered throughout the state (Moran *I* = 0.219, p<0.001) similar to MAC (Figure 2 panel C; Moran *I* = 0.210, p<0.001), especially in the central counties of the Piedmont region and on several peninsulas on Chesapeake Bay in the Tidewater region (Figure 2, panels A, C); we found no clear clustering of *M. abscessus* cases (Moran *I* = 0.01, p = 0.663) (Figure 2, panel E). We did find clustering in rates of self-supplied water use (Moran's *I* = 0.189, p<0.001) and mean annual saturated vapor pressure (Moran *I* = 0.820, p<0.001) (Figure 2, panels D, F). Self-supplied water use appeared to cluster in the more rural south-central parts of the Piedmont region; saturated vapor pressure was highest in the Tidewater region in the southeastern part of the state.

A regression model of county-level prevalence of MAC/*M. abscessus* infections (Table 2) showed saturated vapor pressure to be associated with prevalence of MAC/*M. abscessus* infections. Each 1 millibar increase in mean annual saturated vapor pressure resulted in a 41.4% increase in expected count of MAC/*M. abscessus* infections (prevalence ratio [PR] 1.414, 95% CI 1.011–1.980; p = 0.043), whereas each 1% increase in the proportion of the county population using self-supplied water resulted in a 69.6% decrease in expected MAC/*M. abscessus* infections (IRR 0.304, 95% CI 0.098–0.950; p = 0.041). Other population-level variables included in the model were not significantly related to MAC/*M. abscessus* prevalence rates. A similar model was constructed to evaluate effects of median age, sex, population density, saturated vapor pressure, temperature, precipitation, and proportion of self-supplied water use on prevalence of MAC or *M. abscessus* infections. Saturated vapor pressure was positively associated and self-supplied water use was negatively associated with MAC infection prevalence, but none of those factors was significantly associated with *M. abscessus* infection prevalence. A model constructed to assess relationships between those factors and prevalence of MAC/*M. abscessus* pulmonary disease identified no significant association.

Table 1. Demographic characteristics of case-patients with MAC and *Mycobacterium abscessus*, by isolate, Virginia, USA, 2021–2023*

Variable	All	MAC isolates	*M. abscessus* isolates	p value†
Total	864	714	150	
Age, median, y (IQR)	69 (51–87)	69 (52–86)	64 (35–97)	<0.001
Age group, y				
0–18	18 (2.1)	14 (2.0)	4 (2.7)	
18–64	312 (36.1)	240 (33.6)	72 (48.8)	
≥65	534 (61.8)	460 (64.4)	74 (49.3)	
Sex				
F	497 (57.5)	412 (57.7)	85 (56.7)	0.934
M	366 (42.4)	302 (42.3)	65 (42.7)	

*Values are no. (%) except as indicated. MAC, *Mycobacterium avium* complex; IQR, interquartile range

†p values given for differences in median age and differences in sex distribution between MAC isolates by Mann-Whitney U and *M. abscessus* by χ^2 tests.

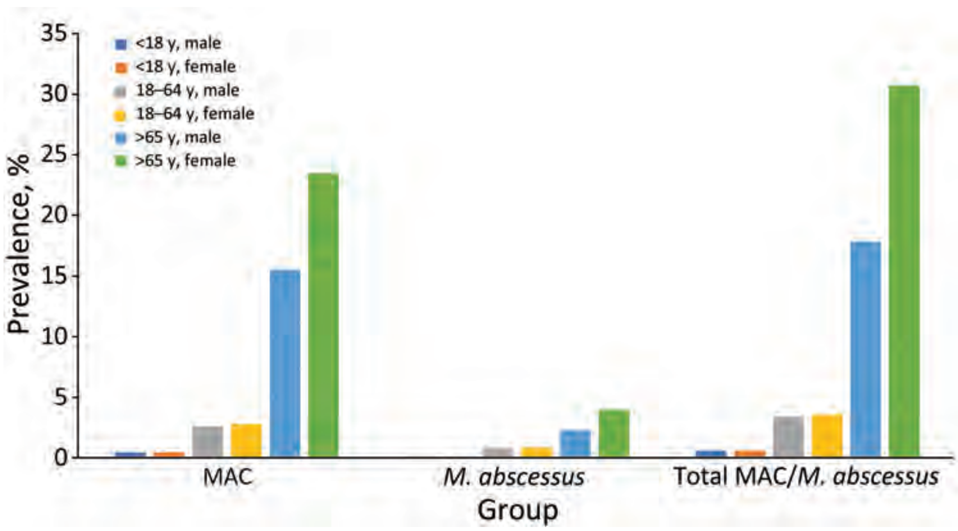

Figure 1. Prevalence of *Mycobacterium avium* complex (MAC), *M. abscessus*, or both (MAC/*M. abscessus*), categorized by age and sex, Virginia, USA, 2021–2023.

Discussion

We report results of our evaluation of local and statewide rates of MAC/*M. abscessus* infection in Virginia using real-time, laboratory-based monitoring. We found that average annual prevalence of MAC/*M. abscessus* in Virginia over the study period was 6.19 cases of MAC/*M. abscessus* infection per 100,000 population and 2.37 cases of MAC/*M. abscessus* lung disease per 100,000 population. More case-patients were female than male, and most were older persons (median age 69 years), consistent with known demographics associated with NTM infection. Of note, we demonstrated significant geographic clustering of MAC/*M. abscessus*. We found increases in saturated water vapor pressure strongly associated with prevalence and self-supplied water use negatively associated with prevalence at the county level, independent of population density.

Characterizing the epidemiology of NTM remains challenging, often because of underreporting. Multiple studies have demonstrated the limitations of using diagnostic billing (International Classification of Diseases [ICD]) codes to identify rates of NTM disease. Barriers include lack of clinician familiarity with NTM diagnostic characteristics and variable rates of need for active antimicrobial therapy, which might not be necessary for treatment of NTM lung disease, unlike for many other infectious diseases (*20*,*21*). Several additional recent studies have evaluated laboratory-based surveillance of NTM, including 1 study from a CDC surveillance program (*22*). Our study differed from that study in multiple ways. Of note, we included data from a state in the southeastern United States, a region not represented in the CDC surveillance data, and gathered comprehensive surveillance data for the entire state from statewide laboratories rather than individual sentinel laboratories. Our prevalence estimate for MAC/*M. abscessus* pulmonary disease (2.37/100,000 population) was lower than overall NTM incidence seen in the CDC study (6.1/100,000 population). That difference might be because we included only MAC and *M. abscessus*, not other NTM, or that we included all laboratories statewide rather than only laboratories serving referral centers. Other recent studies based on statewide data from Missouri (*23*) and Wisconsin (*24*) have used laboratory-based surveillance. Comparing prevalence rates based on our data with rates from those other studies was difficult because of differences in methodology and inclusion criteria. The Missouri study (*23*) reported aggregate period rates. The Wisconsin study (*24*) reported an overall average annual NTM incidence of 22.1–22.4 cases/100,000 persons but included repeat positive samples from individual persons as separate cases. In multivariate modeling across those studies, socioeconomic factors were found to be associated with NTM rates in the Wisconsin study but not the Missouri study. We lacked access to those data from

Table 2. Negative binomial regression model of county-level factors associated with county *Mycobacterium avium* complex and *M. abscessus* case prevalence, Virginia, USA, 2021–2023*

Variable	PR (95% CI)	p value
Sex		
F	1.068 (0.957–1.192)	0.237
M	Referent	
Median age	1.034 (0.968–1.104)	0.319
Population density	0.893 (0.467–1.708)	0.733
Saturated vapor pressure	1.414 (1.011–1.980)	0.043
Groundwater use	0.304 (0.098–0.950)	0.041
Maximum temperature	0.920 (0.771–1.099)	0.358
Precipitation	0.992 (0.976–1.008)	0.312

*NA, not applicable; PR, prevalence ratio

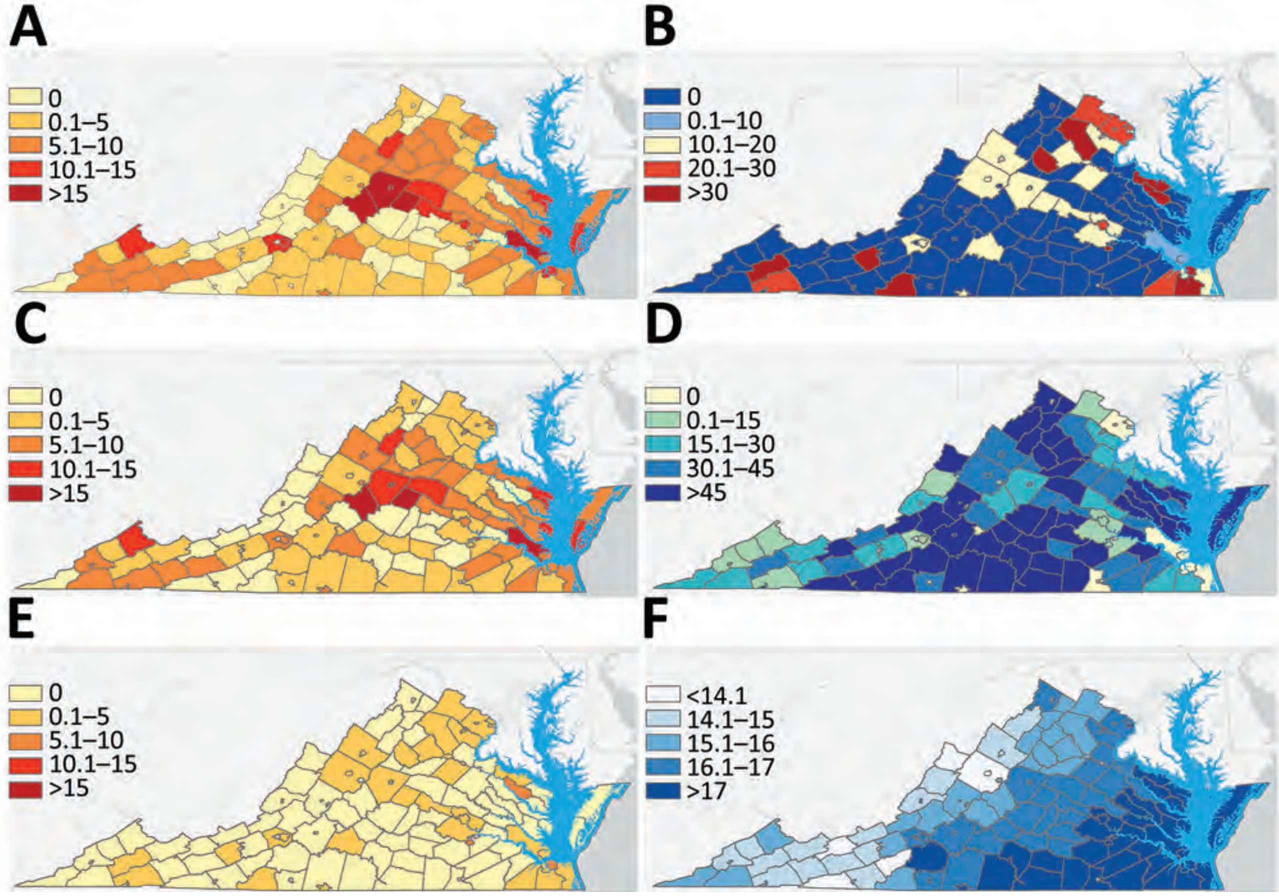

Figure 2. Geographic distribution and variables of interest for *Mycobacterium avium* complex (MAC) and *Mycobacterium abscessus* infections, Virginia, USA, 2021–2023. County-level prevalence (cases/100,000 person-years) of A) MAC/*M. abscessus*; C) MAC; and E) *M. abscessus*. B) *M. abscessus* distribution as a percentage of total MAC/*M. abscessus* infections. D) Percentage of residents using self-supplied water. F) Saturated water vapor pressure in millibars.

patients in our cohort. Our study also differed from the Missouri and Wisconsin studies in that it was set in the southeastern rather than midwestern United States. In addition, we included environmental exposure variables not evaluated in the Missouri and Wisconsin studies (*23*,*24*).

We found a higher percentage of *M. abscessus* (17.4%) among total MAC/*M. abscessus* infections than other studies of distribution of NTM based on aggregate data (*25*), possibly because we excluded NTM species other than MAC and *M. abscessus*. Still, a recent study showed a range of 4.5%–21.7% widely distributed across the United States for *M. abscessus* (*26*). The southeast had the highest proportion of *M. abscessus* among NTM species of any US region (*26*), but particularly given the clinical severity of *M. abscessus* lung disease, its considerable antimicrobial resistance, and the difficulty of managing antimycobacterial therapy, further research is needed to understand why *M. abscessus* appears to be so prevalent in that region.

Our study explored associations between MAC/*M. abscessus* infections and local-level environmental exposures. Previous data have shown that variations between locations in temperature, rainfall, flooding, and drought are associated with prevalence of NTM (*27*). Saturated vapor pressure has been shown to be the climate variable most closely associated with NTM prevalence (*6*,*7*). In our study, mean annual saturated vapor pressure was highest in the Tidewater region in the southeastern part of the state and correlated with higher local prevalence of MAC/*M. abscessus*. Of note, saturated vapor pressure is expected to increase globally with ongoing trends in climate change, highlighting the need to understand how those changes might relate to risks of developing NTM lung disease.

We also examined the relationship between drinking water sources and MAC/*M. abscessus* prevalence. NTM have been more commonly isolated from central water distribution system than groundwater sources, but this comparison has not been tested epidemiologically (*28*). However, several studies have shown piping from central household water sources to be a pathway for NTM infection (*29*,*30*). The source of household water is thought to be critical, with NTM rarely found in samples of clean groundwater (*31*). Here, we found increased use of self-supplied water (mostly well water) to be associated with lower rates of MAC/*M. abscessus* infections in a given locality even after adjusting for population density. Based on our data, the effect size associated with water sources was even larger than with environmental variables, suggesting that water source might constitute a substantial factor in acquiring NTM.

As with many studies based on laboratory surveillance, our study was limited by a lack of individual-level data regarding water sources and behavioral variables, and we assumed that residential postal codes best reflect the location of a person's greatest source of exposure to water for drinking and bathing. However, environmental (*31*) and household (*29*,*32*) surveillance data from our study support that water vapor pressure and types of water source might be factors in acquiring NTM. We also considered that the location of referral centers, particularly the cluster of counties surrounding a large academic hospital in central Virginia. might have biased our observation of geographic clustering. However, 1 study of NTM clustering across the United States found that neither physician-to-patient ratio nor referral center proximity within an area was associated with local variations in clustering of NTM prevalence (*33*). In addition to the modest underestimate of NTM lung disease when considering only laboratory-based microbiologic criteria (*16*), MAC and *M. abscessus* represented only 73.6% of pathogenic pulmonary NTM isolates in Virginia based on earlier data from our group (*34*), and thus NTM lung disease likely carries a greater total population burden than we report. Furthermore, given our study design, we could not conclusively establish causation with regards to the association between exposure variables and outcomes of interest. Finally, although recent data were available, we matched covariates only spatially, not temporally.

In summary, we found a high proportion of NTM isolates in Virginia were MAC. Local clustering of MAC/*M. abscessus* infections within Virginia during the study period might be explained by differences in household water sources and saturated water vapor levels. Future studies of the geographic distribution of NTM should highlight variations in the distribution of different NTM species; additional controlled studies are needed to explore those factors and assess the effects of other individual-level exposures that might be related to developing NTM lung disease. Our findings suggest that a better understanding of geographic clustering and environmental water exposures related to NTM could help inform future monitoring activities and development of prevention and control efforts targeted to populations most at risk.

This work was supported by funding from funding from National Institutes of Health grant R01 HL 155547.

About the Author

Dr. Mullen is a resident physician within the Department of Internal Medicine at the University of Virginia in Charlottesville. His research interests include epidemiology and treatment of mycobacterial infections and HIV.

References

1. Dahl VN, Mølhave M, Fløe A, van Ingen J, Schön T, Lillebaek T, et al. Global trends of pulmonary infections with nontuberculous mycobacteria: a systematic review. Int J Infect Dis. 2022;125:120–31. https://doi.org/10.1016/j.ijid.2022.10.013
2. Winthrop KL, Henkle E, Walker A, Cassidy M, Hedberg K, Schafer S. On the reportability of nontuberculous mycobacterial disease to public health authorities. Ann Am Thorac Soc. 2017;14:314–7. https://doi.org/10.1513/AnnalsATS.201610-802PS
3. Strollo SE, Adjemian J, Adjemian MK, Prevots DR. The burden of pulmonary nontuberculous mycobacterial disease in the United States. Ann Am Thorac Soc. 2015;12:1458–64. https://doi.org/10.1513/AnnalsATS.201503-173OC
4. Dieter CA, Maupin MA, Caldwell RR, Harris MA, Ivahnenko TI, Lovelace JK, et al. Estimated use of water in the United States in 2015 (circular 1441). Reston, VA: US Geological Survey; 2018 [cited 2023 Jul 12]. https://pubs.er.usgs.gov/publication/cir1441
5. Johnson MM, Odell JA. Nontuberculous mycobacterial pulmonary infections. J Thorac Dis. 2014;6:210–20.
6. Adjemian J, Olivier KN, Prevots DR. Nontuberculous mycobacteria among patients with cystic fibrosis in the United States: screening practices and environmental risk. Am J Respir Crit Care Med. 2014;190:581–6. https://doi.org/10.1164/rccm.201405-0884OC
7. Prevots DR, Adjemian J, Fernandez AG, Knowles MR, Olivier KN. Environmental risks for nontuberculous mycobacteria. Individual exposures and climatic factors in the cystic fibrosis population. Ann Am Thorac Soc. 2014;11:1032–8. https://doi.org/10.1513/AnnalsATS.201404-184OC
8. Adjemian J, Frankland TB, Daida YG, Honda JR, Olivier KN, Zelazny A, et al. Epidemiology of nontuberculous mycobacterial lung disease and tuberculosis, Hawaii, USA. Emerg Infect Dis. 2017;23:439–47. https://doi.org/10.3201/eid2303.161827
9. Adjemian J, Olivier KN, Seitz AE, Holland SM, Prevots DR. Prevalence of nontuberculous mycobacterial lung disease in U.S. Medicare beneficiaries. Am J Respir Crit Care Med. 2012;185:881–6. https://doi.org/10.1164/rccm.201111-2016OC

10. Winthrop KL, Varley CD, Ory J, Cassidy PM, Hedberg K. Pulmonary disease associated with nontuberculous mycobacteria, Oregon, USA. Emerg Infect Dis. 2011;17:1760–1. https://doi.org/10.3201/eid1709.101929
11. Cheng Q, Collender PA, Heaney AK, McLoughlin A, Yang Y, Zhang Y, et al. Optimizing laboratory-based surveillance networks for monitoring multi-genotype or multi-serotype infections. PLOS Comput Biol. 2022; 18:e1010575. https://doi.org/10.1371/journal.pcbi.1010575
12. Huang JH, Kao PN, Adi V, Ruoss SJ. *Mycobacterium avium-intracellulare* pulmonary infection in HIV-negative patients without preexisting lung disease: diagnostic and management limitations. Chest. 1999;115:1033–40. https://doi.org/10.1378/chest.115.4.1033
13. Chou MP, Clements AC, Thomson RM. A spatial epidemiological analysis of nontuberculous mycobacterial infections in Queensland, Australia. BMC Infect Dis. 2014;14:279. https://doi.org/10.1186/1471-2334-14-279
14. Donohue MJ, Wymer L. Increasing prevalence rate of nontuberculous mycobacteria infections in five states, 2008–2013. Ann Am Thorac Soc. 2016;13:2143–50. https://doi.org/10.1513/AnnalsATS.201605-353OC
15. Mejia-Chew C, Chavez MA, Lian M, McKee A, Garrett L, Bailey TC, et al. Spatial epidemiologic analysis and risk factors for nontuberculous mycobacteria infections, Missouri, USA, 2008–2019. Emerg Infect Dis. 2023;29:1540–6. https://doi.org/10.3201/eid2908.230378
16. Winthrop KL, McNelley E, Kendall B, Marshall-Olson A, Morris C, Cassidy M, et al. Pulmonary nontuberculous mycobacterial disease prevalence and clinical features: an emerging public health disease. Am J Respir Crit Care Med. 2010;182:977–82. https://doi.org/10.1164/rccm.201003-0503OC
17. US Geological Survey. Factors affecting uncertainty of public supply, self-supplied domestic, irrigation, and thermoelectric water-use data, 1985–2015—evaluation of information sources, estimation methods, and data variability [cited 2023 Dec 12]. https://pubs.usgs.gov/sir/2021/5082/sir20215082.pdf
18. Daley CL, Iaccarino JM, Lange C, Cambau E, Wallace RJ Jr, Andrejak C, et al. Treatment of nontuberculous mycobacterial pulmonary disease: an official ATS/ERS/ESCMID/IDSA clinical practice guideline. Eur Respir J. 2020;56:2000535. https://doi.org/10.1183/13993003.00535-2020
19. US Census Bureau. QuickFacts: Virginia [cited 2023 Jul 11]. https://www.census.gov/quickfacts/VA
20. Winthrop KL, Baxter R, Liu L, McFarland B, Austin D, Varley C, et al. The reliability of diagnostic coding and laboratory data to identify tuberculosis and nontuberculous mycobacterial disease among rheumatoid arthritis patients using anti-tumor necrosis factor therapy. Pharmacoepidemiol Drug Saf. 2011;20:229–35. https://doi.org/10.1002/pds.2049
21. Mejia-Chew C, Yaeger L, Montes K, Bailey TC, Olsen MA. Diagnostic accuracy of health care administrative diagnosis codes to identify nontuberculous mycobacteria disease: a systematic review. Open Forum Infect Dis. 2021;8:ofab035.
22. Grigg C, Jackson KA, Barter D, Czaja CA, Johnston H, Lynfield R, et al. Epidemiology of pulmonary and extrapulmonary nontuberculous mycobacteria infections at 4 US emerging infections program sites: a 6-month pilot. Clin Infect Dis. 2023;77:629–37. https://doi.org/10.1093/cid/ciad214
23. Mejia-Chew C, Chavez MA, Lian M, McKee A, Garrett L, Bailey TC, et al. Spatial epidemiologic analysis and risk factors for nontuberculous mycobacteria infections, Missouri, USA, 2008–2019. Emerg Infect Dis. 2023;29:1540–6. https://doi.org/10.3201/eid2908.230378
24. Vonasek BJ, Gusland D, Hash KP, Wiese AL, Tans-Kersten J, Astor BC, et al. Nontuberculous mycobacterial infection in Wisconsin adults and its relationship to race and social disadvantage. Ann Am Thorac Soc. 2023;20:1107–15. https://doi.org/10.1513/AnnalsATS.202205-425OC
25. Prevots DR, Marras TK. Epidemiology of human pulmonary infection with nontuberculous mycobacteria: a review. Clin Chest Med. 2015;36:13–34. https://doi.org/10.1016/j.ccm.2014.10.002
26. Marshall J, Mercaldo R, Lipner E, Prevots R. Nontuberculous mycobacteria testing and culture positivity in the United States based on Labcorp Data. In: American Thoracic Society International Conference Abstracts, May 19–24, 2023, Washington DC, USA. p. A2955.
27. Thomson RM, Furuya-Kanamori L, Coffey C, Bell SC, Knibbs LD, Lau CL. Influence of climate variables on the rising incidence of nontuberculous mycobacterial (NTM) infections in Queensland, Australia 2001-2016. Sci Total Environ. 2020;740:139796. https://doi.org/10.1016/j.scitotenv.2020.139796
28. Falkinham JO III, Norton CD, LeChevallier MW. Factors influencing numbers of *Mycobacterium avium, Mycobacterium intracellulare*, and other Mycobacteria in drinking water distribution systems. Appl Environ Microbiol. 2001;67:1225–31. https://doi.org/10.1128/AEM.67.3.1225-1231.2001
29. Lande L, Alexander DC, Wallace RJ Jr, Kwait R, Iakhiaeva E, Williams M, et al. *Mycobacterium avium* in community and household water, suburban Philadelphia, Pennsylvania, USA, 2010–2012. Emerg Infect Dis. 2019;25:473–81. https://doi.org/10.3201/eid2503.180336
30. Whiley H, Keegan A, Giglio S, Bentham R. *Mycobacterium avium* complex—the role of potable water in disease transmission. J Appl Microbiol. 2012;113:223–32. https://doi.org/10.1111/j.1365-2672.2012.05298.x
31. Martin EC, Parker BC, Falkinham JO III. Epidemiology of infection by nontuberculous mycobacteria. VII. Absence of mycobacteria in southeastern groundwaters. Am Rev Respir Dis. 1987;136:344–8. https://doi.org/10.1164/ajrccm/136.2.344
32. Falkinham JO III. Nontuberculous mycobacteria from household plumbing of patients with nontuberculous mycobacteria disease. Emerg Infect Dis. 2011;17:419–24. https://doi.org/10.3201/eid1703.101510
33. Adjemian J, Olivier KN, Seitz AE, Falkinham JO III, Holland SM, Prevots DR. Spatial clusters of nontuberculous mycobacterial lung disease in the United States. Am J Respir Crit Care Med. 2012;186:553–8. https://doi.org/10.1164/rccm.201205-0913OC
34. Satyanarayana G, Heysell SK, Scully KW, Houpt ER. Mycobacterial infections in a large Virginia hospital, 2001–2009. BMC Infect Dis. 2011;11:113. https://doi.org/10.1186/1471-2334-11-113

Address for correspondence: Scott Heysell, Division of Infectious Diseases and International Health, University of Virginia, 345 Crispell Dr, Charlottesville, VA 22908, USA; email: skh8r@uvahealth.org

Taenia martis Neurocysticercosis-Like Lesion in Child, Associated with Local Source, the Netherlands

Hendriekje Eggink,[1] Miriam Maas,[1] Judith M.A. van den Brand, Jasja Dekker, Frits Franssen, Eelco W. Hoving, Laetitia M. Kortbeek, Mariëtte E.G. Kranendonk, Linda C. Meiners, Anne E. Rittscher, Jeroen Roelfsema, Elisabeth H. Schölvinck

A neurocysticercosis-like lesion in an 11-year-old boy in the Netherlands was determined to be caused by the zoonotic *Taenia martis* tapeworm. Subsequent testing revealed that 15% of wild martens tested in that region were infected with *T. martis* tapeworms with 100% genetic similarity; thus, the infection source was most likely local.

The zoonotic *Taenia martis* tapeworm lives in mustelid intestines and has been reported across Europe (*1*). Human infection is thought to occur by accidental ingestion of eggs in mustelid feces and can lead to cysticercosis-like lesions, reported for only 6 adults in France, Germany, and Switzerland (*2*–*7*). We report a *T. martis* neurocysticercosis-like lesion in a child in the Netherlands.

The Study

In 2020, an 11-year-old boy was referred to the emergency department of University Medical Center Groningen (Gronigen, the Netherlands). Three days earlier, he had awakened with a frontal headache that intensified within 1 hour and led to nausea and vomiting. Symptoms resolved after sleep. On the evening of his referral to the emergency department, the boy suddenly became nauseous and pale, unable to speak, and in a decreased state of consciousness. His altered mental status continued for 20 minutes and his speech arrest for 90 minutes; a headache followed. No urine incontinence or tongue bite were noted. His medical history revealed only allergic rhinitis. He was an enthusiastic runner in the northern Netherlands woods and spent holidays in different nature areas of western Europe.

At the emergency department, his symptoms had resolved, and initial examination revealed no neurologic or laboratory test abnormalities. Computed tomography of his brain without contrast showed a hypodense area in the left temporal lobe and a barely discernable ringlike lesion with an isointense rim, without calcification (Figure 1, panel A). A cerebral venous sinus thrombosis was excluded. Magnetic resonance imaging (MRI) revealed a 13-mm round lesion with edema in the dorsal left temporal lobe and a hypointense rim on susceptibility-weighted and T2-weighted images (Figure 1, panels B, C), suggesting a fibrotic capsule, enhanced on 3-dimensional T1-weighted images (Figure 1, panel D). On diffusion-weighted images, no central diffusion restriction was seen (Figure 1, panels E, F). Initially, a brain tumor of undefined origin was proposed, but a second viewing suggested neurocysticercosis. Results of serologic testing of 2 samples collected 3 weeks apart, tested for *T. solium* tapeworms via a Centers for Disease Control and Prevention immunoblot recombinant antigen (rT24H antigen and LLGP) (*8*,*9*), were, however, negative.

The boy remained symptom free and because of the differential diagnosis of a brain tumor was referred to the national center for pediatric oncology in the Netherlands, the Princess Maxima Center (Utrecht, the Netherlands). Two weeks after the initial visit to University Medical Center Groningen, the patient

Author affiliations: University Medical Center Groningen, Groningen, the Netherlands (H. Eggink, L.C. Meiners, E.H. Schölvinck); National Institute for Public Health and the Environment, Bilthoven, the Netherlands (M. Maas, F. Franssen, L.M. Kortbeek, J. Roelfsema); Utrecht University, Utrecht, the Netherlands (J.M.A. van den Brand, A.E. Rittscher); Jasja Dekker Dierecologie B.V., Arnhem, the Netherlands (J. Dekker); Princess Maxima Center, Utrecht (E.W. Hoving, M.E.G. Kranendonk)

DOI: https://doi.org/10.3201/eid3003.231402

[1]These first authors contributed equally to this article.

underwent an uncomplicated craniotomy, and a cyst was extirpated in toto (Figure 1, panel G). Macroscopically, the lesion appeared to be an intact cystic round nodule on cut section with a white-greyish central area surrounded by a thin capsule (Figure 1, panel H). Microscopic examination revealed a necrotic core surrounded by fibrin and fibrosis (Figure 1, panel I) with adjacent multinuclear foreign body–type giant cells and an inflammatory infiltrate including plasma cells and eosinophilic neutrophils (Figure 1, panel J).

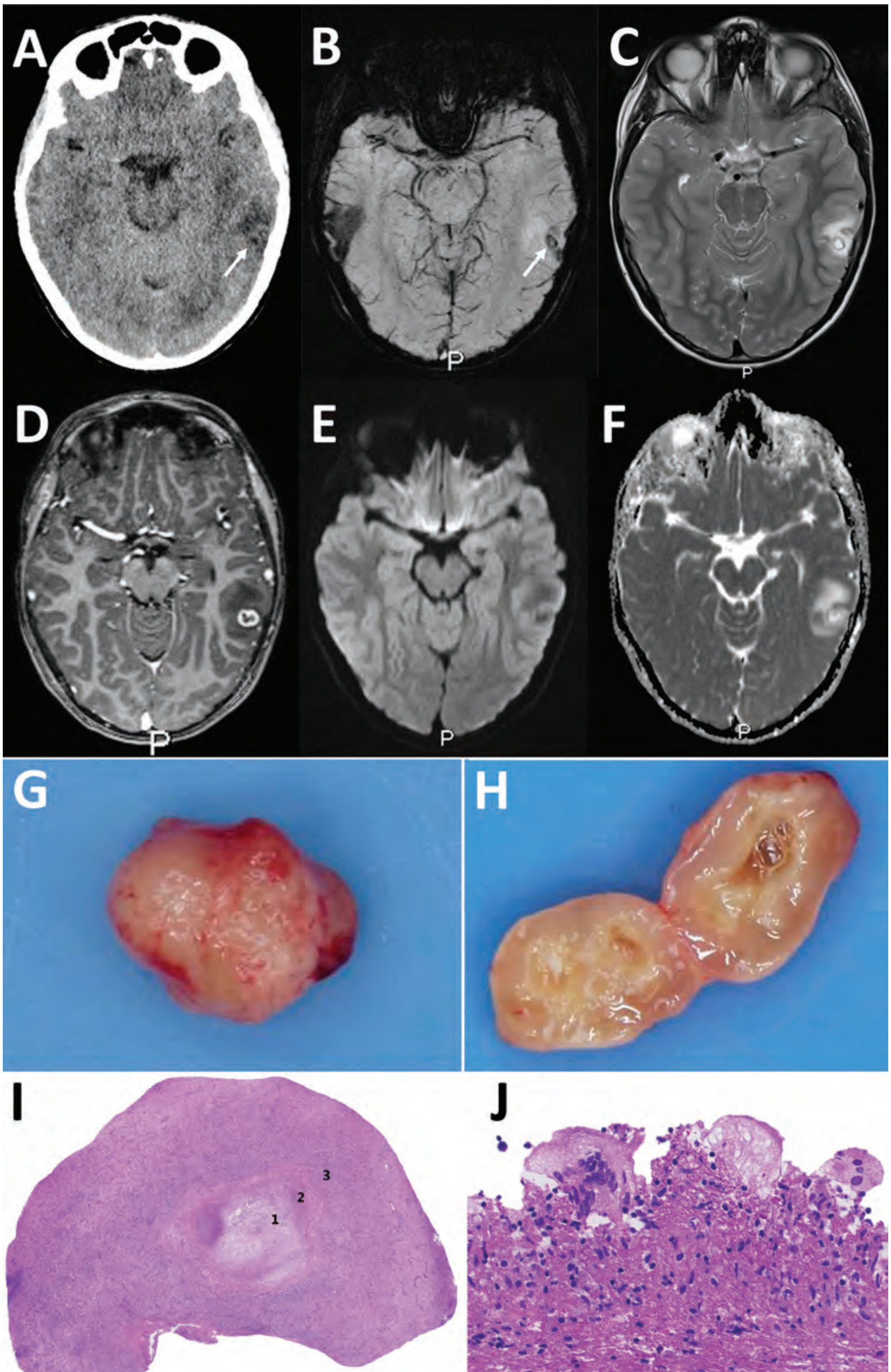

Figure 1. Diagnostic imaging of the brain and cystic lesion resected from boy with neurocysticercosis-like lesion, the Netherlands. A) Axial computed tomography showing edema in the left temporal lobe with a barely visible hypointense round lesion with a noncalcified, isointense rim (arrow). B–F) Axial magnetic resonance images at slightly different levels through the cystic lesion with surrounding edema in the left temporal lobe, showing a hypointense ring on susceptibility-weighted image (B) using minimum intensity projection (arrow) and on T2-weighted image (C), suggestive of a fibrotic capsule. D) Three-dimensional T1-weighted image showing a slightly irregular enhancement of the rim. E, F) On diffusion-weighted image (E) and apparent diffusion coefficient map (F), the rim is isointense and central diffusion restriction is absent, excluding a bacterial abscess. G, H) Macroscopic picture of the lesion showing a round nodule (G) and a cyst-like lesion (H) on cut section with a white-greyish central area surrounded by a thin capsule. I, J) Microscopic images showing a necrotic core (1) surrounded by a rim of fibrosis (2) and a mixed inflammatory response (3) (I) and multinuclear foreign-body-type giant cells (J).

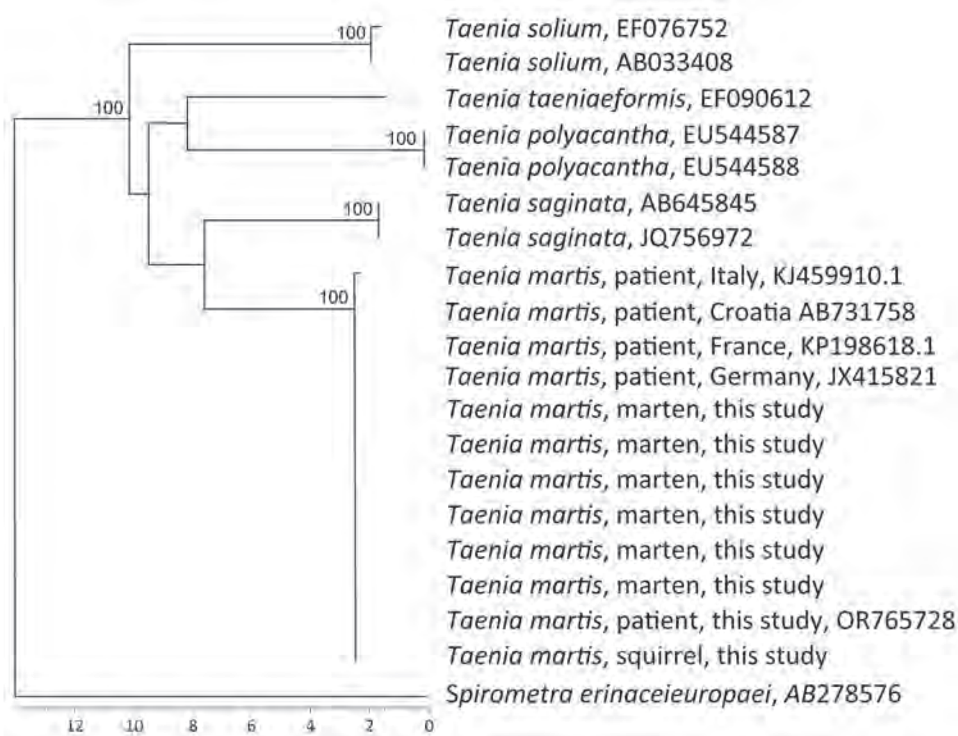

Figure 2. Phylogenetic analysis of the partial *CO1* gene of *Taenia martis* tapeworm samples from a patient, martens, and a squirrel in the Netherlands and reference sequences. GenBank accession numbers are shown when available. The tree is based on multiple alignment with Jukes and Cantor correction and neighbor-joining cluster analysis. Branch quality was determined by bootstrap analysis with 10,000 simulations. Reference sequences were from patients from Italy (GenBank accession no. KJ459910.1), Croatia (accession no. AB731758), France (accession no. KP198618.1), and Germany (accession no. JX415821). Moreover, *T. saginata* (accession nos. AB645845 and JQ756972), *T. solium* (accession nos. EF0767752 and AB033408), *T. polyacantha* (accession nos. EU544587 and EU544588), and *T. taeniaeformis* (accession no. EF090612) were included in the phylogenetic analysis. The cestode *Spirometra erinaceieuropaei* (accession no. AB278576) was included as outgroup. Scale bar indicates nucleotide substitutions/site.

No tegument or calcareous corpuscles were seen. After ruling out common pathogenic microorganisms, we determined that those features could fit well with the second (necrotic) stage of neurocysticercosis (*10*).

PCR analysis of the cyst material was performed by using the 12S rRNA gene as target (*11*) (primers: forward 5′-AAAIGGTTTGGCAGTGAGIGA-3′; reverse 5′GCGGTGTGTACITGAGITAAAC-3′) and with *T. saginata* DNA as positive control. PCR revealed a tapeworm infection, and sequencing indicated *T. martis* (Appendix, https://wwwnc.cdc.gov/EID/article/30/3/23-1402-App1.pdf). Those findings led to the final diagnosis of a stage 2 neurocysicercosis-like lesion, based on the *T. martis* infection. The patient received albendazole (2×/d for 1 week). Follow-up MRI of the brain 1.5 months after surgery showed only the resection cavity, and the boy has remained symptom free.

To explore potential sources, we investigated stone martens (*Martes foina*) that had been killed as part of ongoing predator control in 2020 and 2021 in Friesland, a northern province of the Netherlands. We checked their intestines macroscopically for *T. martis* tapeworms and collected intestinal content from multiple parts of the intestine to submit for molecular detection of *T. martis* tapeworm DNA. We extracted DNA from collected tapeworms and all intestinal scrapings by using the DNeasy Blood and Tissue Kit (QIAGEN, https://www.qiagen.com). We also performed conventional PCR targeting the *CO1* gene on the patient material, using primers previously reported (*12*), with slight modification of the primers (forward, 5′-TTTTTTGGGCATCCTGAGGTTTAT-3′; reverse, 5′-TAACGACATAACATAATGAAAATG-3′), followed by electrophoresis using 1.8% agarose gel PCR. We sequenced samples with bands matching the positive control, obtained from a *T. martis* worm collected at the start of the project, by using BaseClear (Leiden, https://www.baseclear.com) and performed BLAST analysis (http://www.ncbi.nlm.nih.gov/blast/Blast.cgi).

Of the 214 collected stone martens, sequences of 32 (15%, 95% CI 10%–20%) intestinal scraping samples matched *T. martis* sequences from GenBank, including samples from 7 stone martens in which adult tapeworms were macroscopically detected and confirmed by PCR and sequencing to be *T. martis*. Genetic analysis showed 100% similarity between the *T. martis* sequence of the patient (GenBank accession no. OR765728) and those from the martens.

In addition, a *T. martis* sequence from larval cestode from a squirrel collected in 2014 in the Netherlands (provided by Herman Cremers) was 100% identical to the sequence from the patient. Sequences from *T. martis* tapeworms collected in Switzerland, Croatia, France, and Germany were 100% identical and from Italy 99.6% identical to the sequences of the martens from the Netherlands (Figure 2).

Conclusions

To our knowledge, human *T. martis* cysticercosis has been reported for only 6 adults. Two cases involved a *T. martis* neurocysticercosis-like lesion (*2*,*7*), and the others involved the eye, peritoneum, and pouch of Douglas (*3*–*6*). All 6 patients were immunocompetent women: 5 tended and ate from vegetable gardens, 5 lived in rural areas, and 3 were frequent hikers/dog owners. The boy we report also spent a lot of time in the forest.

Stone martens are synanthropic mustelids and will eat fruit or scavenge scraps from compost heaps in gardens and barnyards. It is hypothesized that consuming contaminated vegetables or fruit or accidentally ingesting *T. martis* eggs after contact with contaminated soil may lead to (neuro)cysticercosis-like infection caused by *T. martis* tapeworms.

Neurocysticercosis involves infection of the central nervous system by the larval stage of the pork tapeworm *T. solium* (*13*). The MRI features for the boy with a *T. martis* neurocysticercosis-like lesion and the patient in France resemble those caused by *T. solium* tapeworms (*2*). Features depend on stage of the infection (*14*). No specific serologic test is available for *T. martis* infection, and the extent of cross-reactivity between *T. solium* and *T. martis* antibodies in available serology tests is unknown. Serologic test results for the 6 adult patients showed mixed signals, including positive signals against *Echinococcus multilocularis* crude larval antigen extract (that could not be repeated in confirmatory assays) (*5*) and *T. solium* (*2*,*5*), although others have reported negative serologic test results for those parasites (*3*,*4*). Confirming the diagnosis requires detecting parasite DNA by PCR and sequencing to differentiate between *Taenia* species. The availability of differentiating molecular methods may have resulted in increased diagnoses of *T. martis* infections, possibly previously misdiagnosed as *T. solium* infections (*3*).

The finding of *T. martis* tapeworms in the patient and the stone martens we investigated from the northern part of the Netherlands strongly suggest a local source of infection. Although the prevalence of *T. martis* tapeworms can vary widely regionally (*15*), studies in host and reservoir species suggest widespread appearance of *T. martis* tapeworm in mustelids in Europe (*1*), and underrecognition and underreporting of cysticercosis caused by infection with this tapeworm is probable.

Acknowledgments

The diagnosis in this case was the result of a collaboration between different centers within the Netherlands. We thank contributors Bob Jonge Poerink and Bob van den Brink for their help collecting the stone marten samples; Nahid Nozari and Cecile Dam-Deisz for their help performing the molecular assays for the patient and the martens; Maarten Heuvelmans and Tjomme van de Bruggen for their help finding the diagnosis; Joke van der Giessen for her help with the molecular analyses; and Herman Cremers for his help providing us with the *T. martis* tapeworms from the squirrel from his extensive collection of wildlife parasites.

About the Author

Dr. Eggink is a neurology resident at the University Medical Center Groningen, specializing in pediatric neurology and movement disorders. She combines her residency with a postdoctoral position focusing on recognizing pediatric movement disorders at the Movement Disorders Groningen Expertise Center.

References

1. Deplazes P, Eichenberger RM, Grimm F. Wildlife-transmitted *Taenia* and *Versteria* cysticercosis and coenurosis in humans and other primates. Int J Parasitol Parasites Wildl. 2019;9:342–58. https://doi.org/10.1016/j.ijppaw.2019.03.013
2. Brunet J, Benoilid A, Kremer S, Dalvit C, Lefebvre N, Hansmann Y, et al. First case of human cerebral *Taenia martis* cysticercosis. J Clin Microbiol. 2015;53:2756–9. https://doi.org/10.1128/JCM.01033-15
3. Eberwein P, Haeupler A, Kuepper F, Wagner D, Kern WV, Muntau B, et al. Human infection with marten tapeworm. Emerg Infect Dis. 2013;19:1152–4. https://doi.org/10.3201/eid1907.121114
4. Koch T, Schoen C, Muntau B, Addo M, Ostertag H, Wiechens B, et al. Molecular diagnosis of human *Taenia martis* eye infection. Am J Trop Med Hyg. 2016;94:1055–7. https://doi.org/10.4269/ajtmh.15-0881
5. Mueller A, Förch G, Zustin J, Muntau B, Schuldt G, Tappe D. Case report: molecular identification of larval *Taenia martis* infection in the pouch of Douglas. Am J Trop Med Hyg. 2020;103:2315–7. https://doi.org/10.4269/ajtmh.20-0782
6. Rudelius M, Brehm K, Poelcher M, Spinner C, Rosenwald A, da Costa CP. First case of human peritoneal cysticercosis mimicking peritoneal carcinosis: necessity of laparoscopy and histologic assessment for the correct diagnosis. JMM Case Rep. 2017;4:e005097. https://doi.org/10.1099/jmmcr.0.005097
7. Steinsiepe VK, Ruf M-T, Rossi M, Fricker-Feer C, Kolenc D, Buser BS, et al. Human *Taenia martis* neurocysticercosis, Switzerland. Emerg Infect Dis. 2023;29:2569–72. https://doi.org/10.3201/eid2912.230697

8. Gómez-Morales MÁ, Pezzotti P, Ludovisi A, Boufana B, Dorny P, Kortbeek T, et al. Collaborative studies for the detection of *Taenia* spp. infections in humans within CYSTINET, the European Network on Taeniosis/Cysticercosis. Microorganisms. 2021;9:1173. https://doi.org/10.3390/microorganisms9061173
9. Noh J, Rodriguez S, Lee Y-M, Handali S, Gonzalez AE, Gilman RH, et al. Recombinant protein- and synthetic peptide-based immunoblot test for diagnosis of neurocysticercosis. J Clin Microbiol. 2014;52:1429–34. https://doi.org/10.1128/JCM.03260-13
10. Pittella JEH. Pathology of CNS parasitic infections. Handb Clin Neurol. 2013;114:65–88. https://doi.org/10.1016/B978-0-444-53490-3.00005-4
11. Roelfsema JH, Nozari N, Pinelli E, Kortbeek LM. Novel PCRs for differential diagnosis of cestodes. Exp Parasitol. 2016;161:20–6. https://doi.org/10.1016/j.exppara.2015.12.010
12. Casulli A, Manfredi MT, La Rosa G, Cerbo AR, Genchi C, Pozio E. *Echinococcus ortleppi* and *E. granulosus* G1, G2 and G3 genotypes in Italian bovines. Vet Parasitol. 2008;155:168–72. https://doi.org/10.1016/j.vetpar.2008.04.004
13. Garcia HH, Nash TE, Del Brutto OH. Clinical symptoms, diagnosis, and treatment of neurocysticercosis. Lancet Neurol. 2014;13:1202–15. https://doi.org/10.1016/S1474-4422(14)70094-8
14. Lerner A, Shiroishi MS, Zee C-S, Law M, Go JL. Imaging of neurocysticercosis. Neuroimaging Clin N Am. 2012;22:659–76. https://doi.org/10.1016/j.nic.2012.05.004
15. Borgsteede FH, Tibben JH, van der Giessen JW. The musk rat (*Ondatra zibethicus*) as intermediate host of cestodes in the Netherlands. Vet Parasitol. 2003;117:29–36. https://doi.org/10.1016/j.vetpar.2003.07.015

Address for correspondence: Miriam Maas, Centre for Infectious Disease Control, National Institute for Public Health and the Environment, Antonie van Leeuwenhoeklaan 9, 3721 MA Bilthoven, the Netherlands; email: miriam.maas@rivm.nl

Newly Identified *Mycobacterium africanum* Lineage 10, Central Africa

Christophe Guyeux, Gaetan Senelle, Adrien Le Meur, Philip Supply, Cyril Gaudin, Jody E. Phelan, Taane G Clark, Leen Rigouts, Bouke de Jong, Christophe Sola, Guislaine Refrégier

Analysis of genome sequencing data from >100,000 genomes of *Mycobacterium tuberculosis* complex using TB-Annotator software revealed a previously unknown lineage, proposed name L10, in central Africa. Phylogenetic reconstruction suggests L10 could represent a missing link in the evolutionary and geographic migration histories of *M. africanum*.

The traditional view of restricted diversity among bacterial agents causing human and animal tuberculosis is being revised thanks to wide use of whole-genome sequencing (WGS). Besides *Mycobacterium canettii*, representative of exceptional, nonclonal, early-evolution branching lineages of tubercle bacilli in eastern Africa, several previously unknown lineages of *M. tuberculosis* complex have been identified in Africa during the past decade. *M. tuberculosis* complex lineage 7 (L7) was discovered in the Horn of Africa and L8 in the African Great Lakes region (*1*,*2*). *M. africanum* L9 was found only in Djibouti and Somalia. In contrast, 2 other major *M. africanum*–affiliated lineages contributing substantially to the tuberculosis burden, L5 and L6, are found mostly in western Africa (*3*). The pathway between eastern and western Africa in the evolutionary history of the bacillus remains unclear. We describe a newly identified sister lineage of L6 and L9 associated with central Africa and discuss implications for determining the evolutionary history of related *M. africanum* lineages L5, L6, and L9. We based research on publicly available data and thus required no ethics approval.

Author affiliations: University Bourgogne Franche-Comté (UBFC), Besançon, France (C. Guyeux, G. Senelle); Université Paris-Saclay–AgroParisTech, Gif-sur-Yvette, France (A. Le Meur, G. Refrégier); Institut Pasteur de Lille Center for Infection and Immunity of Lille, Lille, France (P. Supply, C. Gaudin); London School of Hygiene and Tropical Medicine, London, UK (J.E. Phelan, T.G. Clark, L. Rigouts, B. de Jong); Université Paris-Saclay, Saint-Aubin, France (C. Sola); Université Paris Cité, Paris (C. Sola)

DOI: https://doi.org/10.3201/eid3003.231466

The Study

We used the TB-Annotator platform (G. Senelle, unpub. data, https://www.biorxiv.org/content/10.1101/2023.06.12.526393v1) to integrate WGS data from 102,001 *M. tuberculosis* complex isolates in the National Center for Biotechnology Information (NCBI) public domain. This platform identifies genetic variations, including single-nucleotide polymorphisms (SNPs), regions of difference (RDs), and IS*6110* insertions, differentiating selected genomes from *M. tuberculosis* H37Rv. The TB-Annotator database also contains information on genotypic drug resistance and geographic location of variant isolation.

SNPs from an exploratory set comprising 15,699 isolates largely of Africa origin were used to build a phylogenetic tree. Our analysis identified a lineage sister to *M. africanum* L6 and L9, branching between these lineages and the animal lineage A1 (La_A1) (*3*). The newly identified lineage is represented by only 2 genomes: ERR2707158, obtained from a strain isolated in 2008 from a patient residing in Kinshasa, Democratic Republic of the Congo (DRC), now incorporated under reference ITM-501386 (CT2008–03226) in the coordinated collections of microorganisms of the Institute of Tropical Medicine (Antwerp, Belgium); and ERR2516384, obtained from a strain isolated in Belgium in 2013 (V. Mathys, pers. comm., email, 2023 Jul 5). The genomes of the new lineage carried none of the SNP markers described in the latest *M. tuberculosis* complex lineage classification scheme (*4*) and no SNPs that confer drug resistance.

To confirm the phylogenetic position of those 2 genomes, we identified SNPs from 132 isolates covering the genetic and geographic diversity of L5 and L6 and including representatives of all other lineages using the Genotube pipeline (A. Le Meur, pers. comm., email, 2023 Sep 15) and TB-Profiler (*5*). Resulting phylogenetic reconstruction confirmed the clustering of ERR2707158 and ERR2516384 in a branch between L6 and L9 and animal lineage

La_A1 (Figure). The newly designated L10 samples shared 375 specific SNPs with isolates from our selected set of 132 samples; 243/375 specific SNPs were not detected in any of the 102,001 genomes included in TB-Annotator. Among those specific SNPs, 91 were synonymous (Appendix 1, https://wwwnc.cdc.gov/EID/article/30/3/23-1466-App1.xlsx). The pairwise distance between the 2 samples of interest was 382 SNPs (SNPs outside of repetitive regions, manually checked when discordant between 2 pipelines), much shorter than the distance to the other samples of our selection (minimum 1,137 SNPs; average 1,591 ±222 SNPs) (Appendix 2, Figure 1, https://wwwnc.cdc.gov/EID/article/30/3/23-1466-App2.pdf).

We next explored other features of the genomes to corroborate SNP-based phylogenetic inferences. In addition to the deletion of RD9 shared with the L5/L6 branch and animal-associated lineages, the 2 L10 genomes lacked RD7, RD8, and RD10 (*3*). However, they did not show the RD702 (L6/L9) or RD713 (L5) deletions. In contrast, the 2 unclassified

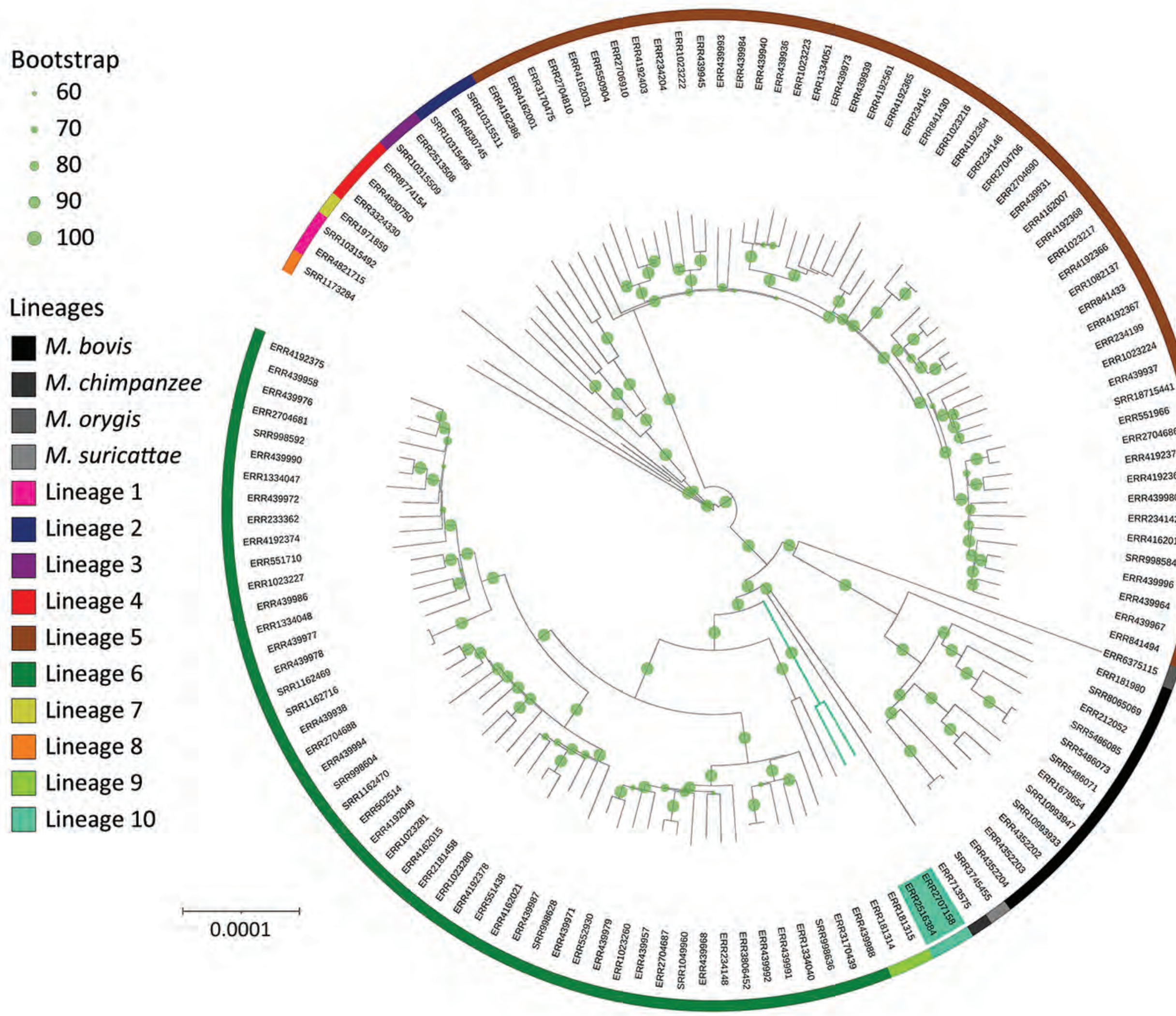

Figure. Global *Mycobacterium* phylogeny including newly identified *M. africanum* L10 (proposed) strains (green shading). We selected *M. africanum* samples for harboring RD9 deletion, having documented country of origin (for the purpose of additional analyses; Appendix 2, Figure 2, https://wwwnc.cdc.gov/EID/article/30/3/23-1466-App2.pdf), and refined our a selection to retain a sole representative of each sublineage for each country. This sample represents the genetic and geographic diversity of *M. africanum* in Africa. Specifically for this phylogenetic reconstruction, single-nucleotide polymorphisms were identified in comparison with an *M. tuberculosis* ancestor (*11*) and reincorporated into the whole genome to avoid biases in the molecular model or need for Lewis correction. Phylogeny was rooted with *M. canettii*, subsequently removed for better visualization. Bootstrap support was computed using 100 replicates and shown when ≥0.6. Circles confirm the large support of almost all branches, especially of L10 and its sister branches. L10 branching point lies between L9 and the La_A1 lineage grouping chimpanzee and Dassie bacillus. Scale bar indicates nucleotide substitutions per site.

Table. Spoligotype patterns of newly identified *Mycobacterium africanum* L10 (proposed) strains from central Africa compared with representative strains of L6, L9, and A1 lineage*

ID	Source†	No.	Spoligotype binary	SIT	Country of isolation
L10-BEL04200301729	SITVITWEB	1	■■■■■■□■□■■■■■■■■■■■■□□□□□□□□□□□□□□□□□□□□□□	Orph	Republic of Congo
L10-ERR2516384	TB-Annotator	1	■■■■■■□■□■■■■■■■■■■■■□□□□□□□□□□□□□□□□□□□□□□	Orph	Belgium‡
L10-ERR2707158	TB-Annotator	1	■■■■■■□■□■■■■■■■■■■■■■■■■□□□□□□□□□□□□□□□□□□	Orph	DRC
L6_SIT181	SITVITWEB	208	■■■■■■□□□■■■■■■■■■■■■■■■■■■■■■■■■■■■■□■■■■	181	Gambia
L9	Coscolla 2021	3	■■■■■■□■□■■■□□□□□□□□□□□□□□□□□□□□□□■■■■□■■■■	Orph	Somalia
L9	Coscolla 2021	1	■■■■■■□■□□□□□□□□□□□□□□□□■■■■■■■■■■□■■■□■■■■	U	Djibouti
L9_FXX01199901706	SITVITWEB	1	■■■■■■□■□□□□□□□□□□□□□□□□■■■■■■■■■■□■■■□■■■■	Orph	France
NLD009501731	SITVITWEB	2	■■■■■■□■□■■■□□□□□□□□□□□□□□□□□□□□□□■■■■□■■■■	Orph	Netherlands
A1_Dassie bacillus	TB-Annotator	1	■■■■■■□■□■■■□□■■■■■□□□□□□□□□□□□□□□□■■■□□■■■	U	South Africa
A1_*M. mungi*	https://mbovis.org, TB-Annotator	1	■■□■■■□■□■■□□□□□□□□□□□□□□□□□□□□□□□□□■■□■■■■	SB 1960	Botswana
A1_chimpanzee bacillus	Coscolla 2013, TB-Annotator	1	■■■□□□□□□□□□□□□□□□□□□□□□□□□□□□□■■■■■■■□■□□■	U	Côte d'Ivoire

*L6, L9, and both L10 samples harbor the same losses of spacer 7 and of spacer 9. DRC, Democratic Republic of the Congo; orph, orphan (single reported occurrence); SIT, spoligotype international type; U, undesignated.
†Coscolla 2021, (*3*); Coscolla 2013, (*12*); SITVITWEB, (*9*); TB-Annotator, G. Senelle, unpub. data, https://www.biorxiv.org/content/10.1101/2023.06.12.526393v1.
‡Origin unknown.

genomes harbored the same specific large 9,134 nt deletion (*Rv0613c–Rv0622*) in *M. tuberculosis* H37Rv (NC_000962.3:706602–715736) not observed in any other lineage. This segment included the toxin/antitoxin gene pair *vapB29*/*vapC29*. Two other shared deletions encompassed *eis* and *dnaE2* (Appendix 1), potentially limiting the ability to acquire aminoglycoside resistance (*6*) and possibly affecting some mutational properties (*7*) of those *M. africanum* strains. The 2 genomes also shared 4 IS*6110* copies at a position found in no other lineage (Appendix 1). In the CRISPR locus of the 2 L10 genomes, reconstructed using CRISPRbuilder-TB (*8*), we found the same absence of spacers 7 and 9 (43-spacer spoligotype format) seen in L6, L9, and La_A1 (Table) and all last spacers starting from spacers 22 (ERR2516384) or 26 (ERR2707158) (Table).

The genetic features of the strains we identified, combining outlying phylogenetic position, genetic distance from the L6/L9 branch and other known *M. tuberculosis* lineages, distinctive regions of deletions and IS*6110* insertions, and specific spoligotype signatures, led us to propose their classification in a newly designated L10 lineage. We propose 3 synonymous SNPs (*gyrA* G7901T, *recN* C1920096T, and *dnaG* C2621730T) compared with the H37Rv 000962.3 reference sequence in housekeeping genes to identify the new lineage.

To evaluate potential regional and global circulation of L10 strains, we searched for similar spoligotype patterns using SITVIT2, which accumulates spoligotypes from >110,000 isolates from 131 countries (*9*). We identified a single instance, BEL04200301729, showing the same spoligotype pattern as ERR2516384, which might represent a third occurrence of L10. Of note, that strain was isolated in the Republic of the Congo, a country neighboring DRC, where ERR2707158 was collected (Appendix 2, Figure 2). We also browsed spoligotyping results from next generation sequencing data, collected from ≈1,500 isolates from a 2016–2017 national survey in DRC, targeted using Deeplex Myc-TB (https://www.deeplex.com) (*10*) but detected no similar pattern. Thus, both global (TB-Annotator and SITVIT2) and local (*10*) datasets suggested that L10 strains are rare at the worldwide level, and aside from migratory dissemination, likely restricted to central Africa. Mapping of *M. africanum* diversity in Africa showed that in addition to L10, central Africa also hosts a relatively large diversity of L5 strains (Appendix 2, Figure 2).

Despite the rarity of L10, its specific phylogenetic positioning and presence in central Africa provide new elements to the complex evolutionary history of *M. africanum*. Currently, the most likely scenario favors western Africa as the place of origin of all *M. africanum* variants (*3*). This scenario implies that L5 and L6 ancestors emigrated from eastern Africa and diversified in western Africa and that L9 migrated back to eastern Africa. Finding L10 in central Africa with intermediate branching between L5 and L6/L9 can fit this scenario but adds an independent migration from western Africa to central Africa. Alternatively, *M. africanum* could have emerged close to central Africa and subsequently migrated westwards and eastwards. This alternative scenario, however, would require greater sampling in central regions of Africa to gain real support.

Conclusions

Through the extensive mining of WGS and genotyping databases, we newly identified a thus far rare *M. tuberculosis* complex lineage, L10 (proposed), present in central Africa. The lineage is characterized by a new region of deletion, IS*6110* insertions, and 243 SNPs, including *gyrA* G7901T, *recN* C1920096T, and *dnaG* C2621730T. L10 represents a sister clade to L6, found mainly in western Africa, and L9, specifically in eastern Africa, and reveals a putative previously missing piece in the evolutionary history and migrations of *M. africanum*. Our findings extend the known diversity of *M. africanum* in Africa.

Acknowledgments

We thank the Institute of Tropical Medicine of Antwerp (Belgium) and Genoscreen (France) for sharing their SRA data on public databases. We thank Vanessa Mathys for providing location of isolation for ERR2516384 sample.

About the Author

Dr. Guyeux is a professor of computer science at the Franche-Comté Électronique Mécanique Thermique et Optique—Sciences et Technologies Institute, University of Franche-Comté in Belfort, France. His research interests include microbial evolution, with a particular focus on extensive sets of genomes.

References

1. Gagneux S. Ecology and evolution of *Mycobacterium tuberculosis*. Nat Rev Microbiol. 2018;16:202–13. https://doi.org/10.1038/nrmicro.2018.8
2. Ngabonziza JCS, Loiseau C, Marceau M, Jouet A, Menardo F, Tzfadia O, et al. A sister lineage of the *Mycobacterium tuberculosis* complex discovered in the African Great Lakes region. Nat Commun. 2020;11:2917. https://doi.org/10.1038/s41467-020-16626-6
3. Coscolla M, Gagneux S, Menardo F, Loiseau C, Ruiz-Rodriguez P, Borrell S, et al. Phylogenomics of *Mycobacterium africanum* reveals a new lineage and a complex evolutionary history. Microb Genom. 2021;7:00047. https://doi.org/10.1099/mgen.0.000477
4. Napier G, Campino S, Merid Y, Abebe M, Woldeamanuel Y, Aseffa A, et al. Robust barcoding and identification of *Mycobacterium tuberculosis* lineages for epidemiological and clinical studies. Genome Med. 2020;12:114. https://doi.org/10.1186/s13073-020-00817-3
5. Phelan JE, O'Sullivan DM, Machado D, Ramos J, Oppong YEA, Campino S, et al. Integrating informatics tools and portable sequencing technology for rapid detection of resistance to anti-tuberculous drugs. Genome Med. 2019;11:41. https://doi.org/10.1186/s13073-019-0650-x
6. Chen W, Biswas T, Porter VR, Tsodikov OV, Garneau-Tsodikova S. Unusual regioversatility of acetyltransferase Eis, a cause of drug resistance in XDR-TB. Proc Natl Acad Sci U S A. 2011;108:9804–8. https://doi.org/10.1073/pnas.1105379108
7. Dupuy P, Ghosh S, Adefisayo O, Buglino J, Shuman S, Glickman MS. Distinctive roles of translesion polymerases DinB1 and DnaE2 in diversification of the mycobacterial genome through substitution and frameshift mutagenesis. Nat Commun. 2022;13:4493. https://doi.org/10.1038/s41467-022-32022-8
8. Guyeux C, Sola C, Noûs C, Refrégier G. CRISPRbuilder-TB: "CRISPR-builder for tuberculosis." Exhaustive reconstruction of the CRISPR locus in *mycobacterium tuberculosis* complex using SRA. PLOS Comput Biol. 2021; 17:e1008500. https://doi.org/10.1371/journal.pcbi.1008500
9. Couvin D, David A, Zozio T, Rastogi N. Macro-geographical specificities of the prevailing tuberculosis epidemic as seen through SITVIT2, an updated version of the *Mycobacterium tuberculosis* genotyping database. Infect Genet Evol. 2019;72:31–43. https://doi.org/10.1016/j.meegid.2018.12.030
10. Kayomo MK, Mbula VN, Aloni M, André E, Rigouts L, Boutachkourt F, et al. Targeted next-generation sequencing of sputum for diagnosis of drug-resistant TB: results of a national survey in Democratic Republic of the Congo. Sci Rep. 2020;10:10786. https://doi.org/10.1038/s41598-020-67479-4
11. Comas I, Chakravartti J, Small PM, Galagan J, Niemann S, Kremer K, et al. Human T cell epitopes of *Mycobacterium tuberculosis* are evolutionarily hyperconserved. Nat Genet. 2010;42:498–503. https://doi.org/10.1038/ng.590
12. Coscolla M, Lewin A, Metzger S, Maetz-Rennsing K, Calvignac-Spencer S,Nitsche A, et al. Novel Mycobacterium tuberculosis complex isolate from a wild chimpanzee. Emerg Infect Dis 2013;19:969–76.

Address for correspondence: Guislaine Refrégier, Ecologie Systématique et Evolution, 12 rue 128, 91190, Gif-sur-Yvette, France; email: guislaine.refregier@universite-paris-saclay.fr

Delayed Diagnosis of Locally Acquired Lyme Disease, Central North Carolina, USA

Ross M. Boyce, Peyton Pretsch, Kay Tyrlik, Abigail Schulz, Dana A. Giandomenico, Alexis M. Barbarin, Carl Williams

Healthcare providers in North Carolina, USA, have limited experience diagnosing and managing Lyme disease because few cases occur annually statewide. We outline the prolonged diagnostic course for a patient with locally acquired Lyme disease in North Carolina. This case highlights the need for greater awareness and professional education.

Historically, the burden of Lyme disease has been concentrated in the Northeast and upper Midwestern regions of the United States (*1*). Recent data suggest a southward expansion into areas of southwestern Virginia and western North Carolina (*2*,*3*). Although North Carolina frequently reports some of the highest incidence rates of spotted fever rickettsiosis and ehrlichiosis (*4*), Lyme disease transmission has been less intense than in neighboring states to the north (*5*). Black-legged ticks (*Ixodes scapularis*) have long been found in North Carolina, and speculation exists that the lower Lyme disease incidence may be attributable to differences in blood-meal seeking behaviors between the northern- and southern-origin ticks (*6*,*7*). Although North Carolina has seen an increase in cases, many clinicians have limited experience with Lyme disease, and diagnostic errors are common (*8*,*9*). We describe a case of Lyme disease diagnosed in an otherwise healthy woman living in central North Carolina who had no history of travel.

The Case

In mid-July, a generally healthy woman in her late 60s went biking around her neighborhood in the suburbs north of Raleigh, North Carolina. After the ride, she felt dehydrated, lightheaded, and excessively fatigued for the level of exertion. Four days later, she noted a large erythematous rash on the right side of her neck (Figure). She also had a fever reaching 38.6°C. Results of an antigen-based COVID-19 rapid test were negative. She treated her symptoms with acetaminophen.

Approximately 5 days after the rash appeared, she went to her primary care physician (PCP) for her annual physical (Table). By that time, the fever had resolved, but the rash was still present. Additional symptoms included a severe frontal headache and bilateral ear pain. Her PCP diagnosed her with cellulitis and prescribed a 10-day course of cephalexin. After starting antibiotics, the patient felt subjectively better. However, the headache returned 2 days later. She contacted her PCP, who changed her antibiotic to double-strength trimethoprim/sulfamethoxazole out of concern that the headache was a side effect of cephalexin.

Figure. Erythematous rash on the right side of the neck of a patient with Lyme disease, central North Carolina, USA.

Author affiliations: University of North Carolina at Chapel Hill, Chapel Hill, North Carolina, USA (R.M. Boyce, P. Pretsch, K. Tyrlik, D.A. Giandomenico); University of Illinois College of Medicine at Peoria, Peoria, Illinois, USA (A. Schulz); North Carolina Department of Health and Human Services, Raleigh, North Carolina, USA (A.M. Barbarin, C. Williams)

DOI: https://doi.org/10.3201/eid3003.231302

Table. Select clinical and laboratory information for a patient with Lyme disease, central North Carolina, USA*

Characteristic	Range	Day of illness (provider)			
		Day 10 (PCP)	Day 28 (PCP)	Day 43 (PCP)	Day 83 (ID clinic)
Signs/symptoms					
Fever ≥38.0°C		X			
Rash		X			
Fatigue		X			
Headache			X		
Itching			X		
Left-sided ear pain			X	X	
Left sided asymmetric smile				X	
Inability to close left eye				X	
Cognitive impairment				X	X
Other					
Laboratory testing					
Complete blood count					
Leukocytes, cells/mm^3	4.0–11.0		6.1		
Hemoglobin, mg/dL	12.9–16.0		13.3		
Platelets, × 10^9/L	150–400		193		
Metabolic panel					
Sodium, mmol/L	136–145		138		
Potassium, mmol/L	3.5–5.5		4.0		
Creatinine, mg/dL	0.6–1.30		0.70		
Liver function, U/L					
Alkaline phosphatase	38–126				
Aspartate aminotransferase	0–39				
Alanine aminotransferase	0–52				
C-reactive protein, mg/L	≤10		10.2		<4.0
Sedimentation rate, mm/h	0–30		42		16
Tick-borne disease testing					
Lyme EIA	<0.91				Positive
Lyme Western blot					
IgM	0 of 3 bands				p41, p39, p23
IgG	0 of 10 bands				p66, p45, p41, p39, p23, p18
SFGR IgG	<1:64				<1:64
Ehrlichia IgG	<1:64				<1:64
α-gal IgE, kUA/L	<0.35†				0.43
Other infectious diseases					
HIV antigen/antibody	Nonreactive				Nonreactive
Syphilis antibody RPR	Nonreactive				Nonreactive
Diagnosis		Cellulitis		Bell's palsy	Lyme disease
Treatment		Cephalexin, bactrim	Erythromycin	Valacyclovir, prednisone	Doxycycline

*EIA, enzyme immunoassay; ID, infectious disease; PCP, primary care provider; RPR, rapid plasma reagin; SFGR, spotted fever group *Rickettsia*; X, present.
†Reference range <0.1 kUA/L (kUA/L level of allergy): <0.35 absent, 0.35–0.69 low, 0.70–3.49 moderate, 3.50–17.5 high, >17.5 very high.

The headaches persisted after the antibiotic change, and the next day the patient visited a local emergency department. Results of basic laboratory evaluations, including a complete blood count and comprehensive metabolic panel, were unremarkable. She underwent a noncontrast computed tomography scan of the head, which was interpreted as without findings that would explain her symptoms. She was subsequently discharged to home.

Ten days later, the patient returned to her PCP for follow-up and was seen by the on-call provider. She still reported pain in her ears and that the pain in the left ear was more severe than the right. She was now experiencing diffuse pruritis, which was thought to be caused by trimethoprim/sulfamethoxazole. The antibiotic was discontinued because the rash appeared to be resolving. However, she also noted more dyspnea with exertion. Additional laboratory testing was ordered, including a complete blood count, comprehensive metabolic panel, C-reactive protein, and erythrocyte sedimentation rate; the erythrocyte sedimentation rate was slightly elevated (Table). The patient was prescribed erythromycin drops for otitis media. A referral to cardiology was placed for evaluation of the exertional dyspnea.

After that visit, the patient became increasingly forgetful, withdrawn, and unable to perform basic cognitive tasks (e.g., simple calculations), which was noticed by her adult children. Two weeks later, ≈1 month after the rash began, she had onset of a left-sided facial droop. On evaluation, her PCP noted that she was unable to close her left eye and her smile was asymmetric on the same side. She was diagnosed with Bell's palsy and prescribed a 1-week course of prednisone and valacyclovir. The facial nerve symptoms slowly improved and eventually resolved over the next week.

The next month, the patient reported more back pain with spasms that radiated into the cervical spine and neck. She underwent magnetic resonance imaging of the spine, which demonstrated degenerative changes but no findings that would explain her symptoms. Her children remained concerned about her cognitive status, anorexia, and unintentional 10-pound weight loss, and they requested additional consultations, including with a subspecialist in infectious diseases.

The patient was seen in an outpatient infectious diseases clinic ≈2 months after the onset of symptoms. Although the patient did not recall any insect bites, her adult son recalled a small punctate lesion in the central part of the initial rash. Other than the bike rides, her only risk factor for tick or mosquito exposure was working in the flower garden in her yard. She did note that there were frequently deer on the property and that the family dog often slept in her bed. She had not traveled outside the local area during the previous year. Vital signs were within reference limits, and her examination was notable only for slow responses to questions and difficulty recalling recent events. Laboratory tests for tickborne and other infectious diseases, including Lyme disease, spotted fever rickettsiosis, ehrlichiosis, and α-gal syndrome, were ordered. No antibiotics were prescribed during the visit.

Results of the Lyme disease enzyme immunoassay were positive. The sample was reflexed to a Western blot, which showed positive results (6 of 10 IgG bands reactive). The patient was prescribed a 28-day course of oral doxycycline. Substantial improvement in her mood, cognitive function, and energy levels were noted within 3 days. She completed the course of doxycycline without issue. At follow-up 1 month later, the patient reported feeling at her recent baseline, and her children no longer expressed concerns over her health. A mildly elevated α-gal result was discussed, but the patient was not experiencing any symptoms associated with the consumption of mammalian meat products.

Conclusions

Given the relatively mild manifestations of early symptoms during Lyme disease, most patients are seen in the outpatient setting. Therefore, primary care providers play an important role in the diagnosis and management of Lyme disease and are key targets for outreach. We believe the following 2 topics merit mention. First, in 2019, the Centers for Disease Control and Prevention approved the use of a modified 2-tier test in which the traditional Western blot is replaced by a second enzyme immunoassay, which is easier to interpret and has improved sensitivity in early disease (*10–12*). Some commercial laboratories in North Carolina have already transitioned to the modified 2-tier test. Second, postexposure prophylaxis with a single 200-mg dose of doxycycline has not routinely been used but warrants consideration in many areas of the state if other criteria are met (*13*,*14*).

Although the patient did not have obvious exposures to ticks, her clinical manifestations were highly suggestive of Lyme disease. In addition to the nonspecific constitutional symptoms, such as malaise, she also had a large erythema migrans rash that appeared within 1 week of the likely exposure, followed by Bell's palsy approximately 1 month later. During that period, she had visits with multiple clinicians and underwent a wide range of testing but never had specific testing or treatment for Lyme disease. Those delays, especially in the context of southward expansion of the disease along the Appalachian Mountains, highlight the need for greater awareness and professional education among healthcare providers in North Carolina (*2*,*3*).

Acknowledgments

We thank the staff of the University of North Carolina Infectious Diseases Clinic for their ongoing compassionate and high-quality care of patients like the one described in this article.

About the Author

Dr. Boyce is an assistant professor of medicine and epidemiology at the University of North Carolina at Chapel Hill. His research and clinical practice are focused on domestic and international vectorborne diseases.

References

1. Fleshman AC, Graham CB, Maes SE, Foster E, Eisen RJ. Reported county-level distribution of Lyme disease spirochetes, *Borrelia burgdorferi sensu stricto* and *Borrelia mayonii* (Spirochaetales: Spirochaetaceae), in host-seeking *Ixodes scapularis* and *Ixodes pacificus* ticks (Acari: Ixodidae) in the contiguous United States. J Med Entomol. 2021;58:1219–33. https://doi.org/10.1093/jme/tjaa283
2. Lantos PM, Nigrovic LE, Auwaerter PG, Fowler VG Jr, Ruffin F, Brinkerhoff RJ, et al. Geographic expansion of Lyme disease in the southeastern United States, 2000–2014. Open Forum Infect Dis. 2015;2:ofv143. https://doi.org/10.1093/ofid/ofv143

3. Barbarin AM, Seagle SW, Creede S. Notes from the field: four cases of Lyme disease at an outdoor wilderness camp—North Carolina, 2017 and 2019. MMWR Morb Mortal Wkly Rep. 2020;69:114–5. https://doi.org/10.15585/mmwr.mm6904a5
4. Centers for Disease Control and Prevention. National Notifiable Diseases Surveillance System, 2016 annual tables of infectious disease data [cited 2023 Nov 12]. https://www.cdc.gov/nndss/infectious-tables.html
5. Levine JF, Apperson CS, Spiegel RA, Nicholson WL, Staes CJ. Indigenous cases of Lyme disease diagnosed in North Carolina. South Med J. 1991;84:27–31. https://doi.org/10.1097/00007611-199101000-00008
6. Apperson CS, Levine JF, Nicholson WL. Geographic occurrence of *Ixodes scapularis* and *Amblyomma americanum* (Acari: Ixodidae) infesting white-tailed deer in North Carolina. J Wildl Dis. 1990;26:550–3. https://doi.org/10.7589/0090-3558-26.4.550
7. Arsnoe IM, Hickling GJ, Ginsberg HS, McElreath R, Tsao JI. Different populations of blacklegged tick nymphs exhibit differences in questing behavior that have implications for human Lyme disease risk. PLoS One. 2015;10:e0127450. https://doi.org/10.1371/journal.pone.0127450
8. Centers for Disease Control and Prevention. Data and surveillance. 2022 [cited 2023 Aug 6]. https://www.cdc.gov/lyme/datasurveillance/index.html
9. Boyce RM, Speight C, Lin JT, Farel CE. Errors in diagnostic test use and interpretation contribute to the high number of Lyme disease referrals in a low-incidence state. Open Forum Infect Dis. 2020;7(1):ofaa009.
10. Mead P, Petersen J, Hinckley A. Updated CDC recommendation for serologic diagnosis of Lyme disease. MMWR Morb Mortal Wkly Rep. 2019;68:703. https://doi.org/10.15585/mmwr.mm6832a4
11. Pegalajar-Jurado A, Schriefer ME, Welch RJ, Couturier MR, MacKenzie T, Clark RJ, et al. Evaluation of modified two-tiered testing algorithms for Lyme disease laboratory diagnosis using well-characterized serum samples. J Clin Microbiol. 2018;56:e01943-17. https://doi.org/10.1128/JCM.01943-17
12. Khan F, Allehebi Z, Shabi Y, Davis I, LeBlanc J, Lindsay R, et al. Modified two-tiered testing enzyme immunoassay algorithm for serologic diagnosis of Lyme disease. Open Forum Infect Dis. 2022 Jul;9(7):ofac272.
13. Nadelman RB, Nowakowski J, Fish D, Falco RC, Freeman K, McKenna D, et al.; Tick Bite Study Group. Prophylaxis with single-dose doxycycline for the prevention of Lyme disease after an *Ixodes scapularis* tick bite. N Engl J Med. 2001;345:79–84. https://doi.org/10.1056/NEJM200107123450201
14. Lantos PM, Rumbaugh J, Bockenstedt LK, Falck-Ytter YT, Aguero-Rosenfeld ME, Auwaerter PG, et al. Clinical practice guidelines by the Infectious Diseases Society of America (IDSA), American Academy of Neurology (AAN), and American College of Rheumatology (ACR): 2020 guidelines for the prevention, diagnosis and treatment of Lyme disease. Clin Infect Dis. 2021;72:e1–48. https://doi.org/10.1093/cid/ciaa1215

Address for correspondence: Ross M. Boyce, Division of Infectious Diseases, University of North Carolina at Chapel Hill, 123 W Franklin St, Ste 2151, Chapel Hill, NC 27516, USA; email: roboyce@med.unc.edu

etymologia revisited

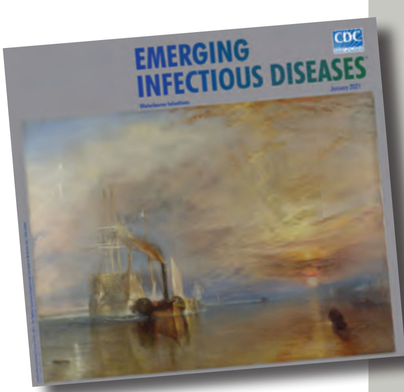

Petri Dish

[pe′tre ′dish]

The Petri dish is named after the German inventor and bacteriologist Julius Richard Petri (1852–1921). In 1887, as an assistant to fellow German physician and pioneering microbiologist Robert Koch (1843–1910), Petri published a paper titled "A minor modification of the plating technique of Koch." This seemingly modest improvement (a slightly larger glass lid), Petri explained, reduced contamination from airborne germs in comparison with Koch's bell jar.

References:

1 Central Sheet for Bacteriology and Parasite Science [in German]. Biodiversity Heritage Library. Volume 1, 1887 [cited 2020 Aug 25]. https://www.biodiversitylibrary.org/item/210666#page/313/mode/1up
2. Petri JR. A minor modification of the plating technique of Koch [in German]. Cent für Bacteriol und Parasitenkd. 1887;1:279–80.
3. Shama G. The "Petri" dish: a case of simultaneous invention in bacteriology. Endeavour. 2019;43:11–6.
4. The big story: the Petri dish. The Biomedical Scientist. Institute of Biomedical Science [cited 2020 Aug 25]. https://thebiomedicalscientist.net/science/big-story-petri-dish

Originally published in January 2021

https//wwwnc.cdc.gov/eid/article/27/1/et-2701_article

Bedaquiline Resistance after Effective Treatment of Multidrug-Resistant Tuberculosis, Namibia

Gunar Günther, Lusia Mhuulu, Azaria Diergaardt, Viola Dreyer, Maria Moses, Kaarna Anyolo, Nunurai Ruswa, Mareli Claassens, Stefan Niemann,[1] Emmanuel Nepolo[1]

Bedaquiline is currently a key drug for treating multidrug-resistant or rifampin-resistant tuberculosis. We report and discuss the unusual development of resistance to bedaquiline in a teenager in Namibia, despite an optimal background regimen and adherence. The report highlights the risk for bedaquiline resistance development and the need for rapid drug-resistance testing.

The development of bedaquiline, and its inclusion in first-line treatment of rifampin-resistant (RR) and multidrug-resistant (MDR, resistance to isoniazid and rifampin) tuberculosis (TB), along with linezolid, pretomanid, and moxifloxacin, the BPaL(M) regimen, has transformed the management of drug-resistant TB (*1*). The World Health Organization (WHO) began recommending BPaL(M) in 2022. However, recent studies have reported the emergence of bedaquiline resistance, which suggests that BPaL(M) may be unable to prevent bedaquiline resistance at population level (*2*,*3*). The mechanisms underlying the selection and spread of bedaquiline resistance are not yet well understood. We describe bedaquiline resistance evolution in a patient with MDR TB who had extensive bilateral pulmonary infiltrates despite a regimen of 6 effective drugs.

Author affiliations: Inselspital Bern, Bern University Hospital, University of Bern, Bern, Switzerland (G. Günther); University of Namibia, Windhoek, Namibia (G. Günther, L. Mhuulu, A. Diergaardt, M. Claassens, S. Niemann, E. Nepolo); Katutura State Hospital, Windhoek, Namibia (G. Günther, M. Moses, K. Anyolo); Research Center Borstel, Borstel, Germany (V. Dreyer, S. Niemann); German Center for Infection Research, Partner Site Hamburg-Lübeck-Borstel-Riems, Borstel (V. Dreyer, S. Niemann); National Tuberculosis and Leprosy Programme, Windhoek, Namibia (N. Ruswa)

DOI: https://doi.org/10.3201/eid3003.240134

The Study

In October 2022, a 16-year-old HIV-negative female patient sought care at a clinic in Windhoek, Namibia. She was severely underweight (BMI 16 kg/m^2) and had radiologic findings of extensive, bilateral destruction of the lung parenchyma (Figure 1). The patient reported treatment for drug-sensitive TB with a standard first-line regimen since December 2021 in neighboring Angola, but she had treatment interruptions caused by stockout (Figure 2, panel A). Initial molecular sputum diagnostics using Xpert MTB/RIF Ultra (Cepheid, https://www.cepheid.com) confirmed an infection with *Mycobacterium tuberculosis* with rifampin resistance. A line probe assay (Genotype MTBDR*plus* and MTBDR*sl*; Hain Lifescience, https://www.hain-lifescience.de) confirmed resistance to rifampin and additional resistance to isoniazid, whereas there was no resistance to fluoroquinolones. Sputum-smear microscopy demonstrated 3+ positive acid-fast bacilli (AFB). Rapid molecular drug-susceptibility testing (DST) was performed on DNA isolated from an initial positive *M. tuberculosis* culture using targeted next-generation sequencing Deeplex Myc-TB assay (Genoscreen, https://www.genoscreen.fr). We identified mutations katG S315T, rpoB L430P, and embB M306I, which indicated resistance to isoniazid, rifampin, and ethambutol (Figure 2, panel B). We confirmed the resistance pattern by phenotypic DST in mycobacterial growth indicator tube (MGIT; Becton Dickinson, https://www.bd.com) at the supranational reference TB laboratory (National Institute for Communicable Diseases, Johannesburg, South Africa).

In response to the patient's extensive lung infiltration and high bacterial load, we initiated a regimen with 6 drugs: bedaquiline, linezolid, levofloxacin, cycloserine, clofazimine, and pyrazinamide (Figure 2, panel A).

[1]These authors contributed equally to this article.

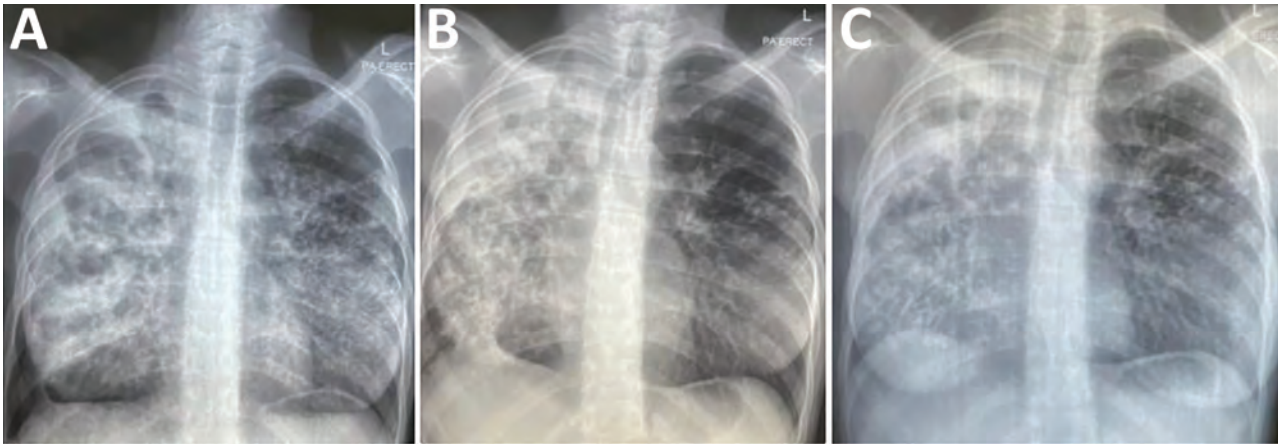

Figure 1. Chest radiographs showing lungs of tuberculosis patient in Namibia who had bedaquiline resistance develop. A) At treatment initiation; B) at culture conversion; C) 3 months after conversion.

We ensured adherence by inpatient directly observed treatment. Clinical and microbiological response was slow; culture and smear microscopy results were negative once after 5 months of treatment (Figure 2, panel C). However, culture reversion occurred, and sustained culture conversion was never achieved despite clinical and transient radiologic improvement (Figure 1). Subsequent molecular DST based on targeted next-generation sequencing documented several frame shift mutations in *Rv0678* at position 779127 with 3.5% variant frequency, at 779130 with 16.0% frequency, and at 779407 with 27.8% frequency. Mutations in *rpoB*, *katG* and *embB* remained unchanged to baseline molecular DST. The de novo mutations were associated with phenotypic resistance to bedaquiline and clofazimine. All other drugs tested remained susceptible in molecular and phenotypic DST (Figure 2, panel B). We stopped bedaquiline and clofazimine administration and added 3 drugs, amikacin, meropenem/amoxicillin/clavulanic acid, and pretomanid, to maximize the probability of achieving conversion and cure. Treatment was ongoing as of February 2024.

Conclusions

Bedaquiline has been shown to be a key drug for improving outcomes in MDR/RR TB patients (*4*). However, recent studies have demonstrated the emergence of bedaquiline resistance in patients failing MDR TB treatment, which, at the population level, points toward rapid bedaquiline resistance evolution and spread (*3*,*5*). Our results are particularly alarming because we demonstrated the evolution of bedaquiline resistance despite the use of an effective background regimen and well-documented adherence to treatment. This result is in line with the findings of recently published work from Mozambique, in which Barilar et al. demonstrated that bedaquiline resistance was found not only in *M. tuberculosis* strains resistant to fluoroquinolones but also in MDR or RR *M. tuberculosis* strains susceptible to other drugs used in the BPaL(M) regimen (*3*).

Taking all evidence together, the data suggest that current MDR/RR TB treatment regimens are unable to prevent the development of bedaquiline resistance in a subset of patients. A specific combination of pharmacokinetic and pharmacodynamic properties of the drug and pathogen or patient markers potentially result in rapid resistance development. Detecting 3 different *Rv0678* variants in the patient sample analyzed, an observation also made for several bedaquiline-resistant strains found previously (*3*,*6*), supports this observation.

In general, bedaquiline and clofazimine cross-resistance can result from underlying pretreatment resistance by infection with an already resistant strain, presence of heteroresistant strains and clonal populations, and de novo evolution of resistance during treatment (*5*). Here we demonstrate the rapid evolution and selection of several bedaquiline resistant subpopulations, despite resistance-appropriate treatment with 6 effective drugs. Our findings suggest a high bedaquiline resistance mutation rate that enables parallel emergence of different bedaquiline-resistant populations with different *Rv0678* mutations in a given patient. That finding is also supported by large-scale sequencing data obtained from patients with bedaquiline resistance in Mozambique (*3*).

In a recent meta-analysis, Mallik et al. reported acquired phenotypic bedaquiline resistance in 2.2%, genotypic resistance in 4.4% of cases (*5*), whereas Perumal et al. reported phenotypic resistance in 2.1% of cases (*7*). Future studies should further investigate mechanisms of bedaquiline resistance development, for example, to identify patients at risk. Bedaqui-

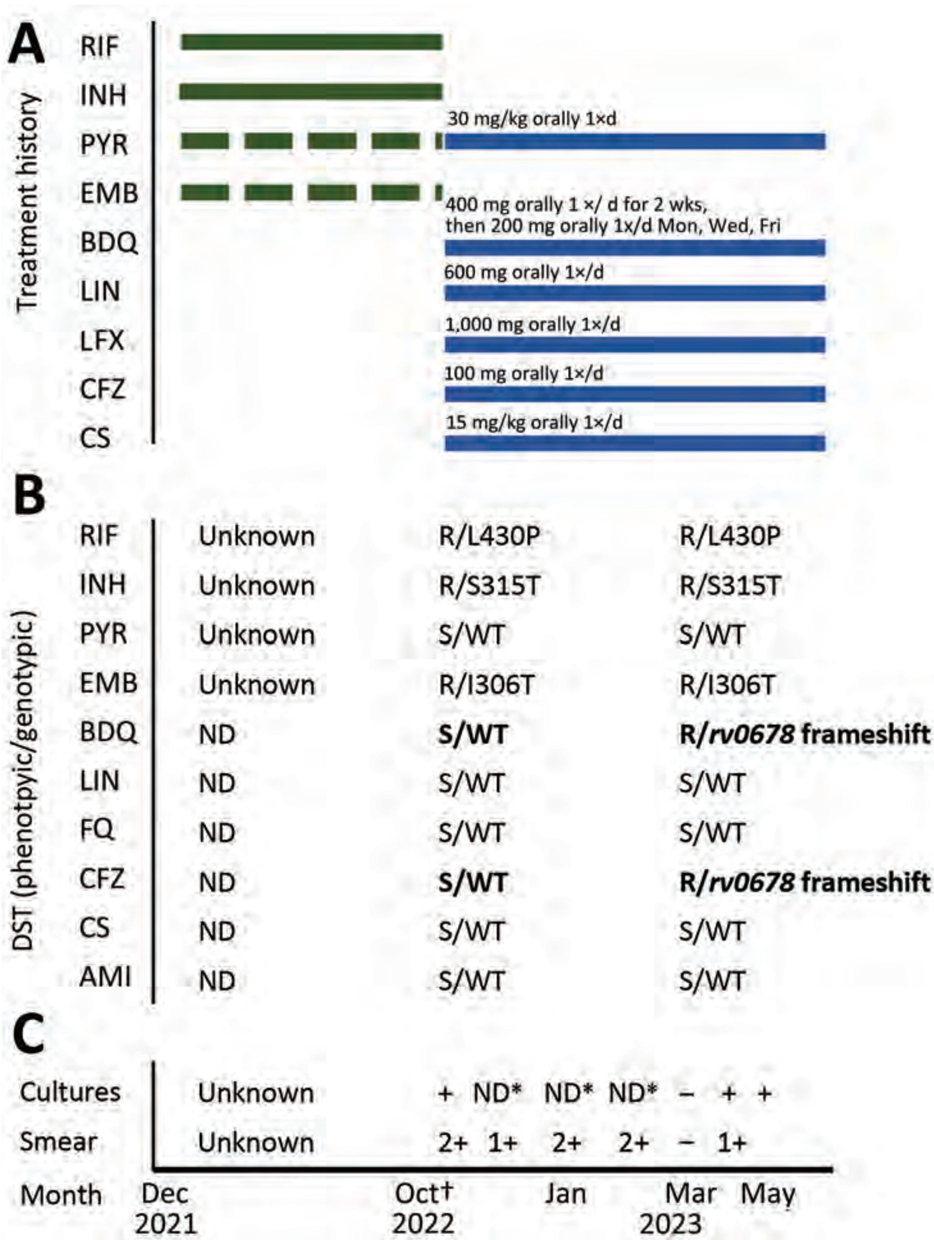

Figure 2. Timeline for a case of tuberculosis in a patient in Namibia whose infection became drug resistant after effective treatment. The case was originally diagnosed and treated beginning in December 2021. Interruptions in treatment were caused by stockout. Second-line drugs were not used. Full detailed treatment history is unknown. The patient sought care in Namibia in September 2022; we diagnosed MDR TB in October 2022. Treatment failed and rv0678 mutation was identified in a culture from June 2023. A) Patient's treatment history. Green bars represent treatment of drug-susceptible TB; blue bars represent treatment of MDR TB. B) Evolution of phenotypic and genotypic drug susceptibility testing with resistance-associated variants using Deeplex Myc TB (https://www.deeplex.com). Testing was done at time of diagnosis of MDR TB and after culture reversion. Bold text indicates de novo mutation Months show time of specimen collection. C) Culture and smear test results. Asterisks indicate that tests were not done because of stockouts. Months show time of specimen collection. Dagger indicates start of MDR TB treatment. AMI, amikacin; BDQ, bedaquiline; CFZ, clofazimine; CS, cycloserine; DS, drug-susceptible; EMB, ethambutol; FQ, fluoroquinolones; INH, isoniazid; LIN, linezolid; LFX, levofloxacin; MDR, multidrug-resistant; ND, not done; PYR, pyrazinamide; R, resistant; RIF, rifampin; S, susceptible; TB, tuberculosis; WT, wild type.

line seems to have a delayed bactericidal response, which could be a risk factor for drug resistance developing during early treatment, particularly in extensive disease (*8*). Some studies suggested the use of highly bactericidal companion drugs in combination with bedaquiline. Van Deun et al. reviewed the regimen composition on the basis of the concept of core drugs and companion drugs (*9*). In accordance with this strategy, our patient received 2 core drugs (bedaquiline and levofloxacin), 1 highly bactericidal companion drug (linezolid) and 2 highly sterilizing drugs (pyrazinamide and clofazimine); we added cycloserine. Despite strictly following van Deun's concept of effective regimen composition, resistance to bedaquiline/clofazimine developed in the patient discussed here, who had severe lung destruction and high bacterial load. Derendinger et al. described acquired bedaquiline resistance in routine care in South Africa and considered use of $\leq$4 effective drugs, fluoroquinolone resistance, and previous or concurrent clofazimine use as risk factors for bedaquiline resistance (*6*). None of those factors were present in the case we describe.

Shao et al. showed in their population pharmocokinetic model that the current WHO recommended dosing of bedaquiline achieves a probability >90% of target attainment (*10*). However, Tanneau et al. proposed an exposure–response relationship for bedaquiline, whereas the half-life of bacterial clearance was longer in pre–extensively drug-resistant (XDR) and XDR TB than in MDR TB. One might speculate that dose adjustments to bedaquiline favorably influence treatment outcomes (*11*), as has been done so far in individual cases applying therapeutic drug monitoring (*12*).

In conclusion, this case demonstrates the rapid evolution of phenotypic and genotypic resistance to bedaquiline and clofazimine, despite an effective individualized regimen. This finding is alarming because the BPaL(M) regimen may not be completely effective in an unknown proportion of patients. In particular, cases of extensive disease might be associated with a high risk for resistance and failure in real-world scenarios. We recommend further research into mechanisms of resistance, and prevention thereof, as well as rapid scale-up of DST capacity to identify and properly treat such cases as quickly as possible.

Acknowledgment

We thank the National Institute for Communicable Diseases, TB Laboratory, Johannesburg, South Africa

About the Author

Dr. Günther is a clinician scientist, working as senior pulmonologist at Inselspital Bern in Switzerland. After working full time from 2015–2019 at the Katutura Tuberculosis Hospital and the University of Namibia in Windhoek, Namibia, he has continued his assignment at both institutions part-time since 2019.

References

1. World Health Organization. WHO consolidated guidelines on tuberculosis. Module 4: treatment—drug-resistant tuberculosis treatment, 2022 update. Geneva: The Organization; 2022.
2. Millard J, Rimmer S, Nimmo C, O'Donnell M. Therapeutic failure and acquired bedaquiline and delamanid resistance in treatment of drug-resistant TB. Emerg Infect Dis. 2023;29:1081–4. https://doi.org/10.3201/eid2905.221716
3. Barilar I, Fernando T, Utpatel C, Abujate C, Madeira CM, José B, et al. Emergence of bedaquiline-resistant tuberculosis and of multidrug-resistant and extensively drug-resistant *Mycobacterium tuberculosis* strains with *rpoB* Ile491Phe mutation not detected by Xpert MTB/RIF in Mozambique: a retrospective observational study. Lancet Infect Dis. 2023;S1473-3099(23)00498-X; [Epub ahead of print].
4. Roelens M, Battista Migliori G, Rozanova L, Estill J, Campbell JR, Cegielski JP, et al. Evidence-based definition for extensively drug-resistant tuberculosis. Am J Respir Crit Care Med. 2021;204:713–22.
5. Perumal R, Bionghi N, Nimmo C, Letsoalo M, Cummings MJ, Hopson M, et al. Baseline and treatment-emergent bedaquiline resistance in drug-resistant tuberculosis: a systematic review and meta-analysis. Eur Respir J. 2023; 62:2300639. https://doi.org/10.1183/13993003.00639-2023
6. Derendinger B, Dippenaar A, de Vos M, Huo S, Alberts R, Tadokera R, et al. Bedaquiline resistance in patients with drug-resistant tuberculosis in Cape Town, South Africa: a retrospective longitudinal cohort study. Lancet Microbe. 2023;4:e972–82. https://doi.org/10.1016/S2666-5247(23)00172-6
7. Mallick JS, Nair P, Abbew ET, Van Deun A, Decroo T. Acquired bedaquiline resistance during the treatment of drug-resistant tuberculosis: a systematic review. JAC Antimicrob Resist. 2022 Mar 29;4:dlac029. https://doi.org/10.1093/jacamr/dlac029
8. Koul A, Vranckx L, Dhar N, Göhlmann HWH, Özdemir E, Neefs JM, et al. Delayed bactericidal response of *Mycobacterium tuberculosis* to bedaquiline involves remodelling of bacterial metabolism. Nat Commun. 2014; 5:3369. https://doi.org/10.1038/ncomms4369
9. Van Deun A, Decroo T, Piubello A, de Jong BC, Lynen L, Rieder HL. Principles for constructing a tuberculosis treatment regimen: the role and definition of core and companion drugs. Int J Tuberc Lung Dis. 2018;22:239–45. https://doi.org/10.5588/ijtld.17.660
10. Shao G, Bao Z, Davies Forsman L, Paues J, Werngren J, Niward K, et al. Population pharmacokinetics and model-based dosing evaluation of bedaquiline in multidrug-resistant tuberculosis patients. Front Pharmacol. 2023; 14:1022090. https://doi.org/10.3389/fphar.2023.1022090
11. Tanneau L, Karlsson MO, Svensson EM. Understanding the drug exposure-response relationship of bedaquiline to predict efficacy for novel dosing regimens in the treatment of multidrug-resistant tuberculosis. Br J Clin Pharmacol. 2020;86:913–22. https://doi.org/10.1111/bcp.14199
12. Koehler N, Andres S, Merker M, Dreyer V, John A, Kuhns M, et al. Pretomanid-resistant tuberculosis. J Infect. 2023;86:520–4. https://doi.org/10.1016/j.jinf.2023.01.039

Address for correspondence: Gunar Günther, University of Bern, Freiburgstrasse 20, 3010 Bern, Switzerland; email: gunar.guenther@insel.ch

High Prevalence of *Echinostoma mekongi* Infection in Schoolchildren and Adults, Kandal Province, Cambodia

Bong-Kwang Jung,[1] Taehee Chang,[1] Seungwan Ryoo, Sooji Hong, Jeonggyu Lee, Sung-Jong Hong, Woon-Mok Sohn, Virak Khieu, Rekol Huy, Jong-Yil Chai

A high prevalence of *Echinostoma mekongi* infection (13.9%; 260/1,876) was found among schoolchildren and adults in Kandal Province, Cambodia, by fecal examination, worm expulsion, and molecular analysis of *cox*1 and *nd*1 genes. The source of infection was consumption of *Pila* sp. snails, a finding confirmed morphologically and molecularly.

Echinostomiasis is a disease caused by infection with echinostome flukes (Echinostomatidae) and is characterized by intestinal inflammation accompanied by mucosal ulceration and bleeding (*1,2*). Echinostomiasis, a typical example of a foodborne helminthiasis, is contracted by consuming raw or improperly cooked snails, bivalves, fish, or amphibians (*1,2*). This disease has been neglected mainly because of underestimated prevalence and worm burden (global prevalence and burden unknown) as well as underrecognized clinical and public health significance. In South Korea and Japan, patients infected with the echinostome *Isthmiophora hortensis* reported gastrointestinal issues, and diagnosis was established after physicians extracted adult worms via gastrointestinal endoscopy (*1*).

Author affiliations: MediCheck Research Institute, Korea Association of Health Promotion, Seoul, South Korea (B.-K. Jung, S. Ryoo, S. Hong, J. Lee); Seoul National University Graduate School of Public Health, Seoul (T. Chang); Seoul National University College of Medicine, Seoul (J.-Y. Chai); Convergence Research Center for Insect Vectors, Inchon National University, Incheon, South Korea (S.-J. Hong); Gyeongsang National University College of Medicine, Jinju, South Korea (W.-M. Sohn); National Center for Parasitology, Entomology and Malaria Control, Ministry of Health, Phnom Penh, Cambodia (V. Khieu, R. Huy)

DOI: http://doi.org/10.3201/eid3003.240001

Echinostoma mekongi was described as a new human-infecting echinostome that emerged in Kratie and Takeo Province, Cambodia, and identified through morphologic and molecular analyses (*3*). The adult flukes were recovered from persons residing along the Mekong River in these provinces, who reported abdominal discomfort, indigestion, and other gastrointestinal troubles (*3*). The metacercarial stage of *E. mekongi* was detected in freshwater snails, *Filopaludina martensi cambodjensis*, a popular food item in Pursat Province (*4*). We found a highly endemic area of *E. mekongi* infection in riverside villages of Kandal Province (surrounding Phnom Penh, the capital; population ≈1.27 million). Adult flukes were expelled after chemotherapy and purging and then analyzed morphologically and molecularly (*cox*1 and *nd*1 genes). Freshwater snails, *Pila* sp., were verified to be the source of infection, but the first intermediate host and the natural definitive host other than humans remain unknown.

The Study

We collected fecal samples in May 2019 from 1,876 villagers, including 1,631 schoolchildren (794 boys and 837 girls, 5–19 years of age) and 245 adults (89 men and 156 women, 20–85 years of age), residing along the Mekong River in Kandal Province, Cambodia (Figure 1, panel A). We examined samples for helminth eggs by using the Kato-Katz thick-smear technique. The overall helminth egg-positive rate was 16.5%. The egg-positive rate of *E. mekongi* was 13.9% and markedly higher (>5 times) in schoolchildren (15.5%) than in adults (2.9%) (Table 1). *E. mekongi* eggs were operculated, oval to ovoid, yellowish,

[1]These authors contributed equally to this article.

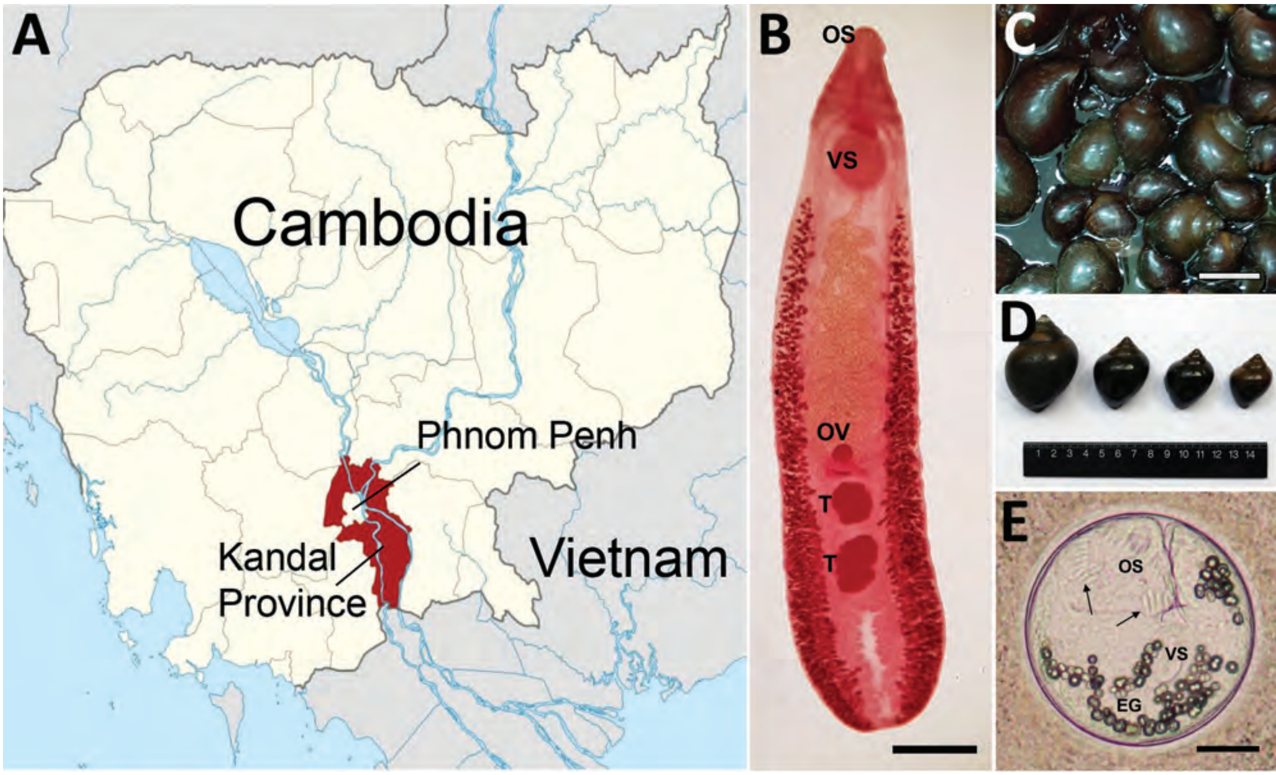

Figure 1. Study area and specimens of *Echinostoma mekongi* flukes and *Pila* sp. snails for study of *E. mekongi* infection in schoolchildren and adults, Kandal Province, Cambodia. A) Study area in Cambodia. B) Adult specimen of *E. mekongi* fluke expelled from a volunteer after chemotherapy and purging. Scale bar = 1.2 mm. C, D) *Pila* sp. snails purchased from a local market in Kandal Province, showing variable sizes. The presence of metacercariae in these snails was confirmed. Scale bar in panel D = 3 cm. E) Metacercaria of *E. mekongi* encysted in the tissue of a *Pila* sp. snail, showing its characteristic structures, including 37 collar spines (arrows), oral sucker, ventral sucker, and excretory granules. Scale bar = 50 m. EG, excretory granules; OS, oral sucker; OV, ovary; T, testis; VS, ventral sucker.

thin-shelled, and 102–130 (average 116) µm long and 62–90 (average 76) µm wide (n = 10). Other helminth species detected were *Opisthorchis viverrini* (0.9%), hookworms (0.7%), *Enterobius vermicularis* (0.7%), *Hymenolepis nana* (0.7%), *Trichuris trichiura* (0.3%), and others (Table 1).

We recruited 8 schoolchildren and 2 adult volunteers for the recovery of *E. mekongi* adult flukes (Table 2) and administered a single oral dose of 10–15 mg/kg praziquantel (Shin Poong Pharm. Co., https://shinpoong.co.kr/en/main/main.php), followed by purging with 20–30 g magnesium sulfate. We collected whole diarrheic stools 3 to 5 times and pooled them individually. We fixed adult flukes in 10% formalin, stained the samples with acetocarmine, cleared each in glycerin-alcohol, and mounted the samples in glycerin jelly. We kept some samples in 70%–80% ethanol for molecular analyses.

We recovered 48 adult and 38 juvenile specimens (86 in total) of *E. mekongi* flukes from the 10 volunteers (Table 2). Schoolchildren (n = 8) expelled a total of 64 worms (8 per child), and adults (n = 2) passed a total of 22 worms (11 per person) (Table 2). The adult flukes (Figure 1, panel B) were elongated and leaflike, with small head collars and small collar spines (37 in 2 alternating rows; 5 corner spines), globular or slightly lobed testes, vitelline follicles not merging near the posterior end, and 7.7–11.2 (average 9.5) mm

Table 1. Results of fecal examinations in study of *Echinostoma mekongi* infection among schoolchildren and adults in riverside villages along the Mekong River in Kandal Province, Cambodia*

		No. (%) egg-positive cases									
Age group	No. examined	Any helminth egg	Em	Ov	Sm	Hw	Al	Tt	Ev	Hn	*Taenia* sp.
Schoolchildren	1,631	290 (17.8)	253 (15.5)	11 (0.7)	1 (0.1)	8 (0.5)	2 (0.1)	5 (0.3)	10 (0.6)	10 (0.6)	1 (0.1)
Adults	245	20 (8.2)	7 (2.9)	6 (2.4)	1 (0.4)	6 (2.4)	0	0	1 (0.4)	1 (0.4)	0
Total	1,876	310 (16.5)	260 (13.9)	17 (0.9)	2 (0.1)	14 (0.7)	2 (0.1)	5 (0.3)	11 (0.6)	11 (0.6)	1 (0.1)

*Em, *Echinostoma mekongi*; Ov, *Opisthorchis viverrini*; Sm, *Schistosoma mekongi*; Hw, hookworms; Al, *Ascaris lumbricoides*; Tt, *Trichuris trichiura*; Ev, *Enterobius vermicularis*; Hn, *Hymenolepis nana*.

Table 2. Worm expulsion after praziquantel treatment and purging from volunteers positive for *Echinostoma mekongi* eggs in fecal examinations in study of *Echinostoma mekongi* infection in schoolchildren and adults, Kandal Province, Cambodia*

Age group and code no.	Age, y	No. *E. mekongi* eggs in Kato-Katz fecal smears†	No. adult *E. mekongi* fluke specimens expelled‡
Schoolchildren			
1	15	168	46
2	15	264	6
3	16	96	4
4	16	480	2
5	14	168	2
6	13	216	2
7	13	168	1§
8	12	48	1
Adults			
1	46	720	15
2	41	120	7§

*All case-patients were female. Fecal samples were collected individually 2–3 h after praziquantel administration and purging with $MgSO_4$.
†Eggs/g of feces; amount in a typical smear was assumed to be 41.7 mg.
‡All recovered worms were adults that contained eggs except for 38 of 46 worms from schoolchildren case 1, which were juvenile or young adults containing no or only a few uterine eggs.
§Adult specimens of *Enterobius vermicularis* (120 female worms in schoolchildren no. 7 and 1 female worm in adult no. 2) were collected simultaneously

by 1.8–2.3 (average 2.1) mm in size (n = 10), all characteristic features of *E. mekongi* flukes (*3*).

We purchased *Pila* sp. snails (Figure 1, panels C and D) at a local market in Kandal Province and examined them for metacercariae by using the crushing method. We detected 10 metacercariae in 5 (7.1%) of 70 snails examined. The metacercariae (n = 5) were round, 165–188 (average 176) µm in diameter (Figure 1, panel E), and encysted with a thin, pinkish, refractile wall. The metacercariae were equipped with a total of 37 collar spines, oral and ventral suckers, excretory granules, and other internal organs.

We obtained mitochondrial cytochrome *c* oxidase 1 (*cox*1) and NADH dehydrogenase subunit 1 (*nd*1) gene sequences for molecular analyses of the adult flukes and metacercariae. We extracted the genomic DNA of each segment by using the DNeasy Blood and Tissue kit (QIAGEN, https://www.qiagen.com/us), following the manufacturer's instructions. We performed PCR amplification and

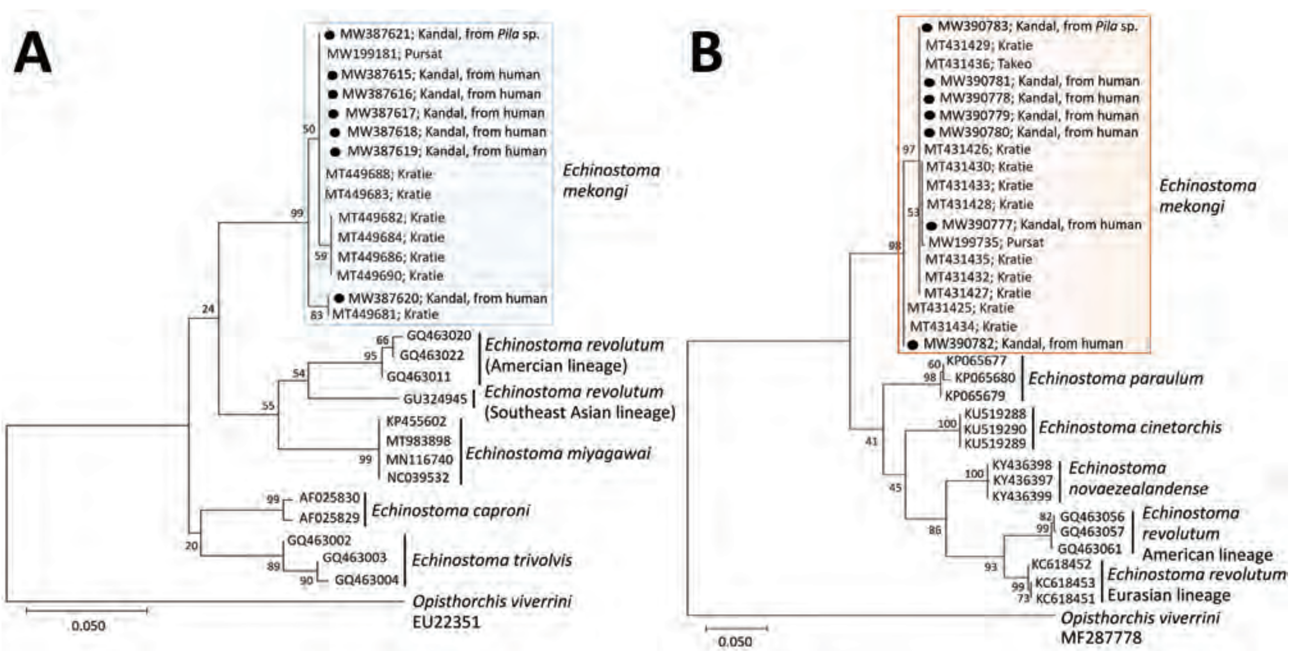

Figure 2. Phylogenetic trees of *cox*1 (A) and *nd*1 (B) genes of *Echinostoma mekongi* adults (n = 6) extracted from volunteers and metacercaria (n = 1) extracted from *Pila* sp. snails for study of *E. mekongi* infection in schoolchildren and adults, Kandal Province, Cambodia. Sequences from this study (shades boxes) are shown in comparison with other 37-collar-spined *Echinostoma* spp. (outgroup; *Opisthorchis viverrini*). The trees were constructed using the maximum-likelihood method, employing the Tamura-Nei model of nucleotide substitution with 1,000 bootstrap replications and viewed in MEGA X (https://www.megasoftware.net). GenBank accession numbers are given for all sequences. Scale bars indicate substitutions per site.

sequencing by using the primers (JB3 and JB13 for *cox*1 and JB11 and JB12 for *nd*1) and conditions described in a previous study (*5*). We constructed phylogenetic trees by using the maximum-likelihood method available in MEGA X (*6*) and also incorporating the Tamura-Nei model of nucleotide substitution with 1,000 bootstrap replications.

Partial sequences of *cox*1 (230 bp) (MW387615-MW387621) and *nd*1 (453 bp) (MW390777–83) genes in our samples (adult flukes and metacercariae) revealed strong identity with *E. mekongi* sequences (Figure 2, panels A and B). The phylogenetic tree of *cox*1 showed that our samples (n = 7) were tightly clustered (99.0%–100% identical) with *E. mekongi* (MT449688; human, Kratie Province, Cambodia) but separated from other 37-collar-spined echinostomes, including *E. caproni* (AF025830; 92.2%), *E. trivolvis* (GQ463003; 91.7%), *E. miyagawai* (KP455602; 90.2%–91.2%), and *E. revolutum* Southeast Asian (GU324945; 90.0%–91.0%) and American lineages (GQ463020; 89.8%). The phylogenetic tree of *nd*1 revealed also that our samples (n = 7) were closely aligned (98.7%–100%) with *E. mekongi* (MT431430; human, Kratie Province, Cambodia) but separated from other 37-collar-spined *Echinostoma* spp., including *E. paraulum* (KP065680; 88.7%–89.4%), *E. cinetorchis* (KU519289; 87.4%–88.1%), *E. novaezealandense* (KY436399; 86.9%–87.6%), and *E. revolutum* American (GQ463056; 86.3%–86.5%) and Eurasian lineages (KC618453; 86.2%–86.4%).

Conclusions

Large trematode eggs, particularly, those of echinostomes, have been detected in various localities of Cambodia (*7–11*). In Pursat Province, echinostome eggs were found in 56 schoolchildren, and the worms expelled from 4 volunteers were assigned as *E. revolutum* by morphologic analysis (*7*). We think, however, that those worms might have been *E. mekongi* because *E. mekongi* and *E. revolutum* are morphologically close and almost indistinguishable (*3*). Molecular studies are necessary to draw a definite conclusion on the species of those echinostomes. In Oddar Meanchey Province, the eggs of echinostomes were detected in 13 persons, and the adult flukes expelled were confirmed to be *Echinostoma ilocanum* flukes, having 49–51 collar spines (*8*). Echinostome eggs were also detected in 71 persons in Kratie Province (*9*) and 52 persons in Takeo Province (*10*), and 6 volunteers were confirmed to be infected with *E. mekongi* flukes by morphologic and molecular analyses (*3*).

A previous study of persons in Kandal Province, Cambodia, found a high prevalence (46.5%; 106/228) of large trematode eggs (suggested to be *Echinostoma* spp.) among schoolchildren (5–18 years of age), but no adult worm recovery nor molecular analysis was performed (*11*). By the time of our study, it was confirmed that *E. mekongi* infection is highly prevalent among schoolchildren and adults in Kandal Province. The recovery of both juvenile and adult flukes may indicate the continuity of infection in this village. Freshwater snails of *Pila* sp. were proven to be the source of infection. It is speculated that *E. mekongi* infection might be prevalent not only in other localities of Cambodia but also in neighboring countries (Thailand, Laos, and Vietnam) along the Mekong River and its tributaries. Avoidance of consuming raw or undercooked *Pila* sp. snails is a preventive measure for this emerging parasitic infection in those areas.

Acknowledgments

We are grateful to the staff of the National Center for Parasitology, Entomology and Malaria Control, Ministry of Health, Cambodia, for their help in collecting fecal specimens from schoolchildren and adults of the surveyed villages. We are also indebted to the members of the MediCheck Research Institute at the Korea Association of Health Promotion for their help in molecular studies.

The National Ethics Committee for Health Research, Ministry of Health, Cambodia (no. 099NECHR), officially approved this study. Informed consent was obtained from all participants, parents, or school guardians.

About the Author

Dr. Jung is the senior researcher at the MediCheck Research Institute, Korea Association of Health Promotion. Taehee Chang, a former research associate at the MediCheck Research Institute, is currently a PhD student at the Department of Public Health Sciences, Graduate School of Public Health, Seoul National University. Their major research interest is molecular analysis of foodborne zoonotic parasites, including echinostomes, heterophyid flukes, and anisakid nematodes.

References

1. Chai JY. Human intestinal flukes: from discovery to treatment and control. Dordrecht, The Netherlands: Springer Nature; 2019. p. 1–549.
2. Chai JY. Echinostomes in humans. In: Fried B, Toledo R, editors. The biology of echinostomes. New York: Springer; 2009. p. 147–183. https://doi.org/10.1007/978-0-387-09577-6_7
3. Cho J, Jung BK, Chang T, Sohn WM, Sinuon M, Chai JY. *Echinostoma mekongi* n. sp. (Digenea: Echinostomatidae) from riparian people along the Mekong River in Cambodia. Korean J Parasitol. 2020;58:431–43. https://doi.org/10.3347/kjp.2020.58.4.431
4. Chai JY, Sohn WM, Cho J, Jung BK, Chang T, Lee KH, et al. *Echinostoma mekongi*: discovery of its metacercarial stage in

snails, Filopaludina martensi cambodjensis, in Pursal Province, Cambodia. Korean J Parasitol. 2021;59:47–53. https://doi.org/10.3347/kjp.2021.59.1.47
5. Morgan JAT, Blair D. Relative merits of nuclear ribosomal internal transcribed spacers and mitochondrial CO1 and ND1 genes for distinguishing among *Echinostoma* species (Trematoda). Parasitology. 1998;116:289–97. https://doi.org/10.1017/S0031182097002217
6. Kumar S, Stecher G, Li M, Knyaz C, Tamura K. MEGA X: molecular evolutionary genetics analysis across computing platforms. Mol Biol Evol. 2018;35:1547–9. https://doi.org/10.1093/molbev/msy096
7. Sohn WM, Chai JY, Yong TS, Eom KS, Yoon CH, Sinuon M, et al. *Echinostoma revolutum* infection in children, Pursat Province, Cambodia. Emerg Infect Dis. 2011;17:117–9. https://doi.org/10.3201/eid1701.100920
8. Sohn WM, Kim HJ, Yong TS, Eom KS, Jeong HG, Kim JK, et al. *Echinostoma ilocanum* infection in Oddar Meanchey Province, Cambodia. Korean J Parasitol. 2011;49:187–90. https://doi.org/10.3347/kjp.2011.49.2.187
9. Sohn WM, Yong TS, Eom KS, Pyo KH, Lee MY, Lim H, et al. Prevalence of *Opisthorchis viverrini* infection in humans and fish in Kratie Province, Cambodia. Acta Trop. 2012;124:215–20. https://doi.org/10.1016/j.actatropica.2012.08.011
10. Yong TS, Shin EH, Chai JY, Sohn WM, Eom KS, Lee DM, et al. High prevalence of *Opisthorchis viverrini* infection in a riparian population in Takeo Province, Cambodia. Korean J Parasitol. 2012;50:173–6. https://doi.org/10.3347/kjp.2012.50.2.173
11. Bless PJ, Schär F, Khieu V, Kramme S, Muth S, Marti H, et al. High prevalence of large trematode eggs in schoolchildren in Cambodia. Acta Trop. 2015;141(Pt B):295–302. https://doi.org/10.1016/j.actatropica.2014.09.007

Address for correspondence: Jong-Yil Chai, Department of Tropical Medicine and Parasitology, Seoul National University College of Medicine, Seoul 03080, South Korea; email: cjy@snu.ac.kr

Potentially Zoonotic Enteric Infections in Gorillas and Chimpanzees, Cameroon and Tanzania

Emily K. Strahan, Jacob Witherbee, Richard Bergl, Elizabeth V. Lonsdorf, Dismas Mwacha, Deus Mjungu, Mimi Arandjelovic, Romanus Ikfuingei, Karen Terio, Dominic A. Travis, Thomas R. Gillespie

Despite zoonotic potential, data are lacking on enteric infection diversity in wild apes. We employed a novel molecular diagnostic platform to detect enteric infections in wild chimpanzees and gorillas. Prevalent *Cryptosporidium parvum*, adenovirus, and diarrheagenic *Escherichia coli* across divergent sites and species demonstrates potential widespread circulation among apes in Africa.

The close phylogenetic relationship between humans and great apes results in similarities in infection susceptibility and a high potential for pathogen exchange (*1*,*2*). Despite this zoonotic potential, previous studies of wild great apes have targeted specific infections (*3*,*4*), failing to establish baselines of the diversity of potentially zoonotic infections in these species. To improve our understanding of which enteric infections great apes are exposed to, we examined biobanked fecal samples from 2 biogeographically and phylogenetically divergent wild great ape species in Africa for an array of viral, parasitic, and bacterial enteric targets using a novel real-time PCR diagnostic platform.

Author affiliations: Emory University, Atlanta, Georgia, USA (E.K. Strahan, E.V. Lonsdorf, T.R. Gillespie); Centers for Disease Control and Prevention, Atlanta (J. Witherbee); North Carolina Zoo, Asheboro, North Carolina, USA (R. Bergl); Jane Goodall Institute Tanzania, Kigoma, Tanzania (D. Mwacha, D. Mjungu); Max Planck Institute for Evolutionary Anthropology, Leipzig, Germany (M. Arandjelovic); iDiv, German Centre for Integrative Biodiversity Research Halle-Jena-Leipzig, Leipzig (M. Arandjelovic); Wildlife Conservation Society Takamanda-Mone Landscape Project, Limbe, Cameroon (R. Ikfuingei); University of Illinois, Urbana, Illinois, USA (K. Terio); University of Minnesota, Minneapolis, Minnesota, USA (D.A. Travis)

DOI: https://doi.org/10.3201/eid3003.230318

The Study

During December 2011–January 2012, a total of 58 fecal samples from critically endangered Cross River gorillas (*Gorilla gorilla diehli*) were noninvasively collected from nest sites and along trails from 2 sites in Cameroon, as detailed in Arandjelovic et al. (*5*). Sampled gorillas experienced infrequent overlap with humans engaged in research or extraction of nontimber forest products (*5*). Fecal DNA extract and microsatellite genotyping identified individual gorilla sample donors, confirming repeated sampling of 18 gorillas: 10 from Kagwene Gorilla Sanctuary (≈50% of population) and 8 from Mone River Forest Reserve (≈35%–40% of population) (*5*). Given that serial sampling can increase chances that an individual tests positive for a target (*6*), only the first sample collected from each gorilla was screened.

During September 2016–February 2018, fecal samples were noninvasively collected from each of 56 individually recognized endangered eastern chimpanzees (*Pan troglodytes schweinfurthii*) (≈50% of population) from Gombe National Park, Tanzania, as detailed in Wroblewski et al. (*7*). Sampled chimpanzees experienced daily overlap with humans engaged in research and tourism following best practices to reduce the risk for pathogen exchange (*2*) and experienced infrequent overlap with humans when consuming crops at the boundary of the protected area (*8*). Fecal DNA extract and microsatellite genotyping were used to identify individual chimpanzee sample donors (*7*).

For all apes sampled, fresh fecal samples were preserved upon collection in Ambion RNAlater (MilliporeSigma, https://www.sigmaaldrich.com) and stored at −20°C until shipping to the United States, where they were stored at −80°C until thawed for extraction. In December 2019, we used the TaqMan

Table 1. Number of individual wild Cross River gorillas (*Gorilla gorilla diehli*) positive for enteric infection targets in Kagwene Gorilla Sanctuary and Mone River Forest Reserve, Cameroon (n = 18), 2011–2012

Assay target	Pathogen group	No. positive gorillas
Cryptosporidium parvum	Parasite	7
All adenovirus serotypes except 40 and 41	Virus	6
Enterococcus faecalis	Bacteria	5
Enterotoxigenic *Escherichia coli: E. coli* carrying virulence gene for heat-labile or heat-stable enterotoxin	Bacteria	1
Enteropathogenic *E. coli: E. coli* carrying gene (*eae*) encoding outer membrane protein intimin and causing pathogenesis through attachment/effacement of epithelial cells	Bacteria	1
Escherichia coli and *Shigella* species carrying invasion plasmid antigen H gene	Bacteria	1
Salmonella bongori and all subspecies of *Salmonella enterica*	Bacteria	1

Array Card (ThermoFisher Scientific, https://www.thermofisher.com), a novel real-time PCR testing platform, to screen ape fecal samples for 39 unique enteric pathogen targets (Appendix, https://wwwnc.cdc.gov/EID/article/30/3/23-0318-App1.pdf). Targets were pathogen-specific genes associated with either virulence or biology (i.e., specific outer membrane protein genes or housekeeping genes). As detailed in Diaz et al. (*8*), we extracted DNA and RNA from each fecal specimen using a Roche MagNA Pure Compact magnetic bead Total Nucleic Acid Kit (Roche, https://www.roche.com). For preprocessing, we incubated sample, lysis buffer, and proteinase (56°C, 15 minutes) before 2 cycles on Precellys bead-beater (Bertin Technologies, https://www.bertin-technologies.com) at 5,000 rpm for 60 seconds. We assayed extracts using the Applied Biosystems ViiA7 Real-Time PCR system (ThermoFisher Scientific) with the following cycling conditions: 45°C for 10 minutes, 94°C for 10 minutes, 45 cycles of 94°C for 30 seconds, and 60°C for 60 seconds (*8*). For validation, we spiked fecal samples with known DNA/RNA concentrations. We evaluated sensitivity with spiked dilution series and specificity through BLAST (https://blast.ncbi.nlm.nih.gov/Blast.cgi), then isolated the panel representing targeted organisms. We evaluated exclusivity using nucleic acid from closely related species.

Analyses confirmed presence of nucleic acids of ≥1 enteric pathogen target in 15 (83%) of the 18 gorillas and 39 (70%) of the 56 chimpanzees. We detected 7 pathogen targets among gorillas (Table 1) and 13 among chimpanzees (Table 2). Adenovirus and *Cryptosporidium parvum* were the most common pathogen targets detected in both gorillas and chimpanzees, occurring in 33% (95% CI 10%–57%) (adenovirus) and 39% (95% CI 15%–62%) (*C. parvum*) of gorillas and 52% (95% CI 39%–65%) (adenovirus) and 13% (95% CI 4%–21%) (*C. parvum*) of chimpanzees. Both adenovirus and *C. parvum* had previously been detected in wild great ape populations and have received attention, given their zoonotic potential (*9*,*10*).

Conclusions

Real-time PCR testing of noninvasively collected wild gorilla and chimpanzee fecal samples from Cameroon and Tanzania provided evidence of widespread enteric infections and demonstrates their potential circulation in ape populations in Africa before 2018. Several pathogen targets detected in the ape species are highly relevant to humans, including those commonly associated with diarrheal disease,

Table 2. Number of individual wild eastern chimpanzees (*Pan troglodytes schweinfurthii*) positive for enteric infection targets in Gombe National Park, Tanzania (n = 56), 2016–2018

Assay target	Pathogen group	No. positive chimpanzees
All adenovirus serotypes except 40 and 41	Virus	29
Enterotoxigenic *E. coli: E. coli* carrying virulence gene for heat-labile or heat-stable enterotoxin	Bacteria	5
Enteroaggregative *E. coli: Escherichia coli* carrying a virulence gene (*aaiC*) associated with causing pathogenesis through aggregation in the intestinal mucosa	Bacteria	4
Enteropathogenic *E. coli: Escherichia coli* carrying gene (*bfpA*) encoding bundle-forming pilus and causing pathogenesis through attachment/effacement of epithelial cells	Bacteria	1
Cryptosporidium parvum	Parasite	7
All Enterovirus serotypes within *Enterovirus* genus	Virus	5
All *Giardia* species infecting humans	Parasite	5
Trichuris trichiura (*Trichocephalus trichiuris)*	Parasite	3
Escherichia coli and *Shigella* species carrying invasion plasmid antigen H gene	Bacteria	2
Aeromonas hydrophila, caviae, veronii, jandaei, salmonicida, schubertii, popofii	Bacteria	1
Enterococcus faecalis	Bacteria	1
Norovirus belonging to genogroup 2	Virus	1
Rotavirus A species from *Rotavirus* genus	Virus	1

such as diarrheagenic *E. coli*, adenovirus, *Shigella* spp., *Giardia* spp., and enterovirus. As human–nonhuman primate contact increases in tropical forest communities, opportunities will continue to arise for both anthroponotic and zoonotic exchange and exposure (*11*).

Adenoviruses and *Cryptosporidium* species infect a broad range of hosts (including humans and nonhuman primates), can cause mild to severe disease, and are also associated with high rates of illness and death in children and immunocompromised persons, especially in developing countries (*12*). Although the pathogenesis of those organisms is less understood in nonhuman primate populations, they are of major zoonotic importance, given the increasing overlap between humans and wild primates and high HIV/AIDS prevalence in humans in regions inhabited by primate populations. Furthermore, because *C. parvum* and adenoviruses can spread through the fecal–oral route and persist in the environment for extended periods, diverse opportunities exist for direct and indirect transmission between humans and great apes (e.g., tourism and research activities, crop-raiding by apes, and events related to humans living in close proximity to parks).

Of note, many of the observed simian adenoviruses show high degrees of sequence relatedness to human strains, suggesting evidence of past cross-species transmission events and potential risk for such events in the future (*10*). Differentiating between strains was beyond the scope of this study, but the high detection rate of this viral target and its zoonotic potential warrants further characterization of this viral group and continued surveillance of great ape populations.

The first limitation of our study is that, because of logistical challenges and budgetary constraints, we were only able to focus our surveillance on 2 populations of great apes at specific points in time. In addition, sex and age classes sampled were representative of each ape population apart from infants, which are nearly impossible to sample noninvasively.

Despite those challenges, our data provide insight into the diversity of enteric infections circulating in wild gorilla and chimpanzee populations before 2018. Detection of gene targets of zoonotic potential in 83% of gorillas and 70% of chimpanzees suggests potential health and disease transmission risks. These results are especially pertinent for monitoring these ape species given the previously documented cases of disease and epizootics (e.g., respiratory infections, polio, mange) in Gombe (*13*), and the lack of such in Cross River gorilla populations. As research, ecotourism, and forest encroachment in wild ape habitat increases, the risk for novel pathogen exposure is heightened, which could have catastrophic impacts on populations. Continued epidemiologic research among wild primate populations has the potential to predict which pathogens might enter both human and great ape populations as contact between species intensifies. Because pathogen exchange occurs across species boundaries, the potential for changes in pathogenicity and host specificity exists, which could have substantial adverse effects on human and wildlife health (*14*,*15*).

Acknowledgments

We thank the Government of Cameroon and the Ministry of Forests and Wildlife for granting permission to conduct research at Kagwene Gorilla Sanctuary and Mone River Forest Reserve. We thank the Government of Tanzania, TANAPA, TAWIRI, and COSTECH for permission to conduct research in Gombe National Park. We thank the Wildlife Conservation Society and Working Dogs for Conservation for logistical assistance in Cameroon and the Jane Goodall Institute and the staff of the Gombe Stream Research Center for logistical support in Tanzania. We thank A. Hurt and N. Richards for technical assistance, B. Hahn for providing samples, and J. Clennon, M. Diaz, M. Parsons, and J. Winchell for helpful discussion and feedback on an earlier draft of this manuscript.

This work was funded by the National Institutes of Health (grants R01 AI58715, R00 HD057992), the National Institutes of Health National Institute on Aging (grant R37-AG049395), the US Fish and Wildlife Great Ape Conservation Fund, the Arcus Foundation, the North Carolina Zoo, the Wildlife Conservation Society, a Robert W. Woodruff Foundation Synergy II Award, and the James G. Lester Fund of Emory University.

About the Author

Ms. Strahan is a recent graduate of the department of environmental sciences at Emory University in Atlanta, Georgia. Her primary research interests relate to wildlife diseases and their implications for public health.

References

1. Calvignac-Spencer S, Leendertz SAJ, Gillespie TR, Leendertz FH. Wild great apes as sentinels and sources of infectious disease. Clin Microbiol Infect. 2012;18:521–7. https://doi.org/10.1111/j.1469-0691.2012.03816.x
2. Gilardi KV, Gillespie TR, Leendertz FH, Macfie EJ, Travis DA, Whittier CA, et al. Best practice guidelines for

health monitoring and disease control in great ape populations. Gland, Switzerland: IUCN SSC Primate Specialist Group; 2015.
3. Mubemba B, Chanove E, Mätz-Rensing K, Gogarten JF, Düx A, Merkel K, et al. Yaws disease caused by *Treponema pallidum* subspecies pertenue in wild chimpanzee, Guinea, 2019. Emerg Infect Dis. 2020;26:1283–6. https://doi.org/10.3201/eid2606.191713
4. Scully EJ, Basnet S, Wrangham RW, Muller MN, Otali E, Hyeroba D, et al. Lethal respiratory disease associated with human rhinovirus C in wild chimpanzees, Uganda, 2013. Emerg Infect Dis. 2018;24:267–74. https://doi.org/10.3201/eid2402.170778
5. Arandjelovic M, Bergl RA, Ikfuingei R, Jameson C, Parker M, Vigilant L. Detection dog efficacy for collecting faecal samples from the critically endangered Cross River gorilla (*Gorilla gorilla diehli*) for genetic censusing. R Soc Open Sci. 2015;2:140423. https://doi.org/10.1098/rsos.140423
6. Miller IF, Schneider-Crease I, Nunn CL, Muehlenbein MP. Estimating infection prevalence: best practices and their theoretical underpinnings. Ecol Evol. 2018;8:6738–47. https://doi.org/10.1002/ece3.4179
7. Wroblewski EE, Norman PJ, Guethlein LA, Rudicell RS, Ramirez MA, Li Y, et al. Signature patterns of MHC diversity in three Gombe communities of wild chimpanzees reflect fitness in reproduction and immune defense against SIVcpz. PLoS Biol. 2015;13:e1002144. https://doi.org/10.1371/journal.pbio.1002144
8. Diaz MH, Waller JL, Theodore MJ, Patel N, Wolff BJ, Benitez AJ, et al. Development and implementation of multiplex TaqMan Array Cards for specimen testing at Child Health and Mortality Prevention Surveillance site laboratories. Clin Infect Dis. 2019;69(Suppl 4):S311–21. https://doi.org/10.1093/cid/ciz571
9. Parsons MB, Travis D, Lonsdorf EV, Lipende I, Roellig DMA, Collins A, et al. Epidemiology and molecular characterization of *Cryptosporidium* spp. in humans, wild primates, and domesticated animals in the Greater Gombe Ecosystem, Tanzania. PLoS Negl Trop Dis. 2015;9:e0003529. https://doi.org/10.1371/journal.pntd.0003529
10. Wevers D, Metzger S, Babweteera F, Bieberbach M, Boesch C, Cameron K, et al. Novel adenoviruses in wild primates: a high level of genetic diversity and evidence of zoonotic transmissions. J Virol. 2011;85:10774–84. https://doi.org/10.1128/JVI.00810-11
11. Estrada A, Garber PA, Rylands AB, Roos C, Fernandez-Duque E, Di Fiore A, et al. Impending extinction crisis of the world's primates: why primates matter. Sci Adv. 2017;3:e1600946. https://doi.org/10.1126/sciadv.1600946
12. Kotloff KL, Nataro JP, Blackwelder WC, Nasrin D, Farag TH, Panchalingam S, et al. Burden and aetiology of diarrhoeal disease in infants and young children in developing countries (the Global Enteric Multicenter Study, GEMS): a prospective, case-control study. Lancet. 2013;382:209–22. https://doi.org/10.1016/S0140-6736(13)60844-2
13. Lonsdorf EV, Travis DA, Raphael J, Kamenya S, Lipende I, Mwacha D, et al. The Gombe Ecosystem Health Project: 16 years of program evolution and lessons learned. Am J Primatol. 2022;84:e23300. https://doi.org/10.1002/ajp.23300
14. Baker RE, Mahmud AS, Miller IF, Rajeev M, Rasambainarivo F, Rice BL, et al. Infectious disease in an era of global change. Nat Rev Microbiol. 2022;20:193–205. https://doi.org/10.1038/s41579-021-00639-z
15. Brook CE, Boots M, Chandran K, Dobson AP, Drosten C, Graham AL, et al. Accelerated viral dynamics in bat cell lines, with implications for zoonotic emergence. eLife. 2020;9:e48401. https://doi.org/10.7554/eLife.48401

Address for correspondence: Thomas R. Gillespie, Departments of Environmental Sciences and Environmental Health, Emory University and Rollins School of Public Health, 400 Dowman Dr, Ste E510, Atlanta, GA 30322, USA; email: thomas.gillespie@emory.edu

Biphasic MERS-CoV Incidence in Nomadic Dromedaries with Putative Transmission to Humans, Kenya, 2022–2023

Brian Maina Ogoti,[1] Victor Riitho,[1] Johanna Wildemann,[1] Nyamai Mutono, Julia Tesch, Jordi Rodon, Kaneemozhe Harichandran, Jackson Emanuel, Elisabeth Möncke-Buchner, Stella Kiambi, Julius Oyugi, Marianne Mureithi, Victor M. Corman, Christian Drosten, Samuel M. Thumbi,[1] Marcel A. Müller[1]

Middle East respiratory syndrome coronavirus (MERS-CoV) is endemic in dromedaries in Africa, but camel-to-human transmission is limited. Sustained 12-month sampling of dromedaries in a Kenya abattoir hub showed biphasic MERS-CoV incidence; peak detections occurred in October 2022 and February 2023. Dromedary-exposed abattoir workers (7/48) had serologic signs of previous MERS-CoV exposure.

Middle East respiratory syndrome coronavirus (MERS-CoV) is endemic in dromedary camels from the Arabian Peninsula and Africa; seroprevalence is >75% (*1*–*3*). Zoonotic transmission to humans has occurred sporadically, mainly on the Arabian Peninsula; >2,400 MERS cases and >800 deaths have occurred (*4*). Despite Kenya being a major camel-breeding country, only 3 potentially autochthonous camel-exposed humans with subclinical MERS-CoV infections were identified in 2019 (*5*). The apparent regional epidemiologic differences might be linked to factors such as limited diagnostics, local risk factors (e.g., human comorbidities, camel herding practices, seasonality), or MERS-CoV strain–specific features (*6*).

In farmed dromedary camels, MERS-CoV outbreaks were associated with annually synchronized camel parturition (*7*). In particular, camel calves tested MERS-CoV RNA–positive upon the loss of maternal antibodies 4–6 months after birth. Because of seasonality and changing food availability, most camels in Africa are nomadic and have variable population density. High population density is correlated with MERS-CoV seropositivity in camels in Kenya (*1*), but detailed insights into MERS-CoV circulation are missing.

Field studies on nomadic camels are hampered by limited infrastructure in remote and resource-restricted regions (*8*). However, nomadic camels are regularly transported to abattoir hubs, enabling sustained daily testing. We performed a continuous 12-month study at an abattoir hub in northern Kenya to investigate MERS-CoV incidence in nomadic camels and explore potential transmission to slaughterhouse workers.

The Study

Our sampling site was an abattoir hub in Isiolo, northern Kenya, where camels from Marsabit, Samburu, and Isiolo counties are slaughtered (Appendix Figure 1, https://wwwnc.cdc.gov/EID/article/30/3/23-1488-App1.pdf). During September 2022–September 2023, we took samples from 10–15 dromedary camels 4–5 days per week (Appendix). The camels (n = 2,711) were originally from 12 different administrative wards, mainly from Laisamis in Marsabit County (n = 1,841, 67.9%) and Burat in Isiolo County (n = 578, 21.3%) (Table; Appendix Figure 1).

Author affiliations: University of Nairobi, Nairobi, Kenya (B.M. Ogoti, V. Riitho, N. Mutono, J. Oyugi, M. Mureithi, S.M. Thumbi); Queen Mary University of London, London, UK (V. Riitho); Charité–Universitätsmedizin Berlin, Berlin, Germany (J. Wildemann, J. Tesch, J. Rodon, K. Harichandran, J. Emanuel, E. Möncke-Buchner, V.M. Corman, C. Drosten, M.A. Müller); Washington State University, Pullman, Washington, USA (N. Mutono, S.M. Thumbi); Food and Agriculture Organization, Dar es Salaam, Tanzania (S. Kiambi); Labor Berlin–Charité Vivantes GmbH, Berlin (V.M. Corman); German Center for Infection Research, Berlin (V.M. Corman, C. Drosten, M.A. Müller); University of Edinburgh, Edinburgh, Scotland, UK (S.M. Thumbi)

DOI: https://doi.org/10.3201/eid3003.231488

[1]These authors contributed equally to this article.

Table. Overview of camel samples and MERS-CoV RNA positivity in study of MERS-CoV incidence in nomadic dromedaries with putative transmission to humans, Kenya, 2022–2023*

Region	MERS-CoV RNA–positive samples/ total samples (%)	Town of origin	MERS-CoV RNA–positive samples/total samples (%)	
			Female camels	Male camels
Isiolo	15/859 (1.75)	Burat	1/252 (0.4)	10/326 (3.1)
		Bulla Pesa	0/2	0/0
		Kinna	0/13	1/19 (5.3)
		Oldo/Nyiro	0/2	2/23 (8.7)
		Garbatulla	0/1	0/1
		Ngare Mara	0/106	0/114
Marsabit	26/1,846 (1.41)	Laisamis	1/250 (0.4)	21/1,591 (1.3)
		Marsabit Central	0/0	0/1
		Sololo	0/1	0/0
		North Horr	0/0	0/2
		not defined	0/0	0/1
Samburu	0/6 (0)	Wamba East	0/0	0/6
Total	36/2,711 (1.3)		2/627 (0.3)	34/2,084 (1.6)

*MERS-CoV, Middle East respiratory syndrome coronavirus.

MERS-CoV RNA was detected in 36/2,711 (1.3%) (Table; Figure 1) camels using quantitative reverse transcription PCR, which amplifies the upstream of the envelope E gene, and confirmed by open reading frame (ORF) 1ab quantitative reverse transcription PCR or sequencing (Appendix). The cumulative RNA positivity rate was higher in September–October 2022 at 19/381 (5.0%) compared with 17/727 (2.3%) in January–March 2023 (Figure 1). Incidence was biphasic, showing detection peaks in the first weeks of October 2022 (7/60, 11.7%) and February 2023 (7/58, 12.1%) (Figure 1, panel B). For 9/36 MERS-CoV–positive samples, we obtained ORF1ab sequences and performed phylogenetic analysis. The 9 ORF1ab sequences were highly similar (>99.93% nucleotide identity) and had 99.75%–99.78% nucleotide identity with the closest MERS-CoV relative identified in Akaki, Ethiopia, in 2019 (*9*). Phylogenetic analysis showed that the 9 sequences clustered as a monophyletic group within clade C2.2, which encompasses East Africa strains initially detected in Kenya in 2018 (*10*) (Appendix Figure 2). Those sequences represent 3 putative MERS-CoV outbreaks occurring contemporarily in camels in Kenya (Appendix Table 1).

To test whether biphasic MERS-CoV RNA–positivity is accompanied by increased MERS-CoV IgG levels, we tested randomized camel serum samples (n = 369/2,711) by MERS-CoV S1 ELISA (Appendix). MERS-CoV IgG levels showed a median optical density ratio (ODR) of 2.14 (95% CI 0.59–3.48) and a seroprevalence of 80.76% (298/369) (Appendix Figure 3, panel A). Lowest IgG levels were identified in June (median ODR 1.28, 95% CI 0.20–3.31),

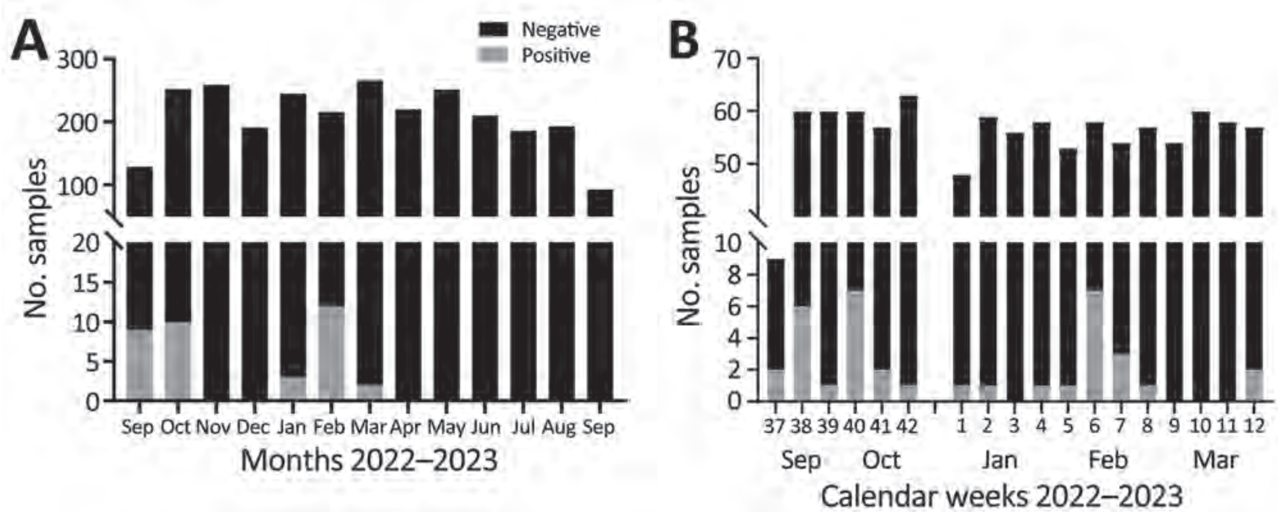

Figure 1. Biphasic Middle East respiratory syndrome coronavirus (MERS-CoV) incidence in dromedaries sampled in an abattoir hub, northern Kenya, 2022–2023. A) MERS-CoV RNA detection rates in nasal swab specimens from dromedary camels tested by MERS-CoV upE quantitative reverse transcription PCR. Continuous 12-month sampling (4–5 days per week) took place in Isiolo abattoir from mid-September 2022 to mid-September 2023. Sampling was suspended for 1 week in December 2022 and 1 week in July 2023. B) Detailed weekly overview of MERS-CoV RNA detections, peaking in October 2022 and February 2023.

whereas the highest levels were seen in March (median ODR 2.72, 95% CI 1.67–3.76). MERS-CoV IgG levels were negatively associated with RNA-positivity (odds ratio [OR] 0.20, 95% CI 0.09–0.44; p<0.0001) (Appendix Figure 3, panel B). RNA-positivity was negatively associated with the season (dry vs. wet, OR 0.14, 95% CI 0.06–0.30; p<0.0001). Male camels were more likely to be RNA positive (OR 3.94, 95% CI 0.86–29.2; p = 0.11) and less likely to be seropositive (OR 0.27, 95% CI 0.08–0.77; p = 0.021) than were female camels. Older animals (>3 years of age) were more likely to be seropositive (86%) than were animals ≤3 years of age (72%), but this difference was not statistically significant.

Seroepidemiologic studies have suggested that abattoir workers in contact with dromedaries are at increased risk for MERS-CoV exposure (*11*). Seroconversion of subclinical MERS cases might be missed when diagnostically implemented ELISA cutoffs of commercial kits (e.g., ODR = 1.1 for IgG positives) are applied (*11,12*). We identified MERS-CoV S1 IgG reactivity (ODR >0.2) in 7/48 (14.6%) of Isiolo abattoir workers (Figure 2, panel A). We excluded SARS-CoV-2 infection– or vaccine–induced antibody cross-reactivity with MERS-CoV S1 by comparison of ELISA ODRs of MERS-CoV S1–based with SARS-CoV-2 S1–based ELISA (Appendix Table 2, Figure 4). A control cohort (n = 12) with no history of camel exposure showed no MERS-CoV S1 IgG reactivity (0/12; 0%) despite high SARS-CoV-2 S1 IgG levels (11/12; 92%) (Appendix Table 2).

Neutralization tests (NT) based on GFP-encoding vesicular stomatitis virus pseudoparticles (VSVpp) carrying the MERS-CoV S protein from clade A EMC/2012 or clade C2.2 (Kenya) showed that 1/7 serum samples (1:20 dilution) had a VSVpp-NT 50% reduction of foci-forming units for EMC/2012 and a 90% reduction for Kenya VSVpp-S (Figure 2, panel B). A MERS-CoV EMC/2012-based plaque-reduction neutralization test (PRNT) showed a 50% PRNT at the 1:20 dilution, fulfilling the World Health Organization criteria for a confirmed MERS-CoV seroconversion. None of 6 selected MERS-CoV S1 ELISA-negative abattoir samples showed neutralizing capacity when tested by VSVpp-NT and PRNT (Appendix Table 2).

Conclusions

Our sustained sampling of dromedary camels showed a biphasic MERS-CoV incidence in northern Kenya not observed in previous studies (*1,10,13*). One explanation might be the short time of virus excretion in MERS-CoV–infected dromedaries (*14*), making viral RNA detection difficult without daily surveillance. Phylogenetic analysis suggests that we identified ≥3 MERS-CoV clusters over 3 different weeks in dromedaries originating from different wards. The first potential factor likely influencing the outbreaks is increased animal-to-animal interactions, because

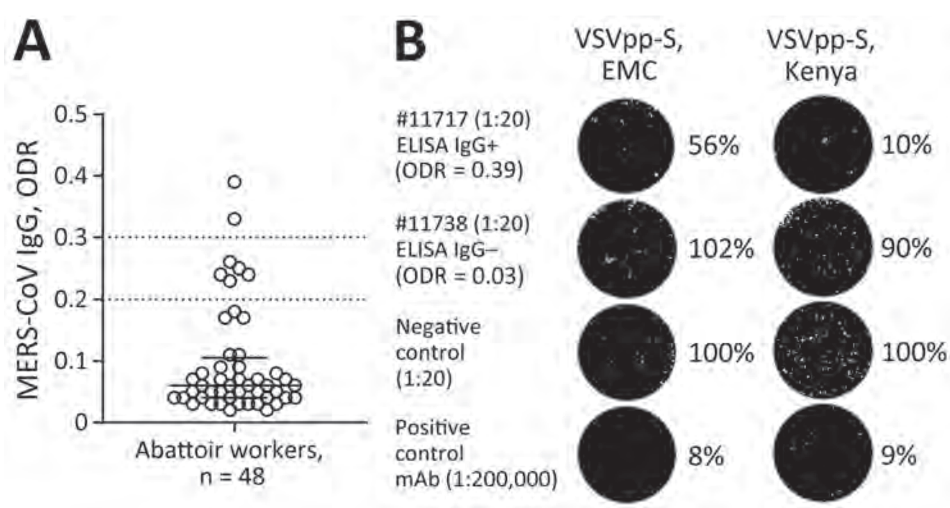

Figure 2. MERS-CoV immune responses in camel-exposed abattoir workers in Isiolo, Kenya. A) Results of commercial MERS-CoV S1-protein ELISA to detect IgG responses in 48 serum samples (diluted 1:100) from Isiolo abattoir workers. Samples with ODR >0.2 were considered ELISA-reactive, suggesting that 7/48 persons had MERS-CoV–reactive IgGs. Of note, all persons tested negative by MERS-CoV quantitative reverse transcription PCR. B) GFP-VSVpp-MERS-CoV S protein-based neutralization test (VSVpp-NT). VSVpp-S (EMC) and VSVpp-S (Kenya) contained human codon-optimized Spikes from prototypic MERS-CoV EMC/2012 clade A and Kenya clade C2.2 (#L00009980). All 7 ELISA-reactive human serum samples were mixed with 200 foci-forming units VSVpp in final serum dilutions 1:20–1:160. Out of the 7 ELISA-reactive persons, 1 showed a VSVpp-NT 50% foci-forming units reduction titer of 1:20 (EMC) and 1:40 (Kenya). The picture shows an example of the 1:20 dilution of an ELISA-reactive (#11717) and ELISA-nonreactive (#11738) abattoir worker. Negative control = ELISA-negative human serum (1:20) was used as reference and set to 100%. Positive control = monoclonal anti-MERS-CoV Spike receptor-binding domain binding antibody (mAb 7.7G6) previously shown to neutralize MERS-CoV at the tested dilution ($1:2 \times 10^5$). For better graphical visibility, all pictures were enhanced in contrast and brightness identically. mAb, monoclonal antibody; MERS-CoV, Middle East respiratory syndrome coronavirus; ODR, optical density ratio; VSVpp, vesicular stomatitis virus pseudoparticles.

camels from different herds are transported to Isiolo and kept in holding pens together before slaughter, which could enhance MERS-CoV outbreaks. Second, increased interactions between immunologically naive and infected animals during transport and in holding pens increases the probability of transmitting MERS-CoV. That hypothesis is supported by the high percentage of IgG–negative adult camels (19.24%, ODR<0.3) (*1*,*7*). Although identifying the exact MERS-CoV transmission scenario between camels is logistically difficult, rapid point-of-care tests might help trace infections even in resource-limited conditions.

The overall biphasic MERS-CoV incidence might be linked to seasonal factors, such as the biannual alternating wet and dry seasons in northern Kenya. During dry seasons, herds congregate using limited forage, then migrate back to the point of origin in wet seasons. Because calves are mainly born during the 2 wet seasons, the loss of protection by maternal antibodies coincides with the dry seasons. Of note, the 2 dry seasons during July–October 2022 and January–February 2023 matched the peaks of MERS-CoV RNA–positivity in October 2022 and February 2023. The combination of immunologically naive, possibly infected camel calves and the dry season–specific increased population density and probability of contact at limited waterholes might encourage MERS-CoV infections and transmissions among camels.

We identified 7/48 abattoir workers with putative MERS-CoV exposure or past subclinical infection by implementing ELISA ODR cutoffs previously shown to be suitable for seroepidemiologic studies outside clinical settings. In 1/7 cases, we confirmed MERS-CoV neutralizing antibodies by VSVpp-based NT and PRNT. None of the abattoir workers experienced severe symptoms in recent years, supporting the hypothesis that clade C strains might have limited pathogenicity and transmissibility (*15*). Identifying defined factors that drive MERS-CoV outbreaks will assist in predictive epidemiology, risk assessment, and timely precautionary interventions for public and occupational health.

Acknowledgments

We thank Patrick Muthui for excellent technical assistance, Muema Mulei for support in the initiation of the abattoir study, and Triza Shigoli, Noel Likalamu, and Andrea Sieberg for logistic and administrative assistance. We thank Gert Zimmer for the VSVpp system. We are grateful to all camel owners and abattoir workers for their help during the sample collection in Kenya. We thank the German FMD reference center at the Friedrich Löffler Institute, Insel Riems, Germany, for testing samples prior to import.

The work was funded by the German Research Foundation (DFG grant MU3564/3-1 to S.M.T and M.A.M.). C.D. received infrastructural support from the German Center for Infection Research (DZIF) and EU ERA-Net Project Durable (GA no. 101102733). The funders had no role in study design, data collection and analysis, decision to publish, or preparation of the manuscript.

M.A.M and V.M.C. are named on patents regarding SARS-CoV-2 serologic testing and monoclonal antibodies.

About the Author

Mr. Ogoti is a virologist at the Center for Epidemiological Modelling Analysis (CEMA), University of Nairobi Institute of Tropical and Infectious Diseases, University of Nairobi, Kenya. His research interests include epidemiology and characterization of highly pathogenic coronaviruses.

References

1. Corman VM, Jores J, Meyer B, Younan M, Liljander A, Said MY, et al. Antibodies against MERS coronavirus in dromedary camels, Kenya, 1992–2013. Emerg Infect Dis. 2014;20:1319–22. https://doi.org/10.3201/eid2008.140596
2. Meyer B, Müller MA, Corman VM, Reusken CB, Ritz D, Godeke GJ, et al. Antibodies against MERS coronavirus in dromedary camels, United Arab Emirates, 2003 and 2013. Emerg Infect Dis. 2014;20:552–9. https://doi.org/10.3201/eid2004.131746
3. Müller MA, Corman VM, Jores J, Meyer B, Younan M, Liljander A, et al. MERS coronavirus neutralizing antibodies in camels, Eastern Africa, 1983–1997. Emerg Infect Dis. 2014;20:2093–5. https://doi.org/10.3201/eid2012.141026
4. World Health Organization. Disease outbreak news: Middle East respiratory syndrome—United Arab Emirates [cited 2024 Feb 4]. https://www.who.int/emergencies/disease-outbreak-news/item/2023-DON478
5. Munyua PM, Ngere I, Hunsperger E, Kochi A, Amoth P, Mwasi L, et al. Low-level Middle East respiratory syndrome coronavirus among camel handlers, Kenya, 2019. Emerg Infect Dis. 2021;27:1201–5. https://doi.org/10.3201/eid2704.204458
6. Peiris M, Perlman S. Unresolved questions in the zoonotic transmission of MERS. Curr Opin Virol. 2022;52:258–64. https://doi.org/10.1016/j.coviro.2021.12.013
7. Meyer B, Juhasz J, Barua R, Das Gupta A, Hakimuddin F, Corman VM, et al. Time course of MERS-CoV infection and immunity in dromedary camels. Emerg Infect Dis. 2016;22:2171–3. https://doi.org/10.3201/eid2212.160382
8. Gikonyo S, Kimani T, Matere J, Kimutai J, Kiambi SG, Bitek AO, et al. Mapping potential amplification and transmission hotspots for MERS-CoV, Kenya. EcoHealth. 2018;15:372–87. https://doi.org/10.1007/s10393-018-1317-6
9. Zhou Z, Ali A, Walelign E, Demissie GF, El Masry I, Abayneh T, et al. Genetic diversity and molecular epidemiology of Middle East respiratory syndrome coronavirus in dromedaries in Ethiopia, 2017–2020. Emerg Microbes Infect. 2023;12:e2164218–27. https://doi.org/10.1080/22221751.2022.2164218
10. Kiambi S, Corman VM, Sitawa R, Githinji J, Ngoci J, Ozomata AS, et al. Detection of distinct MERS-coronavirus strains in dromedary camels from Kenya, 2017. Emerg Microbes Infect. 2018;7:195.

11. Müller MA, Meyer B, Corman VM, Al-Masri M, Turkestani A, Ritz D, et al. Presence of Middle East respiratory syndrome coronavirus antibodies in Saudi Arabia: a nationwide, cross-sectional, serological study. Lancet Infect Dis. 2015;15:559–64. https://doi.org/10.1016/S1473-3099(15)70090-3
12. Ko JH, Müller MA, Seok H, Park GE, Lee JY, Cho SY, et al. Suggested new breakpoints of anti-MERS-CoV antibody ELISA titers: performance analysis of serologic tests. Eur J Clin Microbiol Infect Dis. 2017;36:2179–86. https://doi.org/10.1007/s10096-017-3043-3
13. Ngere I, Hunsperger EA, Tong S, Oyugi J, Jaoko W, Harcourt JL, et al. Outbreak of Middle East respiratory syndrome coronavirus in camels and probable spillover infection to humans in Kenya. Viruses. 2022;14:1743–58. https://doi.org/10.3390/v14081743
14. Haagmans BL, van den Brand JM, Raj VS, Volz A, Wohlsein P, Smits SL, et al. An orthopoxvirus-based vaccine reduces virus excretion after MERS-CoV infection in dromedary camels. Science. 2016;351:77–81. https://doi.org/10.1126/science.aad1283
15. Rodon J, Mykytyn AZ, Te N, Okba NMA, Lamers MM, Pailler-García L, et al. Extended viral shedding of MERS-CoV clade B virus in llamas compared with African clade C strain. Emerg Infect Dis. 2023;29:585–9. https://doi.org/10.3201/eid2903.220986

Address for correspondence: Marcel A. Müller, Charité–Universitätsmedizin Berlin, Institute of Virology, Charitéplatz 1/Rahel-Hirsch-Weg 3, 10117 Berlin, Germany; email: marcel.mueller@charite.de

Highly Pathogenic Avian Influenza A(H5N1) Virus Clade 2.3.4.4b in Domestic Ducks, Indonesia, 2022

Hendra Wibawa, Putut Eko Wibowo, Arif Supriyadi, Lestari, Jessiaman Silaban, Aziz Ahmad Fuadi, Anna Januar Fiqri, Retno Wulan Handayani, Sri Handayani Irianingsih, Zaza Fahmia, Herdiyanto Mulyawan, Syafrison Idris, Nuryani Zainuddin

Highly pathogenic avian influenza A(H5N1) clade 2.3.4.4b viruses were isolated from domestic ducks in South Kalimantan, Indonesia, during April 2022. The viruses were genetically similar to those detected in East Asia during 2021–2022. Molecular surveillance of wild birds is needed to detect potential pandemic threats from avian influenza virus.

The H5N1 subtype of the avian influenza virus A/goose/Guangdong/1/96 (Gs/GD/96) lineage has caused highly pathogenic avian influenza (HPAI) outbreaks in poultry since 1996. In 2008, various novel reassortant viruses were identified in domestic duck and live bird markets (LBMs) in China bearing the genetic backbone of Gs/GD/96 virus clade 2.3.4 hemagglutinin (HA) but different combinations of neuraminidase, such as H5N2, H5N5, H5N6, and H5N8 (*1*). Clade 2.3.4 continued to evolve into 5th order genetic groups (clades 2.3.4.4a–h); reassortment created different genotypes within those clades (*1*). H5N8 clade 2.3.4.4 viruses have predominantly spread across many countries in Asia to Europe, Africa, and North America (*1*,*2*); repeated outbreaks caused by H5N8 clade 2.3.4.4b viruses were reported during 2016 to mid-2020 (*3*,*4*). However, H5N1 clade 2.3.4.4b virus emerged in late 2020, which led to an increase in wild bird and poultry influenza outbreaks worldwide; this virus strain has almost entirely replaced H5N8 clade 2.3.4.4b globally since late 2021 (*5*). Moreover, the eastward movement of H5N1 clade 2.3.4.4b virus outbreaks from Europe to East Asia since late 2021 suggests that wild birds likely play a role in virus introduction (*5*,*6*).

Author affiliations: Disease Investigation Center Wates, Yogyakarta, Indonesia (H. Wibawa, Lestari, J. Silaban, S.H. Irianingsih, Z. Fahmia, H. Mulyawan); Disease Investigation Center Banjarbaru, Banjarbaru, Indonesia (P.E. Wibowo, A. Supriyadi, A.A. Fuadi, A.J. Fiqri, R.W. Handayani); Directorate General of Livestock and Animal Health Services, Jakarta, Indonesia (S. Idris, N. Zainuddin)

DOI: https://doi.org/10.3201/eid3003.230973

The Study

In April 2022, high numbers of poultry deaths were reported from 5 duck farms in Hulu Sungai Utara District, South Kalimantan Province, Indonesia (Appendix Figure 1, https://wwwnc.cdc.gov/EID/article/30/3/23-0973-App1.pdf). Approximately 4,430 of 5,770 (76.8%) ducks of different ages died; younger ducks manifested more severe disease. In July 2023, the deaths of 294 (135 adult and 159 young) of 450 ducks were reported in a Muscovy duck farm in Banjarbaru District of South Kalimantan Province. We collected oropharyngeal swab or tissue samples from ducks in Hulu Sungai Utara in 2022 and Banjarbaru in 2023 for necropsy and hematoxylin/eosin staining; gross and histologic pathology analyses were performed at the Disease Investigation Center Banjarbaru (Appendix). We also collected samples from ducks in LBMs within Banjar District (October 2022), which is located between the Hulu Sungai Utara and Banjarbaru districts where disease was reported (Appendix Figure 1). We sent all influenza A(H5) PCR–positive samples to the Disease Investigation Center Wates in Yogyakarta, where viruses were isolated by using the World Organisation for Animal Health protocol (*7*). However, viruses could only be isolated from 3 pooled swab samples from the initial cases in April 2022 in Hulu Sungai Utara, 1 tissue sample from the July 2023 case in Banjarbaru, and 1 pooled swab sample from LBMs in Banjar. We characterized the virus isolates antigenically by using hemagglutination inhibition assays and

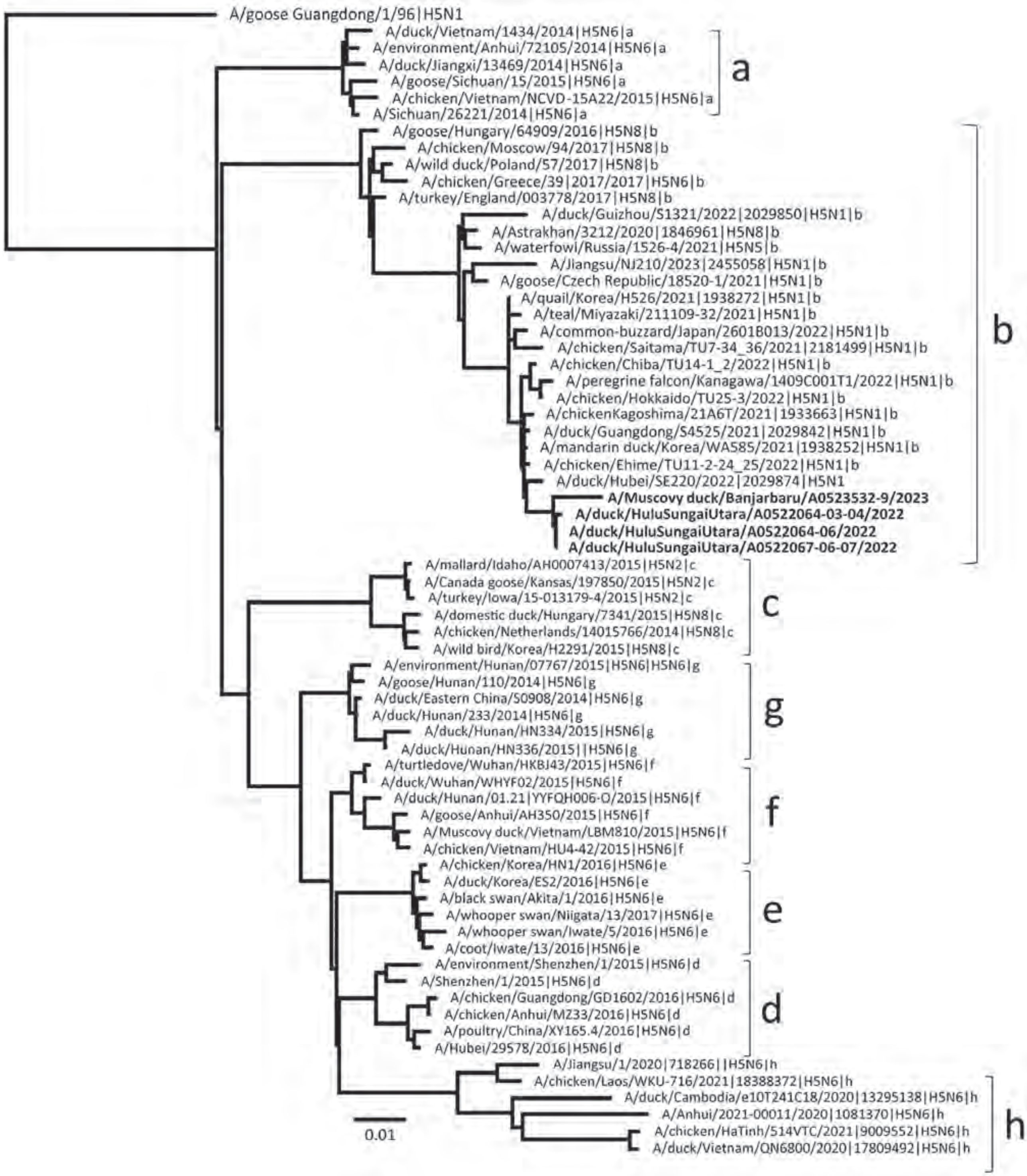

Figure. Phylogenetic analysis of the hemagglutinin gene of highly pathogenic avian influenza A(H5N1) clade 2.3.4.4b viruses isolated from domestic ducks during outbreaks in South Kalimantan, Indonesia, in April 2022 and July 2023 compared with reference sequences. Bold font indicates the viruses isolated from duck farms in this study. Letters at right indicate subclades. Evolutionary history was inferred by using the maximum-likelihood method and best-fit general time reversible plus gamma distribution 4 substitution model involving 67 hemagglutinin H5 sequences from the GISAID database (http://www.gisaid.org); a total of 1,656 positions were in the final dataset. Scale bar indicates nucleotide substitutions per site.

genetically by using whole-genome sequencing on an Illumina sequencing platform (https://www.illumina.com) (Appendix).

We deposited whole-genome sequences of 4 virus isolates into the GISAID database (https://www.gisaid.org) under accession nos. EPI_ISL_17371282 (A/duck/Hulu Sungai Utara/A0522064-06/2022), EPI_ISL_17371283 (A/duck/Hulu Sungai Utara/A0522064-03-04/2022), EPI_ISL_17371284 (A/duck/Hulu Sungai Utara/A0522067-06-07/2022), and EPI_ISL_18438033 (A/Muscovy duck/Banjarbaru/A0523532-9/2023). All 5 identified virus isolates were H5N1 clade 2.3.4.4b viruses, but the virus isolate from LBMs in Banjar District was not included in further analysis or deposited in the GISAID database because of incomplete gene sequences (<50% full-length sequence for each gene segment).

Phylogenetic analysis of the HA gene segment showed that all 4 analyzed viruses clustered with recent HPAI H5 clade 2.3.3.4b viruses from Asia and Europe (Figure). However, they appeared to be more closely related to H5N1 clade 2.3.4.4b viruses from wild birds and poultry from Japan, China, and South Korea isolated during October 2021–February 2022. Phylogenetic trees for the other gene segments (polymerase basic 1, polymerase basic 2, polymerase acidic, nucleoprotein, neuraminidase, matrix protein, and nonstructural segments) also indicated that all 4 viruses were closely related to H5N1 clade 2.3.4.4b from Japan, China, and South Korea (Appendix Figures 2–5). The 3 viruses isolated from the influenza outbreak in April 2022 shared 99.8%–100% nucleotide sequence similarity for each viral segment; however, we observed a lower nucleotide sequence similarity between the viruses from April 2022 and the virus isolated in July 2023 (Table 1), indicating that H5N1 clade 2.3.4.4b continued to mutate resulting in genetic drift. We identified all virus isolates as HPAI on the basis of amino acid sequences within the HA cleavage site (REKRRKR|G); none of those isolates had molecular determinants associated with increased binding affinity or replication efficiency in mammals, including humans (Appendix Table 1) (*8*,*9*). A BLAST search (https://www.ncbi.nlm.nih.gov/blast) and pairwise distance analysis indicated all 8 gene segments from viruses isolated during the first outbreak in April 2022 had 98.4%–99.8% nucleic acid sequence identities to H5N1 clade 2.3.4.4b viruses from Japan, China, and South Korea, suggesting a close common ancestor.

The gross and histologic pathology of naturally infected ducks showed multiorgan hemorrhages

Table 1. DNA sequence homologies between highly pathogenic avian influenza A(H5N1) clade 2.3.4.4b viruses isolated from domestic ducks in Indonesia, 2022, and those from Banjarbaru and East Asia*

Virus name	GISAID no.†	Collection date	% Nucleic acid similarity for each gene segment							
			PB2	PB1	PA	HA	NP	NA	MP	NS
Viruses from first outbreak in Hulu Sungai Utara	EPI_ISL_17371282, EPI_ISL_17371283, EPI_ISL_17371284	2022 Apr	100	100	99.8–99.9	99.9–100	100	100	100	99.8–100
A/Muscovy duck/Banjarbaru/A0523532-9/2023	EPI_ISL_18438033	2023 Jul 7	99.4	99.3–99.4	99.1–99.2	98.9–99.0	99.1	98.8	99.8	98.7
A/mandarin duck/Korea/WA585/2021	EPI_ISL_6959592	2021 Oct 26	99.6	99.5–99.6	99.6–99.7	99.2–99.3	99.6	99.8	99.6	99.4
A/quail/Korea/H526/2021	EPI_ISL_6959593	2021 Nov 8	99.4	99.2	99.2–99.3	99.0–99.1	99.3	99.6	99.3	99.2
A/duck/Guangdong/S4525/2021	EPI_ISL_12572655	2021 Dec 8	99.6	99.6	99.3–99.4	99.2–99.3	99.5	99.7	99.7	99.2
A/duck/Hubei/SE220/2022	EPI_ISL_12572659	2022 Jan 10	99.6	99.5	99.3–99.4	99.0–99.2	99.5	99.5	99.6	99.2
A/duck/Guizhou/S1321/2022	EPI_ISL_12572656	2022 Feb 22	99.6	99.6	99.5–99.6	97.2–97.3	99.5	99.4	99.8	99.2
A/chicken/Kagoshima/21A6T/2021	EPI_ISL_6829533	2021 Nov 12	99.6	99.6	99.6–99.7	99.1–99.2	99.6	99.7	99.8	99.4
A/chicken/Saitama/TU7-34,36/2021	EPI_ISL_15063425	2021 Dec 7	99.6	99.3–99.4	99.1–99.2	98.4–98.6	99.1	99.6	99.3	99.0
A/chicken/Ehime/TU11-2-24 25/2022	EPI_ISL_15063431	2022 Jan 4	99.8	92.0	99.5–99.6	99.2–99.3	99.3	99.6	99.7	99.3
A/common buzzard/Japan/2601B013/2022	EPI_ISL_16831015	2022 Jan 27	99.6	99.2–99.3	99.3–99.4	98.6–98.7	99.3	99.6	99.3	99.2
A/teal/Miyazaki/211109-32/2021	EPI_ISL_15613494	2021 Nov 9	99.4	99.2–99.3	99.3	98.7–98.8	99.1	99.6	99.2	99.2

*H5N1 clade 2.3.4.4b viruses isolated from the initial poultry outbreak in Hulu Sungai Utara in April 2022 were compared with those isolated later from Banjarbaru, Indonesia, in July 2023 and H5N1 clade 2.3.4.b viruses from East Asia isolated during October 2021–February 2022. HA, hemagglutinin; MP, matrix protein; NA, neuraminidase; NP, nucleoprotein; NS, nonstructural; PA, polymerase acidic; PB1, polymerase basic 1; PB2, polymerase basic 2.
†GISAID database (https://www.gisaid.org).

Table 2. Hemagglutinin inhibition assay titers using 2-fold serial dilutions of virus-specific antiserum in study of highly pathogenic avian influenza A(H5N1) virus clade 2.3.4.4b in domestic ducks, Indonesia, 2022*

Antiserum source, clade, GISAID no.†	Antigen source			
	A/duck/Hulu Sungai Utara/A0522064-06/2022	A/duck/Hulu Sungai Utara/A0522064-03-04/2022	A/duck/Hulu Sungai Utara/A0522067-06-07/2022	A/muscovy duck/ Banjarbaru/A0523532-9/2023
A/chicken/West Java/PWT-WIJ/2006, H5N1 clade 2.1.3.2, EPI_ISL_12700530‡	<4	<4	<4	16
A/chicken/Barru/BBVM 41-13/2013, H5N1 clade 2.1.3.2a, EPI_ISL_17767706	16	16	16	16
A /duck/Sukoharjo/BBVW-1428-9/2012, H5N1 clade 2.3.2.1c, EPI_ISL_266808§	16	32	32	32
A/chicken/Tanggamus/031711076-65/2017, H5N1 clade 2.3.2.1c, EPI_ISL_17767763¶	16	32	16	32
A/duck/Laos/XBY004/2014, H5N6 clade 2.3.4.4b, EPI_ISL_168385	8	16	8	16
A/duck/Hulu Sungai Utara/A0522064-03-04/2022, H5N1 clade 2.3.4.4b#	512	512	128	128

*Viruses were isolated by using the World Organisation for Animal Health protocol (*7*). The 3 viruses isolated from Hulu Sungai Utara in April 2022 and the virus isolated from Banjarbaru in July 2023 were used as antigen sources.
†GISAID (https://www.gisaid.org).
‡H5N1 clade 2.1.3.2 vaccine-seed strain used in Indonesia since 2009.
§H5N1 clade 2.3.2.1c vaccine strain used during 2012–2020.
¶H5N1 clade 2.3.2.1c vaccine strain used since 2021.
#Homologous antiserum for H5N1 clade 2.3.4.4b viruses isolated from the initial outbreak in Hulu Sungai Utara, April 2022.

with prominent lesions in tissues and congestion and focal necrosis in parenchymal cells, often accompanied by inflammatory cell infiltrates (Appendix, Figure 6). Hemagglutination inhibition assays revealed the virus isolates from April 2022 had low reactivity with H5N1 antiserum derived from circulating viruses, including the H5N1 vaccine strains used for poultry (Table 2). Those results suggest that new vaccine candidates antigenically matched to circulating viruses might be needed in Indonesia, if H5N1 clade 2.3.4.4b viruses continue to infect poultry.

Wild migratory birds might play a role in the intercontinental spread of HPAI H5Nx clade 2.3.4.4 viruses (*1*,*10*,*11*). Indonesia is situated within the East Asian Flyway's island or oceanic routes linking eastern Russia and Japan to the Philippines and eastern Indonesia (*12*). One stopover site is on the west coast of South Kalimantan, where 23 migratory bird species have been identified and observed (*13*). Migratory birds often use stopover sites for 1 day to several weeks to rest and refuel (*12*), providing opportunities for virus transmission through direct or indirect contacts with local wild birds or aquatic poultry within their shared habitats.

During April 2022–July 2023, we conducted molecular surveillance through a network for influenza virus monitoring in Indonesia (*14*) and did not detect other H5N1 clade 2.3.4.4b outbreaks outside of South Kalimantan. Similar to an earlier virus incursion of H5N1 clade 2.3.2.1c in Java in 2012, which initially also affected ducks (*15*), we could not determine the exact origin of virus incursion. However, genetic evidence and bird migration patterns suggest that migratory birds contributed to the introduction of H5N1 clade 2.3.4.4b into Indonesia.

Conclusion

We identified HPAI H5N1 clade 2.3.4.4b viruses in ducks in South Kalimantan, Indonesia. The role of migratory birds in virus introduction cannot be ruled out because South Kalimantan is situated within the East Asia Flyway corridor, and the infected farms were connected to marshes that provided opportunity for direct or indirect contacts with migratory birds. Limited wild bird surveillance and genome sequence data for avian influenza viruses impeded our ability to determine further transmission and spread of H5N1 clade 2.3.4.4b in Indonesia. Both epidemiologic studies and molecular surveillance of wild birds are needed to better prepare for pandemic threats caused by continued avian influenza virus evolution in Indonesia and elsewhere.

Acknowledgments

We gratefully acknowledge all data contributors, including the authors and their originating laboratories responsible for obtaining the specimens, and their submitting laboratories for generating the genetic sequence and metadata and sharing via the GISAID Initiative (http://www.gisaid.org), on which this research is based (Appendix Table 2). We also thank the staff at the Disease Investigation Center Banjabaru for conducting field investigation and initial laboratory diagnostics and the staff at the Disease Investigation Center Wates for virus isolation, serology testing, and whole-genome sequencing.

This study was supported by the Directorate General of Livestock and Animal Health Services of the Ministry of Agriculture, Indonesia. Some sequencing reagents and the antigen/antiserum for hemagglutination inhibition assays were funded by the United Nations Food and Agriculture Organization Emergency Centre for Transboundary Animal Diseases, Jakarta, Indonesia and CSIRO-Australian Center for Disease Preparedness, Geelong, Victoria, Australia.

About Author

Dr. Wibawa is a veterinarian at the Disease Investigation Centre Wates, Directorate General of Livestock and Animal Health Services of the Ministry of Agriculture, Indonesia. His research interests focus on molecular diagnostics and epidemiology of influenza viruses in animals.

References

1. Lee DH, Bertran K, Kwon JH, Swayne DE. Evolution, global spread, and pathogenicity of highly pathogenic avian influenza H5Nx clade 2.3.4.4. J Vet Sci. 2017;18:269–80. https://doi.org/10.4142/jvs.2017.18.S1.269
2. Kwon JH, Bertran K, Lee DH, Criado MF, Killmaster L, Pantin-Jackwood MJ, et al. Diverse infectivity, transmissibility, and pathobiology of clade 2.3.4.4 H5Nx highly pathogenic avian influenza viruses in chickens. Emerg Microbes Infect. 2023;12:2218945. https://doi.org/10.1080/22221751.2023.2218945
3. Yehia N, Naguib MM, Li R, Hagag N, El-Husseiny M, Mosaad Z, et al. Multiple introductions of reassorted highly pathogenic avian influenza viruses (H5N8) clade 2.3.4.4b causing outbreaks in wild birds and poultry in Egypt. Infect Genet Evol. 2018;58:56–65. https://doi.org/10.1016/j.meegid.2017.12.011
4. Engelsma M, Heutink R, Harders F, Germeraad EA, Beerens N. Multiple introductions of reassorted highly pathogenic avian influenza H5Nx viruses clade 2.3.4.4b causing outbreaks in wild birds and poultry in the Netherlands, 2020–2021. Microbiol Spectr. 2022;10:e0249921. https://doi.org/10.1128/spectrum.02499-21
5. Xie R, Edwards KM, Wille M, Wei X, Wong SS, Zanin M, et al. The episodic resurgence of highly pathogenic avian influenza H5 virus. Nature. 2023;622:810–7. https://doi.org/10.1038/s41586-023-06631-2
6. Yang J, Zhang C, Yuan Y, Sun J, Lu L, Sun H, et al. Novel avian influenza virus (H5N1) clade 2.3.4.4b reassortants in migratory birds, China. Emerg Infect Dis. 2023;29:1244–9. https://doi.org/10.3201/eid2906.221723
7. World Organisation for Animal Health. WOAH terrestrial manual 2021, Chapter 3.3.4. Avian influenza (including infection with high pathogenicity avian influenza viruses) [cited 2023 Jan 2]. https://www.woah.org/fileadmin/Home/eng/Health_standards/tahm/3.03.04_AI.pdf
8. Chutinimitkul S, van Riel D, Munster VJ, van den Brand JMA, Rimmelzwaan GF, Kuiken T, et al. In vitro assessment of attachment pattern and replication efficiency of H5N1 influenza A viruses with altered receptor specificity. J Virol. 2010;84:6825–33. https://doi.org/10.1128/JVI.02737-09
9. Suttie A, Deng YM, Greenhill AR, Dussart P, Horwood PF, Karlsson EA. Inventory of molecular markers affecting biological characteristics of avian influenza A viruses. Virus Genes. 2019;55:739–68. https://doi.org/10.1007/s11262-019-01700-z
10. Caliendo V, Lewis NS, Pohlmann A, Baillie SR, Banyard AC, Beer M, et al. Transatlantic spread of highly pathogenic avian influenza H5N1 by wild birds from Europe to North America in 2021. Sci Rep. 2022;12:11729. https://doi.org/10.1038/s41598-022-13447-z
11. Zhang G, Li B, Raghwani J, Vrancken B, Jia R, Hill SC, et al. Bidirectional movement of emerging H5N8 avian influenza viruses between Europe and Asia via migratory birds since early 2020. Mol Biol Evol. 2023;40:msad019. PubMed https://doi.org/10.1093/molbev/msad019
12. Yong DL, Heim W, Chowdhury SU, Choi CY, Ktitorov P, Kulikova O, et al. The state of migratory landbirds in the East Asian Flyway: distribution, threats, and conservation needs. Front Ecol Evol. 2021;9:1–22. https://doi.org/10.3389/fevo.2021.613172
13. Riefani MK and Soendjoto MA. Birds in the west coast of South Kalimantan, Indonesia. Biodiversitas 2021;22:278–87. https://doi.org/10.13057/biodiv/d220134
14. Hartaningsih N, Wibawa H, Pudjiatmoko, Rasa FST, Irianingsih SH, Dharmawan R, et al. Surveillance at the molecular level: developing an integrated network for detecting variation in avian influenza viruses in Indonesia. Prev Vet Med. 2015;120:96–105. https://doi.org/10.1016/j.prevetmed.2015.02.015
15. Dharmayanti NL, Hartawan R, Pudjiatmoko, Wibawa H, Hardiman, Balish A, et al. Genetic characterization of clade 2.3.2.1 avian influenza A(H5N1) viruses, Indonesia, 2012. Emerg Infect Dis. 2014;20:671–4. https://doi.org/10.3201/eid2004.130517

Address for correspondence: Hendra Wibawa, Disease Investigation Center Wates, Jl. Wates KM 27, Wates, Kulon Progo, Yogyakarta 55602, Indonesia; email: hendra.wibawa@pertanian.go.id

Emergence of Thelaziosis Caused by *Thelazia callipaeda* in Dogs and Cats, United States

Ranju R.S. Manoj, Holly White, Rebecca Young, Charles E. Brown, Renee Wilcox, Domenico Otranto, Manigandan Lejeune

We report 2 autochthonous feline thelaziosis cases caused by the eyeworm *Thelazia callipaeda* and discuss the spread among dogs in the northeastern United States. Phylogenetic analysis suggests the parasite was introduced from Europe. Adopting a One Health approach is needed to limit further spread of *T. callipaeda* eyeworms in North America.

Thelazia callipaeda eyeworm was considered an exotic parasite in North America until an autochthonous case was reported in a dog from New York, USA, in 2020 (*1*). *T. callipaeda* eyeworm has been reported in countries in East Asia and the Soviet Union, later expanding its geographic range into Europe (*2*,*3*). This zoonotic parasite primarily infects the orbital cavity of its host causing thelaziosis (*3*). The zoophilic secretophagous male fly, *Phortica variegata*, is a *T. callipaeda* vector; flies ingest first-stage *T. callipaeda* larvae from the lacrimal secretions of an infected host and redeposit them as infective third-stage larvae, which eventually complete their life cycle by developing into adult worms (*4*). *P. variegata* flies have been found in Orange and Monroe Counties in New York (*5*,*6*), which has likely promoted the emergence of *T. callipaeda* eyeworm in North America (*4*). Since the *T. callipaeda* infection in a dog reported in New York in 2020, a total of 11 canine cases (6 in New York, 3 in New Jersey, 1 each in Connecticut and Nevada) and 2 feline cases (both from New York) (Figure 1) have been confirmed morphologically at the Cornell Animal Health Diagnostic Center (AHDC) in Ithaca, New York, USA. We describe 2 feline thelaziosis cases and discuss new canine cases in northeastern United States (New York/New Jersey border) during February 2021–December 2022 and One Health approaches to limit spread of this emerging disease in the United States.

The Study

Case 1 was in a 16-year-old neutered male, domestic shorthair cat from Greenwood Lake, Orange County, New York, that had been regularly cared for at the Warwick Valley Veterinary Hospital in New York, since October 2019. The animal had a recurrent history of flea infestation, which was managed with selamectin. The cat received routine rabies vaccinations at the clinic and was regularly dewormed with a combination of emodepside (3 mg/kg) and praziquantel (12 mg/kg) applied topically to the skin by the owner. Since June 2021, the animal has been treated for progressive chronic kidney disease. During a visit in April 2022, the cat had crusty lesions on its swollen right eye. Initial treatment with an ophthalmic ointment containing tobramycin resolved the eye infection. In August 2022, the cat manifested squinting, epiphora, and mucus accumulation in the right eye, which did not improve after tobramycin treatment. Detailed examination of the right eye revealed a constricted pupil and an elevated nictitating membrane with 4 thread-like worms, which were recovered mechanically at the clinic by flushing with saline solution. Of the 4 worms collected, 1 intact worm was received at AHDC for identification. The cat did not travel outside of New York. The animal was prescribed an ophthalmic ointment containing neomycin and polymyxin B and a dewormer (combination of emodepside [3 mg/kg] and praziquantel [12 mg/kg]) applied topically to the skin. No relapse was observed after treatment.

Author affiliations: Cornell University, Ithaca, New York, USA (R.R.S. Manoj, H. White, R. Young, M. Lejeune); Warwick Valley Veterinary Hospital, Warwick, New York, USA (C.E. Brown); Countryside Animal Hospital, Staatsburg, New York, USA (R. Wilcox); University of Bari Aldo Moro, Bari, Italy (D. Otranto); City University of Hong Kong, Hong Kong, China (D. Otranto)

DOI: https://doi.org/10.3201/eid3003.230700

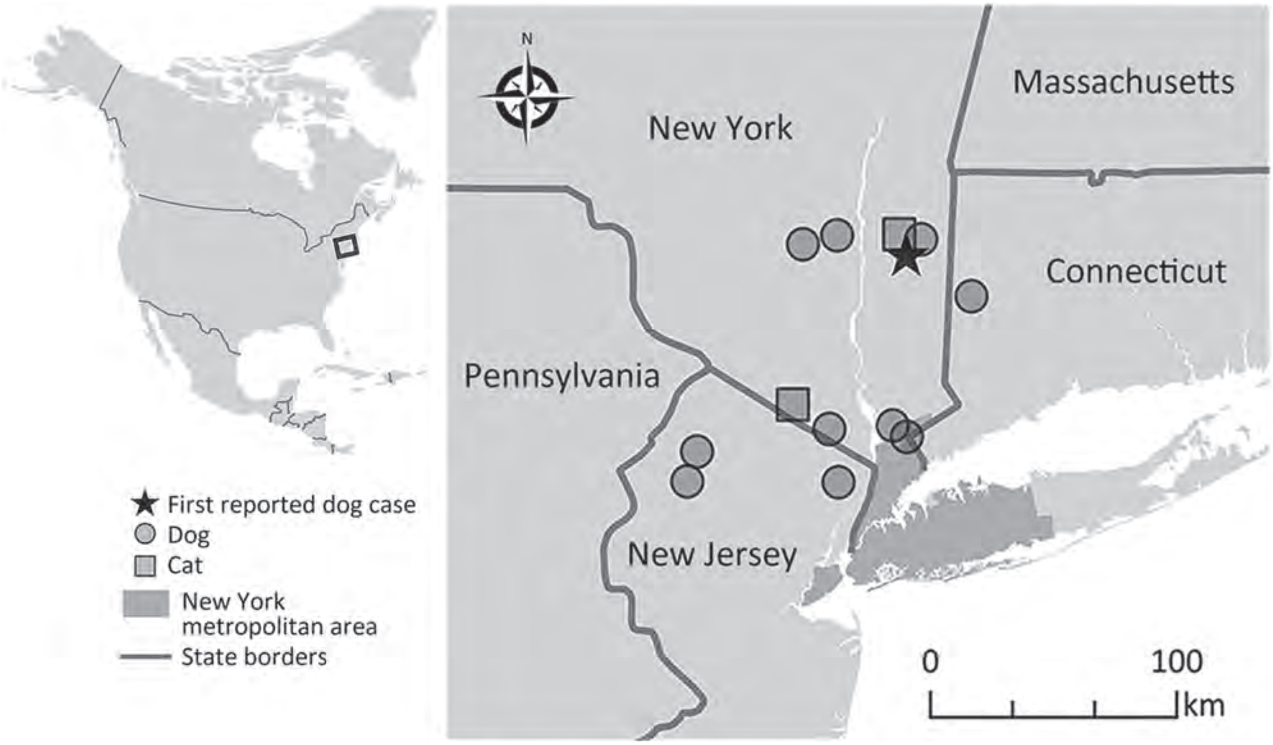

Figure 1. Locations of thelaziosis cases caused by *Thelazia callipaeda* eyeworm in dogs (circles) and cats (squares), New York, New Jersey, and Connecticut, USA. Star indicates the dog case reported in New York in 2020. Inset map indicates the area where *T. callipaeda* infections were reported (box). The dog case reported from Nevada was not included in the map because the travel history for that animal was unknown.

Case 2 was in a 2.5-year-old spayed female, domestic shorthair cat from a multicat household in Clinton Corners, Dutchess County, New York (adopted in Columbia County, New York). The cat did not travel outside of New York and was examined in October 2022 at a pet hospital during a routine rabies vaccination appointment. Ophthalmic examination revealed multiple white thread-like worms on the bulbar conjunctiva of both eyes (Figure 2). The cat had no clinical signs and was prescribed a dewormer (combination of emodepside [3 mg/kg] and praziquantel [12 mg/kg]) applied topically to the skin. Follow-up after 2 weeks revealed the presence of 8 worms, which were manually removed under local anesthesia. Two intact worms were sent to AHDC for identification. The cat was prescribed a combination of imidacloprid (10 mg/kg) and moxidectin (1 mg/kg) applied topically to the skin. Complete recovery was noted during a follow-up visit in November 2022.

At AHDC, we identified 1 male worm from case 1 and 2 female worms from case 2 morphologically as *T. callipaeda* eyeworm, primarily on the basis of transverse cuticular striations. The female worms were 11 and 14 mm long, and the male worm was 8.1 mm long; all 3 had a wide, moderately deep buccal cavity. The number of transverse cuticular striations at the cephalic, midbody, and caudal regions ranged 150–400/mm/region in both male and female worms. In the male worm, the long spicule was ≈2 mm long

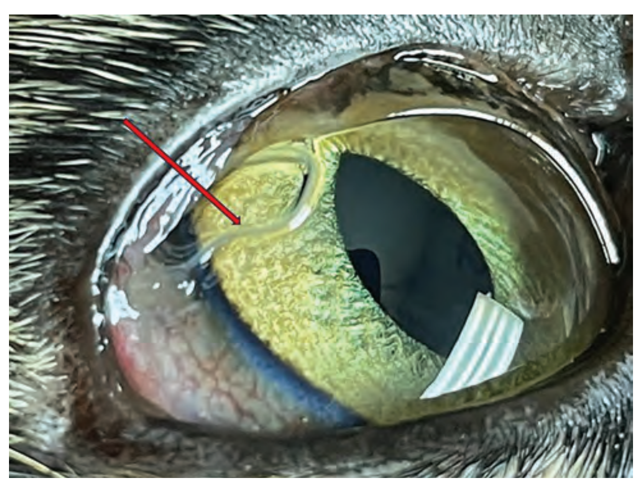

Figure 2. Adult parasites (red arrow) in the bulbar conjunctiva of the left eye of a cat in study of emergence of thelaziosis caused by *Thelazia callipaeda* in dogs and cats, United States. The cat was 2.5-year-old spayed female domestic shorthair cat (case 2) examined in October 2022.

and the short spicule was 0.1 mm long. The vulval opening in the female worms was anterior to the esophageal/intestinal junction (Appendix Figure 1, https://wwwnc.cdc.gov/EID/article/30/3/23-0700-App1.pdf).

We performed PCR on 1 female worm sample from feline case 2 and 1 sample from a dog case targeting 12S rRNA, 18S rRNA, and cytochrome oxidase c subunit 1 (*cox1*) using previously described protocols (*7*–*9*). The amplified PCR products for both worm samples were 421 bp for 12S rRNA, 891 bp for 18S rRNA, and 612 bp for *cox1*. We Sanger sequenced the PCR products, edited and aligned the sequences by using BioEdit (https://bioedit.software.informer.com), and compared them with available GenBank sequences by using BLAST analysis (https://blast.ncbi.nlm.nih.gov). We observed 100% sequence identity with corresponding genes available for *T. callipaeda* in GenBank. We deposited the sequences from this study in GenBank under accession nos. OR545549, OR545261, and OR982681. Phylogenetic analysis of the *cox1* sequences revealed clustering as a monophyletic clade with *T. callipaeda* haplotype 1 from Europe (*10*,*11*) (Appendix Figure 2). This study and the previous report on a dog (*1*) reconfirm the possibility that this parasite was introduced from Europe and subsequently spread in the United States.

Conclusions

The presence of *T. callipaeda* eyeworm in 2 cats and 11 dogs with no travel history outside of the United States suggests that this parasite is emerging in North America. Indeed, a previous study documented the presence of *P. variegata* flies in 2 counties in New York and indicated this fly species is a competent vector for *T. callipaeda* eyeworm, further suggesting an emerging threat by this eyeworm in the northeastern region of the United States (*6*). In addition, a wide variety of wildlife in New York, including coyotes, red foxes, gray foxes, black bears, raccoons, minks, least weasels, striped skunks, cottontail rabbits, and snowshoe hares, might act as potential hosts for *T. callipaeda* eyeworm (*6*); no human cases have been reported from this geographic area. A canine thelaziosis case was also found in the western United States (Nevada), although the travel history is unknown for that dog. Adopting proper diagnosis and surveillance measures is critical to limit the spread of this zoonotic parasite. Studies on control and treatment approaches for dogs suggest mechanical removal of adult and larval *T. callipaeda* nematodes coupled with the administration of diverse deworming drugs is effective (*12*). Because vector control using fly repellents is ineffective (*3*), control of *T. callipaeda* infections mainly rely on diagnosis and timely anthelmintic treatment. The presence of the natural vector, *P. variegata* flies (*4*,*6*), and the potential involvement of the sylvatic cycle promote the spread of this exotic parasite. Most cases in this study were diagnosed in late summer and autumn, which correlates with peak fly activity. Therefore, prophylactic anthelmintic administration coinciding with fly seasons would be an effective control strategy. Furthermore, as indicated in previous reports (*1*,*4*), adoption of a holistic One Health approach will be effective in further limiting the spread of *T. callipaeda* eyeworm in North America.

Acknowledgments

We thank Nicholas A. Hollingshead for his assistance in preparing the map and Antech Diagnostics for sharing information about *Thelazia* infection cases.

About the Author

Dr. Manoj is a postdoctoral associate and Merck parasitology resident at the National Center for Veterinary Parasitology at the Animal Health Diagnostic Center, Cornell University, New York. Her research interests include vectorborne zoonotic diseases, particularly filarioids and their endosymbiont *Wolbachia*.

References

1. Schwartz AB, Lejeune M, Verocai GG, Young R, Schwartz PH. Autochthonous *Thelazia callipaeda* infection in dog, New York, USA, 2020. Emerg Infect Dis. 2021;27:1923–6. https://doi.org/10.3201/eid2707.210019
2. do Vale B, Lopes AP, da Conceição Fontes M, Silvestre M, Cardoso L, Coelho AC. Systematic review on infection and disease caused by *Thelazia callipaeda* in Europe: 2001–2020. Parasite. 2020;27:52. https://doi.org/10.1051/parasite/2020048
3. Otranto D, Mendoza-Roldan JA, Dantas-Torres F. *Thelazia callipaeda*. Trends Parasitol. 2021;37:263–4. https://doi.org/10.1016/j.pt.2020.04.013
4. Otranto D, Cantacessi C, Testini G, Lia RP. *Phortica variegata* as an intermediate host of *Thelazia callipaeda* under natural conditions: evidence for pathogen transmission by a male arthropod vector. Int J Parasitol. 2006;36:1167–73. https://doi.org/10.1016/j.ijpara.2006.06.006
5. Werner T, Steenwinkel T, Jaenike J. The encyclopedia of North American drosophilids: drosophilids of the midwest and northeast. 2018 [cited 2021 May 10]. https://digitalcommons.mtu.edu/cgi/viewcontent.cgi?article=1000&context=oabooks
6. Otranto D, Iatta R, Lia RP, Cavalera MA, Màca J, Pombi M, et al. Competence of *Phortica variegata* from the United States as an intermediate host of the *Thelazia callipaeda* eyeworm. Am J Trop Med Hyg. 2018;98:1175–8. https://doi.org/10.4269/ajtmh.17-0956
7. Floyd RM, Rogers AD, Lambshead PJD, Smith CR. Nematode–specific PCR primers for the 18S small subunit rRNA gene. Mol Ecol Notes. 2005;5:611–2. https://doi.org/10.1111/j.1471-8286.2005.01009.x

8. Casiraghi M, Anderson TJ, Bandi C, Bazzocchi C, Genchi C. A phylogenetic analysis of filarial nematodes: comparison with the phylogeny of *Wolbachia* endosymbionts. Parasitology. 2001;122:93–103. https://doi.org/10.1017/S0031182000007149
9. Morales-Hojas R, Cheke RA, Post RJ. Molecular systematics of five *Onchocerca* species (Nematoda: Filarioidea) including the human parasite, *O. volvulus*, suggest sympatric speciation. J Helminthol. 2006;80:281–90.
10. Tamura K, Stecher G, Kumar S. MEGA11: molecular evolutionary genetics analysis version 11. Mol Biol Evol. 2021;38:3022–7. https://doi.org/10.1093/molbev/msab120
11. Hasegawa M, Kishino H, Yano T. Dating of the human-ape splitting by a molecular clock of mitochondrial DNA. J Mol Evol. 1985;22:160–74. https://doi.org/10.1007/BF02101694
12. Bezerra-Santos MA, Mendoza-Roldan JA, Sgroi G, Lia RP, Venegoni G, Solari Basano F, et al. Efficacy of a formulation of sarolaner/moxidectin/pyrantel (Simparica Trio®) for the prevention of *Thelazia callipaeda* canine eyeworm infection. Parasit Vectors. 2022;15:370. https://doi.org/10.1186/s13071-022-05501-6

Address for correspondence: Manigandan Lejeune, Department of Population Medicine and Diagnostic Sciences, Cornell University College of Veterinary Medicine, Ithaca, NY 14853, USA; email: ml872@cornell.edu

The Last of Us and the Question of a Fungal Pandemic in Real Life

Georgios Pappas, Georgia Vrioni

The television series The Last of Us imagines a postapocalyptic world ravaged by a fungal pandemic caused by a *Cordyceps* species. We evaluate whether a fungal pandemic is possible (and reasons behind its current improbability). We further discuss the series' effect on public perception of fungi, fungal infections, and pandemic response.

The recent release of The Last of Us, a television drama series created for HBO consisting of 9 episodes in its first season (and renewed for a second season), has shed light on the global significance of fungal infections and spurred discussions on their potential to cause a pandemic. The series has met with wide acclaim, even prompting the Centers for Disease Control and Prevention to officially clarify the plausibility of the show's premise in a tweet. Created by Craig Mazin and Neil Druckmann, The Last of Us is based on a successful video game developed in 2013 by the company Naughty Dog. Both the game and the television series take place in a postpandemic world, in which most humans have been either transformed into zombies by a human-adapted, mind-controlling fungal species of *Cordyceps* or killed by zombies, rogue humans, or the totalitarian state. Twenty years after the outbreak, a young girl who is immune to infection crosses the United States, accompanied by her protector, to reach scientists hoping to create a cure or a vaccine by studying her.

Is Such a Scenario, of a Fungal Pandemic, Plausible?

Up to 5.1 million fungal species are estimated to exist in nature (*1*). About 148,000 types have been characterized, a few hundred of which are pathogenic for humans (*2*). A recent fungal priority pathogens list developed by the World Health Organization attributes 1.6 million annual deaths to fungal infections (*3*); considerable illness can also be attributed to fungal infections. In recent years, a rising percentage of emerging infectious diseases has been fungal in nature, including multidrug-resistant species with considerable mortality such as *Candida auris* (*4*) and rapidly disseminating ones such as *Trichophyton indotineae* (*5*). In a planetary health approach, the significance of fungal infections is even broader. Eighty percent of plant diseases are attributed to fungi, including pathogens that bring about substantial species or crop destruction worldwide. *Cryphonectria parasitica* eliminated almost 4 billion sweet chestnut trees in the eastern United States after its geographic introduction (*6*), *Magnaporthe oryzae* has destroyed rice crops (*7*), and *Puccinia graminis* has emerged as a major risk for grains (*8*). Panzootics can be caused by fungi, even threatening to evolve into extinction-level events; a recent example is the emergence of chytrid fungi that have menaced numerous amphibian species (*9*).

In humans, the importance of fungal infections has been increasing because of the increase in susceptible populations, in particular immunocompromised persons of varying immunologic deficits, ranging from transplant patients to persons with diabetes mellitus (which is known to predispose persons to severe mucormycosis) (*10*). Progress in antifungal therapeutic interventions has been slow, partly because of the fungi eukaryotic nature, which can lead to substantial adverse events. At present, only 4 classes of antifungals are available (azoles, polyenes, pyrimidines, and echinocandins), although research toward new antifungal development is promising (*11*). Certain species express a multidrug-resistant profile, though, including *C. auris* and *T. indotineae*.

Selective pressures might account for emergence of novel fungal pathogens, as in the case of *C. auris*, the concurrent worldwide appearance of which might be a consequence of global warming, enabling fungal species to adapt to higher temperatures and subsequently to human body

Author affiliations: Institute of Continuing Medical Education of Ioannina, Ioannina, Greece (G. Pappas); National Kapodistrian University of Athens, Athens, Greece (G. Vrioni)

DOI: https://doi.org/10.3201/eid3003.230684

temperature, a major obstacle to the development of nonsuperficial fungal infections in humans (*2*,*12*). Human practices also induce fungal reemergence, as with the appearance of resistant *Aspergillus* species because of the extensive, uncontrolled use of fungicides in agriculture (*13*).

Fortunately, fungi are relatively slow mutators. The process of species-jumping and host adaptation, such as in the case of *Ophiocordyceps unilateralis* (the prototype for the pathogen in The Last of Us), which adapted from beetle-infecting species to ant fungal pathogen (*14*), is time consuming and would not be expected to occur over just a few years.

Cordyceps species are ubiquitous: >100 have been described, they are species-specific, and >35 of them perform "mind control" in their hosts. The *Cordyceps* name is derived both from Ancient Greek and Latin: *κορδύλη* means truncheon and *ceps* means head. *O. unilateralis*, upon infecting an ant, modifies the host's behavior, leading the ant to move to a specific tree-branch height before it dies; the fungus then destroys the host body and sheds fungal spores (from an ideal height) for further fungal dissemination in the environment.

No vertebrate *Cordyceps* hosts exist, and an evolutionary path leading there would probably require tens of thousands of years. Other brain-modifying or brain-occupying pathogens do exist, however, such as rabies virus, perhaps the most typical. Human behavior can be modified by pathogens to enable their spread in simpler ways: common cold viruses induce coughing and sneezing, essentially enhancing their own transmission, and similarly, gastrointestinal pathogens change human bowel habits and enable them to spread through diarrhea (*15*). Further focusing on neural involvement, primary amoebic meningoencephalitis, caused by *Naegleria fowleri*, might be a more accurate example of a brain-eating pathogen. Bornavirus has in the past been considered a cause of psychiatric disorders (an outcome of brain modification), and the role of toxoplasmosis in the future development of schizophrenia has also been evaluated. Numerous other pathogens can manifest through chronic central nervous system involvement and neuropsychiatric symptomatology, including the fungi *Cryptococcus neoformans*.

The extraordinary success of The Last of Us has implications, because all depictions of epidemics and infection in film and television can affect public perceptions of infectious diseases and outbreaks (*16*,*17*). The video game itself was partly successful because it described a critical dystopia (*18*) but one that included utopian foci that signify hope and resistance (in contrast to classical dystopias) and act as a pathway to catharsis, an escape from the doom, for the player and, subsequently, the viewer. In addition, the game was scripted with valid scientific details and an openness to moral issues (*19*): the enemies were not only the infected persons who had become zombies. The Federal Disaster Response Agency was also an enemy, because it represented a totalitarian force that had little to do with public health and protection (admittedly, this is a television show betting on horror and serves as a worst-case scenario and pessimistic study in social psychology). But surviving humans also, at times, became enemies out of desperation or vile evolution (e.g., the Raiders, survivor gangs attacking other uninfected humans for food and supplies). Even the Fireflies, the citizen group fighting the totalitarian state, could be considered an enemy because their mission includes killing the immune child to use her brain to prepare a vaccine. As Erik English recently stated (*20*), sacrificing a child for the greater societal good represents a broken social contract.

The series is ambitious in its scientific statements to the extent that they align with a compelling narrative. Thus, whereas major scientific issues such as global warming, pandemics, and accelerated mutation and adaptation of pathogens are discussed (things that many viewers with a casual understanding of science will recognize as potential threats even if they do not understand the pathology of fungi), certain details might succumb to the needs of the narrative. The series begins with a televised expert panel discussion in the late 1960s; an expert explains that although humanity has been at constant war with epidemic- and pandemic-causing viruses and bacteria, that war is, eventually, always won, despite casualties and lost battles. However, the same would not be certain if a fungal enemy emerged because of climate change, the expert warns.

Fast forward to the opening of the second episode, which narrates the initial outbreak in Indonesia, describing how the epidemic started in a grain/flour factory, initially infecting persons in contact with infected products but then rapidly disseminating through person-to-person transmission worldwide. This point is where the need of the show runners to impress the viewer diverts from scientific reasoning: apart from the improbably fast dissemination of the nonairborne pathogen worldwide, the series presents an expert Indonesian mycologist who states, when asked what should be done about the outbreak, "Bomb Jakarta," an awe-inducing statement. Bombing was implied as a means of outbreak containment in the 1995 film Outbreak, considered to be one of the most accurate on-screen depictions of an outbreak (*16*), but in that scenario, at least, the army proposed it, whereas here it is a scientist's proposal. One could argue that if Jakarta were bombed in this hypothetical scenario, humanity could have been spared from the apocalypse. However, this statement immediately renders the scientific community useless, possibly indirectly weakening the public's trust in science itself (or reflecting public worries about the ability of science to respond adequately). Similarly, the fact that the human response to the pandemic eventually led to a totalitarian state (complete with quarantine zones and death penalties) might reflect the audience's actual fears, particularly in the context of an actual pandemic, in which necessary initial lifesaving measures (e.g., lockdowns) have been vilified by merchants of disinformation. (One could counter-argue that certain approaches to viral containment in China were, or have been presented in the world media as, dystopic). The choice of Jakarta as the origin of the pandemic might feed inaccurate stereotypes that link emerging infectious diseases specifically with the developing world, but southeast Asia has no relevant outbreak history of emerging fungal infections and would not be considered a fungal hot spot. Jakarta could be considered a megacity, however, and as such could contain areas with hygienic challenges that could favor early infection dissemination.

The Last of Us is not the first work of art depicting a postapocalyptic world caused by a *Cordyceps* species adapted to humans. The 2016 film The Girl With All The Gifts, based on the Mike Carey book of the same title, imagines a world where the pathogen achieves equilibrium with its hosts, resulting in a society that breeds intelligent zombie children ("They had to live with the pathogen, endemicity was unavoidable" echoes the excuses used for our actual pandemic response fatigue). The initial depiction of a human-infecting *Cordyceps* outbreak, though, was in 2011, in the Fox television series Fringe, in an episode titled Alone in the World. In that episode, a variant of the fungus with the capacity for hyper-accelerated growth and nutrition absorption formed an extended neural network and was eventually contained with a specifically developed toxin (after initial partially successful ultraviolet light attempts).

Eventually, is a fungal pandemic a plausible scenario? Fungi are not included in the World Health Organization prioritization criteria for potential biologic weapon development and use, and other prioritization scores for biologic weapons (*21*) would yield a low score for fungi. There is no history of rogue research on fungal weaponization; in addition, a narrow spectrum of the population would be vulnerable to such a pathogen, and person-to-person transmission would be limited (we do inhale fungal spores, but we do not exhale them). On the other hand, a fungal pandemic would find humanity ill-prepared. Our diagnostic capacity for fungal pathogens remains extremely limited, no vaccines are available (although preliminary research has been conducted on a *Coccidioides* vaccine, and a *Candida* vaccine has been tested in a phase 2 clinical trial of vulvovaginal candidiasis) (*22*,*23*), and our therapeutic interventions are limited, costly, and have major side effects. Yet there would be space for preventive use of interventions: would rapid dissemination of antifungal medication be feasible in such a case? And how rapidly would antifungal resistance emerge?

In conclusion, The Last of Us might resonate with audiences because of our current experience with a pandemic unprecedented for the modern scientific world, in addition to the creators' narrative abilities and the minor infusions of scientific accuracy. Does The Last of Us leave viewers with a perhaps dangerous and misconstrued perception about how the preparedness of the scientific and public health community to deal with pathogens and pandemics could lead society into an Orwellian dystopia? One could wish for future depictions of zombie apocalypses that are more optimistic regarding human behavior. An example of more positive messaging depicting such an event was the Center for Disease Control and Prevention Zombie Apocalypse preparedness exercise (now retired), which created a much more optimistic scenario while educating persons on how to be ready for an emergency. The Last of Us is not upon us, neither biologically nor psychologically; humankind's response in reality might, we believe, be far kinder than what is portrayed here.

Acknowledgments

We thank the anonymous reviewers for their insightful and constructive comments.

About the Authors

Dr. Pappas is a physician specializing in zoonoses, epidemic preparedness, and social aspects of infectious diseases. Dr. Vrioni is with the microbiology department of the Medical School of the National Kapodistrian University of Athens; her research interests are primarily focused on fungal infections.

References

1. Blackwell M. The fungi: 1, 2, 3 ... 5.1 million species? Am J Bot. 2011;98:426–38. https://doi.org/10.3732/ajb.1000298
2. Garcia-Bustos V, Cabañero-Navalon MD, Ruiz-Gaitán A, Salavert M, Tormo-Mas MÁ, Pemán J. Climate change, animals, and *Candida auris*: insights into the ecological niche of a new species from a One Health approach. Clin Microbiol Infect. 2023;29:858–62. *PMID 36934871*
3. World Health Organization. WHO fungal priority pathogens list to guide research, development and public health action [cited 2023 May 20]. https://www.who.int/publications/i/item/9789240060241
4. Watkins RR, Gowen R, Lionakis MS, Ghannoum M. Update on the pathogenesis, virulence, and treatment of *Candida auris*. Pathog Immun. 2022;7:46–65. https://doi.org/10.20411/pai.v7i2.535
5. Caplan AS, Chaturvedi S, Zhu Y, Todd GC, Yin L, Lopez A, et al. Notes from the field: first reported U.S. cases of Tinea caused by *Trichophyton indotineae*—New York City, December 2021–March 2023. MMWR Morb Mortal Wkly Rep. 2023;72:536–7. https://doi.org/10.15585/mmwr.mm7219a4
6. Roane MK, Griffin GJ, Elkins JR. Chestnut blight, other *Endothia* diseases, and the genus *Endothia*. St. Paul (Minnesota, USA): The American Phytopathological Society; 1986.
7. Fernandez J, Orth K. Rise of a cereal killer: the biology of *Magnaporthe oryzae* biotrophic growth. Trends Microbiol. 2018;26:582–97. https://doi.org/10.1016/j.tim.2017.12.007
8. Singh RP, Hodson DP, Huerta-Espino J, Jin Y, Njau P, Wanyera R, et al. Will stem rust destroy the world's wheat crop? Adv Agron. 2008;98:271–309. https://doi.org/10.1016/S0065-2113(08)00205-8
9. Fisher MC, Garner TWJ. Chytrid fungi and global amphibian declines. Nat Rev Microbiol. 2020;18:332–43. https://doi.org/10.1038/s41579-020-0335-x
10. Steinbrink JM, Miceli MH. Mucormycosis. Infect Dis Clin North Am. 2021;35:435–52. https://doi.org/10.1016/j.idc.2021.03.009
11. Osherov N, Kontoyiannis DP. The anti-*Aspergillus* drug pipeline: is the glass half full or empty? Med Mycol. 2017;55:118–24. https://doi.org/10.1093/mmy/myw060
12. Casadevall A, Kontoyiannis DP, Robert V. Environmental *Candida auris* and the global warming emergence hypothesis. MBio. 2021;12:e00360–21. https://doi.org/10.1128/mBio.00360-21
13. Friedman DZP, Schwartz IS. Emerging fungal infections: new patients, new patterns, and new pathogens. J Fungi (Basel). 2019;5:67. https://doi.org/10.3390/jof5030067
14. Araújo JPM, Hughes DP. Zombie-ant fungi emerged from non-manipulating, beetle-infecting ancestors. Curr Biol. 2019;29:3735–3738.e2. https://doi.org/10.1016/j.cub.2019.09.004
15. Alberts B, Johnson A, Lewis J, Raff M, Roberts K, Walter P. Molecular biology of the cell. 4th edition. New York: Garland Science; 2002.
16. Pappas G, Seitaridis S, Akritidis N, Tsianos E. Infectious diseases in cinema: virus hunters and killer microbes. Clin Infect Dis. 2003;37:939–42. https://doi.org/10.1086/377740
17. Pappas G. Ebola in your living room. Lancet Infect Dis. 2019;8:820. https://doi.org/10.1016/S1473-3099(19)30343-3
18. Farca G, Lavedeze C. The journey to nature: The Last of Us as critical dystopia [cited 2023 May 20]. http://www.digra.org/digital-library/forums/13-digra-fdg2106
19. Green AM. The reconstruction of morality and the evolution of naturalism in The Last of Us. Games Cult. 2016;11:745–63. https://doi.org/10.1177/1555412015579489
20. English E. The real horrors of "The Last of Us" may already be here [cited 2023 May 20]. https://thebulletin.org/2023/03/the-last-of-us
21. Pappas G, Panagopoulou P, Akritidis N. Reclassifying bioterrorism risk: are we preparing for the proper pathogens? J Infect Public Health. 2009;2:55–61. https://doi.org/10.1016/j.jiph.2009.03.002
22. Galgiani JN, Shubitz LF, Orbach MJ, Mandel MA, Powell DA, Klein BS, et al. Vaccines to prevent coccidioidomycosis: a gene-deletion mutant of *Coccidioides posadasii* as a viable candidate for human trials. J Fungi (Basel). 2022;8:838. https://doi.org/10.3390/jof8080838
23. Edwards JE Jr, Schwartz MM, Schmidt CS, Sobel JD, Nyirjesy P, Schodel F, et al. A fungal immunotherapeutic vaccine (NDV-3A) for treatment of recurrent vulvovaginal candidiasis-a phase 2 randomized, double-blind, placebo-controlled trial. Clin Infect Dis. 2018;66:1928–36. https://doi.org/10.1093/cid/ciy185

Address for correspondence: Georgios Pappas, Institute of Continuing Medical Education of Ioannina, Greece, H. Trikoupi 10, 45333, Ioannina, Greece; email: gpele@otenet.gr

Burkholderia pseudomallei Bacteria in Ornamental Fish Tanks, Vientiane, Laos, 2023

Tim Venkatesan, Vannavong Siritana, Joy Silisouk, Tamalee Roberts, Matthew T. Robinson, David A.B. Dance

Author affiliations: Lao-Oxford-Mahosot Hospital-Wellcome Trust Research Unit, Vientiane, Laos (T. Venkatesan, V. Siritana, J. Silisouk, T. Roberts, M.T. Robinson, D.A.B. Dance); London School of Hygiene and Tropical Medicine, London, UK (T. Venkatesan, D.A.B. Dance); University of Oxford Centre for Tropical Medicine and Global Health, Oxford, UK (T. Roberts, M.T. Robinson, D.A.B. Dance)

DOI: https://doi.org/10.3201/eid3003.231674

In 2019, a melioidosis case in Maryland, USA, was shown to have been acquired from an ornamental fish tank contaminated with *Burkholderia pseudomallei* bacteria, likely derived from Southeast Asia. We investigated the presence of *B. pseudomallei* in ornamental fish tanks in the endemic area of Vientiane, Laos.

Burkholderia pseudomallei is a saprophytic gram-negative bacillus that resides in the soil and surface water of many tropical and subtropical environments (*1*). This bacterium causes the potentially life-threatening infection melioidosis, a major cause of death in endemic areas (*1*).

In 2019, a 56-year-old woman from Maryland, USA, was hospitalized with melioidosis despite having no travel history to a *B. pseudomallei*–endemic region. She was infected with a *B. pseudomallei* isolate found within a recently purchased ornamental fish tank (*2*). Whole-genome sequencing demonstrated genome clustering associated with Southeast Asia. An earlier study had also detected *B. pseudomallei* bacteria in water used to import tropical fish from Singapore to France (*3*). A large overlap exists between *B. pseudomallei* bacteria endemicity and sources of ornamental fish exportation, and Southeast Asia accounts for 57% of global trade (*4*).

We sampled retail and residential fish tanks in Vientiane Capital, Laos, where *B. pseudomallei* bacteria has been shown to be widespread (*5*,*6*). We defined a fish tank as a container (glass, plastic, or ceramic) with water containing ornamental fish. Samples were collected during the Laos rainy season (June–July), when melioidosis incidence is highest (*7*). Each site completed a questionnaire detailing tank water sources and maintenance procedures.

Sampling methods mirrored those used by the investigational team from the Maryland case (*2*), alongside established methods for environmental sampling of *B. pseudomallei* bacteria in Laos (*6*). From each tank, we took a 1-L water sample, 10 g of sediment, and 2 swab samples (Medical Wire & Equipment, https://www.mwe.co.uk) of biofilm. We vacuumed 500-mL water samples that had been filtered in succession through 5 µm– and 0.2 µm–pore-sized cellulose acetate filters (Sartorius Stedim Biotech, https://www.sartorius.com) to capture suspended particulates and planktonic bacteria. We placed the water filters, the sediment, and swab tips directly in *B. pseudomallei*–selective broth containing colistin (50 mg/mL) and incubated them aerobically at 37°C for 48 hours and 168 hours before culture and molecular detection. We then subcultured 10 µL of enriched sample on Ashdown agar containing gentamicin (8 mg/L). We tested any colony with an appearance consistent with *B. pseudomallei* bacteria by using both *B. pseudomallei*–specific latex agglutination (Mahidol University Faculty of Tropical Medicine, https://www.tm.mahidol.ac.th) and Vitek MS matrix-assisted laser desorption/ionization time-of-flight mass spectrometry (bioMérieux, https://www.biomerieux.com). We conducted molecular detection by using real-time quantitative PCR (qPCR) after 7 days of enrichment in *B. pseudomallei*–selective broth. We performed DNA extraction by using a GeneJET Genomic DNA Purification Kit (ThermoFisher Scientific, https://www.thermofisher.com). The qPCR targeted the *B. pseudomallei* type 3 secretion system using a protocol based on a previously published methodology (*8*). To control for the presence of inhibitors, we used a parallel *Orientia tsutsugamushi* bacteria inhibition control PCR to check delay in amplification of a 47-kDa *O. tsutsugamushi* gene plasmid in the presence of each sample. We processed 2 positive controls using tank water samples we inoculated with 3 and 30 CFU/mL using the same methods. We isolated *B. pseudomallei* bacteria on culture and detected it by qPCR in both cases.

We sampled a total 111 tanks from 14 sites, including 82 tanks from 6 fish retailers and 29 tanks from 8 residents. Eleven (9.9%) tanks were kept outside, 39 (35.1%) were kept outside under cover, and 60 (54.1%) were kept inside. All sites used tap water as the primary water source without the addition of disinfectants, except 1 that used rainwater. We detected *B. pseudomallei* bacteria by qPCR only within a single covered outdoor retailer tank water sample, a finding we confirmed on repeat qPCR testing (cycle threshold value 34.9). The absence of positive culture and the high qPCR cycle threshold value suggested that a low concentration of *B. pseudomallei* bacteria was present in the sample (<1 CFU/500 mL).

Our study has confirmed that *B. pseudomallei* bacteria can contaminate ornamental fish tanks in an endemic area, yet its presence is not widespread in Vientiane Capital, Laos. Our findings probably underestimate the presence of *B. pseudomallei* bacteria, given the limitations in the sensitivity of environmental sampling methods, which have not been optimized for ornamental fish tanks. Because untreated tap water was the primary water source for tanks, the absence of *B. pseudomallei* bacteria suggests it is not widely present in tap water in Vientiane Capital. To our knowledge, no formal analysis of tap water samples in Vientiane has been performed; however, 2 studies undertaken in rural Thailand found *B. pseudomallei* bacteria present within some tap water samples (*9*,*10*). Our positive finding on qPCR does not prove the existence of viable organisms, but it is a possibility. Further studies are needed to investigate possible contamination of tanks in other regions and to determine the risks this might imply for the international ornamental fish trade. We suggest that susceptible persons having contact with fish tanks should take precautions and wear protective gloves while minimizing contact with fish tanks.

The work was completed at the Lao-Oxford-Mahosot Hospital-Wellcome Trust Research Unit, Mahosot Hospital, Vientiane, Laos. This research was funded in whole, or in part, by the Wellcome Trust (grant no. 220211).

About the Author

Dr. Venkatesan is junior doctor from the United Kingdom and MSc student at London School of Hygiene & Tropical Medicine. His research interests include infectious diseases, microbiology, and global health.

References

1. Limmathurotsakul D, Golding N, Dance DAB, Messina JP, Pigott DM, Moyes CL, et al. Predicted global distribution of *Burkholderia pseudomallei* and burden of melioidosis. Nat Microbiol. 2016;1:15008. https://doi.org/10.1038/nmicrobiol.2015.8
2. Dawson P, Duwell MM, Elrod MG, Thompson RJ, Crum DA, Jacobs RM, et al. Human melioidosis caused by novel transmission of *Burkholderia pseudomallei* from freshwater home aquarium, United States. Emerg Infect Dis. 2021;27:3030–5. https://doi.org/10.3201/eid2712.211756
3. Galimand M, Escallier G, Dodin A. Les risques sanitaires de l'importation des poissons tropicaux. Ref Fr Aquariol. 1981;8:19–22.
4. Evers HG, Pinnegar JK, Taylor MI. Where are they all from? Sources and sustainability in the ornamental freshwater fish trade. J Fish Biol. 2019;94:909–16. https://doi.org/10.1111/jfb.13930
5. Rachlin A, Luangraj M, Kaestli M, Rattanavong S, Phoumin P, Webb JR, et al. Using land runoff to survey the distribution and genetic diversity of *Burkholderia pseudomallei* in Vientiane, Laos. Appl Environ Microbiol. 2021;87:e02112-20.
6. Zimmermann RE, Ribolzi O, Pierret A, Rattanavong S, Robinson MT, Newton PN, et al. Rivers as carriers and potential sentinels for *Burkholderia pseudomallei* in Laos. Sci Rep. 2018;8:8674. https://doi.org/10.1038/s41598-018-26684-y
7. Bulterys PL, Bulterys MA, Phommasone K, Luangraj M, Mayxay M, Kloprogge S, et al. Climatic drivers of melioidosis in Laos and Cambodia: a 16-year case series analysis. Lancet Planet Health. 2018;2:e334–43. https://doi.org/10.1016/S2542-5196(18)30172-4
8. Kaestli M, Mayo M, Harrington G, Watt F, Hill J, Gal D, et al. Sensitive and specific molecular detection of *Burkholderia pseudomallei*, the causative agent of melioidosis, in the soil of tropical northern Australia. Appl Environ Microbiol. 2007;73:6891–7. https://doi.org/10.1128/AEM.01038-07
9. Limmathurotsakul D, Kanoksil M, Wuthiekanun V, Kitphati R, deStavola B, Day NP, et al. Activities of daily living associated with acquisition of melioidosis in northeast Thailand: a matched case-control study. PLoS Negl Trop Dis. 2013;7:e2072. https://doi.org/10.1371/journal.pntd.0002072
10. Thaipadungpanit J, Chierakul W, Pattanaporkrattana W, Phoodaeng A, Wongsuvan G, Huntrakun V, et al. *Burkholderia pseudomallei* in water supplies, southern Thailand. Emerg Infect Dis. 2014;20:1947–9. https://doi.org/10.3201/eid2011.140832

Address for correspondence: David Dance, London School of Hygiene & Tropical Medicine, Keppel St, London WC1E 7HT, UK; email: David.d@tropmedres.ac

Staphylococcus succinus Infective Endocarditis, France

Louise Ruffier d'Epenoux, Erwan Fayoux, Frédéric Laurent, Pascale Bémer, Raphaël Lecomte, Thierry Le Tourneau, Aurélie Guillouzouic, Stéphane Corvec

Author affiliations: Centre Hospitalier Universitaire, Nantes, France (L. Ruffier d'Epenoux, E. Fayoux, P. Bémer, R. Lecomte, T. Le Tourneau, A. Guillouzouic, S. Corvec); Université de Nantes, INSERM INCIT UMR 1302, Nantes (L. Ruffier d'Epenoux, S. Corvec); Université de Nantes, CNRS, INSERM UMR 1087, l'Institut du Thorax, Nantes (T. Le Tourneau); Université Claude-Bernard Lyon 1, Lyon, France (F. Laurent); Groupement Hospitalier Nord, Lyon (F. Laurent); Hôpital Croix Rousse, Lyon (F. Laurent)

DOI: http://doi.org/10.3201/eid3003.230986

Infective endocarditis is a rare condition in humans and is associated with high illness and death rates. We describe a case of infective endocarditis caused by *Staphylococcus succinus* bacteria in France. We used several techniques for susceptibility testing for this case to determine the oxacillin profile.

Staphylococcus succinus was first described in 1998 and was isolated from 25- to 35-million-year-old Dominican amber (*1*). Members of this species are widespread in nature. Studies have reported the frequent isolation of *S. succinus* bacteria from various sources, such as cheeses, dry or fermented meat products, the Dead Sea, and occasionally human specimens (*2*–*4*). We report a case of *S. succinus* infective endocarditis in a patient in France who had many cardiovascular risk factors: age, sex, hypertension, dyslipidemia, diabetes, and weight. In accordance with legislations in France and Europe, the use of anonymous data does not need approval of an ethics committee.

On hospital day 1, an 83-year-old man sought care for dyspnea and chest pain for 72 hours; he had evidence of global cardiac decompensation for a severe ischemic heart disease with preserved left ventricular ejection fraction. Cardiac blood marker analysis revealed an increased troponin level to 250 ng/L and thereafter 350 ng/L (reference range <14 ng/L). Electrocardiogram results showed ST-segment depression in the lateral leads. In this context of non–ST-segment elevation myocardial infarction, the patient was hospitalized in the cardiology unit. On day 6, transthoracic echocardiography revealed an aortic valve bioprosthesis, reshaped, with a thickening of the cusps and a vibratory element attached on the ventricular side (7 × 4 mm), suggesting vegetation suspicious for infective endocarditis (Appendix Figure, https://wwwnc.cdc.gov/EID/article/30/2/23-0986-App1.pdf). The patient became febrile. We collected a total of 7 sets of aerobic and anaerobic blood bottle cultures during days 9–12; all showed a gram-positive coccus in clusters. Matrix-assisted laser desorption/ionization time-of-flight mass spectrometry identification (VitekMS; bioMérieux, https://www.biomerieux.com) indicated *S. succinus* with a 99.9% index.

The patient initially received 6 g intravenous cefazolin; on day 13 we changed the antimicrobial treatment to intravenous daptomycin (10 mg/kg) and gentamicin (3 mg/kg) every 48 h. Finally, after a dedicated endocarditis multidisciplinary consultation, we changed the patient's regimen on day 22 to daptomycin (10 mg/kg) and rifampin (900 mg) for 6 weeks. The patient returned home; follow-up care was scheduled with a hospital at home. The patient outcome was favorable without relapse or side effects from daptomycin/rifampin. His last cardiology appointment was 11 months after his initial treatment; no sequelae of endocarditis were present.

S. succinus susceptibility testing was a challenge. We performed methicillin resistance testing with cefoxitin screen and oxacillin testing using the AST-P668 bioMérieux card with a VitekXL automated system. However, we observed a discrepancy between the results from the 2 tests. To confirm oxacillin resistance, we tested by agar diffusion method using impregnated disks and interpreted them in accordance with EUCAST (European Committee on Antimicrobial Susceptibility Testing) criteria (https://www.eucast.org/fileadmin/src/media/PDFs/EUCAST_files/Breakpoint_tables/v_13.0_Breakpoint_Tables.pdf). We used oxacillin (1 µg) and cefoxitin (30 µg) disks (Bio-Rad, https://www.bio-rad.com). The oxacillin (1 µg) disk diffusion method detected oxacillin resistance. In contrast, the isolate was susceptible when we used the cefoxitin (30 µg) disk test. In addition, we performed an oxacillin MIC strip test; MIC of 0.5 (mg/L), indicated that the strain was susceptible according to the EUCAST 2022 criteria.

A retrospective study (*5*) of penicillin-binding protein (PBP) assays indicating antimicrobial drug resistance has shown that preinduction with cefoxitin/oxacillin and reading of the test after 10 min (instead of 5 min) substantially improve the sensitivity, specificity, and robustness of the immunochromatographic assay PBP2a (Abbott, https://www.globalpointofcare.abbott) for coagulase-negative staphylococci.

We performed PBP2a detection from bacterial culture after a preinduction with cefoxitin, but results were negative. Thereafter, we performed *mecA* gene detection by PCR to identify oxacillin-resistant *Staphylococcus* (*6*); however, we did not detect the *mecA* gene by PCR.

Finally, we sent the isolate to the French Reference Center for *Staphylococci* (Lyon, France) on day 19 for detection of other *mec* genes; this test result was negative. Staff at the reference center performed whole-genome sequencing of the strain as previously described (*7*); results revealed no site-specific insertion sequences comprising direct-repeat sequences typical of a staphylococcal cassette chromosome–like cassette (*8*). To evaluate the possibility of resistance by PBP modification, we performed a disk diffusion method for antimicrobial susceptibility of imipenem (PBP1), cefotaxime (PBP2), oxacillin (PBP3), and cefoxitin (PBP4) (*9*,*10*). The cefotaxime diameter was reduced, indicating resistance in a strain, most likely by a modification of PBP2 (Figure; Appendix Table).

In conclusion, we identified environmental *S. succinus* behaving as an opportunistic pathogen as the cause of infective endocarditis in a patient with many cardiovascular risk factors. The source of *S. succinus* was not clearly established. Virulence factors contributing to *S. succinus* pathogenicity are not yet well defined. We further described the difficulty of determining the resistance profile of this rarely pathogenic species mimicking either the borderline oxacillin-resistant *S. aureus* phenotype with an elevated oxacillin MIC value, or to a lesser extent the modified *S. aureus* phenotype in the absence of *mec* gene–mediated resistance. Our findings highlight the importance of a multiple-technology approach for laboratories assessing methicillin resistance using a combination of phenotypic and genotypic methods.

Figure. Disk diffusion testing for antimicrobial susceptibility testing of *Staphylococcus succinus* from a patient in France with infective endocarditis. Agar diffusion method using impregnated disks was interpreted according to the criteria of the European Committee on Antimicrobial Susceptibility Testing 2022 (version 13.0) breakpoints for oxacillin susceptibility testing (https://www.eucast.org/fileadmin/src/media/PDFs/EUCAST_files/Breakpoint_tables/v_13.0_Breakpoint_Tables.pdf). CEF, cephalotin; CRO: cefotaxime (PBP2); FOX, cefoxitin (PBP4); IMP, imipenem (PBP1); OXC, oxacillin (PBP3); PBP, penicillin-binding protein.

Acknowledgments

We thank Patricia Martin for her technical assistance in the whole-genome sequencing of the clinical strain. We thank Julie Marraillac, Caroline Consent, Jihane El Khobzi, and Gaëlle Croizier, for their technical assistance.

This study has been recorded in the Nantes Hospital by the local Data Protection Officer under reference TS005-BIO-AP-2019_20. In accordance with legislation in France and Europe, use of anonymous data does not need approval of an ethics committee.

About the Author

Dr. Ruffier d'Epenoux is a medical microbiologist at Nantes University Hospital, Nantes, France. Her primary research interests are device-related infections, especially bone and joint infection (*Cutibacterium acnes*) and prosthetic infective endocarditis.

References

1. Lambert LH, Cox T, Mitchell K, Rosselló-Mora RA, Del Cueto C, Dodge DE, et al. *Staphylococcus succinus* sp. nov., isolated from Dominican amber. Int J Syst Bacteriol. 1998;48:511–8. https://doi.org/10.1099/00207713-48-2-511
2. Place RBE, Hiestand D, Burri S, Teuber M. *Staphylococcus succinus* subsp. casei subsp. nov., a dominant isolate from a surface ripened cheese. Syst Appl Microbiol. 2002;25:353–9. https://doi.org/10.1078/0723-2020-00130
3. Stabnikov V, Chu J, Ivanov V, Li Y. Halotolerant, alkaliphilic urease-producing bacteria from different climate zones and their application for biocementation of sand. World J Microbiol Biotechnol. 2013;29:1453–60. https://doi.org/10.1007/s11274-013-1309-1
4. Nováková D, Sedláček I, Pantůček R, Štětina V, Švec P, Petráš P. *Staphylococcus equorum* and *Staphylococcus succinus* isolated from human clinical specimens. J Med Microbiol. 2006;55:523–8. https://doi.org/10.1099/jmm.0.46246-0
5. Kolesnik-Goldmann N, Bodendoerfer E, Röthlin K, Herren S, Imkamp F, Marchesi M, et al. Rapid detection of PBP2a in *Staphylococci* from shortly incubated subcultures of positive blood cultures by an immunochromatographic

assay. Microbiol Spectr. 2021;9:e0046221. https://doi.org/10.1128/Spectrum.00462-21
6. Okuma K, Iwakawa K, Turnidge JD, Grubb WB, Bell JM, O'Brien FG, et al. Dissemination of new methicillin-resistant *Staphylococcus aureus* clones in the community. J Clin Microbiol. 2002;40:4289–94. https://doi.org/10.1128/JCM.40.11.4289-4294.2002
7. Durand G, Javerliat F, Bes M, Veyrieras JB, Guigon G, Mugnier N, et al. Routine whole-genome sequencing for outbreak investigations of *Staphylococcus aureus* in a national reference center. Front Microbiol. 2018;9:511. https://doi.org/10.3389/fmicb.2018.00511
8. Ito T, Ma XX, Takeuchi F, Okuma K, Yuzawa H, Hiramatsu K. Novel type V staphylococcal cassette chromosome mec driven by a novel cassette chromosome recombinase, ccrC. Antimicrob Agents Chemother. 2004;48:2637–51. https://doi.org/10.1128/AAC.48.7.2637-2651.2004
9. Herold BC, Immergluck LC, Maranan MC, Lauderdale DS, Gaskin RE, Boyle-Vavra S, et al. Community-acquired methicillin-resistant *Staphylococcus aureus* in children with no identified predisposing risk. JAMA. 1998;279:593–8. https://doi.org/10.1001/jama.279.8.593
10. Tomic V, Svetina Sorli P, Trinkaus D, Sorli J, Widmer AF, Trampuz A. Comprehensive strategy to prevent nosocomial spread of methicillin-resistant *Staphylococcus aureus* in a highly endemic setting. Arch Intern Med. 2004;164:2038–43. https://doi.org/10.1001/archinte.164.18.2038

Address for correspondence: Stéphane Corvec, Institut de Biologie des Hôpitaux de Nantes, Service de Bactériologie et des contrôles Microbiologiques, CHU de Nantes, 9 quai Moncousu, 44093 Nantes CEDEX 01, France; email: stephane.corvec@chu-nantes.fr

Inadvertent Platelet Transfusion from Monkeypox Virus–Infected Donor to Recipient, Thailand, 2023

Jiratchaya Puenpa, Duangnapa Intharasongkroh, Sompong Vongpunsawad, Dootchai Chaiwanichsiri, Yong Poovorawan

Author affiliations: Center of Excellence in Clinical Virology, Chulalongkorn University Faculty of Medicine, Bangkok, Thailand (J. Puenpa, S. Vongpunsawad, Y. Poovorawan); National Blood Center, Thai Red Cross Society, Bangkok (D. Intharasongkroh, D. Chaiwanichsiri); FRS(T), The Royal Society of Thailand, Sanam Sueapa, Dusit, Bangkok (Y. Poovorawan)

In Thailand, platelet product from a blood donor was transfused to a recipient who had dengue. Two days later, the donor was confirmed to have monkeypox virus infection. Monkeypox virus DNA was undetectable in recipient specimens up to 2 weeks after transfusion. The recipient remained asymptomatic at 4 weeks of monitoring.

DOI: http://doi.org/10.3201/eid3003.231539

Monkeypox virus (MPXV), a double-stranded DNA virus that primarily infects rodents in sub-Saharan Africa, causes mpox disease. MPXV is a member of the genus *Orthopoxvirus* in the family *Poxviridae*. MPXV clade I is endemic to Central Africa and clade II to West Africa. Clade II is further subdivided into IIa and IIb. Strains from the recent global emergence appear to belong to clade IIb (https://nextstrain.org/mpox/all-clades).

The potential to unknowingly transmit MPXV from donated blood products exists despite routine stringent screening of bloodborne pathogens at donation centers. Thailand first reported mpox in a 27-year-old male tourist from Africa in Phuket province on July 21, 2022; nonoutbreak sporadic infections have since been identified (*1*). By May 2023, ≈40 infections had been laboratory-confirmed. Infections surged after Pride Festivals, which took place in Bangkok and Pattaya City in June 2023; infections peaked in August and then declined. As of November 4, 2023, the Ministry of Public Health Thailand (MoPH) had identified 582 infections (563 male and 19 female patients; median age 33 years, age range 1–64 years) and 2 deaths. Here, we describe an unintended administration of platelets from an MPXV-infected donor to a dengue-infected recipient and the subsequent follow-up to monitor for potential MPXV transmission.

On July 24, 2023, an apparently healthy 22-year-old man donated whole blood at the National Blood Center (NBC) of the Thai Red Cross in Bangkok (Figure). That afternoon, he experienced fever and malaise. On July 26, itchy skin rash and lesions appeared on his hands, feet, and anus, which prompted him to go to a hospital. His doctor sought consultation with the Department of Disease Control at MoPH, where samples of the skin lesion, oropharyngeal swab, and plasma were tested for MPXV by real-time PCR to detect the F3L gene region (BioPerfectus, https://www.bioperfectus.com). MPXV DNA was detected only in the lesion (cycle threshold [Ct] 21.7) and oropharyngeal (Ct 31.5) swab samples.

NBC processes blood donations individually and routinely screened for hepatitis B/C and syphilis. Derived products from donations are primarily leukocyte-poor red cells, leukocyte-depleted pooled plate-

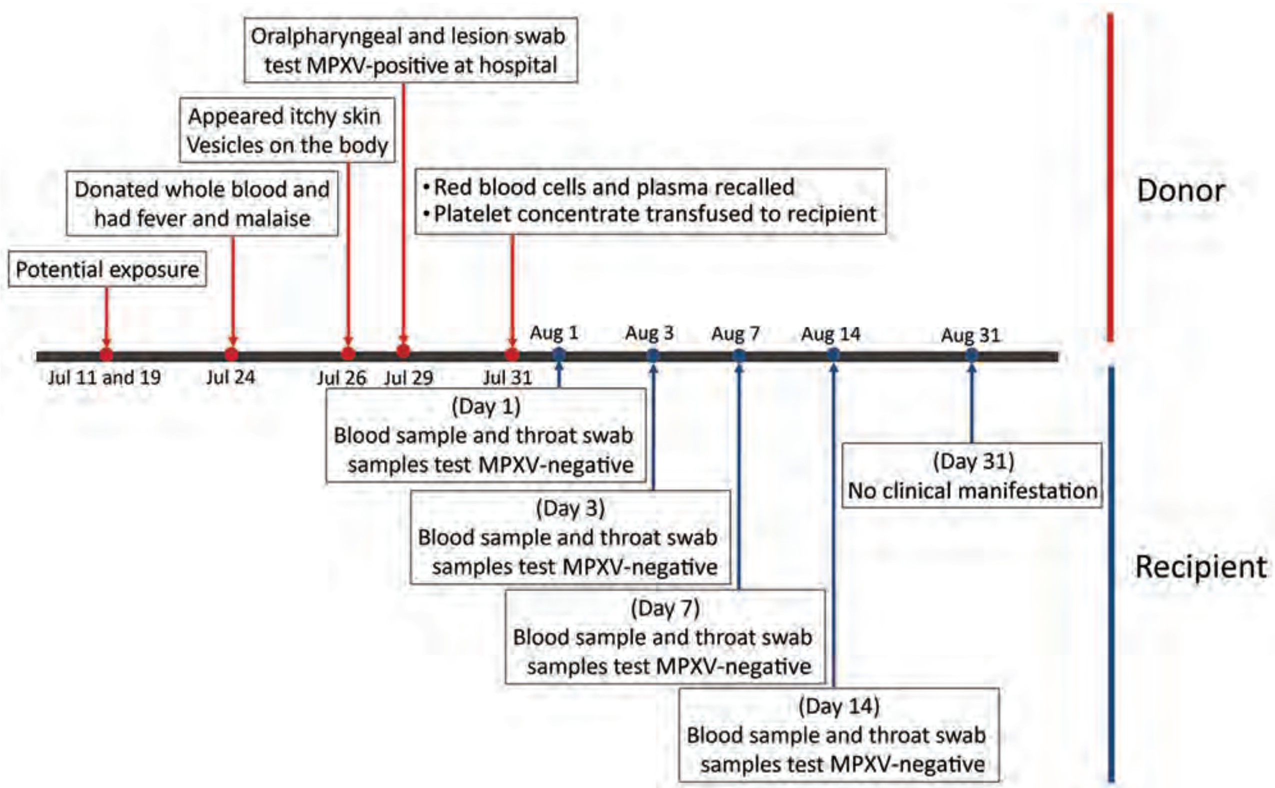

Figure. Timeline of MPXV-infected blood donor (red) and platelet recipient (blue), Thailand, 2023. MPXV, monkeypox virus.

let concentrate, and fresh frozen plasma, prepared in accordance with guidelines of the European Directorate for the Quality of Medicines & Healthcare (*2*). Specifically, the platelet concentrate is prepared from a pool of 4 donor buffy coats of the same ABO blood group, diluted with either plasma from one of the buffy coat donations or a platelet additive solution, centrifuged to separate the platelets, filtered to deplete leukocyte, and stored for bacterial testing before distribution.

On July 31, the NBC was alerted to the potential of an MPXV-contaminated donation, which prompted recalls of all blood components derived from the 22-year-old donor. That same day, red blood cells and plasma derived from the donor materials were successfully retrieved and destroyed; however, the platelet concentrate had already been administered to an 11-year-old female recipient who had ongoing dengue infection.

To characterize MPXV in the donation, our laboratory received residual donor plasma and red cells that the NBC had, from which we extracted DNA by using the magLEAD 12 gC instrument (Precision System Science, https://www.pss.co.jp) according to the manufacturer's instructions. We tested for MPXV DNA by generic real-time PCR to detect the tumor necrosis factor receptor gene located at the terminal inverted repeat region on the MPXV genome, in accordance with the US Centers for Disease Control and Prevention protocol (*3*). We confirmed the result using conventional PCR to amplify the DNA helicase and Schlafen protein genes (Appendix, https://wwwnc.cdc.gov/EID/article/30/3/23-1539-App1.pdf). We Sanger sequenced amplicons, and deposited nucleotides into GenBank (accession nos. OR790439–40).

Plasma yielded detectable MPXV DNA (Ct ≈35); red blood cells did not. Phylogenetic analysis of the DNA helicase gene sequence suggests that the MPXV strain in the donor belonged to clade IIb (lineage B) and genetically clustered with strains previously identified in Taiwan, Japan, and the United States (88% bootstrap support) (Appendix Figure).

MPXV DNA was undetectable in serum and throat swab samples collected from the platelet recipient on August 1, 3, 7, and 14. No mpox-associated symptoms were evident 4 weeks posttransfusion. Incubation period for mpox is 3–17 days (mean 8.5 days) (*4*,*5*).

We posit that there was a low risk for transfusion-transmitted infection for several reasons. First, detection of MPXV DNA in the residual donated plasma does not indicate infectious virus, as was shown in a viral load study using cell culture as surrogate for infectivity (*6*). Thus, nucleic acid detection does not prove the presence of viable or infectious virus, as Cohen et al. demonstrated in a smallpox-vaccine study (*7*). We pooled and extensively prepared platelet products from multiple donors, which may have diluted out any residual virus before transfusion 1 week later. In conclusion, our study shows that a blood donation from a donor with detectable MPXV viral DNA did not appear to transmit the infection to a pooled-platelet recipient.

This work was supported by the Health Systems Research Institute, the National Research Council of Thailand, the Center of Excellence in Clinical Virology, Chulalongkorn University, King Chulalongkorn Memorial Hospital, the MK Restaurant Group and Aunt Thongkam Foundation, and the BJC Big C Foundation. J.P. reports financial support from the Second Century Fund Fellowship of Chulalongkorn University.

About the Author

Dr. Puenpa is a postdoctoral fellow at the Center of Excellence in Clinical Virology in the Faculty of Medicine at Chulalongkorn University. Her primary research interests are molecular epidemiology and evolution of human enteroviruses.

Reference

1. Ministry of Public Health Thailand (MoPH). Thailand's first monkeypox case identified in Phuket tourist [in Thai]. 2022 Jul 22 [cited 2023 Nov 1]. https://pr.moph.go.th/?url=pr/detail/2/04/176575
2. European Directorate for the Quality of Medicines & HealthCare. Guide to the preparation, use and quality assurance of blood components. 21st edition [cited 2023 Oct 11]. https://freepub.edqm.eu/publications/AUTOPUB_48/detail
3. Li Y, Zhao H, Wilkins K, Hughes C, Damon IK. Real-time PCR assays for the specific detection of monkeypox virus West African and Congo Basin strain DNA. J Virol Methods. 2010;169:223–7. https://doi.org/10.1016/j.jviromet.2010.07.012
4. Centers for Disease Control and Prevention. Clinical recognition [cited 2023 Oct 24]. https://www.cdc.gov/poxvirus/mpox/clinicians/clinical-recognition.html
5. Miura F, van Ewijk CE, Backer JA, Xiridou M, Franz E, Op de Coul E, et al. Estimated incubation period for monkeypox cases confirmed in the Netherlands, May 2022. Euro Surveill. 2022;27:2200448. https://doi.org/10.2807/1560-7917.ES.2022.27.24.2200448
6. Lim CK, McKenzie C, Deerain J, Chow EPF, Towns J, Chen MY, et al. Correlation between monkeypox viral load and infectious virus in clinical specimens. J Clin Virol. 2023;161:105421. https://doi.org/10.1016/j.jcv.2023.105421
7. Cohen JI, Hohman P, Preuss JC, Li L, Fischer SH, Fedorko DP. Detection of vaccinia virus DNA, but not infectious virus, in the blood of smallpox vaccine recipients. Vaccine. 2007;25:4571–4. https://doi.org/10.1016/j.vaccine.2007.03.044

Address for correspondence: Yong Poovorawan, Center of Excellence in Clinical Virology, Faculty of Medicine, Chulalongkorn University, 1873 Rama 4 Rd, Pathumwan, Bangkok 10330, Thailand; email: yong.p@chula.ac.th

Detection of Invasive *Anopheles stephensi* Mosquitoes through Molecular Surveillance, Ghana

Yaw A. Afrane, Anisa Abdulai, Abdul R. Mohammed, Yaw Akuamoah-Boateng, Christopher M. Owusu-Asenso, Isaac K. Sraku, Stephina A. Yanney, Keziah Malm, Neil F. Lobo.

Author affiliations: University of Ghana, Accra, Ghana (Y.A. Afrane, A. Abdulai, A.R. Mohammed, Y. Akuamoah-Boateng, C.M. Owusu-Asenso, I.K. Sraku, S.A. Yanney); Ghana Health Service, Accra (K. Malm); University of Notre Dame, Notre Dame, Indiana, USA (N.F. Lobo)

DOI: https://doi.org/10.3201/eid3003.231638

The invasive *Anopheles stephensi* mosquito has rapidly expanded in range in Africa over the past decade. Consistent with World Health Organization guidelines, routine entomologic surveillance of malaria vectors in Accra, Ghana, now includes morphologic and molecular surveillance of *An. stephensi* mosquitoes. We report detection of *An. stephensi* mosquitoes in Ghana.

Anopheles stephensi is an invasive mosquito species originating from parts of Southeast Asia and the Arabian Peninsula (*1*). Over the past decade, *An. stephensi* mosquitoes have been expanding in range and have now been documented in several countries in Africa (*2*). First detected in Djibouti, on the Horn of Africa, in 2012, this vector has been implicated in urban malaria outbreaks (*3*). They were also detected in Ethiopia in 2016 and 2018 (*4*,*5*). *An. stephensi* mosquitoes were subsequently detected in Sudan (2016), Somalia (2019), Nigeria (2020), and Kenya (2023) (*2*,*3*,*5*–*7*). This invasive vector poses a major threat to current malaria control and elimination efforts. The ability of *An. stephensi* mosquitoes to breed in artificial containers enables them to thrive in urban areas, setting them apart from other major

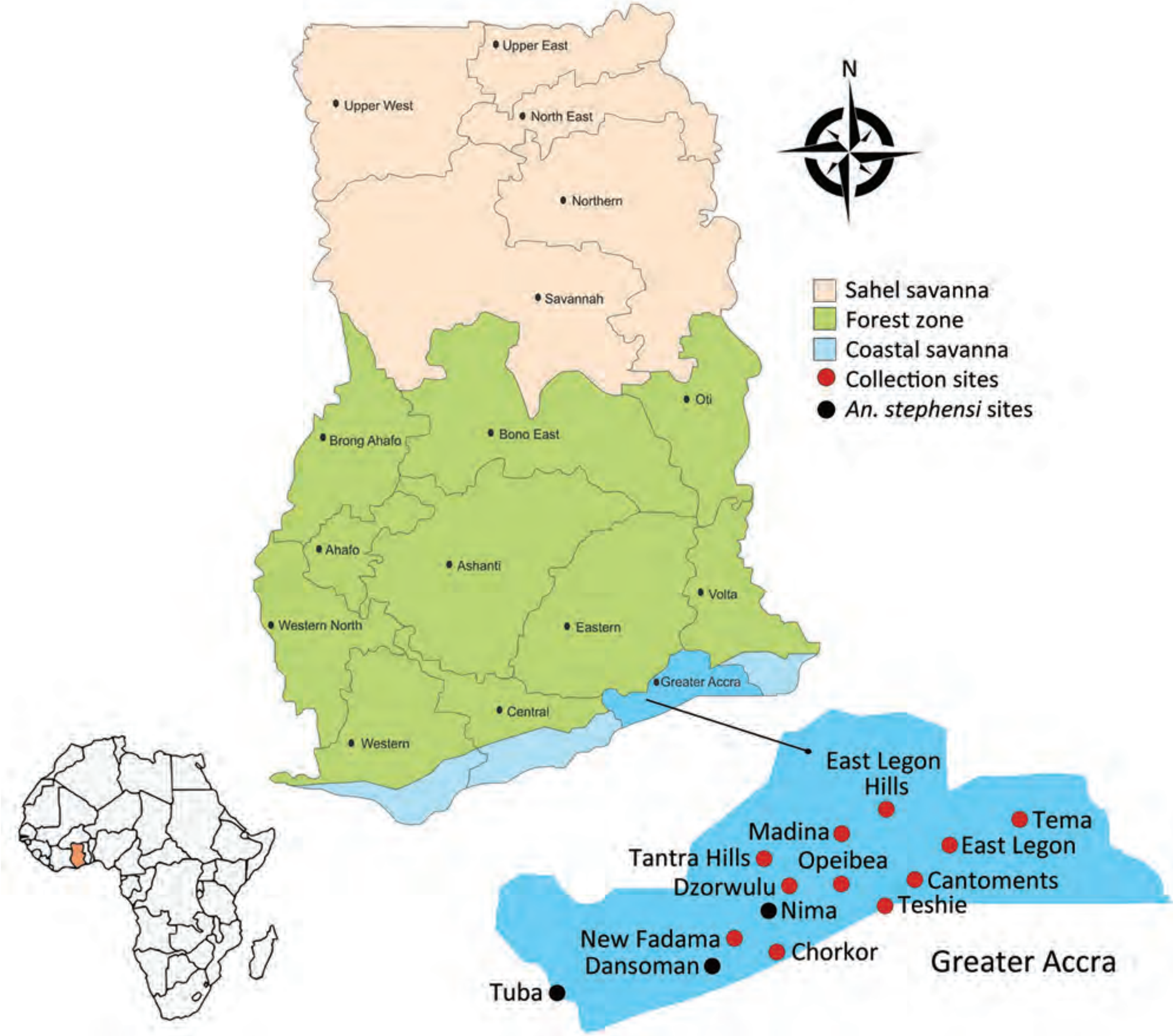

Figure. Routine entomologic surveillance sites, Accra, Ghana, January 2022–July 2022. Inset map shows location of Ghana in Africa.

malaria vectors (*8*). This species can also transmit both *Plasmodium falciparum* and *P. vivax* protozoa (*1*). Although malaria is widely a rural disease, transmission in urban areas may rise because of the establishment of *An. stephensi* mosquitoes, putting ≈126 million persons at risk of malaria (*2*,*8*). The World Health Organization issued an initiative in 2022 aimed at strengthening surveillance to help stop the spread of *An. stephensi* mosquitoes in sub-Saharan Africa (*2*). Morphologic and molecular surveillance of *An. stephensi* mosquitoes were incorporated into routine entomologic surveillance of malaria vectors in the city of Accra, Ghana, after the World Health Organization initiative (*2*). This study outlines the entomologic surveillance that documents the identification of this invasive species in Ghana.

Table. Sequencing results of suspected *Anopheles stephensi* mosquito samples, Accra, Ghana

Sample	ITS2 contig	BLAST result†	GenBank accession no. of best match	% Identity match	Final species identification	GenBank accession no.
DN 035	283	*An. stephensi* voucher	MH650999.1	100	*An. stephensi*	OR711900
TP 002S	283	*An. stephensi* voucher	MH650999.1	100	*An. stephensi*	OR711899

*ITS2, internal transcribed spacer 2 region.
†BLAST, https://blast.ncbi.nlm.nih.gov/Blast.cgi.

We conducted routine entomologic surveillance in 8 sites within the city of Accra, Ghana, during January 2022–July 2022 (Figure). We conducted larval sampling in all mosquito larval breeding habitats encountered in each of the sites. We recorded the total number of dips, larvae, and pupae, and we calculated the larval density as the ratio of the number of larvae collected per dip. We conducted larval sampling in the dry (February–March) and rainy (June–July) seasons of 2022. We transported larval samples to the insectary at the Department of Medical Microbiology, University of Ghana Medical School (Accra, Ghana), where we raised them into adults for morphologic and molecular species identification. We further identified members of the *An. gambiae* sensu lato. complex and sibling species by using PCR. We performed PCR amplifications to detect *An. stephensi* mosquitoes by using primers targeting the internal transcribed spacer region on the basis of on previously described protocols by Singh et al. (*9*). After PCR, were subjected 2 mosquitoes to Sanger sequencing of the internal transcribed spacer 2 regions and analyzed them on the basis of comparisons to the National Center for Biotechnology Information database.

We identified a total of 1,169 mosquitoes obtained from the larval sampling by using morphologic keys and PCR methods for speciation. Out of that number, 551 (47.13%) were *An. gambiae* sensu stricto, 582 (49.79%) *An. coluzzii*, and 32 (2.74%) hybrids of both species. We identified 4 samples (0.34%) as *An. stephensi* by using a modified PCR-based method by Singh et al. (*9*) and sequencing (Appendix Table 1, https://wwwnc.cdc.gov/EID/article/30/2/23-1638-App1.pdf). Results from BLAST analysis (https://blast.ncbi.nlm.nih.gov/Blast.cgi) showed that the *An. stephensi* mosquito samples had 100% sequence similarity with *An. stephensi* voucher A268 5.8S ribosomal RNA gene and internal transcribed spacer 2 (GenBank accession no. MH650999.1) (Table).

We found *An. stephensi* mosquitoes in larval samples from urban areas of Accra, Ghana, specifically the suburbs of Tuba, Dansoman, and Nima. We found *An. stephensi* mosquitoes breeding in dugout wells within irrigated vegetable farms and roadside ditches (Appendix Figure), habitats that are distinct from the typical ones observed in Asia and East Africa. In addition, *An. stephensi* larvae were present alongside *An. gambiae* s.s. and *An. coluzzii* mosquitoes, even though *An. stephensi* larvae are usually present alongside *Aedes* mosquitoes.

The spread of *An. stephensi* mosquitoes in Africa is thought to have occurred through land borders, air travel, or seaports. However, we discovered the mosquitoes at considerable distances from those points of entry, suggesting possible earlier introductions. Expanding surveillance efforts for *An. stephensi* mosquitoes is crucial to curbing the dissemination of this invasive species within Ghana, which could potentially elevate malaria prevalence in the city of Accra, traditionally considered a low malaria transmission zone within Ghana.

This report of the invasion of *An. stephensi* mosquitoes in Accra, Ghana, represents a major public health concern, given the heightened risk of urban malaria outbreaks. It is imperative to reinforce surveillance and response strategies in both rural and urban settings across Ghana, with specific attention directed toward *An. stephensi* mosquitoes, to mitigate the spread of this invasive species.

Acknowledgements

We thank the Eck Institute for Global Health, University of Notre Dame, for support with sequencing.

This study was supported by grants from the National Institute of Health (NIH grant nos. R01 A1123074 and D43 TW 011513).

Author contributions: Y.A.A., K.M. ,and N.F.L. were r esponsible for the study design, supervised the data collection, and contributed to the writing of the manuscript. A.A., A.R.M., Y.A.B., C.M.O.-A., S.A.Y., and I.S. performed the data collection, laboratory work, and analysis. A.A., Y.A.A., and NFL drafted the manuscript. All the authors read and approved the final manuscript.

About the Author

Dr. Afrane is a professor of vector biology at the University of Ghana. His research focuses on vector and parasite biology and epidemiology.

References

1. Sinka ME, Bangs MJ, Manguin S, Chareonviriyaphap T, Patil AP, Temperley WH, et al. The dominant *Anopheles* vectors of human malaria in the Asia-Pacific region: occurrence data, distribution maps and bionomic précis. Parasit Vectors. 2011;4:89. https://doi.org/10.1186/1756-3305-4-89
2. World Health Organization. WHO initiative to stop the spread of *Anopheles stephensi* in Africa. 2023 Aug 15 [cited 2023 Aug 22]. https://www.who.int/publications/i/item/WHO-UCN-GMP-2022.06
3. Faulde MK, Rueda LM, Khaireh BA. First record of the Asian malaria vector *Anopheles stephensi* and its possible role in the resurgence of malaria in Djibouti, Horn of Africa. Acta Trop. 2014;139:39–43. https://doi.org/10.1016/j.actatropica.2014.06.016
4. Balkew M, Mumba P, Dengela D, Yohannes G, Getachew D, Yared S, et al. Geographical distribution of

Anopheles stephensi in eastern Ethiopia. Parasit Vectors. 2020;13:35. https://doi.org/10.1186/s13071-020-3904-y
5. Carter TE, Yared S, Gebresilassie A, Bonnell V, Damodaran L, Lopez K, et al. First detection of *Anopheles stephensi* Liston, 1901 (Diptera: culicidae) in Ethiopia using molecular and morphological approaches. Acta Trop. 2018;188:180–6. https://doi.org/10.1016/j.actatropica.2018.09.001
6. Ahmed A, Khogali R, Elnour MB, Nakao R, Salim B. Emergence of the invasive malaria vector *Anopheles stephensi* in Khartoum State, Central Sudan. Parasit Vectors. 2021;14:511. https://doi.org/10.1186/s13071-021-05026-4
7. Ochomo EO, Milanoi S. Molecular surveillance leads to the first detection of *Anopheles stephensi* in Kenya. 2023 [cited 2023 Sep 9]. https://www.researchsquare.com/article/rs-2498485/v1
8. Sinka ME, Pironon S, Massey NC, Longbottom J, Hemingway J, Moyes CL, et al. A new malaria vector in Africa: predicting the expansion range of *Anopheles stephensi* and identifying the urban populations at risk. Proc Natl Acad Sci U S A. 2020;117:24900–8. https://doi.org/10.1073/pnas.2003976117
9. Singh OP, Kaur T, Sharma G, Kona MP, Mishra S, Kapoor N, et al. Molecular tools for early detection of invasive malaria vector *Anopheles stephensi* mosquitoes. Emerg Infect Dis. 2023;29:36–44. https://doi.org/10.3201/eid2901.220786
10. Thomas S, Ravishankaran S, Justin NA, Asokan A, Mathai MT, Valecha N, et al. Resting and feeding preferences of *Anopheles stephensi* in an urban setting, perennial for malaria. Malar J. 2017;16:111. https://doi.org/10.1186/s12936-017-1764-5

Address for correspondence: Yaw Asare Afrane, University of Ghana, Department of Medical Microbiology, University of Ghana Medical School, University of Ghana, PO Box KB 4236, Accra, Ghana; email: yafrane@ug.edu.gh

Streptobacillus moniliformis and IgM and IgG Immune Response in Patient with Endocarditis[1]

Philipp Mathé, Katja Schmidt, Viktoria Schindler, Ahmad Fawzy, Tilman Schultze, Reinhard E. Voll, David Pauli, Milena Popova, Franziska Schauer,[2] Tobias Eisenberg[2]

Author affiliations: University Medical Center Freiburg, Freiburg, Germany (P. Mathé, V. Schindler, R.E. Voll, D. Pauli, M. Popova, F. Schauer); German Cancer Research Center, Heidelberg, Germany (K. Schmidt); Cairo University, Giza, Egypt (A. Fawzy); Hessian State Laboratory, Giessen, Germany (A. Fawzy, T. Schultze, T. Eisenberg)

DOI: https://doi.org/10.3201/eid3003.230917

We describe a case of endocarditis caused by *Streptobacillus moniliformis* bacteria, a known cause of rat-bite fever, in a 32-year-old woman with pet rats in Germany. The patient had a strong serologic response, with high IgM and IgG titers. Serologic analysis is a promising tool to identify *S. moniliformis* bacterial infection.

Rat-bite fever (RBF) is a rare disease that typically manifests with fever, rash, and arthritis (*1*). Possible complications are abscess formation, endocarditis, and death if left untreated (*1*,*2*). *Streptobacillus moniliformis* bacteria is the main causative pathogen of RBF (*3*). Norway rats (*Rattus norvegicus*) are the natural host and usually carry *S. moniliformis* bacteria asymptomatically in their nasopharynx (*3*,*4*). Transmission occurs typically by rat bite or scratch but also by nontraumatic indirect contact.

We describe a case of a 32-year-old woman who came to an emergency department in Germany in May 2022 with fever, fatigue, and migrating arthralgia in the large and small joints of all 4 extremities, without signs of joint swelling or rash. She had a short history of diarrhea, and her first set of blood cultures were negative. She was initially diagnosed with reactive arthritis and transferred to the rheumatology department. We initiated treatment with 20 mg prednisolone and etoricoxib. The patient had initial relief of symptoms and was discharged after 6 days in the hospital. A small papule on her right foot

[1]Preliminary results from this study were presented at the 51st Congress of the German Rheumatological Society, August 30–September 2, 2023, Leipzig, Germany.

[2]These senior authors contributed equally to this article.

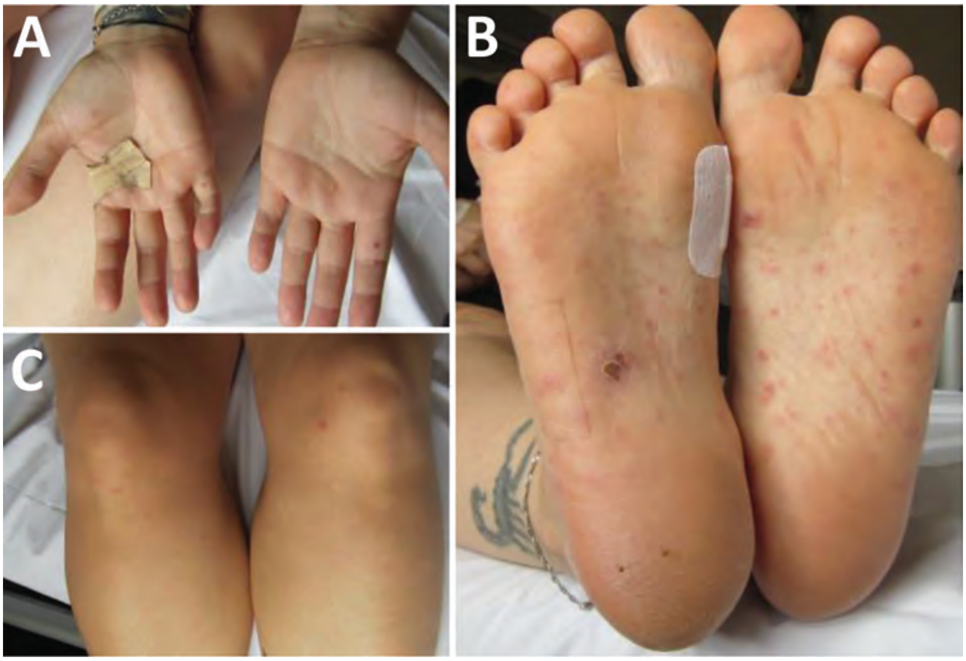

Figure 1. Rat bite fever lesions on 32-year-old female patient, Germany, 2022. At the time of patient's readmission, reddish papules appeared on the palms of the hands (A), soles of the feet (B), and legs (C).

appeared immediately after discharge. A few days later, she went to the dermatology department with a fever and red, nonitching papules on hands, legs, and feet (Figure 1). We examined the papules, finding them comparable to Janeway lesions, and took a biopsy from the right hand. We collected a second blood culture that was positive within 18 hours with growth of a gram-negative bacilli. We identified *S. moniliformis* bacteria by using matrix-assisted laser desorption/ionization time-of-flight mass spectrometry.

The patient was readmitted. In an extended history, she reported having 3 Norway rats as pets. Our further investigation revealed an 11-mm size vegetation on the right coronary cusp of the aortic valve; we observed no signs of insufficiency during echocardiography. The patient was diagnosed with RBF and probable aortic valve endocarditis because of meeting 1 major criterion (positive echocardiography) and 2–3 minor criteria (fever, positive blood culture, and suspected Janeway lesions) of the modified Duke criteria (*5*).

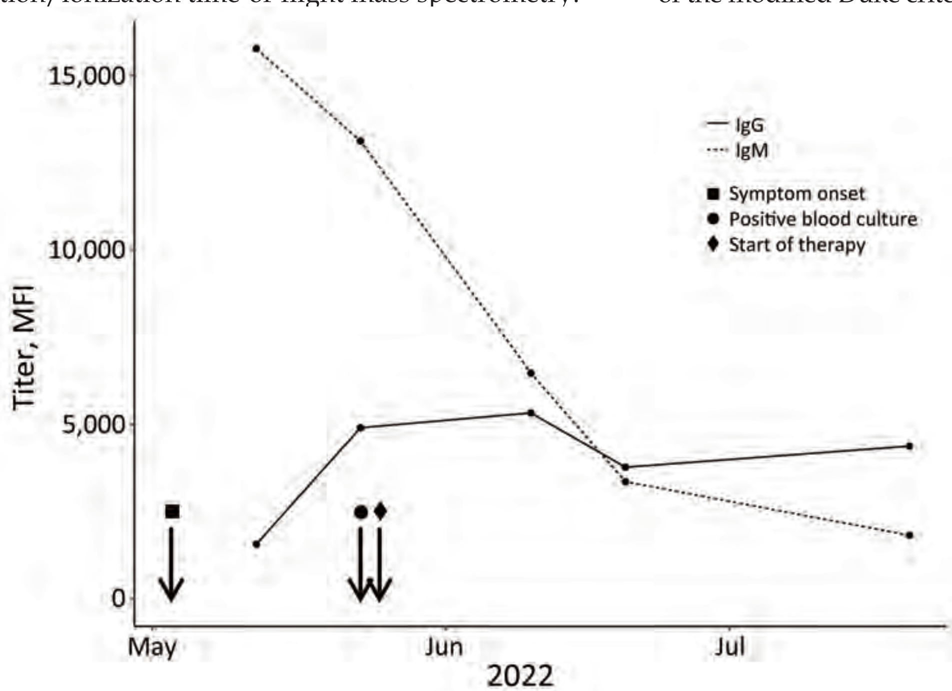

Figure 2. Antibody response to *Streptobacillus moniliformis* infection over time on 32-year-old female patient, Germany, 2022. The graph displays the dynamics of IgM (serum dilution 1:100) and IgG (serum dilution 1:250) levels in MFI values analyzed by *Streptobacillus* multiplex serologic tests (y-axis) and plotted against the time point of infection (x-axis). MFI, median fluorescence intensity.

After we identified the causative pathogen, we began an intravenous therapy with penicillin G (4 × 5 million IU) for 14 days. Because endocarditis was discovered late in the diagnostic process and no further complications arose, we continued monotherapy under frequent clinical and echocardiographic controls. After 14 days, we changed the therapy to oral amoxicillin (4 × 1 g) for another 4 weeks. Two weeks after the start of oral therapy, we no longer detected the aortic vegetation. Two weeks after therapy concluded, the patient reported well-being and no persistent symptoms.

We used a phylogenetic approach to group the microorganism from this study to closely related taxa (Appendix, https://wwwnc.cdc.gov/EID/article/30/3/23-0917-App1.pdf). The resulting tree confirmed the taxonomic position of the isolate from this study as a member of *S. moniliformis* bacteria.

In addition to microbiologic work-up, we analyzed serum samples from different time points for *S. moniliformis* bacteria–specific antibodies by using *Streptobacillus* multiplex serologic analysis. We found high IgM and IgG antibody levels in the patient's serum 9 days after symptom onset. IgM levels of subsequent measurements decreased, and IgG levels initially increased before declining approximately 3 weeks after the onset of symptoms (Figure 2).

Several aspects hamper the diagnosis of RBF, including unawareness of the disease among most clinicians, lack of reliable diagnostics, fastidious growth of the microorganism, susceptibility to most antibiotics used for empiric therapy (*3*), and unnoticed animal contact (*6*). Therefore, the incidence of RBF is unknown and difficult to estimate, especially because RBF is a nonnotifiable disease worldwide. Most of the published case reports do not properly identify the causative organism because they rely solely on 16S rRNA gene sequencing, which is insufficient for an accurate identification at species level (*6*).

In cases where direct detection methods, such as pathogen isolation or molecular testing, are not successful, serologic analysis could be a useful tool for clinical decision-making. High initial IgM and IgG levels of *S. moniliformis* bacteria–specific antibodies were measured in the patient by using *Streptobacillus* multiplex serologic analysis. However, because serologic tests for *S. moniliformis* bacteria are not commercially available nor readily accessible, the prevalence of RBF among humans is unknown. Further serologic studies could help to estimate the occurrence of RBF by shedding light on a largely unknown and underreported disease (*6*). Novel PCR tools could help to reduce the number of undetected infections and enable appropriate treatment.

This case report highlights the benefits of a One Health approach to healthcare in daily practice. Veterinary healthcare provided valuable information for clinicians regarding this rare disease and provided a serologic assay originally developed for the health monitoring of laboratory rodents and adapted for human application. Population-level serologic studies are needed to assess disease prevalence in high-risk groups. This case shows the possibility of species-specific RBF diagnosis in cases where direct diagnostic tools prove to be negative.

Acknowledgments

We thank Ulrike Kling for her support in the microbiologic analysis.

No external funding was received for conducting the analysis and drafting the paper.

About the Author

Dr. Mathé is an infectious disease resident at the Department of Internal Medicine, University Medical Center Freiburg, in Freiburg, Germany. His research focuses on bloodstream infections, climatic influences on diseases, and public health.

References

1. Gaastra W, Boot R, Ho HTK, Lipman LJA. Rat bite fever. Vet Microbiol. 2009;133:211–28. https://doi.org/10.1016/j.vetmic.2008.09.079
2. Eisenberg T, Poignant S, Jouan Y, Fawzy A, Nicklas W, Ewers C, et al. Acute tetraplegia caused by rat bite fever in snake keeper and transmission of *Streptobacillus moniliformis*. Emerg Infect Dis. 2017;23:719–21. https://doi.org/10.3201/eid2304.161987
3. Elliott SP. Rat bite fever and *Streptobacillus moniliformis*. Clin Microbiol Rev. 2007;20:13–22. https://doi.org/10.1128/CMR.00016-06
4. Kimura M, Tanikawa T, Suzuki M, Koizumi N, Kamiyama T, Imaoka K, et al. Detection of *Streptobacillus* spp. in feral rats by specific polymerase chain reaction. Microbiol Immunol. 2008;52:9–15. https://doi.org/10.1111/j.1348-0421.2008.00005.x
5. Otto CM, Nishimura RA, Bonow RO, Carabello BA, Erwin JP III, Gentile F, et al.; Writing Committee Members. 2020 ACC/AHA Guideline for the management of patients with valvular heart disease: a report of the American College of Cardiology/American Heart Association Joint Committee on Clinical Practice Guidelines. J Am Coll Cardiol. 2021;77:e25–197. https://doi.org/10.1016/j.jacc.2020.11.018
6. Eisenberg T, Ewers C, Rau J, Akimkin V, Nicklas W. Approved and novel strategies in diagnostics of rat bite fever and other *Streptobacillus* infections in humans and animals. Virulence. 2016;7:630–48. https://doi.org/10.1080/21505594.2016.1177694

Address for correspondence: Philipp Mathé, Hugstetter St 55, 79106 Freiburg im Breisgau, Germany; email: philipp.mathe@uniklinik-freiburg.de

Source Tracing of *Leishmania donovani* in Emerging Foci of Visceral Leishmaniasis, Western Nepal

Pieter Monsieurs, Kristien Cloots, Surendra Uranw, Megha Raj Banjara, Prakash Ghimire, Sakib Burza, Epco Hasker, Jean-Claude Dujardin, Malgorzata Anna Domagalska

Author affiliations: Institute of Tropical Medicine, Antwerp, Belgium (P. Monsieurs, K. Cloots, E. Hasker, J.-C. Dujardin, M.A. Domagalska); BP Koirala Institute of Health Sciences, Dharan, Nepal (S. Uranw); Tribhuvan University, Kathmandu, Nepal (M.R. Banjara, P. Ghimire); London School of Hygiene and Tropical Medicine, London, UK (S. Burza)

DOI: http://doi.org/10.3201/eid3003.231160

We sequenced *Leishmania donovani* genomes in blood samples collected in emerging foci of visceral leishmaniasis in western Nepal. We detected lineages very different from the preelimination main parasite population, including a new lineage and a rare one previously reported in eastern Nepal. Our findings underscore the need for genomic surveillance.

Leishmania spp. are parasitic protozoans that cause human leishmaniasis in multiple forms, including visceral leishmaniasis (VL), which affects the internal organs. For decades, the Indian subcontinent (ISC)—a geographic region that includes Bangladesh, Bhutan, India, Maldives, Nepal, Pakistan, and Sri Lanka—was the most endemic region for VL in the world. In 2005, a regional elimination program was launched in India, Nepal, and Bangladesh, aiming to reduce VL annual incidence to <1 case/10,000 population at subdistrict and district levels (*1*). Before the start of the program, VL in Nepal was confined mainly to 12 VL endemic districts (out of 77), located in the eastern lowlands. Recently, VL cases in Nepal have spread westward, as well as from lowlands to hilly and even mountainous areas, resulting in a current total of 23 official VL endemic districts, with many more districts reporting likely indigenous cases (*1*). Cutaneous leishmaniasis is also becoming more common (*2*), and combined cases of VL and cutaneous leishmaniasis have been reported, without any information to date on the parasite species and genotype involved. There is clearly a need for a postelimination surveillance system adapted to this new epidemiologic profile.

Molecular surveillance of infectious diseases may provide the most relevant information for control programs, such as following the evolution of epidemics in time and space, characterizing of new transmission cycles, conducting outbreak studies and source identification, and detecting new variants with new clinical features (*3*). Currently, no molecular surveillance is being implemented for leishmaniasis in the world, despite the existence of suitable technologies. We previously showed the feasibility and added value of direct whole genome sequencing (SureSelect sequencing [SuSL-seq]; Agilent Technologies, https://www.agilent.com) of *L. donovani* in host tissues, without the need for parasite isolation and cultivation (*4*).

Here, we demonstrate the proof-of-principle of SuSL-seq for genome surveillance of leishmaniasis, in the context of the reported expansion of VL to the western regions of Nepal. We collected blood samples in 2019 and stored them on DNA/RNA Shield (Appendix). We performed sequencing on 3 samples with the highest amounts of DNA, positive for *Leishmania*, and originating from 3 different districts in Nepal (Dolpa, Darchula, and Bardiya) (Appendix Table 1, Figure 1) and compared them with our database of *L. donovani* genome sequences from the ISC. All samples showed a high genome coverage (Appendix Table 2). The database comparison samples originated from 204 cultivated isolates (2002–2011) from Nepal, India, and Bangladesh (*5*); 52 clinical samples (2000–2015) from Nepal (*4*); and 3 isolates (2002, 2010) from Sri Lanka (*6*,*7*). Altogether, these earlier studies reported 4 main genotypes: a large core group (CG), genomically very homogeneous, in the lowlands of India, Nepal, and Bangladesh; a small ISC1 population, genomically very different from CG, in hilly districts of Eastern Nepal; a single divergent isolate from Nepal, BPK512; and a Sri Lanka (SL) cluster. New phylogenomic analyses (Figure) revealed that the samples from the 3 new foci from western Nepal were clearly distinct from CG and SL: one ISC1-related lineage (024) had not been reported previously, and the 2 other lineages (022 and 023) clustered together with BPK512.

It is premature to conclude that ISC1-related (024) and BPK512-like (022, 023) parasites are expanding, spreading, and replacing CG in a postelimination phase. However, a study based on single-locus genotyping showed a much higher proportion of ISC1 and unclassified genotypes (and a strong decrease of CG) during 2012–2014 compared with 2002–2011 (*9*). Considering the genomic differences between these lineages and CG and their transmissibility by *Phlebotomus argentipes* (*10*), we recommend particular attention to the further evolution of parasites in regions of the ISC. Our previous work evidenced several important functional differences between isolates from

ISC1 and CG (Appendix), and we found in this investigation allele differences in 8 of 10 genes previously shown to be involved in *L. donovani* drug resistance (Appendix Figure 2). Of particular interest, those genetic variants are common in the ISC1 group and in the BPK512 but never found in CG parasites. Without experimental confirmation, it is difficult to speculate about the exact impact of this polymorphism on the resistance to antileishmanial drugs, but it is clear that these parasites are genetically (and, likely, functionally) very diverse from the CG parasites, which were the main target of the recent elimination efforts.

Molecular surveillance requires a method applicable on routine samples collected in any type of field settings. We demonstrate that small amounts of blood from routine examination of patients with VL could be successfully used for direct, sensitive, and untargeted whole-genome analysis of *Leishmania*. Our optimized SuSL-seq protocol enables highly discriminatory genotyping and targeted analysis of the genetic variation within selected loci as well as untargeted searching for new markers related to a clinical or epidemiologic question. Our research supports the need for genomic surveillance of VL—in particular in

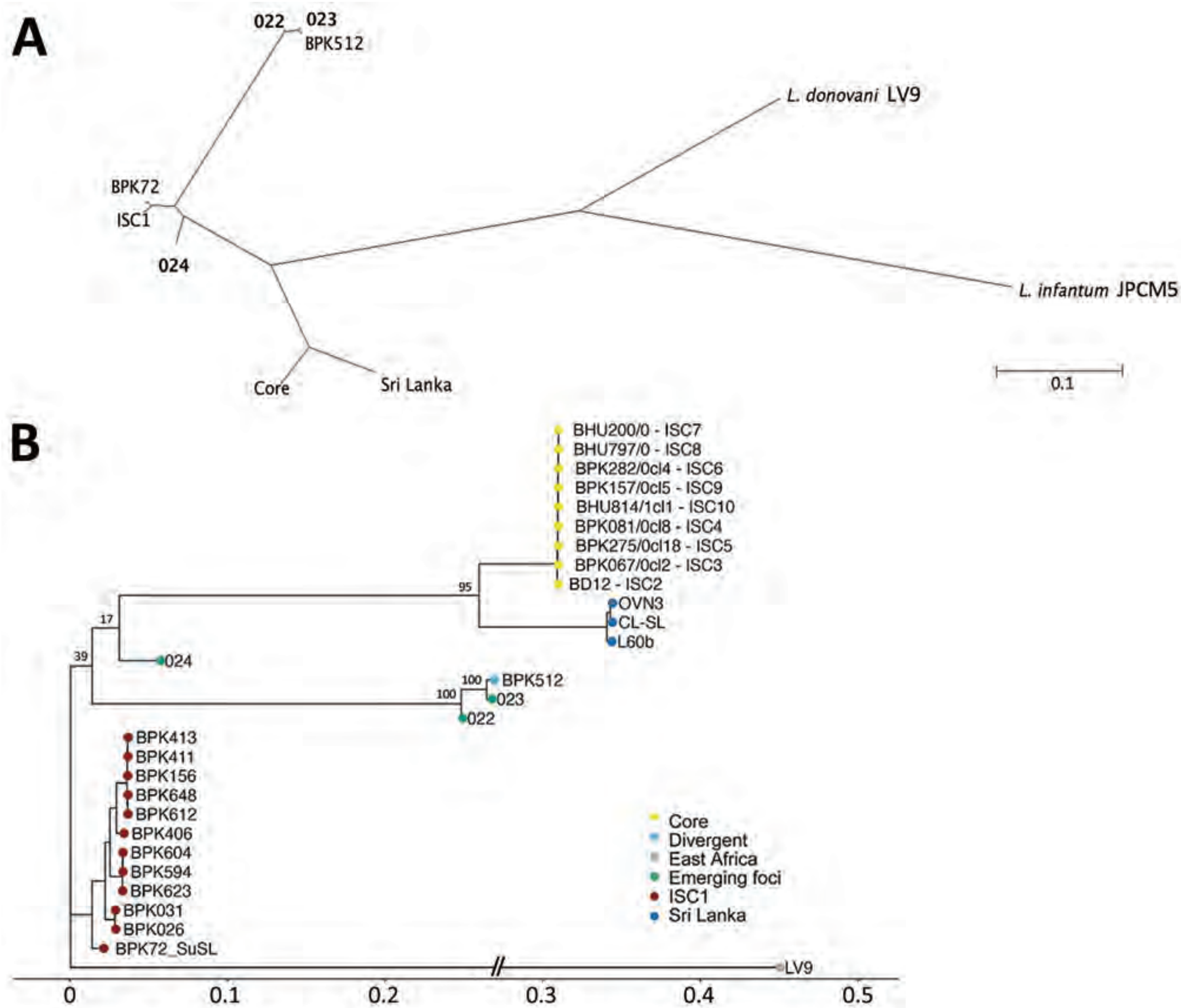

Figure. Phylogenetic analyses of *Leishmania donovani* from the ISC, including Nepal, and reference sequences. Trees were based on genomewide single-nucleotide polymorphisms using RAxML (*8*). A) Unrooted phylogenetic network of the *L. donovani* complex, showing samples representing the emerging foci (bold text). B) Rooted phylogenetic tree of reference strains of *L. donovani* from the ISC, showing the branching of 3 samples (022, 023, and 024) originating from emerging foci. Important bootstrap values are indicated on the branches. The West-African LV9 strain is included as an outgroup. BPK72_SuSL represents an ISC1 sample analyzed using SureSelect sequencing (Agilent Technologies; https://www.agilent.com), confirming that the branching of the emerging foci is not a result of a technical artifact. Scale bars indicate number of single-nucleotide polymorphism differences. ISC, Indian subcontinent.

the context of the current elimination program in the ISC—and demonstrate the applicability of SuSL-seq to molecular surveillance of blood. Continued collaborations will be required to translate these new approaches for VL surveillance to the specific needs of the region.

This article was published as a preprint at https://www.biorxiv.org/content/10.1101/2023.08.22.554278v1.

Genomic sequence reads of the parasites from the 3 new foci are available on the European Nucleotide Archive (https://www.ebi.ac.uk/ena) under accession no. PRJNA991731.

This study was financially supported by the Belgian Directorate-General for Development Cooperation (program FA4), and the UK Department for International Development (KALACORE project).

About the Author

Dr. Pieter Monsieurs is senior scientist in computational biology at the Institute of Tropical Medicine, Antwerp, Belgium, and an expert in genomics and transcriptomics of microbial organisms. He contributed to several studies on the genomic diversity of *Leishmania*, *Trypanosoma*, *and Plasmodium* in molecular epidemiology, evolutionary, and experimental contexts.

References

1. Pandey K, Dumre SP, Shah Y, Acharya BK, Khanal L, Pyakurel UR, et al. Forty years (1980–2019) of visceral leishmaniasis in Nepal: trends and elimination challenges. Trans R Soc Trop Med Hyg. 2023;117:460–9. https://doi.org/10.1093/trstmh/trad001
2. Pandey K, Bastola A, Haiyan G, Pyakurel UR, Pandey BD, Dumre SP. Emergence of cutaneous leishmaniasis in Nepal. Trop Med Health. 2021;49:72. https://doi.org/10.1186/s41182-021-00359-3
3. Domagalska MA, Dujardin JC. Next-generation molecular surveillance of TriTryp diseases. Trends Parasitol. 2020;36:356–67. https://doi.org/10.1016/j.pt.2020.01.008
4. Domagalska MA, Imamura H, Sanders M, Van den Broeck F, Bhattarai NR, Vanaerschot M, et al. Genomes of *Leishmania* parasites directly sequenced from patients with visceral leishmaniasis in the Indian subcontinent. Rogers MB, editor. PLoS Negl Trop Dis. 2019;13:e0007900. https://doi.org/10.1371/journal.pntd.0007900
5. Imamura H, Downing T, Van den Broeck F, Sanders MJ, Rijal S, Sundar S, et al. Evolutionary genomics of epidemic visceral leishmaniasis in the Indian subcontinent. eLife. 2016;5:e12613. https://doi.org/10.7554/eLife.12613
6. Franssen SU, Durrant C, Stark O, Moser B, Downing T, Imamura H, et al. Global genome diversity of the *Leishmania donovani* complex. eLife. 2020;9:e51243. https://doi.org/10.7554/eLife.51243
7. Zhang WW, Ramasamy G, McCall LI, Haydock A, Ranasinghe S, Abeygunasekara P, et al. Genetic analysis of *Leishmania donovani* tropism using a naturally attenuated cutaneous strain. PLoS Pathog. 2014;10:e1004244. https://doi.org/10.1371/journal.ppat.1004244
8. Kozlov AM, Darriba D, Flouri T, Morel B, Stamatakis A. RAxML-NG: a fast, scalable and user-friendly tool for maximum likelihood phylogenetic inference. Bioinformatics. 2019;35:4453–5. https://doi.org/10.1093/bioinformatics/btz305
9. Rai K, Bhattarai NR, Vanaerschot M, Imamura H, Gebru G, Khanal B, et al. Single locus genotyping to track *Leishmania donovani* in the Indian subcontinent: Application in Nepal. PLoS Negl Trop Dis. 2017;11:e0005420. https://doi.org/10.1371/journal.pntd.0005420
10. Seblova V, Dujardin JC, Rijal S, Domagalska MA, Volf P. ISC1, a new *Leishmania donovani* population emerging in the Indian sub-continent: Vector competence of *Phlebotomus argentipes*. Infect Genet Evol. 2019;76:104073. https://doi.org/10.1016/j.meegid.2019.104073

Address for correspondence: Malgorzata Anna Domagalska, Institute of Tropical Medicine, Nationalestraat 155, 2000 Antwerpen, Belgium; email: mdomagalska@itg.be

Enterocytozoon bieneusi Infection after Hematopoietic Stem Cell Transplant in Child, Argentina

Cristian Javier Mena,[1] Magalí Pérez Garófalo,[1] Juliana Perazzo, Carolina Epelbaum, Gonzalo Castro, Paola Sicilia, Andrés Barnes, Lorena Guasconi, Verónica L. Burstein, Ignacio Beccacece, Mariel A. Almeida, Laura Cervi, Monica Santin, Laura S. Chiapello

DOI: http://doi.org/10.3201/eid3003.231580

Author affiliations: National University of Córdoba Faculty of Chemical Sciences, Center for Research in Clinical Biochemistry and Immunology, Córdoba, Argentina (C.J. Mena, L. Guasconi, V.L. Burstein, I. Beccacece, M.A. Almeida, L. Cervi, L.S. Chiapello); Dr. Juan P. Garrahan Pediatric Hospital, Buenos Aires, Argentina (M. Pérez Garófalo, J. Perazzo, C. Epelbaum); Central Laboratory of the Province of Córdoba, Córdoba (G. Castro, P. Sicilia); Microbiology Laboratory, Complementary Diagnostic Area, Hospital Rawson, Córdoba (A. Barnes); USDA Agricultural Research Service, Beltsville, Maryland, USA (M. Santin)

[1]These authors contributed equally to this article.

We report a case of *Enterocytozoon bieneusi* infection in a pediatric hematopoietic stem cell transplant recipient in Argentina. Spores were visualized in feces using Calcofluor White and modified trichrome stainings. PCR and sequencing identified *E. bieneusi* genotype D in fecal samples and liver samples, confirming extraintestinal dissemination of the parasite.

Microsporidia, fungal-related single-cell parasites, infect a broad range of vertebrates and invertebrates. The most identified species of Microsporidia in humans are *Enterocytozoon bieneusi* and *Encephalitozoon intestinalis*, which have emerged as opportunistic pathogens in immunosuppressed persons, such as those infected with HIV, organ transplant recipients, and cancer patients. The infective forms of these parasites are the resistant spores that persist in the environment, causing infections through direct contact with infected persons, infected animals, or ingestion of contaminated water and food (*1*). Human microsporidiosis is characterized primarily by chronic diarrhea and wasting, with less frequent occurrences of extraintestinal disseminated disease. Identification to the genus and species level is crucial for tailored treatments, especially in cases of chronic diarrhea (*2*).

Pediatric patients undergoing allogeneic hematologic stem cell transplantation (HSCT) may experience gut-localized or extraintestinal microsporidiosis by *Encephalitozoon* spp (*3*). In patients with leukemia or lymphoma who receive cytotoxic treatments, intestinal infections are predominantly associated with *E. bieneusi*, and rare cases of extraintestinal dissemination also have been reported (*1*,*4*).

More than 500 worldwide genotypes of *E. bieneusi* have been identified based on genetic polymorphisms in the internal transcribed spacer of the rRNA gene. They are distributed into 11 distinct phylogenetic groups, with groups 1 and 2 comprising genotypes with zoonotic potential that infect humans and various mammalian and avian species (*2*).

Although intestinal microsporidiosis is prevalent in children residing in developing countries, scarce studies have been reported in Argentina (*1*,*5*,*6*). We present a case of *E. bieneusi* (genotype D) infection in a child who underwent unrelated allogeneic HSCT in Buenos Aires, Argentina.

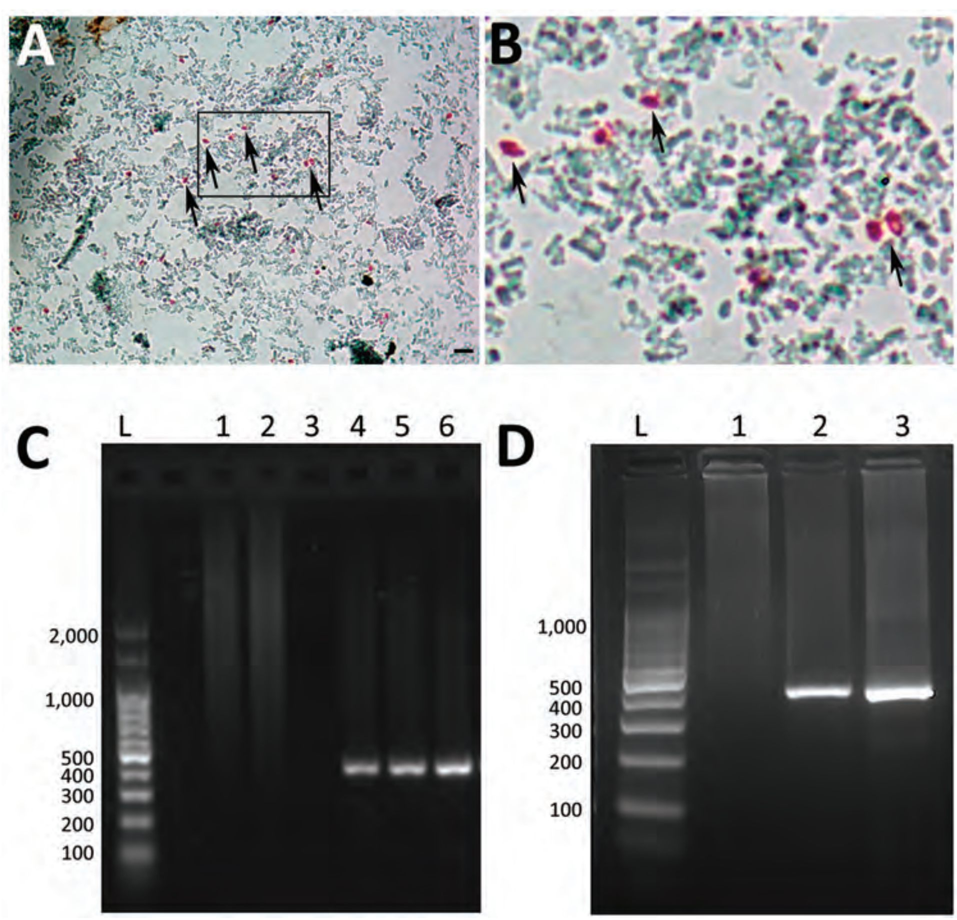

Figure. *Enterocytozoon bieneusi* detection in fecal sample and liver aspiration biopsy sample from a child with hematopoietic stem cell transplant, Argentina. A) Light microscopy of fecal samples after Weber's modified trichome staining showing ovoid shaped-spores with a pinkish-red stained wall (arrows). Original magnification × 1,000; scale bars = 5 μm. B) Closer view of boxed area in panel A, showing spores (arrows). C) Agarose gel electrophoresis (2%) showing amplification products (≈390 pb) from nested PCR with inner primers EBITS1 and EBITS2 from patient fecal sample. Lane L, molecular weight ladder; lane 1, negative control (water); lanes 2 and 3, fecal samples from healthy donors; lane 4, positive feces control for *E. bieneusi*; lanes 5 and 6, fecal samples from patient. D) Nested PCR products from liver aspiration biopsy sample. Lane L, molecular weight ladder; lane 1, fecal sample from healthy donor; lane 2, fecal sample from patient; lane 3, liver aspiration biopsy sample from patient.

The Study

A 12-year-old boy from Buenos Aires who had a January 2018 diagnosis of intermediate-risk pre-B acute lymphoblastic leukemia received an unrelated allogeneic HSCT in February 2022. A month after HSCT, the child was treated with antiviral therapy for reactivation of cytomegalovirus, adenovirus, and Epstein-Barr virus infections. Three months post-HSCT, under immunosuppressive therapy with tacrolimus (0.1 mg/kg/d), he received antimicrobial treatment with meropenem (60 mg/kg/d), linezolid (30 mg/kg/d), and liposomal amphotericin B (3 mg/kg/d) to combat prolonged fever and abdominal symptoms. Videoendoscopy of the upper digestive tract confirmed gastrointestinal graft-versus-host disease, and ultrasound showed splenomegaly with multiple rounded hypodense images in the spleen and liver. We also noted distension of the ileal and colonic loops, predominantly in the right colon, and ascites.

We treated the child with liposomal amphotericin B (3 mg/kg/d) to address persistent febrile symptoms and visceral lesions compatible with chronic disseminated candidiasis. Four months after HSCT, the child sought treatment for chronic diarrhea (>1 month) and abdominal pain. Prior to microbiological documentation, we prescribed empirical treatment of metronidazole (30 mg/kg/d), which produced no improvement of symptoms.

Coproanalysis revealed typical polymicrobial bacterial flora, with no detection of bacterial toxins, adenovirus, rotavirus, or parasites. Calcofluor White and Weber's modified trichrome staining revealed structures compatible with microsporidian spores in single and serial fecal specimens (Figure, panels A, B). Analysis of liver aspiration biopsy samples rendered no conclusive results. On the basis of microscopic results, we immediately initiated albendazole treatment (400 mg/d) for microsporidiosis (*7*).

We conducted molecular biology studies based on fecal samples and liver aspiration biopsy samples. We determined *E. bieneusi* and genotype identification by using a nested PCR protocol that targeted the entire internal transcribed spacer and also amplified portions of the flanking large and small subunits of the ribosomal RNA (≈400 bp) gene (*8*,*9*) (Figure, panels C, D). We confirmed the presence of *E. bieneusi* genotype D based on Sanger sequencing using the inner-nested PCR primers (*2*). We named the nucleotide sequence generated BsAs1 and deposited it into GenBank (accession no. OP650902). Despite a decrease in diarrhea symptoms, the child died 18 days after initiation of albendazole treatment due to fulminant hyperacute lymphoproliferative syndrome, before identification of *E. bieneusi* was determined.

Conclusions

E. bieneusi has been reported commonly in cancer patients undergoing chemotherapy (*1*,*3*,*4*,*10*). We report a case of *E. bieneusi* genotype D microsporidiosis, with intestinal and hepatic localization, in a child with leukemia and immunosuppression after a bone marrow transplant in Argentina. Our findings highlight the need to incorporate microsporidiosis in the differential diagnosis of immunosuppressed children after transplant surgery, as well as for other patient populations at high risk for opportunistic infections. Our report also emphasizes the critical importance of microsporidia identification because albendazole is effective against some *Encephalitozoon* species but not against *E. bieneusi* (*1*,*7*). Genotyping isolates of clinical *E. bieneusi* may help to identify potential environmental sources. Although nitazoxanide could be used as an alternative treatment, fumagillin has a wider range of activity effectively targeting *E. bieneusi* (*7*). The unavailability of fumagillin for treating human infections in several countries, including Argentina, underscores the need for enhanced accessibility to microsporidia treatment options, especially for vulnerable populations.

This study was approved by the Research and Ethics Committee of Hospital de Pediatría J.P. Garrahan (Buenos Aires, Argentina). This work was supported by Agencia Nacional de Promoción Científica y Tecnológica, Fondo para la Investigación Científica y Tecnológica (FONCyT), Argentina, PICT 2019-4101 and SECyT-UNC. C.J.M is a Fellow from CONICET. L.S.C. is Researcher of CONICET.

About the Author

Bioq. Mena is a biochemist and PhD student at the National University of Cordoba and fellow of CONICET, Córdoba, Argentina. His research interests include development and improvement of molecular tools for diagnosis and epidemiology of parasite and fungal human pathogens causing infections in South America. Bioq. Pérez Garófalo is biochemist at the Laboratorio Central, Hospital de Pediatría S.A.M.I.C. "Prof. Dr. Juan P. Garrahan," Buenos Aires, Argentina. Her research interests include improvement of diagnosis techniques for infectious diseases in pediatric patients.

References

1. Han B, Pan G, Weiss LM. Microsporidiosis in humans. Clin Microbiol Rev. 2021;34:e0001020. https://doi.org/10.1128/CMR.00010-20
2. Li W, Feng Y, Santin M. Host specificity of *Enterocytozoon bieneusi* and public health implications. trends Parasitol. 2019;35:436–51. https://doi.org/10.1016/j.pt.2019.04.004

3. Ambrosioni J, van Delden C, Krause KH, Bouchuiguir-Wafa C, Nagy M, Passweg J, et al. Invasive microsporidiosis in allogeneic haematopoietic SCT recipients. Bone Marrow Transplant. 2010;45:1249–51. https://doi.org/10.1038/bmt.2009.315
4. Jiménez-González GB, Martínez-Gordillo MN, Caballero-Salazar S, Peralta-Abarca GE, Cárdenas-Cardoz R, Arzate-Barbosa P, et al. [Microsporidia in pediatric patients with leukemia or limphoma]. Rev Invest Clin. 2012;64:25–31. Spanish.
5. Velásquez JN, di Risio C, Etchart C, Chertcoff AV, Astudillo OG, Carnevale S. Multimethodological approach to gastrointestinal microsporidiosis in HIV-infected patients. Acta Parasitol. 2019;64:658–69. https://doi.org/10.2478/s11686-019-00095-z
6. Valperga SM, de Jogna Prat SA, de Valperga GJ, Lazarte SG, de Trejo AV, Díaz N, et al. [Microsporidian spores in the stool specimens of toddlers, with or without diarrhea, from Tucumán, Argentina]. Rev Argent Microbiol. 1999;31:157–64. Spanish.
7. Han B, Weiss LM. Therapeutic targets for the treatment of microsporidiosis in humans. Expert Opin Ther Targets. 2018;22:903–15. https://doi.org/10.1080/14728222.2018.1538360
8. Buckholt MA, Lee JH, Tzipori S. Prevalence of *Enterocytozoon bieneusi* in swine: an 18-month survey at a slaughterhouse in Massachusetts. Appl Environ Microbiol. 2002;68:2595–9. https://doi.org/10.1128/AEM.68.5.2595-2599.2002
9. Mena CJ, Barnes A, Castro G, Guasconi L, Burstein VL, Beccacece I, et al. Microscopic and PCR-based detection of microsporidia spores in human stool samples. Rev Argent Microbiol. 2021;53:124–8. https://doi.org/10.1016/j.ram.2020.04.005
10. Desoubeaux G, Nourrisson C, Moniot M, De Kyvon MA, Bonnin V, De La Bretonniére ME, et al. Genotyping approach for potential common source of *Enterocytozoon bieneusi* infection in Hematology unit. Emerg Infect Dis. 2019;25:1625–31. https://doi.org/10.3201/eid2509.190311

Address for correspondence: Laura S. Chiapello, Departamento de Bioquímica Clínica (Lab 105), Facultad de Ciencias Químicas, Universidad Nacional de Córdoba, CIBICI, CONICET, Ciudad Universitaria, Haya de la Torre y Medina Allende, X5000HUA Córdoba, Argentina; email: laura.chiapello@unc.edu.ar

Subdural Empyema from *Streptococcus suis* Infection, South Korea

Sejin Choi, Tae-Hwan Park, Hyun-Jeong Lee, Tae Hyoung Kim, Jin-Deok Joo, Jisoon Huh, You Nam Chung, Sang Taek Heo, Eui Tae Kim, Jong-Kook Rhim

Author affiliations: Seoul National University Hospital, Seoul, South Korea (S. Choi, T.-H. Park); Jeju National University College of Medicine, Jeju, South Korea (H.-J. Lee, T.H. Kim, J.D. Joo, J. Huh, Y.N. Chung, S.T. Heo, E.T. Kim, J.-K. Rhim); Jeju National University Graduate School, Jeju (T.H. Kim); Jeju National University Core Research Institute, Jeju (E.T. Kim)

DOI: https://doi.org/10.3201/eid3003.231018

In Jeju Island, South Korea, a patient who consumed raw pig products had subdural empyema, which led to meningitis, sepsis, and status epilepticus. We identified *Streptococcus suis* from blood and the subdural empyema. This case illustrates the importance of considering dietary habits in similar clinical assessments to prevent misdiagnosis.

Streptococcus suis is a zoonotic pathogen that affects pigs and humans when they handle pigs or eat undercooked pork products. Globally, an outbreak of infection occurred in China in 2005, and *S. suis* is a common cause of bacterial meningitis in Vietnam and Hong Kong (*1*,*2*). High-risk eating habits of ingesting raw or undercooked pork also have been reported in Thailand (*2*).

Although *S. suis* infection traditionally is associated with pig contact or consumption of undercooked pork, South Korea reported its first human infection in 2012, with subsequent cases not explicitly linked to pigs (*3*). Of note, consuming raw pork is rare in South Korea because of cultural taboos. In South Korea, the prevalence of *S. suis* infection was 12.6% among slaughtered pigs and 16.4% among diseased pigs; serotypes 2 and 14 were predominant in the Jeju area compared with other regions (*4*).

Common manifestations of *S. suis* infection are meningitis, endocarditis, septicemia, and arthritis but not subdural empyema (*2*). Subdural empyema is a rare but serious infection that causes a collection of pus between the dura and arachnoid layers of the meninges (*5*). We describe a case of subdural empyema caused by to *S. suis* infection after the consumption of raw pig products in Jeju Island, South Korea, where the pork industry has been an economic pillar for over 500 years.

The patient, a 76-year-old man, visited the emergency department exhibiting dysarthria, neck stiffness, and right-sided weakness with motor grade III. He did not have hearing loss, a common symptom of human *S. suis* infection, or signs of increased intracranial pressure such as papilledema. His medical history included a fall 3 months prior and recent headache and dizziness. Initial brain computed tomography and magnetic resonance imaging showed chronic subdural hematoma (cSDH) with recurrent bleeding and an inflamed subdural sac (Figure 1). Concurrently, he exhibited septic symptoms, such as fever, hypotension, marked thrombocytopenia, and elevated inflammatory markers, necessitating immediate administration of antibiotics (vancomycin, ceftazidime, and metronidazole). Further studies showed that he did not have endocarditis, sinusitis, or otitis media (all possible causes of subdural empyema) (*5*). We drew blood cultures on admission day and on hospital days 4 and 7 and incubated them for >5 days. On hospital day 4, we detected *S. suis* from a blood culture. Subsequent inquiries into the patient's dietary habits revealed recent consumption of Ae-Jeo-Hoe, a traditional dish from Jeju Island, made by slicing open the belly of a pregnant pig, finely chopping or grinding the fetus, and eating it raw with various seasonings. Consequently, we conducted further microbiologic investigations to rule out other conditions, such as severe fever with thrombocytopenia syndrome and cysticercosis, which all turned out negative.

Upon confirmation of *S. suis* infection, treatment shifted to ceftriaxone. Results of blood cultures from days 4 and 7 were negative, but neurologic deficits persisted. On day 10, we evacuated a subdural empyema through left frontal and parietal burr hole trephinations. Intraoperatively, we identified a multiseptated pus-like tissue and a bloody subdural fluid. Despite the negative swab and fluid culture results, PCR confirmed *S. suis gdh* and *thrA* genes in the subdural empyema sample (Figure 2). We extracted total genomic DNA from blood-cultured bacteria and from the patient's subdural hematoma by using the Solg Genomic DNA Prep Kit (SolGent,

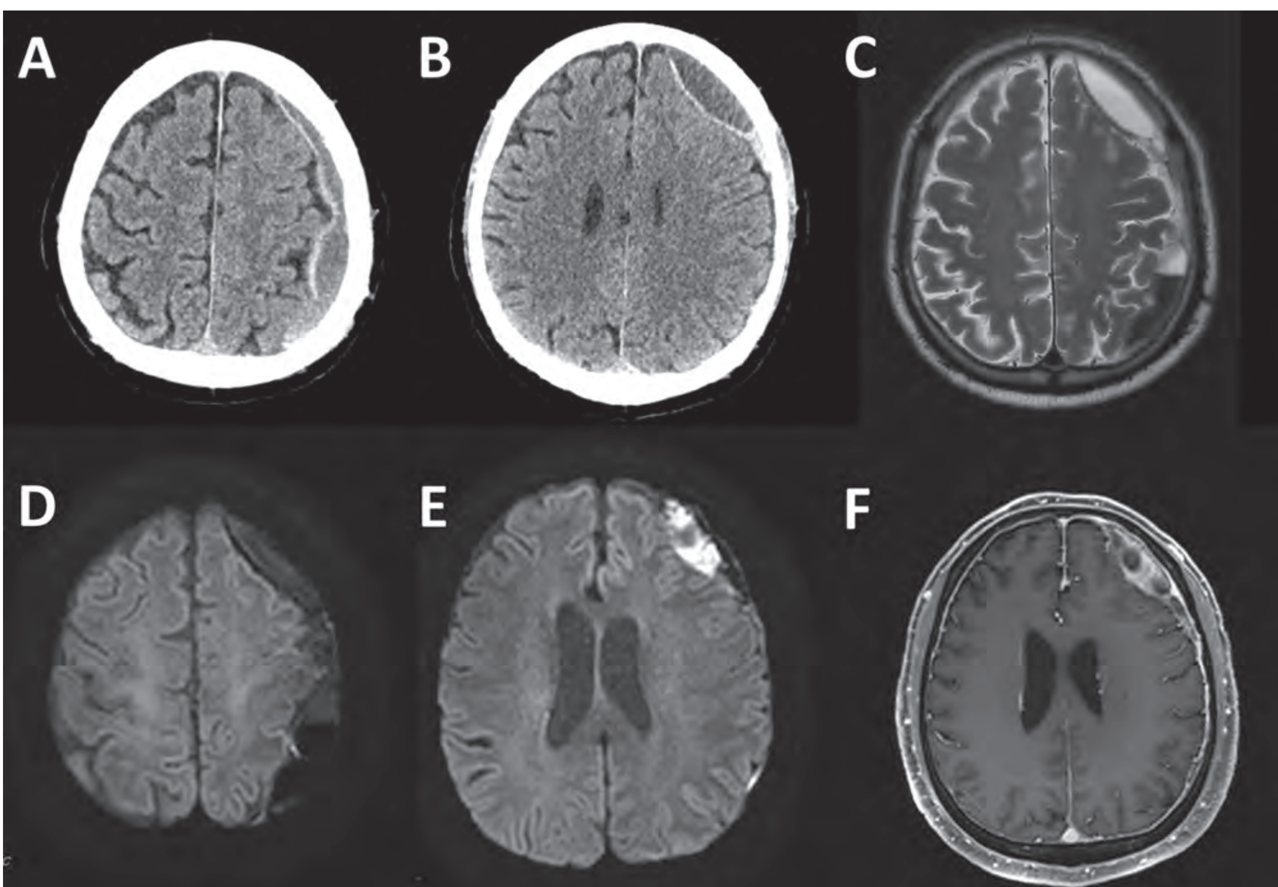

Figure 1. Initial image findings of subdural empyema in a patient with *Streptococcus suis* infection, Jeju Island, South Korea. A, B) Computed tomography scans. D–F) Magnetic resonance imaging: diffusion weighted (D, E), T2 (C), and enhanced T1 (F).

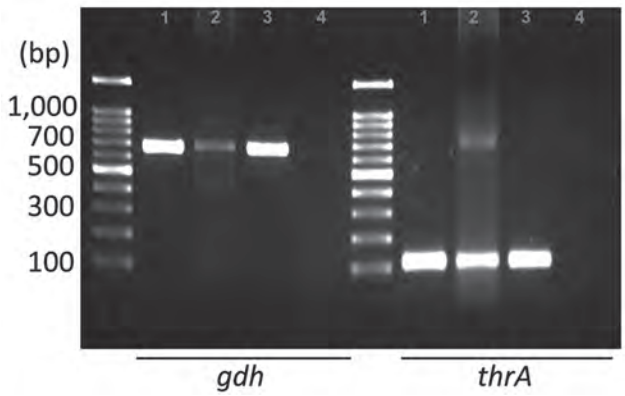

Figure 2. Detection of *Streptococcus suis* in a patient with *Streptococcus suis* infection, Jeju Island, South Korea, performed by using PCR with specific primers for *gdh* and *thrA*. Size marker, 1 kb DNA ladder (LugenSci, https://www.lugensci.com). Lane 1, blood culture, DNA from patient's blood culture; lane 2, subdural empyema, DNA from patient's subdural pus; lane 3, positive control, DNA from previously isolated *S. suis* stock; lane 4, negative control, no template PCR condition.

http://www.solgent.com) according to the manufacturer's instructions. We detected *S. suis* DNA by using the *gdh*-specific primers GCAGCGTATTCTGTCAAACG (forward) and CCATGGACAGATAAAGATGG (reverse) (*6*), and the *thrA*-specific primers GAAAATATGAAGAGCCATGTCG (forward) and GACAACGAACATAACAGAAACTTC (reverse) (*7*). In addition, we conducted next-generation whole-genome sequencing (Theragen Bio, https://www.theragenbio.com), which identified the isolate as serotype 2, which closely matched the genetic sequence of the ISU2614 strain (GenBank accession no. ASM1348816v1), known for its high virulence (*8*,*9*) (Appendix Figure, https://wwwnc.cdc.gov/EID/article/30/3/23-1018-App1.pdf).

On day 16, the patient had onset of convulsive status epilepticus potentially attributable to meningitis, which was managed by a continuous infusion of propofol. The patient was subsequently stabilized, and his neurologic symptoms improved.

This case is noteworthy because it represents a neurosurgical condition, specifically subdural empyema, which required surgery, associated with *S. suis* infection. In addition, severe conditions such as sepsis and status epilepticus after the infection underscore the lethality of this zoonotic pathogen.

The role of the patient's cSDH caused by prior trauma warrants further discussion in the pathogenesis of the infection. The vascularized membrane of the cSDH may have served as a seeding bed for the hematogenous spread of the infection and development of the subdural empyema (*10*), suggesting increased susceptibility in patients with cSDH or older patients with a trauma history and emphasizing the need for prompt diagnosis and treatment.

This report highlights a unique correlation to consuming a traditional dish prepared from raw pig fetuses and underscores the importance of considering dietary habits in the clinical assessment. It also raises public health concerns about the potential risks associated with consuming raw or undercooked pork products and possible *S. suis* endemic in Jeju Island, where extensive pig rearing and consumption take place. Increasing disease awareness among clinicians and laboratories can prevent undiagnosed or misdiagnosed cases.

E.T.K. was supported by the National Research Foundation of Korea grant, funded by the Ministry of Science and Information and Communication Technology (grant no. 2021R1A2C1010313) and the Ministry of Education (grant no. RS2023-00270936), South Korea.

About the Author

Dr. Choi is a neurosurgery resident at Seoul National University Hospital. His primary research interests include neurosurgical diseases and public health.

References

1. Wertheim HF, Nghia HD, Taylor W, Schultsz C, Taylor W, Schultsz C. *Streptococcus suis*: an emerging human pathogen. Clin Infect Dis. 2009;48:617–25. https://doi.org/10.1086/596763
2. Huong VTL, Ha N, Huy NT, Horby P, Nghia HDT, Thiem VD, et al. Epidemiology, clinical manifestations, and outcomes of *Streptococcus suis* infection in humans. Emerg Infect Dis. 2014;20:1105–14. https://doi.org/10.3201/eid2007.131594
3. Kim J-G, Seong GM, Kim YR, Heo ST, Yoo JR. *Streptococcus suis* causes bacterial meningitis with hearing loss in patients without direct exposure to pigs in a regional pork industry territory. J Med Life Sci. 2023;20:43–7.
4. Oh SI, Jeon AB, Jung BY, Byun JW, Gottschalk M, Kim A, et al. Capsular serotypes, virulence-associated genes and antimicrobial susceptibility of *Streptococcus suis* isolates from pigs in Korea. J Vet Med Sci. 2017;79:780–7. https://doi.org/10.1292/jvms.16-0514
5. Baek SH, Choi SK, Ryu J, Lee SH. Subdural empyema treated by continuous irrigation and drainage catheter insertion in a young adult patient with hemiparesis: a case report. Nerve. 2017;3:85–8.
6. Okwumabua O, O'Connor M, Shull E. A polymerase chain reaction (PCR) assay specific for *Streptococcus suis* based on the gene encoding the glutamate dehydrogenase. FEMS Microbiol Lett. 2003;218:79–84. https://doi.org/10.1111/j.1574-6968.2003.tb11501.x
7. Liu Z, Zheng H, Gottschalk M, Bai X, Lan R, Ji S, et al. Development of multiplex PCR assays for the identification of the 33 serotypes of *Streptococcus suis*. PLoS One. 2013;8:e72070. https://doi.org/10.1371/journal.pone.0072070

8. Fan H-j. Advances in pathogenesis of *Streptococcus suis* serotype 2. Journal of Integrative Agriculture. 2017;16: 2834–47.
9. Nicholson TL, Waack U, Anderson TK, Bayles DO, Zaia SR, Goertz I, et al. Comparative virulence and genomic analysis of *Streptococcus suis* isolates. Front Microbiol. 2021;11:620843. https://doi.org/10.3389/fmicb.2020.620843
10. Shapiro M, Walker M, Carroll KT, Levitt MR, Raz E, Nossek E, et al. Neuroanatomy of cranial dural vessels: implications for subdural hematoma embolization. J Neurointerv Surg. 2021;13:471–7. https://doi.org/10.1136/neurintsurg-2020-016798

Address for correspondence: Eui Tae Kim or Jong-Kook Rhim, Jeju National University College of Medicine, Aran 13gil 15 (Ara-1 Dong) Jeju-si, Jeju Self-Governing Province, 63241, South Korea; email: tae@jejunu.ac.kr or nsrhim@gmail.com

Incursion of Highly Pathogenic Avian Influenza A(H5N1) Clade 2.3.4.4b Virus, Brazil, 2023

Andreina Carvalho de Araújo,[1] Laura Morais Nascimento Silva,[1] Andrew Yong Cho,[1] Márcio Repenning, Deyvid Amgarten, Ana Paula de Moraes, Fernanda Malta, Michael Miller, Erick G. Dorlass, Soledad Palameta, Daniele Bruna L. Oliveira, Jansen de Araújo, Clarice Weis Arns, Edison L. Durigon, João Renato R. Pinho, Dong-Hun Lee, Helena Lage Ferreira

Author affiliations: University of São Paulo, Pirassununga, Brazil (A.C. Araujo, L.M.N. Silva, D.B.L. Oliveira, J. De Araujo, E.L. Durigon, J.R.R. Pinho, H.L. Ferreira); Konkuk University, Gwangjin-gu, South Korea (A.Y. Cho, D.-H. Lee); FURG, Rio Grande, Brazil (M. Repenning); Albert Einstein Israelite Hospital, São Paulo, Brazil (D. Amgarten, F. Malta, E.G. Dorlass, D.B.L. Oliveira, J.R.R. Pinho); UNICAMP, Campinas, Brazil (A.P. de Moraes, M. Miller, S. Palameta, C.W. Arns); Institut Pasteur, São Paulo, Brazil (E.L. Durigon)

DOI: http://doi.org/10.3201/eid3003.231157

[1]These authors contributed equally to this article.

We report 4 highly pathogenic avian influenza A(H5N1) clade 2.3.4.4.b viruses in samples collected during June 2023 from Royal terns and Cabot's terns in Brazil. Phylodynamic analysis revealed viral movement from Peru to Brazil, indicating a concerning spread of this clade along the Atlantic Americas migratory bird flyway.

Highly pathogenic avian influenza viruses (HPAIVs) have caused substantial economic losses in the poultry industry and potentially threaten public health. Since its first identification in 1996, H5Nx HPAIVs, Gs/GD lineage, have evolved into multiple genotypes through reassortment across decades (*1*–*3*).

In late 2020, novel reassortant clade 2.3.4.4b H5N1 HPAIVs emerged and became predominant in Europe (*1*). The first detection of clade 2.3.4.4 b H5N1 viruses in North America occurred through transatlantic spread via wild birds in late 2021 (*2*). From late 2021 to early 2022, multiple reassortant viruses have been naturally generated by recombination with North American low pathogenicity avian influenza virus (LPAIV) internal genes. In late October 2022, South America countries including Argentina, Bolivia, Brazil, Chile, Colombia, Ecuador, Paraguay, Peru, Uruguay, and Venezuela reported clade 2.3.4.4 b H5N1 HPAIV detection in domestic and wild birds (*3*,*4*). Human infections were also reported for the first time in South America (*3*,*5*). We report 4 clade 2.3.4.4b H5N1 HPAIVs sequenced from wild bird carcasses collected in Brazil in June 2023.

In June 2023, we collected swab samples from Royal terns (*Thalasseus maximus*) and Cabot's terns (*Thalasseus acuflavidus*) in Brazil, from which we detected and sequenced 4 H5N1 HPAIVs: A/Thalasseus_maximus/Brazil-ES/23ES1A0008/2023 (TM/BR08/23), A/Thalasseus_acuflavidus/Brazil-ES/23ES1A0009/2023 (TA/BR09/23), A/Thalasseus acuflavidus/Brazil-ES/23ES1A0025/2023 (TA/BR25/23), and A/Thalasseus maximus/Brazil-ES/23ES1A0026/2023 (TM/BR26/23) (Appendix 1, https://wwwnc.cdc.gov/EID/article/30/3/23-1157-App1.pdf). We obtained complete genome sequences for TM/BR08/23 and TM/BR09/23 and partial sequences for TA/BR25/23 and TM/BR26/23 (GISIAD [https://www.gisaid.org] accession nos. EPI_ISL_18130597, EPI_ISL_18130622, EPI_ISL_18130627, and EPI_ISL_18130628) (Appendix 1 Table 1).

All H5N1 isolates possessed polybasic amino acid sequences at the hemagglutinin (HA) cleavage site (PLREKRKKR/GLF). The isolates shared high sequence identities (99.59%–100%) across all 8 genes. BLAST search (https://blast.ncbi.nlm.nih.gov) showed all 8 genes shared high identities (99.59%–

100%) to the recent H5N1 HPAIVs isolated from samples obtained in Chile and other South American countries. Using maximumplikelihood phylogenies, we noted that all internal genes (polymerase basic [PB] 2, PB1, polymerase acidic [PA], nucleoprotein [NP], matrix [M], nonstructural [NS]) clustered with the B3.2 genotype, a reassortant genotype identified in the United States in early 2022. The B3.2 genotype comprises North America–origin PB2, PB1, NP, and NS and Eurasia–origin PA, HA, NA, and M. We observed no evidence of reassortment, indicating the viruses were direct descendants of genotype B3.2 (Appendix 1 Figure 1) (*6*). Bayesian phylogeny of the HA gene revealed the H5N1 viruses from Brazil formed a well-supported cluster. We estimated the time to most recent ancestor to be May 13, 2023 (95% highest posterior density April 15, 2023–June 10, 2023), suggesting the H5N1 HPAIVs emerged ≈1 month before the detection in the carcasses of wild terns (Figure).

We estimated the incursion of genotype B3.2 into South America to be around August 14, 2022 (95% highest posterior density July 3, 2022–September 21 2022). Discrete trait analysis of geographic location suggested the source of H5N1 HPAIV was from North America, with frequently observed viral movement from Peru to Chile (Figure). The viral transition from Chile to Brazil was highly supported. However, the long branch between the two countries suggests a lack of data to be filled (Figure; Appendix 1 Tables 2, 3). Discrete trait analysis after minimizing the sampling bias showed similar results to the initial analysis (Appendix 1 Figure 2).

We evaluated mammalian molecular markers by using the H5N1 HPAIVs and the human virus from Chile (A/Chile/25945/2023) (*5*). The HA protein sequences of the H5N1 HPAIVs had amino acids related to those with a binding affinity to avian-like (α-2,3 sialic acid) receptors (188T, 210A, 222Q, and 224G in H5 numbering) (*7*,*8*). The HA protein sequences had 3 minor substitutions associated with increased binding affinity of the HA receptor to a human-like receptor (α-2,6 sialic acid) (S123P, S133A, and T156A in HA) (Appendix 1 Table 4). All isolates exhibited L89V, K389R, and V598T in PB2; N30D, I43M, and T215A in M; and P42S and ESEV PDZ binding motif mutations in NS, known to increase virulence in mice. The Chilean virus harbored more amino acid substitutions known to be associated with increased viral replication in mammals, including Q591K and D701N in PB2, A515T in PA, and L98F and I101M in NS (Appendix 1 Table 4).

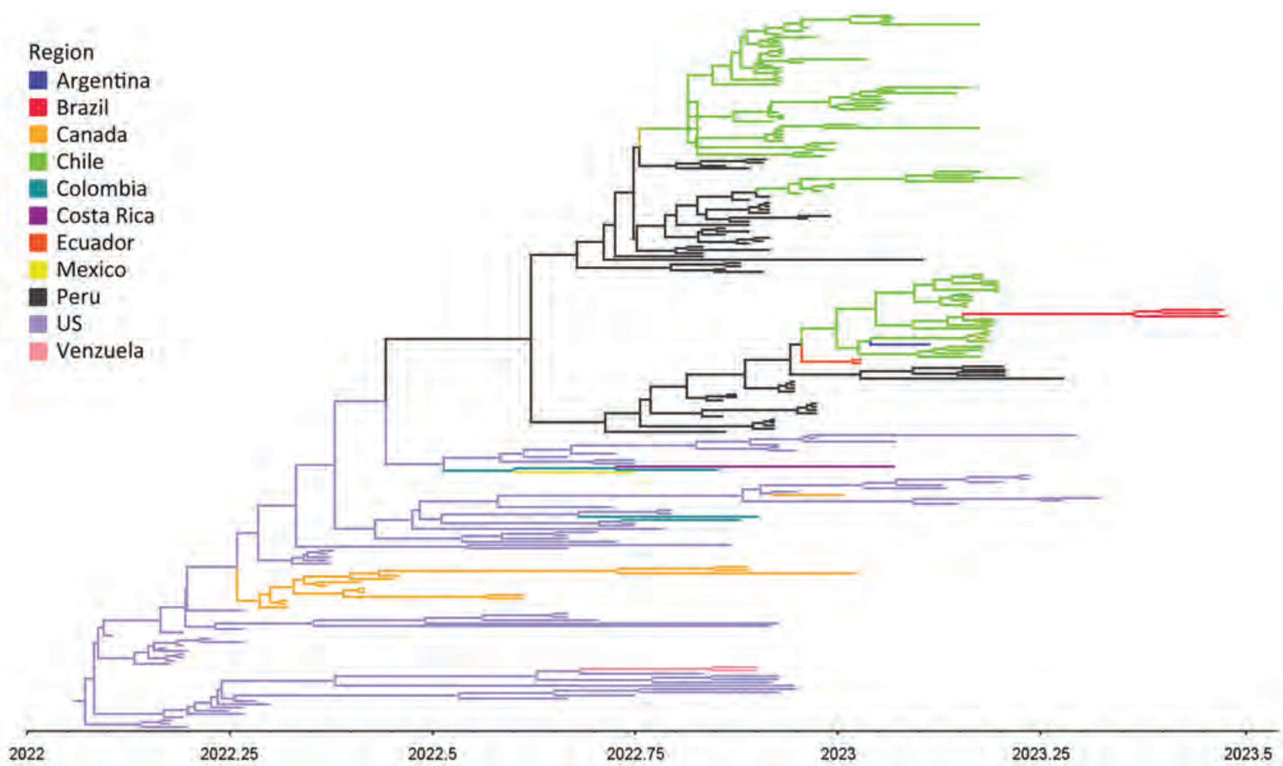

Figure. Maximum clade credibility phylogenetic tree of hemagglutinin gene based on discrete trait analysis of geographic location of wild bird carcasses identified as harboring highly pathogenic avian influenza A(H5N1) clade 2.3.4.4b virus, Brazil, 2023. The time scale is shown on the horizontal axis. Each branch is colored according to geographic region.

The reassortment of H5Nx clade 2.3.4.4b HPAIVs, containing segments from both HPAIVs and LPAIVs, created a diverse genetic pool of H5 clade 2.3.4.4 that is continuously emerging in various countries (*9*). Novel reassortment of Eurasian clade 2.3.4.4 HPAIV with North America LPAIVs was reported in 2014–2015 and 2022–2023 (*6*,*10*). South America has been largely unaffected by the HPAIV epizootic in the past decade, but more countries are reporting HPAIV since its first detection in October 2022. Royal terns and Cabot's terns are mainly coastal birds, staying on shore areas all year (P. Yorio et al., unpub. data, https://doi.org/10.1675/1524-4695-31.4.561). The terns are known to use the Atlantic Americas Flyway and move along the coast, which raises concern for the spread of H5N1 HPAIV in this region. The unprecedented global distribution and continuous generation of novel reassortant clade 2.3.4.4b HPAI H5Nx viruses call for heightened monitoring of HPAIV movement and reassortment to improve prevention and control policies.

Acknowledgments

The authors gratefully acknowledge Julia Cristina Benassi Bueno and Alessandra Greatti for their technical assistance and Cristian M. Joenck for fieldwork assistance. We thank the support of the Brazilian Post and Telegraph Company (Correios) for transporting our fieldwork supplies and samples. We also thank the National Network for Virus Surveillance in Wild Animals (PREVIR Network). We gratefully acknowledge all data contributors (i.e., the authors and their originating laboratories responsible for obtaining the specimens and their submitting laboratories) for generating the genetic sequence and metadata and sharing via GISAID (https://www.gisaid.org), on which this research is based (Appendix 2, https://wwwnc.cdc.gov/EID/article/30/3/23-1157-App2.xlsx).

This work is funded by the Ministry of Science, Technology, and Innovation (MCTI-Brazil) and by the National Council for Scientific and Technological Development (CNPq: 403761/2020-4, 400172/2022-4, and 405786/2022-0). A.G., H.L.F., and C.W.A. are recipients of the CNPq scholarship. L.M.N.S. is the recipient of the CAPES scholarship.

About the Author

Dr. Araujo is a veterinarian and postdoctoral fellow at the University of São Paulo, Brazil. Her research focuses on the epidemiology and diagnosis of infectious and parasitic diseases.

References

1. Pohlmann A, King J, Fusaro A, Zecchin B, Banyard AC, Brown IH, et al. Has epizootic become enzootic? evidence for a fundamental change in the infection dynamics of highly pathogenic avian influenza in Europe, 2021. MBio. 2022;13:e0060922. https://doi.org/10.1128/mbio.00609-22
2. Caliendo V, Lewis NS, Pohlmann A, Baillie SR, Banyard AC, Beer M, et al. Transatlantic spread of highly pathogenic avian influenza H5N1 by wild birds from Europe to North America in 2021. Sci Rep. 2022;12:11729. https://doi.org/10.1038/s41598-022-13447-z
3. Adlhoch C, Fusaro A, Gonzales JL, Kuiken T, Melidou A, Mirinavičiūtė G, et al; European Food Safety Authority, European Centre for Disease Prevention and Control, European Union Reference Laboratory for Avian Influenza. Avian influenza overview, April–June 2023. EFSA J. 2023;21:e08191.
4. World Organisation for Animal Health. World Animal Health Information System (WAHIS) Events Management. Search: High pathogenicity avian influenza viruses (poultry) and South American countries. Accession date 2023 Nov 7 [cited 2023 Nov 23]. https://wahis.woah.org/#/event-management
5. Castillo A, Fasce R, Parra B, Andrade W, Covarrubias P, Hueche A, et al. The first case of human infection with H5N1 avian Influenza A virus in Chile. J Travel Med. 2023;30:taad083. https://doi.org/10.1093/jtm/taad083
6. Youk S, Torchetti MK, Lantz K, Lenoch JB, Killian ML, Leyson C, et al. H5N1 highly pathogenic avian influenza clade 2.3.4.4b in wild and domestic birds: introductions into the United States and reassortments, December 2021–April 2022. Virology. 2023;587:109860. https://doi.org/10.1016/j.virol.2023.109860 PMID: 37572517
7. Suttie A, Deng YM, Greenhill AR, Dussart P, Horwood PF, Karlsson EA. Inventory of molecular markers affecting biological characteristics of avian influenza A viruses. Virus Genes. 2019;55:739–68. https://doi.org/10.1007/s11262-019-01700-z
8. Burke DF, Smith DJ. A recommended numbering scheme for influenza A HA subtypes. PLoS One. 2014;9:e112302. https://doi.org/10.1371/journal.pone.0112302
9. Gu M, Liu W, Cao Y, Peng D, Wang X, Wan H, et al. Novel reassortant highly pathogenic avian influenza (H5N5) viruses in domestic ducks, China. Emerg Infect Dis. 2011;17:1060–3. https://doi.org/10.3201/eid/1706.101406
10. Lee DH, Criado MF, Swayne DE. Pathobiological origins and evolutionary history of highly pathogenic avian influenza viruses. Cold Spring Harb Perspect Med. 2021;11:a038679. https://doi.org/10.1101/cshperspect.a038679

Address for correspondence: Helena Lage Ferreira, Department of Veterinary Medicine, FZEA-USP, University of São Paulo, 225 Av Duque de Caxias Norte, 13635900, Pirassununga, SP, Brazil; email: hlage@usp.br

Betacoronavirus Infection Outbreak, São Paulo, Brazil, Fall 2023

Tânia do Socorro Souza Chaves, Ana H. Perosa, Gabriela Barbosa, Diogo B. Ferreira, Nancy Bellei

Author affiliations: Universidade Federal do Pará, Belém, Brazil (T.D.S.S. Chaves); Universidade Federal de São Paulo, São Paulo, Brazil (T.D.S.S. Chaves, A.H. Perosa, G. Barbosa, D.B. Ferreira, N. Bellei)

DOI: http//:doi.org/10.3201/eid3003.230990

We report a human coronavirus OC43 infection outbreak in hospitalized patients and healthcare workers in São Paulo, Brazil, occurring after SARS-CoV-2 cases disappeared. Infection was associated with healthcare workers in 5 (29.4%) patients. Routine surveillance including a respiratory virus panel can improve coronavirus detection in both healthcare professionals and patients.

The COVID-19 pandemic has caused major human and social behavior changes. Human coronavirus (HCoV) OC43, a common human coronavirus, remains a major cause of respiratory infections. HCoV-OC43 can infect humans at any age, causing lower respiratory tract infections that can be severe in patients who have concurrent conditions (*1*,*2*). Until May 2023, a total of 2,533 patients were hospitalized with COVID-19 at Hospital São Paulo (São Paulo, Brazil). We report an unexpected HCoV-OC43 infection outbreak among patients and healthcare workers at Hospital São Paulo. We conducted this observational study in compliance with institutional guidelines and approval by the Ethics Committee of Universidade Federal de São Paulo (CEP/UNIFESP no. 29407720.4.00 00.5505).

During March–June 2023 (fall season), we collected swab specimens from patients and screened those specimens for influenza A/B virus, respiratory syncytial virus, SARS-CoV-2, and HCoV in the laboratory at our hospital as a routine surveillance method used since 2020. We evaluated samples from 927 persons who had acute respiratory infections: 446 hospitalized patients and 481 healthcare workers. We detected HCoV by using multiplex real-time PCR with specific primers and probes for HCoV-OC43, HCoV-229E, HCoV-40 HKU-1, and HCoV-NL63 (*3*,*4*). Among tested samples, 7.7% (71/927) were positive for HCoV: 10.6% (51/481) for healthcare workers and 4.5% (20/446) for hospitalized patients (Table).

Of the 71 HCoV-positive samples, 28.2% (20/71) were obtained from hospitalized patients (mean age 34.5 years; interquartile range 6–64 years) and 71.8% (51/71) from healthcare workers (mean age 41.9 years; interquartile range 32–52 years). Among healthcare workers, 46 (90.2%) samples were positive for HCoV-OC43, 4 (7.8%) for HCoV-NL63, and 1 (2%) for HCoV-229E. Among hospitalized patients, 16 (80%) patients were positive for OC43, 3 (15%) for NL63, and 1 (5%) for HKU-1. Co-infections were identified in only 4 (5.6%) case-patients: 1 patient had both HCoV-NL63 and SARS-CoV2, 1 patient had both HCoV-OC43 and respiratory syncytial virus, and 2 patients each had both HCoV-OC43 and influenza A(H1N1)pdm09 virus.

All 16 inpatients who had HCoV-OC43 had risk factors for more severe illness, such as immunosuppression (3 patients) and underlying conditions (8 patients); 5 (31.2%) patients had both. Two (2/16; 12.5%) immunosuppressed patients required admission to an intensive care unit and died (1 child, 1 adult).

Radiologic images were obtained for 14 of 16 inpatients who had HCoV-OC43, and 62.5% (10/16) had an alteration detected by chest computed tomography. Radiologic findings included lung opacities, bilateral interstitial infiltrate, consolidations, and centrilobular micronodules with a unifocal or multifocal ground glass pattern, all of which were predominantly distributed within the lower lobes.

A probable nosocomial acquisition might have occurred because the infection rate among healthcare workers peaked earlier (May) than the observed inpatient peak rate (June) (Table). Five (31.2%) inpatients who had HCoV-OC43–positive samples were

Table. HCoV-positive case-patients by month, age, and participant groups during the betacoronavirus infection outbreak in Hospital São Paulo, São Paulo, Brazil, March–June 2023*

Characteristic	Total	Hospitalized patients	Healthcare workers
Total	71/927 (7.7)	20/446 (4.5)	51/481 (10.6)
March	4/295 (1.3)	2/128 (1.6)	2/167 (1.2)
April	5/195 (2.6)	2/104 (1.9)	3/91 (3.3)
May	28/218 (12.8)	4/102 (3.9)	24/116 (20.7)
June	34/219 (15.5)	12/112 (10.7)	22/107 (20.6)
Adults (>12 y old)	63/813 (7.7)	12/332 (3.6)	51/481 (10.6)
Children	8/114 (7.0)	8/114 (7.0)	NA

*Values are no. positive/no. tested (%). HCoV, human coronavirus; NA, not applicable.

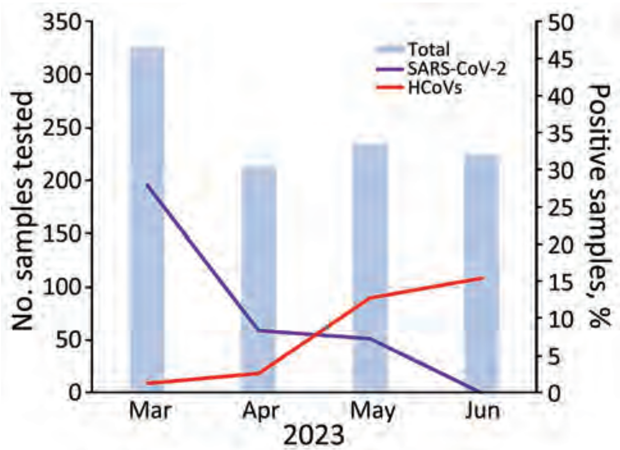

Figure. Positivity rates for SARS-CoV2 and HCoV in Hospital São Paulo during betacoronavirus infection outbreak, São Paulo, Brazil, March–June 2023. Blue bars indicate the number of samples tested each month. Purple and red lines indicate the percentage of samples that were positive for each virus. HCoV, human coronavirus.

housed within different wards several days after admission; thus, it was possible to confirm nosocomial acquisition. In those cases, HCoV-OC43 transmission took place within inpatient wards, specifically during activities involving direct contact with a healthcare worker. Contact tracing connected patient cases to interactions with healthcare workers.

The SARS-CoV-2 positivity rate during the outbreak period (March–June) varied from 7.3% to 27.9% (Figure); no cases were reported in June. To provide background for the outbreak, we conducted surveillance testing for respiratory viruses collected 2 months before (January–February) and after (July–August) the outbreak; no HCoV was detected during those periods. In previous studies conducted at our hospital before the COVID-19 pandemic, we did not observe >5% monthly circulation of HCoVs during the study years under investigation (*5*). The HCoV-OC43 outbreak peak occurred after the disappearance of SARS-CoV-2 cases (Figure).

In this outbreak, hospitalized patients showed evolution of a severe form of infection caused by HCoV-OC43. Nirmatrelvir/ritonavir is a promising antiviral drug combination in preclinical studies that inhibits the proteolytic activity of SARS-CoV-2 M^{pro}, a cysteine protease found in the family Coronaviridae (*6*), and might be useful for treating HCoV-OC43 infections.

At the end of March 2023 in Brazil, the National Health Surveillance Agency (Agência Nacional de Vigilância Sanitária) updated guidelines for mask use in healthcare settings. Since April 2023, the hospital committee has relaxed the requirement for universal mask use, making them obligatory only in areas designated for patient care (*7*). Relaxing mask use by healthcare workers who provide care to high-risk patients likely contributed to nosocomial acquisition of HCoV-OC43. Furthermore, healthcare workers who had respiratory infections other than SARS-CoV-2 infections were likely less vigilant in using personal protective equipment during patient care. In addition, an unconscious relaxation in maintaining precautions might have occurred, possibly because persons did not perceive themselves as potential transmitters.

In conclusion, we report the occurrence of HCoV-OC43 causing severe acute respiratory infection that might be underestimated because of a lack of better diagnostic approaches for viral respiratory infections, particularly in high-risk patients. Routine surveillance using a diagnostic panel of respiratory viruses can improve detection in both healthcare workers and patients and can help determine prevalence and prevent transmission of different viruses.

T.S.S.C was supported by the Evandro Chagas Institute at the Ministry of Health of Brazil and the School of Medicine at the Federal University of Pará.

N.B., A.H.P., and T.S.S.C. conceived and designed the study and contributed to data analysis; A.H.P., D.B.F., and G.B. contributed to diagnostic, patient, and public health surveillance data analysis; and N.B., T.S.S.C., and G.B. wrote the first draft. All authors contributed and approved the final manuscript.

About the Author

Dr. Chaves is an infectious and tropical diseases research scientist at the Evandro Chagas Institute/Secretariat of Health and Environment Surveillance at the Brazilian Ministry of Health, professor at the Faculdade de Medicina da Universidade Federal do Pará, Belém, Brazil, and a postdoctoral research scientist at the Federal University of São Paulo, São Paulo, Brazil. Her primary research interests are epidemiologic and clinical studies of infectious and tropical diseases, emerging and reemerging diseases, public health¸ and travel medicine.

References

1. Chow EJ, Uyeki TM, Chu HY. The effects of the COVID-19 pandemic on community respiratory virus activity. Nat Rev Microbiol. 2023;21:195–210. https://doi.org/10.1038/s41579-022-00807-9
2. Vabret A, Mourez T, Gouarin S, Petitjean J, Freymuth F. An outbreak of coronavirus OC43 respiratory infection in Normandy, France. Clin Infect Dis. 2003;36:985–9. https://doi.org/10.1086/374222

3. Kesheh MM, Hosseini P, Soltani S, Zandi M. An overview on the seven pathogenic human coronaviruses. Rev Med Virol. 2022;32:e2282. https://doi.org/10.1002/rmv.2282
4. Dare RK, Fry AM, Chittaganpitch M, Sawanpanyalert P, Olsen SJ, Erdman DD. Human coronavirus infections in rural Thailand: a comprehensive study using real-time reverse-transcription polymerase chain reaction assays. J Infect Dis. 2007;196:1321–8. https://doi.org/10.1086/521308
5. Cabeça TK, Granato C, Bellei N. Epidemiological and clinical features of human coronavirus infections among different subsets of patients. Influenza Other Respir Viruses. 2013;7:1040–7. https://doi.org/10.1111/irv.12101
6. Owen DR, Allerton CMN, Anderson AS, Aschenbrenner L, Avery M, Berritt S, et al. An oral SARS-CoV-2 M^pro^ inhibitor clinical candidate for the treatment of COVID-19. Science. 2021;374:1586–93. https://doi.org/10.1126/science.abl4784
7. ANVISA. Technical Note GVIMS/GGTES/ANVISA No.04/2020. Guidelines for health services: prevention and control measures that must be adopted when providing care to suspected or confirmed cases of COVID-9 infection [in Portuguese] [cited 2024 Jan 3]. https://www.gov.br/anvisa/pt-br/centraisdeconteudo/publicacoes/servicosdesaude/notas-tecnicas/2020/nota-tecnica-gvims_ggtes_anvisa-04_2020-25-02-para-o-site.pdf

Address for correspondence: Tânia do Socorro Souza Chaves, Universidade Federal de São Paulo, Rua Pedro de Toledo 781, São Paulo CEP 04039-032, Brazil; Evandro Chagas Institute/Secretariat of Health and Environment Surveillance/Brazilian Ministry of Health, Rodovia BR-316 km 7 s/n, Ananindeua CEP 67030-000, Brazil; or Universidade Federal do Pará/Instituto de Ciências Médicas, Avenida Generalíssimo Deodoro número 1, Belém CEP 66050-060, Brazil; email: tania.chaves@uol.com.br

Larone's Medically Important Fungi: A Guide to Identi ication, 7th Edition

Lars F. Westblade, Eileen M. Burd, Shawn R. Lockhart, Gary W. Procop Larone;
John Wiley & Sons, Inc., Hoboken, NJ, USA, 2023;
ISBN: 978-1-683-67440-5 (print);
ISBN: 9781683674436 (ebook); Pages: 506; Price: US$135

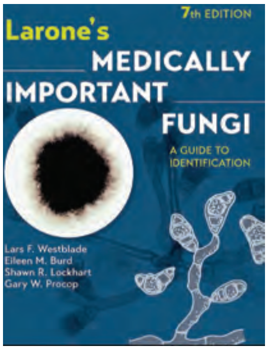

The French chemist and microbiologist Louis Pasteur famously stated that "in the fields of observation, chance favors only the prepared mind." How better then to be prepared for a journey into the challenging and often perplexing world of clinical mycology than with a copy of *Larone's Medically Important Fungi* in hand? Composed with the needs of the medical mycology technician in mind (which, fortunately, translate equally well to the needs of laboratorians, physicians, and trainees alike) and written in the style of a field guide to identification, Larone's guide serves as an easily accessible yet surprisingly granular compendium of medically important fungi.

As stated in the book's preface, this manual does not include an exhaustive account of the epidemiology, pathophysiology, diagnosis, and therapeutics for each fungal pathogen, nor is it designed to replace more comprehensive mycology textbooks. There are other well-known and exhaustive references for that. The aim of this guidebook is to help provide a rapid preliminary diagnosis within the trenches of the microbiology laboratory, based only on the colony and microscopic morphology of a cultured organism or, at times, its morphology on direct stains.

In keeping with this purpose, this newest (7th) edition's format adheres to an ergonomic design, with a color-coded layout that increases its usability in real time. The book begins with a Basics section to orient readers on how to wield the guide and ends with a highly useful image appendix and glossary of commonly used, but sometimes nebulous, terms (e.g., blastoconidium, the technical term for a unicellular yeast). The Basics section begins ominously, by cautioning that readers "should understand several points" before using the guide; such counsel is justified, given that the practice of fungi identification in the medical setting is highly nuanced and requires strict adherence to standard laboratory procedures of quality and safety for favorable results. The meat of the matter lies in the middle of the book, which features 4 core sections on direct identification of fungi from clinical specimens, identification of fungi from cultured isolates, basics of molecular methods of fungal identification, and laboratory techniques. The first 2 sections stand out as outstanding compendia of clinically important fungi, with pithy descriptions of each pathogen, its taxonomy, pathogenicity, site of infection, accompanying tissue reactions, and microscopic and colony morphologies. Each fungi discussion is accompanied by a hand-drawn sketch of the organism's distinct morphology alongside one or more representative photomicrographs. Many of the photos are in color, but a large number are unfortunately monochrome, making them less visually appealing and rendering the depicted structures harder to discern. A full-color image appendix partially makes up for this concern.

Importantly, most organisms are arranged according to their morphological similarities rather than alphabetically to make comparisons between similarly appearing structures easier. This categorization works well with the included discussion of nonfungal pathogens (e.g., actinomycetes and *Prototheca*), which closely resemble fungi microscopically.

One of the reasons Larone's guide is such an effective mycology handbook is because it takes nothing for granted. Replete with explanations of basic histological terms, ranging from abscess to Splendore-Hoeppli phenomenon, and descriptions of fundamental tissue reactions to fungal infection (e.g., granulomatous inflammation)—all complemented by helpful summary tables and explanatory figures—the book achieves the remarkable feat of being simultaneously concise and complete. Although the emphasis is on usability, readers will enjoy the breadth of information provided. The book is well edited, and the newest edition now includes information on emerging pathogens, such as *Emergomyces* and *Emmonsia* species.

Larone's guide is not meant to be the sort of book one peruses cover to cover nor the subject of a leisurely read, but the kind of book that is never far away from the bench, the microscope, or the office. It appeals to all levels of expertise—from mycologists-in-training to seasoned experts and from academic to commercial laboratories—because it provides the actionable information needed to make a diagnosis. I was gifted a copy of an earlier edition as a budding clinical mycologist and have since reached for it countless times. Joining the pantheon of revered medical tomes is no small feat, yet Larone's guide successful formula has enabled it to accomplish just that.

Marwan M. Azar

DOI: http://doi.org/10.3201/eid3003.231623

Author affiliation: Yale School of Medicine, New Haven, Connecticut, USA

Address for correspondence: Marwan M. Azar, Department of Medicine, Section of Infectious Diseases and Department of Laboratory Medicine, Yale School of Medicine, 135 College St, New Haven, CT 06510, USA; email: marwan.azar@yale.edu

Paulina Siniatkina (1989–), *Don't speak*! *(detail).* Tempera on canvas (2016), 37.4 in × 41.3 in/100 cm × 105 cm. http://www.paulinasiniatkina.com

Mental Health and Tuberculosis—Holding Our Breath in Isolation

Rena Fukunaga, Patrick K. Moonan

Paulina Siniatkina, an artist and activist, is a survivor of tuberculosis (TB). In 2015, in a TB hospital on the outskirts of Moscow, the treating physician advised her to never talk about her TB diagnosis to anyone—further reinforcing the longstanding stigma associated with the disease. During her 7 months of treatment in isolation, Paulina experienced firsthand the suffering and loss associated with TB and turned to art to express her emotions and frustrations. She now uses her artistic talent and personal experience to advocate in the global fight against TB, and her work has drawn international recognition by the American Medical Association and World Health Organization. This month's cover image, *Don't speak!*, by Ms. Siniatkina, exemplifies the poignant psychology associated with TB. At the center, a young woman with

Author affiliation: Centers for Disease Control and Prevention, Atlanta, Georgia, USA

DOI: https://doi.org/10.3201/eid3003.AC3003

sullen eyes draws your attention with her gaze, using a silent expression of longing to tell her story from behind the mask. Her unspoken feelings of hopelessness and depression appear to be subtly calmed by her nervous plucking of white petals from the single daisy protected by her hand, as the surrounding community dissolves into the background with looks of fear and judgement.

TB remains one of the leading causes of death by an infectious disease agent. Each year, more than 10 million people suffer from TB, and 1.5 million die as a result. Although curable, TB is a chronic multisystem infectious disease with well-documented, and often life-changing, disability and reduced quality of life. Treatment requires a multidrug, multimonth course of antibiotics; drug-resistant forms of TB extend the duration of treatment and in many communities require the patient to spend months in hospital or respiratory isolation. Not surprisingly, an estimated 40%–70% of persons treated for TB experience clinical anxiety or depression.

Beyond stigma and social isolation, mental illness persists as a silent driver of the global TB epidemic. Mental illness is associated with acquired drug resistance, TB transmission, disease recurrence, and TB-related death. Mental illness and TB are often exacerbated by homelessness and HIV co-infection. Integrated services for persons with TB and concurrent psychiatric conditions such as addiction, anxiety, or depression are now considered an essential component of global TB elimination efforts. However, in many countries with high burdens of TB, access to psychiatric services, including routine mental health screening and treatments, remain extremely limited.

Each year on March 24, we commemorate World TB Day in honor of the day Robert Koch announced to the Berlin Physiologic Society that he had discovered the cause of tuberculosis. World TB Day is a time to remember the millions of persons who suffer from TB, often in silence. It is also a time to break the silence, raise greater awareness, take specific actions to reduce the impact of mental health on our ambitions for global TB elimination, and not hold our breath in isolation.

Acknowledgments

We thank Paulina Siniatkina, the artist discussed in this article, for her review of the manuscript and for permission to republish her work. More of her work can be viewed at http://www.paulinasiniatkina.com.

Bibliography

1. Alene KA, Wangdi K, Colquhoun S, Chani K, Islam T, Rahevar K, et al. Tuberculosis related disability: a systematic review and meta-analysis. BMC Med. 2021;19:203. https://doi.org/10.1186/s12916-021-02063-9
2. Bamrah S, Yelk Woodruff RS, Powell K, Ghosh S, Kammerer JS, Haddad MB. Tuberculosis among the homeless, United States, 1994–2010. Int J Tuberc Lung Dis. 2013;17:1414–9. https://doi.org/10.5588/ijtld.13.0270
3. Chang SH, Cataldo JK. A systematic review of global cultural variations in knowledge, attitudes and health responses to tuberculosis stigma. Int J Tuberc Lung Dis. 2014;18:168–73, i–iv. https://doi.org/10.5588/ijtld.13.0181
4. Egelund EF, Bucciarelli AL. Art and the fight against tuberculosis. JAMA. 2022;328:509–10. https://doi.org/10.1001/jama.2021.24029
5. Hayward SE, Deal A, Rustage K, Nellums LB, Sweetland AC, Boccia D, et al. The relationship between mental health and risk of active tuberculosis: a systematic review. BMJ Open. 2022;12:e048945. https://doi.org/10.1136/bmjopen-2021-048945
6. Kim L, Moonan PK, Heilig CM, Yelk Woodruff RS, Kammerer JS, Haddad MB. Factors associated with recurrent tuberculosis more than 12 months after treatment completion. Int J Tuberc Lung Dis. 2016;20:49–56. https://doi.org/10.5588/ijtld.15.0442
7. Koch R. Die Atiologic der Tuberkulose. Berliner Klinische Wochenschrift. 1882;15:221–30.
8. Lee G, Scuffell J, Galea JT, Shin SS, Magill E, Jaramillo E, et al. Impact of mental disorders on active TB treatment outcomes: a systematic review and meta-analysis. Int J Tuberc Lung Dis. 2020;24:1279–84. https://doi.org/10.5588/ijtld.20.0458
9. Oeltmann JE, Kammerer JS, Pevzner ES, Moonan PK. Tuberculosis and substance abuse in the United States, 1997–2006. Arch Intern Med. 2009;169:189–97. https://doi.org/10.1001/archinternmed.2008.535
10. The Global Fund to Fight AIDS. Tuberculosis and malaria. fighting pandemics and building a healthier and more equitable world: Global Fund Strategy (2023–2028) [cited 2023 Sep 5]. https://www.theglobalfund.org/en/strategy
11. Thornicroft G, Ahuja S, Barber S, Chisholm D, Collins PY, Docrat S, et al. Integrated care for people with long-term mental and physical health conditions in low-income and middle-income countries. Lancet Psychiatry. 2019;6:174–86. https://doi.org/10.1016/S2215-0366(18)30298-0
12. Volkmann T, Moonan PK, Miramontes R, Oeltmann JE. Excess alcohol use and death among tuberculosis patients in the United States, 1997–2012. J Tuberc Res. 2016;4:18–22. https://doi.org/10.4236/jtr.2016.41003
13. World Health Organization. Hold your breath, paintings made by Russian artist while in a TB clinic [cited 2023 Dec 21]. https://www.who.int/news-room/feature-stories/detail/hold-your-breath-paintings-made-by-russian-artist-while-in-a-tb-clinic
14. World Health Organization. Global tuberculosis report, 2022. Geneva: The Organization; 2022.

Address for correspondence: Patrick K. Moonan, Centers for Disease Control and Prevention, 1600 Clifton Rd NE, Mailstop H21-6, Atlanta, GA 30329-4018, USA; email pmoonan@cdc.gov

EMERGING INFECTIOUS DISEASES®

Upcoming Issue

- Crimean-Congo Hemorrhagic Fever Virus Diversity and Reassortment, Pakistan, 2017–2020
- Single-Center, Retrospective Study Showing *Clostridium butyricum* Bacteremia Associated with Probiotic Use, Japan
- Geographic Disparities in Domestic Pig Population Exposure to Ebolaviruses, Guinea
- A One Health Perspective on *Salmonella infantis*, the Emerging Human Multidrug-Resistant Pathogen
- Alfred Whitmore and the Discovery of Melioidosis
- Case Report of Nasal Rhinosporidiosis in South Africa
- Concurrent Outbreaks of Hepatitis A, Invasive Meningococcal Disease, and Mpox, Florida, USA, 2021–2022
- Breaking Through: My Life in Science
- Co-Circulating Monkeypox and Swinepox Viruses, Democratic Republic of the Congo, 2022
- Phylogenetic Characterization of *Orthohantavirus dobravaense*
- Effects of Shock and Vibration on Last Mile Transportation of Ebola Vaccine Regimen under Refrigerated Conditions
- Novel Oral Poliovirus Vaccine 2 Safety Evaluation during Nationwide Supplemental Immunization Activity, Uganda, 2022
- Reemergence of Sylvatic Dengue Virus Serotype 2 in Kedougou, Senegal, 2020
- Case Management of Imported Crimean-Congo Hemorrhagic Fever, Senegal, July 2023
- Chlamydia pneumoniae Upsurge at a Tertiary Hospital, Lausanne, Switzerland
- Isolation of Diverse Simian Arteriviruses Causing Hemorrhagic Disease

Complete list of articles in the April issue at
https://wwwnc.cdc.gov/eid/#issue-307

Earning CME Credit

To obtain credit, you should first read the journal article. After reading the article, you should be able to answer the following, related, multiple-choice questions. To complete the questions (with a minimum 75% passing score) and earn continuing medical education (CME) credit, please go to http://www.medscape.org/journal/eid. Credit cannot be obtained for tests completed on paper, although you may use the worksheet below to keep a record of your answers.

You must be a registered user on http://www.medscape.org. If you are not registered on http://www.medscape.org, please click on the "Register" link on the right hand side of the website.

Only one answer is correct for each question. Once you successfully answer all post-test questions, you will be able to view and/or print your certificate. For questions regarding this activity, contact the accredited provider, CME@medscape.net. For technical assistance, contact CME@medscape.net. American Medical Association's Physician's Recognition Award (AMA PRA) credits are accepted in the US as evidence of participation in CME activities. For further information on this award, please go to https://www.ama-assn.org. The AMA has determined that physicians not licensed in the US who participate in this CME activity are eligible for AMA PRA Category 1 Credits™. Through agreements that the AMA has made with agencies in some countries, AMA PRA credit may be acceptable as evidence of participation in CME activities. If you are not licensed in the US, please complete the questions online, print the AMA PRA CME credit certificate, and present it to your national medical association for review.

Article Title

Molecular Epidemiology of Underreported Emerging Zoonotic Pathogen *Streptococcus suis* in Europe

CME Questions

1. *Streptococcus suis* is endemic in which of the following countries?

A. Vietnam and Thailand
B. Germany and Spain
C. Tanzania and Kenya
D. Ecuador and Colombia

2. Which serotype of *S. suis* is associated with the greatest proportion of zoonotic infections historically as well as in the current study?

A. Serotype 2
B. Serotype 4
C. Serotype 7
D. Serotype 9

3. What was the main clinical syndrome associated with *S. suis* infections in the current study?

A. Endocarditis
B. Sepsis
C. Enteritis
D. Meningitis

4. Which of the following statements regarding genetic characteristics of *S. suis* isolates in the current study is most accurate?

A. Most strains were part of the major zoonotic clade CC20
B. Strains from clades CC1 and CC20 had more accessory genes overrepresented in zoonotic isolates
C. All pathogenic clades featured the sly, mrp, and fhb genes
D. Overrepresented genes generally increased zoonotic potential

Earning CME Credit

To obtain credit, you should first read the journal article. After reading the article, you should be able to answer the following, related, multiple-choice questions. To complete the questions (with a minimum 75% passing score) and earn continuing medical education (CME) credit, please go to http://www.medscape.org/journal/eid. Credit cannot be obtained for tests completed on paper, although you may use the worksheet below to keep a record of your answers.

You must be a registered user on http://www.medscape.org. If you are not registered on http://www.medscape.org, please click on the "Register" link on the right hand side of the website.

Only one answer is correct for each question. Once you successfully answer all post-test questions, you will be able to view and/or print your certificate. For questions regarding this activity, contact the accredited provider, CME@medscape.net. For technical assistance, contact CME@medscape.net. American Medical Association's Physician's Recognition Award (AMA PRA) credits are accepted in the US as evidence of participation in CME activities. For further information on this award, please go to https://www.ama-assn.org. The AMA has determined that physicians not licensed in the US who participate in this CME activity are eligible for AMA PRA Category 1 Credits™. Through agreements that the AMA has made with agencies in some countries, AMA PRA credit may be acceptable as evidence of participation in CME activities. If you are not licensed in the US, please complete the questions online, print the AMA PRA CME credit certificate, and present it to your national medical association for review.

Article Title

Disseminated Leishmaniasis, a Severe Form of *Leishmania braziliensis* Infection

CME Questions

1. Which of the following statements regarding disseminated leishmaniasis (DL) is most accurate?

A. DL is defined by lesions in ≥ 4 anatomic locations
B. The prevalence of DL has increased > 20-fold in the past 30 years
C. DL is generally caused only by Leishmania amazonensis
D. DL is characterized by a high number of parasites in situ in lesions

2. What were the respective rates of clinical cure of leishmaniasis associated with one course of meglumine antimoniate (MA) for cutaneous leishmaniasis (CL) and DL in the current study?

A. 91% for CL; 84% for DL
B. 78% for CL; 82% for DL
C. 60% for CL; 44% for DL
D. 35% for CL; 31% for DL

3. Which of the following variables is most significantly associated with a higher risk of more than 50 lesions of DL (DL > 50) vs less than 40 lesions of DL (DL < 40) in the current study?

A. Longer duration between appearance of the first lesion and dissemination
B. Older age
C. Longer duration of illness
D. Higher rates of mucosal disease

4. Which of the following statements regarding treatment with amphotericin B, miltefosine, or miltefosine plus MA in the current study is most accurate?

A. The number of lesions was highest in the miltefosine-plus-MA cohort
B. Miltefosine plus MA was associated with the fastest mean healing time
C. Amphotericin B was associated with the highest cure rate
D. No treatment group had a superior cure rate vs MA alone

Emerging Infectious Diseases
Photo Quiz Articles

Volume 14, Number 9
September 2008

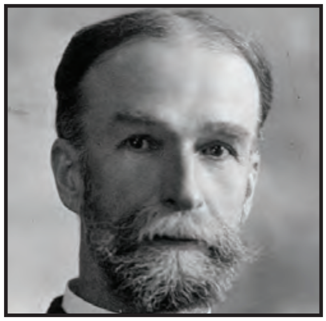

Volume 14, Number 12
December 2008

Volume 15, Number 9
September 2009

Volume 15, Number 10
October 2009

Volume 16, Number 6
June 2010

Volume 17, Number 3
March 2011

Volume 17, Number 12
December 2011

Volume 19, Number 4
April 2013

Volume 20, Number 5
May 2014

Volume 21, Number 9
September 2015

Volume 22, Number 8
August 2016

Volume 28, Number 3
March 2022

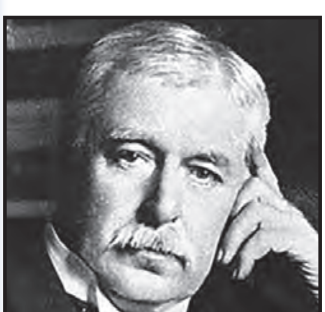

Volume 28, Number 7
July 2022

Click on the link below to read about the people behind the science.

https://bit.ly/3LN02tr

See requirements for submitting a photo quiz to EID.

https://bit.ly/3VUPqfj

EID Journal